Validating the techno-economic viability of hemp lime construction for passive and low energy moisture control in museum storage

Leskard, Marta

Award date:
2021

Awarding institution:
University of Bath

Validating the techno-economic viability of hemp lime construction for passive and low energy moisture control in museum storage

Marta Kristine Leskard

A thesis submitted for the degree of Doctor of Philosophy

University of Bath

Department of Architecture and Civil Engineering

February 2021

Signed:……..

Abstract

Museums require storage for cultural heritage collections that provide stable environments, ensuring that risks of deterioration from environmental conditions are reduced as far as possible. Incorrect levels of relative humidity (RH) can lead to physical, chemical and biological degradation, devaluing historic collections and damaging institutional reputations. Analysing the historical development of RH guidelines for the storage of museum collections through a review of literature on the risks and effects of incorrect RH, past and current recommendations for RH levels and fluctuations, and past and current practices to control RH clarifies the current approach to provide suitable and sustainable storage for cultural collections. Standard practice has been to regulate RH by relying on large-scale heating, ventilation and air conditioning systems which has had significant impact on institutional carbon footprint, energy use and operating expenditure but which has not always achieved the required stability. Contemporary research on biobased construction materials has highlighted the potential for their transient hygrothermal behaviour to buffer internal environment, providing good indoor air quality and energy savings. A key knowledge gap is the lack of assessment to identify the extent to which such hygrothermal behaviour can moderate RH levels and fluctuations under dynamic museum storage conditions.

This thesis explores the hygrothermal performance of hemp lime concrete (HLC), in augmenting the regulation of RH within a museum storage building in a temperate climate. The key objectives of the investigation were to assess the moisture management capacities of HLC through a literature review of relevant studies and *in situ* monitoring of a museum store utilising HLC as part of a low energy RH control system and to put the findings of the assessment into the context of conventional museum RH control practices by comparing performance and operational costs with other low energy museum stores. The assessments were carried out using a case study, the Science Museum's Hempcrete Museum Store (HMS). By evaluating the performance of the case study over several years, from 2012 to 2020, through transient, first and second steady states of building use, the moisture management capacity of HLC as used in the building's wall construction has been shown to augment the moderation of RH to meet the museum requirements by reducing reliance on energy consuming mechanical systems. The comparison with the effectiveness achieved in controlling RH in other low energy storage buildings during the same period demonstrated that the hygroscopic properties of HLC decreased the need for mechanical control, cutting operational expenditure by a minimum of 30% while still maintaining levels in the museum's specified range of 40% RH to 60% RH. Buffering capacity of the HLC has been shown to reduce the effects of mechanical system function and malfunction and to sustain specified conditions through passive means. One of the most important findings during the *in situ* monitoring has been the effect of the thermodiffusion phenomenon across the porous HLC walls, which results in internal RH rising during periods of higher external temperatures, confirming the feasibility of using dehumidification rather than heating and ventilation as active controls to achieve specified conditions.

Acknowledgements

I am greatly indebted to Dr Stephen Lo for his meticulous supervision and continuous support throughout what has been one of the most challenging endeavours of my career.

I am grateful to Dr Mike Lawrence who encouraged me to take up the challenge and enter the field of Civil Engineering, a discipline in which I had little experience but great interest. I would also like to thank both examiners, Dr Andy Shea and Dr Mervyn Smyth for their detailed analysis and constructive criticism of my thesis.

I would like to thank the Science Museum Group for offering me the opportunity to undertake the challenge by financing my studies throughout, allowing me the time to pursue research and letting me use the Hempcrete Museum Store as the case study. Particular thanks and gratitude go to Louisa Burden, Head of Conservation, SMG, as I would never have been able to succeed in this challenge without her assistance, guidance, support, advice, encouragement and good humour.

I could not have carried out this challenge while still working without the support of my SMG colleagues in Conservation and Collections Care, and in particular, the National Collections Centre CCC team who managed beautifully without me. I would particularly like to thank Simon Stephens and Jonathan Hobbs for their invaluable assistance when manufacturing the sensors for the Dampwatch and Jessica Crann, who deputised for me during my extended study breaks, keeping all the balls in the air.

Without Matt Moore, there might never have been a Hempcrete Museum Store and so I am indebted to him. Thanks also must go to Dr Lubo Jankovic and Ian Pritchett for encouraging me in this work.

I would like to thank the team at Hanwell for their support and quick response to my many queries.

This thesis would not have been possible without the belief from my family and friends that I was up to the challenge and that I would make it through to the end.

To my parents

Table of Contents

List of Figures and Tables

List of Abbreviations

AHU	Air Handling Unit
AIC	American Institute for Conservation of Historic & Artistic Works
AAC	Autoclaved Aerated Concrete
AICCM	Australian Institute for the Conservation of Cultural Materials
ASHRAE	American Society for Heating, Refrigerating & Air-Conditioning Engineers
BESTEST	Building Energy Simulation Test
BM	British Museum
BMFA	Boston Museum of Fine Arts
BMS	Building Management System
BSI	British Standards Organisation
$Ca(OH)_2$	Calcium hydroxide
$CaCO_3$	Calcium carbonate
CAL	Conservation Analytical Laboratory (Smithsonian)
CaO	Calcium oxide
CAPEX	Capital Expense
$CaSO_4$	Calcium Sulphate
CCA	Canadian Council of Archives
CCI	Canadian Conservation Institute
CLT	Cross-Laminated Timber
CMA	Canadian Museums Association
CO_2	Carbon dioxide
CSH	Calcium Silicate Hydrate
CSV	Comma-separated Values
DSY	Design Summer Year
DVS	Dynamic Vapour Sorption
EE	Embodied Energy
EMC	Equilibrium Moisture Content
EMS	Environmental Monitoring System
EN	European Standards
EU	European Union
FGD	Flue Gas Desulphurisation
FPRL	Forest Products Research Laboratory
GCI	Getty Conservation Institute
GUI	Graphical User Interface
H_2O	Water
HAM	Heat, Air & Moisture
HAMT	Heat, Air, Moisture & Temperature
HLC	Hemp lime Concrete
HMS	Hempcrete Museum Store
HVAC	Heating, Ventilating & Air Conditioning
ICCROM	International Centre for the Study of the Preservation and Restoration Cultural Property
ICOM	International Council of Museums
ICOM-CC	International Council for Museums- Committee for Conservation
IES<VE>	Integrated Environmental Solutions Virtual Environment
IIC	International Institute for Conservation of Historic & Artistic Works
ISO	International Standards Organisation

JIS	Japanese Industrial Standard
L&A	Library & Archives
LCA	Life Cycle Assessment
LWC	Lightweight Concrete
M&E	Mechanical & Engineering
MBV	Moisture Buffer Value
MC	Moisture Content
$MgCl_2$	Magnesium Chloride
MgO	Magnesium Oxide
NCC	National Collections Centre
NG-L	National Gallery, London
NISO	National Information Standards Organization
NMDC	National Museum Directors Conference
NMR	Nuclear Magnetic Resonance
NRM	National Railway Museum
NTC	Negative Temperature Coefficient
NWC	Normal Weight Concrete
O&M	Operation & Maintenance
OPC	Ordinary Portland Cement
OPEX	Operating Expense
PAS	Publicly Available Specification
PCB	Printed Circuit Board
PD	Published Document
Pt	Platinum
PTC	Positive Temperature Coefficient
PV	Photovoltaic
RH	Relative Humidity
RH/T	Relative Humidity/Temperature
RINA	Rail Industry National Archive
RTD	Resistance Temperature Detector
SCM	Science Museum
SiO_2	Silicon Dioxide
SMG	Science Museum Group
SPARK	Simulation Problem Analysis & Research Kernel
T	Temperature
UNESCO	United Nations Educational, Scientific and Cultural Organization
V&A	Victoria & Albert Museum
VC	Vapour Content
VOC	Volatile Organic Compound
VP	Vapour Pressure
VPN	Virtual Private Network
WME	Wood Moisture Equivalent
XRPD	X-ray Powder Diffraction

Nomenclature

A	area, m^2
A	adsorbate, mg/l
b_m	moisture effusivity, kg/(m^2·Pa·$s^{½}$)
C	concentration of solute, mg/l
c	specific heat capacity, J/kg·K
D	moisture diffusion coefficient, m^2/s
D_H	diffusion coefficient dependent on pore relative humidity, kg/(m^2·s·K)
D_{HT}	coupling coefficient for mass diffusion resulting from the thermal gradient, kg/(m^2·s·K)
D_T	thermal diffusion coefficient, m^2/s·K
H	pore relative humidity, %
J	mass flux, kg/(m2·s)
K	adsorption equilibrium constant, mg/g
K_B	BET constant, l/mg
K_L	Langmuir equilibrium constant, l/mol
K	permeability coefficient, darcy: derived unit = 9.869233 $(\mu m)^2$
L	length, m
m	mass, kg
MBV	moisture buffer value, g·(m^2·%RH)
N	unit of force, kg·m·s^{-2}
n	adsorption equilibrium constant, mg/l
P	water vapour pressure, Pa
P_0	saturation vapour pressure, Pa
Q	flow rate, m^3/s
q_e	equilibrium adsorbent-phase concentration of adsorbate, mg/l
q_m	maximum monolayer adsorption capacity, mg/g
R	molar gas constant, J/(kg·K)
r	radius of curvature, m
T	temperature, °K
t	time, s
u	humidity or moisture ratio, (kg/kg)
V	volume, m^3
V_m	molar volume, m^3/mol
w	moisture content, kg/m^3
X	distance, m
γ	surface tension, N/m
δ_ρ	water vapour permeability, kg/(m·s·Pa)
δ_α	water vapour permeability of air, kg/(m·s·Pa)
η	viscosity, Pa·s
θ	angle, °
κ	areal heat capacity, kJ/m^2·K
λ	thermal conductivity, W/(m·K)
μ	water vapour resistance factor
ξ	thermal effusivity, J/$s^{1/2}$·m^2·K
ρ	density, kg/m^3
φ	relative humidity, %

Chapter 1 Thesis Preface

1.1 Introduction

This chapter identifies the economic, environmental and reputational issues facing museums currently in providing suitable and sustainable storage for cultural collections. It describes the risks to cultural collections if nothing is done to replace the standard practices for regulating relative humidity (RH) that have significant impacts on institutional carbon footprint and energy use. It sets out the objectives of the research project and provides a framework for the written thesis.

1.2 Background

This thesis explores the potential of a selected hygroscopic building material, hemp lime concrete (HLC), to augment the regulation of RH within museum storage buildings in temperate climates. The rationale for the research is based on directives to provide long-term sustainable storage for cultural heritage collections, reducing energy use and carbon footprint while still ensuring continuous stability of the preservation environment.

1.2.1 The mandate for sustainable storage of museum collections

According to the ICOM (International Council of Museums, 2007) a museum is:

> "*a non-profit, permanent institution in the service of society and its development, open to the public, which acquires, conserves, researches, communicates and exhibits the tangible and intangible heritage of humanity and its environment for the purposes of education, study and enjoyment*".

Tangible heritage is the legacy of physical objects - works of art, ethnographic, archaeological and historic artefacts, natural history specimens, industrial, technical and maritime objects, scientific and musical instruments, textiles, coins, stamps, archival material - that the institution has deemed to be of scientific, historical or artistic value. Collections can easily include hundreds of thousands of objects in a larger museum.

Museums hold the majority of their collections in storage with major institutions frequently showing less than 5% on public display at any given time (Groskopf, 2016) (Figure 1.1). While this might be as a result of limited display space, not all museum objects are potentially exhibitable. Retention is justified by such as the UK's National Museums Directors' Conference (NMDC, 2003) for their value as representative specimens of natural and cultural history, to be used for education and research rather than for public exhibit.

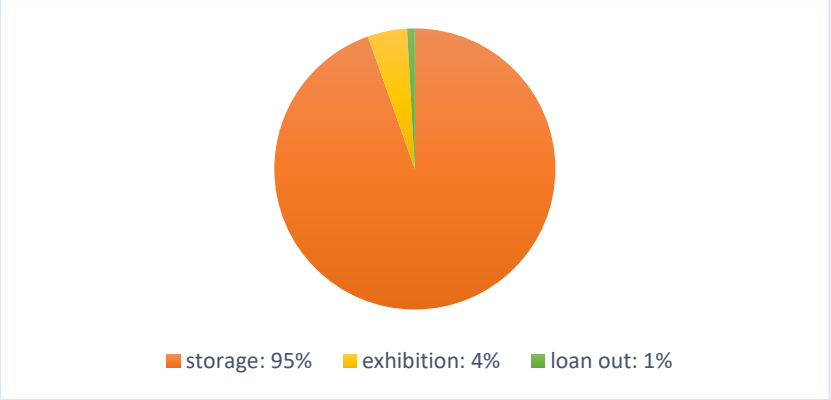

Figure 1.1 Locations of Science Museum collections by percentage, drawn from the SMG collections management database, 2018

However, while it is acknowledged that looking after these stored collections is a crucial responsibility for museums, providing suitable storage space has not had as high a priority as developing public gallery space despite the greater number of heritage objects concerned. Museum collections management practices have advanced since UNESCO felt it crucial to publish a technical handbook to redress the lack of attention paid to museum collection storage but international and national surveys undertaken since 2010 (ICCROM-UNESCO, 2011; CMA, 2013; Prislan, Cerar & Živković, 2014) still support the comment that:

> *"In fact, probably more harm has been done to museum collections through improper storage than by any other means." (Johnson & Horgan, 1979)*

Many museums now assess the suitability of their collections storage using a preventive conservation management system championed by Waller (Waller, 1994, 1995, 2002) based on work undertaken by earlier researchers (Cameron, 1968; Michalski, 1990). This identifies ten agents of deterioration that can be used to determine the level of risk to collections preservation. While catastrophic damage to collections is more likely from physical forces (fire, flood) and criminal activity, the cumulative effects of inappropriate environments, (temperature, RH, light levels and light wavelength), pests and pollution can also lead to material deterioration, object damage and loss of heritage fabric and information. RH can adversely affect heritage materials when maintained at or fluctuating between high and low levels. RH may be the most difficult environmental factor to control in museum environments, as Henry noted at a summit on museum preservation held at the Smithsonian (Image Permanence Institute, 2016), as it is a consequence of combined factors such as the outdoor climate, the building envelope, building use and the capabilities of any installed mechanical environmental control system. Since low temperatures (10°C to 18°C) are preferable when storing cultural heritage collections, the control of RH is jeopardised by its thermodynamic link to RH; as temperature rises, RH decreases, and as temperature decreases, RH increases, for the same atmospheric moisture content.

Close control of RH to prevent deterioration to museum collections has become prescriptive guidance given to architects and engineers over the course of the last 90 years. Insufficient understanding of the dynamics of moisture interaction with objects

of widely different materials and past uses has led to the blanket use of stringent environmental recommendations for the storage and exhibition of archival documents such as *BS 5454:2000, Recommendations for the storage and exhibition of archival documents* being applied to museum collections as a whole. This close control of RH has historically been achieved by installing and operating mechanical heating, ventilating and air conditioning (HVAC) systems rather than through applying a synergistic approach that considers all factors influencing moisture levels. However, HVAC system capabilities are limited by the system design, size, supply and extract fans, filter efficiency, and sensor reliability, placement and settings. They can be expensive to install, operate and maintain and are unreliable when not consistently maintained and repaired. No system is capable of running continuously as there will always be periods of enforced down-time for maintenance or repair. Poor comprehension of demand may result in the specification and subsequent installation of an inappropriate system. As a conventional HVAC system only dehumidifies incidentally as it cools the internal temperature, it may be unable to control RH during periods of high humidity. Other equipment such as humidifiers and dehumidifiers may be needed. Human activity in the building, (increasing public access, opening windows and doors, adjusting thermostats, leaving lights and equipment on), will affect the temperature, humidity and heat load and thus the effectiveness of a system of a specified capacity. The thermal performance of the building envelope, (level of insulation, number of exposed windows, airtightness, and roof design), affects the efficiency of a system. Running HVAC systems to maintain a consistent indoor environment impacts hugely on institutional carbon footprint and energy use. As an example, the Victoria & Albert Museum identified that 62% of its utility carbon footprint in the museum was due to heating, ventilating, air conditioning and humidification/dehumidification (V&A, 2015).

The current objective for museums to embrace sustainability comes from the acknowledgement that long-term care of collections should not come at the expense of global climate conditions (Conrad, 2007; Cassar, 2009; Brophy & Wylie, 2008). By understanding that there are a number of factors that affect moisture levels in museum storage, more holistic and less energy intensive methods of moisture control are being explored. Re-evaluating the sensitivity of materials to changes in RH is challenging the previous narrow, all-encompassing guidance for levels of RH (BSI, 2012a; NMDC, 2008), leading to better-tailored recommendations for wider bands for RH levels although not for fluctuations within those bands (IIC; ICOM-CC, 2014). By tailoring the use of the building and the dynamic performance of its fabric to the design of mechanical systems for heating, ventilating and conditioning of air (BSI, 2012a, 2018b), more appropriate apparatus for efficient energy use can be specified and installed.

1.2.2. The role of construction materials in achieving sustainable storage systems

A building envelope that limits heat transfer and absorbs and stores both heat energy and moisture is a significant part of a sustainable low energy RH control system. Low energy control of RH in museum storage buildings has been tested in Denmark at Ribe and Vejle, using conventional building materials (concrete and brick) and insulation (mineral wool) to provide well-insulated walls and roofs. (Ryhl-Svendsen et al., 2011; Janssen & Christensen, 2013; Christensen & Kollias, 2015).

Computer modelling of the Ribe store, adding a simulated 50mm veneer of unfired brick, indicated improved buffering of the RH, slowing the seasonal rise and reducing the need for dehumidification. Unfired brick, measured in tests by Padfield and Jensen, had shown better buffering capability than wood or cellular concrete (Padfield & Jensen, 2011). A renewable hygroscopic building material was chosen for the prototype storage building built at the Science Museum's main storage facility in Wiltshire, England. The material was chosen for its excellent hygroscopic capability which was anticipated to contribute to low energy regulation of RH to the museum's specifications.

The construction industry accounts for around half of all non-renewable resources used worldwide (Willmott Dixon, 2010), consuming raw materials such as earth minerals, metal ores and fossil fuels, with the greatest demand for cement-related non-metallic minerals (sand and gravel). Extraction and transport of raw materials adversely impacts the environment, damaging landscape and creating pollutants. Industrial manufacture of conventional building materials (concrete, steel, fibreglass, plastics, etc.) involves toxic processes and produces large quantities of unrecyclable waste, including hazardous substances. The embodied energy consumption of the construction industry, both the direct energy used to transport building products and construct buildings and the indirect energy used to acquire, process and manufacture the building materials, has been estimated to account for 4.5% of total UK usage (Willmott Dixon, 2010). The total energy consumption of buildings rises to around 50% of total usage when considering the whole life cycle, adding the recurring embodied energy of buildings (the energy consumed in maintaining and renovating a building through its lifespan), and the demolition energy to the initial embodied energy usage (McAlinden, 2015; Berardi, 2017). CO_2 emissions generated by energy consumption adversely affect the environment, contributing to global warming (Murphy et al., 2010). In the UK, the construction industry activity accounts for almost 10% of the total national CO_2 emissions (Lawrence et al., 2012) with use of buildings (heating, cooling, lighting, powering appliances) accounting for a further 47%. Carbon emissions from construction industry activity can be broken down into percentages, with 70% coming from mineral extraction, product and material manufacture, 17% from transport and 13% from construction site processes (Lawrence, 2013).

Reducing building operational energy use by increasing the thickness of insulating materials can actually increase the embodied energy if non-recyclable insulating materials are derived from non-renewable resources requiring industrial manufacturing techniques (Crawford et al., 2016). Blengini and Di Carlo (2010) have proposed that, based on the life cycle assessment (LCA) of new low energy buildings, the correct choice of building materials and the proper recycling processes may lower life cycle impacts. They noted that natural materials which sequestered carbon could potentially increase recycling potential and lower greenhouse gas emissions. Renewable building materials, produced from regenerational resources such as trees and crops, can be used as sustainable alternatives to conventional materials if they are managed and processed responsibly (Hirst et al., 2012) with the rate of use not exceeding replacement of resource. While conventional building materials require large amounts of fossil fuels for production and transport, biobased materials generally require less industrial processing, with the potential of manufacture on-site, greatly reducing energy needs and greenhouse gas emissions

(Melia et al., 2014). Traditional rather than industrial production methods reduce or eliminate toxic processes and large amounts of unrecyclable waste. Building materials are biodegradable and emit few if any volatile organic compounds (VOCs), further reducing the embodied impact on the environment over their lifespan.

Many crop-based construction materials have demonstrated good hygroscopic capability (Holcroft & Shea, 2013; Dubois et al., 2014) with the potential to successfully moderate internal RH. HLC, considered to be carbon-negative due to its low embodied energy and carbon sequestering capability (Walker & Pavia, 2014a) has been shown to have a higher buffering capacity than conventional hygroscopic building materials such as brick or gypsum (Maalouf et al., 2013). In its exposed state, HLC's moisture buffer value has been rated as either Good or Excellent by several researchers (Collet et al., 2013; Rahim et al., 2015; Latif et al., 2015). Based on on-going research and initial results from warehouse construction (Betts, 2010), the Science Museum specified HLC for their first low energy controlled environment storage facility, the Hempcrete Museum Store (HMS).

The HMS was used as the case study for this thesis. The building had shown good buffering characteristics during early operation but a number of construction and operational issues compromised qualifying or quantifying the hygroscopic capability of the HLC. A heating and ventilation system and portable dehumidifiers and air conditioners have been required to stabilise the RH. More testing to determine the adsorption/desorption function and moisture buffering values of HLC under low storage temperatures was required as was further monitoring of the dynamic performance of the prototype store in order to obtain robust data on HLC's functional in-use performance.

Primary data was acquired through *in situ* environmental monitoring of the HMS. The key contribution to knowledge will be identifying through qualitative and quantitative analysis how the hygroscopic performance of HLC can support the design of low energy museum storage.

1.3 Research hypothesis

The research hypothesis has been based on the key performance criteria, which are to maintain suitable control of RH levels and fluctuations in museum storage buildings while reducing the operational energy costs of storage building operation. The following hypothesis has been formulated and tested:

> *Does hemp lime concrete have the hygroscopic performance potential to augment the regulation of relative humidity within museum storage buildings in temperate climates?*

1.4 Objectives and desired outputs of the research

The primary aim of the research was to evaluate the moisture control and buffering performance of HLC in the context of museum storage recommendations.

In line with the aim of the research, key objectives were identified in order to:

- Analyse the historical development of RH guidelines for the storage of museum collections in order to clarify causes and consequences of ambiguity. This was achieved by reviewing the historic and current literature on the risks and effects of incorrect RH, past and current recommendations for RH levels and fluctuations, and past and current practices to control RH.

- Evaluate the moisture management capacity of HLC over a range of hygrothermal boundary conditions relevant to museum storage conditions.This was done through a literature review, *in situ* monitoring and evaluation of the dynamic operation of the case study.

- Compare the ability of HLC to buffer RH with that of conventional building materials. This was achieved through *in situ* monitoring of other low energy museum repositories on the same site.

- Acquire data that support the design of low energy museum storage facilities. This was achieved through the dynamic *in situ* environmental monitoring.

- Evaluate the economic impacts of HLC on the CAPEX and OPEX of the case study and assess the consequences for achieving sustainable museum storage.

1.4.1 Thesis Chapter Structure

This thesis essentially utilises the thesis structural model as outlined by Holliday (2007) (Table 1.1):

Table 1.1 Thesis structural model

ABSTRACT	• summary of basic argument
INTRODUCTION	• statement of topic • vision & motivation for research located within broader context • research setting and data collection strategy • plan for rest of written study
LITERATURE REVIEW / RESEARCH METHODOLOGY	• conceptual framework • assessment of current thought • what has been learnt • position of work
DESCRIPTION OF RESEARCH PROCEDURES	• evidence for choice of core settings & relevant data sources • description of setting • development of research strategy related appropriately to setting • process of access & data acquisition • catalogue of research activities & data collection • analysis structure • data system presentation
DISCUSSION OF DATA	• what has been learnt from the data • how data provides evidence • summary of findings throughout written study • what it all means
CONCLUSION	• summing up • recommendations from all basic points in argument

Table 1.2 shows the key objectives and desired outputs mapped to the most appropriate research methodologies:

Table 1.2 Thesis structure mapped to objectives & ouputs

Abstract		
Chapter:	**Key Objectives:**	**Desired Outputs:**
1 Introduction	Set scene Establish key performance criteria State research hypothesis Outline research & data collections strategy Plan for rest of written work	Objectives of research placed within wider context Identification of desired outcomes
2 Literature Review Risks of incorrect RH to museum collections	Review risks to museum collections Analyse historical development of RH control Evaluate drivers for sustainability in museums	RH risks to collections identified & tabulated RH control needs assessed & tabulated Historical guidance chronologically sequenced Historical engineering influence summarised Historic & current recommendations clarified Risks of current practice qualified Costs of current practice quantified Challenges to low energy & passive solutions specified
3 Literature Review Hygroscopic capabilities of HLC	Establish moisture control potential of HLC Verify sustainable performance credentials Identify key knowledge gap	Adsorption/desorption & absorption properties identified Moisture buffering potential assessed Current research summarised
4 Research Methodology Monitoring methods, materials & equipment	Develop a monitoring strategy to evaluate potential of HLC to regulate RH	Construction materials & methods summarised Equipment sourced, tested to monitor RH, T, air velocity & moisture content as part of existing environmental monitoring system
5 Research Procedures The HMS case study: 1st monitoring phase	Describe setting Assess data acquired during transient & 1st steady state 2012- 2016	Project parameters & specifications reviewed M&E design & operation assessed Effects of mechanical system failures on RH fluctuations quantified Effects of HLC on RH levels & fluctuations quantified

6 Research Procedures The HMS case study: 2nd monitoring phase	Extend monitoring strategy Acquire and analyse data for 2nd steady state 2016-2019 Evaluate monitoring system for functionality	Comparative RH data obtained Additional environmental data obtained for HMS Data evaluated under operational variations Reciprocal effects of moisture/RH assessed Monitoring strategy validated
7 Discussion	Statistical significance of data Implications of research Environmental impact Economic consequences Benefits to the collections Limitations of the research	Replication potential of monitoring schedule Applications for future SMG storage facilities Replication of manufacture Energy use, embodied energy & sustainability quantified Manufacturing, maintenance & lifetime costs compared to conventional SMG solutions Impact on longevity of collections qualified Geographical, climatic & scope limits identified
8 Conclusions	Present the main points of the research. Validate the research hypothesis.	Chapter conclusions summarised Hygroscopic performance of HLC quantified for museum storage in temperate climates
References		
Appendices		Related tables & graphs Technical data sheets

1.5 Aim of the research

The aim of this research is to evaluate the moisture control and buffering performance of HLC as used in a case study against the criteria recommended for museum storage environmental conditions.

Hygroscopic properties of the material have been studied through a review of current research and a case study of a prototype museum storage building. The *in-situ* monitoring of the museum storage building provided long-term data during dynamic operational phases. The effects of additional building materials, such as concrete, fire rated lining boards and external cladding, were appraised for their effects on the capability of the HLC to moderate RH.

1.6 Boundaries of the research

The research hypothesis has been tested within the limitations of the following boundaries.

1.6.1 Boundaries of research activity

The boundaries of this research are found within the context of climate change, museum sustainability and environmental control of storage environment, limited to what is achievable by means of the research methodology (Table 1.3).

Table 1.3 Boundaries of research

Climate Change	Museum Sustainability	Environmental control
Government directives	**Preservation of collections**	**Storage environment**
Reduced CO_2 emissions	Reduced construction costs	RH levels
Reduced embodied energy	Reduced energy costs	RH fluctuations
Low carbon construction	Reduced risks to collections	Moisture content
Biobased materials	Collections storage	Mechanical RH control
Hygroscopic materials	New builds	Passive RH control
Hemp lime concrete	Hempcrete Museum Store	Monitoring

A 980 m^2 museum storage building, constructed using prefabricated HLC panels for wall infill, was used to assess the hygroscopic performance potential of HLC to augment the regulation of RH. This prototype store, used as the case study, was built within a 3000m^2 1940s aircraft maintenance hangar, repurposed for museum storage. The store was built to house four specific environmentally-sensitive cultural heritage collections.The outer building was uninsulated and unheated with interior RH conditions reflecting those of the external environment. Building within a building was intended to allow an additional layer of protection from the elements (Moore, 2013). The control of RH within two other low energy storage buildings on the same site, a library and archival store, built within the same hangar as the HMS, and a free-standing collection objects store, was assessed for comparative purpose.

The environmental parameters against which the performance of the buildings were assessed have been provided through a literature review of the development of recommendation by the museum sector over the last 100 years.

The museum's telemetric environmental monitoring system was used to obtain data from the storage buildings. Additional monitoring capability was added to the system to obtain moisture content and air velocity as well as RH and temperature data from the prototype store. Monitoring was carried out while the storage buildings contained cultural heritage collections and over full seasonal changes.

Due to the constraints of time and building design, the following issues and applications could not be addressed:

- Assessment of the effect of coatings and linings on the hygroscopic ability of HLC.
- Assessment of the effect of hygroscopic cultural heritage collections on RH.
- Assessment of the effect of hygroscopic construction materials on cultural heritage collections.
- Effectiveness of natural versus forced ventilation in assisting desorption of moisture from the HLC.
- Extent of dust emission from uncoated HLC and effects on cultural heritage collections.

1.6.2. Geographic Boundaries of the location

The case study was based in a UK temperate maritime climate, that of the south-west of the UK. In addition, the prototype store was located within another (unheated) building. Both these factors may affect the study's relevance to other climates or building structures.

1.7 Contributions to knowledge

This thesis attempts to fill the gap in knowledge regarding the hygroscopic capability of HLC to augment the regulation of RH levels and fluctuations within the environmental parameters required to prolong preservation of cultural heritage collections.

As a result of this research, the following are the key contributions made to current knowledge, drawn from the desired outputs of the objectives:

1.7.1 Literature Review Outcomes

- Development of a red, amber and green (RAG) key performance indicator chart for allowable RH ranges for cultural heritage collections.
- Development of a RAG key performance indicator chart for allowable RH fluctuations for cultural heritage collections.
- Development of time-lines charting the progression of RH range recommendations linked to the literature review.

1.7.2 Research Outcomes

- To define the potential of the hygroscopic ability of HLC to moderate the RH fluctuations caused by mechanical environmental control of RH levels.
- To identify the extent to which HLC can control levels of RH within optimal museum storage ranges under dynamic operation.
- To verify how the hygroscopic performance of HLC can augment control of RH in order to support the design of very low energy museum storage facilities.
- To validate the economic viability of HLC construction as part of a low energy moisture control system that regulates RH to current museum recommendations.

1.8 Summary of the thesis preface

The progression of recommendations for RH levels and fluctuations for historic materials held by museums has led to non-sustainable energy-consuming systems of control. While RH levels are currently being reviewed, passive or low energy solutions, such as the use of hygroscopic building materials, are being endorsed as a means to reduce reliance on mechanical environmental control systems. However, there is limited information on how hygroscopic building materials interact with moisture to control and/or buffer RH levels to the levels required in museum storage facilities. An investigation into the performance of a highly hygroscopic material under dynamic situations will lead to a more sustainable method to preserve cultural heritage collections through building design in future. The research hypothesis for this study was based on key performance criteria, to maintain suitable control of RH levels and fluctuations in museum storage buildings while reducing the operational energy costs of storage building operation.

Boundaries of the research have placed the research objectives within the context of sustainable preservation of cultural heritage collections and thus within the wider circumstances of climate change, energy use and carbon emissions. Defined limitations were within the area of environmental control, specifically the control of RH levels and fluctuations, within the framework of building storage repositories for museum collections. A low carbon hygroscopic construction material, HLC, was delineated as the focus of the research study. A case study, the HMS, was designated as the research and data collection strategy.

The desired outcome from a review of the literature on museum environment was identified as the key contribution to the understanding of the development of recommendations for allowable RH ranges and fluctuations for cultural heritage collections.

A research hypothesis was formulated, based on the key performance criteria to maintain suitable control of RH levels and fluctuations in museum storage buildings while both reducing the carbon footprint of building construction and the operational energy costs of storage building operation.

> *Does hemp lime concrete have the hygroscopic performance potential to augment the regulation of relative humidity within museum storage buildings in temperate climates?*

The key objectives for the rest of the written work were correlated to the desired research outcomes in order to define the extent to which the research hypothesis could be proved.

Chapter 2 The risks and control of RH in museum storage: literature review

2.1 Introduction

In this chapter, the risks to museum collections through incorrect RH in storage are assessed through a comprehensive review of historic and current literature, from the earliest published identification of the problem to current recommendations and solutions for RH control. The sequences of RH guidelines developed by researchers over the past decades are critically reviewed and guideline ambiguities are highlighted in order to clarify past and current approaches to controlling RH in museum storage. The gaps in the present knowledge related to passive and low energy control strategies are identified and discussed.

2.2 Risks to collections by uncontrolled RH

> *"For each material, there is a level of environmental moisture content, related to the associated relative humidity, which is consistent with its physical, chemical or biological stability."* (ASHRAE, 2011)

Humidity is the amount of water vapour or moisture in the air. It can be expressed in a number of ways:

- Absolute humidity is the actual mass of water vapour present in a given volume of air, at a given temperature and pressure, expressed as grams of water per cubic metre of air (kg/m^3). Absolute humidity is greater at higher temperatures with an approximate maximum of 30 g/m^3 at 30°C and an approximate maximum of 5 g/m^3 at 0°C.

- Specific humidity is the ratio of the actual mass of water vapour in the air to the total mass of the mixture of air and water vapour, expressed as kilograms of water to kilograms of air (kg/kg). With decreasing temperature, the amount of moisture required to reach saturation also decreases.

- Relative humidity can be expressed as the ratio of actual mass of water vapour in the air to the maximum mass of water vapour the air is able to hold at a particular temperature. It can also be expressed as a ratio of vapour partial pressure in the air to the saturation partial pressure in the air at a specific temperature or as a ratio of vapour density. It is expressed as a percentage (% RH). Warm air will hold more water vapour than cold air so, with the same amount of absolute humidity, air will have a higher RH if the air temperature is cooler and a lower RH if the air temperature is warmer. When air can hold no more moisture at a given temperature, the air is said to be saturated, with the RH at 100%.

- Dew point temperature is the temperature to which the air must be cooled (at constant pressure and constant water vapour content) in order for it to be saturated with water vapour. At air temperatures below the dew point, water will leave the air and condense on solid surfaces. The dew point temperature

is never greater than the air temperature but the higher the dew point temperature is, the higher the moisture content of the air at a given temperature will be. If the dew point temperature is constant, when the RH goes down, the air temperature goes up and when the RH goes up, the air temperature goes down. If the % RH is 100%, then the dew point and air temperatures are the same (Figure 2.1).

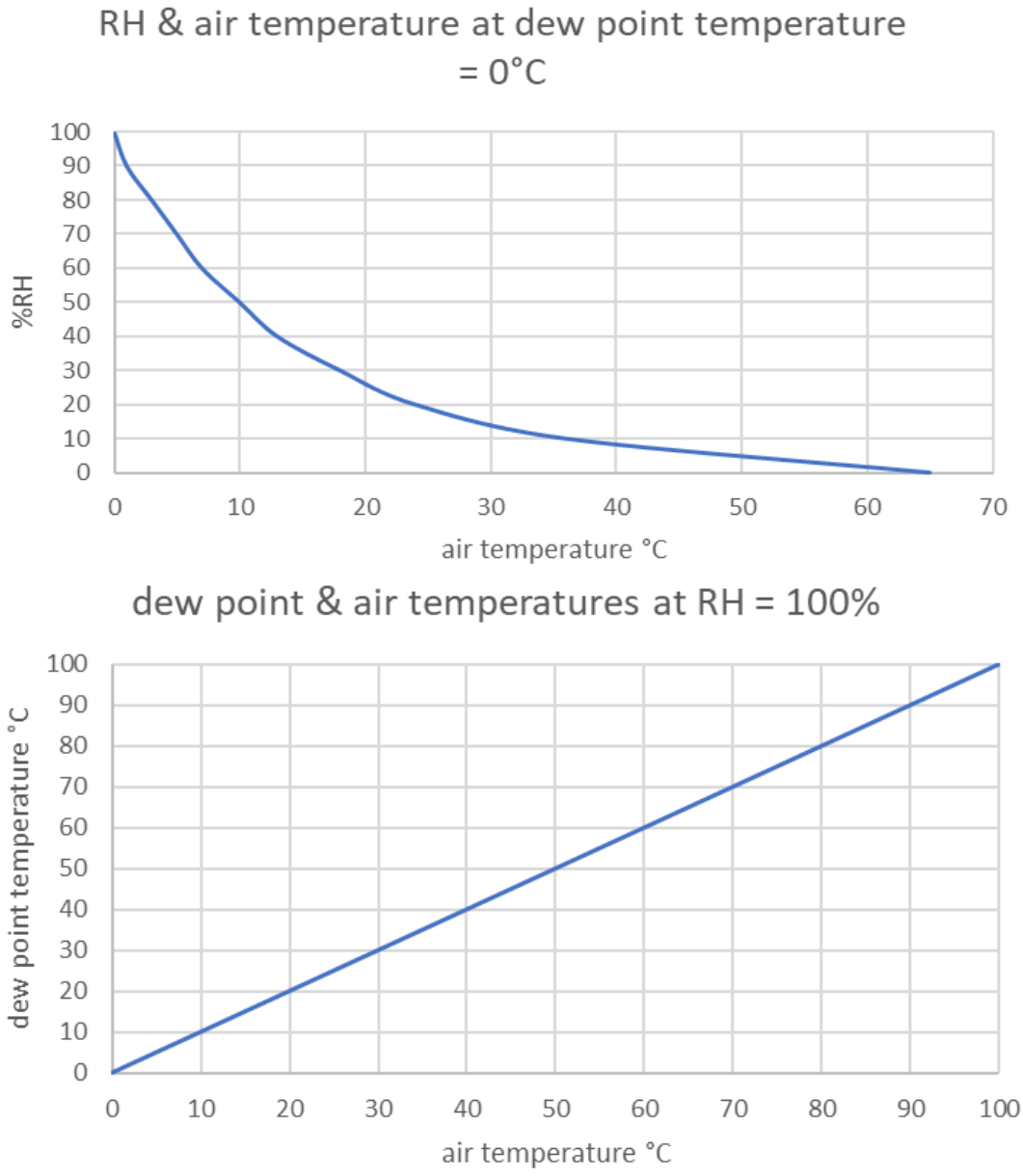

Figure 2.1 Relationship between RH & air temperature when dew point = 0°C & between dew point and air temperatures when RH = 100%
Graphs plotted using on line Dew Point Calculator (www.dpcalc.org)

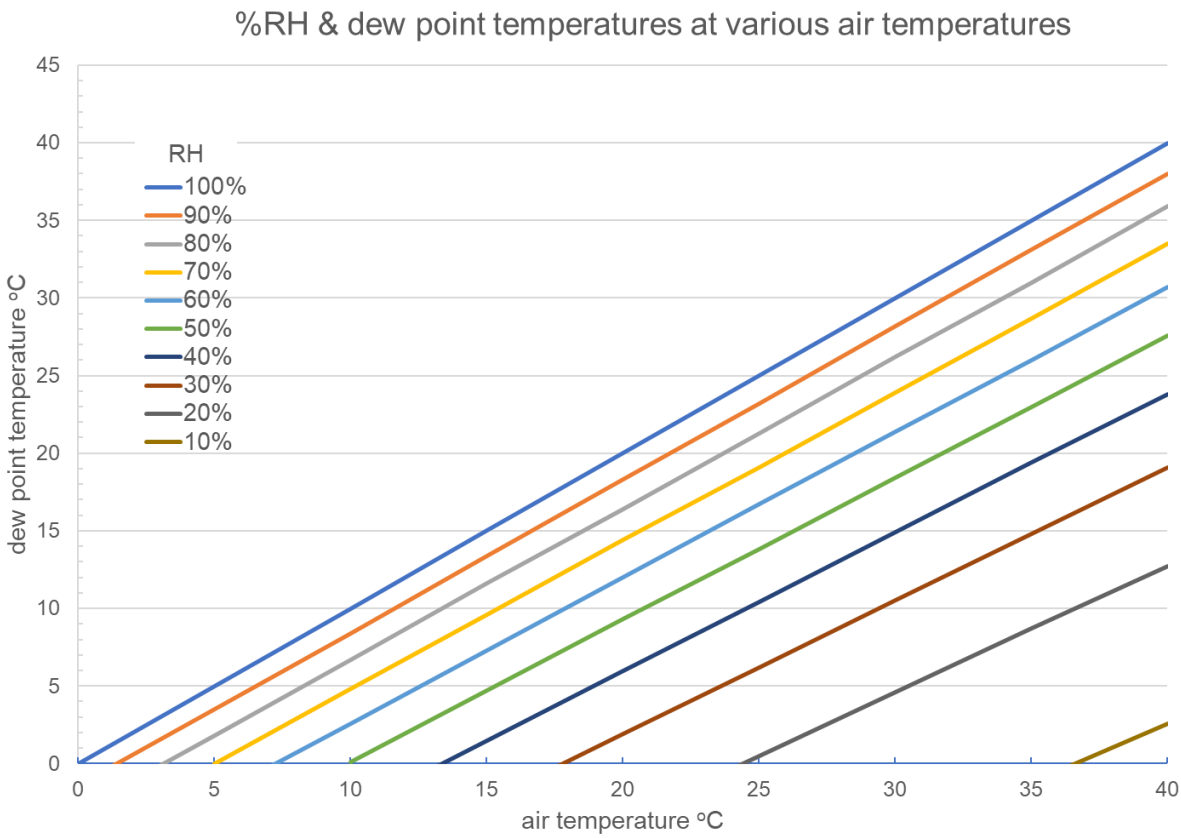

Figure 2.2 Relationship between dew point & RH at various temperatures
Graphs plotted using on line dew point calculator (www.calculator.net)

The relationship between RH and the dew point temperature at any given air temperature is non-linear (Figure 2.2) although the relationship does become almost linear above 50% (Lawrence, M.G., 2005). Lawrence proposed a simple calculation to give an approximation conversion of RH to dew point temperature above RH values of 50%:

$$\boldsymbol{T_d \approx T - \left(\frac{100-RH}{5}\right)} \qquad \text{[equ.2.1]}$$

where,
T = air temperature, °C
T_d = dew point temperature,°C
RH = relative humidity, %

Dew point converters are available online to convert known RH and air temperature values to more accurate dew point temperatures (for example: http://www.dpcalc.org/;https://www.calculator.net/dew-point-calculator.html). While measuring the dew point is a more accurate way to identify the actual air moisture content, monitoring RH has historically been the conventional method of measuring moisture content in the air in museums.

The relationship between moisture content (humidity), temperature and enthalpy of the moist air can be demonstrated using a psychrometric chart. According to ASHRAE (2008), the chart is based on two concepts:

- Indoor air is a mixture of dry air and water vapour
- There is a specific amount of enthalpy or total heat content (sensible plus latent heat) in the mixture at a specific temperature

A psychrometric chart is a graph of the physical properties of moist air at a constant absolute pressure (Figure 2.3) The dry-bulb temperature of the air, which indicate sensible heat changes, is typically the x-axis, measuring from left to right. Temperature readings in SI metric psychrometric charts are in °C. Readings are plotted vertically. The y-axis is the humidity ratio, expressed as kg of water vapour per kg of dry air, and measuring upwards. Readings are plotted horizontally. A latent heat change occurs when moisture in the air increases or decreases. The saturation curve, running from the lower left up to the top of the graph, represents the maximum amount of humidity that air can hold at a given temperature. Temperature values on the curve are constant dew point and are plotted horizontally. Wet-bulb temperature readings, which indicate the total heat content of air, are plotted on the upward left sloping lines. Relative humidity readings are plotted aong the curving lines in 10% steps, with the saturation curve equaling 100% humidity. Constant specific volume, which is the space occupied by dry air at a given temperature and moisture content in m^3/kg, is plotted on the nearly-vertical sloping lines. Enthalpy, in kJ/kg of air, is plotted from a scale to the left of the saturation curve along left sloping lines. Change in enthalpy can be determined by changes solely to sensible heat or to latent heat or to simultaneous changes in humidity ratio and dry bulb temperature.

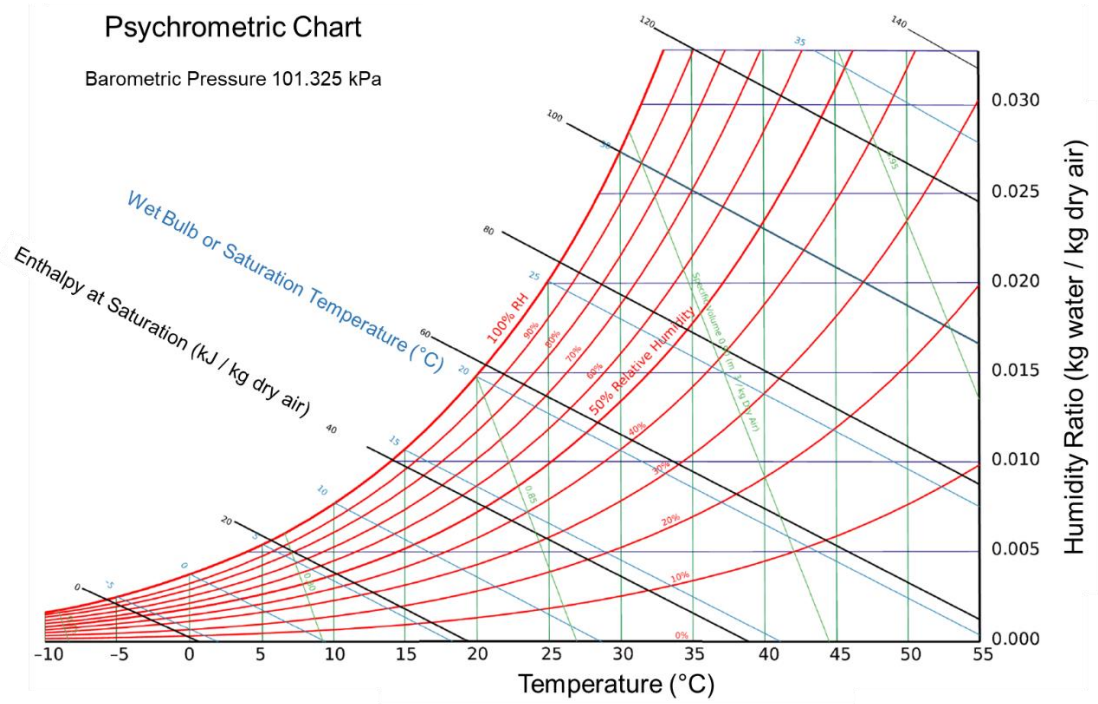

Figure 2.3 SI metric unit psychrometric chart for normal temperatures at sea level (after Padfield, 2010)

By measuring two of three variables, RH, temperature and humidity ratio, and plotting them on the psychrometric chart, the third can be found. As an example, if a room temperature is measured at 20°C and the relative humidity measured at 55%, the humidity ratio will be 0.0073 (kg/kg) (Figure 2.4).

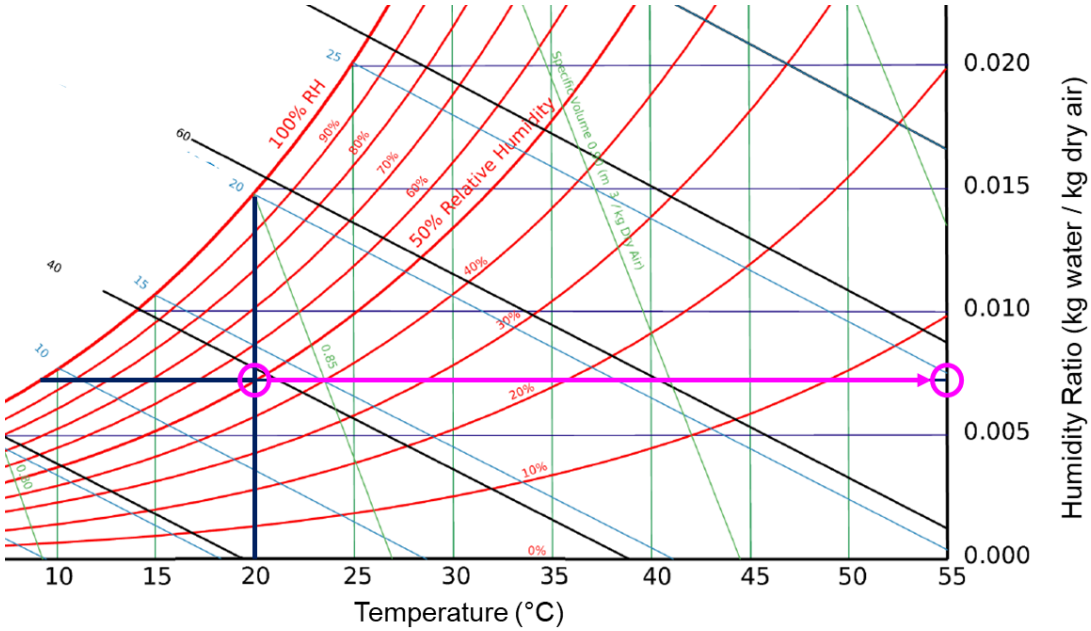

Figure 2.4 Humidity ratio found from known temperature & RH

As the density of dry air is 1.2041 kg/m^3 at 20°C, the water vapour concentration or absolute humidity can be calculated as 0.0073 x 1.2041 = 0.0088 kg/m^3. If the the absolute humidity remains at 0.0088 kg/m^3 but the temperature rises to 25°C , the RH drops below 40% (Figure 2.5). This is an RH level considered by some conservation professionals as too low for the preservation of certain organic materials held under tension.

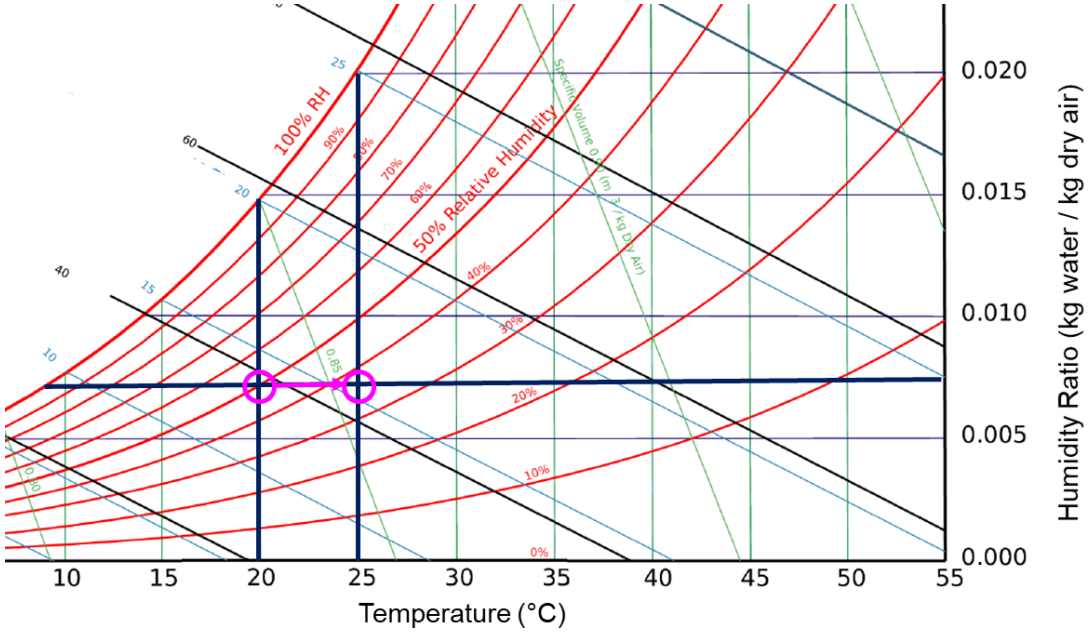

Figure 2.5 Increase in temperature with drop in RH at constant absolute humidity

If the temperature drops to 15°C, the RH rises to almost 70%, an RH level considered too high for the preservation of cultural heritage collections as it supports mould growth and promotes corrosion in some metals (Figure 2.6).

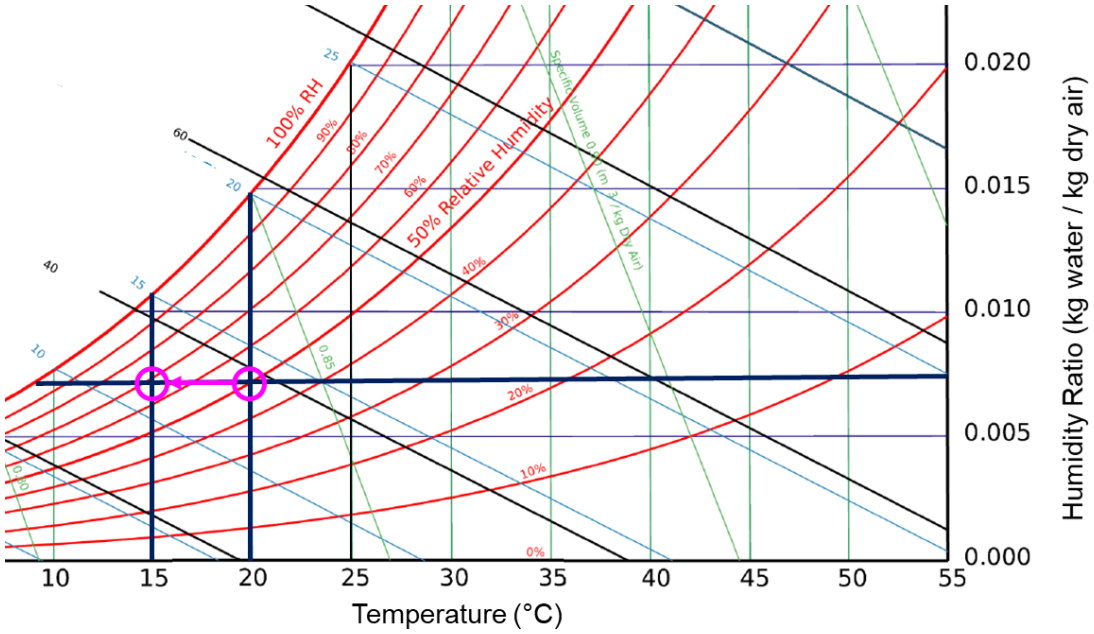

Figure 2.6 Drop in temperature with increase in RH at constant absolute humidity

The psychrometric chart can be used to determine what parameters need to be altered to maintain the preservation environment. In order to raise the RH back up to 50% at 25°C, the humidity ratio would have to be raised to 0.011 (kg/kg), absolute humidity 0.013 kg/m^3 (Figure 2.7).

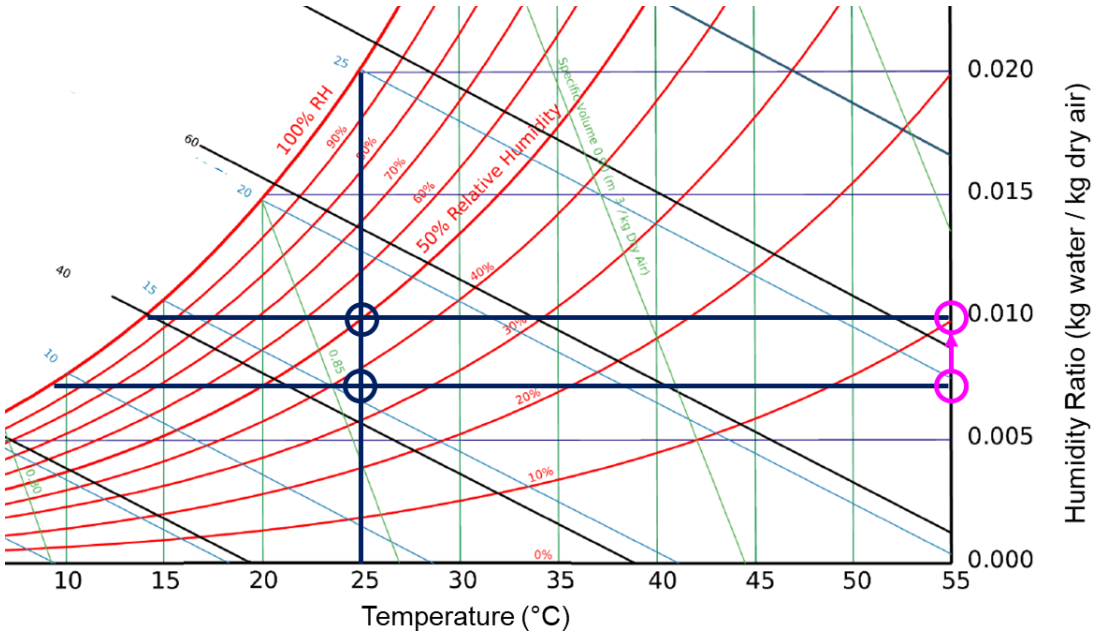

Figure 2.7 Rise in humidity to obtain 50% RH at 25°C

To reduce the RH to 50% at 15°C, the humidity ratio would have to be dropped to 0.006 (kg/kg), absolute humidity 0.0073 kg/m^3 (Figure 2.8). In order to keep temperatures constant, moisture would have to be added by humidification in the first case and removed by dehumidification in the second case.

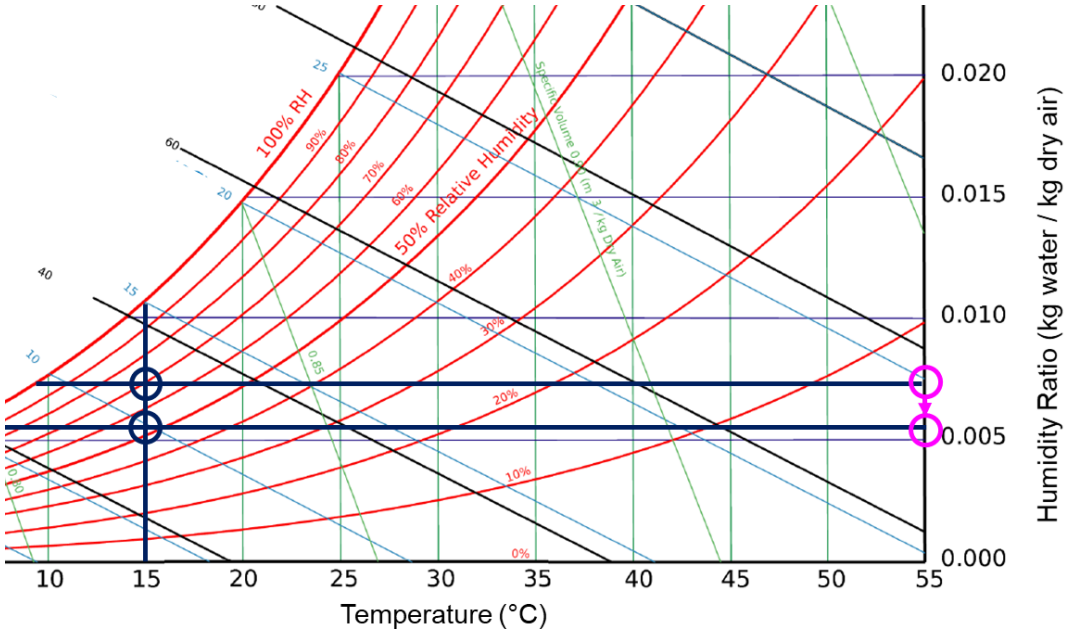

Figure 2.8 Drop in humidity ratio to obtain 50% RH at 15°C

The dew point can also be calculated from the chart. As the temperature drops, the air is less able to hold moisture and eventually reaches saturation, at 100% RH (Figure 2.9). Condensation starts at this point. If the temperature continues to fall, the absolute humidity will also fall although it still remains saturated.

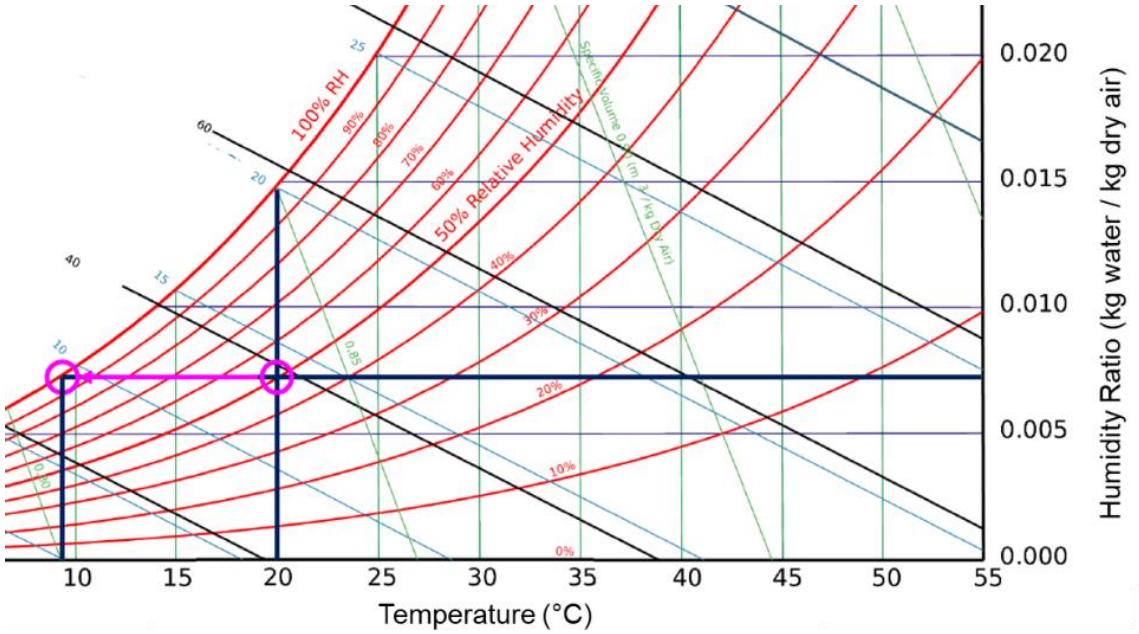

Figure 2.9 Calculation of dew point at 20C and humidity ratio 0.0073 kg/kg

Controlling humidity is more important than controlling temperature in the museum storage environment (Thomson, 1986). Measuring the humidity using the RH scale, which is independent of temperature, is the primary method used, whether data is acquired through sling hygrometers and thermometers and plotted on a psychrometric chart, or charted by mechanical hair hygrometers or by continuous

electronic data loggers and transmitters (Cassar & Hutchings, 2000). Identifying the ranges of RH at which potential deterioration to historic materials may occur requires an understanding of the effects of environmental moisture content, related to the associated RH, on physical, chemical or biological stability.

2.2.1 Equilibrium moisture content and physical damage

All organic materials naturally contain water, thus are hygroscopic and will adjust moisture content to equilibrate with the RH of the environment. They are able to attract and hold water molecules from the atmosphere either by absorption (within the cell) or adsorption (against the cell wall), with resultant changes in dimension or physical characteristic causing mechanical damage. Changes include swelling, cockling, warping, plasticising, hydrolysing, leaching, dissolving, fading, staining, weathering, cracking and weakening. Or they can lose their moisture by giving up water molecules to the atmosphere (desorption). This leads to shrinking, splitting, cracking, breaking, crumbling, delaminating, stiffening and weakening. By responding to changes in levels of RH by absorption, adsorption or desorption, an organic material will reach a state of equilibrium moisture content (EMC) with the environment after a period of time dependent on a number of factors (Image Permanence Institute, 2014).

Organic materials exhibit different hygroscopic properties due to their physical structure, not just from each other, but also within the individual materials themselves. Wood will swell or shrink more across the grain than along it; sapwood will respond more than heartwood, softwood more than hardwood (Hoadley, 1978). Ivory (the tusks and teeth of mammals such as elephant, walrus, boar, narwhale and mammoth) will react more across the dentinal tubules than along them (Lafontaine & Wood, 1982). Bone and antler will react more across the collagen fibres as will other collagen-containing materials such as leather and parchment (Hansen & Lee, 1991). Thinner sections will react more quickly to change in RH than thicker pieces.

Objects made of the same material from different sources such as veneered furniture and musical instruments may crack or break as the sections react (Thomson, 1978). Objects made from a number of different organic materials may undergo mechanical damage as the various materials respond differently to changes in moisture. In composite objects such as paintings on canvas, glue sizing will swell and lose strength in high humidity but the linen support will shrink due to increased fibre crimp, with resultant loss of the painted surface. Materials which are held under tension can undergo severe strain which can ultimately result in breakage so a painting canvas, tacked to a wooden stretcher, may crack or split at the corners due to the expansion or contraction of the wood (Mecklenburg, 2007).

2.2.2 Chemical damage

Chemical deterioration of organic compounds may be produced through hydrolysis and oxidation. Hydrolysis, where a molecule of water is added to a substance causing the formation of one or two new compounds, can break down the bonds in molecular chains. Hydrolyses of polymeric materials such as leather, paper and textiles, as well as cellulosic plastics, can be catalysed by acids or alkalies from the atmosphere and the materials may lose strength, colour, shape and flexibility.

Oxidation, where an atom loses an electron to an oxidizing agent, promotes hydrolysis in the presence of moisture when acids are produced in the process. Organic dyes will fade more rapidly through oxidation when atmospheric moisture levels are high (MacIntyre & Buckley, 1930; Padfield & Landi, 1966).

Reduction-oxidation (redox) reaction in the presence of moisture causes corrosion in inorganic materials such as iron. Other metals such as magnesium, aluminium, zinc, lead, tin and silver and their alloys oxidize but do not corrode as rapidly as iron since the initial oxidation layer protects the surface of the metal Contaminants such as those found in dust will accelerate deterioration at RH above 75%, as they aggravate the phenomena of increased water adsorption leading to the formation of a liquid film on metal surfaces above that RH level (ASHRAE, 2011).

Glass with an incorrect proportion of sodium and potassium is highly reactive and will deteriorate in high humidity with the hygroscopic metals being leached to the surface where they attract atmospheric moisture, forming droplets and causing cracks and flakes. Efflorescence of soluble salts through hydration caused by high RH will obscure or damage surfaces or even promote the disintegration of contaminated stone, ceramics, metals and geological specimens. Minerals and fossils containing iron pyrite material will deteriorate in high humidity, converting the iron sulphide to ferrous sulphate and sulphuric acid (Waller, 1985).

High RH levels will lead to condensation when warmer air, coming in contact with cooler surfaces, has its moisture temperature lowered below dew point. This can be not only a problem for storage building structures, with moisture condensing on or within walls and on windows and floors, but also for stored objects. In unheated storage areas moisture will also condense on cold object materials, usually metals. A film of moisture contaminated with chlorides or sulphates from the atmosphere can provide an aggressive electrolyte for corrosion promotion. The film can also become alkaline from contact with metal surfaces or acidic from picking up carbon dioxide molecules, leading to the deterioration of both the organic and inorganic materials with which it comes into contact. Lack of air circulation may prevent pockets of moisture from returning to ambient levels even when the air temperature rises. High RH levels may arise from condensation, atmospheric conditions, water leakage through the building envelope, retained construction moisture, damp ground, plumbing issues or occupational activities such as washing, cooking or even breathing.

2.2.3 Biological damage

While wet materials are susceptible to some forms of biodeterioration such as bacteria, algae and lichens, many materials dampened by high RH levels will support active micro fungal growth (mould). As long as there are suitable nutrients, temperatures, pH and exposure times, the moulds most commonly affecting museum collections (the conidial fungi) may begin to grow around 70% RH; growth depends on the moisture content of the materials rather than the RH of the atmosphere (Florian, 2000). Nutrients are provided by hygroscopic materials, often sugars or salts, and the substrate biodegradability may continue to support growth at low RH (Sterflinger, 2010). Lower temperatures will inhibit but not prevent the growth of most moulds if critical moisture levels are increased; since critical moisture levels are

different for each specific substrate, not all materials are equally susceptible to mould growth (Johansson et al., 2012). pH is considered a minor influencing factor, as is spore availability, oxygen, light and roughness of the surface but most moulds prefer an acidic to slightly acidic (pH 2-7) range (Vereecken et al., 2011). Mould can grow on both organic and inorganic materials. Organic binders in paints and glues can be degraded by enzymatic digestion; paper can be stained and weakened through the secretion of cellulases; mould mycelia can penetrate cracks and crevices in paint layers, textiles, wood, ceramic and stone. Mould growth is also a significant health factor and can cause respiratory illnesses, skin and eye irritation and infections (Vereecken & Roels, 2012).

As many insects rely on high moisture content in order to obtain the water required for survival, some will prefer areas of high RH. Museum pests such as furniture boring beetle larvae prefer a wood moisture content about 12%, which is equivalent to an RH of 65% (Child, 2007); silverfish, which will feed on starches in glues and textiles, prefer a range from 75% RH to 95% RH; booklice feed on microscopic moulds so thrive above 75% RH. Brown and white house moth larvae will attack damp wool, fur, feathers and skin but the webbing and case bearing clothes moth larvae will survive much drier conditions as will most dermestids such as common and carpet beetles.

2.2.4 Fluctuations of RH

Fluctuations in RH may deleteriously affect hygroscopic objects as they attempt to come to equilibrium with the changing moisture levels in the environment

Brief and small fluctuations may cause little harm as materials need time to respond; response time depends on the equilibrium moisture content values of each material as well as other factors such as thickness, coatings or presence of buffers. Slow fluctuations over a long period of time within the critical RH values of polymeric materials may not cause permanent damage (Erhardt & Mecklenburg, 1994) or damage may be limited due to the lowered stress response to the reduced strain. Stress relaxation, a decrease in stress and force over time with a constant strain, results in the material showing a decreased tendency to return to its original shape after the strain is removed (Michalski, 1993) and may result in diminished response under the next series of similar fluctuations. Stresses below the critical value necessary to fracture an assembly in one cycle are still able to cause incremental growth of cracks from microscopic flaws inherent in real materials (Figure 2.10) resulting in a fatigue lifetime which depends logarithmically on stress reduction. According to Michalski, the greatest amount of damage may occur when fluctuations are shorter than the stress relaxation time but longer than the response time.

Figure 2.10 Fractures along cover paper fault lines caused by RH fluctuations (SCM Library collection)

2.3 Historical development of RH control in museums

In the nineteenth century, coal-gas central heating systems improved levels of comfort within museum buildings. Daily and seasonal extremes of high, low and fluctuating RH were likely as systems used warm air buoyancy to expel sulphurous gases and soot from furnaces. Air drawn in at lower levels was warmed over hot pipes to rise up through ducts and grilles to heat, dry and vent rooms. Solar gain could also contribute to daily RH fluctuations with daytime high indoor temperatures reducing moisture levels but low night temperatures allowing the humidity to rise. According to Brown and Rose (1996) in the summer months without heating, European and North American museums would likely have had RH levels between 60% to 90%; in the winter, heating might have driven the RH levels to as low as 10%.

2.3.1 Early observations and recommendations

In Munich's oldest art museum, the Alte Pinakothek, the hot air heating system installed in 1836 was observed almost immediately to be causing severe damage to paintings hung at height. High temperatures rather than excessive dryness and large fluctuations in RH were initially identified to be the cause and the system was shut down in 1841 in an attempt to preserve the collections (Eibl & Burmester, 2013). Perceiving that incorrect humidity was a contributing factor to the deterioration of the collections, in 1891 a low-pressure steam heating system was installed instead, with basins of water placed above the heating pipes, in order to achieve the recommendation that:

> *"the humidity level of the air should be permanently kept close to 50% saturation"* (Eibl & Burmester, 2013, p.223).

The RH value was based on an evaluation of existing climate control systems in other prominent European museums according to a report on the Bavarian State

Picture Collections (Bayerische Staatsgemäldesammlungen München BStGS registry file 16/3 No.314 c.1872).

A contemporary technical manual described damage to paintings from heating systems with the dynamics of RH levels being identified along with those of temperature as deteriorating factors:

> *"… the picture is still liable to injury from alteration in the size and form of the canvas or panel- alterations which may arise from excess of dryness as well as of damp, or from inequality of temperature. ..extreme dryness of the air is as much to be dreaded as extreme damp. …the coloured films of the painting are submitted to an injurious strain, which may end, as the binding medium of the pigments becomes more brittle, in a multitude of minute fissures, and the final flaking off of portions of the paint."* (Church, 1872, p.247)

In order to reduce the movement of paintings under fluctuations of RH, Church recommended that a picture gallery should be kept at a "*mild*" and consistent temperature with enough moisture in the air to keep the hygroscopic materials at equilibrium. He advised monitoring the moisture for stability by using a piece of primed canvas held under light tension, connected to a calibrated balance, but did not give a value of RH to maintain the equilibrium moisture content.

By the 20th century, purification of sooty external air was carried out with water sprays and air washing equipment with humidification noted as a bonus of installation. After installing water sprays in the Huntington Building (Boston Museum of Fine Arts, BMFA) in 1908, the humidity engineer and building maintenance team observed the RH conditions in the galleries for two years. They concluded, based on their observations, that:

> *"the humidity best adapted for paintings and other works of art ranged from 55 to 60 percent regardless of the temperature or the time of the year"* (McCabe, 1931, p.7).

In Cleveland, during the first year (1916-1917) of operation of the Museum of Art's new building, the building superintendent (James F. McCabe, formerly of the BMFA) tested the plenum (fan-driven) heating system with *"the latest improved air washers"* to ensure that it maintained *"the proper percentage of humidity desired in the exhibition galleries and store-rooms"* (McCabe, J.F., 1917) which he determined to be between 50% RH to 55% RH (McCabe, J.W., 1931). Dehumidification was provided by constant heating throughout the summer months, in order to keep the internal RH eight to ten percent below external conditions. His successor (and brother) J.W. McCabe felt that heating to reduce RH was not effective enough to protect certain types of object, recommending the installation of a dehumidifying plant to control the RH in the Egyptian and the arms and armour galleries. However, he acknowledged that the costs of installation might be prohibitive and the costs of maintenance unknown.

Tests to determine the effect of RH fluctuation on the movement of wood was carried out by researchers from the Forest Products Research Laboratory (FPRL), the Office of Works and the National Gallery of London (NG-L) after severe deterioration

occurred to a number of panel paintings during the exceptionally dry year of 1929 (Stillwell & Knight, 1931). Their research report concluded that long term fluctuations would cause more damage than short ones and that waterproofing the back of panel paintings would reduce warping. A test using small samples of various woods, placed around the gallery spaces and weighed monthly, was used to determine annual variations in moisture gain in wood. From data obtained they deduced that the average annual moisture content was 11%, and thus the optimum range for RH to maintain equilibrium moisture content would be 55% to 60% (Keeley & Rawlins, 1951). While a scheme to introduce water spraying in the NG-L was designed (MacIntyre, 1934a) no control of humidification was undertaken until almost twenty years later (Keeley & Rawlins, 1951) and the NG-L relied on glazing and backing paintings to reduce reactions to changes in air moisture content.

MacIntyre, a researcher with the Office of Works, appended the FPRL report in his introduction to the Courtauld publication of a conference on atmospheric humidity held in 1929 (MacIntyre, 1934a). He assumed the effects of fluctuating RH on canvas paintings, despite lack of experimentation, and recommended that all new galleries should be provided with either an air spray or a contact washer in order to avoid low RH. MacIntyre endorsed the RH level of 55% to 60% as optimal for galleries, except for those exhibiting water colours where a lower RH was required to prevent fading of pigments. He added specifications for storage, with a temperature at 60°F (consistent with gallery temperature) and an RH at 60% or 55% if no spraying plant was installed. In the same year he installed an HVAC system in the Hampton Court Orangery, using water sprays and 1740 pounds of old canvas fire hose as a cost-effective way to reduce the levels and fluctuations of RH which were damaging a series of massive paintings on canvas. The unlined canvas hose was intended to absorb or desorb moisture as required to limit the fluctuations of the RH to within 20% overall, with the range of RH being maintained at 55% to 75% in the summer, with closer limits in the winter despite noting that:

> *"…At present there are no data available from which the best conditions for the pictures, as now treated, can be deduced."* (Waterhouse et al., 1934b, p.114).

MacIntyre hoped to attain close to the *"assumed ideal 60 per cent"* in the winter months by running both the pump of the water spray and an air circulating fan whenever the RH fell below 55%. In the summer, when external RH could rise to over 90%, the fan would be run to reduce the RH to no more than 75%, although he suspected the need for additional absorbing material (silica gel, salt hydrates) or refrigeration. Unfortunately, he never published a report on the success or failure of his system.

The U.S. National Bureau of Standards studies on the permanence of paper (1928 - 1934) led Scribner (1934) to recommend optimum environmental parameters of 70°F to 85°F and 45% RH to 55% RH for the preservation of records in libraries. Research undertaken by Groom and Panisset (1933), for the British Public Record Office, on the minimum hygrometric conditions required for the mildewing of book materials, showed that the mould species (conidia) which affected the most susceptible of binding materials (tanned skins) only started to grow at about 72.6% RH at a temperature between 68°F to 77°F. This prompted an upper limit of 70% RH at any

temperature to be set at the British Museum (BM) by Plenderleith (1943). Based on MacIntyre's observations and a 1929 experiment which monitored RH fluctuations in a large exhibition case, Plenderleith also recommended a constant 60°F at 60% RH for paintings and collections of any kind, although he allowed that museum and library collections could likely withstand ±5°F and ±5% RH. As excessive changes in RH could potentially be more damaging than high RH, he recommended using closed showcases to mitigate fluctuations (Plenderleith & Werner, 1971). This was considered more achievable than adding humidification and dehumidification equipment to the existing heating systems as:

> *"putting air conditioning into most of the galleries would conflict with the fine architecture of the building"* (Bradley, 1989, p.68)

A publication, *La Conservation des Peintures* (Office International des Musees, 1938) was drawn from various papers presented at an international conference held in Rome in 1930 on the conservation of works of art. Recommendation for a stable RH levels within a range from 40% RH to 60% RH, came from J.W. McCabe who agreed with MacIntyre that, while 60% RH to 65% RH was the easiest range to achieve in temperate climates and most suitable for the preservation of most objects in museums, it was too high for watercolours. He observed that progressive acclimatisation was necessary to prevent deterioration since many objects came into museums from other places where the RH levels were very different. Examples of humidification systems were given, including MacIntyre's Orangery system, but it was concluded that the best way to obtain a very stable environment was to construct a well-insulated airtight building such as the new wing of the British Library.

Between 1917 and 1938, most recommendations for RH levels were in a tight band between 50% to 65%; lower ranges were considered acceptable for records and works of art on paper (Figure 2.11).

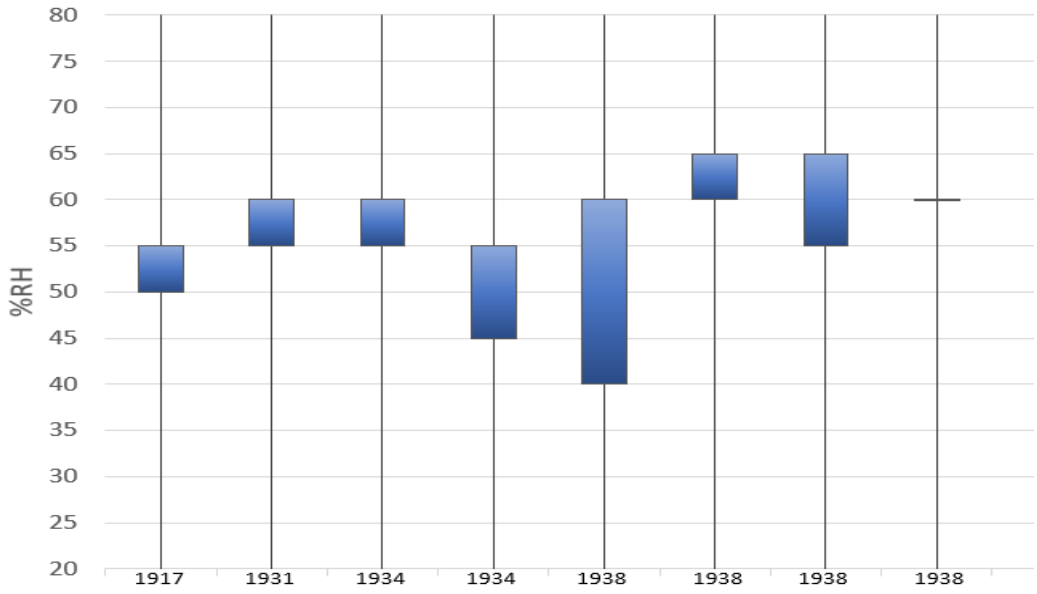

Figure 2.11 RH range recommendations as found in the literature, 1917-1938

2.3.2 Influence of WWII underground collections storage on RH guidelines

During the First World War, the BM evacuated important collections into the disused underground tunnels of the Holborn Post Office. Although ventilation, heating and environmental monitoring equipment had been installed, the environment was *"strange, rather damp and overheated"* (Plenderleith, 1998). When the objects were returned to the museum two years later, many were found to be deteriorating from the high humidity levels, with significant metal corrosion, mould growth and salt efflorescence, some to the point of total loss. By the Second World War, although the major British museums again ultimately had to evacuate their most valuable collections to underground storage, the research into the effects of RH levels and fluctuations led to more effective measures to control storage environments. Initially a tunnel constructed under the National Library of Wales was used to store books, manuscripts, prints and drawings from the BM. A stable RH of around 65% was maintained by an air conditioning system using fans and heaters (Plenderleith, 1943). By 1940, it was decided to move collections from both the BM and the Victoria & Albert Museum (V&A) into a purpose-built underground repository in the Westwood limestone quarry in Wiltshire. The quarry walls were waterproofed with a silica-based paint and an extensive heating, ventilating and dehumidifying system, using chilled water, was installed to control the naturally cold and very damp conditions. Continuous set points of 65°F and 58% RH were tested so that:

> *"before any valuables could be stored, it had to be demonstrated that conditions of 60°F, 60 per cent R. H. could be continuously maintained…It was a question of perfection or nothing"* (Plenderleith, 1943, p.97).

Continuous monitoring and maintenance of the system was initially needed to sustain the required conditions but subsequent modification used dehumidified cold air from the unoccupied areas of the quarry. The condenser of the cooling system provided sufficient heat to warm the dehumidified air so that the boilers were no longer required resulting in more stable hygrothermal conditions for collections from the British Museum and thirty other institutions (Pallot, 1946).

The NG-L collections were stored in the Manod slate quarry in Wales, where the natural conditions were a temperature of 47°F and an RH of 95% to 100%. Rawlins, the NG-L's Scientific Advisor, dismissed the "traditional" values of 60°F and 60% RH which he considered had been adopted more for the comfort of museum visitors rather than for the benefit of collections:

> *"It seems likely that a range of between 50-55 percent at around 60˚F is nearly ideal"* (Rawlins, 1942, p.112).

Basing his RH values on the thermodynamic relationship drawn from the FPRL wood moisture content experiments, Rawlins (1943) set RH levels at 55% to 60% with an allowed deviation within the range of up to 3% at a temperature of 62°F. Free-standing brick storage buildings were built inside the quarry, each with its own plant room. RH levels were generally maintained by raising or lowering the temperature some 2°F to 3°F; the system operated on almost full recirculation of air (Pallot, 1946).

The significant reduction in deterioration rates of the collections in storage in comparison to those on gallery prior to the war had great impact on the levels of RH recommended for European museum collections. The narrow RH range of 55% to 60% was perceived to be responsible for the improved condition of paintings on both wood panels and canvas (Clarke, 1943) and for a large variety of objects including furniture (Plenderleith & Philippot, 1960). However, as Brown and Rose (1997) pointed out, the stability of the RH was not taken into consideration; nor was Plenderleith's assumption that an RH ideal for paintings was also ideal for all other objects questioned. Both Rawlins (1943) and Plenderleith (1943) believed the extensive body of monitoring data being gathered from the stores would be invaluable for future design of museum buildings. Rawlins (1942, 1947) was decisive in his belief that only full air conditioning would achieve his preferred environmental conditions and his opinion influenced a government commission reporting on the care of paintings in the NG-L to recommend that:

> *"For the purposes of proper conservation it is essential to bring the relative humidity to a close range of 55 per cent to 60 per cent, and to maintain it around these figures, which is considered to be the theoretical optimum. This can only be effected by the provision of FULL CONDITIONING at the Gallery…"* (Weaver et al., 1950, p.30)

From 1940 through 1950, RH recommendations were for narrow bands with very limited fluctuations, within the range 50% RH to 60% RH, based predominately on results from British museum storage conditions during WWII (Figure 2.12).

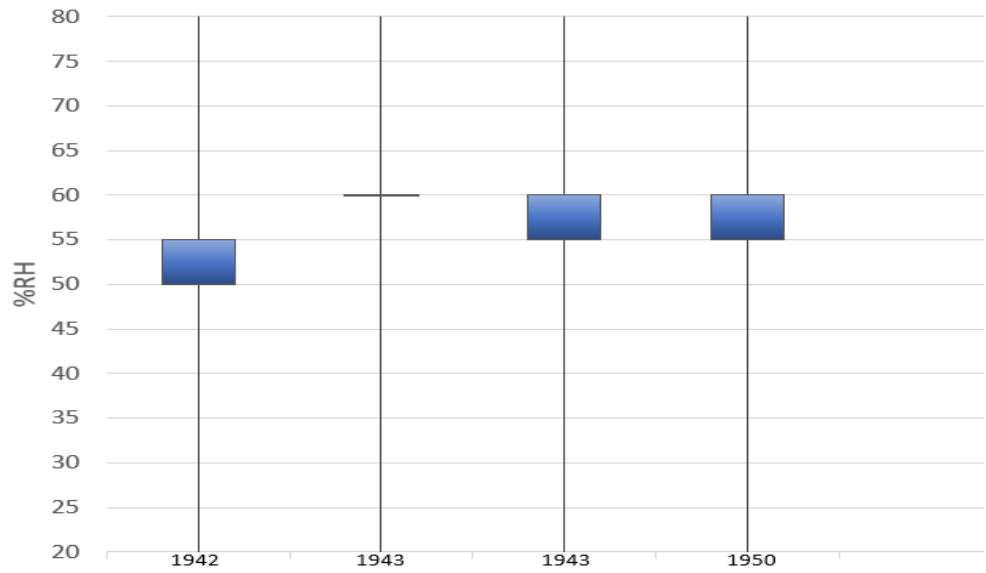

Figure 2.12 RH range recommendations as found in the literature, 1942-1950

2.3.3 Growing reliance on air conditioning to control RH

Plenderleith's 1956 textbook, *Conservation of Antiquities and Works of Art: Treatment, Repair and Restoration,* became the established reference for the conservation of museum objects, particularly throughout Europe (Oddy, 2011) by the end of the 1950s. He based his recommended RH range of 50% to 60% on the BM's

war-time storage conditions, advising that 50% RH was the absolute lowest limit as levels below 40% would allow "*dangerous*" desiccation (of parchment); levels above 68% would lead to mould growth (Plenderleith, 1956). Reporting on the results of a questionnaire sent out to 64 museums and archives in 11 countries by the International Council of Museums (ICOM) in the late 1950s, he and Philippot based their interpretation of the variety of RH guidelines received (from 40% to 60% up to 65% to 70%) on the experiences at Westwood and Manod:

> *"…there is a strong measure of agreement that relative humidity should lie between 50 and 70 per cent; the scientists' preference being for approximately 60 per cent."* (Plenderleith & Philippot, 1960, p.254)

Plenderleith and Philippot asserted that it would be impossible to achieve 60% RH without installation of a complete air conditioning plant:

> *"…it is so effective for the conservation of the most delicate material that it has come to be regarded not as a luxury but, indeed, as an essential for the protection of the heritage of easel paintings"* (p.273).

In the United States, air conditioning systems using chilled water sprays had been installed in galleries, archives and libraries as early as 1932 as in the Huntington Library, San Marino, California. The Washington Art Gallery (West Building), opened in 1941, was one of the first museums in the world to include air conditioning as an integral part of the design, with refrigerating compressors and a continuous flow of air used to manage the temperature and humidity throughout the entire building (National Gallery of Art, 2016). Scribner believed that the only possible way to obtain the recommended environmental parameters was through an effective mechanical control system:

> *"…the only safe and efficient means of maintaining such conditions is through the use of a complete air-conditioning system with which the air can be humidified, dehumidified, and washed."* (Scribner, 1934, p.382).

However, while many such systems installed in North American museums were practically capable of controlling RH to 55% in the summer, those in colder regions could only supply 35% to 45% in the winter as higher RH levels were likely to promote condensation in the building envelope (Brown & Rose, 1996).

In Britain, while Rawlins, Plenderleith and Philippot, and Weaver had all considered full air conditioning essential at the very least for the preservation of easel paintings, it wasn't until 1951 that the NG-L began to install a spray-wash air-conditioning system. The system, installed to:

> *"maintain a temperature of 64°± 3°F (1.7*°C*) and 54%± 4% RH: …24 hours per day throughout the year…"* (Learmonth, 1968. P.52)

took over forty years to be installed throughout the gallery and was only completed during the construction of the Sainsbury Wing in the 1990s (The National Gallery, 2016).

Despite improvements to electric motors and fan technology, which increased air supply pressures allowing the use of narrower ducts, it was difficult to retrofit historic European museums with air conditioning systems without damaging original building fabric (Brown & Rose, 1996). Full air conditioning was installed in new extensions, such as the Tate Gallery in 1979, or in new buildings, such as the Museum of the Twentieth Century in Vienna in 1962 (Learmonth, 1968), but limited partial air conditioning was more likely, as the financial and cultural costs of retrofitting air conditioning equipment in historic buildings negated the desire to keep the internal environment as stable as possible (Legnér & Luciani, 2013).

Advice on controlling RH levels and fluctuations in museum storage through air conditioning was given in UNESCO's *The Protection of Cultural Property in the Event of Armed Conflict* (Noblecourt, 1958). Noblecourt referred to Rawlins for recommended temperature and RH ranges, accepting that air conditioning of shelters should provide two types of conditions:

> *"…for works of extremely great cultural value …a 'refined' environment… a temperature of about 18˚C and a relative humidity of 58 ±3 per cent" …for most works of art of great cultural value…a 'rough' environment of temperature 5˚-20°C and an RH of 40 - 60 per cent"* (p.303).

Noblecourt specified that the RH should never exceed 80% to 85%, although he emphasized that the safe upper limit could be no more than 68%, or drop lower than 40%. Repeated fluctuations within those limits might be no less harmful than those caused by extremes of RH.

In North America, advice for engineers on climate specifications for libraries and museums, specifying a range of 72°F/22°C and 35% RH to 40% RH in winter and 78°F/26°C and 45% RH to 50% RH in summer, was published in the American Society for Heating, Refrigerating and Air-Conditioning Engineers' *Guide and Data Book* (ASHRAE, 1964). An RH range of 45% to 65% (55% RH ±10% RH) was proposed by Buck, based on his perceptions of the limitations of air conditioning systems as most museums, in his opinion, found it difficult to limit the annual humidity range to within 20%. However, he warned that:

> *"if winter humidities cannot be maintained above 45 percent RH and held below 65 percent RH, unnecessary damage to some parts of almost any museum collection may be anticipated."* (Buck, 1964, p.56)

Brommelle, in UNESCO's *Museums and Monuments Series* (UNESCO, 1968), considered air conditioning by refrigeration essential to control RH in tropical museums although he was pragmatic that the levels recommended for temperate climates (an average of 50% RH to 60% RH ±3% RH) were less likely to be obtained. While recognising the cost of such control, he felt it was justified in the long run as it reduced the need for restoration and the loss of value of the cultural objects. Brommelle considered it important to stay within a broad range of 40% RH to 65% RH but even more important to limit fluctuations as much as possible; however, he suggested that the limits of tolerance could be extended in order to reduce costs.

Between 1950 to 1970, the installation of air conditioning systems to control ranges of RH became more common. Recommendations for ranges and fluctuations were often based on what the systems could achieve rather than on what conditions were suitable for the preservation of museum and library collections (Figure 2.13).

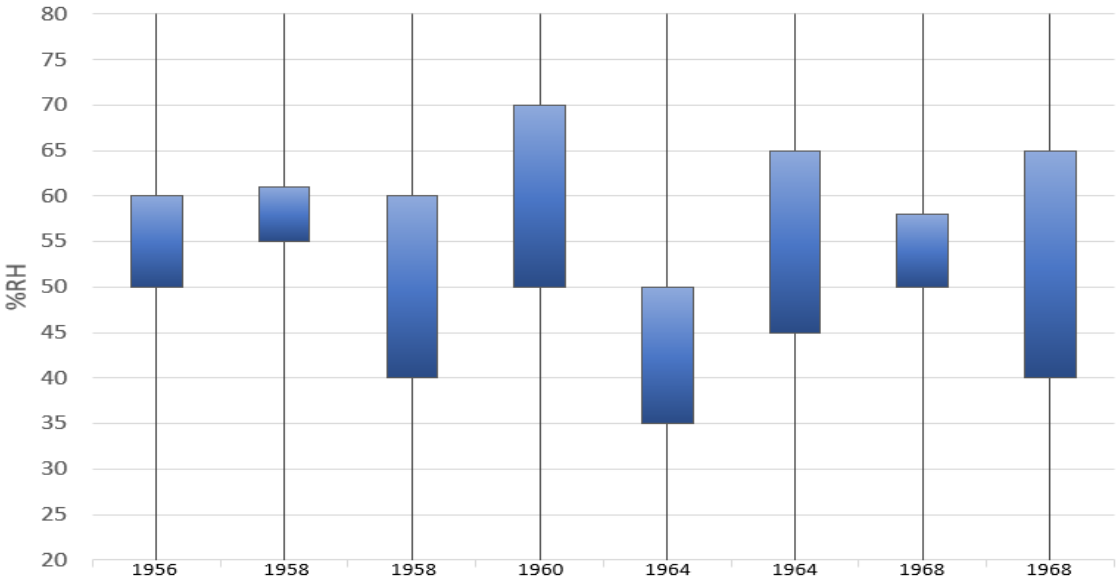

Figure 2.13 RH range recommendations as found in the literature, 1956-1968

2.3.4 Developing RH range recommendations into museum standards

In the Canadian Conservation Institute's (CCI) first Technical Bulletin, *Relative Humidity: Its Importance, Measurements and Control in Museums* (Macleod, 1975), Macleod endorsed Buck's RH range of 45% to 65% but noted that 45% might be unattainable in Canadian winters depending on building construction. If a lower limit of 35% RH had to be accepted, the upper limit must then be reduced to 55% RH so that the extent of fluctuations (20%) remained the same as:

> *"the imperative is to keep the range of seasonal variations as small as possible"* (Macleod, 1975, p.8)

Daily variations should be much less than seasonal variations. By 1979, CCI had revised their recommended optimum rate of change to a daily variation not exceeding ±2% around a constant set point between 47% RH to 53% RH. But, again acknowledging that a more practical range might be required for the severe Canadian climate, a minimally acceptable rate of change could be 38% RH (winter) to 55% RH (summer) with diurnal ±3% RH fluctuations (very occasional variable of up to 5% RH) with a monthly set point changeover no faster than 5% RH per month (Lafontaine, 1979).

In the first edition of *The Museum Environment* (Thomson, 1978), Thomson recommended an RH level of 50% RH to 55% RH with a seasonal tolerance of ±4% RH or ±5% RH. Referring to works he considered "standard textbooks, *The Conservation of Antiquities and Works of Art* (Plenderleith & Werner, 1971), *The Conservation of Cultural Property* (UNESCO, 1968) and *Textile Conservation*,

(Leene, 1972), he noted they agreed on mould growth and metal corrosion occurring above 65% RH to 70% RH and on the embrittlement of organic materials at low RH (40% RH to 45% RH). He also recommended lower RH levels to reduce possible condensation in building envelopes for those areas with very cold winters. In his 2nd edition (Thomson, 1986), Thomson divided RH specifications into two classes:

- *Class 1 as appropriate for major national museums, old or new, and also for all important new museum buildings*

- *Class 2 as essential for avoiding major damages while keeping costs and alteration to a minimum.*

Class 1 was 50% RH or 55% RH ±5% RH, day and night, throughout the year, with the caveat that the level might be fixed higher or lower but for mixed collections should be in the range 45% RH to 60% RH. For Class 2, the range was:

> *"to be kept within the danger limits 40% and 70%"* (Thomson, 1986, p.269)

Thomson's Class 1 became a standard specification for museum architects and engineers despite his own view that there was still too little information on how much RH variation could be tolerated by different materials or his conviction that there could be more simple, reliable and cheap ways of stabilising RH than installing a mass of energy-consuming air conditioning machinery. Further limitations to his recommended daily fluctuations occurred as conservators, believing that very limited variation in RH was necessary to avoid dimensional change in hygroscopic materials, asked for tighter and tighter controls.

> *"There was the general feeling that if ±5% was good then ±3%, or even ±2%, must inevitably be better."* (Brown & Rose, 1997, p.15)

Many conservators, told that sophisticated air conditioning systems could achieve tight daily tolerances, misunderstood that the tight tolerances would be in the return air duct, where the RH sensor for the system was located, rather than in the room they were monitoring. A ±2% RH tolerance in the return air duct would likely only control room RH to ±5% at the very most, given flow and volume of air and room use. Precise monitoring of the fluctuations was also not possible since mechanical equipment such as psychrometers and hygrothermographs were only accurate to ±5% RH even when properly calibrated. While electronic sensors might be more precise, sensor drift could limit the accuracy to ±2% RH to 3% RH (Appel, 2010). As Brown (1994) explained, specifications less than ±5% RH were unrealistic without a credible permissible absolute error for the level and variation. However, tight tolerance specifications became standard.

A literature search undertaken by ASHRAE consultant engineers (Ayres et al., 1988) to identify design criteria for museum environmental conditions found that detailed information on RH specifications came from conservation rather than engineering publications. They found that the permissible daily RH fluctuations varied widely, with values varying from ±2%, ±3%, ±5%, ±6% to ±10%, within what they described as the "safe" range of RH of 45% to 65% for most objects, being suitable for material preservation. But they considered that conservators lacked an understanding of the

operational issues in maintaining daily close control. Based on their study, they used computer simulation to analyse the costs of HVAC control of RH (Ayres et al., 1989). They concluded that the least expensive RH to maintain was 50% and the different energy costs associated with maintaining the daily tolerances between ±2% RH to ±7% RH were not particularly significant. The underlying museological concern that tight control was essential for reducing damage to hygroscopic materials was not addressed.

Despite resource and operational implications, full air conditioning was still considered the best way to maintain specified RH 'standards'. The desired level of control could be unrealistic; even if installed systems could maintain very tight parameters, monitoring equipment and methods were less precise, with sensor drift factors between ±2% RH to ±5% RH and measurements not representative of the over-all conditions (Brown, 1994). Even with the most sophisticated and extensive air conditioning systems, maintaining ±5% RH for 95% of the time was probably the best obtainable result. Unintended consequences of enforcing standards were no or delayed environmental condition upgrades due to cost, system installations that damaged building structures, or resources wasted by attempts to meet published standards rather than to preserve collections (Weintraub, 2006).

By the end of the 1980s, varying RH 'standards' were being recommended for museums. In the United States, many museums aimed for 50% RH in general collections areas. European museums tried for a range of 55% RH to 65% RH, in line with local conditions and as specified in publications such as *Recommendations for storage and exhibition of archival documents* (BSI, 1991). Museums in cold climates, such as Canada, were still being advised to maintain lower winter values of 40% RH to 45% RH in order to reduce condensation in building envelopes (Erhardt & Mecklenburg, 1994). Strict specifications could be impossible to achieve in museums which held mixed collections especially if objects, some requiring a low RH and others an RH of 55% to 60%, had to be stored, displayed or studied in the same room (Bradley, 1991). When international loans specified almost flat-line institutional RH tolerances, many museums prevaricated about their own ability to control RH in their galleries and stores (Ashley-Smith et al., 1994).

Through the 1970s to 1980s, very tight control of RH was recommended although RH ranges could vary, depending on geographical location. Expectations were for fluctuations of no more than ±5% RH within collections areas despite the limitations of air conditioning and monitoring equipment (Figure 2.14).

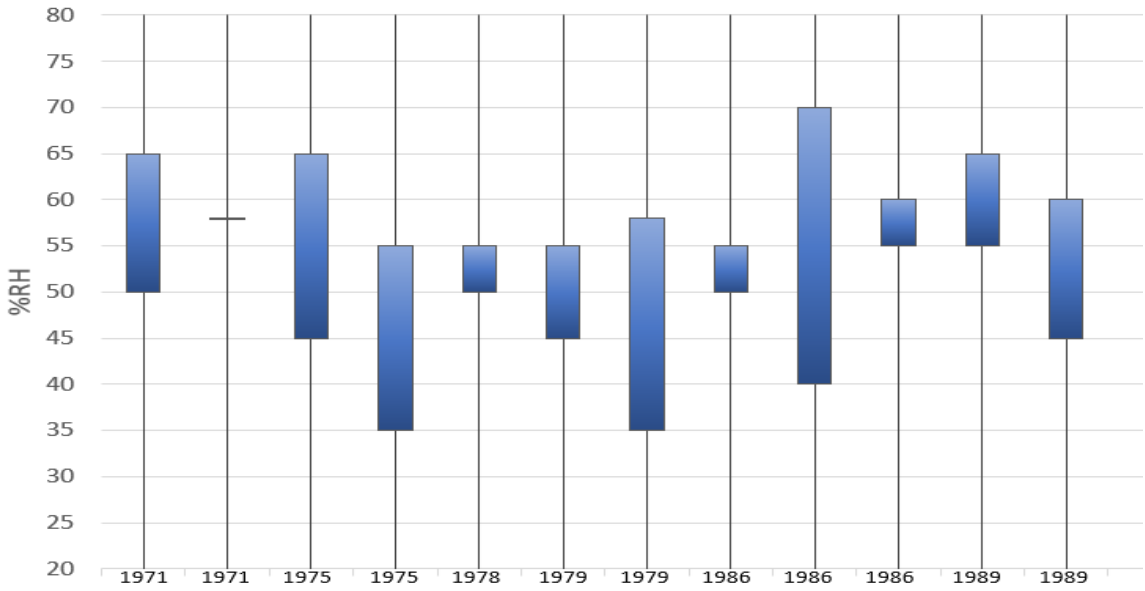

Figure 2.14 RH range recommendations as found in the literature, 1971-1989

2.3.5 Researching rates of change in material response

While architects and engineers incorporated RH standards and mechanical control of those standards into museum building design, satisfied that they were responsibly responding to the concerns of museum professionals, some professionals more closely involved with the deterioration of collections were beginning to challenge the established approach. Hoadley (1978), studying the relationship between stress and strain in wood during RH changes, had dismissed Plenderleith and Werner's assumption that all organic materials were susceptible to damage by desiccation under 50% RH. He considered that Buck (Buck, 1964) had incorrectly cited other researchers on *"incipient damage"* in wood at low RH, misidentifying low RH as the principal cause of damage to museum collections in northern climates. In his view, desiccation damage was unlikely if a limit lower than 50% RH was set where climate conditions and history of the object suggested some lower value and that dimensional change in wood was a greater danger at high RH than mould growth. He concluded that an optimum level was not necessarily the midpoint between high and low endpoints and the breadth of the range was more important than the average level; thus a 10% RH variation in a range of 55% RH to 65% RH was the limit to protect against elastic strain limits, rather than an average RH level of 60%. Hoadley was of the opinion that moisture barriers, cases and even plastic bags could be used to minimise the response of hygroscopic materials to changes in RH since:

> *"maintaining total environmental control to a close tolerance is expensive and difficult (if not impossible) in the face of widely fluctuating climate extremes"* (Hoadley, 1978, p.6)

Michalski, at CCI, had reviewed the stringent RH recommendations of the 1960s and 70s, using what he considered relevant data to consider a wider range. He predicted, based on analysis of potential vulnerability, that high risk only occurred outside the range 25% RH to 75% RH as long as the middle 50% RH remained the local norm (Michalski, 1993). Researchers at the Conservation Analytical Laboratory (CAL) of

the Smithsonian (Colville et al., 1982; Mecklenburg et al., 1994) modelled stress/strain behaviour in order to predict patterns of damage from RH fluctuations on canvas supported oil paintings. Mecklenburg (1991) showed that the strain/stress curves of each painting component was a function of RH, with each painting layer undergoing continual change with RH fluctuation. Comparisons between resultant cracking of modelled and actual paintings showed good correlation. Based on modelled predictions and additional mathematical calculations of stress/strain responses of materials to changes in environment (Erhardt & Mecklenburg, 1994), the CAL scientists concluded that stringent standards of 50% RH and 21°C were excessive. They believed that, within a reasonable range of RH, from 30% to 60%, most unrestrained organic materials would absorb and desorb moisture with little to no damage or stress, with a reversible return to original shape on a return to original environment (Erhardt et al., 1995). They felt confident they could predict larger allowable although still conservative RH fluctuation values for a material under restraint by knowing the stress/strain curve for that material, allowing *"as much as 15% fluctuation in relative humidity"* (Office of Public Affairs, Smithsonian Institution, 1994). This value was later clarified as *"moderate fluctuations within the range 50% ±15% RH"* (Erhardt et al., 2007). The revised guidelines were predicted to save millions of dollars in energy costs for museums.

Advice on expanded RH ranges was received skeptically by many conservators and consultants who disbelieved the science and the predicted costs savings (Real, 1994; Lull, 1994; McCrady, 1994). But Michalski reaffirmed that CCI also recommended a wider range, based on his own review of monitoring data. He advised that the most effective global advice was not to recommend ±15% RH around a set point of 50% RH but to stay within 20% of the local historic average RH (McCrady, 1995). Reducing the steps to ±10% RH or ±5% RH would bring smaller benefits but any failure of a mechanised control system would increase risk. Like Hoadley, Michalski considered that critical values for RH fluctuations should be based on an object's past exposure and materials and manner of composition. Based on the work at CCI and CAL, Brown and Rose (1997) suggested "*organic artifacts be acclimated to mid-range humidity"* and that 45% RH to 55% RH ±10% RH was a more acceptable range than the traditional museum humidity specifications of 55% RH to 60% RH which had been a result of codification of earlier practice in specific climates.

A meeting on collections' environment was held at the Smithsonian in 1997, where Michalski, Mecklenburg and other participants from the conservation profession discussed the decision-making process for environmental parameters. The conclusion of the meeting was that the safest environment for collections was well-controlled with humidity fluctuations of ±5% but within the stipulation that:

> *"…before deciding on the set points of humidity and temperature, permissible fluctuations, and seasonal drifts one has to understand if the deterioration of the collection is mostly chemical or mechanical One also should know what percentages of the collection are of very high, high, medium, or low vulnerability to environmental damage."* (Preusser, 1997, p.2)

Further research into the hysteretic behaviour of wood and other hygroscopic materials such as ivory under large changes in RH (Mecklenburg & Tumosa, 1999),

showed that the materials responded less in the 35% RH to 65% RH range than in wider fluctuations. Tests indicated that the moisture coefficient of various woods was not a constant but had the lowest values within the range 30% RH to 70% RH, allowing significant fluctuations without damage when the ambient RH was centred between 35% and 65%.

Research on the chemical deterioration of paper (Michalski, 1993; Banks, 1999; Michalski, 2000) indicated that archival materials were better preserved when stored in colder and drier environments:

> *"the key words for preservation of records are clean, cool, dry, and stable."* (Banks, 1999, p.67)

The *American National Information Standards Organization (NISO) Technical Report 01-1995* (Wilson, 1995) recommended 30% RH to 50% RH ±3% RH, depending on ambient climatic conditions, for archival storage. Other published guidelines at the end of the 20th century supported lower RH values. RH ranges previously recommended in *BS:5454 1989* of 55% RH to 65% RH were revised to 45% RH to 60% RH ±5% RH (BSI, 2000). *ISO 11799:2003* (International Standards Organisation, 2003) recommended storage RH of 20% to 50%, with tolerable diurnal fluctuations of ±3% RH to ±5% RH within the limits, depending on the type of material. The Canadian Council of Archives (CCA) summed up the varying recommendations and suggested a compromise for mixed collections of 45% RH ±10% RH at 18˚C to 20°C (Canadian Council of Archives, 2003).

The *2003 ASHRAE Handbook* repeated the seasonal and daily fluctuation ranges as recommended by Michalski in an earlier (1999) edition and as issued by CCI in 2000 (Michaski, 2000). These varied between:

- '*AA': no seasonal changes or adjustments with short duration ±5%*
- *'A': ±10% seasonal change OR seasonal adjustment with short duration ±5%*
- *'B': ±10% seasonal change and some seasonal adjustment with short duration ±10%*
- *'C': within 25%-75%*
- *'D': prevent dampness*

Despite the research into stress/ strain response in organic material and the development of risk assessment and risk modelling of past environmental damage, there was still reluctance by some conservators to depart from strict standards. Posting on the Conservation DistList (ConsDistList), McManus, a paper conservator from Israel, asked:

> *"I am interested to know what are American conservators' position on the "2003 ASHRAE's Applications Handbook--Chapter 21--Museums, Libraries, and Archives", and is it generally endorsed by AIC and other groups? Are the temperature and RH specifications presented in the document recommended by conservators? I present this question because the RH and temperature bandwidths seem rather large — are these performance targets presently*

applied in institutions or are they only representing what ASHRAE considers achievable and acceptable." (McManus, 2003)

In the 1990s, research into the effects of RH ranges and fluctuations on cultural heritage collections was carried out to give better defined recommendations (Figure 2.15). Despite advice based on research results, many museum professionals felt uneasy with the wider RH bands and allowable fluctuations.

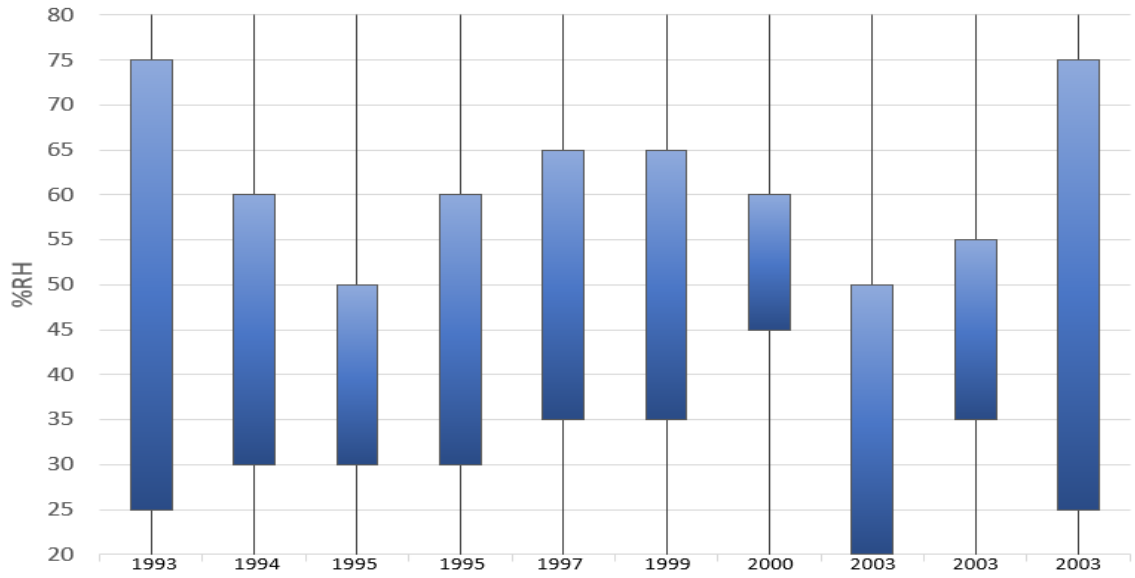

Figure 2.15 RH range recommendations as found in the literature, 1993-2003

2.3.6. Impact of sustainability policies on RH control

The move towards more sustainable operations to maintain museum environments had grown as energy costs increased and funding declined. The potential impact of climate change on stewardship decisions indicated that a more sustainable approach to the issues of RH control was required. In 2007, the Getty Conservation Institute (GCI) organised a roundtable on sustainable climate management strategies (*Experts' Roundtable on Sustainable Climate Management Strategies*, Tenerife, Spain) where conservation and other museum professionals discussed current strategies, emerging trends, the meaning of sustainability in the context of cultural preservation and whether cultural institutions had a role in the debate on energy consumption (GCI, 2007). The panel concluded that there was a need to manage environmental conditions to reduce climate-related risks but that management must be accomplished in a responsible manner, taking into account "*proofed*" RH and temperature fluctuations (most extreme historic fluctuations), building design and performance, financial costs, energy consumption and global climate change.

During the revision to the international agreement on *Loans Guidelines* (Bizot Group, 2009), a group of UK conservators and other stakeholders amended environmental recommendations to reflect the wider ranges of RH that were being considered as tolerable. The *"Interim Guidelines"* called for a stable RH with set points 40% to 60%, at a stable temperature of 16°C to 25°C, with fluctuations of no more than ±10% RH per 24 hours within the range, with a proviso that more sensitive materials would

require specific and tight RH control. Additional guiding principles for reducing museums' carbon footprint stipulated that passive methods and lower energy solutions should be considered before air conditioning in order to maintain suitable environments. Further research into the effectiveness of passive buffering and hygroscopic building materials and finishes was endorsed to find ways of moderating changes in RH (National Museum Directors' Conference, 2008). More than 50 heads of conservation departments from museums in North American and the UK adopted the *"Interim Guidelines"* after "*two days of wrangling*" (Michalski, 2011) at a meeting held at the BMFA, although some felt that changing from ±5% RH or ±10% RH or ±15% RH to a box of 40% RH to 60% RH could easily cause misinterpretation if the values were not understood as end-points. The meeting endorsed improvements in passive methods to control RH and developing standards for building design, taking into account preservation needs, sustainability, climate change and future energy costs (IIC, 2010).

The European Standard *EN 15757:2010, Specification for temperature and relative humidity to limit climate-induced mechanical damage in organic hygroscopic materials* (BSI, 2010) cited Thomson, Mecklenburg et al., Michalski and the 2007 *ASHRAE Handbook.* Recommendations were for a mid RH range unless the material had become acclimatised to other conditions, in which case analysis of the material's needs were required before altering the environment. RH should be stable around average values or typical seasonal cycles, with a 10% threshold considered acceptable. The methodology allowed flexible target values of temperature and RH which in turn allowed less and simpler equipment and reduced maintenance costs, with further mechanical control reduced through enhancement of a building's passive control capability (BSI, 2010).

BS 5454:2000, Recommendations for the storage and exhibition of archival documents (BSI, 2000), which had specified RH ranges for archival materials, was replaced by two publications. *PAS 198:2012, Specification for managing environmental conditions for cultural collections* (BSI, 2012a) gave parameters for RH for cultural collections, taking into account the material and structure of objects and sensitivities to ranges and fluctuations of RH. The upper permissible RH limit was set at 75% although 65% RH was given as a precautionary limit due to mould growth. The lower permissible limit was set at 30% RH; lower RH set points could be recommended for materials such as corroding metals. Specific ranges and rates of fluctuation for material types were listed in Annex D, based on Michalksi's work. Padfield, et al. (2007) were cited for the potential for passive environmental control in temperate climates using large scale RH buffers. Archival storage recommendations were revised and reissued as *PD 5454:2012, Guide for the storage and exhibition of archival materials* (BSI, 2012b). A range of 35% RH to 60% RH was recommended for mixed collections, with 25% RH to 60% RH for boxed papers, with a preference for moderating fluctuations rather than allowing slow seasonal drift.

The AIC accepted the *Interim Guidelines*, with an allowable seasonal drift of ±5% RH within the 40% RH to 60% RH parameters, for the majority of loans of cultural material, with the proviso that some materials could require different environmental conditions for their preservation and that fluctuations must be minimised (Kerschner, 2013). The Australian Institute for the Conservation of Cultural Materials (AICCM) recommended an RH between 45% to 55% with an allowed diurnal fluctuation of

±5% RH as acceptable storage and display conditions, after taking into consideration the points of view from both supporters and opponents of the Bizot Group *Interim Guidelines* (Bickersteth, 2014). Dissenting opinion against the perceived relaxed guidelines came from some European conservators (predominately German, Austrian and Swiss), who argued that the *Interim Guidelines* were more politically than environmentally motivated and more useful for organizing large exhibits than saving either energy or sensitive collections. In their view, poor energy control was a result of poor museum design which could not be resolved through adopting less stringent specifications. In a statement issued from the Doerner Institut Munich (*Stable is safe. The Munich Position on Climate and Cultural Heritage*), Burmester and Eibl (2014) declared that, rather than depart from stable climates with tight ranges for RH and temperature which they considered had been largely responsible for the excellent condition of their collections,:

> *"Future energy savings can only be achieved through hygro-thermally optimized building fabric (moisture-buffering surface materials, thermal mass etc.) and changed climate control strategies"* (Burmester & Eibl, 2014)

In 2014, the International Institute for Conservation of Historic and Artistic Works (IIC), in conjunction with the International Council for Museums - Committee for Conservation (ICOM-CC) released a declaration on environmental guidelines at the conclusion of their joint conference in Hong Kong. They announced that the interim RH guidelines agreed by AIC, AICCM and the Bizot Group should be accepted as guidelines for international loans: RH 40% to 60% with no more than ±10% RH/24 hrs within the range. The RH range thus ratified was narrower than those recommended in the European standards (Figure 2.16).

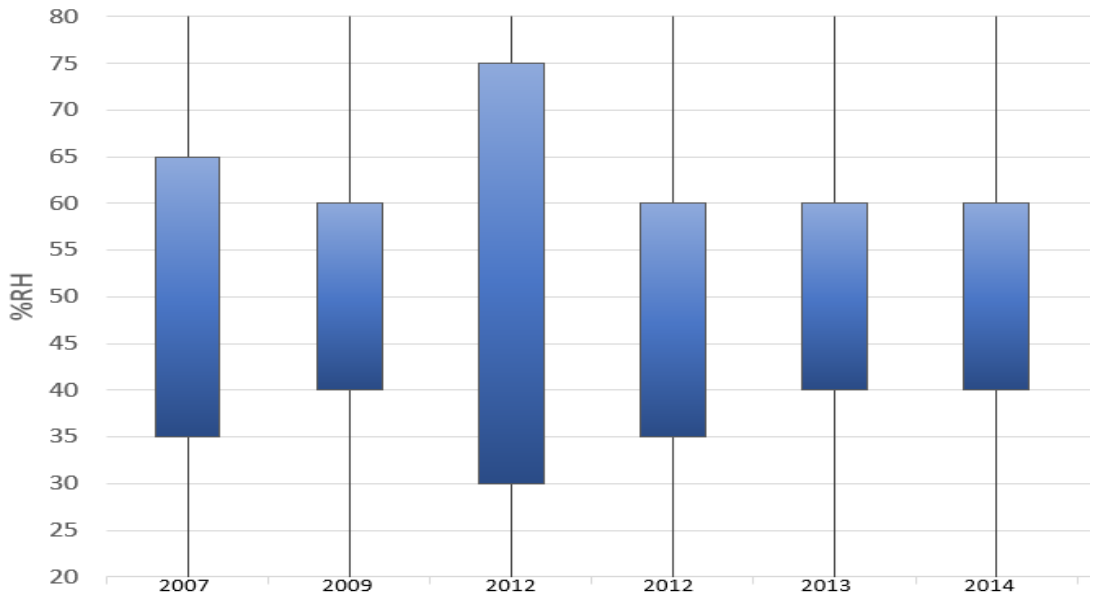

Figure 2.16 RH range recommendations as found in the literature, 2007-2014

The guidelines were also accepted by the AICCM and AIC for storage and exhibition conditions. While not as stringent as some of the RH recommendations from 1917 to

1989, the revised guidelines were not as wide as those suggested by Mecklenburg, Michalski and others through the 1990s and into the early 2000s.

A timeline of the RH recommendations illustrates the trend developing from narrow bands into broader ranges as research into materials' deterioration was incorporated, then settling into a mid-range that has been accepted internationally by many in the conservation profession (Figure 2.17).

Currently (up to 2020) European museum environment management guides (*PAS 198:2012, Specification for managing environmental conditions for cultural collections* (BSI, 2012a); *ISO 11799:2015, Information and documentation- Document storage requirements for archive and library materials* (EN, 2018); *BS 4971:2017, Conservation and care of archive and library collections* (BS, 2017); *EN 15759-2:2018, Conservation of cultural heritage- Indoor climate* (BSI, 2018a); *EN 16893:2018, Conservation of Cultural Heritage- Specifications for location, construction and modification of buildings or rooms intended for the storage or use of heritage collections* (BSI, 2018b); *PD ISO/TR 19815:2018, Information and documentation- Management of the environmental conditions for archive and library collections* (ISO, 2018) recommend basing institutional guidelines on the needs of a collection, the resources of the institution, the operational context and the local climate and to minimise the use of energy and non-renewable resources, rather than to rely on simplified standards. The RH band, 40% to 60%, with diurnal fluctuations of ±10% RH within the band and even allowing seasonal fluctuations of ±5% RH outside the band, is not suitable for all classes of cultural heritage collections (Table 2.1; Table 2.2).

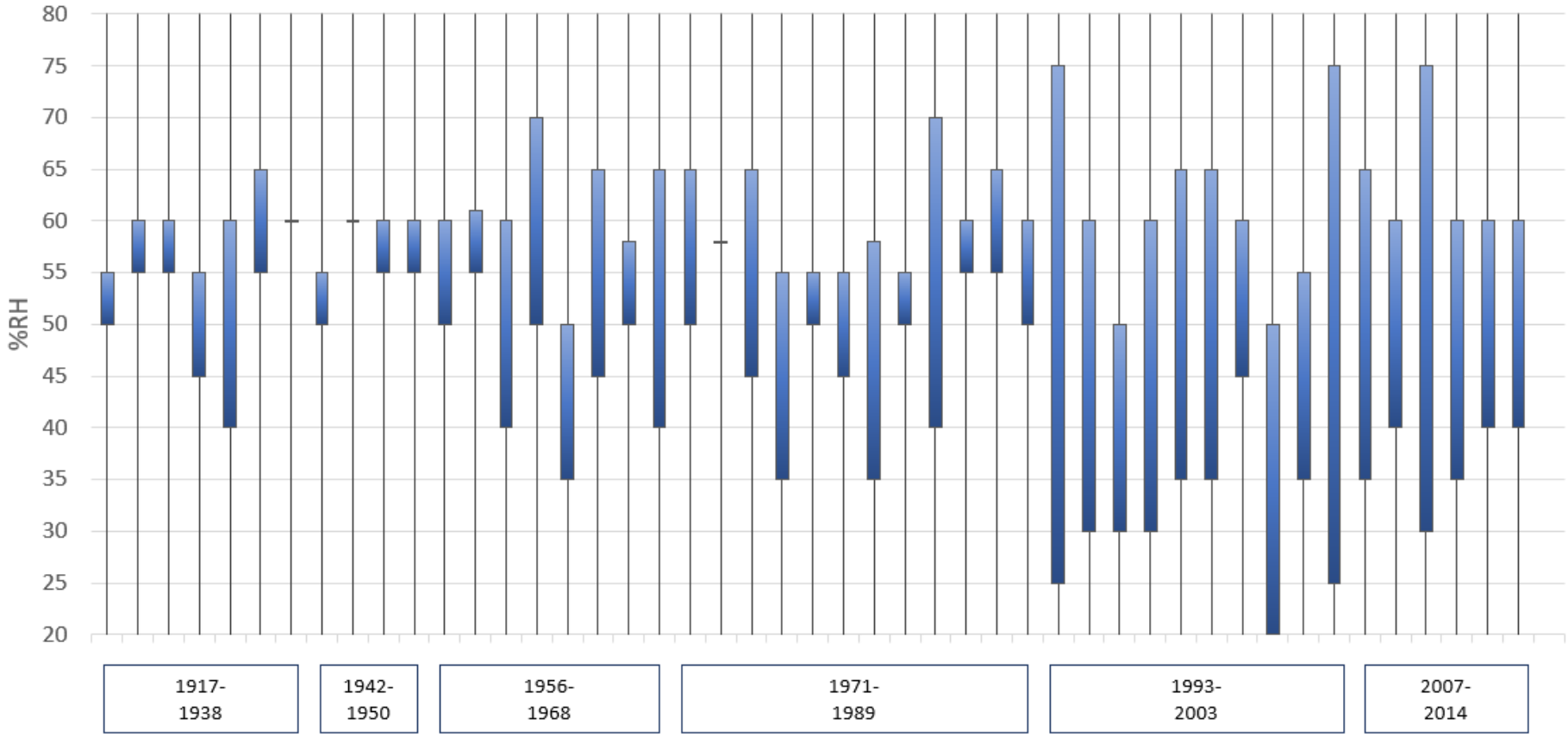

Figure 2.17 Timeline of trends in the historic development of RH recommendations for the preservation of cultural heritage collections, 1917-2014

Table 2.1 Potential deterioration of materials by incorrect RH ranges found in conservation literature

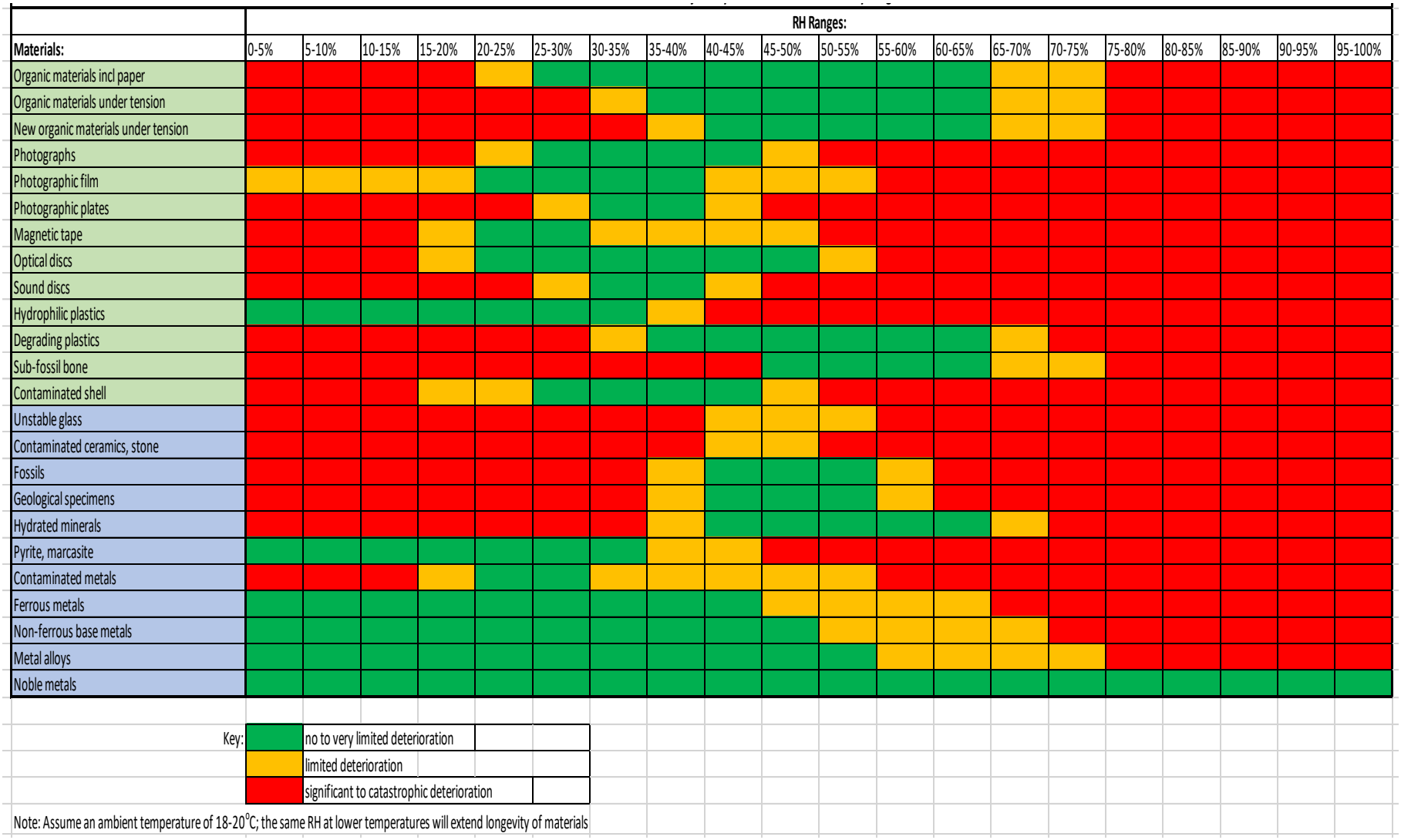

	RH Ranges:																			
Materials:	0-5%	5-10%	10-15%	15-20%	20-25%	25-30%	30-35%	35-40%	40-45%	45-50%	50-55%	55-60%	60-65%	65-70%	70-75%	75-80%	80-85%	85-90%	90-95%	95-100%
Organic materials incl paper																				
Organic materials under tension																				
New organic materials under tension																				
Photographs																				
Photographic film																				
Photographic plates																				
Magnetic tape																				
Optical discs																				
Sound discs																				
Hydrophilic plastics																				
Degrading plastics																				
Sub-fossil bone																				
Contaminated shell																				
Unstable glass																				
Contaminated ceramics, stone																				
Fossils																				
Geological specimens																				
Hydrated minerals																				
Pyrite, marcasite																				
Contaminated metals																				
Ferrous metals																				
Non-ferrous base metals																				
Metal alloys																				
Noble metals																				

Key:
- no to very limited deterioration
- limited deterioration
- significant to catastrophic deterioration

Note: Assume an ambient temperature of 18-20°C; the same RH at lower temperatures will extend longevity of materials

References:

BSI, 2012a; Grattan & Michalski, 2014; NatSCA & ICON, 2013; Mecklenburg, 2007; Morse, 2014; Stauderman & Tompkins, 2016

Table 2.2 Potential deterioration of materials by RH fluctuations found in conservation literature

	RH fluctuations/ 24 hours			
Materials	**up to ±5%**	**up to ±10%**	**up to ±20%**	**up to ±40%**
Organic materials:				
ivory, parchment; lacquers				
bone, horn, tortoiseshell, antler; plastics				
textiles, basketry; leather, skin; feathers, hair, fur; wood; grasses, fibres, bark; paper; shell; waxes				
degrading organic materials				
Organic materials under tension:				
paper adhered to support; inlaid wooden furniture; composite objects; taxidermy				
panel & tightly keyed paintings on canvas; globes; veneered wooden furniture; musical instruments				
oil paintings on canvas; vellum & wood book bindings; jointed wooden furniture; leather & textile seat coverings; taut drumskins; books				
New organic materials under tension:				
acrylic paintings on canvas, board				
Photographs:				
mounted photographs				
loose photographs				
Photographic film				
Photographic plates				
Magnetic tape				
Optical discs				
Sound discs				
Hydrophilic plastics				
Sub-fossil bone				
Contaminated shell				
Unstable glass				
Contaminated ceramics, stone				
Fossils				
Geological specimens				
Hydrated minerals				
Pyrite, marcasite				
Metals:				
contaminated metals				
ferrous metal				
non-ferrous base metals				
metal alloys				
noble metals				

Key:		no to very limited deterioration
		limited deterioration
		significant to catastrophic deterioration

References:
Vici et al., 2006; Kozlowskii et al., 2007; Mecklenburg, 2007; Erhardt et al., 2007; Thickett et al., 2011; BSI, 2012; Radon et al., 2013; NatSCA & ICON, 2013; Grattan & Michalski, 2014; Morse, 2014

2.4 Improving the sustainability of RH control

While discussion about values and ranges of RH continues, there has been agreement that objects should be stored in environments similar to those to which they have become accustomed, bearing in mind the potential mechanical, chemical and biological deterioration caused by too high or too low RH. Reducing the fluctuations within the chosen range of RH, thus reducing or eliminating stress/strain reactions in hygroscopic materials, also prolongs the preservation of organic historic materials. If ways can be found to design museum storage buildings that effectively maintain RH levels and fluctuations within the wider bands recommended in current guidance without expending the substantial amount of energy required for the full-time operation of extensive HVAC systems, significant energy savings can be made. HVAC systems have typically used close to 50% of the total energy consumption in a non-domestic building (Korolija, 2011) and up to 60% in museums (Mitchell, 2014). According to the *CIBSE 2008 Energy Benchmarks* referenced by Hawkins (Hawkins, 2011; BSRIA, 2018), the average energy (electricity and natural gas) consumption for UK cultural venues (museums, art galleries, libraries) was 270k Wh/m^2 with electrical use at 70 kWh/m^2. Total energy consumption benchmarks for storage facilities (non-food, cold storage, and distribution warehouses) was listed between 195 kWh/m^2 to 240 kWh/m^2 with electrical use between 35 kWh/m^2 (distribution warehouse) to 145 kWh/m^2 (cold storage). Annual total energy costs were benchmarked at £11/m^2 (electricity £6/m^2) for cultural venues and between £7/m^2 to £10/m^2 (electricity £3/m^2 to £12.30/m^2) for warehouses from distribution to cold storage facilities.

Moore estimated that an excellent annual electricity consumption for a conventional museum storage facility with an HVAC control system would be 44 kWh/m^2 and a poor electricity consumption would be 120 kWh/m^2 (Moore, 2013). Basing costs on an average electricity tariff of £0.13/kWh, he calculated that annual electricity costs of a conventional museum store would be in the range of £5.72/m^2 to £15.60/m^2.

Reducing energy consumption through building design and operational changes not only saves money but also reduces the associated fossil fuel emissions and mitigates climate change. Fossil fuels (coal, oil and natural gas) emit from 0.056 kgCO_2/kWh to 1.133 kgCO_2/kWh whereas renewables (solar PV, biomass, water, wind) and nuclear emit an average of 0.005 kgCO_2/kWh (World Nuclear Association, 2011). While CO_2 emissions in the UK have declined by approximately 38% since 1990, due to a greater proportion of electricity being generated from natural gas and renewables than from fossil fuels and a reduced industry demand, further reductions will continue to be required in order to meet the UK's climate goals and net-zero emissions in line with the 2016 Paris Agreement to combat climate change (McLaren, 2019).

Greenhouse gases (GHGs) emitted from refrigerants used in HVAC systems have contributed both to the depletion of the ozone layer and to global warming. The Montreal Protocol (1987) brought in the ban of chlorofluorocarbons (CFCs) and hydrochlorofluorocarbons (HCFCs) in order to protect the ozone layer. The Kyoto Protocol (effective 2005) brought in reduction targets for the refrigerant gases CO_2, N_2O, CH_4, HFCs and perfluorocarbons (PFCs). In 2016, the Kigali amendment to the Montreal Protocol was adopted to phase down the production and use of hydrofluorocarbons (HFCs), as they contribute to global warming although not to

ozone layer depletion. A second commitment of the Kyoto Protocol (Doha Amendment 2012) was made to further reduce GHGs by 18% by 2020 but Low Globe-Warming Potential (LGWP) alternative refrigerants such as hydrocarbons (HCs), hydrofluoroolefins (HFOs), ammonia and CO_2 have issues of flammability, toxicity or high energy use in production. The high costs for conversion of existing systems as well as the stockpiling of HFCs from 2014 has reduced the progress of transition to GWP refrigerants (House of Commons, 2018).

Sustainability of RH control through full HVAC system operation requires a fully reliable and functional system at all times (Myrefelt, 2004). If a system is not robust enough to function with minimal maintenance or capable of operating during maintenance or if remedial work is delayed or takes long periods of time to complete, it will not maintain the required environmental conditions. The more complex the total system, the lower the reliability as the potential for component failure is greater. The availability of the system to control the environment is reduced with less knowledgeable and experienced maintenance staff, as repairs may exceed allowable periods of time. Operational variables such as supply air temperature, air flow rate and the set points of the heating system also affect the functional availability of the system (Neuhaus & Schellen, 2007).

According to Neuhaus (2012), the most common HVAC malfunctions which cause disruption in RH control are ineffective system monitoring, lack of redundancy or duplication of critical and failure-prone components, failure to seasonally adjust temperature and RH set-points, scheduling maintenance during high demand seasons and defective room and/or control sensors. A failure of system design for creating stable climate conditions throughout a storeroom comes from control sensors being placed in the return air duct and not in the storeroom. While HCFC systems can be run using HFCs, they cannot be run using LGWP refrigerants without extensive conversion. Lack of planning for a conversion project or improper conversion will also result in failure of the HVAC system to control RH.

While full HVAC systems were still considered essential by many to maintain institutionally specified RH levels for collections despite growing energy costs and recognition of system failures, passive and low energy control measures were beginning to be explored by the latter part of the 20th century. The impetus came from:

> *"…the growing scepticism of museum conservators as well as museum and archive managers towards the traditional solution of complete climate control"* (Christoffersen, 1993, p.603).

The 2014 IIC & ICOM-CC declaration on environmental guidelines noted that:

- *"The issue of museum sustainability is much broader than the discussion on environmental standards, and needs to be a key underlying criterion of future principles.*
- *Museums and collecting institutions should seek to reduce their carbon footprint and environmental impact to mitigate climate change, by reducing their energy use and examining alternative renewable energy sources.*

- *Care of collections should be achieved in a way that does not assume air conditioning (HVAC). Passive methods, simple technology that is easy to maintain, air circulation and lower energy solutions should be considered."* (IIC & ICOM-CC, 2014)

2.4.1 Applying seasonal adjustment to control mechanisms

Gradual seasonal adjustment of RH was considered permissible by Buck (1964) who identified the ability of hygroscopic materials to adjust to changes in moisture content without damage as long as plastic limits were not exceeded. In his opinion, it was safe to allow a 10% RH rise above an ideal specification of 55% RH in the summer and a 10% RH drop below 55% RH in the winter, along with a corresponding rise or drop in temperature, in order to reduce the load on air conditioning systems and cut costs of equipment and maintenance. Macleod (1975) and Kerschner (1991) both suggested a low set-point of 35% RH if the outside temperature was below 0°F (-18°C). Conservators in Ontario (Royal Ontario Museum, 1978) gave a set point of 25% RH when heating to 21°C in the winter. Wilson (1995) included a table on the use of *'seasonal drift'* to protect a building and its contents which gave an allowable fluctuation of 3% RH and 3°F per month, from a low of 35% RH in January and February to a high of 50% RH in July and August for poorly-insulated buildings, since:

> *"the environments of buildings with thermal weaknesses may be allowed to drift (change slowly) to coincide with the changes of the seasons."* (Wilson, 1995, p.15)

CCI suggested a transition of no more than 5% RH per month from a low of 35% RH in the winter to a high of 58% RH in the summer, with a permitted daily fluctuation of no more than 5% RH as well, in an air-conditioned building where paintings were stored (CCI, 1993).

Seasonal drift as a method to mitigate deterioration by incorrect RH began to be used in historic house museums in North America and the United Kingdom as the environmental guidance for preserving the collections was identified as being at odds with the necessary conditions for preserving the buildings (Kerschner, 1991). Even if full air conditioning systems could be installed without damaging historic fabric, maintaining RH levels around 50% throughout the winter could result in serious building damage due to condensation within the building structure. Practical climate control measures included dropping internal temperatures through the autumn to winter then gradually increasing it from spring into summer, allowing the RH to drift within an acceptable range, generally 40% RH to 60% RH (Padfield et al., 2017). RH fluctuations could be moderated and RH levels reduced or raised to specified ranges in individual storage and exhibit spaces by localised heating or humidification/dehumidification.

In addition to preventing deterioration to building structure, seasonal drift along with dehumidification was found to reduce energy use and costs. The National Trust (UK) concluded that dehumidification used one-fifth of the energy for the same measure of RH reduction using heating (Staniforth & Hayes, 1987). As overall dehumidification in leaky buildings was less effective in controlling RH, in 1987 the National Trust began

experimenting with low level heating to see if RH could be maintained between 50% RH to 65% RH in historic houses by raising internal temperatures five degrees above external average conditions (Staniforth et al., 1994). The term *'conservation heating'* was introduced to describe using a humidistat to control the heating system (Staniforth, 2008). High RH was prevented by operating the heating system and low RH avoided by limiting the heating to a lower temperature set-point. While conservation heating could maintain RH levels suitable for the preservation of cultural heritage collections and reduce energy use, the strategy affected occupant thermal comfort as heating levels might need to be raised during the summer and lowered in the winter (Neuhaus & Schellen, 2007). By increasing the hygrothermal buffering capacity of the store and reducing the ventilation, Padfield et al. (2007) thought it possible to improve thermal comfort while still maintaining a constant RH using conservation heating. Ryhl-Svendsen et al. (2010) found that dehumidification in hygrothermally buffered airtight stores could maintain a stable RH at temperatures between 10°C to 15°C whereas conservation heating needed to operate between 15°C to 25°C, making dehumidification the better choice for energy savings. Temperature however, could have an effect on the operation of the dehumidifier with compressor dehumidifiers functioning less well than desiccant dehumidifiers at temperatures under 15°C, since the compressor could potentially ice up (Michael, 2013). Drainage could also affect the efficiency of the dehumidifier to control RH levels, with continuous drainage preferable as a full water collection tank would stop the unit from functioning.

Analysis into the mechanical properties and dimensional responses of historic wooden objects under cyclic humidity variations (Vici et al., 2006; Bratasz et al., 2007; Kozłowski, 2007; Jakieła et al., 2008) continued in order to predict a target band of tolerable RH fluctuations around a defined seasonal value. Results from modelling indicated that fluctuations centred around a yearly average RH were less damaging than those at seasonal extremes and that fluctuations of short duration, less than 24 hours, within the average band caused no evident deterioration. Modelling of wooden panel supports indicated that even thin (10 mm) panels were able to tolerate RH fluctuations in excess of 20% with a duration of less than 24 hours (Łukomski, 2012) with lower temperatures reducing moisture diffusion coefficients, increasing response time. Michalski (2007) labelled a similar predictive approach "*proofed RH*" where he assumed that, as long as future climate conditions did not exceed those to which an object had been exposed in the past, the risk of mechanical damage beyond that already accumulated would be almost negligible. This approach enabled him to develop risk models to find the point of minimum total risk of all environmental factors on cultural heritage collections, enabling an evaluation of mitigation methods and costs against the perceived loss of value.

2.4.2 Applying operational strategies for low energy RH control

Altering operational schedules of HVAC systems has been used as a strategy to reduce energy consumption while still controlling RH levels and fluctuations to acceptable levels in storage. A four-year experiment on the impact of HVAC shut-downs on storage environments was undertaken by the IPI and an energy consulting firm (Linden, 2014). While impact varied depending on geographic location and building structure, the research indicated that HVAC systems did not have to be run continuously in order to provide desired RH ranges and that a systematic shut-down

programme could provide significant energy savings and operational costs without affecting cultural collections.

In 2010, a number of different building management strategies for the National Archives storage facility at Kew were simulated in order to identify potential energy cost reduction strategies and potential impact of climate change (Hong et al., 2012). A week-end shut-down of the HVAC system, the running of which accounted for 70% of the repository's total annual energy load, was shown to potentially reduce the energy load by 14%. By combining the shut-down with seasonally- adjusted thermostat and humidistat set-points, RH 35% to 55% from February to September then back to 35% by December, it was estimated that the energy load could be reduced by 43% but still ensure an acceptable and slightly improved control of RH, due to a reduced seasonal variation. Projected climate change was found to have no impact on the store's environmental conditions but the energy load was predicted to increase due to increased cooling needs. Part-time operation with seasonal adjustment was implemented and, after three years of operation, the revised schedule surpassed the target of a 25% reduction in CO_2 emission reductions (Ntanos, 2014).

Implementing HVAC operational strategies to reduce energy consumption requires the HVAC system to be designed, controlled and maintained properly. As Myrefelt (2004) pointed out, the more complex the system, the less reliable the environmental control provided by that system. A malfunction in any part of the system can have consequences if it is not detected and remedied in an allowable period of time. Climate change could also increase the energy demand if cooling demands have to rise in order to maintain current RH guidelines (Hong et al., 2012).

2.4.3 Applying design and materials in low energy RH control strategies

Museum galleries need to accommodate both the requirements of the collections and the needs of people, regulating the internal environment not only to prevent accelerated deterioration of materials but also to provide thermal comfort and air quality for people. Museum storage buildings generally do not have to balance the environmental needs of both collections and people as there is reduced access and activity, unless there is some form of public access programme. Using design and materials as a way to reduce the reliance on mechanical plant in storage buildings can be a cost-effective way to provide sustainable solutions for maintaining suitable levels and fluctuations of RH while still preserving the greater proportion of museum collections.

Thermal mass and thermal insulation can be used to reduce the energy consumption needed to heat and cool buildings. Thermal mass, the ability of a material to store heat, depends on the density, specific heat capacity and thermal conductivity of that material. As thermal mass buffers by storing or releasing heat, the internal temperature rises and falls less rapidly than the external temperature, reducing the need for heating or cooling. This reduces energy demand and CO_2 emissions (Fraser, 2009). Heavy-weight conventional construction materials, such as concrete, stone and brick, provide thermal inertia through high specific heat capacity along with moderate thermal conductivity (Greenspec, 2019a). The stored heat requires adequate ventilation in order to prevent a buildup of heat during summer months

(Fraser, 2009) but sudden influxes of external air combined with the thermal inertia of the building will destabilise internal RH through the differences between internal and external temperatures (Padfield, 2008). Thermal insulation reduces the flow of heat through the building envelope, minimising the energy consumption needed to maintain the internal temperature. A good insulator has a high specific heat capacity as well as low thermal conductivity, contributing to thermal buffering (Greenspec, 2019). Continuity of insulation eliminates the cold spots caused by a thermal bridge, an area that allows loss of heat from inside to outside, which can lead to surface condensation, damp and mould (Carbon Trust, 2018). Thermal buffering requires the addition of moisture buffering, either by the construction materials or by the contents of the building such as a mass quantity of paper, along with airtightness and reduced ventilation in order to effectively contribute to passive control of moisture content (Padfield, 2008).

The energy efficiency now required by many building regulations is often achieved by reducing the air permeability of the building envelope. In the UK, *Approved Document Part L2A 2006 Building Regulations* allows a maximum air permeability of 10.0 $m^3/(h{\cdot}m^2)$ @ 50 Pa. The Airtightness Testing & Measurement Association (ATTMA, 2010) benchmarked best and normal practice for museum and archival stores at 1.0 and 1.5 $m^3/(h{\cdot}m^2)$ @ 50 Pa. The costs of achieving high airtightness may be affected by the complexity of building design as well as by building materials, competency of construction and testing schedules (de Selincourt, 2013; Bomberg et al., 2016). Airtightness reduces unwanted air leakage through the building envelope and is provided by a continuous air barrier formed from a set of construction materials excluding the insulation (Burrell, 2015). Design and construction must minimise penetrations, eliminate gaps and use appropriate robust and durable materials in order to reduce heat loss by up to 10% (Kraus & Kubečková, 2014). Airtightness can prevent moisture moving into the building envelope as barriers are placed on the warm side of insulation, ie.the interior in the case of cold climates, but can also trap moisture (Bomberg et al., 2016). If inadequate provision is made for return air, internal areas can become depressurised, with moist air being drawn into the building envelope, resulting in damage from interstitial condensation and mould growth (Larsson et al., 2007). Moist air can also be drawn in through leaks in the airtight barrier by internal positive pressure, leading to mould growth on interior walls and elevated RH levels (Bomberg et al., 2016).

If ventilation rates are also reduced in order to achieve a stable RH, the use of vapour permeable and hygroscopic materials to provide airtightness can help to reduce the effects of high RH (May, 2005). Vapour permeability is related to the pore structure of the material and the size and weight of the water vapour molecule. A vapour permeable airtight layer such as a breather membrane will allow excess moisture to be transported away from internal areas if the internal vapour pressure is higher than the external vapour pressure (May, 2005). Used outside the insulation layer, it reduces the amount of sealing to all penetrations, is potentially easier and more robustly installed and can act as secondary weather protection (Proctor, 2016). Hygroscopic capacity is also related to the material's porous structure, volume and size as well as its equilibrium moisture content (EMC). According to May, hygroscopic materials can stabilise internal RH, reduce surface condensation and potentially absorb moisture interstitially. The buffering action of hygroscopic building materials requires controlled low ventilation and increased airtightness in the building

envelope in order to be effective (Padfield, 2008). A description of the theory of RH control by hygroscopic capability is presented in Chapter 3, Section 3.2.

In 1971, the Municipal Archive (Stadtarchiv) of Cologne in 1971 was designed to replicate the conditions in the basement under Cologne Cathedral where the archival materials, stored for several centuries in a non-mechanically ventilated or air-conditioned environment, had survived in good condition. The municipal archive building's internal environment was thermally buffered by massive masonry walls with an air gap between them and the building's granite facade. The RH was buffered by the mass of archival material (Larsen et al., 2014). Despite the walls providing adequate thermal buffering, heating and natural ventilation affected the building's energy consumption (Christoffersen, 1995). The Repository at the Regional Archive of Schleswig-Holstein was a modification of the Cologne Archive. Built in 1991, it had massive brickwork, mineral wool insulation and an air gap between wall and brickwork façade. Both the ventilation rate and heating were kept at low levels to maintain the RH and staff activity was limited to reduce energy usage, ventilation needs and overheating from lighting. The RH was intended to drift from 40% to 60% and subsequent monitoring showed effective buffering from the building mass and the hygroscopic archival material (Christoffersen, 1995).

With a design based in part on the Cologne Municipal Archive, the Suffolk Record Office in Ipswich was intended to have both low energy and passive RH control. Built in 1990, it was a heavily thermally buffered two storey concrete frame building, with double cavity brick walls with insulation and airbrick layers and with narrow recessed windows. The building was heated to 14°C in the winter and the buffering afforded by the archival contents was intended to stablise the RH within 55% RH ±5% RH throughout the year (Padfield et al., 2013). The building failed to achieve a stable lower temperature revision and various modifications were undertaken, including installing an air conditioning plant, blocking and insulating fire doors and windows and removing the hot water pipes originally installed to provide winter heating. The air conditioning improved the stability of the temperature but the amount of fresh air and air circulation introduced during the summer as well as the rate of air infiltration through the building's structure increased the level and instability of the RH (NCS Suffolk, 2017).

At the National Museum of Denmark , Padfield and Jensen (1990) analysed various methods of RH control in museum stores, including stored objects in calculations of heat and moisture variation, while planning new low energy museum storage facilities. Their modelling predicted that an air-tight room filled with hygroscopic materials could not be controlled to a constant RH through heating as an increased room temperature would lead to moisture being released from the stored objects in the process known as thermal diffusion or thermodiffusion. Despite their conclusions, the new store at Ørholm, built in 1991 with walls of expanded concrete block with lime wash coating, insulation and black-painted tongue and groove timber cladding and a roof of gypsum board, insulation and black asphalt paper on a base of uninsulated concrete and compressed gravel, was provided with heating to control RH. A dehumidifier had to be installed in order to stabilise the RH. When the dehumidifier broke down, Padfield and Jensen's prediction of rising internal RH with rising external temperature was confirmed by the environmental data. Padfield (1996) attributed the phenomenon to the warming of the concrete block by solar radiation on

the black cladding, with water evaporating from the concrete into the store and being adsorbed by the hygroscopic contents rather than being vented outside.

In Copenhagen, a small archival store was constructed in 2003 within the university's new Humanities building in order to house the Arnamagaean Institute's collection of manuscripts. The storage space, on the second floor, was thermally buffered by an additional concrete shell and outside and inside layers of insulation, with the inside layer thicker in order to maintain a lower temperature range. The walls inside the store were lined with 50 mm of porous lime silicate blocks to buffer RH fluctuations. Internal RH could be controlled by introducing external air with the desired moisture content or, in the winter, from heat leaking in from the office spaces, with RH inertia from the hygroscopic contents providing shoulder seasonal passive control (Padfield & Larsen, 2005). The RH varied between 50% and 57% with the temperature cycling between 16°C to 22°C (Padfield, 2008) once deviations from the original specifications, including painting the silicate brick with two coats of acrylic paint, had been rectified.

A highly-insulated storage building intended to provide full passive control of RH was completed at Vejle, Denmark, in 2003. Thermal inertia was provided by thick walls, mineral wool insulation and an uninsulated but waterproofed concrete floor sitting on drainage. Hygric inertia was provided by the lightweight concrete construction of the thick walls. The design anticipated that after a few years, once the moisture content of the fresh concrete had been reduced, passive controls would eliminate the need for dehumidification. However, the yearly average internal RH remained unacceptably high, requiring a continuing need for dehumidification. Further investigation concluded that fully passive conditioning was impossible in Denmark's climate as, without interior heat or moisture gain, interior average temperature and vapour pressure would equilibrate with the external environment (Christensen & Janssen, 2011; Janssen & Christensen, 2013). An extension to the storage building was planned in 2009 with *'passive air conditioning'* (Christensen et al., 2016) incorporating thermal insulation, an extremely airtight building envelope and an uninsulated floor as well as concentrated dehumidification to keep the RH close to 50% at a temperature below 18°C. Dehumidifiers were run at night, two in the extension for three hours and two in the older building for six hours, and this was found sufficient to maintain a stable RH throughout the remainder of the day. Due to the night-time overproduction of electricity from the wind turbines, which provided the building's energy, the building's operation was considered to be virtually carbon neutral (Christensen et al., 2016).

A storage building at Ribe, in use from 2007, was constructed with 740 mm thick walls formed of layers of brick and concrete with mineral wool insulation in between, all separated by small air gaps. There was mineral wool insulation installed in the roof but not under the concrete floor so as to use the ground's thermal buffering ability. The building was virtually airtight with a low air change rate, about 0.7 air changes/day. Heating was limited to the offices, with some leakage into the storage area (Ryhl-Svendsen et al., 2011). Dehumidification was required in summer to reduce the high RH caused by the low internal temperature. No deliberate buffering was included which would have reduced the need for dehumidification but not necessarily influenced the RH fluctuations which were already minimal due both to

the annual temperature cycle having a smaller average value than one produced by conservation heating and to the low ventilation (Ryhl-Svendsen et al., 2011).

At Randers, a storage facility was constructed in 2007 with walls of pre-cast concrete walls, mineral wool insulation and steel cladding, roof of metal deck, mineral wool insulation and bitumen roofing, and an uninsulated concrete floor. It also relied on dehumidification to maintain RH levels although indirect heating from adjacent staff areas and from the desiccant dehumidifiers helped in reducing the RH. In order to decrease the number of short-term fluctuations produced by the activation of the dehumidifier, the set-point for the basic storage area was raised to 55% RH from 50% RH. Mechanical intake of external air was eliminated in 2009 (Ryhl-Svendsen et al., 2012).

A comparison of the energy used to maintain an RH in the range 55% ±5% showed that the stores with high thermal insulation, low air changes and dehumidification (Velje, Ribe and Randers) performed better than the thermally inert, insulated, ventilated and passively-heated Arnamagnaean store (Ryhl-Svendsen, 2012). However, the Randers store performed no better than the partly underground airtight solid concrete bunker used for storage by the Royal Danish Arsenal Museum, which relied on thermal mass and dehumidification to maintain RH levels around 50%. The results confirmed the theory that a one-storey well-insulated lightweight building with an uninsulated floor would be as thermally-stable as a more heavily built one. The control of RH by dehumidification would be enhanced by adding humidity buffering to the interior wall cladding and improving airtightness (Larsen et al., 2014).

Reduction of ventilation was found by Ryhl-Svendsen et al. (2010) to not just reduce energy consumption but also reduce RH fluctuations. However, while a low air change rate would reduce the concentration of external air pollutants such as ozone, it would allow the accumulation over time of internal air pollutuants such as organic acids and hydrogen sulphide, which can be emitted not only from building materials and building systems (Seppänen, 2002) but also from cultural heritage collections (Ryhl-Svendsen & Clausen, 2009). Ryhl-Svendsen and Clausen's investigation into potential mitigation methods found that the most effective way to avoid high pollution levels was a combination of low air change rates and internal recirculation with adequate filtration. Larsen et al. (2014) found that, in a building with an air change rate of less than one per day, infiltration of air pollutants was reduced by the building fabric. They advised that internal pollutants could be restricted by using inert construction and storage furniture materials and finishes and by air recirculation through carbon filters.

Modifications to existing buildings to provide passive moderation of RH through environmental buffer zones were suggested by Bordass (Bordass, 1996). Buffer zones through building layout, with storage areas placed centrally and offices and circulation routes around the edge, would reduce proximity to external walls. Access doors should be insulated and as airtight as possible. Other buffer zones could be provided by creating a roof cavity or through the use of containers such as polythene tents, portacabins and conventional plasterboard or blockwork structures. In his guide to the use of industrial buildings for museum storage, Bordass also recommended methods for upgrading function and performance and for reducing operational costs while noting that alterations and upgrading might be less cost-

effective than rebuilding if construction elements were difficult to modify or access for services constrained.

A thermal buffer zone was created through the design of the Library & Archives Canada Preservation Centre, which opened in 1997 in Gatineau, Québèc. In order to reduce the energy required to maintain specific environmental zones within 48 storage vaults, it was designed as a building-within-a-building, with an outer shell of glass and steel creating an environmental buffer zone for the interior reinforced concrete vaults. Each vault was supplied by one of two different air systems which delivered a specific humidity range depending on the materials stored within. Each vault also had its own heating coil and humidifier in order to precisely adjust internal conditions. Humidity from the glass-enclosed galleria was buffered by the 300 mm thick concrete slabs, with additional insulation and vapour barriers added for those vaults where the required conditions were -18°C and 20% RH (Heissler, 1998).

2.4.4 Applying the buffering potential of hygroscopic building materials in low energy RH control strategies

The use of hygroscopic materials, either building contents or building materials, to buffer RH in museum stores has been explored by researchers, particularly from the National Museum and Technical University of Denmark who have studied the potential of full passive conditioning in museum stores. Padfield and Jensen (1990) modelled various methods of air conditioning in a museum store filled with hygroscopic objects to devise control strategies which took into account the buffering capacity of the store's contents. Christoffersen (1995) and his colleagues modelled the interactions between outside and inside climate, physical qualities of the building and the objects stored within to develop concepts for natural climate control. Further investigation by Padfield et al. (2007) led them to consider that passive climate control of storerooms was possible but not so much through the use of hygroscopic contents as through the use of absorbent walls with a high exposed surface area, as moisture diffused too slowly and only to a limited (10 mm) depth into absorbent materials. They concluded that the principle reason passive RH control was not yet being applied in museum storage was due to the lack of quantitative experiments on exposed hygroscopic wall surfaces.

In a continuing program of the Research, Analysis and Consulting group in the Conservation Department of the National Museum of Denmark, performance of both modelled and actual stores were evaluated using climate data from Danish churches built of calcareous tufa or porous medieval brick, with limewash surface treatments (Eshøj & Padfield, 1993; Padfield et al., 1994; Larsen, 2004). The data, which indicated good moisture buffering capability of porous hygroscopic walls, prompted evaluation of construction materials for museum buildings:

> *"The RH stabilisation provided by porous walls can surely be used in museum architecture."* (Eshøj & Padfield, 1993, p.608)

Padfield (1998) evaluated various construction materials for their RH buffering capability in museum buildings, including end grain wood, unfired clay brick, fired brick, unbaked clay tile, cellular concrete, wood planks, wool insulation, gypsum board and lime plaster. He concluded that the best buffer materials were wood and

clay but that neither was effective in their usual form. His experimental tile, bentonite clay mixed with perlite, showed the best overall performance but was very dusty and required a surface finish. He recommended porous lime painting, a traditional finish generally confined to churches in northern Europe. His experimental tile was never commerically produced.

Padfield and Jensen (2009; 2010; 2011) undertook analysis of the sorption properties of commonly available building materials in order to describe moisture buffering capacity, proposing a measure of buffer performance called the *Buf (B).* They claimed an indicator of good moisture buffering capacity was *"complicated labyrinthine geometries"* or an interconnected and varied porous structure. They evaluated unfired massive and perforated clay brick, fired perforated clay brick, end grain wood and a porous calcium-aluminium-silicate block (also referred to as cellular concrete) and concluded that unfired perforated clay brick had the best buffer performance. The actual buffer performance was cut by one-half when coated to reduce the brick's dustiness but they concluded that there was still capability to provide sufficient RH buffering, reducing reliance on mechanical dehumidification in museum stores. Cellular concrete was assessed as a poor buffer although it performed better than fired brick. Other very porous but less readily obtainable materials were considered for their buffer potential but were not evaluated for buffering capacity, including clay-rich diatomaceous earth, cement bonded earth bricks, cement bonded wood chip boards, compressed wood chip boards and a lime-sand mixture filled with hemp fragments.

A *Moisture Buffer Value (MBV)*, a number which could indicate the rate and amount of moisture flowing between a construction material and its surrounding climate under changes of humidity, and a test method, to determine the moisture buffer performance of the material, were the aims of the NORDTEST project (Rode et al., 2004; Rode, 2005; Rode et al., 2006; 2007). Round Robin tests were carried out during the project on a number of porous, absorbent conventional construction materials in climate chambers under diurnal cycles of high and low RH. MBVs were found for concrete, brick, lightweight aggregate concrete with stucco, cellular concrete, gypsum, laminated and varnished wood, birch panels and spruce boards. Untreated spruce and birch boards and cellular concrete performed best as buffers, with concrete and brick performing less than half as well (Rode et al., 2006). The practical buffering performance of each material on fluctuations of RH would be affected by the exposure area of the surface materials, the ventilation rate, the vapour content of both indoor and outdoor air, the surface temperature and the surface moisture transfer coefficients of the surfaces (Rode, 2005). A more detailed description of moisture buffering capacity and determination of moisture buffer values is found in Chapter 3 of this thesis.

PD 5454:2012 (BSI, 2012a) recomended a selection of hygroscopic building materials to be used for museum and archival storage in order to reduce the energy use required to stabilise internal conditions:

> *"Walls, floors and ceilings inside the repository should be made of a material such as dust-sealed concrete block or unfired brick, or from combinations of materials that have a high thermal and hygroscopic capacity, with insulation materials appropriate to the system of construction selected. Internal finishes*

should not impede the function of the thermal and hygroscopic capacity of the building to stabilize conditions." (PD 5454:2012b, p.35)

2.4.5 Assessing the buffering potential of a non-conventional very hygroscopic building material

Through the literature review on the development of museum RH guidelines and the attempts to regulate RH to those guidelines, the application of hygroscopic building materials to buffer RH in museum storage to current guidelines has been limited to conventional materials. The following key gaps in knowledge are identified:

- There is a lack of data on the augmentation of RH buffering in dynamic museum storage through the incorporation of non-conventional very hygroscopic building materials

- There is a lack of data on the extent to which energy use and costs are reduced when RH regulation is augmented by incorporating a very hygroscopic building material

- There is a lack of data on the relationship between moisture storage and buffering capability of a very hygroscopic building material under dynamic operation

This thesis will attempt to fill the key knowledge gaps identified in the literature review with a case study of a museum storage building constucted using a non-conventional very hygroscopic building material, hemp lime concrete.

In 2010 this researcher, while employed at the Science Museum, attended a workshop on low energy museum storage led by Padfield and colleagues at the National Museum of Denmark. Knowledge gained from the workshop was used by the museum in selecting a very hygroscopic material to be included in the construction of a new storage facility for cultural heritage collections that required stable RH levels. The building had to meet institutional directives for sustainability and reduced energy consumption (Moore, 2013). Based on initial results from studies on the hygrothermal performance of hemp lime concrete (HLC) carried out at the University of Bath on an experimental building (University of Bath, 2010) and from a case study of a brewery distribution warehouse (Betts, 2010), the museum sought construction proposals incorporating HLC. The principle factors influencing the choice of material were the hygrothermal performance and the construction technique, promoting good airtightness and minimal thermal bridging in the building envelope as described by Bevan & Woolley (2008). HLC's renewable low carbon credentials were considered valuable contributors to the sustainability of the museum's built environment (Moore, 2013) with the research indicating that HLC significantly reduced the environmental impact of construction despite the need for lime binder and substantial amounts of water due to renewability, CO_2 sequestration, replacement of high environmental impact construction materials and a hygrothermal performance which could lower energy consumption during occupation (Sutton et al., 2011).

Industrial hemp is a fast-growing natural renewable material that requires little irrigation, fertilisation or pest control. The stalk or shiv, formerly considered a waste by-product, has found a use as a natural aggregate to provide a lightweight concrete building material when mixed with lime-based binders (Bevan & Woolley, 2008). As hemp grows, it sequesters atmospheric CO_2 through photosynthesis and, when used with a lime binder as HLC, locks up the CO_2 for the lifetime of the building (Shea et al., 2012). According to Bevan and Woolley (2008), the construction technique of casting or spraying HLC around timber frames produces not only a strong and solid composite weatherproof mass providing thermal insulation and thermal storage but also simplifies construction methods and costs by reducing the need for additional layers of insulation, breather membranes and external cladding. The solid walls promote good airtightness by minimising thermal bridging and air leakage (Lawrence et al., 2012). Airtightness was tested around 2 $m^3/(h{\cdot}m^2)$ @ 50 Pa without the need for additional layers (Bevan & Woolley, 2008). The pore structure of the matrix and pore connectivity of the shiv increase the effective thermal mass as well as providing a hygric buffer through absorption/desorption characteristics which produce thermal effects through responses to changes in RH and vapour pressure gradients (Lawrence et al., 2013). The material's high vapour permeability reduces potential moisture build-up and mould growth, with the alkalinity of the lime binder also limiting mould growth (BRE, 2011). Specific material and hygrothermal properties of HLC is to be found in Chapter 3 of this thesis, in a literature review of the pertinent research.

The initial proposal considered by the Science Museum in 2011 was developed in a collaborative process with partners from Lime Technology Ltd., an HLC manufacturer and constructor, and Emission Zero LLP, a building performance research and design practice, with academic input on RH buffering by hygroscopic materials from the BRE Centre for Innovative Construction Materials at the University of Bath (Eberlin & Carter, 2011). The proposal included using pre-dried HLC panels wherever possible in order to buffer RH and temperature, reduce energy requirements and increase the use of a sustainable low-embodied carbon material (Eberlin & Carter, 2011). Walls were to have a U-value of 0.22 $W/m^2{\cdot}K$ with the roof having a U-value of 0.15 $W/m^2{\cdot}K$. Thermal modelling was undertaken to design low energy temperature control in the range 13°C to 16°C ±1°C. Empirical data from a variety of sources (Lime Technology Office, Oxford; Renewable House, BRE; Hempod, Bath University) was used to predict that the RH would meet the range 45% RH to 60% RH ±5% RH, with a slow rate of change, using the passive performance of the building. The aim was to produce a building which operated at half the energy consumption of a conventional museum storage facility of the same size rather than a building which would maintain its environment entirely by passive means, so a mechanical ventilation with heat recovery (MVHR) system was proposed to ensure a stable RH. The modelled energy use of the system was 15 $kW/m^2/yr$. An energy cost of £1,176/yr, based on £0.08/kW, was predicted for a 980 m^2, six room, three storey facility with an air permability of 1.0 $m^3/(h{\cdot}m^2)$ @ 50 Pa.

Construction costs for the building, including a provisional cost for the design and installation of the M&E system, were contracted at £885,019 in February, 2012 (Pritchett, 2012). The overall costs of construction were anticipated by the Science Museum to be around 10% higher than that of a traditionally constructed museum store. Based on the Glasgow Museums costs for the Kelvingrove extension (Merriman, 2008), it was estimated that a conventional museum storage building

would cost £1000/m^2. As higher costs were also expected as a result of the building specification for long-term low operational costs, the project was budgeted at 14% over costs for a conventional build (Moore, 2013). The overall spend for the Hempcrete Museum Store (HMS) project was, in the end, 15% higher than the estimated overall cost of a conventional museum storage building, at £1,152.75/m^2. Total construction costs as quoted by Moore, excluding the M&E, were £980,058 or £1000/m^2, with 12% (£118,000) being the cost of the HLC panels. A breakdown of construction costs based on the final budget and valuation will be found in Chapter 4, Section 4.4.1.

Redesign of the M&E system contributed to the increase to the capital costs of the project (Chambers, 2012). During the design phase, the proposed M&E system was altered to control RH and temperature to very tight specifications through cooling, dehumidification, heating and ventilation (Jankovic, 2012b). This compromised the original intent of the building design as well as affecting the costs. Further modelling was undertaken incorporating the buffering potential of the HLC walls. This reduced the design of the M&E to two air handling units for heating and for circulation of cool nighttime or warm daytime air in order to use external temperature and/or moisture content to manage humidity levels to the revised specifications, which allowed a gentle drift within set parameters of 50% RH ±5% RH (Moore, 2013). Final costs of the system including design and install were £111,222.83, an uplift of 35% on the original cost. The remodeled system had a revised energy requirement of 28 kW/m^2/yr which was still considered to minimse long-term operational costs, estimated by Moore (2013) to be a 46% decrease on the best running consumption of a conventional museum store. Capital costs of the M&E system are found in Chapter 4, Section 4.4.1, details of the air handling system design and subsequent operation in Chapters 5 and 6 and operational expenditure in Chapter 7.

The HMS was constructed within another building on the SMG storage site near Swindon, Wiltshire, in 2012. Full details of the design and construction of the store will be found in Chapter 4. As using the passive performance of the building envelope to assist in the regulation of RH and temperature was considered by the contractors to carry some risk, they undertook monitoring of the building environment from completion in May 2012, through the transient state and into the first year of steady state operation (Jankovic, 2012). Routine RH and temperature monitoring was also undertaken by the museum's conservation team when the museum's telemetric environmental monitoring system was installed in the HMS in July 2012.

Through the course of this investigation, this researcher has accessed and analysed data acquired from the museum's environmental monitoring system. The system was expanded during the course of this study to include moisture content and air velocity as well as RH and temperature monitoring. The data acquired during the case study has been used to attempt to fill the key knowledge gaps identified from the literature review in order to validate the techno-economic viability of HLC construction to augment RH control in a low energy museum storage building.

2.6 Summary of the literature review on the effects of RH on museum collections

The risks to museum collections through incorrect RH in storage are assessed through a comprehensive review of historic and current literature, from the earliest published discussion of the problem to current recommendations and solutions for RH control. The sequences of RH guidelines developed by researchers over past decades are critically reviewed and guideline ambiguities are highlighted in order to clarify past and current approaches to controlling RH in museum storage.

Key objectives were to review the potential risks through incorrect RH levels and fluctuations, analyse the historical development of RH guidelines for the storage of museum collections and clarify causes and consequences of ambiguity, and evaluate the museum drivers for sustainability. Published RH recommendations, guidelines and standards for museum storage buildings revealed inconsistent recommendations from decade to decade from the beginning of the twentieth century through to the twenty-first and was demonstrated graphically. The influence of mechanical systems of heating, ventilation and air conditioning on the development of recommendations for ranges and fluctuations of RH in museum storage was evaluated to show that recommendations reflected the effectiveness of mechanical control rather than the requirements of cultural heritage collections. Reliance on mechanical systems resulted in high operational costs and unachievable expectations. Institutional drivers towards sustainability prompted the development of environmental risk management strategies. Studies on the effects of RH on specific cultural heritage collections increasingly demonstrated that there could not be one ‘correct’ standard for the storage of all museum collections. By the end of the twentieth century, wider bands of RH levels and fluctuations were recommended than previously, based on identification of material and condition of cultural heritage collections. Key performance indicator tables for both RH levels and RH fluctuations were developed as a result of the review of the contemporary recommendations in order to clarify the risks to the main classes of materials found in cultural heritage collections.

While conservative museum practice still relied strongly on mechanical systems to achieve these levels, with high financial, environmental and operational costs, by the twenty-first century institutional sustainability directives emphasized low energy and passive RH control measures. While the design of a limited number of low energy museum stores in temperate climates utilised thermal insulation and airtightness, studies showed that the hygroscopic materials had a greater potential to augment RH regulation. The key knowledge gaps preventing the incorporation of very hygroscopic construction materials into low energy museum RH regulation strategies were identified through the literature review. Data from the research case study, the HMS, constructed with a walls of a very hygroscopic building material, HLC, will be used to fill the knowledge gaps in order to validate the techno-economic viability of HLC construction to augment RH control in a low energy museum storage building.

Chapter 3 Theoretical and defined hygroscopic capabilities of HLC: literature review

3.1 Introduction

In this chapter moisture transfer, moisture storage and moisture sorption mechanisms of hygroscopic materials are described in order to explain how a porous construction material might affect the RH of an internal environment. The buffering properties of HLC are compared to an ideal material and to those in current use by a review of the research literature on numerical, simulation and experimental studies pertinant to the potential for HLC's to moderate internal environment. The review identifies the gap in the present knowledge related to the augmentation of RH control by HLC specified for museum storage under dynamic conditions.

Sustainability credentials, including environmental, social and economic, will be reviewed to identify how HLC meets such criteria and where the criteria contribute to current museum directives on low impact construction and low energy operation.

3.2 Theory of RH control by hygroscopic building materials

A hygroscopic material has the ability to take up and release moisture as water vapour to and from the surrounding air. Its sorption behaviour describes the extent of this ability until a state of equilibrium has been reached. Uptake of water vapour is achieved through absorption or adsorption and release of water vapour through desorption mechanisms. A sorption isotherm graphically represents the sorption behaviour of a material, showing equilibrium with the ambient air at a particular temperature. A highly hygroscopic material will show a steep sorption isotherm while a less hygroscopic material will demonstrate a flatter profile.

Water content in strongly hygroscopic materials may vary widely as a consequence of variations in RH. Water may be stored in vapour or liquid form depending on the maximum storage capacity of the material. Storage capacity will affect the material's ability to buffer changes in RH. A hygroscopic material may demonstrate a different water content characteristic under dynamic than under potential conditions. Hygroscopic material property data is obtained experimentally through measurement of the water vapour diffusion at different humidity gradients (Barclay et al., 2014).

RH levels in the internal environment have an effect on human comfort and health (Fang et al., 1998) as well as on the durability of construction materials and preservation of historic materials (Simonson et al., 2004). Levels below 25% RH and above 60% RH can cause respiratory problems, aggravate allergies and affect skin humidity. By maintaining levels around the RH mid-range of 25% to 60%, perceived air quality is deemed acceptable even when control of temperature and ventilation rates are reduced (Osanyintola & Simonson, 2006). Various building materials have been evaluated through experimental, field and modelling studies to determine their potential in moderating indoor RH levels in order to the reduce the energy consumption required for mechanical control. These have included hygroscopic materials such as wood and crop-derived cellulose-based materials as well as

mineral-based construction materials such as concrete, brick and gypsum which are less hygroscopic but have other properties conducive to moisture transfer and absorption (Rode, 2005; Cerolini et al., 2009).

3.2.1 Sorption mechanisms in hygroscopic materials

A water (H_2O) molecule, with the hydrogen (H) end permanently positive and the oxygen (O) end permanently negative, is a polar molecule which is attracted to many other molecules in both liquid and vapour phases. Van der Waals Forces define the attraction of the intermolecular forces between the water and another molecule in the following equation:

$$\boldsymbol{P = \frac{RT}{V_m - b} - \frac{a}{V_m{}^2}} \qquad \text{[equ.3.1]}$$

where,

P = pressure, Pa;
V_m = molar volume, m^3/mol
T = temperature, °K
R = gas constant, J/(kg·K)
a, b = specific gas constants

Where another molecule is also permanently polar, the force is strong and is described as dipole-dipole. A weaker force is formed with molecules that can become polarised by the displacement of electrons and is known as the London Dispersion Force of attraction.

The surfaces of a hydrophilic material capture and physically bind water vapour molecules, forming a film, in a surface phenomenon known as physical adsorption or physisorption. The spontaneous accumulation of the vapour molecules (adsorbate) takes place on a solid surface, usually a porous material with a large specific surface (adsorbent), with the degree of adsorption increasing with decreasing temperature and increasing partial pressure as a function of increasing RH, making the process reversible (Figure 3.1).

A highly hygroscopic material will have extensive connected internal porosity with large areas available for moisture adsorption. Water vapour molecules from the air will be adsorbed on the internal surfaces and the moisture content of the material will rise. Physically adsorbed molecules will form a monolayer on the surface of the adsorbent as the pressure increases, then further increase in pressure will cause the beginning of multilayer coverage. Smaller pores will fill first with further increasing pressure eventually causing complete filling of all accessible pores.

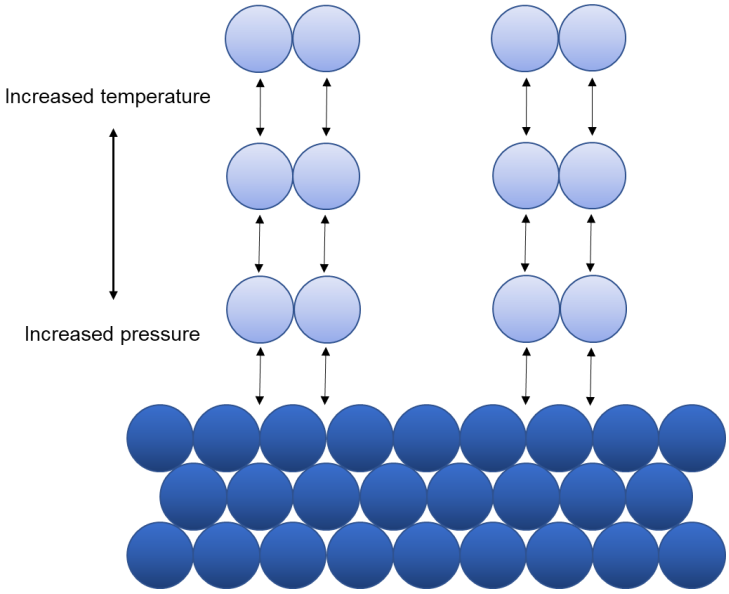

Figure 3.1 Reversible physisorption of molecules under temperature & pressure changes

Dynamic equilibrium is established between the adsorbate and the adsorbent when the same number of molecules undergo adsorption and desorption in the same time period at a constant temperature. The equilibrium process can be written as:

$$\mathbf{A} \leftrightarrow \mathbf{A}_{ads} \qquad \text{[equ.3.2]}$$

where,

A = adsorbate molecule in vapour phase

A_{ads} = adsorbate molecule in adsorbed state

The equilibrium constant of adsorption can be written as:

$$\boldsymbol{K} = \frac{[\mathbf{A}_{ads}]}{[\mathbf{A}]} \qquad \text{[equ.3.3]}$$

where,

K = adsorption equilibrium constant

$[A]$ = bulk concentration of adsorbate molecules in vapour phase

$[A_{ads}]$ = bulk concentration of adsorbate molecules in adsorbed phase

After considerable adsorption of vapour molecules on the adsorbent surface, adsorbent equilibrium is reached. On a homogenous surface, the concentration of adsorbate on the surface layer is constant over the whole surface. At a constant temperature, the equilibrium condition can be expressed by:

$$\boldsymbol{C^s} = \frac{\boldsymbol{Kf}}{\boldsymbol{f^s}}\boldsymbol{C} \qquad \text{[equ.3.4]}$$

where,

C^s = adsorbate concentration on the surface layer

C = vapour concentration

f^s, f = activity coefficients

K = adsorption equilibrium constant

The adsorption isotherm is a graphical representation of the amount of adsorbate adsorbed on an adsorbent as a function of pressure or concentration under isothermal conditions. According to the International Union of Pure and Applied Chemistry (IUPAC) classification, there are six types of isotherm for gas/solid equilibria, which are based on the five types classified by Brunauer in 1945 (Donahue & Aranovich, 1998). These six types of isotherm are characteristic of adsorbents that are microporous, macroporous, mesoporous or non-porous. The IUPAC classification of isotherms show both the adsorption and desorption pathways. Adsorption isotherms can be predicted by diffusion equations based on the kinetic theory of gases and the conservation of mass and energy.

In a Type I adsorption isotherm, after saturation pressure Ps has been reached, adsorption does not occur any further as there are limited numbers of vacancies on the adsorbent surface. At high pressure, all sites are occupied and further increase in pressure does not alter the adsorption process (Figure 3.2). Type 1 adsorption isotherms are used to describe adsorption on microporous adsorbents, that is, a material having pore diameters up to 2 nm.

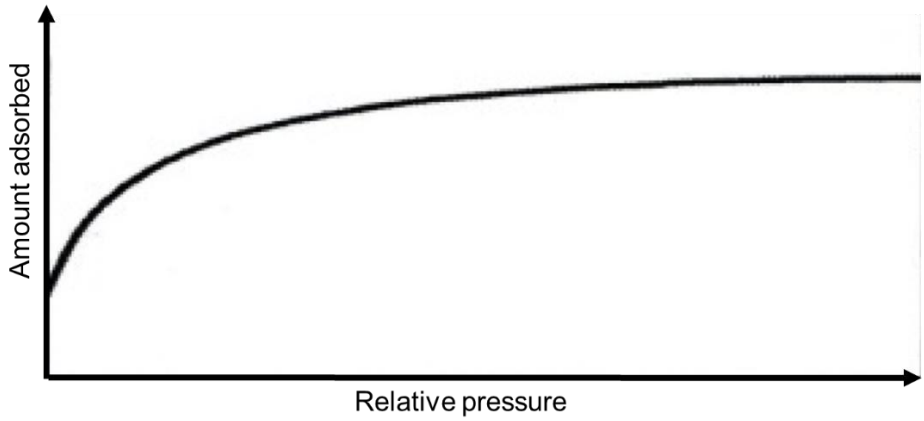

Figure 3.2 Type I adsoprtion isotherm, IUPAC classification

Type I adsorption isotherms can be predicted by the Freundlich adsorption isotherm which empirically descibes the multilayer adsorption of molecules to a heterogeneous adsorbent with non-uniform adsorption heat distribution, as follows:

$$q_e = K_F C_e^{1/n} \qquad \text{[equ.3.5]}$$

where,

q_e = equilibrium adsorbent-phase concentration of adsorbate, mg/l
C_e = equilibrium concentration, mg/l
n = Freundlich constant, indicates adsorption strength or intensity, mg/l
K_f = Freundlich constant, indicates relative adsorption capacity, mg/g

A value of n higher than 1 indicates a favorable adsorption of the molecules onto the adsorbent surface as it reflects the higher intensity of adsorption.

The Langmuir adsorption model assumes a homogeneous surface, with adsorption occurring at specific localised and identical binding sites on the surface of the adsorbent. There is no interaction between the adsorbed molecules and just a

monolayer is formed as molecules only adsorb onto the free surface of the adsorbent. According to Ghosal & Gupta (2017), the Langmuir adsorption isotherm was theoretically derived from the dynamic equilibrium between the adsorption and desorption reactions, with the rate of surface coverage being zero at equilibrium:

$$\boldsymbol{q_e = \frac{q_m K_L C_e}{1 + K_L C_e}} \quad \text{[equ.3.6]}$$

where,

q_e = equilibrium adsorbent-phase concentration of adsorbate, mg/l
q_m = maximum monolayer adsorption capacity, mg/g
K_L = Langmuir constant, binding energy of the adsorption system, l/mol
C_e = equilibrium concentration of solute, mg/l

The Langmuir adsorption isotherm is only valid for low RH levels, where RH < 20% altough the constant K_L obeys an Arrhenius law where the magnitude of adsorption enthalpy reflects the strength of binding the adsorbate to the adsorbent (Colinart & Glouannec, 2017).

The Brunauer-Emmett-Teller (BET) mulitilayer adsorption model applies the Langmuir theory to each layer. All molecules in the second and higher layers are assumed to be the same as in bulk liquid where their heat of adsorption is equal to the heat of moisture condensation and can be written as:

$$\boldsymbol{q_e = \frac{q_m K_B C_e C_s}{(C_s - C_e)[C_s + (K_B - 1) C_e]}} \quad \text{[equ.3.7]}$$

where,

q_e = equilibrium adsorbent-phase concentration of adsorbate, mg/l
q_m = maximum monolayer adsorption capacity, mg/g
K_B = BET constant representing the adsorption intensity, l/mg
C_e = equilibrium concentration of solute, mg/l
C_s = saturation concentration of solute, mg/l

The BET equation can yield Type I isotherms when the heat of adsorption is greater than the heat of condensation and the constant K_B consequently greater than 1, leading to monolayer adsorption. Type II isotherms are obtained when the constant is extremely large and represents reversible unrestricted monolayer to multilayer adsorption on a macroporous (pore diameter >50 nm) or non-porous adsorbent (Figure 3.3).

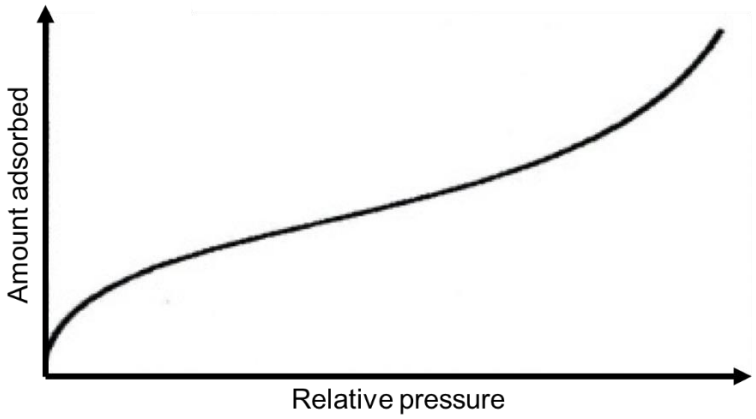

Figure 3.3 Type II adsoprtion isotherm, IUPAC classification

The reversible Type III isotherm can be obtained from the BET equation when the constant is equal to or less than 1. It represents unrestricted multilayer adsorption with lateral interactions between molecules stronger than interactions between adsorbent and adsorbate and is characteristic of macroporous adsorbents (Figure 3.4).

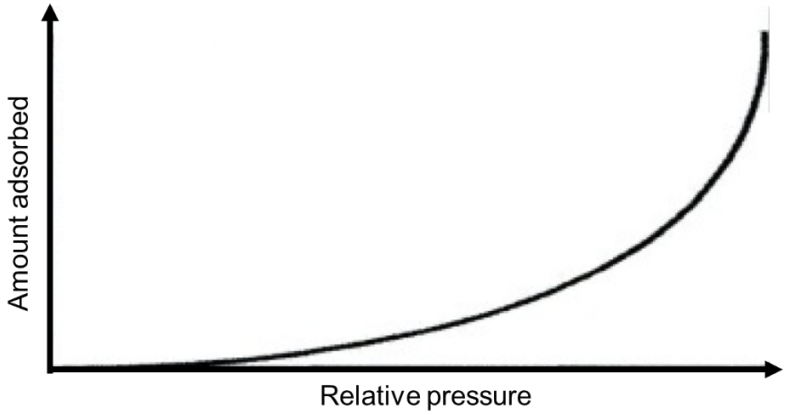

Figure 3.4 Type III adsoprtion isotherm, IUPAC classification

Adsorption on mesoporous (2 nm ~ 50 nm) materials progresses through multilayer adsorption followed by capillary condensation. A characteristic feature of the Type IV and Type V adsorption isotherms, known as sigmoidal adsorption isotherms due to their S shape, is the hysteresis loop, which is associated with capillary condensation in the mesopores and a limiting uptake over a range of high relative pressure. In Type IV adsorption isotherms, at lower relative pressure, there is a formation of monolayer to multilayer adsorption, as in Type II. Adsorption levels off before the saturation pressure is reached, as in Figure 3.5. Type V isotherms correspond similarily to Type III (Figure 3.6).

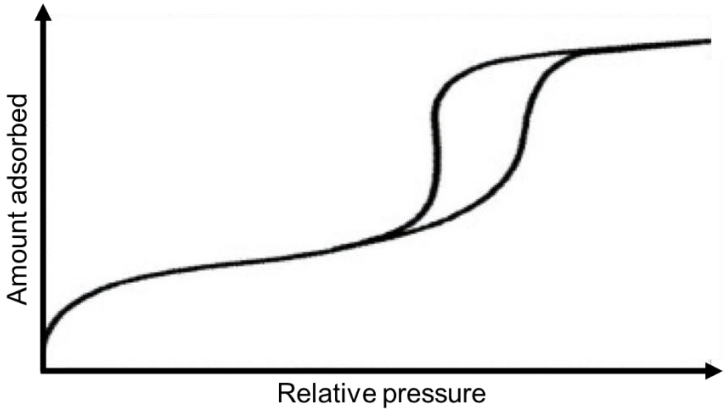

Figure 3.5 Type IV adsorption isotherm IUPAC classification

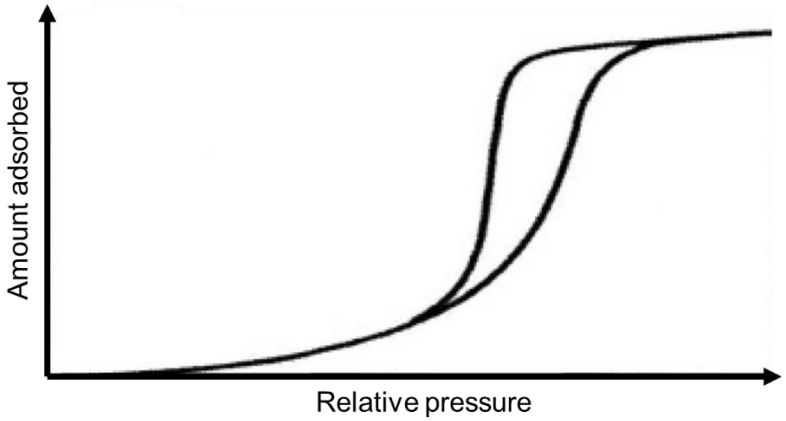

Figure 3.6 Type V adsorption isotherm, IUPAC classification

While the BET isotherm model can represent the equilibrium adsorption isotherm, according to Xi et al. (1994), it does not cover the RH range from 5% to between 30% to 50%.

Fick's first law of diffusion can be used to illustrate moisture transport in the hygroscopic range under isothermal conditions, when the flux of moisture is proportional to the moisture gradient, as shown in the following equation:

$$\boldsymbol{J = -D_H \frac{\partial H}{\partial X}} \qquad \text{[equ.3.8]}$$

where,

J = flux of moisture, kg/(m^2·s)
H = pore relative humidity, %
D_H = diffusion coefficient dependent on pore relative humidity, kg/(m^2·s·K)
$\partial H/\partial X$ = concentration gradient

Pore relative humidity H is a combination of liquid water and water vapour in the pore of the hygroscopic material. The diffusion coefficient depends on moisture and the characteristics of the material pore structure and varies as a function of time and material mix design parameters, such as water-material ratio and aggregate volume fraction. According to Wang and Xi (2017), moisture content, which must be reflected

in the conservation of mass, can be expressed as:

$$\frac{\partial w}{\partial t} = -\nabla \cdot J \qquad \text{[equ 3.9]}$$

where,

J = flux of moisture, kg/(m^2·s)
w = moisture content, kg/m^3
t = time, s

By combining equations [2] and [3], moisture transport under isothermal conditions can be expressed as:

$$\frac{\partial w}{\partial H} \cdot \frac{\partial H}{\partial t} = \nabla \cdot D_H \frac{\partial H}{\partial x} \qquad \text{[equ.3.10]}$$

where,

D_H = diffusion coefficient dependent on pore relative humidity, kg/(m^2·s·K)
H = pore relative humidity, %
t = time, s
w = moisture content, kg/m^3
$\partial H / \partial x$ = concentration gradient
$\partial w / \partial H$ = moisture capacity

Under isothermal conditions, elevated temperatures have been shown to have only a minor effect on moisture transport (Wang & Xi, 2017). Under non-isothermal conditions, moisture transfer in porous media is driven by the moisture gradient, a difference in moisture content between a material's surface and internal matrix, and the temperature gradient $\partial T/\partial x$, a change in temperature over a specified distance between two locations. The phenomenon is called thermodiffusion, thermal diffusion or "Soret effect" and the mass diffusion coefficient defined as:

$$S_T = \frac{D_T}{D} \qquad \text{[equ.3.11]}$$

where,

S_T = Soret coefficient
D = moisture diffusion coefficient, m^2/s
D_T = thermal diffusion coefficient, m^2/s·K

The Soret coefficient may be positive or negative depending on the migration of the reference component to the hot or the cold side. According to Löwgren et al. (2020), the Soret effect in porous media only occurs during dynamic operations and is relevant as long as the dynamic change in temperature outlasts the dynamic change in moisture concentration, which critically impacts on the dynamic part of the drying process.

If a system in equilibrium is subjected to a temperature gradient, a mass transfer occurs and the system reaches a new equilibrium. The effect of the temperature gradient becomes more significant as the temperature gradient increases. According to Wang and X1 (2017), the flux of moisture under a non-isothermal condition can be described as:

$$\boldsymbol{J = -D_H \frac{\partial H}{\partial x} - D_{HT} \frac{\partial T}{\partial x}} \qquad \text{[equ.3.12]}$$

where,

J = flux of moisture, kg/(m^2·s)
D_H = diffusion coefficient dependent on pore relative humidity, kg/(m^2·s·K)
D_{HT} = coupling coefficient for mass diffusion resulting from thermal gradient, kg/(m^2·s·K)
H = pore relative humidity, %
T = temperature, °K

Three material parameters, the moisture capacity $\partial w/\partial H$, the moisture diffusion coefficient D_H and the coupling coefficient D_{HT} are used in the equation which governs the moisture transfer under non-isothermal conditions:

$$\boldsymbol{\frac{\partial w}{\partial H}\frac{\partial H}{\partial t} = \nabla \cdot \left(D_H \frac{\partial H}{\partial x} + D_{HT} \frac{\partial T}{\partial x} \right)} \qquad \text{[equ.3.13]}$$

where,

D_H = diffusion coefficient dependent on pore relative humidity, kg/(m^2·s·)
D_{HT} = coupling coefficient for mass diffusion resulting from thermal gradient, kg/(m^2·s·K)
H = pore relative humidity, %
t = time, s
w = moisture content, kg/m^3
T = temperature

At equilibrium, the amount of adsorbed water vapour per m^2 of pore surface, being a function of temperature and RH of the ambient air, will never be static (Janz & Johannesson, 2001). The number of molecules leaving will be the same as the number becoming bound to the surface. When a porous material has reached full capacity for adsorbed water vapour, to the limit of its hygroscopic storage range which generally corresponds to a moisture range from 0% RH to 95% RH, capillary condensation of water molecules will occur. Surface tension will cause menisci to start forming in microvoids such as the necks of pores and narrow spaces. The vapour pressure of the water in these microvoids is less than that of the saturation vapour pressure of pure water, a result due to the increased number of van der Waals interactions between vapour phase water molecules inside the confined space. With condensation, a meniscus formed at the liquid/vapour interface allows for equilibrium below the saturation vapour pressure. For each pore of radius r, there is a threshold pressure for condensation. Viscous saturated flow in the porous material is driven by the difference in water pressure but also depends on the pore geometry of the material as illustrated by Darcy's equation:

$$\boldsymbol{Q = -\frac{kA(P_1 - P_2)}{\eta L}} \qquad \text{[equ.3.14]}$$

where,

Q = flow rate, m/s
k = permeability, darcy
A = area of flow, m^2
P_1 = initial pressure, Pa

P_2 = final pressure, Pa
η = fluid viscosity, Pa·s
L = length of fluid path, m

The Kelvin equation can be used to describe capillary condensation due to the change in vapour pressure in the presence of a curved meniscus:

$$ln\left(\frac{P}{P_0}\right) = \frac{-2\gamma V_m cos\theta}{rRT} \quad \text{[equ.3.15]}$$

where,
ln = number of moles per volume of water
P = pressure, Pa
P_0 = saturated pressure, Pa
γ = surface tension, N/m
V_m = molar volume, m^3/mol
θ = contact angle, °
r = radius of curvature, m
R = gas constant, J/(kg·K)
T = temperature, °K

Capillary action or suction will force liquid to permeate the pores and diffuse into the material itself in the process known as absorption. Absorption of water follows the Young-Laplace equation for a non-spherical curved surface which relates the pressure difference across the interface of two static fluids such as water and air due to surface tension:

$$\Delta P = \gamma\left(\frac{1}{r_1} + \frac{1}{r_2}\right) \quad \text{[equ.3.16]}$$

where,
P = water vapour pressure, Pa
γ = surface tension, N/m
r_1, r_2 = radii of curvature, m

As explained by Wendler and Charola (2008), a balance between both the surface tension of the water and adsorption forces to a material and the surface energy of that material defines the contact angle (θ) that water will form on that material (Figure 3.7). For a highly polar material, the θ value will be close to 0°, resulting in water entering the pore system of the material through capillary action, allowing total wetting.

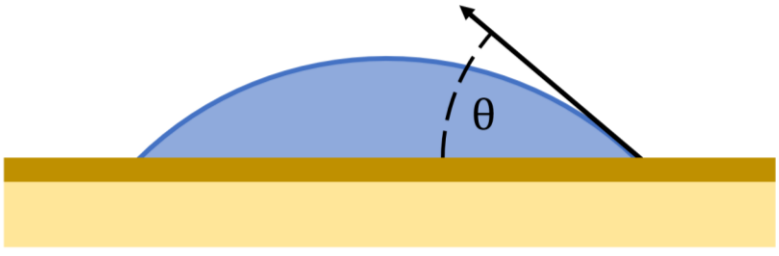

Contact angle < 90°

Figure 3.7 Wettability

According to Straube (2006), as an example, wood will adsorb vapour from the air to raise its moisture content to between 25% to 30% at 98% RH but will absorb two to four times as much liquid water through capillary water uptake. At supersaturation, when all pores are filled with water, capillary suction ceases. Additional water can only be forced into the material through external pressures such as gravity and air.

The drying mechanism or desorption of absorbed and adsorbed water is evaporation and diffusion, as drainage will only remove excess free water above the material saturation point. At saturation, initial drying takes place through evaporation from the exposed material surface. Diffusion through capillary transport will continue to move available liquid water to the surface from the pores of the material but it will be a much slower process than during absorption due to the attraction of the water molecules to the material molecules. The drying rate remains constant as long as capillary action continues, with evaporation from the surface by diffusion through external conditions of temperature and RH or by convection caused by air movement. The critical moisture content is reached when there is no longer sufficient liquid to sustain continuous capillary action at which point the drying rate falls.

The next phase of drying may include some capillary action as there may still be liquid water in areas with smaller pores but where there are larger pores, drying depends on evaporation of any remaining liquid water with subsequent water vapour diffusion. The drying rate may change as the drying progresses. Finally, drying is only by diffusion of water vapour to the surface and removal from the surface by diffusion and convection. The drying rate becomes constant again but is very slow as the moisture content of the material approaches the hygroscopic moisture content at a particular RH. However, the EMC during desorption will always be higher than the EMC noted during adsorption at a given RH (Janz & Johannesson, 2001; Hill et al., 2009). As the drying process is not linear, a moisture diffusion coefficient must be determined through experimentation to predict the time-dependent phenomena.

A flowchart showing the sorption & desorption mechanism stages is presented in Figure 3.8.

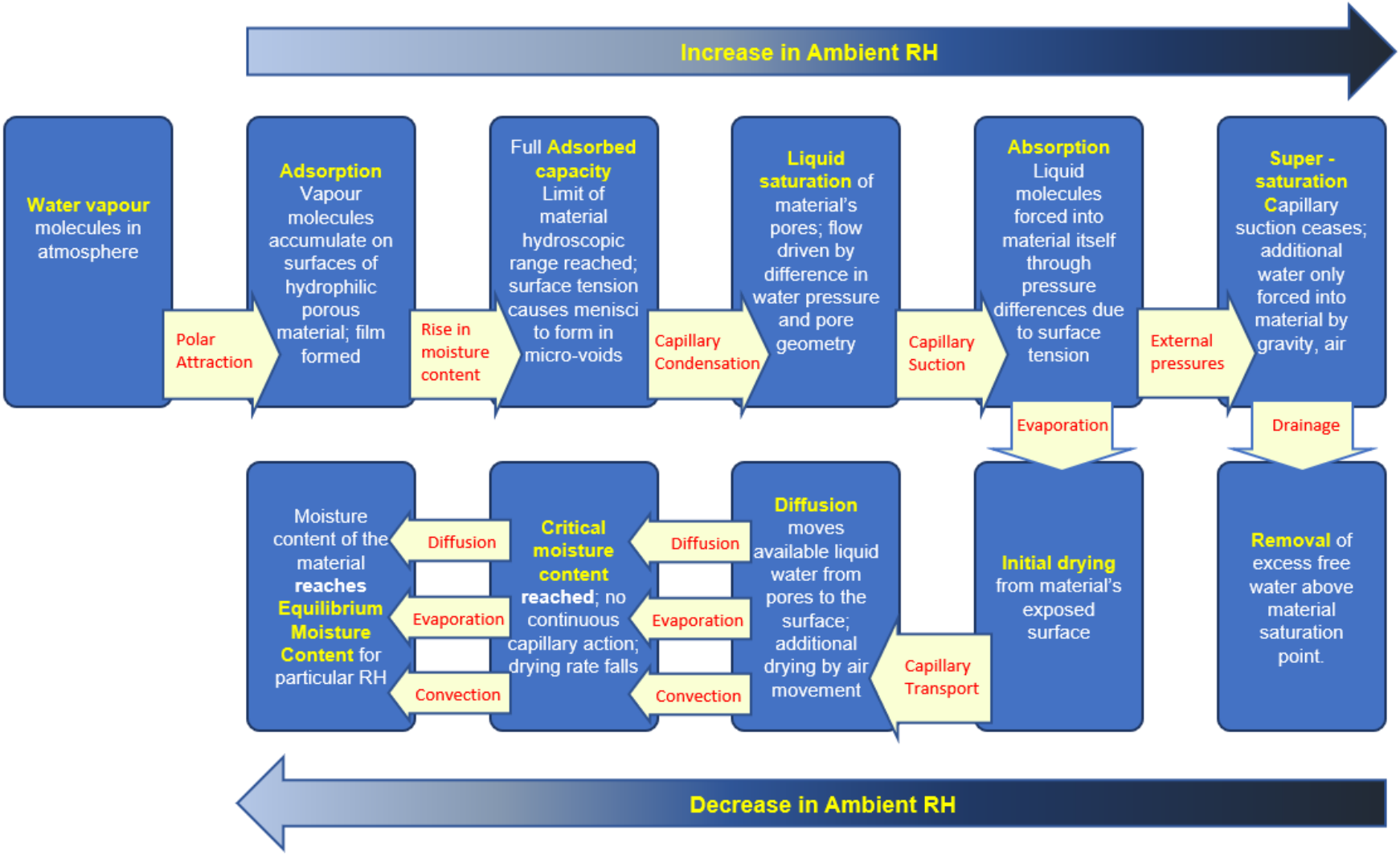

Figure 3.8 Flowchart of sorption & desorption mechanism stages

3.2.2 Moisture storage

Moisture sorption isotherms can be used to evaluate the hygroscopic moisture storage capacity of a particular porous material. It is a graphic representation of adsorption and desorption at a set temperature. Isotherms can be used to plot the relationship between the EMC in a material against the vapour content (VC), vapour pressure (VP) or RH at a given temperature (Figure 3.9). The isotherm is a curved line joining the points where, for each VC, VP or RH value, the corresponding moisture content has reached equilibrium. Each porous material will have its own unique isotherm due to different interactions between water and the material's components and structure at different moisture contents.

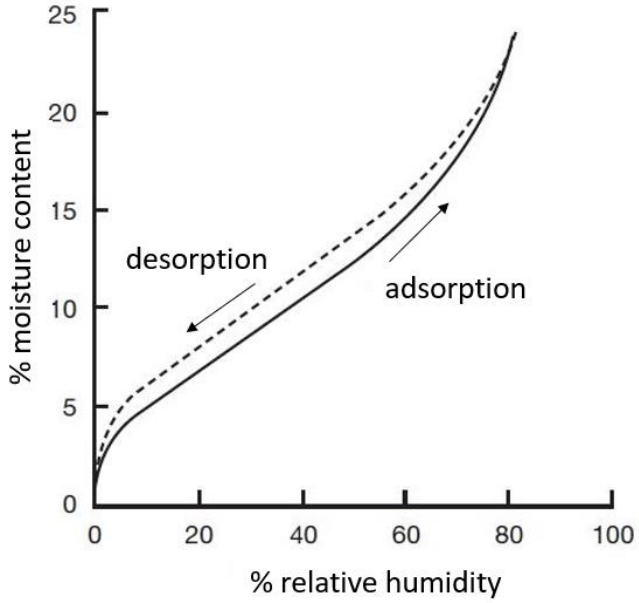

Figure 3.9 Typical sigmoidal moisture sorption isotherm for mesoporous materials (after Hill et al., 2009, p.1527)

For mesoporous materials, the curve typically will be sigmoidal:

- at low RH values from 0% to 15%, there will be monolayer adsorption of water vapour molecules against the internal cell walls
- at median RH values from 15% to 70%, there will be multiple layers of adsorbed water vapour molecules which might lead to capillary condensation in microvoids
- at high RH values from 70% to 95%, capillary condensation is the dominant mechanism
- at RH values from 95% to 100%, the cell walls are assumed to be saturated and above the hygroscopic range, resulting in a very steep curve
- there will be different MC values for adsorption and desorption at the same RH and thus different curves

Moisture sorption isotherms can be determined by exposing a material sample to a specific RH, waiting until equilibrium is reached and gravimetrically confirming the moisture content. There are two methods of carrying out the experiment, both being specified in *ISO 12571* (BSI, 2013). One is to place a dried sample within a climatic chamber under isothermal conditions where the RH can be adjusted and the sample

weighed automatically. Janz and Johannesson (2001) presented a schematic diagram of a complete device, which they termed a dynamic vapour sorption instrument (DVS), where the sample, placed on a microbalance, is exposed to a continuous air flow at a pre-established and continuous RH supplied by a vapour humidifier. The complete set-up is housed in a temperature-controlled incubator.

Moisture storage properties in the hygroscopic range can be determined using the *ISO 12571:2013* cup test method. This method uses standard salt solutions to achieve the necessary RH levels in a chamber (desiccator) into which specimens are placed, under isothermal conditions. Dry specimens are used to determine the adsorption curve; wet specimens (at an RH of no less than 95%) are used to determine the desorption curve. At each chosen RH, the specimen is weighed until equilibrium with its environment in the chamber is reached. Equilibrium at each RH generally takes from two to four weeks, with constant mass identified when three subsequent weighings, each made at least 24 hours apart, show a change in mass less than 0.1% of the total mass. A minimum of three specimens is specified by ISO 12571 so measurements for the sorption isotherm can take considerable time. The moisture content is taken as the mean of the calculated moisture contents for the specimens:

$$\boldsymbol{u} = \frac{\boldsymbol{m} - \boldsymbol{m_0}}{\boldsymbol{m_0}} \qquad \text{[equ.3.17]}$$

where,

u = moisture ratio by dry weight, kg/kg
m = mass of test specimen, kg
m_0 = mass of dried test specimen, kg

Moisture storage in the super-hygroscopic range cannot be measured using saturated salt solutions. Pressure plate methods, adapted from soil physics (ISO, 2014), can be used to force retained moisture from a saturated specimen, measuring the water mass after equilibrium is reached at each predetermined lower pressure. This directly measures suction and the relationship between suction and EMC, giving a water retention curve for the absorbed water. According to Hill et al. (2009), while there is an assumption that there is a neat limit for cell wall saturation so that further sorption can only happen within macro voids such as lumens, this does not happen in reality. Extrapolating the fibre saturation point from the sorption isotherm will give a lower value than measuring it from a saturated sample.

3.2.3 Hysteresis

A porous material's moisture adsorption isotherm will not be exactly the same as its moisture desorption isotherm. The EMC will be higher at the same RH during the drying cycle than the wetting cycle (Figure 3.10).

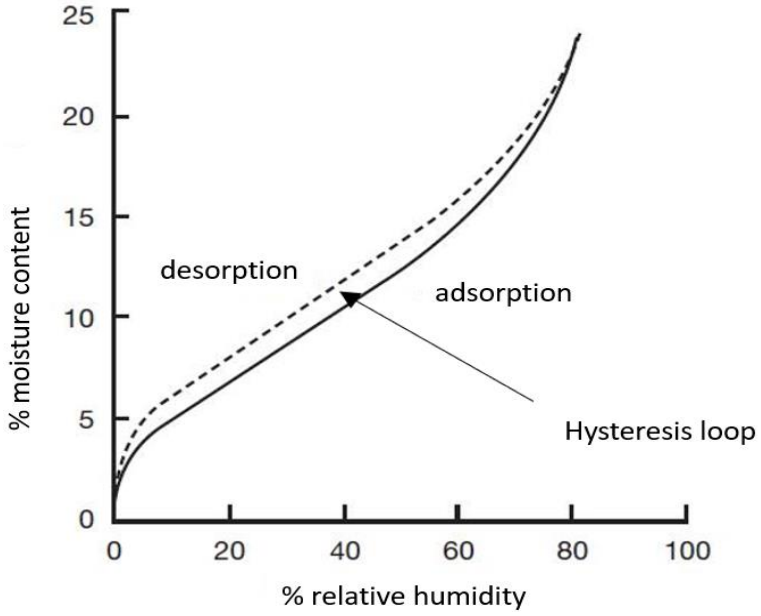

Figure 3.10 Typical hysteresis loop in porous material moisture isotherm (after Hill et al., 2009)

The cause of the hysteresis effect has been explained through various theories:

- incomplete wetting theory, where hysteresis is assumed to be due to θ being greater during adsorption than desorption due to the competitive attraction of air molecules with the material's molecules at low RH (Chen & Wangaard, 1968)
- ink-bottle effect, where the water in the smaller neck of the pore blocks water moving out from the larger pore interior until the capillary pressure drops low enough to allow diffusion from the neck (Carmeliet et al., 2005)
- sorption site availability, where hydroxyl adsorption sites in green or wet organic porous material are reduced in availability for water attachment as they bond with each other (Time, 1998)
- open pore theory, where a meniscus cannot be formed during adsorption, since the pore is open at both ends, but once the pressure has been reached to allow condensation and the pore to be completely filled, a meniscus is present (Cohan, 1938)
- evolution of surfaces in lignocellulosic materials where, as the cell wall swells with increased moisture content, new sorption sites are exposed so that by desorption there are increased numbers of accessible hydroxyl sites associated with water molecules (Hill et al., 2009)
- swelling stresses in lignocellulosic materials, where irreversible plastic deformation can break weak bonds between groups of cellulose molecules, creating additional hydroxyl groups for moisture adsorption (Carmeliet et al., 2005)

Immediate past history and temperature also have an effect on the extent of the hysteresis effect. Understanding the hysteresis effect in a porous material is necessary for modelling potential moisture contents under different RH values.

3.2.4 Moisture buffering

While the effect of hysteresis in a particular porous material has a bearing on modelling the moisture content of that material at a particular RH, according to Carmeliet et al. (2005) it seems that the effect itself is only of minor importance in determining a hygroscopic material's overall buffer capability. The ability of building materials to buffer indoor environment has been identified as a positive way to support the moderation of low RH in winter and high RH in summer and during high occupancy loads (Cerolini et al., 2009). The dynamic interaction of buffering materials with the internal air is thought to help moderate extremes in RH ranges to improve air quality, human comfort and material preservation, reduce energy consumption for heating and cooling, and prevent damage to building structure.

Moisture buffer capacity is theoretically based on the heat-moisture transfer relationship, where moisture effusivity, the ability of a material to sorb or desorb moisture, is determined by its relationship to material density, RH and VP through the following equation:

$$\boldsymbol{b_m} = \sqrt{\frac{\boldsymbol{\delta_p} \cdot \boldsymbol{\rho_0} \cdot \frac{\partial \boldsymbol{u}}{\partial \boldsymbol{\varphi}}}{\boldsymbol{P_0}}} \qquad \text{[equ.3.18]}$$

where,

b_m = moisture effusivity, kg/(m²·Pa·s½)
δ_p = water vapour permeability, kg/(m·s·Pa)
ρ_0 = material dry density, kg/m^3
u = moisture ratio by dry weight, kg/kg
φ = relative humidity, %
P_0 = saturation vapour pressure, Pa

Water vapour permeability values, which measure how easy it is for water vapour to pass through a material under isothermal conditions, can be determined using the method outlined in *ISO 12572* (ISO, 2016). The method is again based on cup tests, with a sample contained in either a dry or wet cup that is then placed in a temperature and RH controlled test chamber. A vapour flow should take place through the permeable sample due to the different partial VP between the test cup and climate chamber. Periodic weighing of the assembly is done to determine the rate of water vapour transmission under steady state conditions. Values are expressed as kg/(m·s·Pa).

The μ-value is a measure of the resistance of the material to allow water vapour to pass through it and is measured in comparison with air. It gives an indication of impedence by adsorption effects at pore walls and by the complexity of the porosity architecture. It can only be quoted for a particular thickness of a material as it is also a property of the bulk material and has no unit. Measurement of μ is through dry cup and wet cup tests. A μ-value close to 1 indicates high permeability of a material. The equation for the conversion of water vapour permeability to water vapour resistance factor is expressed as:

$$\boldsymbol{\mu} = \frac{\boldsymbol{\delta_\alpha}}{\boldsymbol{\delta_\rho}} \qquad \text{[equ.3.19]}$$

where,

μ = water vapour resistance factor

δ_α = water vapour permeability of air, kg/(m·s·Pa)

δ_ρ = water vapour permeability, kg/(m·s·Pa)

As has been pointed out by Hagentoft et al. (2004) and Rode (2005), a steady-state method is inadequate for assessing all the parameters that affect moisture buffer capacity under dynamic conditions. The NORDTEST protocol for determining a practical Moisture Buffer Value ($MBV_{practical}$), to indicate the amount of moisture taken up or released during diurnal variations between two levels of RH, was devised to define a numerical value (MBV_{ideal}) (Figure 3.11).

A unit value for the $MBV_{practical}$, g·(m^2·%RH), was obtained by plotting the mass change ($m_{8\,hours} - m_0$) per m^2 and per ΔRH.

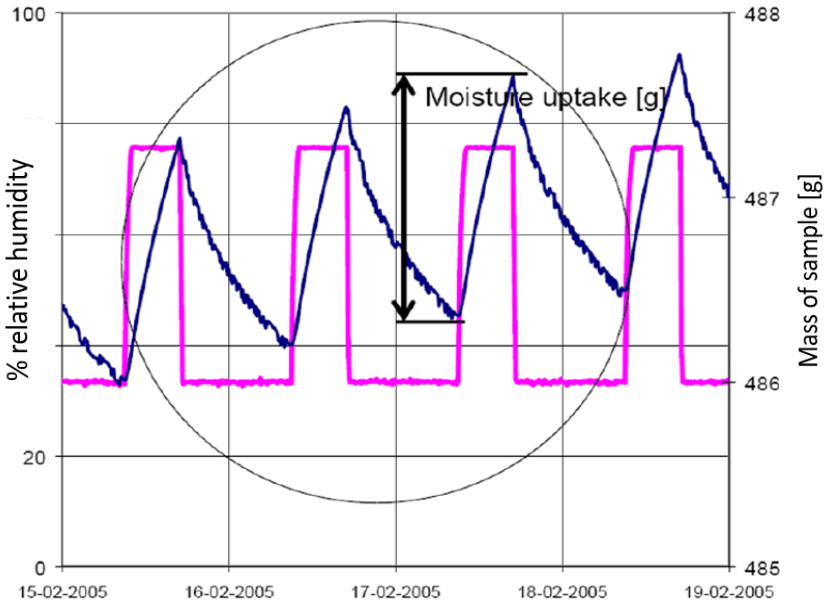

Figure 3.11 Determination of $MBV_{practical}$ from dynamic measurements (Rode, 2005, p.19)

The $MBV_{practical}$ indicates the rate and amount of moisture movement between a hygroscopic material and its environment under dynamic conditions, with values classified as Negligible, Limited, Moderate, Good and Excellent (Table 3.1; Figure 3.12).

Table 3.1 Ranges for $MBV_{practical}$ classes (Rode et al., 2006)

$MBV_{practical}$ class	Minimum MBV level [g·(m^2·%RH)@ 8/16h]	Maximum MBV level [g·(m^2·%RH)@ 8/16h]
Negligible	0	0.2
Limited	0.2	0.5
Moderate	0.5	1.0
Good	1.0	2.0
Excellent	2.0	3.5+

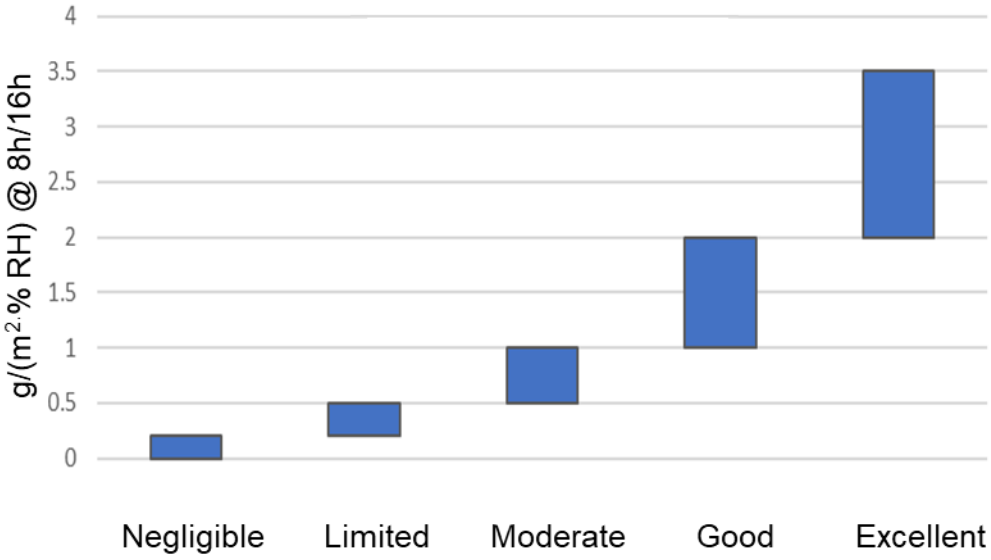

Figure 3.12 Graph of $MBV_{practical}$ classes (after Rode et al., 2006)

The NORDTEST project proposed reference measurements of the $MBV_{practical}$ using a limited number of building materials which were exposed to repeated daily cycles of 16 hours at low RH (33%) and 8 hours at high RH (75%), at 23°C (Rode, 2005). Samples were sealed on all but one or two surfaces with a minimal surface exposure, conditioned to 33% RH, subjected to isothermal RH cycles in a climate chamber, and weighed regularly. Sample thickness was determined to be at least the moisture penetration depth for daily humidity fluctuations. A minimum of three samples of each material was weighed either continuously or intermittently throughout the cycles with a minimum of three cycles. Values are found in Table 3.2.

Table 3.2 $MBV_{practical}$ for conventional building materials (after Rode, 2005)

Building material	**$MBV_{practical}$**
spruce plywood	1.106 g·(m^{2}·%RH)
birch panels	0.49 g·(m^{2}·%RH)
concrete	0.38 g·(m^{2}·%RH)
brick	0.47 g·(m^{2}·%RH)
ligtweight aggregate concrete	0.76 g·(m^{2}·%RH)
autoclaved aerated (cellular) concrete	1.07 g·(m^{2}·%RH)
gypsum	0.64 g·(m^{2}·%RH)

Similar methods to evaluate moisture buffering performance of building materials were developed for both *Japanese Industrial Standard (JIS) A1470-1:2002* and *International Standards Organization (ISO) 24353:2008*. While these tests also use dynamic climate chamber tests of pre-conditioned building material samples (Roels & Janssen, 2006) there are differences in the length of cycles, levels of humidity, number of cycles, sample thicknesses and surface exposure. All tests yield a single value which would allow for a qualitative comparison of buffering ability between different materials (Janssen & Roels, 2009). Hysteretic effect is not taken into account in any of the tests.

Quantitative assessment of moisture storage and moisture transport functions can be carried out by computerised hygrothermal modelling using standard material properties, moisture storage and liquid transport functions (Kwiatkowski et al., 2009). Heat, air and moisture (HAM) transfer simulations using data from outdoor and indoor climate and material properties including vapour permeability and sorption isotherms can also qualitatively assess moisture buffering potential of whole room enclosures (Janssen & Roels, 2009), or whole building performance (Barclay et al., 2014).

The moisture buffering performance of an ideal construction material for museum storage purposes should fall in the Good-Excellent MBV range. A critical buffering property is the rate of adjustment to changes in RH over time in order to reach equilibrium, with an ideal material adsorbing and desorbing quickly to moderate abrupt peaks and drops of internal ambient RH. The moisture storage capacity is also key to the buffering performance, so that an ideal material is able to store a significant volume of water vapour at very high RH without becoming saturated. Vapour permeability being a function of porosity, a very porous material will have a high vapour permeability, providing a better buffer performance. A material with a significant interconnected porous structure will have a more effective penetration depth, allowing for the long-term buffering required to maintain stable storage conditions.

3.3 Material characteristics of HLC

HLC has been demonstrated to have a higher buffering capacity than conventional hygroscopic building materials such as concrete, brick or gypsum (Maalouf et al., 2013). In its exposed state, HLC's moisture buffer value has been rated as either Good or Excellent by several researchers (Collet et al., 2013; Rahim et al., 2015; Latif et al., 2015). Its hygroscopic behaviour and buffering capacity are a result of its components and the process of formulation. The key material characteristics that make HLC an excellent buffering material influence are its mechanical, thermal and hygroscopic properties and performance.

3.3.1 Components and formulation

Hemp lime concrete (HLC), also known as lime-hemp concrete (LHC), hempcrete, lime-hemp, hemp concrete, green concrete and vegetable concrete (Strandberg-de Bruijn & Johansson, 2014) is a mixture of an aggregate derived from industrial hemp, with a lime-based binder and water. Industrial hemp (*Cannabis sativa* L.) is a annually-renewable, fast-growing (three to four months) carbon absorbing and sequestrating broad-leafed bast fibre plant, grown for fibre and grain as a single or dual-purpose crop. Breeding over centuries for tall slender plants with long fibres has reduced the tetrahydrocannabinol (THC) content to less than 0.3%, making the plant a poor source of drug material. In the UK, it must be grown under a *Home Office Law THC Cannabis (Hemp)* licence.

It can be grown with a minimum of fertilisation as it aerates the soil and deposits CO2, although studies have shown that liberal fertilization with organic matter improves fibre yield (USDA, 2000). Few pests or diseases cause problems so use of

pesticides is limited and the hemp canopy from the close-growing plants naturally supresses weed growth. It requires only moderate amounts of moisture for good grain yield (BCMAF, 1999) but needs more moisture for high fibre yield.

The hemp stalk comprises 20% to 40% bast fibre and 60% to 80% wood pith with a hollow core except at the joints (Figure 3.13). After harvesting, the stalks are retted (rotted) naturally by rain and dew or by mechanical or chemical processes to remove the fibre. The wood pith (also known as shiv, shive or hurd), a by-product of the fibre industry, is separated from the fibre during decortication (removal of bark), then shredded into chips with an average dimension of 2 cm x 0.5 cm x 0.2 cm (Cerezo, 2005). The chips, originally considered a low-value waste product of the fibre industry, have begun to be used in biobased construction materials and, by 2004, about 4% of the hemp shiv produced in the EU was used in construction (Karus & Vogt, 2004).

Figure 3.13 Cross section of hemp stalk

Hemp shiv has a lignin content of around 24%, holocellulose content of 74% (hemicellulose content of 30% and cellulose content of 44%) and <2% ash and silica (Cigasova et al., 2014). It is more resistant to biological decay than other biobased materials such as straw and its silica content makes it fire-retardant. The porous water and solute transport structures (xylem vessels and xylem parenchyma cells) of the shiv are, according to Amziane et al. (2017), unaffected by harvesting and production processes. Lawrence et al. (2012) found a trimodal pore structure with pore sizes ranging from 50 µm in diameter connnecting to 10 µm pores via 1 µm pores (Figure 3.14), when investigating the microstructure of hemp shiv. According to Jiang et al. (2018) the high total porosity of hemp shiv is a result of the vessels, approximately 50 µm to 80 µm in diameter, and the bimodal pore size distribution, with the main pore radius range between 0.01 µm to 1 µm and the second pore radius range between 2 µm and 60 µm. The pore structure affects the rate of adsorption and desorption as a partial pressure differential across the 1 µm pore is required to force moisture through the structure. As a result of hydrophilic hydroxyl groups, hemp shiv can absorb large large amounts of water, up to 400% increase in its original mass (Hussain et al., 2018).

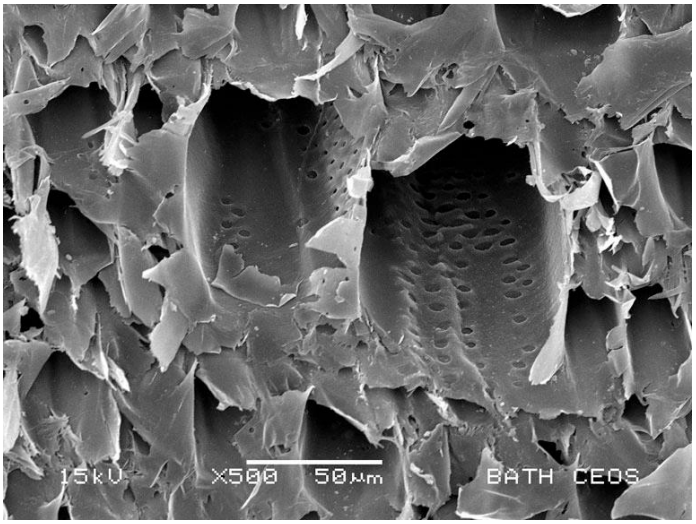

Figure 3.14 Interlinked pore structure of hemp shiv (photomicrograph x 500) (from Lawrence et al., 2012)

Most commonly lime binders specifically formulated for use with hemp shiv are used in construction. Formulated lime based binders typically contain a varying proportion of natural hydraulic lime (calcium oxide (CaO) plus impurities) which sets under water and is quick setting, hydrated or slaked lime (calcium hydroxide ($Ca(OH)_2$) which sets on exposure to carbon dioxide from the air and is slow setting (carbonation), a hydraulic component such as Portland cement produced by heating calcium carbonate ($CaCO_3$) with alumina-silicates and pozzolanic (siliceous) admixtures such as fly (flue) ash, a residue of coal burning commonly added to cement mixtures to enhance setting by forming calcium silicate hydrate (CSH). Fly ash also improves the workability of the mix due to its fine round grains and reduces the required water content (de Bruijn & Johansson, 2013). Generally, proportions are in the range of 75% hydrated lime, 15% natural hydraulic lime and/or hydraulic components and 10% pozzolans. Hydrated lime has good water vapour permeability due to small particle size and high porosity but increasing the cement (hydraulic) content reduces the permeability and thus the buffering capacity (Walker & Pavia, 2014b). Evrard and De Herde (2010) analysed electronic microscope results to determine a pore size with dimensions around 1 µm in lime matrix.

HLC can be used to replace non-structural elements of walls that traditionally use concrete, brick, gypsum board or wood. HLC can be produced as a wet mix on site which may be cast into shuttering around framework or sprayed against a vapour permeable lining board. In casting, water is added to the dry shiv and binder before the mixture is poured and tamped into the shuttering. Spraying uses lime binder in a slurry with water forced through a nozzle to mix with shiv being blown from a separate hose. According to Bevan & Wooley (2008), spraying tends to produce a more consistent and more porous structure than casting; however Duffy et al. (2013) reported a lack of control in the consistency of sprayed HLC. Panels for insertion into framework can also be prefabricated off-site (Daly & Woolley, 2009; Jankovic, 2013). Blocks, produced either on- or off-site, can be self-supporting but are also generally inserted into a supporting frame structure (Arrigoni et al., 2017). The ultimate desired result is a very porous material, an interconnected matrix of various sizes of thinly coated shiv particles, with strong bonds between the particles only where they touch,

leaving air voids between the particles (Figure 3.15)

Figure 3.15 Interconnected matrix of cast HLC

The drying rate is influenced by the composition of the binder, the amount of water used during construction and ambient conditions during the curing period. Using enough water to sufficiently hydrate the lime to achieve an initial hydraulic set may result in a high quantity of retained moisture, up to 70% (Duffy et al., 2013). Recommended drying times for a 300 mm thick HLC wall are from four to eight weeks depending on the ambient atmospheric conditions although the material will hold its form after 24 hours (Sutton et al., 2011). Forced drying may prevent proper setting of the hydraulic components of the binder. Moisture, which might promote rot and mould growth, is less likely to be trapped from the production process given the interconnected porous structure of HLC.

The carbonation process continues over time, with the hemp shiv slowly encapsulated and mineralised by the conversion of calcium hydroxide in the lime binder to calcium carbonate by the presence of carbon dioxide ($Ca(OH)_2 + CO_2 \rightarrow CaCO_3 + H_2O$). X-ray powder diffraction (XRPD) of HLC samples by Arrigoni et al. (2017) showed that, while the amount of carbonates increased with sample age, the extent of carbonation depended on the sampling depth. Carbonation was found to be negligible at 60 mm after eight months. Studies of HLC mixtures have found total carbon sequestration of 275.7 $kgCO_2/m^3$ to 307.26 $kgCO_2/m^3$ (Jami & Kumar, 2017) over its lifetime although lower estimations are generally given by suppliers, from 110 to 160 $kgCO_2/m^3$ (UK Hempcrete, 2019), using a proprietary binder of hydraulic lime, Portland cement and other additives. The amount of CO_2 locked into the HLC compensates for the amount of CO_2 generated during transport, manufacturing process, construction and demolition. Carbon emissions are measured using a standard unit, the carbon dioxide equivalent (CO_2e), which is expressed as parts per million by volume per unit. According to Lawrence et al. (2012) the predicted total life cycle CO_{2e} emissions of HLC mixed with a binder of hydrated lime and natural hydraulic lime or Portland cement can be caculated as -35.5 kg/CO_{2e} per m^3 of HLC, making the material carbon negative. The production of lime, by heating $CaCO_3$ sources such as limestone, chalk and shell to a temperature of approximately 900°C,

is considered to produce fewer CO_2 emissions than the temperature required for cement production (1200°C to 1400°C) but proprietary lime binders also contain cement. The carbon sequestration of HLC is considered to compensate for the production of the binder (Bevan & Woolley, 2008). Replacing non-structural conventional construction materials that have higher CO_{2e} emssions over their life cycle with HLC would contribute to initiatives in lowering CO_2 emissions from construction.

The construction methods result in airtight monolithic walls, contributing to the buffering of internal RH by reducing air changes, as well as preventing condensation, mould growth and building material deterioration, reducing energy consumption and operating costs and excluding drafts, dust and environmental pollutants (Cammalleri & Lyon, 2003). Airtightness tests have achieved air leakage figures around <2 $m^3/(h \cdot m^2)$ @ 50 Pa (Bevan & Wooley, 2008; Abbott, 2014). Durability tests of HLC under freeze and thaw conditions, salt exposure and biodeterioration have shown that the material is resistant to salt damage or microbial infestation (Walker et al., 2014). Small losses in compressive strength result from freeze-thaw action but this is mitigated by the construction technique.

HLC is considered to be a non-toxic building material despite the hemp plant requiring fertilisation. The shiv must be as dust-free as possible but, during the mixing process, significant quantities of caustic dust can come from the dry lime binder. When wet, the material is slightly caustic but once the HLC mixture has dried, there is no off-gassing as there are no volatile organic compounds due to synthetic materials derived from petrochemicals. HLC is anti-microbial, antifungal and fire-resistant due to the presence of the lime binder, eliminating the need for additional chemicals. Any potential for dusting decreases as carbonisation increases.

The costs of HLC can be variable as the main ingredient, the hemp shiv, is not a common building material being a by-product of another industry, with the hemp plant being grown for fibre or for seed. As there is a high yield from the industrial hemp crop, estimated at 2.3 to 7.9 tonnes per acre (USDA, 2000), there can be a large volume of biomass available for construction use from a single crop. Transport can add significantly to the cost if cultivation is at a distance from the processing plant. In 2019 in the UK only 900 hectares were under cultivation (https://sensiseeds.com).

Average material cost for HLC, excluding transport, is estimated between £76/m^2 to £99/m^2, based on current (2019) information from supplier websites in the UK, Australia and the US. A table of costs compared with some conventional insulating materials will be found in Section 3.3.3.

3.3.2 Mechanical properties

Mechanical properties of a building material are responsible for the behavior of that material when used in construction. HLC is considered to be a non-load bearing construction material and is typically used with a load bearing frame (Bevan & Woolley, 2008; Walker et al., 2014). It has a low compressive strength with values found for mixtures with various lime binders of 0.2 MPa to 0.5 MPa (Evrard, 2003), 0.4 MPa to 1.2 MPa ((Arnaud & Cerezo, 2001) and 0.057 MPa to 0.093 MPa (Hirst

et al., 2010). Hirst et al. (2010) found that the compressive strength was low at 28 days when compared with that at three and six months but, according to Arnaud and Cerezo (2001), maximum compressive strength might not be reached for decades. Stiffness is also considered low but again was found to increase with time (Hirst et al., 2010). Ductile behaviour is high initially due to the nature of the hemp particles in the mix along with the long term setting of the binder but decreases over time, although ductility remains higher than in conventional concretes (Arnaud & Gourlay, 2012).

Increase in compaction can lead to increase of mechanical strength as compaction can align the shiv in a series of layers, forming an anisotropic material. According to Dartois et al. (2017), both the slender, rectangular shape and flattened structure of the hemp shiv and its orthotropic behaviour caused by its microtubular ducts contribute to the overall anisotropy. Delayed hardening and subsequent low material strength has been attributed to the slow carbonisation setting behaviour of lime by Colinart et al. (2012) and an insufficient quantity of water during the mixing phase (Colinart et al., 2013; Arizzi et al., 2015). Poor adhesion between binder and aggregate leading to low mechanical strength or unhardened binder may also be caused by the hydrophilic nature of the shiv which can reduce the amount of water available to set the lime binder. However, Sinka et al. (2015) dismiss the insufficient water theory, claiming that unhardened lime binder is a result of the reaction between the organic shiv and the alkaline lime which extracts pectins and other polysaccharides. Amziane et al. (2017) believe that the water content of the shiv, which is affected by the ambient RH at the time of bagging or mixing, strongly influences the mix proportions and final density and porosity of the material.

With differing proportions of binder to hemp, HLC can be used for a number of building uses from insulation (low density) to walls (medium density) and ground slabs (high density). Typically, mixture proportions for wall construction are two parts by mass of binder to one part shiv and three parts water but current practice can reduce the amount of binder and water to one and a half and two parts respectively in order to decrease costs, embodied carbon and density. Densities generally range from a low of 300 kg/m^3 to a high of 500 kg/m^3. The bulk density of the hemp shiv will influence the density of the final product (Arnaud & Gourlay, 2012) as will the choice of binder (Hirst et al., 2010; Arnaud & Gourlay, 2012; Walker et al., 2014) and extent of compaction (Holcroft & Shea, 2015).

3.3.3 Thermal properties

Thermal properties, the abilities of a material to conduct heat, are affected by the porosity of that material (Balabanov & Mishchenko, 2016). Increasing the density of HLC by reducing porosity through increasing the quantity of lime or extent of compaction has a significant effect on the thermal properties of the material, with lower densities resulting in lower thermal conductivity and therefore better thermal performance (Barclay et al., 2014).

Thermal conductivity is the amount of energy flow or heat transferred through a material due to a temperature gradient and is measured in watts per metre Kelvin, W/(m·K), also known as k-value, k-factor or lambda value (λ). Dry thermal conductivity of different densities of HLC has been measured by researchers, with

lower densities, from 220 kg/m^3 to 275 kg/m^3, around 0.06 W/(m·K) (Arnaud & Gourlay, 2012; Lawrence et al., 2012) and higher densities, from 400 kg/m^3 to 600 kg/m^3, around 0.11 W/(m·K) to 0.13 W/(m·K) (Evrard, 2008; Arnaud & Gourlay, 2012; Collet & Pretot, 2014). Cerezo (2005) showed the near linear dependence of increased conductivity as a function of increased density. Benfratello et al. (2013) assessed samples of varying density to demonstrate that thermal conductivity depended on the percentage of shiv in the mixture. Collet and Pretot (2014) demonstrated that density has a much greater impact on thermal conductivity than moisture content, showing that when density was increased by two-thirds, thermal conductivity increased by more than 50% but when the RH was increased from 0% to 90%, thermal conductivity increased by less than 15% to 20%.

Thermal resistance or R-value measures a material's resistance to conductive heat flow through a given thickness and is calculated by dividing the thickness of the material in metres by the thermal conductivity in W/(m·K). The standard measurement is given in m^{2}·K/W. A higher R-value indicates a greater thermal resistance, resulting in better insulating properties. HLC R-values provided by suppliers on-line (2019) are 1.43 m^{2}·K/W for 100 mm (Lime Technology) to 4.35 m^{2}·K/W for 300 mm to 7.14 m^{2}·K/W for 500 mm (Hempsteads) with variations depending on the density of the mix. HLC R-values compare favourably with those of building materials such as clay brick and concrete block but less well with those of insulation materials such as wood fibre batt, mineral wool or polystyrene.

U-value or thermal transmittance is the rate of transfer through a material divided by the difference in temperature across that material. It is calculated from the thermal resistance and measured in W/(m^{2}·K). It represents how effective materials are as insulators. The lower the U-value of a building material, the more slowly heat will transmit through it, enabling a better performance as an insulator. A typical U-value for a thermal conductivity of 0.07 to0.09 W/mK for a 300 mm thick HLC wall is given as 0.21 W/m^{2}K (Sutton et al., 2011), indicating that HLC is a moderate insulating material.

According to Arnaud and Gourlay (2012), HLC has a high thermal inertia due to the internal porosity which retards the rate of heat transfer, stores heat and slows down responses to thermal shock, giving the lightweight material characteristics of high thermal mass. Thermal mass, which can be used to buffer extreme changes in temperature by absorbing and desorbing heat, can be quantified by the Standard Assessment Procedure (SAP) thermal mass value (kappa value or κ-value). κ-value refers to the heat capacity, the amount of heat required to change the temperature of a material by a certain degree and which varies per amount of that material, per square metre of the material, and is measured in kJ/m²K. The higher the κ-value, the greater the thermal mass. κ-value is calculated using the thickness, density and specific heat capacity *c,* the amount of heat needed to raise the temperature of a material per unit mass of that material, derived from the ratio of the heat capacity to the mass of the material, of a layer of the material (Patience, 2016). Values reported for dry thermal or specific heat capacity for HLC densities between 413 kg/m^3 to 627 kg/m^3 range between 1000 J/kg·K to 1800 J/kg·K (Tran Le et al., 2010; Evrard, 2008; Abbott, 2014). The limiting factor for thickness, measured from the inside to the outside, is a maximum of 100 mm in a period of 24 hours. This is based on the assumption that under a 24 hour thermal cycle, such as occurs in the UK, heat

energy can only penetrate up to 100 mm into thermal mass such as concrete and masonry. Under *BS EN ISO 13786:2017* (BSI, 2017b) thermal conductivity, effective material thickness and period of temperature variations are added as identifiers for κ-values.

Using the Dynamic Thermal Properties Calculator, (https://www.concretecentre.com/Publications-Software/Publications/Dynamic-Thermal-Properties-Calculator.aspx), with software methodology based on *ISO 13786* and default settings for a 24 hour period and surface resistances, an HLC wall with a maximum thickness of 100 mm, a density of 413 kg/m^3 , a specific heat of 1000 J/(kg·K) and a thermal conductivity of 0.11 W/(m·K) (values obtained from Tran Le et al., 2012) would have a thermal mass parameter of 21 kJ/m²K. This is a low value, similar to κ-values of a timber-framed external wall with two layers of plasterboard, a solid external masonry wall with dense plaster and internal insulation or a twin timber-framed interior wall with double plasterboard on each side but less than a lightweight AAC block wall at 70 kJ/m²K or a dense concrete block wall with a plaster finish at 190 kJ/m²K (BRE, 2012). Increasing the binder content would improve the κ-value but would decrease the thermal performance. Thermal properties of the dry wall mixture can also be quantified using the calculator, with a low value obtained for thermal admittance or measurement of the material's ability to absorb and release heat over time of 1.36 W/(m^2·K), and with a high decrement factor, or attenuation of thermal gain, as 0.93 and decrement delay, or slowing of the passage of heat, of 2.27 hours. These thermal properties are similar to lightweight insulators such as plastic foams.

Thermal diffusivity of the wall mixture, which measures how fast a material temperature adapts to ambient temperature by dividing thermal conductivity by density and specific heat capacity at constant pressure using the calculation $\lambda/\rho c$, was calculated by Evrard and De Herde (2005) at an average of 1.4 x 10^{-7} m^2/s. A simulated sudden temperature change of 20°C resulted in a linear temperature distribution through 250 mm of HLC not fully completing after 48 hours, compared to 24 hours for cellular concrete and five hours for mineral wool. Thermal effusivity, the measure of a material's ability to exchange thermal energy with its surroundings using the calculation $(\lambda\rho c)^{1/2}$ and defined as the square root of the product of thermal conductivity and heat capacity, was averaged at 320 J/s$^{1/2}$·m^2·K, also lower than mineral wool and and concrete block. A low thermal effusivity results in the material being found warm to the touch, increasing thermal comfort at lower room temperatures.

According to Bevan & Woolley (2008), computer simulations and laboratory tests can only indicate thermal performance. Monitoring the dynamic operation of a real building, they showed that a very stable internal temperature was achieved in a building with 500 mm thick HLC walls. They postulated that the moisture stored within HLC contributed to the thermal stability with a phase change between liquid and vapour storing or releasing energy, slowing down the quick flow of heat from temperature changes and resulting in HLC demonstrating a characteristic of heavyweight construction.

Table 3.3 compares thermal properties, taken from the literature, and average costs, taken from building suppliers (2019-2020) of HLC to some conventional insulation

materials. While HLC as it stands alone does not compare favourably with some other insulating materials in terms of thermal resistance and cost, it should be noted that many of the conventional construction materials would be used as elements in a multi-layered wall structure and that comparative values may therefore have little practical validity. Each element of a layer must be taken into account when calculating both the thermal mass value and the cost.

Table 3.3 Comparison of thermal properties & costs of HLC to some conventional insulation materials

Material	Density ρ Kg/m^3	Thermal conductivity λ W/(m·K)	Specific heat capacity c J/kg·K	Thermal diffusivity α m^2/s	Thermal resistance K·m^2/W	Cost £/ m^2
HLC	275-600	0.06-0.13	1500-2700	1.5E-07	1.43-7.14	76-132
Mineral wool batts	10-70	0.032-0.044	840-1030	13.3E-07-3.4E-06	2.70-2.85	20-30
Fiberglass batts	10-20	0.035	1030	1.6E-06	2.85	13-20
Polystyrene board	20-40	0.033-0.035	n/a	n/a	3.0	16-20
Expanded polystyrene foam	15-30	0.034-0.038	1300		3.52	40-70
Polyurethane board	30-40	0.023-0.026	n/a	n/a	4.50	5-15

3.4 Hygroscopic properties of HLC

HLC characteristically has an open porosity between the binder and aggregate and both the binder and the aggregate themselves have highly porous microstructures. Both porosity and the hydrophilic properties of hemp shiv and hydrated lime binder contribute to the hygroscopic behaviour of HLC.

3.4.1 Water vapour permeability and moisture content

The high water vapour permeability resulting from the material's interconnected porosity reduces potential for condensation and mould growth as well as buffers internal RH levels through moisture transfer (Cerolini et al., 2009). A high water vapour permeability also reduces the need for ventilation to reduce moisture gain (Woloszyn et al., 2009). Measurement of the internal RH of HLC buildings under dynamic conditions has shown very stable levels (Lawrence et al., 2012) but the drying mechanism and the buffering behaviour of the material is still not completely understood. The porous structure affects how water vapour is adsorbed, absorbed, desorbed or stored, which in turn affects the drying rate of the material and its buffering capability. The porous structure is affected by binder properties and

production methods and is reduced over time due to the carbonation process of lime.

Initial total porosity of 71.1% was measured by Evrard and De Herde (2005) on dry samples using a helium pycnometer but pore size distribution in the binder and the shiv could not be differentiated. Open porosity values were obtained both experimentally by measuring air volume in samples of HLC and through theoretical calculations by Cerezo (2005) to give values of 80% to 85%. Pore size distribution in two different HLC mixtures was determined by mercury porosimetry and computed from water sorption isotherms (Collet et al., 2008). Their computed results for total porosity (76.5%) and open porosity (70.6%) were larger than the accessible porosity measured by mercury porosimetry (64.4%) as the latter was only able to penetrate mesospores and macropores and did not take into account micropores in either the binder or the shiv. Evrard & De Herde (2010) analysed porous structure using electron microscopy, revealing three pore sizes: air voids in the mix from 1 nm to 10 mm; larger micropores in the hemp shiv around 10 µm; smaller micropores in the lime binder around 1 µm. Sorption curves were again used by Collet et al. (2013) to determine total and open porosity of three densities of HLC. Both sprayed and moulded (cast *in situ*) HLC showed a similar total porosity of about 79% with a slightly lower percentage (72%) for pre-cast HLC. Open porosity was higher (77%) for the moulded material than for the pre-cast or sprayed HLC (70%). Measurement of porosity was carried out by Rahim et al. (2015) using the pycnometer method with toluene for matrix density. Total porosity was determined from both the matrix density and the dry bulk density to give 76.4% ±0.1% for HLC.

Evrard and De Herde (2005) investigated the hygrothermal properties of HLC following *EN ISO 12572* to measure water vapour permeability. They anticipated that liquid transport would follow a time dependency similar to that shown by wood, cellular concrete or brick. By simulating hygric shock, they demonstrated a specific buffer behaviour due to the material's very low resistance to vapour diffusion against a pronounced hygroscopic uptake. Evrard (2008) determined a water vapour diffusion resistance factor (µ-value) of 4.85 ±0.24 using the wet cup method. Walker and Pavia (2014b) obtained measurements using the test protocol of *EN 12086:1997* which gave slightly higher resistance factors, thus lower permeability values, for six different mixes of hemp and binder (µ-value 5.47 to 5.71). Collet and Pretot (2014) quoted µ-values of 5 to 12, from Collet (2004), Evrard (2008) and Walker and Pavia (2014b), comparing them to those obtained for concrete (130), lightweight aggregate concrete (50) and aerated autoclaved concrete (10). Barclay et al. (2014) also used *EN ISO 12572* to determine a range of water vapour diffusion resistance factors for a HLC with bulk density of 304 kg/m^3. Porosity was extrapolated linearly to be 80% by plotting values obtained from Cerezo (2005) and Collet et al. (2013) against density. Experimental data obtained from measuring the rate of water vapour diffusion under changes of RH were combined with RH relationship parameters to give µ-values from 6.58 at 0% to 0.46 at 100% RH. Rahim et al. (2015) obtained a vapour resistance factor of 8.98 by the standard cup method for an HLC sample with a dry density of 480 ±8 kg/m$^{3.}$

Collet et al. (2013) obtained water vapour permeability values for three HLC samples with densities ranging between 430 kg/m^3 and 460 kg/m^3 using *EN ISO 12572* cup method and obtained a value of 1.7 x 10^{-11} to 6.2 x 10^{-11} kg/(m·s·Pa) for moulded HLC and 2.5 x 10^{-11} kg/(m·s·Pa) for sprayed and pre-cast HLC. Rahim et al. (2015)

reported a water vapour permeability value of 2.2310 x 10^{-11} kg/(m·s·Pa).

Initial water absorption by capillary action was demonstrated to be high in the first 24 hours, then to decrease with time, in all six samples as investigated by Walker and Pavia (2014b), who identified the capillary behaviour as a function of the binder. Capillary action increased with a lower hydraulic content. All water absorption coefficients obtained were lower than those observed by both Evrard (2008) and de Bruijn et al. (2009) who used samples with higher densities. The values found ranged from 2.65 kg/(m^2·$h^{1/2}$) to 9 kg/(m^2·$h^{1/2}$), similar to those found for cement lime mortar and aerated concrete (5.4 kg/(m^2·$h^{1/2}$) and 5.88 kg/(m^2·$h^{1/2}$) respectively but much lower than the value of 21 kg/(m^2·$h^{1/2}$) for fired brick found by Janz (2001). Moisture storage potential was calculated by Barclay et al. (2014) from the sorption isotherms obtained by Evrard and De Herde (2010), which showed that the water content at equilibrium at a very high RH (117 kg/m^3 at 99% RH) was much lower than that at saturation (546 kg/m^3 at 100% RH). Evrard and De Herde also compared the moisture retention curve of HLC to those of concrete, autoclaved aerated concrete, brick and wood and found that only HLC showed an incremental increase after 99% RH. Moisture retention by wood and concrete was much higher in the initial stages than in HLC; all four conventional materials assumed exponential rises to saturation from 93% RH under the effect of capillary condensation, indicating that the hygroscopic capacity was reached at RH <95%. The hygroscopic capacity of HLC appeared not to be reached until 99% RH.

Cup tests were undertaken by Strandberg-de Bruijn and Johansson (2014) to determine the water vapour diffusion coefficient and capillary water uptake for two HLC mixtures with densities of 394.8 ±9.9 kg/m^3 and 298.1 ±6.4 kg/m^3. The tests were combined to determine moisture transport properties over the complete moisture range. The mixture containing a higher proportion of lime binder had a slightly higher moisture transport value at higher RH (>95%); both mixtures had a higher moisture diffusion coefficient in the range 35% to 95% than conventional building materials as reported in literature. Values reported for the two HLC mixes were 4.9 to 12.7 x 10^{-6} m^2/s and 5.4 to 15.4 x 10^{-6} m^2/s, which they compared to 1 x 10^{-6} m^2/s to 2.5 x 10^{-6} m^2/s for lime-based render, 0.2 x 10^{-6} m^2/s to 3.5 x 10^{-6} m^2/s for spruce timber and 3.5 x 10^{-6} m^2/s to 6.4 x 10^{-6} m^2/s for cellular concrete. Collet et al. (2013) found that both sprayed and moulded HLC showed a similar variation in moisture diffusivity, decreasing in value as water content increased, from 7.8 x 10^{-6} m^2/s to 3.7 x 10^{-9} m^2/s. Rahim et al. (2015) found a value of 1.54 x 10^{-9} m^2/s.

Adsorption and desorption isotherms were produced by Cerezo (2005) to show the moisture storage capacity of different formulations of HLC, varying the quantities of binder and water. Samples were placed in a climate chamber at a constant temperature of 20°C and subjected to 25%, 40%, 50% 75% and 95% RH. Measurements were incomplete due to equipment failure and time limitations but the results showed hysteresis loops over the range of RH (Figure 3.16).

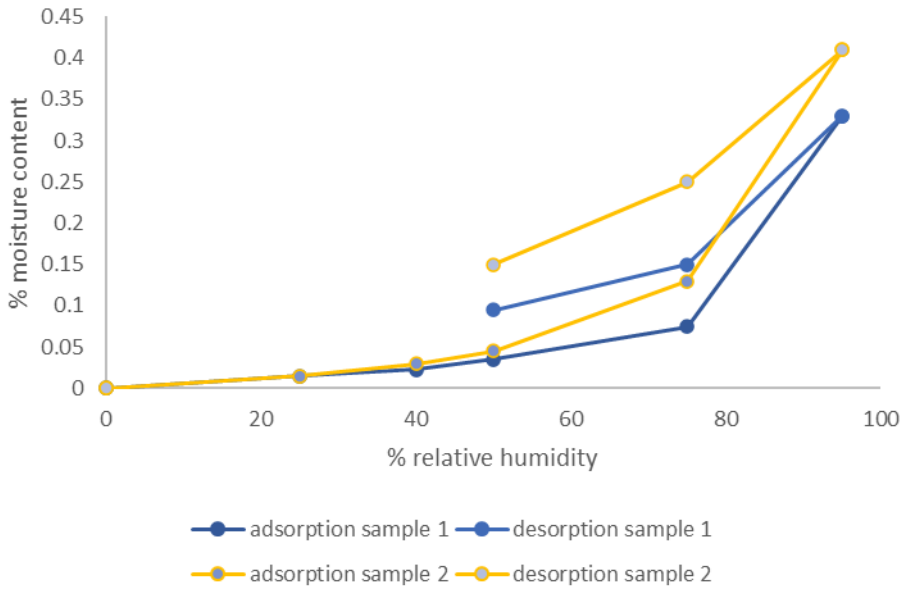

Figure 3.16 Sorption/desorption isotherm of two HLC formulations at 20°C (after Cerezo, 2005, p.166)

Adsorption-desorption isotherms showing hysteresis were measured by Collet et al. (2008) (Figure 3.17) in order to characterise HLC material porosity, using the climate chamber method at 23°C to 25°C. They identified the isotherm as an S-shaped type II physisorption isotherm according to the IUPAC classification and the hysteresis loop as type H3 or H4 as the two branches were nearly parallel over a wide range of relative humidity. The isotherm and hysteresis types related to pore size and pore structure, indicating the presence of macropores and mesopores.

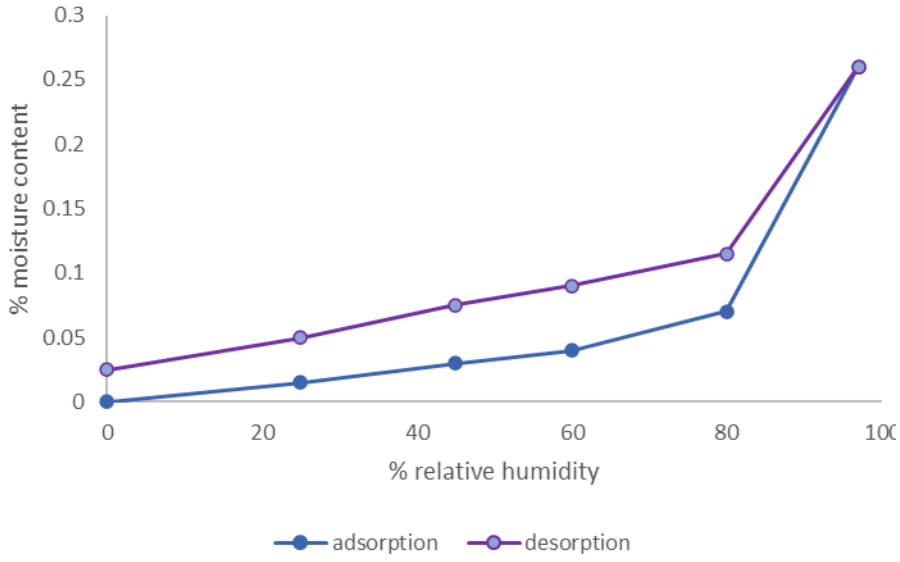

Figure 3.17 Adsorption/desorption isotherm of hemp mortar (after Collet et al., 2008, p.1278)

De Bruijn and Johansson (2013) used the cup (glass jar) test method at ambient temperature for RH <95% and a pressure plate test at 21.6°C for RH >95% to obtain sorption isotherms for two HLC mixtures (Figure 3.18), varying the amount of hemp

shiv, in order to assess the influence of the binder to shiv ratio on thermal properties.

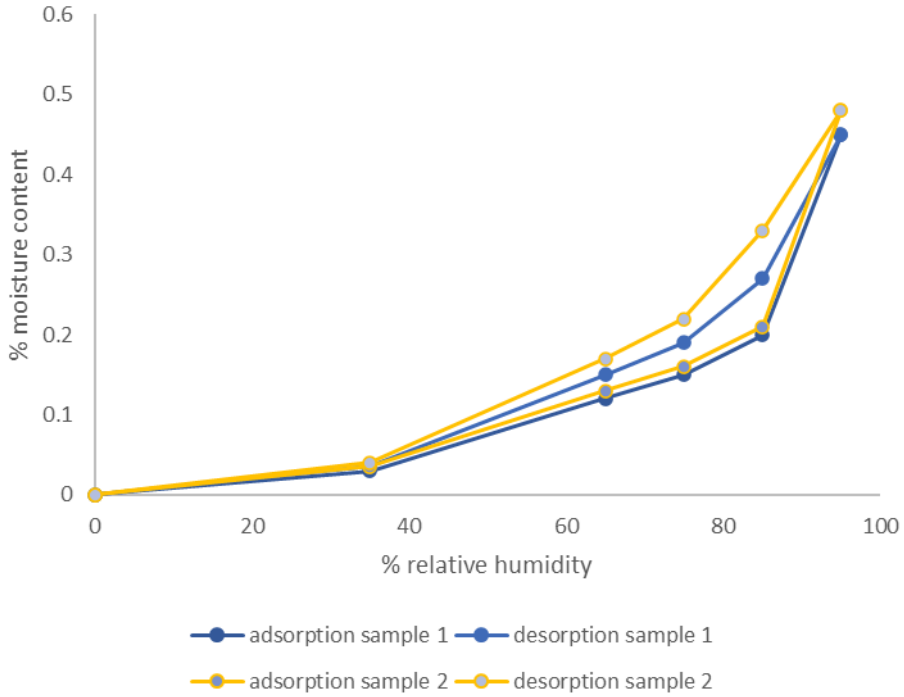

Figure 3.18 Sorption/desorption isotherms for two HLC samples to 95% (after de Bruijn & Johansson, 2013, p.1240)

Adsorption-desorption isotherms were determined by Latif et al. (2015), using the DVS system, up to 95% RH and by the gravimetric method, using a climate chamber, up to 98% RH, both at 23°C. Similar curves were obtained by the two methods to the adsorption-desorption isotherm determined by Collet et al. (2008).

Collet et al. (2008) thought a partial VP differential across the face of the interconnecting pore, required to force through moisture (ink bottle effect), might account for the demonstrated hysteresis. According to Lawrence et al. (2013), the open pore architecture, with 50 µm pores connected to 10 µm pores via 1 µm pores, affects the rate of moisture sorption and desorption as a partial pressure differential is necessary to force through moisture across the 1 µm pore. This slows down the rate of adsorption and desorption so that, under dynamic situations where the ambient RH is never constant, the HLC water vapour content never achieves equilibrium. This results in significant hysteresis occurring in the sorption process with the EMC depending on moisture history as well as RH. Rahim et al. (2015) summarised current explanations for the existence of hysteresis as capillary condensation hysteresis, contact angle hysteresis and ink-bottle effect due to entry pores with small diameters.

Moisture transport within an HLC wall has been investigated through simulation by Tran Le at al (2010) using a mathematical model with an equation system describing the heat and mass transfer solved through the software SPARK (Simulation Problem Analysis and Research Kernel). Simulations were undertaken to analyse the impact of HLC on indoor RH and air-conditioning loads in a room with exterior and interior walls. The impact of the mass transport coefficient associated to a temperature

gradient on indoor RH was investigated in terms of predicting building performance. The simulation results showed decreasing internal RH from the increase in moisture flow through HLC walls from the internal side to the external side under winter conditions. Neglecting moisture transfer led to significant errors when profiling the indoor RH. A ventilation strategy to reduce energy use and improve indoor conditions in winter was proposed by decreasing the air change rate in order to increase the RH.

A HAM transfer model was used by Colinart et al. (2013; 2016) and the simulation results compared with those obtained by monitoring an HLC wall placed between two spaces, one replicating outdoor environment and the other indoor environment. They found that their numerical results roughly agreed with their experimental results under different environmental conditions. They concluded that vapour pressure was largely responsible for moisture transport across the wall, with liquid water evaporating in the macropores.

Moisture transport was also investigated by nuclear magnetic resonance (NMR), particularly to investigate the mechanism of the initial drying phase, but also as a potential technique to obtain clearer information on the links between the porous structure and moisture transfer under different RH values (Faure et al., 2012). The distribution of water content indicated that initial water absorption was by the hydrophilic shiv. Then the smallest pores in the mixture filled with water, with the water finally progressing to the larger pores under increasing RH. Under decreasing RH, it appeared that some of the initial MC in the shiv pores resulting from preparation was also extracted through capillary action and evaporation so that the material at the end of the process was drier than at the beginning.

Temperature has been shown to influence the EMC. Ait Oumeziane et al. (2016) took sorption isotherm measurements of HLC samples at two temperatures and compared them to measurements derived from two simulated models, one based on the physical sorption mechanism and the other on moisture transport. The results showed that the EMC decreased when the temperature increased over the chosen RH range. MC at high RH differed slightly at 10°C and 23°C but buffer capacity was reduced by about 20% at the lower temperature compared to that at 23°C. Colinart & Glouannec (2016) found that temperature differences alter the shape of the sorption isotherm which influences the results of hygrothermal simulations for predicting water vapour permeability and moisture diffusivity

Monitoring of the temperature and RH of a building encorporating HLC (HemPod Building, University of Bath) showed that internal humidity variations were significantly dampened inside the building compared to the external environment (Shea et al., 2012; Lawrence et al., 2012). The experimental building was an unoccupied and airtight single zone with 200 mm thick HLC walls cast against an internal 9 mm thick magnesium silicate board. The RH dampening, with the RH held around 55% RH to 60% RH, was considered to be a result of limited air permeability through the building fabric rather than through hygric performance of the HLC. BESTEST (Building Energy Simulation Test) simulated performance of a whole building with 200 mm HLC walls using a HAMT model with and without humidity transport demonstrated the capability of HLC’s hygric material properties to buffer internal moisture bursts during occupied hours (Barclay et al., 2014). The hygric

model had an RH fluctuation of 17% within the range 30% to 47% while the closed model had a 36% variation in the RH range of 24% to 60%. The researchers noted a reduced risk of mould growth as a result of reduced diurnal variation, as well as improved energy performance due to reduced need for humidification or dehumidification, from the more stable internal conditions of the hygric model. Maalouf et al. (2014) studied the hygrothermal behaviour of an HLC building envelope under various summer conditions using simulations of an occupied room in a heat and moisture transfer model and also found that it was necessary to include moisture transport coefficients in order to accurately predict moisture buffering capacity. When included, indoor RH fluctuations were shown to be reduced by 20% over 24 hours, remaining within the range of 60% RH ±5% RH. Simulations of rooms made with an envelope of HLC alone and with HLC layered with lime plaster showed the plaster reduced the buffering capacity by up to 5% during daytime ocupation. Results from a layered concrete envelope model compared to the layered HLC envelope model showed much more effective buffering of the indoor RH by the HLC case, with a difference of 10% in the upper RH levels.

HLC's properties of rapid moisture transfer, high moisture storage capacity and high water vapour permeability reduce the potential for condensation on interior wall surfaces during periods of high humidity and thus reduce the potential for mould growth. This limits the requirement for mechanical ventilation to regulate the moisture content of the internal environment. Limiting the ventilation rate can be a strategy to reduce energy use during the winter. The moisture effusivity caused by the absorption of moisture by the hydrophillic hemp shiv and the adsorption and desorption of moisture through the extensive and complex porous structure of the hemp and binder mixture has been demonstrated through experimentation and simulation to buffer the internal environment to an RH range considered suitable for stable museum collections.

3.4.2 Moisture Buffer Value of HLC

A value that describes the moisture buffer capacity of hygroscopic building materials would characterise HLC's ability to exchange moisture with the surrounding climate and its resistance to moisture fluctuation, enabling prediction of RH control of the indoor climate.

Evrard (2006) assessed buffering capacity using a process inspired by the NORDTEST protocol project, using 17.5 mm thick samples of commercially available shiv and binder, modifying the production process for each group of samples. The sample thickness underestimated penetration depth. Comparisons with values obtained through simulation showed that water content in the samples was neither as high nor as low as that predicted in the simulation; however, Evrard considered buffering values obtained in his experimental sorption tests as "good", being 1.39 g/(m^{2}·%RH). He concluded that high moisture capacity and specific porous structure possibly slowed down the sorption function and recommended further research be undertaken to analyse pore size distribution. Evrard and De Herde (2010) simulated MBVs for a 300 mm HLC wall assemblage, achieving a value of 2.11 g/(m^{2}·%RH). They found that simulated results were not precise enough as hysteresis had not been considered and the modelling overestimated the hydric capacity of HLC, giving inaccurate predictions of moisture transfer.

Moisture buffering capacity of HLC was investigated as per the NORDTEST protocol by Collet and Pretot (2012) who obtained an average MBV of 2.15 g/(m^{2}·%RH) from a range of 2.08 g/(m^{2}·%RH) to 2.22 g/(m^{2}·%RH) measured from a number of samples from 70.8 mm to 82.9 mm thick and with an average density of 420 kg/m^{3}. These results put HLC into the $MBV_{practical}$ classification of Excellent. They noted their experimental values were somewhat higher than Evrard's due to increased thickness of sample. Penetration depth was estimated at 58 mm, leading them to recommend a wall thickness of at least 60 mm for effective moisture buffering since the MBV would drop when the thickness was less than penetration depth. Moisture penetration depths were measured for samples 120 mm thick with an average density of 290 kg/m^{3} by Latif et al. (2015) who found a range of true moisture penetration depth values depending on the methodology. Values for penetration depth of 73.2 mm were determined by using gravimetric sorption (dry cup); 69.9 mm using DVS (dry cup); 94.7 mm using gravimetric sorption (wet cup) and 90.4 mm using DVS (wet cup). The MBV_{ideal} was calculated to be from 3.24 g/(m^{2}·%RH) to 4.40 g/(m^{2}·%RH), based on the penetration values, with a $MBV_{practical}$ of 3.47 g/(m^{2}·%RH). After experimentally assessing the moisture penetration depth of two samples of different thicknesses using the NORDTEST protocol, they concluded that it was possible for the moisture penetration depth to be closer to 120 mm than 70 mm, based on the amplitude of RH variation which, for a true moisture penetration depth, should be at 0.37%. Variations found were 23.0% at 7 mm and 0.28% at 120 mm.

Dubois et al. (2012; 2013) used the NORDTEST protocol to obtain experimental measurements of an HLC wall mix sample block 75 mm thick. These were compared with mathematical modelling results and good agreement between simulated and measured results was found:

- $MBV_{experimental}$ *2.36 g/(m^{2}·%RH)*
- $MBV_{simulated\ real\ cycle}$ *2.51 g/(m^{2}·%RH)*
- $MBV_{simulated\ ideal\ cycle}$ *2.67 g/(m^{2}·%RH)*

The researchers noted that the study

> *"confirms the general idea of agro-sourced material being good indoor climate regulator*s." (Dubois, Evrard & Lebeau, 2012, p.6)

Figure 3.19 shows $MBV_{experimental}$ plotted against sample thickness as found in the literature with Table 3.4 setting out attribution for MBV, thickness and density. As can be seen in the graph, most $MBV_{experimental}$ for thicknesses greater than 45 mm but less than 120 mm were found to be in the Excellent range, between 2.0 g/(m^{2}·%RH) to 2.2 g/(m^{2}·%RH). Values still in the Good range were found for thinner samples despite underestimation of penetration depth. Values above 3.0 g/(m^{2}·%RH) were found for samples over 100 mm thick.

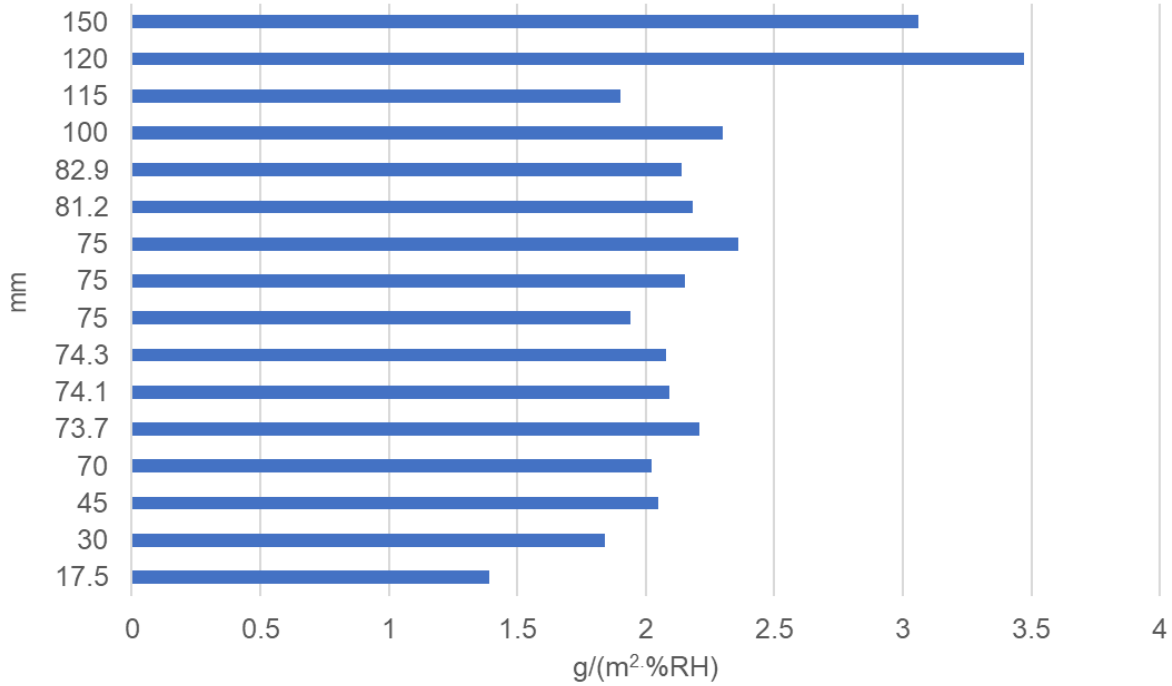

Figure 3.19 HLC $MBV_{experimental}$ plotted against sample thickness

Table 3.4 $MBV_{experimental}$ for HLC samples of various thicknesses and densities, as found in the literature

$MBV_{practical}$ g/(m²·%RH)	Sample thickness mm	Sample density kg/m³	Reference
1.39	17.5	400	Evrard 2006
2.18	81.2	412	Collet & Pretot 2012
2.21	73.7	428	
2.08	74.3	434	
2.09	74.1	440	
2.14	82.9	451	
2.15	70-80	430	Collet et al. 2013
1.94	70-80	460	
2.36	75	480	Dubois et al. 2012
3.06	150	383.5	Dubois et al. 2013
2.3	100	450±20	Lelievre et al. 2014
2.05	45	450	Ait Oumeziane et al. 2014
1.84	30	478	Rahim et al. 2015
2.02	70	478	
3.47	120	290	Latif et al. 2015
1.9	115	450	Colinart et al. 2016

All sorption isotherms obtained for HLC mixes over the whole moisture range by researchers (Collet et al., 2008; Collet & Pretot, 2012; de Bruijn & Johansson, 2013; Colinart et al., 2013; Colinart & Glouannec, 2014) showed similar plotted adsorption

and desorption curves with significant hysteresis between adsorption and desorption. Ait Oumeziane et al. (2014) analysed the performance of two hysteresis models in keeping with the MBV test protocol, using the experimental set up as described by Collet et al. (2008). From the results, Ait Oumeziane concluded that it seemed more reasonable to give a range of 1.85 g/(m²·%RH) to 2.65 g/(m²·%RH) for the MBV rather than a single value.

Moisture buffering capacity of HLC was carried out by Holcroft and Shea (2013) in accordance with *ISO 24353*, exposing 90 mm thick HLC samples with a density of 304 ±14 kg/m^3 to a cycle of step changes in RH between 53% and 75% at 23°C. While the researchers acknowledged that their tests were not directly comparable to those conducted under the NORDTEST protocol, they felt their results matched well to the measurements obtained by Collet et al. (2013). Barclay et al. (2014) also conducted moisture buffer measurements according to *ISO 24353* and compared them to those obtained through simulation in order to assess accuracy of simulation results. Samples were similar in size and density to those used by Holcroft and Shea. Hygrothermal performance of a whole building with 200 mm thick HLC walls of 304 kg/m^3 density was then simulated. Results showed the material's moisture buffering ability to mitigate peaks of high RH, producing more stable internal conditions and reduced risk of mould, with less need for humidification or dehumidification and consequent improved energy performance.

MBVs for different thicknesses of HLC were obtained by Rahim et al. (2015) since the NORDTEST protocol did not give strict guidelines for sample thickness, specifying only that the thickness should be as in intended use or the moisture penetration depth over daily humidity fluctuations. It was found that the MBV increased with the increased thickness of the sample with 1.84 g/(m²·%RH) for 30 mm to 2.02 g/(m²·%RH) for 70 mm. A lower humidity range was also tested, 8 hours at 55% followed by 16 hours at 33%, with the MBVs obtained being lower, from 1.83 g/(m²·%RH) to 1.98 g/(m²·%RH).

Coatings and linings on the internal surface of HLC walls influence the moisture buffering capability of the material. Holcroft and Shea (2013) found that a surface finish of 15 mm lime or clay plaster greatly reduced moisture buffering capacity. Experimental and numerical analysis on HLC samples coated with lime-based plasters by Lelievre et al. (2015) showed that the lime plasters were less hygroscopic and permeable than the HLC and that the MBV of coated HLC was reduced by 40% to a value of 1.2 g/(m²·%RH). Latif et al. (2015) tested ten variations of HLC wall assemblies, some of which were also coated with a water based white emulsion trade paint. Only the HLC and HLC with lime plaster demonstrated an Excellent MBV. The MBV of the other assemblies were decreased to 61% to 69% of the HLC assembly but they still were within the range of Good moisture buffer classes, making them analogous to conventional materials such as exposed wood, concrete and brick. The trade paint had a limited effect on the MBV but the researchers concluded that a clay-based paint would have even less effect. Latif et al. also determined MBV and moisture penetration depths for wood wool board and plasterboard and found that the moisture penetration depth was greater than the thickness of wall assembly samples under testing. This resulted in a lower MBV since moisture moved through these materials into the next layer of the wall assemblies.

A wall constructed of HLC, plastered on both sides with a lime-sand mixture and then on the interior with a lime-hemp mixture, provided samples for comparative analysis between experimental and simulated hygric response by Colinart et al. (2016). A mean value of 1.9 g/(m²·%RH) was found for a base sample of HLC with the plaster surface treatments decreasing the MBV to 1.2 g/(m²·%RH).

As demonstrated in Figure 3.20, less dense HLC mixtures were found to have a greater MBV as determined using the NORDTEST protocol. Results show that densities around 400 kg/m^3 have $MBV_{experimental}$ in the range of 2 g/(m²·%RH). The sample with the lowest density, 290 kg/m^3, had a $MBV_{experimental}$ of almost 3.5 g/(m²·%RH). This is similar to the results obtained by Holcroft and Shea (2015) who obtained MBVs under *ISO 24353* protocol for a number of samples with dry densities ranging between 192 kg/m^3 and 365 kg/m^3. Samples were cast using a mix with a ratio of 1 part hemp shiv to 1.65 parts lime binder to 2.1 parts water, using different degrees of compaction into formwork, from gravity to full force pounding. Increasing the density to 278 kg/m^3 reduced the MBV by 6% but compacting it to 333 kg/m^3 reduced it by 39%. Based on the fragility of the lightest samples, they concluded that an optimum target density for HLC would be between 238 kg/m^3 and 278 kg/m^3, with a MBV between 2.9 g/(m²·%RH) and 3.1 g/(m²·%RH).

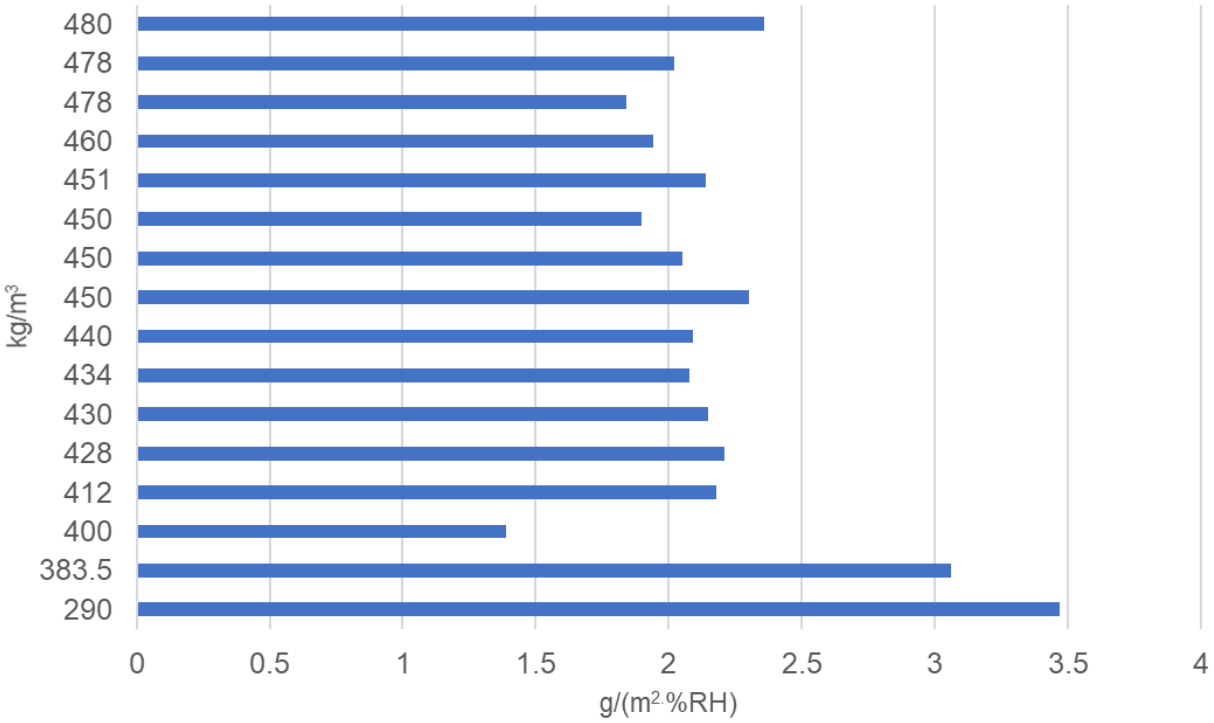

Figure 3.20 HLC $MBV_{experimental}$ plotted against sample density

3.5 Buffering properties of conventional hygroscopic building materials

The key aim up to now in delineating the buffering effectiveness of HLC has been to find a sustainable low energy solution to augment the moderation of internal environment for occupant health and comfort and to control potential moisture

damage to building structure. The potential of HLC to moderate RH in order to meet museum requirements in the storage of cultural heritage collections has not been a focus for exploration until this thesis. But, in reviewing the written research literature on the hygrothermal properties of HLC, it is evident that the material's hygroscopic behaviour has the potential to augment the regulation of RH to current requirements for a stable museum storage environment as identified through the literature review in Chapter 2. Its properties satisfy many of the current directives for environmentally-responsible construction of museum storage facilities, reducing the carbon footprint of construction and energy use in operation:

> *"natural and sustainable environmental controls should be explored and made maximum use of, including…maximising the moisture buffering effect of the building and the materials used within it…..using hygroscopic building materials and finishes to moderate changes in relative humidity…the investigation of new designs for museums and improved methods of building is needed."* (NMDC, 2008)

The following comparison of the key moisture buffering properties of conventional hygroscopic construction materials, as found in the literature, to those of HLC indicates that HLC could be a more effective buffer under museum storage conditions. The material could replace the hygroscopic materials recommended in current guidance (BSI, 2012b), such as concrete block and unfired brick, used as infill materials in wall construction. Design would have to take into account HLC's low structural strength, reducing overall building height or integrating other materials such as timber or steel. Consideration would also have to be made in the design in order to either allow surface exposure to the material, as finishes have been demonstrated to reduce HLC's buffering effectiveness, or to use vapour permeable finishes such as lime or clay plasters. HLC's potential for dusting has yet to be quantified so use in museum storage may require the material to be coated.

3.5.1 Concrete

Concrete is the most used man-made material in the world, with a world average per capita consumption of 563 kg (Armstrong, 2018). It is considered a sustainable construction material by the industry for its strength, durability and excellent thermal mass as well as being:

> *"a friend to the environment in all stages of its life span, from raw material production to demolition"* (Balogh, 2018)

However, Andrew (2018) estimated that manufacture may be responsible for up to 8% of the world's total carbon emissions with 30% to 40% of the emissions derived from the use of energy and 60% to 70% a result of the thermal decomposition of $CaCO_3$.

Concrete is a mixture of fine and coarse inorganic aggregates, cement and water and sets predominately by hydration. Materials of composition include limestone, shell, chalk or marl combined with shale, clay, slate, blast furnace slag, silica sand, and iron ore (Portland Cement Association, 2017). More sustainable concretes are being developed using recycled industrial by-products such as fly-ash, slags or

crushed concrete and adding fibres, water-reducing super-plasticisers (Burridge & Clear, 2014), or low carbon binders to replace conventional aggregates and reduce the use of Portland cement.

Normal weight concrete (NWC), also known as Ordinary Portland Concrete (OPC), composed of Portland cement, sand, gravel and rock, has high compressive strength but requires internal metal (steel) reinforcement due to its heavy weight. The high compressive strength contributes to increased brittleness and loss of tensile strength and shear capacity so reinforcement fibres, either natural material or manufactured products, are often also added to improve flexural capacity, ductility, toughness and crack control (Hassanpour et al., 2012). NWC requires a high proportion of water to aggregate ratio and must be sufficiently agitated to remove air pockets trapped during mixing and pouring. Prolonged setting time (more than 100 days) is required if construction occurs during periods of dampness. Too much water or over-working the wet mix results in dusting, fine flakes spalling from the surface of the set concrete.

Very porous conventional concrete is considered undesirable as it allows water penetration into the concrete structure along with other agents which can promote corrosion of internal steel components. Compressive strength is reduced with increased porosity. A higher initial water to concrete ratio results not only in higher porosity but a greater volume of large pores which allow rapid air penetration. Moisture diffusion and moisture sorption increase with increased porosity (Kim et al., 2014). Pore structure in NWC is composed of randomly arranged and connected gel (nano) pores (<10 nm), capillary pores (10 nm to 1000 nm) and air voids. The initial connected pore structure alters with hydration, with pores becoming smaller as they are filled with hydration products and the structure gradually becoming only partially connected. Moisture transport properties decrease with increased degree of hydration (Sun et al., 2011). Moisture transport in NWC occurs via the gel pores with capillary pores being involved only at high (>75.5%) RH. Moisture transport is not significantly affected by increasing RH until the capillary pores are filled at very high RH (Saeidpour & Wadso, 2016) so dense NWC has very limited transport capability in the hygroscopic range. While NWC is hygroscopic, the material uses available water to continue the hardening process indefinitely rather than storing and desorbing water during periods of lower ambient RH.

While overall porosity, and therefore vapour permeability, is reduced by carbonation, there is an increase in the proportion of capillary pores which results in increased chloride diffusivity leading to steel reinforcement corrosion (Ngala & Page, 1997; Sun et al., 2011). Carbonation rate is affected by ambient RH, with the highest rate occurring between 50% to 70% RH. Diffusion of CO_2 into the concrete matrix is not consistent, being affected by the presence of silicates and the pore structure. Sequestration of CO_2 likely only occurs when the material is fresh as the CO_2 penetration depth of matured concrete is minimal due to the dense microstructure (Ashraf, 2016). Carbonation in low carbon binders which use an alkali source (sodium silicate, sodium hydroxide) with aluminosilicates, such as fly ash and slags, can cause disintegration of the binding matrix and induce loss of strength due to an initial rapid reaction. Other binders containing hydrated lime or non-hydraulic calcium silicates have a slower rate which has a beneficial result on the mechanical properties of the binder (Ashraf, 2016).

Cracking in concrete can occur during curing through shrinkage as the water evaporates from the matrix, with the shrinkage rate greater with higher proportions of water to binder and aggregate. Thermal contraction (internal and external), restraint, subgrade settlement and applied loads during curing can lead to cracking (CFA, 2005). Cracks can be caused by freezing and thawing of saturated concrete, alkali-aggregate reactivity, sulphate attack or corrosion of reinforcing steel as the concrete ages. Cracking occurs at the interface between coarse aggregate and cement since coarse aggregate has a higher crushing strength than cement (Wu et al., 2016). Cracking increases the potential for water permeability, increased moisture transport and moisture - chemical ingress which can promote corrosion of structural components. Mould growth is likely where the cracking is sufficient for water ingress and pooling.

NWC has low vapour permeability so structures are only open to water vapour transport to a very limited depth, resulting in a greater potential for condensation and mould growth since the moisture cannot pass through the material. Vapour barriers used to prevent the possibility of internal air-borne moisture being adsorbed or absorbed can also trap moisture from construction within the concrete's porous structure. Buffering capability by NWC is rated as Limited (<0.5 g/(m^2·%RH) (Rode, 2006) but becomes Negligible with the use of vapour barriers.

Lightweight concrete (LWC) uses porous aggregates, such as pumice, expanded shale, clay, slate, wood, plastics and vermiculite or industrial by-products including blast furnace slag and sintered fly ash, in a mix with cement and water. According to Wu et al. (2016), LWC's prominent characteristics are low unit weight, low permeability, high absorption, good thermal insulating capacity and excellent durability. It is considered a relatively 'green' building material for its superior thermal, acoustic and fire-resistant properties and positive impact on operational energy use (He et al., 2014). Mechanical properties of the concrete are largely controlled by those of the aggregate rather than by the mortar matrix (Wu et al., 2016). Compressive strength depends on aggregate types but increases with an increase in density caused by increasing the ratio of cement mortar. Higher brittleness and lower mechanical properties of LWC compared to NWC at the same compressive strength prevent it from being used as widely in the construction industry (Hassanpour et al., 2012).

The microstructure of LWC is affected by the porous surface of the aggregate and the nature of the interface between aggregate and cement as the high absorption rate of the aggregate can cause the cement to diffuse into the aggregate pores to a certain extent (Lo & Cui, 2004). Capillary pores larger than 50 nm can affect the strength and permeability of the concrete as can larger air pockets in the cement. Extent of carbonation also depends on the type of aggregate and the porous structure of the concrete. A lower water to cement or aggregate to cement ratio mitigates the carbonation process but reduces porosity (Lo et al., 2008). Compressive strength is less than that of NWC due to the increased porosity but LWC provides higher thermal and acoustic insulation. The low density reduces structural weight and need for internal structural reinforcement (Kurpinska & Ferenc, 2017). Inclusion of fibres increases density along with compressive and flexural strength so toughness increases but hygrothermal benefit decreases. The comparative low density of LWC offers better thermal insulation properties compared

to NWC and reduces thermal bridging. LWC has a lower resistance to water vapour diffusion than NWC due to the greater number of pores with radii > than 10 µm (Ducman & Mirtič, 2014) so is much more vapour permeable, leading to a Moderate MBV of 0.76 g/(m²·%RH) (Rode et al., 2006).

Autoclaved Aerated Concrete (AAC) (also known as Cellular Concrete) is considered to be a more environmentally-friendly material than concrete as it uses up to 70% less energy to volume of material in its production (Qu & Zhao, 2017). Raw cementitious materials such as Portland cement, lime, fine silica sand or pulverised fly ash and gypsum are mixed with fine aluminium powder and water to form a slurry which is then poured into moulds. As the cement hydrates, the mix stiffens and rises in the mould due to the evolution of hydrogen gas formed from the reaction of the aluminium particles and the alkaline liquid. The gas bubbles give the material its overall cellular structure. The hardened mix is cut into blocks and heated in an autoclave which results in tobermorite as the principal hydration product (Aidan et al., 2009). The dried blocks are load bearing with high heat insulation parameters (Rubene et al., 2014). Due to the high proportion of air (at least 20%) within the concrete, compressive strength is very low, in the region of 0.7 MPa to 15 MPa depending on density.

The pore volume of AAC is between 65% to 90%, consisting of large aeration pores, capillary pores and nanopores.The large aeration pores are almost spherical in shape and in the millimetre size range. In lowest density AAC, they may touch each other or be interconnected. Interconnection can also be caused by an expansion crack structure inside the air pores. Much smaller pores (nm scale) are in the matrix material around the aeration pores, from the formation of tiny tobermorite and calcium silicate hydrate crystals (Schober, 2011).

Carbonation severely weakens long-term durability as tobermorite reacts with CO_2 in the presence of moisture, decomposing to silica gel and $CaCO_3$ (Matsushita et al., 2004). The polymerisation results in shrinkage, decreasing strength and increasing cracking. The key to improving durability is preventing water entering AAC as much as possible. However, excessive amounts of moisture can be stored in the porous structure during construction as water can be absorbed both in capillary and in aeration pores with a low absorption velocity due to the large number of aeration pores slowing down the capillary forces (Rubene et al., 2014). Moisture migration through AAC is also affected by the uneven pore distribution which is a result of the manufacturing process. Total drying of AAC can take from one to two years, depending on climate conditions (Schoch & Kreft, 2011).

A limited amount of testing has been done on AAC's hygric capabilities for moderating indoor climate conditions. Koronthalyova et al. (2008) found an MBV of 1.6 g/(m²·%RH) which puts it into the Good range. A lower value of 0.99 g/(m²·%RH) was determined by Zhang et al. (2017), closer to the 1.07 g/(m²·%RH) found in the first round-robin tests undertaken by the NORDTEST project (Rode et al., 2006), putting it at the low end of the Good range. It was considered an unimpressive buffer when tested by Padfield and Jensen (2010). Padfield (1998) assessed its buffer capacity as Moderate in earlier work, considering it to have high permeability but modest capacity.

3.5.2 Brick

Fired clay bricks are used world-wide in construction, wherever there are clay earth deposits. Clay deposits contain a mixture of several minerals and so the raw material composition as well as the manufacturing process affects the final hygric properties of the ceramic block (Freyburg & Schwarz, 2007). Four clay types were determined by Freyburg and Schwarz as kaolinitic (mostly containing kaolinite), illitic-kaolinitic (mostly containing mica/illite), mixed layer (alternating mineral layers) and carbonate-containing (containing >9% calcite and dolomite). Raw clay materials have also been divided into lime-rich (containing calcite, dolomite or gypsum), red-firing (containing mica), quartz-rich and carbonaceous (high organic content) (Gualtieri et al., 2010).

Clay is mixed with water and extruded (10% to 15% water), moulded (20% to 30% water) or pressed (<10% water) into brick shapes (Brick Industry Association, 2006). After drying and firing, each clay type displays different amounts and sizes of pores, with carbonate-containing clay bricks being the most porous. Secondary organic or inorganic materials, often industrial waste, added to reduce firing temperatures and reduce clay consumption, also affect the porous structure of the fired product. An increase in porosity results in an increase in water absorption, which results in an increase in freeze-thaw damage in bricks used to form exterior walls. Rode et al. (2006) found a Limited to Moderate MBV range of 0.39 g/(m²·%RH) to 0.69 g/(m²·%RH) for fired brick.

Unfired clay brick is considered to be more sustainable due to low energy production but must incorporate a stabiliser such as Portland Cement or lime to improve durability to long-term water exposure. Unfired clay bricks are more vapour permeable than fired clay brick and therefore have a greater moisture buffering potential (Padfield, 1998). MBVs were determined using the NORDTEST protocol for unfired clay brick samples made from various clays, both natural and artificial, using different manufacturing processes (McGregor et al., 2014). Values varied between 1.13 g/(m²·%RH) and 3.73 g/(m²·%RH), from Good to Excellent, with the greatest range occurring in compressed earth blocks made from an experimental mixture of six clay soils from the UK and France, from 1.6 g/(m²·%RH) to 3.73 g/(m²·%RH). This mixture also had the lowest water vapour resistance factor, indicating a correlation between that and buffering capability. Samples made using a single natural clay with a stabiliser showed MBVs in the range 2 g/(m²·%RH).

3.5.3 Gypsum board

Conventionally, gypsum ($CaSO_4.2H_2O$) is produced from a soft sulphate ore which is mined or quarried, then transported in rock form to processing plants where it is crushed and screened. The crushed ore is fed into a dryer to evaporate all surface moisture prior to grinding. The fine powder is dehydrated to remove chemically-bound water, approximately 20.9% by mass (Yu & Brouwers, 2012). This very dry powder, mixed with water, additives and foaming agents to form a slurry, is sandwiched between recycled paper, cut into panels and dried to make wall board. In the last 20 years, flue gas desulphurisation (FGD) or synthetic gypsum, a by-product of the desulphurisation process of fossil fuels used in power stations, has replaced up to 50% of the mined ore (Gypsum Association, 2014).

The microstructure of gypsum board is a network of interlocked fine needle-shaped gypsum crystals, 5 µm to 10 µm long and 1 µm to 2 µm in width. Macropores are spherical, bordered by a thick crust of gypsum crystals, and are a result of production foaming agents forming air bubbles in the matrix. Mesopores are irregular and are formed by the dissolution of large hemihydrate grains during setting. Interstitial porosity is provided by micropores (<1µm) between the gypsum crystals (Payraudeau-Le Roux et al., 2016).

Hygric buffering capabilities of both uncoated and coated gypsum board were carried out by Roels et al. (2006) as gypsum board is more commonly coated when used as part of a building envelope. They found that, while the paper layers were much more hygroscopic than the gypsum layer, their thinness meant that the overall buffer capacity of the board was determined by the gypsum layer. Coating the board significantly increased the vapour resistance at lower RHs but this reduced with increasing RH. Acrylic paints had less effect on the vapour openess of the gypsum board than latex paints. A moisture buffer value of 0.22 g/(m²·%RH) to 0.63 g/(m²·%RH) was determined depending on thickness (5 mm to 15 mm) (Roels & Janssen, 2005) which agreed with the MBV found during the NORDTEST project of 0.57 g/(m²·%RH) to 0.69 g/(m²·%RH) for a minimum thickness of 13 mm (Rode et al., 2006). This placed gypsum board at the low end of the Good range.

3.5.4 Wood

While wood is considered a very hygroscopic material (Padfield, 1998), wood products are not generally recommended for the construction of museum stores due to flammability and potential for acetic acid, formaldehyde and other VOC off-gassing. Wood panels and plywood or wood chip boards can be used to form interior walls. Glue-laminated (Glulam) timber, made from the main species of softwoods such as spruce and larch, can replace structural steel or concrete uprights and beams and cross-laminated timber (CLT) be used as structural panels for ceilings and floors. Wood sealers, applied to protect the surface of wooden construction elements, are intended to prevent moisture penetration and thus reduce the buffering capability of the wood.

Wood has different moisture permeability depending on its cut orientation. Wood cut across its cell walls will be far more permeable than wood cut parallel to its cells but by far the most common method of milling lumber is to slice a log into lengths along the grain. Flat sawn timber is cut along the tangential plane of the log, resulting in face grain; quarter sawn and rift sawn timber are cut along the radial plane, resulting in edge grain. Plywood veneers are thinly sliced along the radial plane as the log is rotated. The end grain, the most hygroscopic orientation, is produced by cutting across the growth rings and is rarely used in modern construction, although historically end grain boards were used for flooring in high traffic area (factories, boardwalks) due to their durability (Smith, 2018) rather than their hygroscopic capability.

Wood is a cellular material with the cell walls comprised of cellulose and hemicellulose, impregnated with lignin. Softwoods have a simple cellular structure, being 90% to 95% longitudinal tracheids with 5% to 10% horizontal rays. Hardwood

structures are composed of 7% to 55% longitudinal vessels in addition to tracheids (27% to 76%) and rays (5% to 25%).

Moisture in wood can be held within the cell walls by bonding forces between water and cellulose molecules or be contained in cell lumens, held by surface tension. Bound water is transported via vapour diffusion. Free water is transported up the trunk via vessels and tracheids in hardwood and tracheids in softwood and across the trunk via rays. Moisture content of green wood is considered to be 100%. Air or kiln-dried wood contains <20% moisture with all free water and some bound water lost during the drying process. Dried wood will reach an EMC with ambient moisture conditions through diffusion (Simpson, 1993).

Testing under different ambient RH levels by Osanyintola et al. (2006) resulted in a range of MBV for spruce plywood, from 0.55 g/(m²·%RH) to 0.69 g/(m²·%RH). The testing was done in conjunction with the initial round for the NORDTEST protocol prior to the Round Robin, where all laboratories involved in that project tested spruce plywood samples to assess the protocol (Rode et al., 2005). Their tests resulted in an average MBV of 0.58 g/(m²·%RH). During the Round Robin, tests were done on spruce boards, with a resulting average MBV of 1.106 g/(m²·%RH) (Rode et al., 2006), giving the boards a Good grade as opposed to a Moderate grade for the plywood.

Comparisons between average $MBV_{practical}$ values for HLC and other hygroscopic building materials found in the literature are presented in Figure 3.21 and Table 3.5. The MBV for HLC as been taken as an average from values found in the literature; the MBV for all other materials has been taken from Rode et al. (2006).

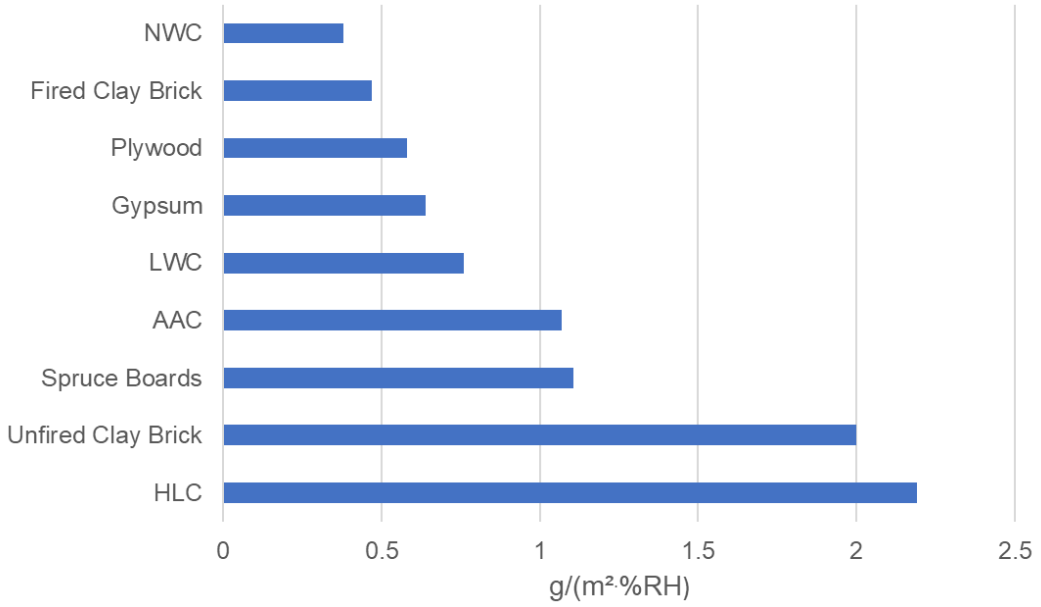

Figure 3.21 MBV of HLC compared to other hygrosopic construction materials

Table 3.5 MBV of HLC compared to other hygroscopic construction materials, as found in the literature

Material	MBV g/(m²·%RH)	Grade
HLC	2.19	Excellent
Unfired Clay Brick	2.0	Excellent
Spruce Boards	1.106	Good
AAC	1.07	Good
LWC	0.76	Moderate
Gypsum	0.64	Moderate
Plywood	0.58	Moderate
Fired Clay Brick	0.47	Limited
NWC	0.38	Limited

Tables comparing the thermal and hygroscopic properties of HLC compared to those of conventional hygroscopic construction materials commonly used in the construction of museum storage, as found in the literature, will be found in Appendix A.

3.6 Potential for augmenting moisture control in museum storage through use of HLC in construction

The hygroscopic parameters of HLC have been investigated by researchers in order to establish the material's credentials in moderating ranges and variations in internal RH. The material has been found to be highly porous, with a complex interconnected architecture of pores ranging in size from 1 µm to 10 mm. Experiments which have provided data on isotherm sorption curves, water vapour permeability values and water vapour diffusion resistance factors have shown that the material's moisture storage and moisture transfer functions are high. Its high vapour permeability has the potential to both reduce the need for ventilation, saving energy that would be required for heating and cooling, and to hinder mould growth and condensation on the interior of the building envelope.

Moisture buffer values have been characterised experimentally and numerically using protocols developed to quantify the amount of moisture stored or released by a hygroscopic material under changes of RH. MBVs were identified as Excellent when the material was uncoated and either Excellent or Good when coated, depending on surface treatment type and thickness. Experimental research results on samples of various densities and formulations of HLC have shown the material's propensity to hysteresis with the material's EMC dependent not only on RH but on moisture history but practical effects of hysteresis have been shown to have only a limited efffect on moisture buffering capacity. The effective moisture penetration depth has a greater influence on the moisture parameters but must be less than the thickness of the material for effective buffering. A limited range of temperatures has been tested with results showing that HLC's buffering ability is reduced but still effective under lower temperatures. Whole building performance analysis through simulation has demonstrated that incorporating exposed internal HLC components into the building

envelope stabilises internal RH, reducing the need for humidification or dehumidification.

Current mechanical control systems of RH in the museum storage environment utilise HVAC systems with environmental control provided through heating, ventilating and air conditioning, the latter including cooling, humidification and dehumidification, in order to achieve the recommended RH range. Fluctuations in the RH can be caused by mechanical methods adding or extracting moisture in order to maintain required RH ranges as well as by the introduction and velocity of external air through ventilation. Current guidance for environmental control stipulates that all available options for achieving specified conditions should be investigated before assuming that mechanical environmental control systems are required (BSI, 2018b). Recommendations are for the incorporation of hygroscopic materials in the construction of museum stores to moderate internal RH fluctuations, in addition to good insulation, low air infiltration and moisture barriers. The moisture buffer values found for HLC indicate that it can play a significant role in moderating fluctuations in RH as long as a suitable density and thickness of material is used. By replacing a less hygroscopic wall infill material such as concrete or brick with a very hygroscopic material such as HLC, buffering of the RH fluctuations caused by mechanical control systems would be improved, resulting in a very stable environment. Indications are that the hygrothermal behaviour of HLC under transient conditions could reduce the energy requirements for mechanical control with moisture transfer maintaining the required internal RH level with limited need for heating in winter. As HLC has been demonstrated to still have an effective MBV at temperatures as low as 10°C, the lower temperatures would be beneficial in the preservation of cultural heritage collections. The high moisture storage capability of HLC should mitigate the potential for internal condensation and mould growth under cold conditions.

The buffering capacity from HLC incorporated into wall structures could reduce potential damage to cultural heritage collections during a failure of mechanical systems by maintaining RH levels through the absorption/desorption of moisture. This would enhance the non-mechanical strategy of seasonal drift by reducing the gain or loss of moisture within the storage area. With its rapid moisture transfer function, HLC would respond more quickly to changes in RH than any hygroscopic organic cultural heritage collections themselves, reducing still further the potential for damage to those materials. This could lessen the requirement for additional enclosures for all but the most RH-sensitive cultural heritage collections, as identified in Table 2.1.

As the ventilation rate also affects RH levels and fluctuations, the high water vapour permeability of HLC could reduce the need to ventilate storage spaces to eliminate occupational and /or activity RH gain, so that ventilation could be kept at the minimum required for abatement of internally-generated pollutants from cultural heritage collections and other construction materials. Being an inert material due to the action of the lime binder gradually mineralising the hemp shiv (Arrigoni et al., 2017), HLC would not contribute to internal pollution. Lawrence (2014), has also suggested that HLC may also passively improve internal air quality by interacting with pollutants. Reducing the ventilation rate also reduces the energy cost for fan operation.

The extent to which a building envelope is airtight also affects the internal RH. Moist outside air can unintentionally be brought in through a combination of pressure differences caused by wind pressure or by the difference between internal and external temperatures (stack pressure) (Younes et al., 2011). Tests have shown HLC to have good airtightness as a result of the monolithic construction method although the measured performance of <2 $m^3/(h \cdot m^2)$ @ 50 Pa falls below the *EN 16893:2018* (BSI, 2018b) recommendation for no more than 1 full air change in 24 hours in museum storage. Airtightness would be improved by adding a vapour permeable airtight barrier on the exterior of the building envelope.

Through the literature review of numerical, simulation and experimental studies on the hygrothermal behaviour of HLC it has been demonstrated that HLC has a greater potential to augment low energy control of RH in museum storage environments than currently recommended conventional hygroscopic building materials. However, knowledge on the extent to which HLC could enhance a low energy control strategy under dynamic storage conditions is limited. HLC is used in combination with other materials as part of a building envelope. Building design, structural materials and construction methods, density and thickness of HLC, area of surface exposure, thickness and type of surface coatings may affect moisture buffering and moisture storage capabilities of HLC. Heating, ventilation, air filtration rates and duration of activity may influence the buffering effectiveness and so dynamic operation may compromise a low energy RH control strategy. The limitations to the techno-economic viability of HLC construction for augmenting RH control under dynamic museum storage conditions are assessed in this study through an *in situ* assessment of an HLC museum storage building, the HMS.

3.7 Summary of the hygroscopic capabilities of HLC related to the control of museum storage environment

The key objectives defined for Chapter 3 were to establish the moisture control potential of HLC and identify its sustainable performance credentials through a review of current numerical, simulation and experimental studies. Through the review, the key knowledge gap on the performance potential of HLC to augment RH control to deliver recommendations for museum cultural heritage collections preservation under dynamic storage conditions was highlighted.

A review of the research on the material characteristics of HLC revealed it to be highly porous, with a complex interconnected architecture of pores. A comparison between HLC and conventional hygroscopic materials concluded that the high vapour permeability and transient moisture transfer rate of HLC would have the potential to reduce the need for ventilation and heating, saving energy while hindering mould growth and condensation. The MBV of HLC was demonstrated to be at GOOD to EXCELLENT and better than materials conventionally used in the construction of museum storage. Buffering capability was shown to be a function of moisture effusivity, the ability to sorb or desorb moisture related to material density, RH and vapour pressure, and moisture storage capacity. Moisture buffer values for conventional hygroscopic building materials were presented for comparative purposes.

HLC's sustainable performance credentials in controlling moisture were identified from the review. Experimental research results on samples of various densities and formulations of HLC showed the material's propensity to hysteresis with the material's EMC dependent not only on RH but on moisture history. A limited range of temperatures were also tested and indicated that HLC's buffering ability might be slightly reduced under lower temperatures. However, the simulation of moisture transfer under transient environmental conditions indicated that the hygrothermal performance would maintain RH levels under lower temperatures, reducing energy costs for heating and ventilation. Analysis of simulated whole building performance analysis indicated that HLC walls could stabilise internal environments, reducing the need for humidification or dehumidification.

A lack of studies under dynamic museum conditions has revealed the key knowledge gaps. The prediction of the HLC buffering performance could be influenced by the location, design and use of museum storage facilities. Indicators are that HLC should provide augmentation of regulation of RH as part of a low energy environmental control system but the extent of effectiveness under actual conditions requires testing under dynamic conditions.

Chapter 4 Research Methodology: Methods, Materials and Equipment

4.1 Introduction

This chapter presents the research methodology, the methods and the materials used to develop a guideline system for obtaining data to support the research hypothesis. It describes the design, methods, materials and costs for the construction of the case study, the Hempcrete Museum Store (HMS). Information is provided on the two other low energy storage buildings on the NCC site which have been used for comparative purposes. The research procedures used to acquire monitoring data for assessment of the hygrothermal capability of the material to control and moderate the RH ranges within the case study are outlined. The monitoring equipment, specifications and operation are detailed.

4.2 Research methodology

A research methodology is a strategy used to collect information and data in order to solve a problem. It sets out the procedures for describing, explaining and predicting events and results. It can also be described as the study of relevant methods, materials, tools and techniques for gaining knowledge leading towards a solution to the chosen problem (Rajasekar et al., 2006). Approaches to developing a research methodology can be descriptive, reporting on what has happened or is happening, or analytical, critically evaluating available facts and information. Strategies can be either applied, finding a solution for a current problem, or fundamental, gathering knowledge for the sake of knowledge. Research can be conceptual, relating to an abstract idea or theory, or empirical, relying on experimentation and observation (Nallaperumal & Krishnan, 2013).

Research methodologies basically fall into two approaches, quantitative and qualitative. Quantitative research gathers information through a structured approach with a theory that relates to the topic being studied, hypotheses based on the theory, and tests on those hypotheses with data either confirming the hypotheses or not. Data are numerical, being the primary raw output of volumetric, gravimetric, colourimetric and instrumental systems, and are physical and measurable. Results are often presented in tables and graphs and generally require analysis and evaluation to support recommendations for solutions. Quantitative research investigates what, where and when.

Qualitative research gathers information through less structured approaches such as case studies and field observations in order to explore the problem. Data derived from visual observation define the meaning, feeling and description of the situation using words and reasoning. Results are non-numerical and cannot be graphed. Qualitative research investigates why and how.

Case studies have a contextual nature with their strength lying in defining concurrent phenomena in real-life contexts (Meyer, 2001). They are well-suited to mixed methods research, combining quantitative and qualitative research methods to take advantage of the multiple ways in which a research problem can be explored. A case

study was chosen as the research methodology for this thesis in order to provide analytical and empirical strategies into investigating the actual performance of HLC during dynamic museum storage operation. The design of the research programme data collection system was tailored to the research question in order to achieve the objectives.

The objectives of the case study were to address the key knowledge gaps identified in the literature reviews by:

- Obtaining data from the dynamic operation of a case study building to compare with contemporary data from other low energy museum stores.

- Evaluating the moisture management capacity of HLC over a range of hygrothermal boundary conditions relevant to museum storage conditions.

- Quantifying the extent to which the hygrothermal performance of HLC can support the research hypothesis:

  Does hemp lime concrete have the hygroscopic performance potential to augment the regulation of relative humidity within museum storage buildings in temperate climates?

4.3 Research methods

The qualitative approach to research analysed environmental monitoring data obtained during dynamic operation of SMG museum storage facilities on one site, using the museum's environmental monitoring system. Longitudinal and in-depth studies on the effectiveness of the regulation of RH were carried out on the case study through transient and first and second steady states of operation. RH data was analysed from other museum storage areas for comparative purposes during the steady state periods. Data on moisture storage in the HLC walls, air velocity and duration of access to the storerooms of the case study were recorded and assessed for correlations to the RH data. Observation was used to determine if variables in operation had any deleterious effect on historic collections housed in the stores. Quantitative analysis on the correlation of moisture content to RH was carried out using linear regression modelling.

While laboratory-based experiments are necessary to produce standard steady state material data, there has been sufficient data obtained by other researchers, detailed in the literature review in Chapter 3, to determine the hygrothermal capabilities of HLC and overall the material has been shown to be effective at buffering RH levels under laboratory conditions. Therefore, upon evaluation, the decision was made not to attempt to replicate those experiments but to accept published findings to inform the development of the research methodology.

Similarly results obtained by several researchers using building simulation software programmes to investigate the effects that the hygric behaviour of HLC wall assemblages and whole building hygrothermal performance has on indoor RH have been discussed in the literature review. Results using computational numerical

values, constructing an artificial environment where the dynamic behaviour of a system under controlled conditions can be observed, have been compared to experimental data obtained from laboratory tests in order to corroborate the buffering effect of HLC on internal RH. Discrepancies demonstrated between modelled and experimental RH performance have shown that accurate values for hygric properties such as adsorption and desorption hysteresis, water vapour resistance factor and moisture transfer coefficient as well as material thickness, material porosity and initial moisture content of all layers must be used if the model is to simulate real hygrothermal behaviour (Ait Oumeziane et al., 2011; Colinart et al., 2016). To predict accurately a variation in RH, the model must also take into account the effects of climate and internal conditions as a result of building use. The most commonly used models which include moisture transport are effective capacitance (EC), effective moisture penetration depth (EMPD) and combined heat and moisture transfer (HAMT) model (Wan et al., 2017) but, according to Hong et al. (2018), no programme is perfect in terms of accuracy. Modelling errors are found if the simulation tool does not calculate moisture transport, as shown by Tran Le (2010) and Maalouf (2014), or if simplified mathematical models used for input parameters do not match the actual structure and properties of the materials, as demonstrated by Colinart (2016). Results of simulation have demonstrated that the use of HLC in building envelopes may reduce daily variations of internal RH, reducing energy use and improving indoor air quality.

The case study, a long-term in-depth assessment of the dynamic operation of an museum storage building built with HLC walls, will attempt to provide data which will support the moisture buffering potential found in both experimental and numerical studies by other researchers.

4.3.1 Design of the data collection programme

The focus of the case study is a museum storage building, the Hempcrete Museum Store (HMS), built within one of the WWII hangars on the site of the SMG's National Collection Centre (NCC) at Wroughton, Wiltshire. The HMS was built in order to store three discrete RH-sensitive cultural heritage collections and a nationally important archive. Another low energy storage building, for the reserve collections of the Science Museum Library & Archives (L&A), had been built within the same hangar some years previously. Both buildings were intended as low energy repositories for the storage of discrete collections which required specific environmental controls. Building within a building was intended as a way to augment passive regulation of temperature and RH changes by using the thermal mass of the hangar as a buffer. The aim in using a highly hygroscopic construction material was to meet the museum's directive for a more sustainable way to regulate storage conditions than had been achieved in the L&A store, The choice of HLC was based on contemporaneous research which indicated that the material's hygroscopic characteristics could be capable of moderating the internal environment.

Data from telemetric monitoring of temperature and RH in the case study, from pre-conditioning to full operation, was available for analysis. The environmental monitoring system used was an accurate (RH ±2% to ±3%; temperature ±0.1°C - ±0.3°C) and flexible telemetric system, installed at SMG sites in order to enhance and validate the controls of building management systems in galleries and storage

areas. The museum agreed that the system could be utilised for the research study by this researcher as data obtained would also be used to inform decisions for future storage projects on the NCC site. This eliminated the need to resource and install another monitoring system. The RH/T data was collected continuously, with sample rates every 10 s and logging intervals every 15 minutes, and was transmitted wirelessly for analysis, without the need to download data from stand-alone data loggers. The wireless system included a logging facility to prevent data loss should radio communication fail.

Data was assessed in two phases. The first phase was during the transient and first steady state of the building's operation, from June 2012 to June 2016, through four heating seasons. RH data was consistently collected from three HMS storerooms. RH data was also acquired from telemetric units in both the L&A store and one other low energy storage building, the A Store. In the second phase, during the second steady state from June 2017 to January 2020, the telemetric system was expanded to provide additional monitoring data for the purposes of this study. More RH/T transmitter units, as well as a moisture detection system to measure moisture penetration within walls and an air flow sensor to determine effects of air velocity, were added to the environmental monitoring system. A logged access procedure was implemented to assess potential influence of duration of access in the HMS storerooms.

RH data was obtained during the transient and first steady state periods from data loggers in hangar D2 and externally. Data loggers were replaced with transmitter units as museum budget permitted so that comparative data could be obtained as part of the monitoring strategy. Initially, weather data was also obtained from weather stations in Wiltshire, at Marlborough (Windrush), approximately 11 km south of the Wroughton site at 144 m above sea level, and at Lyneham, (RAF Lyneham) 14.5 km to the west at 145 m above sea level, but was found not to be fully consistent with the data acquired from the external data logger on the site, despite the short distance from either weather station.

4.3.2 Data collection assessment process

RH and temperature data from the transient and initial steady state operation of the building, June 2012 to June 2016, was assessed on a regular basis after building and mechanical system issues caused unacceptable RH regulation performance during pre-conditioning, necessitating modifications in operational procedures in order to reach hygrothermal equilibrium. A history of the issues is more thoroughly discussed in Chapter 5. Data acquired during this phase was used to revise initial operational procedures in order to meet SMG guidelines on RH levels and fluctuations.

In the second steady state, the dynamic operation from June 2016 until January 2020, the monitoring programme of the case study was extended and operational procedures were further modified but without compromising the agreed specification parameters. Data from the other two low energy stores was used through this phase to validate initial findings from the first phase on improved RH regulation for lower operational and energy expenditure in the HMS. Data was assessed on a monthly

basis, to ensure environmental parameters stayed within SMG specifications, and annually, to update SMG storage and display benchmarks.

Data acquired during the second phase was used to inform the design of new storage facilities for SMG. SMG guidelines (SMG Conservation & Collections Care, 2018) for RH levels and fluctuations were revised, using information based on the literature review for this research project. Assessment of the regulation of RH in the HMS was disseminated in peer-reviewed publications, conference papers, posters and seminars during the PhD research period.

4.4 Research Materials - the museum stores

The NCC site is a former Ministry of Defence maintenance airfield 6.5 km south of Swindon, Wiltshire (Figure 4.1). It is 220 hectares (545 acres) in size and 200 m above sea level at its highest point. Wiltshire, in the south-west of England, has a temperate climate, being generally wetter and milder than the rest of the country, with an average mean temperature of 10°C and an RH of 80% (WorldWeatherOnline, 2018). Due to its elevation, the site can frequently be windy, damp and cold which results in low temperatures and high RH in unheated storage buildings.

The museum stores at the NCC facility are diverse, including unheated hangars, heated purpose-built repositories and unheated storage shelters with and without dehumidifiers. In them are stored cultural heritage collections from all the museums that comprise the SMG - the Science Museum (SCM) in London, the National Railway Museum (NRM) in York, the National Science and Media Museum (NSMM) in Bradford and the National Science and Industry Museum (SIM) in Manchester. This section presents the intent, design and build specifications for the case study, including description and costs of materials. The other stores which have provided comparative RH data are described.

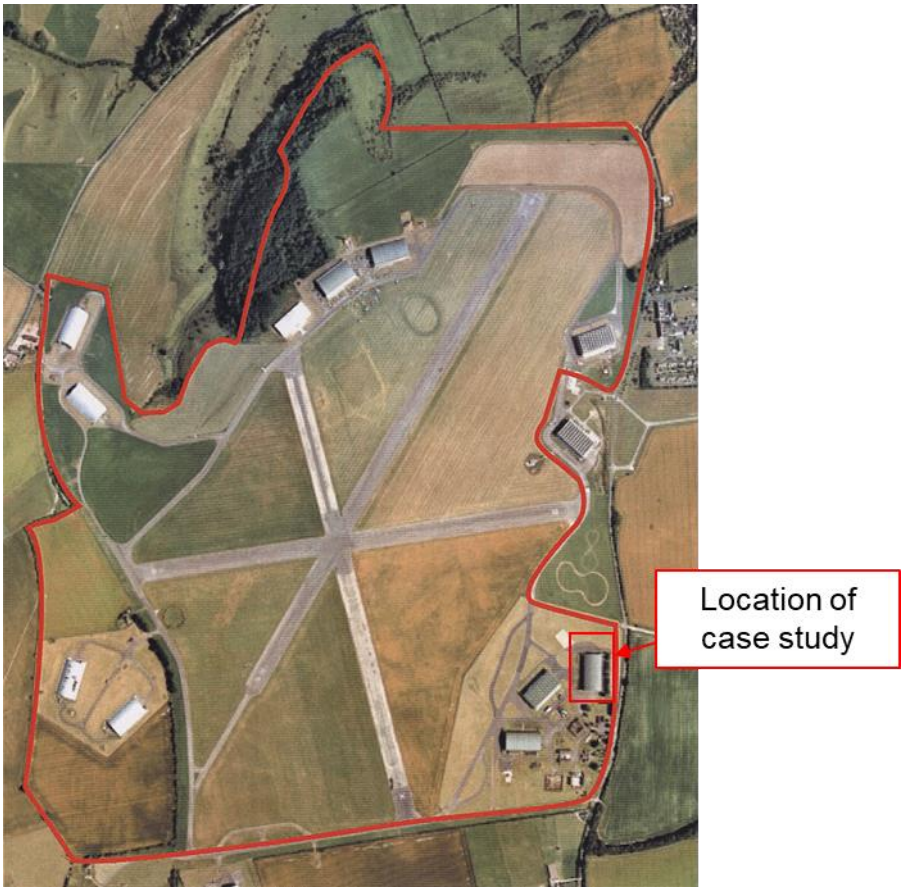

Figure 4.1 Location of the case study on the SMG NCC site, Wroughton, Wiltshire

4.4.1 Case study - The HMS

The HMS was designed and constructed in 2011 to 2012 within a 1940's concrete D-type unheated aircraft hangar. It was built in response to several needs of the SMG. A large and important archive, the Rail Industry National Archive (RINA), was being transferred to the NRM but neither their archive stores nor those of the SCM had sufficient available space. An exhibition gallery in the SCM was being transformed, requiring the decant of large ship models and framed paintings but with no suitable storage available at either their storage building in Kensington Olympia (Blythe House) or the NCC site. Horse-drawn carriages, stored in the same building as the Conservation facility at NCC, needed to be moved as the space was required for the treatment of objects for the new gallery. The SCM framed art work collection was stored in two separate buildings with only some of the works on suitable storage furniture.

The 17.92 m x 17.15 m building was erected in the south-east area of hangar D2 (Figure 4.2). A previous low energy storage repository for the SCM Library and Archives (L&A) (discussed in section 4.4.2.2) had been built in the north half of the hangar a few years previously. Construction within another structure was intended to provide an additional layer of protection from the elements. Specifications for the store were for a stable RH and temperature suitable for the storage of highly

sensitive hygroscopic materials. Low energy consumption was a key criterion with limited reliance on mechanical and engineering (M&E) systems.

The building was positioned next to the L&A store, being oriented with room access at the centre of the hangar and perpendicular to the hangar's south external sectional overhead door. Access to each of the three larger storerooms was through a sectional overhead door as well as a personnel door at the front of the building, with a fire exit door, or in the case of the ground floor two fire exits, at the rear. The three smaller rooms had a personnel door at the front and a fire exit at the rear.

Figure 4.2 Location of the HMS within hangar D2

In order to house the specific cutural heritage collections, the building was designed to have three 17.45 m x 12.4 m rooms (the **BOX**) and three 17.45 m x 4.0 m rooms (the **RINA**), one of each on three floors, with an overall internal floor area of approximately 860 m^2 (Figure 4.3). The BOX was designated for the storage of horse-drawn carriages, large ship models and framed art works while storage in the RINA was reserved for the RINA archive.

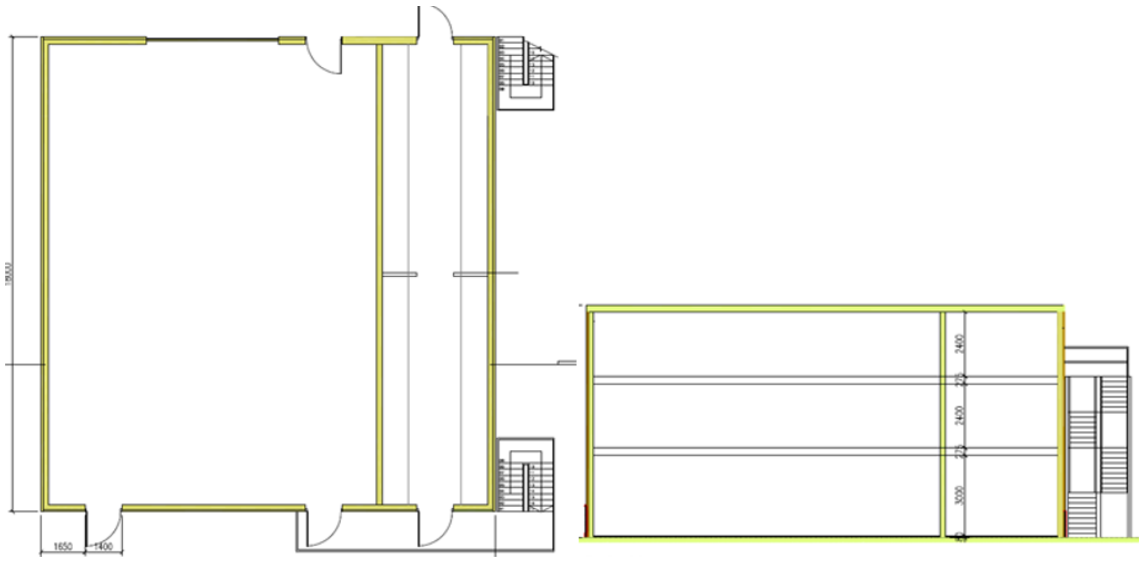

Figure 4.3 Room layout and building elevation (Emission Zero, 2011)

The rafters of the hangar limited the over-all height of the building to 8.9 m. Due to the height of some of the carriages, the ground floor ceiling was set at 3.31 m, with a useable storage height of 3.08 m, which reduced the ceiling height of the two other floors to 2.51 m, giving a useable storage height of 2.26 m. This resulted in a overall usable storage capacity of 2,179 m^3. With a view to future repurpose for archive storage, the overall design complied with archival standards for not only RH and temperature but also lighting and floor-loading.

The environmental remit for the initial proposal was to meet specifications from *BS 5454:2000* (BSI, 2000) with a temperature at a fixed point in the range 13°C to 16°C ±1°C and an RH at a fixed point in the range 45% RH to 60% RH ± 5% RH (Eberlin & Carter, 2011). SMG environmental guidelines were revised during the design process to a daily temperature between 16°C to 19°C ±1°C and 40% RH to 55% RH ±5% RH, with allowance for limited seasonal drift between low and high limits.

Tradical® Hemcrete® (Appendix C), a proprietary formulation of HLC produced by Lime Technology (Lhoist UK), was chosen for its documented thermal and hygroscopic properties in order to achieve stable conditions within the store without reliance on continuous use of mechanical air conditioning and heating. Empirical data was obtained from a variety of sources (including contemporary results from the DEFRA research project on Hemcrete® at the University of Bath) to demonstrate that the moisture buffering ability of Tradical® Hemcrete® would be capable of creating a stable internal RH, at both a lower level and a slower rate of change than externally. The initial construction proposal, detailed in Chapter 3, proffered exceptionally low operating costs, inherent thermal inertia and humidity buffering even in the event of a power or control failure and an airtight structure by using Tradical® Hemcrete® in pre-cast wall panels (Eberlin & Carter, 2011).

Tradical® HF, an aggregate produced from the stem of industrial hemp grown in the UK (Figure 4.4), was processed for construction purposes by removing the fibre, then chopping, grading and de-dusting the shiv (Figure 4.5).

Figure 4.4 Industrial hemp grown in Suffolk for Tradical® HF

Figure 4.5 Shiv processed for construction mix

This was then mixed with Tradical® HB, a pre-formulated binder based on a high purity hydrated lime blended with cement (hydraulic lime), pozzolanic and mineral additions, and water to produce Tradical® Hemcrete® (Tradical, 2014) (Figure 4.6).

Figure 4.6 Mixing shiv with binder

The panels used to construct the store walls were a modification of the pre-cast wall product Hembuild® (Appendix C), produced by Lime Technology. The standard wall system incorporates internal softwood timber studs within a timber cassette formed from a Glulam base and head member and plywood side pieces. 9 mm thick Multi-Pro XS Board, a white medium density magnesium silicate fire retardant board, is used for the inner face. Manufactured from inorganic minerals (SiO_2, $CaCO_3$, MgO, $MgCl_2$) and fibreglass mesh, Multi-Pro XS has an A1 fire rating, low thermal conductivity, moisture and water resistance, rodent and mould resistance and breathability (Resistant Building Products, 2015) (Appendix C). 120 mm of Tradical® Hemcrete® (Appendix C), with a density of 330 kg/m^3 (Tradical, 2014) is cast against the Multi-Pro XS, then 90 mm to 180 mm Breathe™ hemp fibre insulation and a breathable airtightness membrane added. A cladding system completes the outer face.

The panels used for the storage building were modified by increasing the thickness of Tradical® Hemcrete® to 195 mm and eliminating the insulation layer as the emphasis was to be on greater humidity control than temperature regulation (Pritchett, (*pers.comm*), 25.02.2014). Panels used for the interior walls were lined on both sides with Multi-Pro XS which eliminated the need for plastering and painting. Panels used for the exterior walls were lined on the outer face with a breathable airtightness membrane (Figure 4.7; Figure 4.10). Testing based on *BS 476: Part 22:1987* for fire resistance integrity achieved 88 minutes for the exterior panels (BRE Global test report number 269397) and 180 minutes for the interior panels (BRE Global test report number (269398).

Figure 4.7 Example section of the modified exterior wall panel

After casting and light tamping to finish the exterior face (Figure 4.8) the HLC panels were air-dried for several days (Figure 4.9).

Figure 4.8 Finishing off process for cast panel

Figure 4.9 Panels air drying

A total of 742 m^2 HLC panels were used, 606 m^2 for the external walls and 136 m^2 for the interior walls. Panels were given a U-value of 0.22 $W/m^2 \cdot K$.

Figure 4.10 Completed exterior and interior wall panels

In order to support the high floor loading required for archival storage as specified in *BS 5454:2000* (10 kN/m^2 to 12 kN/m^2), groundworks were required to cut a 17.88 m by 18.78 m hole out of the existing concrete floor slab (Figure 4.11) to allow foundations to be laid on the harder chalk soil found approximately one metre below the slab. Column pads were founded on the firm chalk at a minimum depth of 1150 mm with foundation trenches dug at a minimum depth of 875 mm. An initial layer of 25 mm sand, followed by a layer of 100 mm rigid insulation (Celotex rigid polyurethane foam) sandwiched between 1000 gauge damp proof membrane was

laid under the new 150 mm GEN 3 concrete floor slab (Figure 4.12) (Sylva Group, 2011). Concern was expressed by the contractors prior to pouring that drying of the concrete would be an issue. The concrete slab was poured mid-February 2012 and painted prior to racking installation in mid-May 2012. No specification for the paint used was documented. The original design had been provided a CLT floor over the slab but this would have caused a lip which would hinder movement of large objects in and out of the store.

Figure 4.11 Groundworks for HMS foundations & floor slab

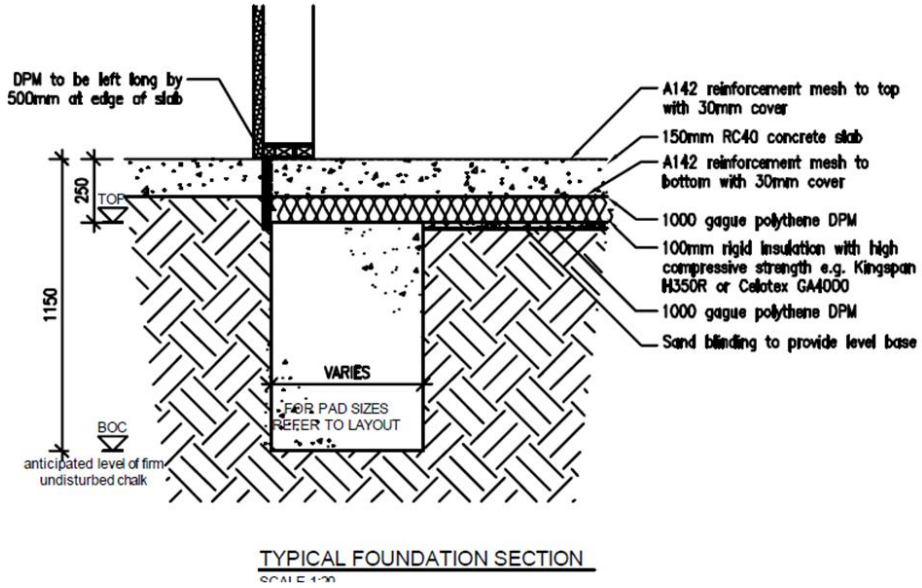

Figure 4.12 Detail of column footings & floor slab (Sylva Group, 2011)

The prefabricated panels were used to clad a three-storey high steel superstructure (Figure 4.13). They were slotted into place then tied back to the steel frame with coach or wood screws. The structural steelwork used universal beams (UB) and

universal columns (UC) for the framework with circular hollow sections (CHS) used for bracing. The steel framework was coated with intumescent paint.

Figure 4.13 HLC panel installation on steel framework

All paper joints and laps were sealed with 60 mm wide breather membrane (Siga Sicrall) lap tape to enhance airtightness. Interior joints were faced with additional strips of Multi-Pro (Collins, 2012). The HLC panels were externally clad with a layer of vapour permeable 80 mm thick Pavatex (Hofatex® Therm) (Appendix C) wood fibre insulation board (Figure 4.14) and a layer of 'rat mesh' (Figure 4.15).

Figure 4.14 External cladding of wood fibre insulation board

Figure 4.15 Detail of "rat mesh"

A 1200 mm high skirting board of Multi-Pro XS board was installed at ground level for additional rodent resistance. Figure 4.16 is a schematic of the wall layers at ground floor level. The total U-value of the wall panels, at an overall thickness of 285 mm, was given as 0.22 W/m^{2}·K.

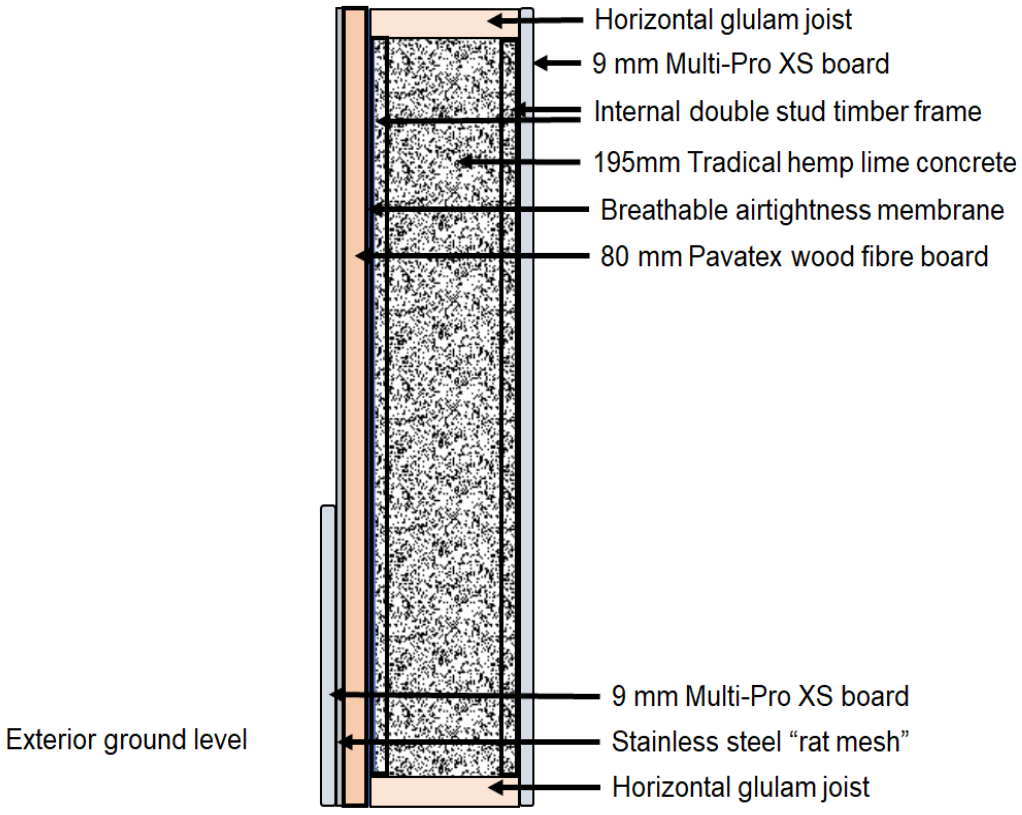

Figure 4.16 Schematic of exterior wall layers

The roof layers included 95 mm Cross Laminated Timber (CLT) between steel beams, 100 mm hemp fibre insulation between the rafters, with a breathable airtight membrane over the timber structure, then 100 mm Pavatex® Hofatex® Therm and 15 mm plywood decking, with a weight load of 2.5 kN/m^2 (Sylva Group, 2011). The U-value of the roof was given as 0.15 W/m^{2}·K. Double skinned steel doors and sectional overhead doors insulated to a U-value between 0.8 and 0.9 W/m^{2}·K were provided with extra lip seals to reduce air and heat loss and installed into steel frames. Overall the building envelope met the design air permeability target of 1.0 $m^3/(h{\cdot}m^2)$ @ 50 Pa when tested for airtightness upon completion (Chambers, 2012).

Intermediate floors were formed using sustainably-sourced spruce 162 mm thick CLT planks, chosen for high structural strength, excellent dimensional stability and vapour permeability, to span the structural steel beams. In order to increase floor-standing space in the BOX storerooms, the floor weight specification was reduced and access spaces left for future installation of additional steel columns were capped (Figure 4.17). After installation, the CLT planks were treated with Envirograf Product 92 clear fire protection coating (Appendix C). As no information on vapour permeability is available, its use likely affected the vapour permeabilityof the CLT, reducing potential buffering.

Figure 4.17 CLT intermediate floor with floor cap in place

Access to the upper storerooms was provided via external free-standing steel frame staircases, one at each north corner of the building, with steel frame balconies floored with insulation board (Powerdeck). Each BOX room had a personnel door and sectional overhead door at the front and a rear fire exits (two fire exits on the ground floor); each RINA room had a personnel door at the front and a fire exit at the rear (Figure 4.18); all doors opened directly into the hangar. Doors were edged externally with Multi-Pro board strips for wall protection. Gates were inserted into the railings of the decks in front of each store on the first and second floors to allow archives and objects to be delivered on pallets using a reach truck. A small lift, suitable for conveying art works and archival material, was later installed at the SW corner

Figure 4.18 Front face of the HMS with external access framework & doors

Breakdown costs for the total project, including construction works and materials, drawn from the final valuation of 31 March 2012 and budget update of 26 April 2012, are given in Table 4.1. Final project costs, including costs for the lift, were £1152/m^2 which was a 1% increase on the intial projected costs of £1140/m^2. Figure 4.19 charts the breakdown of percentage costs for the project for construction, fit out and services installation, professional fees, enabling works and contingencies. Figure 4.20 charts the percentage breakdown for the construction materials, with the Hembuild walls being 24% of the material costs or 11.5% of the total project costs. Costs per m^2 are included for the materials of the building structure with the exception of the steel frame, which are given in costs per tonne.

Table 4.1 Costs for construction works & materials

Nature of work:	Project Cost £	£ per
Groundworks & foundation	48,000.00	156/m^2
External Hembuild walls	98,172.00	159/m^2
Internal Hembuild walls	19,828.80	
Ground floor- concrete	12,000.00	130/m^2
First floor- CLT	39,320.00	128/m^2
Second floor- CLT	39,320.00	
Roof structure, insulation & covering	43,042.05	140/m^2
Steel portal frame	95,000.00	3.65/tonne
Wood fibre board	12,000.00	20/m^2
Rodent mesh	6,000.00	10/m^2
Vapour Control Layer tape	1,636.20	
Doors	24,333.70	
Stairs & galleries	41,660.00	
Erection of superstructure	62,000.00	
Scaffolding/MEWPS/access	33,750.00	
Floor painting	2,000.00	
Construction costs	103,452.50	
Delivery	10,000.00	
Cranage/plant	10,800.00	
Racking	27,062.00	
Lift	30,935.00	
Low level robust finish	8,100.00	
Air tightness test	1,350.00	
Engineers fee	55,350.00	
Architects fee	16,200.00	
Other Professional fees	62,030.10	
Consultancy	6,592.00	
Contingency	46,793.50	
Prelims & overhead	49,800.00	
Other project costs	4,250.00	
Security upgrade	7,700.00	
Total	**1,129,700.68**	

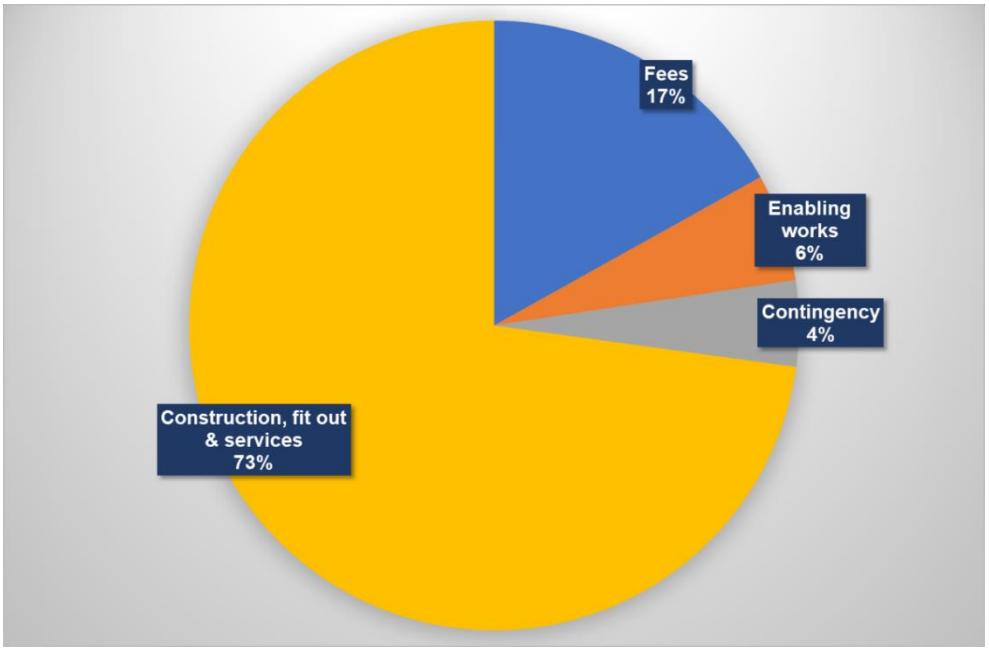

Figure 4.19 Breakdown of percentage project costs

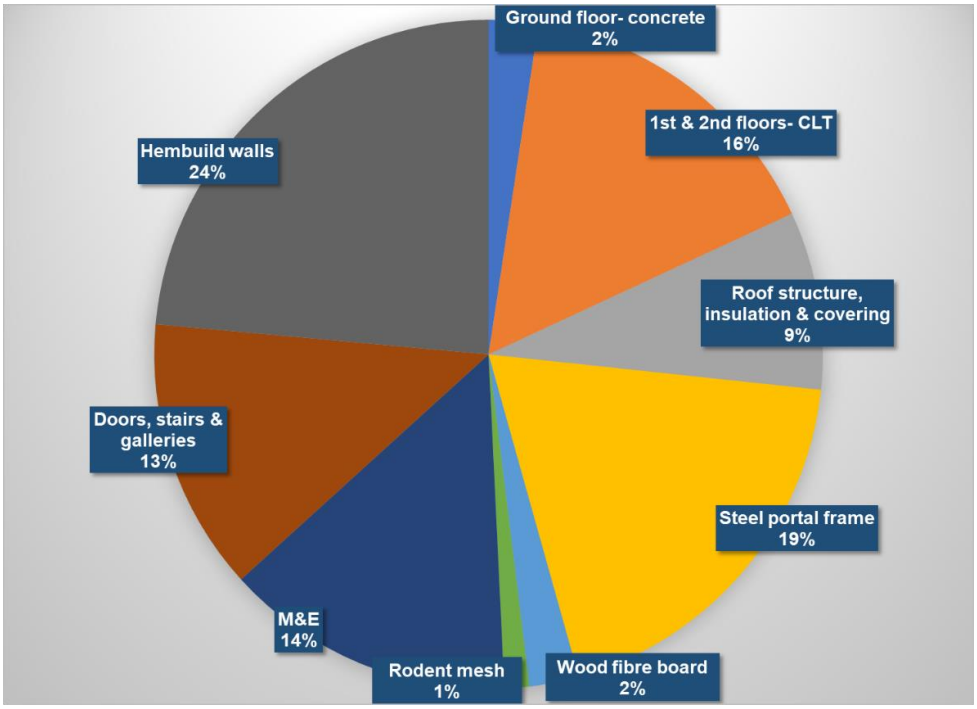

Figure 4.20 Breakdown of percentage construction materials costs

The internal environment was to be maintained to SMG recommendations for temperature and RH with low reliance on AHU plant, anticipating passive regulation of temperature and RH by the HLC walls (Jankovic, 2012c). There was to be limited heating and cooling was to be achieved only by free cooling, bringing in external air cooler than ambient store temperature. The air handling system was to run continuously only during the winter months with passive seasonal drift allowed through more temperate periods. Initally, as the RINA and the BOX were intended for the storage of different materials, each section was to have its own AHU and

separate ducting system but this was altered in the final design as a result of value engineering undertaken during the final design review. Two mechanical ventilation heat recovery units with cross flow plate heat exchanger were installed on the roof of the building with one handling the ventilation to HMS 5 and 6, the other to HMS 1, 2, 3 and 4 (Figure 4.21). A schematic of the MVHR unit is provided in Figure 4.22. Breakdown costs of the total M&E system, including design, installation of equipment and environmental monitoring, are given in Table 4.2. Costs of the M&E system accounted for not quite 10% of the total project costs.

Figure 4.21 AHU1-FF, unit supplying HMS 1, 2, 3 & 4

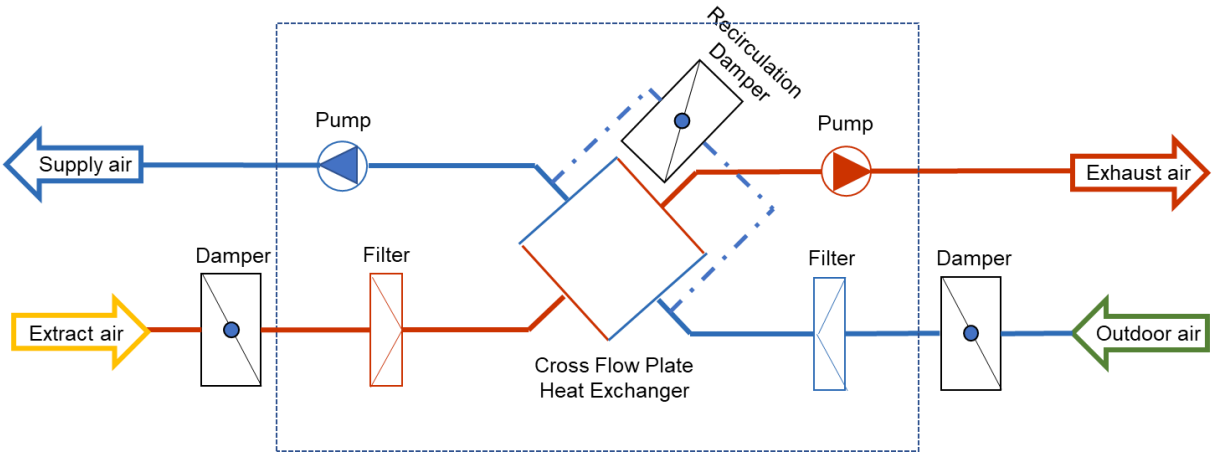

Figure 4.22 Schematic of air handling system

Table 4.2 Total costs of M&E system

Nature of works	Cost £
AHUs	9,723.04
Ductwork, BMS	60,500.00
Lighting, power	11,951.93
Fire detection	6,628.00
Monitoring	7,479.00
Electrical upgrade	8,348.86
Design & consultancy	6,592.00
Total:	**111,222.83**

Labelling on the final plans for the air handling system (Figure 4.23), which showed both AHU units supplying the second floor, along with the change in zoning, resulted in confusion when assessing system operation during the transient and first steady states of the HMS. The conservation team was unaware that there had been design changes resulting in a cross-over of the system and that the original intent to provide two separate environments, one for archives and the other for museum objects, had been lost. In the BMS, the units were labelled as AHU1 – RINA and AHU2 – FF and the facilities (Estates) team assumed that one AHU served the RINA and one served the BOX. This resulted in operational errors during the initial steady state period when the Estates team took over the running of the HMS system from the contractor. RH/T monitoring data was used to clarify the system design and operation.

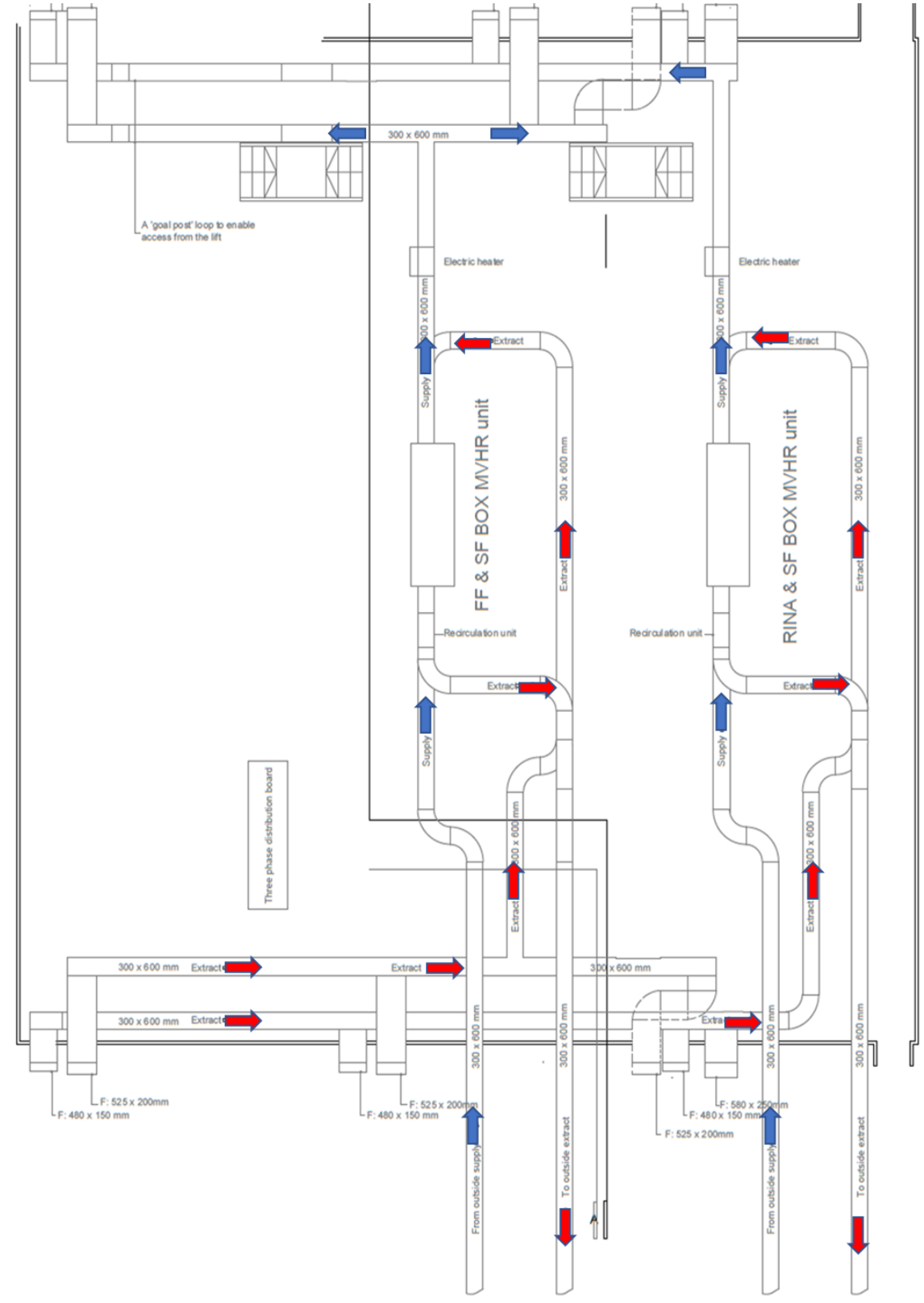

Figure 4.23 Air handling system as installed (Emission Zero, 2012)

From the AHUs, ducts ran along the front edge of the roof, with vertical supply duct risers installed externally on the front face and extract risers on the back face of the building. A horizontal air duct at ceiling height with four 300 mm x 150 mm supply

grilles ran from the supply duct through HMS 1, 2 and 3 with a 480 mm x 150 mm extract grille connected to the extract duct at the rear. In HMS 4, 5 and 6, air was introduced through the supply duct risers through three 480 mm x 150 mm supply grilles at intervals along the front of each room, at ceiling height, and extracted through three 480 mm x 150 mm extract grilles along the back, at ceiling height (Figure 4.24). Supply and extract grilles were fitted with balancing dampers as well as fire dampers. The system both admitted and recirculated air. The potential impact of air movement or temperature stratification on RH was anticipated to be regulated through the high thermal inertia and hygroscopic properties of the HLC (Jankovic, 2012c).

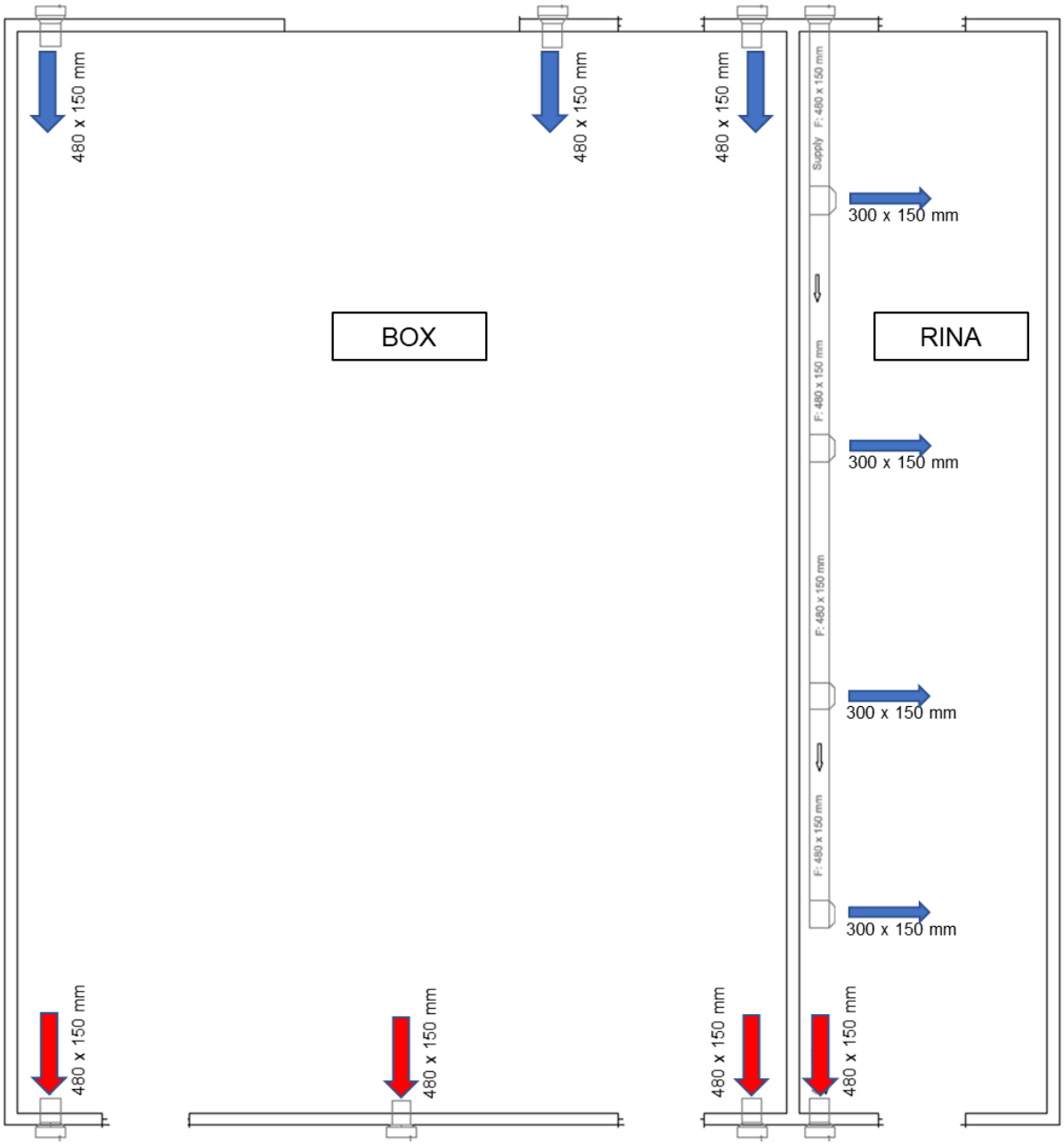

Figure 4.24 Location & size of supply & extract grilles in the HMS

The air handling system as installed was revised from a system proposed during the design phase which had included heating, cooling, humidifying and dehumidifying in order to achieve the very tight environmental parameters initially requested by the NRM Archivist for the storage of the RINA archive. Broadening the environmental specifications and including the anticipated passive performance of the building envelope to augment RH and temperature regulation led to the design changes and a much-reduced plant type. A description of the development of the air handling system will be found in Chapter 5 along with the operational issues of the installed system during the transient and initial steady states of the HMS.

After construction was completed, the storerooms were given location codes in the collections management database (Figure 4.25). The three RINA rooms were numbered HMS 1, 2 and 3, from ground to second floor. The three BOX rooms were numbered HMS 4, 5 and 6 which fortuitously followed the AHU zoning.

Figure 4.25 Completed building showing location codes

During the transient state, storage furniture was installed in four of the storerooms. Static shelving for archival material storage was installed in HMS 1, 2 and 3. Open mesh art racking, suspended from rails secured to the ceiling, was installed in HMS 4. While the initial reason for constructing the HMS had been for storage of the RINA archives, by the end of this research project they had still not been delivered to site. HMS 1 was temporarily repurposed for the storage of HR records and taken out of the research project scope as access was restricted. A limited amount of ephemeral material was stored in HMS 2 during the second steady state.

The first collections to be moved into the HMS, during the first steady state of operation, were the very large historic ship models coming out of the museum's Shipping Gallery. Predominately scale models of fully rigged sailing vessels, they dated from as early as the 1670s up to the 1950's, with over half being made between 1820 and 1920. Ship models are inherently fragile composite objects,

composed mostly of organic materials such as wood and textiles but also metals, glass, ceramics and paints. They are very susceptible to changes in RH, with potential for physical deterioration to organic materials, such as lifting, warping and swelling in high RH and cracking, delaminating and splitting in low RH. High RH can lead to metal corrosion and paint discolouration. Fluctuations in RH will accelerate deterioration as components are generally thin and held under tension.

The models had been on exhibit in the gallery since the 1960s, and had become acclimatised to a stable environment below 35% RH. In order to remove them safely from the museum, each model was packed inside a bespoke crate. The crates were lightweight timber frames on pallet bases, with a cover of 250 mm clear polythene sheeting secured to the inside of the frame and sealed on the outside with aluminium tape. The crates were tested prior to use and found to minimise RH fluctuations sufficiently to prevent deterioration during transport. All ship models were photographed and their condition recorded before removal from the gallery, with conditions being assessed and recorded again on delivery to the HMS. As the RH in the HMS was intended to be regulated between 40% and 60%, higher than in the gallery, it was decided to leave the ship models in their crates as this would slow down any material reactions to the change in humidity levels. It was still possible to inspect their condition through the polythene. The large ship models were stored in HMS 5 with the exception of three very large models, which were stored on the ground floor, in HMS 6.

Half-block ship models were moved to the HMS from the Science Musuem's Blythe House store in Olympia, West Kensington, during the second steady state of operation. These had been stored on shelves in a number of different storerooms at varying levels and fluctuations of RH. Half-block models are largely made of painted wood with metal fittings, mounted on wooden backing boards. Due to past use such as display in shipping company offices, they can be in poor condition and susceptible to cracking, splitting, warping, paint lifting and loss and metal corrosion. Each half-block model had a condition assessment after delivery to site. Half-block models were hung uncovered on the art racking in HMS 4.

The horse-drawn carriages had been stored for a number of years in the unheated hangars on the NCC site.There had been biological deterioration caused by mould growth and insect (moth) activity on textiles, leather and wood and chemical deterioration through corrosion of iron and brass components. Physical deterioration of leather, textile and wood components had resulted in splitting, warping, delamination and loss of strength. Surface varnishes and waxes had turned cloudy under exposure to prolonged periods of high RH. A six-month conservation cleaning project undertaken in 2010 had stabilised their condition with a full condition report produced for each carriage treated. The carriages were stored for two years after treatment in the conservation facility, at an RH that fluctuated seasonally between 30% to 70%, before being moved into HMS 6 during the first steady state of operation. As space was tight in the storeroom, most were left uncovered in order to be able periodically to review their condition.

The framed works of art had been exhibited or stored in three main locations prior to being moved to the HMS. Many of the works were oil on canvas, painted from the 1700s to the 1900s. Oil paintings on canvas are susceptible to damage by changes

in RH. Canvas, held under tension on the stretcher, can warp, twist, split, lift, tear, buckle, cockle or sag. Each layer of the painting, from the ground layer through the paint layers to the varnish, can react to RH fluctuations in different ways by swelling, lifting or cracking, Other works of art were on paper, art board or wooden panel supports, each likely to be affected by fluctuation in RH in the same ways as canvas supports. Most significantly, paper under high RH loses strength but under low RH become brittle. Discolouration through chemical deterioraton or biological deterioration by mould growth are likely under high RH. Many of the framed works had been exhibited in the Shipping Gallery and were moved into HMS 4 during the same period as the ship models. These had been acclimatised to an RH level below 40% for decades. Some framed works of art had been stored in a location in the museum's basement where there was an overhead waterpipe and a constant risk of water damage. Annual RH in the basement of the museum fluctuated seasonally from less than 20% to over 60%. The third main location was on the ground floor of the museum's Blythe House.The seasonal RH in the storeroom fluctuated between 25% to 60%. The framed works of art were moved from the Science Museum and Blythe House onto the art racking in HMS 4 over both steady state periods as time and resources allowed. Each work was assessed for condition when delivered to the store. While framed works were protected from RH fluctuations by glazing and backing boards, most of them had been displayed or stored for decades at RH levels much lower than anticipated in the HMS. Hanging the framed works on art racking allowed for condition checking of both front and back of each work.

By the end of the research project, 401 framed works of art, 30 carriages and 238 rigged and half-block ship models were stored in the three large storerooms of the HMS. The condition of all collections in HMS 4, 5 and 6 were periodically reviewed throughout both steady states of operation, with a final condition assessment carried out at the end of the research project.

4.4.2 Other museum stores on NCC site

Environmental monitoring data from other stores on the NCC site has been used for comparative purposes in this research. These were the unheated hangar building itself (hangar D2), the low energy repository constructed for the library and archive reserve materials and an unheated collection objects storage shelter, both in hangar D2, and a free-standing low energy storage building, the A Store.

4.4.2.1 Hangar D2

Hangar D2 was situated in the lower south-east area of the NCC site on a N-S orientation. Built circa 1940 of reinforced cast concrete, it had a footprint of 41.6 m by 91.2 m, with a useable internal height of 10 m due to the rafters but an overall volume of 45,527 $m^{3.}$ Walls were *in situ* cast concrete to the high-level window sills, with pairs of internal concrete piers supporting the concrete bow-strung roof trusses which provided drainage from the roof to internal storm drains. The curved roof decking was concrete as was the floor, both cast *in situ*. Externally at roof level, a deep concrete canopy projected above the concrete transom over a row of windows on the long sides of the hangar, continuing in the wall line to form a parapet. At the short ends, the parapet merged with horizontal projecting rails which carried the

track for the suspension of 6 full-height steel doors. A channel drain ran the full width of the hangar at each end just inside the doors.

Refurbishment to the hangar had occurred in two phases. The first, undertaken in 2006, was limited to cleaning the interior, removing asbestos cladding and lead paint, and sealing shut the north hangar doors. In 2011, the hangar doors at the south end were replaced with 81 mm Kingspan KS1000RW composite wall panels (50 mm insulated core; U-value 0.38 W/m^{2}·K) (Appendix C) and a sectional overhead door. The hangar doors at the north end were removed and the space filled in with Kingspan panels. Door projecting rails were removed as was the asbestos-clad annex on the west side. The windows were blocked in and some concrete repairs undertaken (Figure 4.26). The roof was not replaced nor was there any additional insulation added to the walls or ceiling. Subsequent to the refurbishment, wire mesh was attached over the external face of all the walls due to continuous spalling of the concrete exterior. While both phases of refurbishment were enabling works for the construction of, firstly, the L&A store and, secondly, the HMS, the costs of neither phase were included in the capital costs for the storage building projects.

The original hangar heating system had been made redundant in 2004 and was not replaced. There was therefore no mechanical control of RH. The thermal mass of the building was inadequate in mitigating the external environment to meet SMG requirements as the building only afforded protection from wind, rain and extreme external conditions. RH levels averaged between 60% RH and 75% RH in summer to 75% RH to 90% RH in the winter.

Figure 4.26 South end of hangar D2 with completed renovations

4.4.2.2 Library & Archive Reserve Collections Store (L&A store)

In 2006, a single storey 1968 m^{2} structure, with a ceiling height of 4.5 m, overall volume 8,856 m^{3}, was erected within the north half of hangar D2 for the storage of the SCM's reserve L&A collections. The specifications were for a temporary (25 year life span) single storey free-standing storage structure, consisting of a highly-insulated, water-sealed and pest resistant perimeter wall and ceiling, on the sealed hangar slab (no groundworks).The structure was to be as airtight as possible in order

to assist in maintaining a stable storage environment for books and paper, with a total energy load of less than 80 kWh/m^2 (Leitch, 2006). While the museum's sustainability team had suggested that the building incorporate floor insulation, airtightness and passive humidity control through the use of hygroscopic building materials (Zammit, 2006), the end product was a traditional mezzanine floor construction, with steel columns mechanically fixed to the hangar's concrete structural slab. The original budget was £800,000.00 with final costs being £1,039,210.00 or £528/m^2 (2007 valuation).

The free-standing structure had a service/ fire corridor running around the perimeter on three sides, with fire exits on the south face from the entrance vestibule and the store itself opening directly into the hangar (Figure 4.27; Figure 4.28).

Figure 4.27 South end of L&A store, in hangar D2

The non-load-bearing roof was 38 mm chipboard decking with a membrane covering, laid on the upper side of a free-standing steel framed structure bolted to universal steel beams supported by the steel columns. Tthe ceiling was formed by two layers of moisture resistant Gyproc Fireline board (Appendix C) on the lower side of the steel framework. The cavity contained an insulation quilt with a U-value of 0.34 W/m^2K. Walls were 146 mm galvanised steel stud partitioning clad with two layers of standard wallboard on the inner side and one layer of Gyproc Duplex board (standard gypsum plasterboard backed with a vapour control layer) (Appendix C) and one of standard wallboard, with cavity insulation of 0.34 W/m^2K (odbcontracts, 2006). When tested for airtightness in accordance with BS EN 13829:2001, it was given an air permeability rate of 0.84 $m^3/(h{\cdot}m^2)$ @ 50 Pa, which satisfied the BSRIA (1998) requirement to achieve an air leakage rate of 2 $m^3/(h{\cdot}m^2)$ @ 50 Pa.

A 400 mm high impervious PVC skirting was installed internally to reduce the chance of water ingress and a 400mm high stainless-steel mesh was sandwiched within the outer skin to discourage rodents. Doors were steel construction. Initially, due to a budget shortfall, the interior plasterboard was not sealed or coated and dusting became a major issue in the store. Painting the interior was undertaken some time

after the 3.75 m high, high-density mobile shelving storage furniture and the collections had been installed.

The internal environment was to be kept at 13°C to 18°C with an RH within 55% to 65%. The original intent had been to use as little mechanical plant as possible but an HVAC system was installed. The plant (Appendix B), with a biomass (KWB USV Woodchip) boiler and a VES Ecovent air handling unit, was housed in an external container unit on the west side of hangar D2 (Figure 4.28). The biomass boiler was chosen for its sustainability credentials and because both gas and electrical supplies were limited in the area (Zammit, 2006). The air handling plant supplied heated air at a rate of 3.3 m^3/s, with a minimum air change rate of 5 ach/hr and was run continuously despite the initial intent to limit operation. The ducting ran from the plant through a housing built against the west wall of the hangar and through the perimeter corridor into the store itself (see Appendix B). Supply ducting ran along the west and south walls, with five supply grilles spaced evenly along the south run, one supplying the vestibule. The return ducting ran along the north and west walls, with five exhaust grilles on the north run. The air intake for the ventilation plant proved to be undersized, so velocity drew in moisture from rain and snow into the AHUs with significant mould growth on the pre-filters, leading to contamination of the filters (Flower, 2018).

Figure 4.28 Plan of L&A store, external location of M&E & internal corridor

From May 2017, the RH was sustained at a high enough range, between 65% RH to 75% RH ±5% RH, to support mould growth on a number of book spines and covers. Mould growth was further exacerbated by poor air circulation where the aisles of the high-density mobile book shelving were left closed. Paper percentage moisture content readings showed an average of 11% to 16%, with 13% being considered extremely high for paper. Dehumidification units were introduced into the store from

October 2017 but mould outbreaks persisted. A permanent solution to the high humidity and mould issues of the store was still not implemented by February 2020.

4.4.2.3 The A Store

The only free-standing purpose-built storage building on site, the A Store was built in 1992-1993 at the north end of the NCC site, at a cost of £2.9 million, to hold medium-sized scientific and industrial heritage collections (Figure 4.29). It consisted of a 35 m by 90 m by 10 m high insulated (68.6 mm polystyrene) structural steel frame set on insulated concrete pad bases with double polythene damp proof membranes, with external horizontal composite cladding panels hung on the mainframe and mullion supports from ground to roof. It had a flat steel deck roof with a single ply synthetic felt membrane laid over insulation and a vapour retardant. There were two large storage areas on either side of a central loading and reception area. The outer double loading bay had two overhead sectional doors to outside and one overhead sectional door to the inner reception bay. Overhead sectional access doors, one on either side of the reception bay, led into the two stores. There were two mezzanine floors, one at the front of the building with office (converted to textile storage in 2010) and welfare spaces, and one at the back, with two AHUs and a cooling and humidification (steam)/dehumidification (desiccant) plant. Another plant room for two oil-fueled boilers and one AHU was located on the ground floor, to the rear of the reception area and below the mezzanine plant room. The finished building envelope had an area of 3,150 m^2 and an overall volume of approximately 32,000 m^3. Just over two-thirds of the volume could be considered usable storage space, with the two main stores each being just over 11,000 m^3. The two ground floor stores were furnished with eight metre high racking, 28 rows of mobile pallet racking on the west side (A1) and 10 rows of static pallet racking on the east side (A2). A floor plan is presented in Chapter 6, Section 6.3.2. Airtightness testing by BSRIA was reported by Laurin & Scott (1994) to show an excellent air-leakage rate performance based on BSRIA standard of 2 $m^3/(h{\cdot}m^2)$ @ 50 Pa but no figures were recorded. Infiltration rate was set at 0.15 air changes/hour in the stores (Read, 2011).

The HVAC system was intended to provide separate zones of specified conditions for the two ground floor storerooms, with sensors for the BMS located throughout, and fresh air supply and extraction from the two AHUs on the mezzanine. The ground floor AHU provided fresh air supply and extract to the rooms on the mezzanine. Jet nozzle diffusers, high capacity diffusers with jet-type airflow, introduced supply air from ceiling height (10 m) ductwork in the ground floor storerooms. Extraction grilles were at low level. This was intended to provide recirculation of air throughout the rooms but air flow from the supply nozzle diffusers was blocked by the racking, with the result that the floors were subject to condensation since the heated air could not reach the lower level of the stores. The boilers served the low temperature hot water (LTHW) coils within all AHUs as well as a number of radiators located throughout the building. Heating to the external loading bay was provided by two warm air blowers which operated when the external sectional overhead doors were opened. These were undersized, allowing external conditions to affect both the inner bay and main stores. The original specifications of the building were for 55% RH ±5% RH and a temperature of 14°C ±2°C but the tight parameters were never achieved. The original brief was for:

> *“a comprehensive and computerized building management system which would control and monitor the plant. The system should maintain appropriate environmental conditions such as relative humidity and temperature…* (Laurin & Scott, 1994, p.154)

However, the humidistat system was never completed as designed. The desiccant dehumidification wheel system failed within the first two years of operation and was disconnected without repair or replacement since access was severly restricted as a result of initial installation. The condensers utilised for cooling were no longer operational by 2011 and air leakage rates through the AUHs were regarded as unacceptable (Read, 2011). Original design criteria stated that the external temperature was 0°C in winter but monitoring data showed that design conditions should be closer to -10°C, meaning the LTHW coils were undersized. The BMS could not be monitored or operated remotely. A seasonal RH drift within the range of 30% to 70% was achieved through continuous low-level heating but any failure to maintain boiler function resulted in periods of high RH and/or continuously fluctuating RH. The boilers reached their indicative life expectancy in 2019 and the circulating pumps in 2014. A survey for boiler and HVAC replacement but not dehumidification plant was undertaken in 2011 with capital project costs ranging between $276,000 and £587,000. The system was not replaced. Further details of the replacement costs are given in Chapter 7.

Figure 4.29 Front face of the A Store

4.4.2.4 Free-standing storage shelter

The RH level in hangar D2 was generally slightly lower than in other hangars on the NCC site with a slightly higher internal temperature possibly due to heat escaping through the perimeter corridor around the L&A store. Both the RH level and amount of fluctuation exceeded SMG recommendations for storage of cultural heritage collections, either temporary or long-term. In order to provide an additional level of protection for objects in temporary storage, in 2017 a free-standing steel framed

shelter was erected next to the library and archive store and across from the HMS. The 7.3 m d x 7.3 m w x 4.2 m h unit had a galvanised steel frame with a heavy duty 610 g/m^2 polyvinyl chloride (PVC) cover and a large roll-up door which could be more or less sealed shut using a velcro strip system (Appendix C) (Figure 4.30). The storage shelter in hangar D2 was unheated and without dehumidification so objects remained wrapped for additional protection.

Figure 4.30 Free-standing collections storage shelter in D2

4.5 Environmental Monitoring Equipment

A wireless telemetric environmental monitoring system, Hanwell Pro (Hanwell Solutions), had been installed by SMG Conservation in two locations in London, the SCM in South Kensington and the Blythe House storage facility in Kensington Olympia, to monitor RH and temperature in galleries, exhibition cases and storage rooms. The system was extended to the NCC site during the transient state of the HMS. Prior to the install of the telemetric system, monitoring of site storage conditions was undertaken using Hanwell data loggers, which used the same software programme for recording and downloading data as the telemetric system, and Tinytag data loggers, which used Tinytag Explorer software.

Over the period of this research, the telemetric monitoring system was modified, updated and extended. Hanwell and Tinytag data loggers were replaced by telemetric units. As the Hanwell Pro wireless system could be used to map and verify other environmental parameters as well as temperature and RH, transmitters to monitor moisture storage and air flow were added to the HMS monitoring programme. Data sheets for the equipment and software used for environmental monitoring will be found in Appendix D.

4.5.1 Telemetric monitoring system

A Hanwell Pro network-enabled smart base station receiver, SR2 (Figure 4.31), which collects and logs environmental monitoring data from multiple points within a site or across multiple sites, was connected to a 240V AC power source in HMS 5 and to the SMG environmental monitoring system via a local area network (LAN) point.

Figure 4.31 SR2 receiver (Hanwell, 2018)

4.5.2 Transmitter units

Three radio transmitter unit formats encorporating RH and temperature sensors were used to collect RH data for this research project (Figure 4.32). The units used were from the ML4000 RH/T range. ML4106 units are for internal use whereas ML4109 units are used to log external RH/T data. ML4114 units can be equipped with either 3 or 5m probe extension leads in order to reach less accessible areas. Temperature probes are either negative temperature coefficient (NTC) or resistance temperature detector (RTD) thermistors and RH probes are capacitive polymers (Table 4.3). The EE07-02 probe, used in the ML4109 and ML4114 loggers, combines capacitive RH and Pt1000 temperature sensors and is optimised for very low power consumption, so is well-suited for use in battery powered measurement units (E + E Elektronik, 2018). The nominal capacitance of the polymer HC105 used in the capacitive sensor is 160 ±16 pF (1.6×10^{-7} mF) at 30°C, making errors over the range 0% - 98% RH lower than ±1.5%/year (E+E Elektronik, 2018). The units were calibrated on-site annually using standard saturated salt solutions.

(a) (b) (c)

Figure 4.32 (a)ML4106; (b)ML4109; (c)ML4114 transmitter units (Hanwell 2108)

Table 4.3 RH/T transmitter unit specifications (Hanwell, 2018)

	ML4106 (a)	**ML4109 (b)**	**ML4114 ©**
T probe	NTC Thermistor	RTD- Pt1000	RTD-PT1000
Range	-20°C to +60°C	-40°C to +60°C	-40°C to +60°C
Accuracy	±0.3°C	±0.1°C at 20°C	±0.1°C at 20°C
Humidity probe	Capacitive Polymer	Capacitive Polymer	Capacitive Polymer
Range	10% to 90% RH non-condensing	0% to 100% RH non-condensing	0% to 100% RH non-condensing
Accuracy	±3% RH	±2% (0 – 90%); ±3% (90 – 100%)	±2% (0 – 90%); ±3% (90 – 100%)
T dependence	<(0.025 + 0.0003 x RH) [$[(\%RH)/°C$]	<(0.025 + 0.0003 x RH) [$[(\%RH)/°C$]	<(0.025 + 0.0003 x RH) [$[(\%RH)/°C$]

Logging intervals were set at 15 minutes for all transmitters, as per SMG monitoring protocol, which extended sensor battery life. The logging interval allowed enough reading updates to effectively chart the RH conditions for monitoring and research purposes. The SMG's system originally used RadioLog8 (rl8), an early software platform that ran on a variety of Microsoft based platforms. The system was not web based so access to the data was only through a portal installed on a site PC. Data files were exported in CSV format (IMC Group Ltd., 2007) with data viewable in tabular, graphical or plan views. The graphical view had a limited number of line colours and required editing for reporting purposes. While rl8 software was superseded by the Synergy software platform (HanLog32) in 2013, the SCM's monitoring system was not upgraded until August 2018, when Hanwell replaced Synergy with the Environmental Monitoring Software (EMS). EMS provided all the software features of RadioLog8 and was a more robust platform, employing a browser based Graphical User Interface (GUI) separate from the underlying hardware. Users could connect via any commercially available browser and access data via an Intranet or over the Internet. EMS also offered tabular, graphical and plan

views as well as an overview and exported data in CSV format. The software programmes continuously sampled the data received by the SR2 with daily, weekly, monthly, three-monthly, six-monthly or yearly graphical views. Historic RH/T data was in comparable format with current data altough the scales in the archived data could not be recalibrated, resulting in temperature scales overlying RH scales. In this thesis, graphical views of data from the Hanwell system prior to August 2018 have used rl8 software due to this issue.

4.5.3 Moisture monitor

In 2017, a moisture detection unit was added to the HMS monitoring programme, in order to see if a relationship between levels of internal RH and the moisture content within the HLC matrix could be determined. The Hanwell 16 Channel WME Sensor Unit (Dampwatch) (Figure 4.33), operated over a range of -20°C to +65°C in a non-condensing RH environment. The unit accepted up to 16 dampness sensors. However, sensors were not provided with the purchase of the unit and so this researcher manufactured sensors in-house. Internet research provided a blueprint (Frueh, 2017).

Figure 4.33 Dampwatch unit (Hanwell, 2018)

A 4 mm diameter stainless steel rod was cut into pins 100 mm in length, slightly sharpened on one end to facilitate insertion into the HLC walls, the other end keyed to allow soldering. Two pins were attached to a length of two core braided copper wire insulated cabling. The initial attempt at soldering the pins to the copper wire was not very successful given the small size of the wire and difficulty in soldering to stainless steel, with a propane torch being required to achieve the correct temperature. Instead, 4 mm red female bullet connectors were used as they fitted the pins perfectly and provided a secure push fit connection. This made a more user-friendly product as one end of a pin could be inserted into a connector after the other end was inserted into a wall. Their continuity was tested with a multimeter and was found to be good. The wire was soldered to the bullet connectors as well as crimped for the best connection. Making the sensors in-house allowed cable lengths up to a

maximum of 5 m in length, as signal loss could occur at >5 m. Varying cable lengths were attached to the pairs of pins so that the pins could be inserted into walls from floor to ceiling without excess cable in the way. The other end of the cable was inserted into the wall-mounted Dampwatch unit, with each braided wire strand connected to the terminal strip, two to each channel.

A template was made for drilling holes in the HLC walls to ensure the pins were inserted 20 mm apart (Figure 4.34). A marker made from red insulation tape was placed on each pin to ensure the pins were inserted 50 mm into the HLC matrix. A trial was run using the HLC exterior wall sample (Figure 4.35; Figure 4.36) under varying ambient humidities in the conservation facility, ranging from 30% RH to 70% RH The trial proved that the sensors were sensitive enough to provide data to the unit.

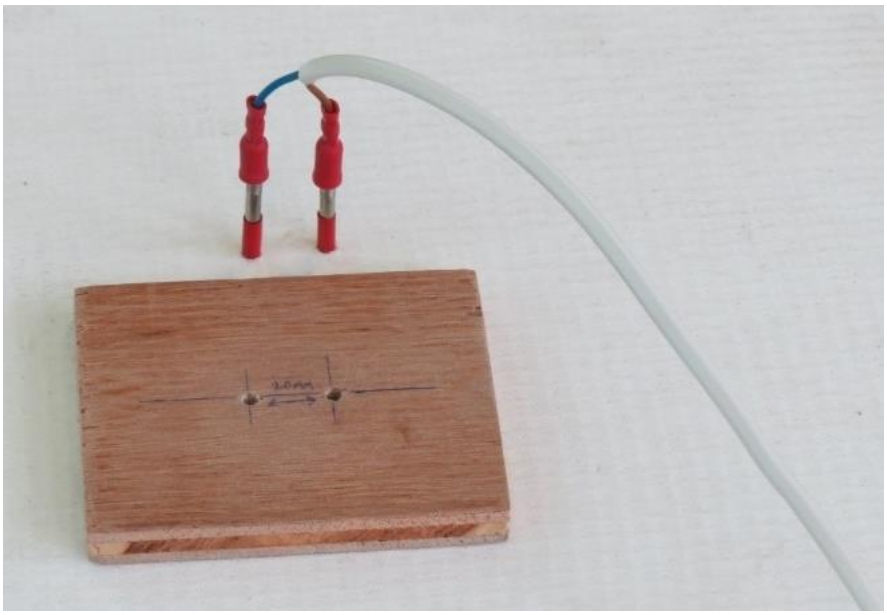

Figure 4.34 Sensor pair with drilling template

Figure 4.35 Components for sensor trials

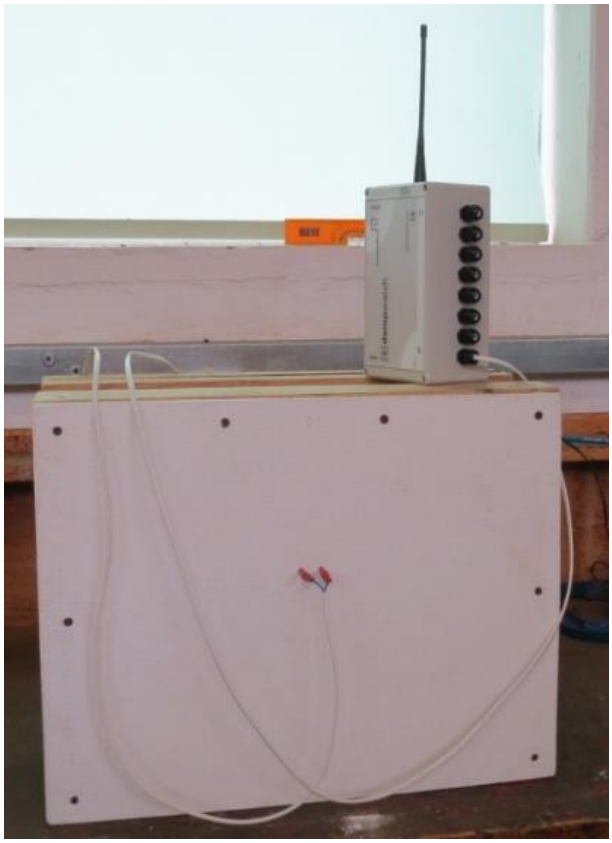

Figure 4.36 Sensor trial set up in ambient conditions in conservation facility

The Dampwatch unit uses construction industry-recognised Wood Moisture Equivalent (WME) measurements. WME is the moisture level in any building material as if it were in close contact and in moisture equilibrium with wood, expressed as percentage moisture content, MC (%), of wood (Figure 4.37). The construction industry uses the percentages from a generic wood as a relative scale. The Dampwatch sensor unit measures the resistance between the pins and converts the resistance value into the water content of beechwood. The water content levels are relative rather than actual as the theoretical WME is unlikely to be the same as the actual water content of the specific material being monitored (Hanwell, 2018).

The Dampwatch unit reads the WME (%) from a channel's sensor for an hour, transmits the reading for the following hour and then moves consecutively to the next channel, returning to a value of zero for a further hour after all channels have had readings taken. The sensor type is 'Dual Linear' with Channel **A** (red) representing the WME (%) and Channel **B** (blue) representing the Sensor/ Channel numbers.

Initially the Dampwatch unit logging interval was incorrectly set up with one reading every 15 minutes which resulted in graphs being improperly configured. Once the logging interval was reset to every 60 minutes, it allowed all of the channels' outputs to be shown consecutively on one chart. As each full cycle had one chartline, it was necessary to know the identity and location of each sensor to interpret the data (Figure 4.38).

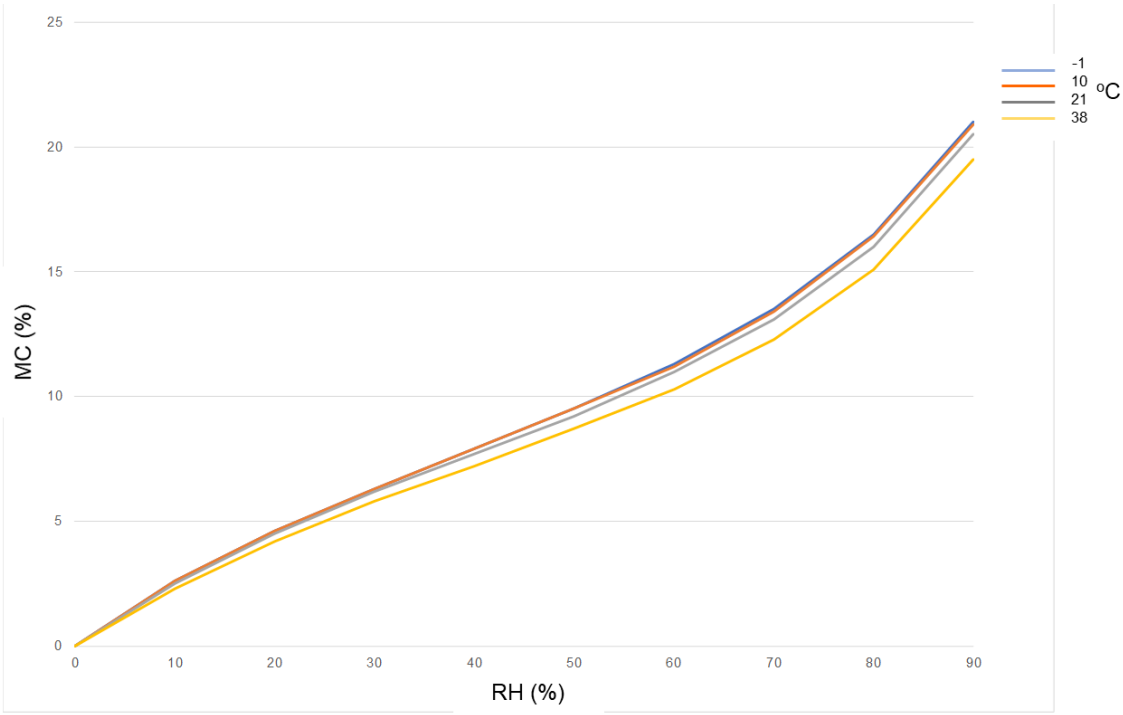

Figure 4.37 Generic wood equilibrium MC (%) under changes of RH & temperature

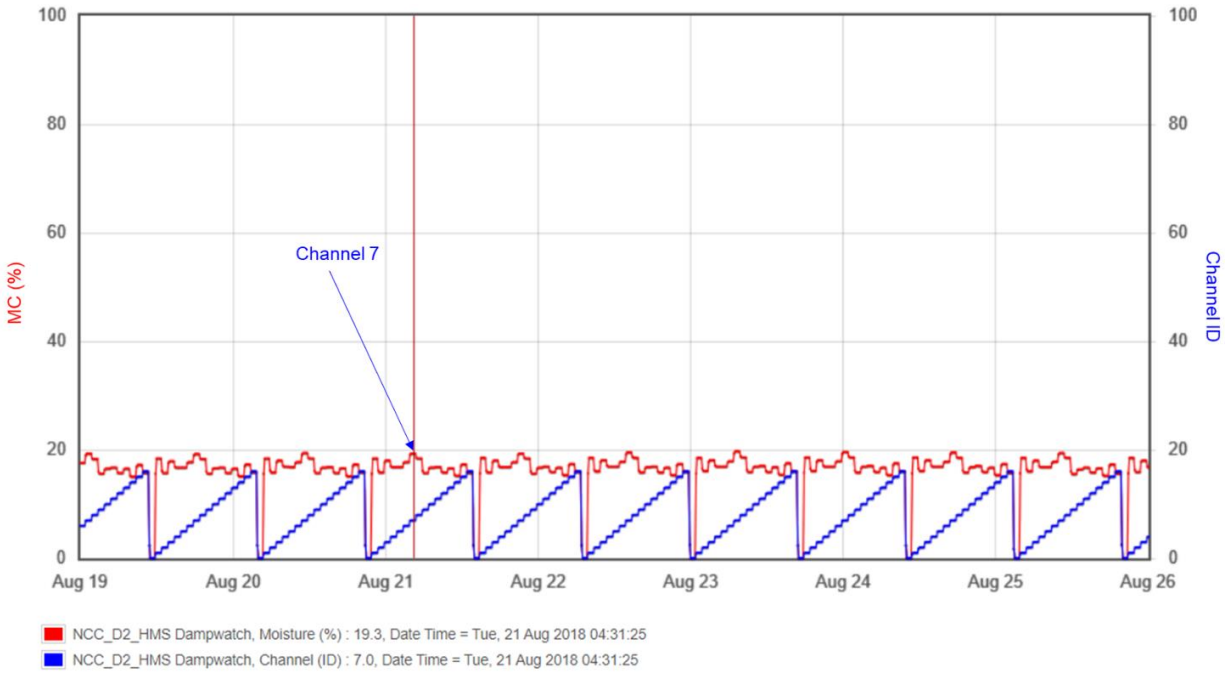

Figure 4.38 Dampwatch graph showing channel identification (Hanwell EMS)

4.5.4 Air flow meter

An ML4810 air flow tranmsitter (Figure 4.39) was added to the Hanwell monitoring system in the HMS in 2018 to identify operational problems with the air handling system. It was thought that data might also be used to identify the effects of ventilation on storage environment although, typically, air flow meters are used to

monitor air flow levels and alerts for door openings/closings and HVAC systems operation/failure. The data produced from the air flow meter was mapped to the data from the RH/T transmitters to see if a correlation could be made between an increase in RH fluctuations and an increase in ventilation rate.

Figure 4.39 Air flow transmitter & sensor (Hanwell, 2018)

Three probe operating ranges were available, with decreasing accuracy with increasing working range. The air flow sensor option J189-0, with an operating range of 0-10 m/s, accuracy ±(0.3 m/s + 4% of measuring value), was picked as its supplied cable was of sufficient length to enable the sensor to be suspended from the ceiling. The sensor was a thermoelectric (hot-wire) anemometer probe which produces accurate data when measuring low air velocity in the range 0 m/s to 10 m/s, making it suitable for use inside museum stores.

Tabulated specifications for the environmental monitoring equipment used in this study are to be found in Appendix D.

4.5.5 Location of sensors

At the start of the transient period, a Hanwell ML4106 RH/T transmitter unit was placed on the floor of each of the empty BOX storerooms (HMS 4, 5 and 6), against the internal (north) wall in order for the site conservators to monitor the ambient storage environment before delivery of any collection objects. As storage furniture and objects were installed in the rooms, the three units were repositioned within the same areas. In HMS 5 and 6, they were placed on top of conveniently located ship model crates, at 1400 mm m above the floor near the centre of the north wall (Figure 4.40; Figure 4.41). In HMS 4, the sensor was placed on the central flange of the art racking framework, on the north side of the centre aisle at a height of just over 1000 mm (Figure 4.42). Unit locations were not identical in each storeroom due to storage furniture and object placement within each room but were as close as practicable. The units remained in these locations throughout both phases of the research project in order to retain consistency of data.

Figure 4.40 ML4106 unit location, HMS 6

Figure 4.41 ML4106 unit location, HMS 5

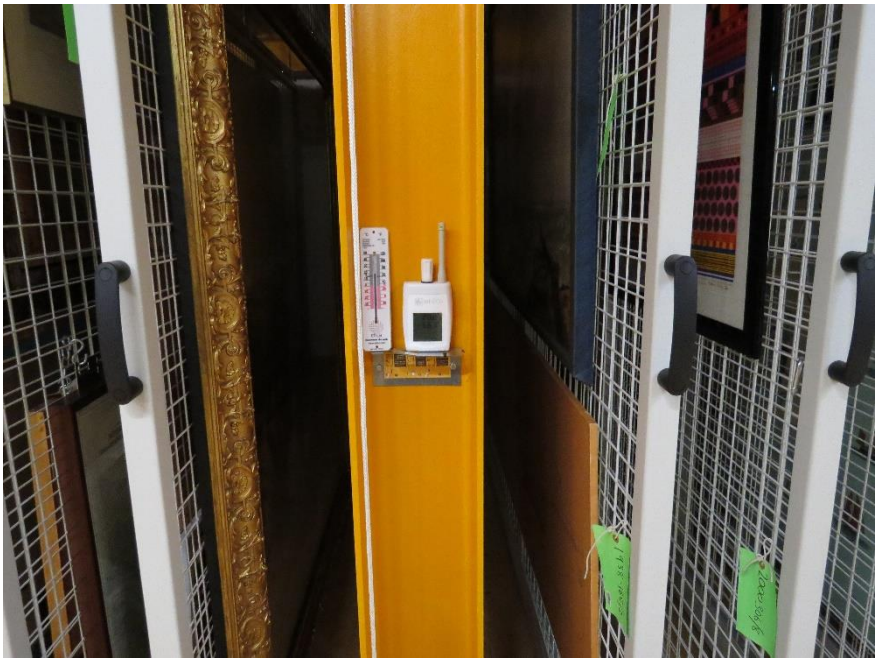

Figure 4.42 ML4106 unit location, HMS 4

No telemetric units were installed in HMS 1, 2 and 3 during the transient and first steady states as those storerooms remained empty of objects but data loggers were placed on shelving near the front of the rooms on the ground and second floor. Data loggers were also used in hangar D2 and externally. Hanwell ML 4106 units were installed in the A Store and L&A store in 2013.

Figure 4.43 shows the locations of the sensors used to obtain RH and temperature data in and around the HMS during the transient and first steady state period of operation of the case study. A location map showing the extended telemetric system used in the second research period of the case study will be found in Chapter 6.

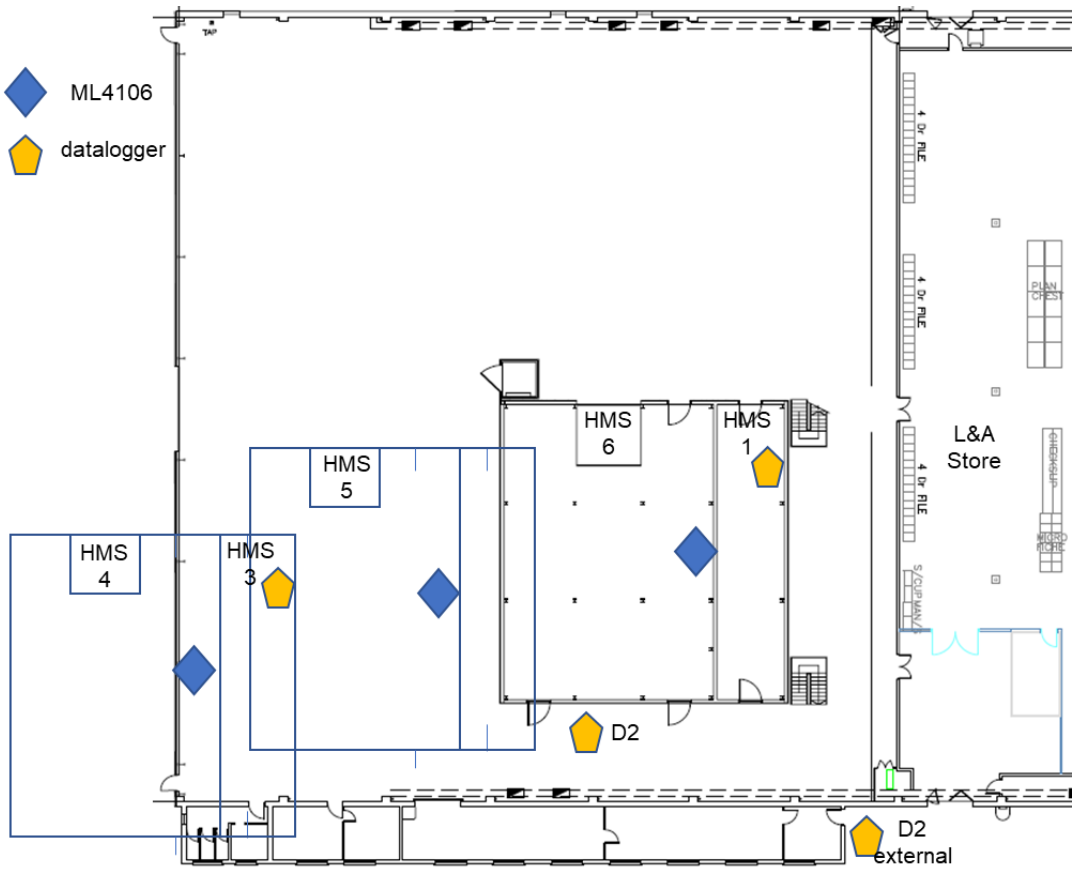

Figure 4.43 Location of RH/T sensors used during transient & 1st steady state of building operation

In the first steady state, two ML4106 units replaced the data loggers in the L&A store. One was placed in the high-density mobile shelving in the north area and one on a cabinet in the south area at approximately the same height of 1400 mm from the floor (Figure 4.44). Just before the second steady state period starting in June 2016, the external data logger on the north-east external wall of hangar D2's annex was replaced with an ML4109 RH and temperature unit at 2000 mm from the ground (Figure 4.45).

Figure 4.44 ML4106 unit location, L&A store

Figure 4.45 ML4019 unit location, exterior of D2

During the second steady state period, additional Hanwell telemetric sensors were acquired to augment data acquisition for the second phase of the case study. In March 2017, the data logger in hangar D2 was replaced with an ML4106 unit and another ML4106 unit positioned within an object shelter. The shelter unit was inadvertently moved out into the hangar in mid-April 2018, being left on a pile of pallets close to the north-west corner of the HMS, and not replaced in the shelter until January 2019. While the move resulted in a lack of data for the shelter, the unit

fortuitously provided monitoring data for the hangar during the period from November 2018 to January 2019 when the hangar D2 ML4106 unit stopped transmitting.

Two ML4114 RH and temperature units were installed in January 2018 in the north-west corner of HMS 6. Three metre probe extension leads allowed one sensor to be installed just above floor level and one at the ceiling height of 3080 mm, in order to collect data on potential stratification of RH levels and fluctuations (Figure 4.46). Positioning was due to the location of carriages and ship model crates in the room. The probe at ceiling height was placed to the side and slightly behind the supply vent in order to reduce any effects of direct air velocity on the sensor. Data was compared to that from the room's median ML4106 RH and temperature unit.

Figure 4.46 ML4114 unit & sensor locations, HMS 6

From August 2019, an ML4106 unit was positioned on the east wall of HMS 6 at the same height as the median sensor and sealed over with a section of polythene (Figure 4.47). This provided data for a definitive comparison between the response of RH within the room and within the HLC wall as a result of internal and external influences, in order to clarify the dynamic infuence of the HLC.

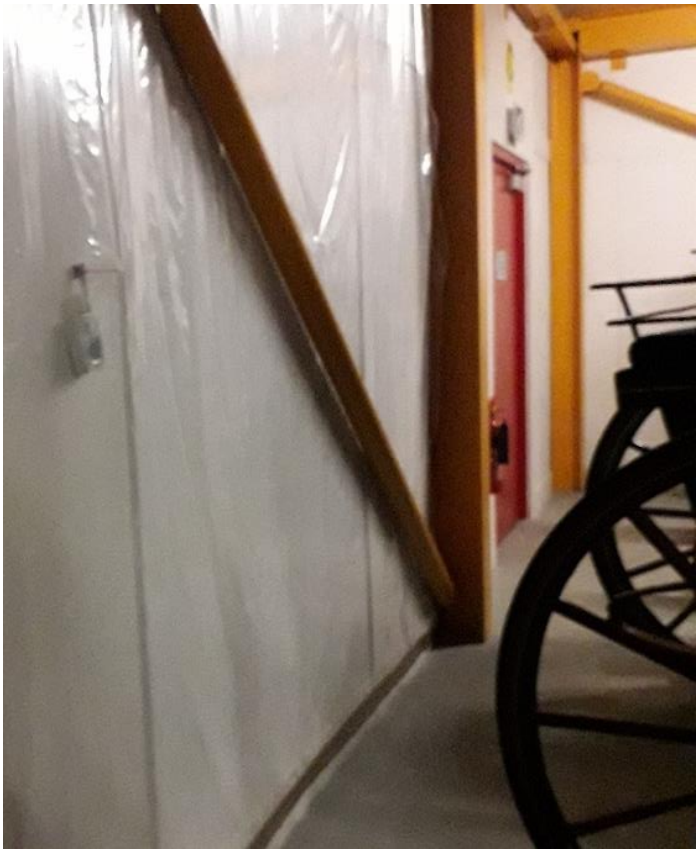

Figure 4.47 ML4106 unit location, under polythene, east wall HMS 6

The 16 channel Dampwatch moisture detection unit was installed in HMS 6 (Figure 4.48) in April 2017, to determine if there was a relationship between the moisture content, MC (%), of the HLC walls and the room RH. The 16 pairs of sensors were inserted into the HLC walls at the north-east corner of the room with half the sensor pairs inserted into the east wall and the other half into the north wall. The area was chosen as access to both interior and exterior walls was not hindered by carriages or ship model crates. Pairs of sensors were installed 20 mm apart at intervals of 410 mm, with sensors **1** to **8** from floor to ceiling on the east exterior wall and **9** to **16** from floor to ceiling on the interior north wall.

Figure 4.48 Installation of Dampwatch unit & sensors, HMS 6

Sensors could not be inserted directly at ceiling height due to the steel framework of the building so the highest sensors were inserted at 280 mm from the ceiling, just under the ceiling beam. The lowest sensors were inserted 160 mm from the floor. Sensors were inserted 50 mm deep through the Multi-Pro XS facing boards and into the HLC walls. Holes only had to drilled through the Multi-Pro board as the pins could then be pushed into the HLC matrix. This gave the pins enough contact with the HLC to ensure good thermal conductivity and uniform heat transfer. Sensors were sealed into the holes using the cable bullet connectors and the cables were run to the Dampwatch unit mounted on the east wall.

Usable data was acquired from the Dampwatch from August 2017 once operational diagnosis identified that the Dampwatch sensor reading and transmitting intervals had been set incorrectly. Once the reading and transmitting intervals were corrected, consistent readings were obtained. Data was assessed to see if changes in internal or external RH levels had a reciprocal effect on MC (%). Data was also evaluated to see if moisture transfer had any effect on RH levels or fluctuations.

The Dampwatch unit was moved from the ground to the first floor in January 2018 in order to see if MC (%) in the HLC would differ compared to overall levels in room RH, as the RH in HMS 5 was 5% lower than in HMS 6. The unit was placed directly above the previous position on the ground floor and in the same configuration but

intervals were reduced due to the lower ceiling height in HMS 5. (Figure 4.49). Data was obtained from this location until the end of this research project. The unit was not installed in HMS 4 as access to wall space was limited due to the art racking.

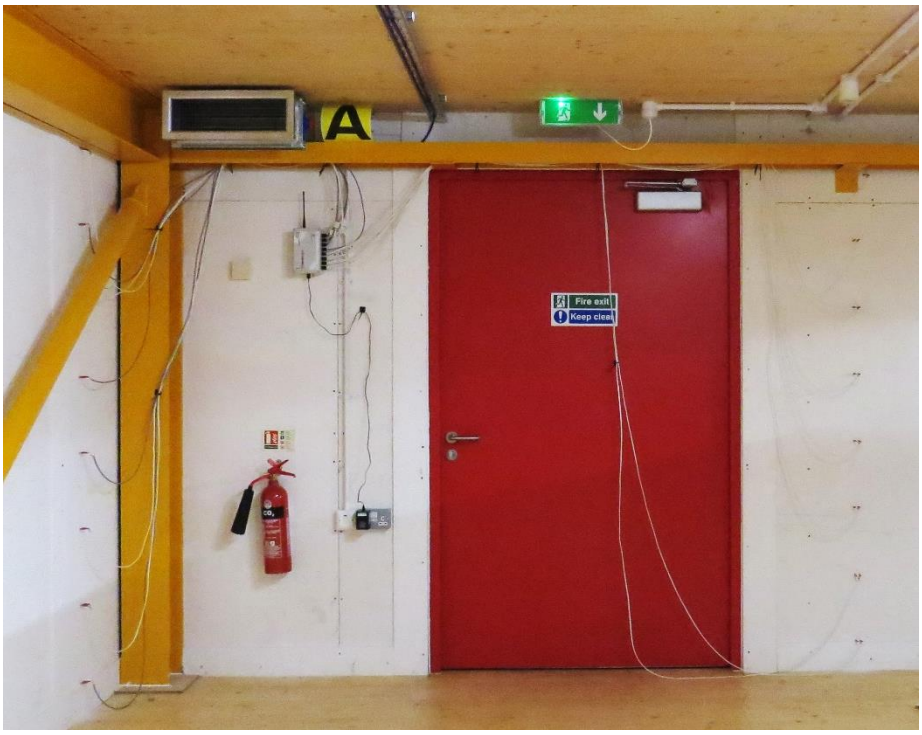

Figure 4.49 Dampwatch location, HMS 5

The Hanwell Air Flow meter RL 4810 was installed in January 2018 in HMS 6 to verify and evaluate the operation of the air handling system by monitoring the air velocity in the storeroom. Data was assessed for ventilation and air velocity effects on RH control. The air flow probe J189-07 was initially suspended from the ceiling quite close to the air distribution supply grille in the north-west corner of the storeroom but then was moved half-way along the north end of the room to obtain more comprehensive monitoring data.The sensor was suspended from the ceiling in the same area as the median RH and temperature sensor (Figure 4.50) as this was one of the few areas of the storeroom that could be accessed without having to move carriages.

Figure 4.50 Air flow meter & probe location, HMS 6

Figure 4.51 show the locations of the environmental monitors used in and around the HMS during the second steady state.

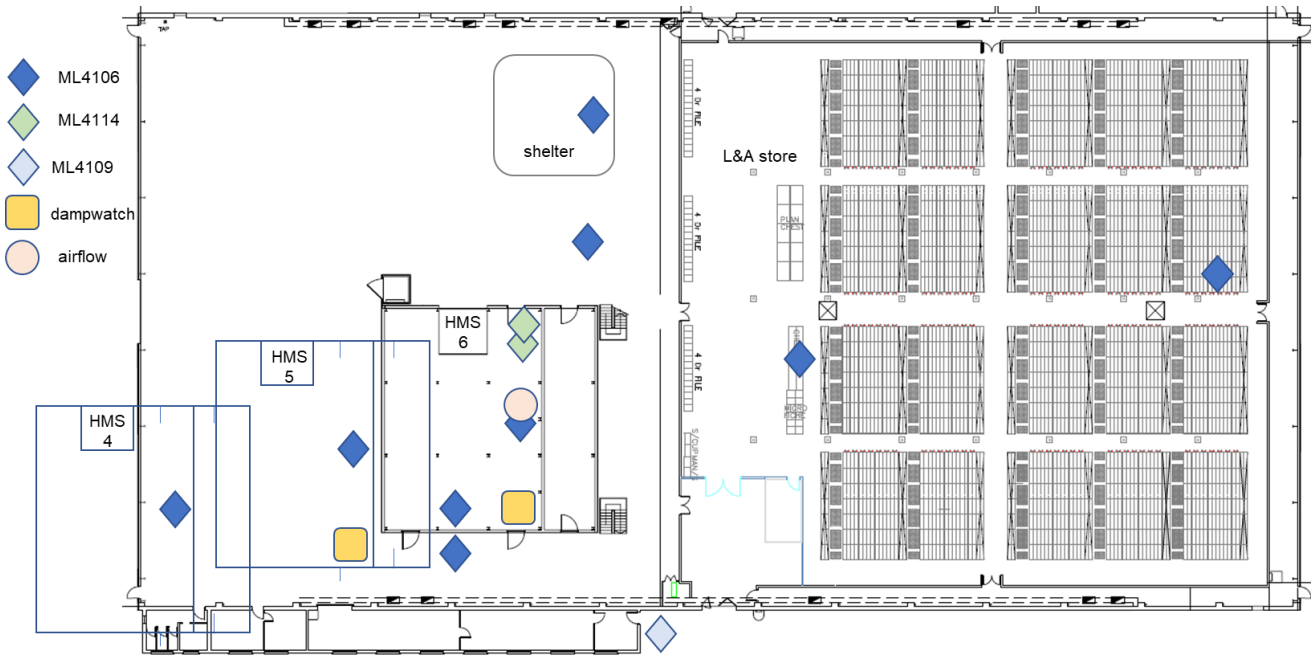

Figure 4.51 Location of sensors in & around the HMS during 2nd steady state

The Hanwell telemetric environmental monitoring system was installed in the A Store in May 2013. Figure 4.52 show a floor plan of the A Store with Hanwell sensor locations. ML4106 units were located in the three stores as well as in the loading and reception bays. All units were placed at 1400 mm from the floor. Additionally, Tinytag units were placed in A1 racking in May 2015, at low and high levels, in order to identify the extent of stratification of RH.

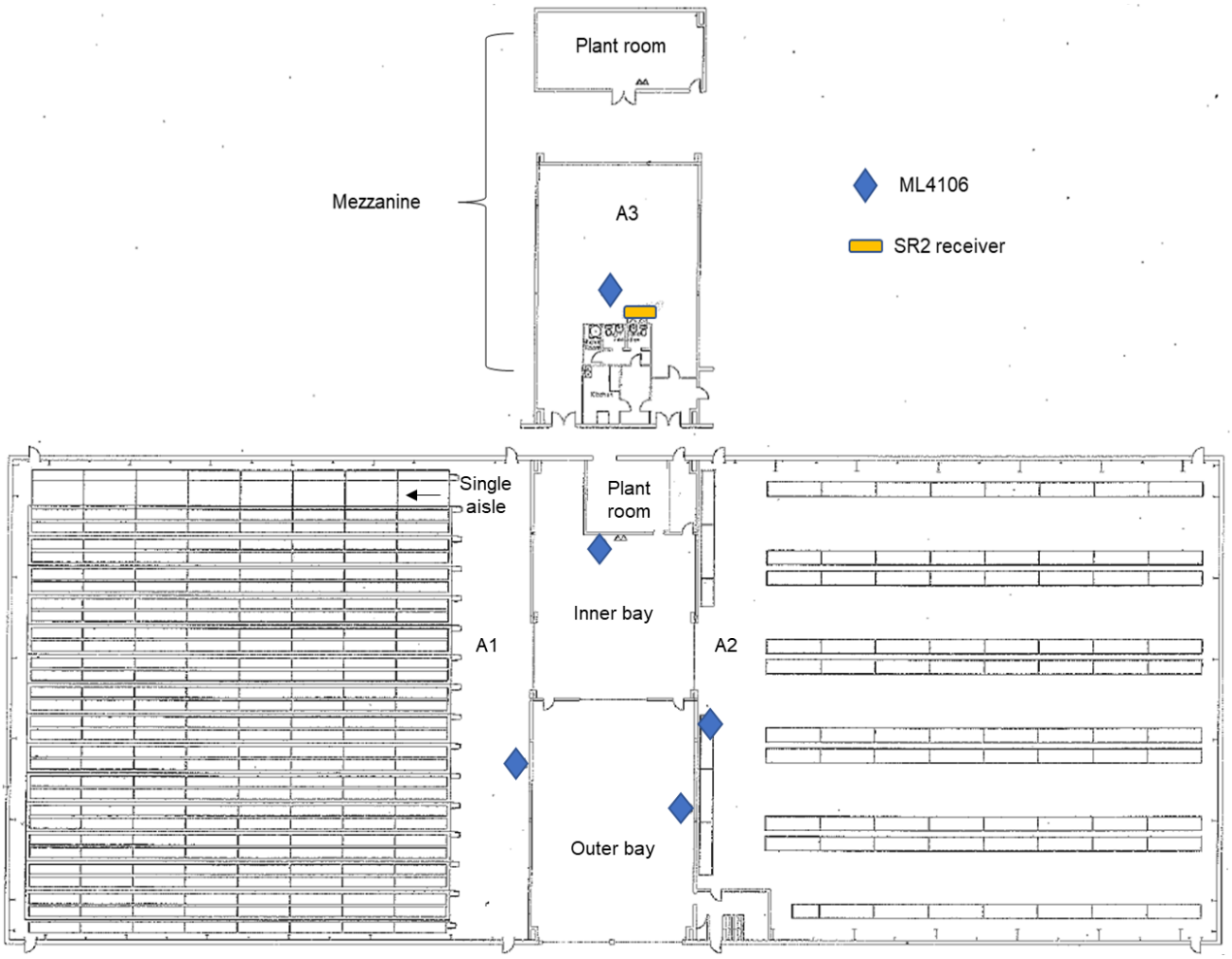

Figure 4.52 ML4106 units & SR2 receiver locations, the A Store

4.6 Summary of the research methodology

This chapter presents the research methodology and the methods and materials used to develop a guideline system for obtaining data to support the research hypothesis. The research methodology developed used both qualitative and quantitative methods to evaluate the potential of HLC to augment the regulation of RH within a museum storage building under dynamic operation.

The intent, design, methods, materials and costs for the construction of the case study, the Hempcrete Museum Store (HMS) are described. Details of the building design, construction materials and methods were obtained from project records as well as sourced from suppliers. Details of design and schematic of the mechanical air handling system as installed are provided. Object collections requirements are detailed to provide a context for building intent and design. The objectives of the case study were to address the key knowledge gaps identified in the literature reviews by:

- Obtaining data from dynamic operation to compare with contemporary data from other museum stores.

- Evaluating the moisture management capacity of HLC over a range of hygrothermal boundary conditions relevant to museum storage conditions.

- Quantifying the extent to which the hygrothermal performance of HLC can support the research hypothesis

Information is given on the construction of other buildings on the site, the hangar in which the HMS was built and the two other low energy stores which were used for comparative purposes throughout the research study.

The research procedures used to acquire monitoring data for assessment of the hygrothermal capability of the material to control and moderate the RH ranges within the case study are outlined. The monitoring equipment, specifications and operation are detailed. The Hanwell environmental monitoring system hardware and software were evaluated to ensure suitability for the monitoring programme. Moisture content sensors were designed by this researcher and fabricated and tested on the NCC site. Data collection and assessment was divided into two phases of dynamic building operation. The first phase covered the transient and first steady states, from 2012 to 2016, when RH data was collected from three storerooms in the HMS as well as from the two other low energy stores. The second phase covered the second steady state of operation, from 2016 until 2020, with an augmented monitoring strategy which included obtaining data on moisture content, air flow and activity duration from the HMS.

Chapter 5 Case study - the HMS: transient and initial steady state performance, May 2012 to May 2016

5.1 Introduction

This chapter presents the results of the first monitoring phase of the case study, from the transient state through initial steady state. The consequences of the design and construction methods on the storage building's environment are discussed. The design and operational plan of the mechanical air handling plant, the operational failings due to installation and construction factors and subsequent modifications undertaken to rectify these deficiencies are described. Influence of the hygroscopic capability of HLC on the building's environment is discussed. The effectiveness of RH regulation and operational expenditure, including energy usage, by the HLC walls is assessed against other low energy stores.

The initial M&E design entailed environmental control through a full heating, ventilation, humidification and dehumidification (air conditioning) system in order to achieve tight environmental parameters. In order to comply with low energy directives from the museum, subsequent alterations to the software modelling and in environmental recommendations led to the design of a reduced capacity (no cooling, humidification or dehumidification) mechanical plant. A description of the modelling process, final design and discussion on the success of the design in controlling the internal environment of the HMS are presented.

The monitoring programme was evaluated and limitations identified. The preliminary conclusions on the efficiency of HLC in moderating RH levels and fluctuations in the case study are presented.

5.2 The case study- the HMS

The materials and construction of the HMS have been described in Chapter 4. This section reviews the design intent of the building project and details the specification of the environmental parameters required to achieve that intent.

5.2.1 Intent of the storage project

The HMS was conceived, designed and built from 2011 to 2012 in order to provide climate-controlled storage for four distinct collections of moisture-sensitive cultural heritage collections, described in Chapter 4, being:

- The RINA archives
- Framed art works
- Whole and half-block ship models
- Horse-drawn carriages

The intent of the project was to design storage in line with the museum's sustainability development policy (Moore, 2010) to reduce energy consumption. Evaluation of low energy projects utilising hygroscopic building materials to moderate

internal environment instead of large-scale heating and air conditioning systems resulted in the choice of HLC. The benefits of the choice were considered to be long term operational sustainability as well as very stable RH although building costs were anticipated to be approximately 10% higher than that of a conventionally constructed museum store (Moore, 2013).

A small team of SMG stakeholders, comprised of the NRM Archivist, the SCM's Director of Estates, Heads of Conservation and Sustainable Development, and the site's Conservation (this researcher) and Estates Managers, worked with external specialist contractors and consultants to reduce the energy loads normally associated with controlling the storage environment to museum specifications.

5.2.2 Parameters for storage environment

Initially the environmental parameters were based solely on the needs of the RINA archive collection and were required by the NRM Archivist to be compliant with *BS 5454:2000*, as advised by the Archives and Records Association (UK & Ireland) (Eberlin & Carter, 2011). This standard recommended a storage environment with a fixed point for temperature between 13°C to 16°C ±1°C and for RH between 45% RH to 60% RH with a tolerance of no more than 5% RH on either side and with no rapid changes (BSI, 2000). While it was acknowledged that the collections objects would require less stringent storage conditions, with no need for compliance with the archival recommendations, the entire store was to be designed to meet these parameters. This would allow a future change of use should the entire building eventually be turned over to the storage of archival material. Fixed points for temperature were specified at 15.5°C ±1°C in summer and 14.5°C ±1°C in winter and 50% RH ±5% RH year-round (Jankovic, 2012a) within all storerooms. Fresh air intake rate was also taken from *BS 5454:2000*, which recommended a daily rate of 5% to 10%. The proposed air flow for the plant supplying the RINA storerooms was 0.35 m^3/s which would have given an air exchange rate of 5/hr on the ground floor and 7/hr on the other two floors. For the plant supplying the BOX storerooms, the proposed air flow was 1.08 m^3/s, giving an air change rate of 5/hr on the ground floor and 7/hr on the other two floors. Air change rates were calculated using the following equation:

$$\boldsymbol{n} = \left(\frac{\boldsymbol{3600Q}}{\boldsymbol{V}}\right) \qquad \text{[equ.5.1]}$$

where,

n = air changes per hour
Q = volumetric flow rate of air per second
V = volume of room

5.2.3 Evolution of the mechanical and engineering system

In order to achieve the narrow RH and temperature controls desired by the NRM Archivist, the original low energy approach proposed by the contractors was revised to include a full HVAC system to supplement the passive regulation provided by the building envelope. In order to achieve 97% compliance with the fixed RH and temperature points, a *"safe and conventional approach to M&E design"* (Jankovic,

2012a) with heating, cooling, humidification and dehumidification was proposed, based on an analysis using CIBSE local (SwindonDSY05) baseline climate data and CIBSE Swindon future weather data, (modelled from the UK Climate Impacts Programme (UKCIP)), in .fwt (IES) file format and .epw (EnergyPlus Weather) file format in IES software. Climate tables and graphs from Jankovic's analysis are reproduced in Appendix E.

Jankovic characterised the year 2050 with the greatest extremes in temperature range, 1.5°C lower and 2.3°C higher than the baseline climate, and chose it as the design year for the M&E system, anticipating that the M&E plant would last until 2050 as it was protected from outside conditions. The system proposed was a cross flow plate heat exchanger and reversible air source heat pump, but with an added humidifier and a reheater. The air source heat pump system would be used for both heating and cooling modes. Humidification would be provided using a water humidifier in the AHU and would require a cold water supply, taken from the D2 hangar toilet block. Dehumidifying would be a part of the normal operation of the evaporator working as a chiller with the condensate water routed to the toilet block's drainage system. A reheater was included in the AHU in order to achieve the required humidity controls. Fresh air intake would be between 5% to 10% with the remainder of air coming from recirculation. As the RINA and the BOX were to be used for storage of different materials, each space would have a dedicated AHU and separate ducting. In the RINA, there were to be four ceiling supply diffusers above the central aisle at one approximately every four metres, with one duct extract at the end of the sequence and, in the BOX, three rows of ceiling supply diffusers in a similar sequence with one extract at the end of each duct run. The initial M&E plant and ductwork plans are reproduced in Appendix D.

The M&E system was based on dynamic simulation modelling in Integrated Environmental Solution Virtual Environment (IES VE), undertaken by the engineering design consultant (Jankovic, 2012a). IES is a software package with a number of energy related simulation tools which address dynamic thermal properties, air flow, lighting, etc., in relation to buildings. The information obtained on cooling loads was used for plant sizing.

The HMS construction materials were used in the model (Table 5.1) with the geometry of the storage building obtained from architectural drawings. The location of the building, within hangar D2, meant that the store geometry had to be sectioned out of the hangar geometry in order to obtain a volume within a volume for the simulation model. Views of the simulation model geometry are reproduced in Appendix E.

Table 5.1 Construction materials used in simulation (Jankovic, 2012a)

External walls	Ground floor	Intermediate floors	Roof
40 mm wood fibre board	Sand	162 mm CLT	15 mm PLY deck
195 mm Hembuild panel	DPM membrane	160 mm structural steel zone	100 mm Hofatex SYS THERM
Airtightness membrane	100 mm Cellotex polyurethane foam		100 mm CLT
6 mm Multipro board	150 mm concrete		

Parameters in the model were set in accordance with occasional use as one hourly visit per month and up to six visits per year lasting between three to seven hours, and with the initial desired internal environmental specifications (Table 5.2). Thermal comfort during occupancy was not taken into account so functions of clothing and mean relative air movement were ignored. Metabolic heat production and heat gain from lighting and any equipment were calculated from assumed occupancy. Worst case scenarios of the highest internal heat gain on the hottest day and no heat gain on the coldest day in 2050 were taken into account and factored into the M&E design.

Table 5.2 Internal environmental parameters used in simulation (Jankovic, 2012a)

	Air temperature		RH
	Summer	Winter	
RINA	15.5°C±1.0°C	14.5°C±1.0°C	50% ± 5%
BOX	15.5°C±1.0°C	14.5°C±1.0°C	50% ± 5%

The intended volume of hygroscopic contents was estimated in the RINA by assuming predominately paper stored on 1.5 m deep linear shelves running on both sides of a central aisle, with a 50 mm gap from the external wall for ventilation, and in the BOX with large objects, with properties assumed similar to softwood/pine and with 30% solid mass, taking up 60% of the storage volume. Thicknesses of each material were calculated to represent full room loading and used as additional interior wall layers in the environmental design simulations in order to retain the heat gain/loss characteristics of the building but allow their influence on thermal mass. Material property tables as used in the modelling are reproduced in Appendix E.

Ambient lighting was provided by high efficiency fluorescent luminaires controlled by passive infrared (PIR) sensors in order to eliminate superfluous operation. Specific connected loads for ambient lighting, compliant with *BS 5454:2001*, were calculated for five luminaires in each RINA storeroom and 15 luminaires in each BOX storeroom with the fluorescent luminaires positioned between the supply diffusers and duct extract. General gains for the luminaires are found in Appendix E.

Heating and cooling loads were analysed on an hourly basis for 2050 with the cumulative frequency of occurance revealing a differentiation between frequent and infrequent loads. The equipment size was derived from the output on cooling loads that occurred for 98% of the time. AHU sizing was also carried out in conjunction with duct sizing, volume flow rate and required fan pressure with two sizes of AHU specified. Equipment rating and sizing tables are found in Appendix E.

The impact by winter and summer failure of the M&E system on temperature in the rooms both with and without contents was simulated. The stored materials were shown to influence the change of internal temperature but the changes were considered insignificant, being no more than 0.4°C in the summer and 1°C in the winter in the RINA and almost negligible in the summer and no more than 0.4°C in the winter in the BOX. However, as the standard IES output did not support moisture transport, the effect of the hygric properties of the HLC building envelope on the internal RH was not calculated and the resultant M&E design moved away from the

original intent to use HLC to moderate RH. The museum asked for a redesign to reduce the size and energy requirements of the M&E system by taking into account the potential capability of the HLC building envelope to regulate RH as well as temperature.

Simulation modelling was carried out on the redesign which returned to the approach originally accepted by the museum (Jankovic, 2012c). Active control of humidity and mechanical cooling was eliminated so there was no requirement for water supply or drainage**.** While the museum issued revised specifications for RH, based on the SMG current (2012) recommendations which were for a stable RH range between 40% RH to 60% RH with seasonal and diurnal fluctuations no more than ±5% RH and a temperature between 13°C to 24°C with no more than 4°C fluctuation over 24 hours, the *BS 5454:2000* (BSI, 2000) parameters for RH, temperature and air changes were still used in the modelling of the revised system.

With IES not having the capability to use hygric behaviour to simulate the RH buffering effect of a hygroscopic building material, the engineering design consultant took:

> "*a ground breaking and pioneering approach to the thermal/humidity modelling of the building*" (Jankovic, 2012c).

Jankovic predicted the attenuation of internal temperature and RH by HLC by appling a mathematical algorithm/filter to the standard IES output in order to correct it for the passive performance potential of the HLC walls (Jankovic, 2014). He used the relationship between IES simulated temperature and RH and actual data from temperature and RH monitoring of an unheated HLC test cell (the HemPod at the University of Bath) to provide a ratio in the form of a Fourier filter. Monitoring data for the simulation was taken from periods with stable external conditions and the input weather data file was amended to include external parameters. While there was a noticeable fluctuation in simulated internal conditions, the monitored values appeared quite stable. Jankovic found a root mean squared error (RMSE) between simulated and measured temperature values of 6.47°C and between simulated and measured RH of 12.33%. Jankovic's graph showing the performance gap between simulated and measured temperature and RH in the HemPod is reproduced in Appendix E.

When used for the modelling for the revised M&E system, the Fourier filter had been tested only as far as assessing IES results obtained from a simulation of an unheated HLC terraced house. Jankovic concluded that his method would more closely represent actual building internal temperature and RH than standard IES simulation results (Jankovic, 2012c) and used it to determine the extent to which mitigation of RH fluctuations could be anticipated using the buffering potential of HLC without any active cooling or humidity regulation by the M&E system. The results of Fourier filtering showed a mitigation of the fluctuations in IES simulated temperature and RH, with temperature fluctuations maintained within ±1°C of the required design temperature and RH held generally within ±5% on either side of 50% RH throughout the year. Jankovic's graphs showing the application of the Fourier filter to IES simulated temperature and RH in the RINA are reproduced in Appendix E. It was concluded that the HLC building envelope would substantially buffer temperature and RH and therefore a simplified design of the M&E system was possible, reducing

the amount of mechanical and electrical equipment and capital and running costs while meeting the environmental specifications of the museum.

The revised design was for two cross plate heat recovery exchanger air handing units, one for the RINA and one for the BOX, to supply heat and ventilation. The plant would be sized to cope with 90% of the predicted peak demands. Airflow remained the same but there would be minimal ducting and no supply diffusers, just supply grilles. Ambient lighting would be provided to 100 lux at floor level. The design year would be based on 2005 climate data. Additional options were added to the modelling to determine the effect on equipment ratings. The first option included cooling and humidification control for the RINA but not for the BOX and an adherence to the *BS 5454:2001* RH specifications for that space and the second option extended the specifications to include the BOX. Free cooling in summer months, using nighttime external air to offset internal heat gains through mechanical ventilation, was also calculated to show that between 2 kW and 6 kW of cooling capacity could be achieved. Heating loads were analysed on an hourly basis throughout the design year to determine the equipment rating (Table 5.3).

Table 5.3 Revised equipment rating based on cooling & heating loads (Jankovic, 2012a)

		Base case- 90% of all loads	**Option 1- 95% of all loads**	**Option 2- 97.5% of all loads**
		kW	kW	kW
RINA	Heating	3.6	4.1	4.4
	Cooling	0	4.0	7.0
BOX	Heating	3.8	4.4	4.7
	Cooling	0	0	13.0

The reduced M&E system specification, without the air conditioning and humidifying/dehumidifying modules, was expected to reduce the capital cost by a third (Jankovic, 2013) although this was not reflected in the final project costs. As a result of value engineering undertaken for the M&E system design, the zoning for the AHUs was altered with one AHU serving HMS 1, 2, 3 and 4 and the other serving HMS 5 and 6. The AHUs installed were the same size rather than one being larger than the other as in the previous design. Total room volumes served by each AHU were 1,124 m^3 for AHU1 - RINA and 1,259 m^3 for AHU2 - FF. Ductwork was run across the front and back of the building from AHU1, crossing under the ductwork from AHU2, in order to serve HMS 4 (see Figure 4.22). Air flow for the AHUs was set at 1.08 m^3/s with supply and extract fan pressure set at 180 Pa, leaving the air change rate the same in the BOX storerooms but doubling it in the smaller RINA storerooms. Uniformity of the systems was intended to facilitate operation and maintenance as well as reduce installation costs.

A building management system (BMS), Trend IQ3 (Appendix C), with both daily and weekly on/off settings was installed to control the heating. Control functions were set and performed remotely via a web-based dashboard with the controller itself installed in a moisture-proof box on the outside north-east wall of the store. The two Airflow MVHR units *Duplexvent Flexi DV3600* (Airflow Developments) (Appendix C) had

their own control systems linked to the IQ3 controller so that control parameters could also be checked online. A schematic of the M&E system linked to the control units is found in Figure 5.1. Both the Trend BMS and the Airflow AHU dashboards were accessed by the contractor through a virtual private network (VPN) provided by the museum as it was:

> *"especially important to have the network connectivity for IQ3 from the start, before the building is loaded with artefacts. This will enable the start-up control programme to be executed and manually adjusted if needed, so as to achieve the gradual change to the required conditions within the required period of one week from the start."* (Jankovic, 2012)

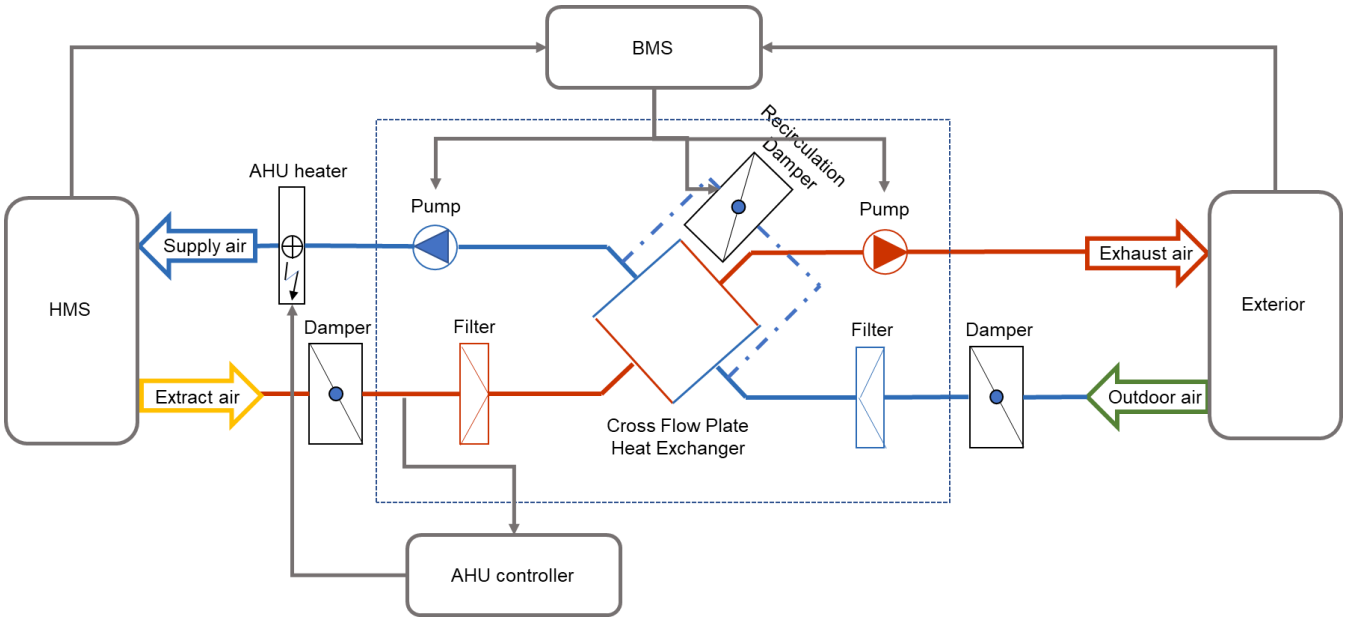

Figure 5.1 Schematic of the air handing system linked to controllers

A bespoke environmental monitoring system (Carnego Systems) with a web-based interface, independent from the Trend IQ3 BMS, was installed so the design engineer could remotely monitor environmental conditions, since the SMG Hanwell telemetric system software, rl8, was not browser based technology. The bespoke system used a Tridium M2M JACE data logger with HDH-FL-RH (SyxthSense) transmitters. The transmitters had sensors with a stated accuracy of T ±0.5°C but no stated RH accuracy (SyxthSense Ltd., 2010). Fourteen combined RH/T transmitters, two in each storeroom, one in the hangar and one outside, were wired into the power supply, connecting them to the data logger (Jankovic, 2013). The conservation team found the Hanwell system to be more accurate and easier to access and use of the Carnego system ceased at the end of the transient state with no data archived.

5.3 Transient state

The Museum accepted the M&E design revision in April 2012 and installation of the system was completed by early May, with the commissioning of the AHUs and Trend BMS starting mid-May. The original programme had specified the establishment of

stable internal conditions for one month before the first delivery of ship models, scheduled for early May (Chambers, 2012) but the redesign of the M&E system delayed completion of the building. The revised programme estimated that the '*stable month*' would not occur until mid-June at the earliest or potentially the end of June, so deliveries were postponed until the end of August. It was anticipated by the design team that this would allow enough time to achieve stable conditions in the building. However, it took a full year before the operation of the building entered the first steady state.

5.3.1 RH history during transient state, May 2012 to May 2013

A number of faults and problems with the M&E system had to be resolved before the '*stable month*' was achieved. Prior to the commissioning period which began in the last week of May, the internal RH in the HMS had reached a high of 95%, then fluctuated between 55% RH to 75% RH, following external conditions as the doors to the storage building and to the hangar were open during installation of M&E equipment and storage furniture. During the commissioning period, the internal RH fluctuated between 65% RH to 85% RH. Faults found during commissioning included a malfunctioning printed circuit board (PCB) in one of the AHUs, missing duct sensors and defective outside temperature and RH sensors in the BMS. Design flow rates in the ductwork were exceeded and the AHUs were found to change the flow rate unpredictably, despite being in manual override. Delays to commissioning and fault diagnosis resulted as internet connectivity was not arranged until the beginning of June. Then online access was made available to the engineering designer but only to the BMS and not the AHUs. Full on-line access was provided to the design engineer by the end of June but not to the Airflow contractors who were still unable to remotely commission the AHUs. Remote access allowing fault diagnosis was finally established in mid-July by which time the design engineer had initiated the pre-conditioning operation in order to establish stable internal conditions to meet the revised object delivery schedule.

The RH was in the range of 80% RH to 85% RH when, at the end of June, the engineering designer attempted to reduce the temperature inside the HMS from around 17°C in order to achieve the specification for summer temperature of 15°C ±1°C. The AHUs were set to operate from 22:00 to 04:00 every day of the week in order to use nighttime air for free cooling. As there was no programme in the M&E operational system to turn off the ventilation if external humidity rose above room humidity, the design engineer monitored conditions remotely, using data sent from the Trend BMS. Figure 5.2 shows the RH and temperature data from the HMS, obtained using SMG Tinytag data loggers as data from the Carnego system was not achived, prior to the transient state, during the installation and initial commissioning of the M&E, and in the early stage of the transient state, during pre-conditioning.

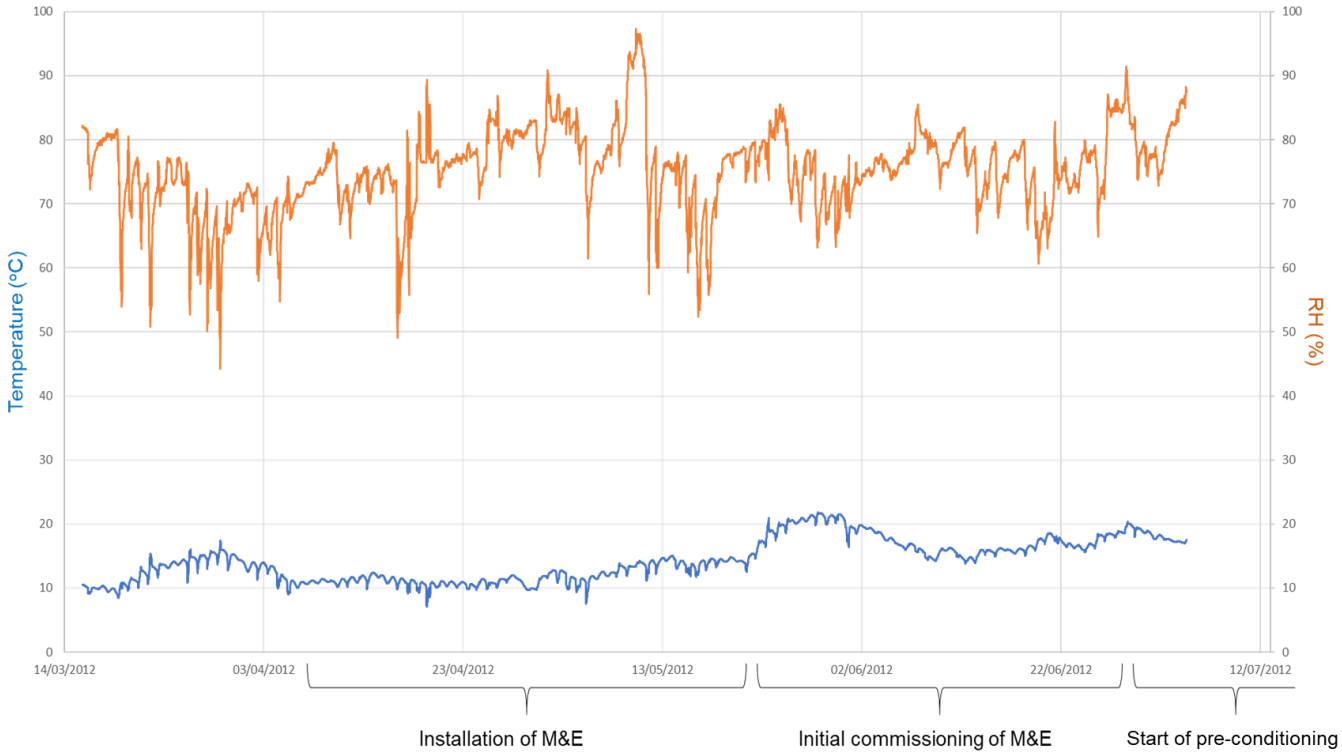

Figure 5.2 RH & temperature into transient state, HMS 6 (Tinytag)

Issues with the system continued as the AHUs were found to operate at 30% of fan speed between 04:00 and 22:00 despite the BMS sending a zero-speed signal. Any cooling achieved by introducing nighttime air was reversed by the inadvertent introduction of warmer daytime air. Due to the very high external RH levels at night, which ranged between 90% RH to 100% RH, and only slightly lower daytime ranges, 70% RH to 95% RH, from the beginning of June through to almost the end of July (Figure 5.3), the introduction of external air contributed greatly to an increase in the internal RH of the building. The focus on reducing the temperature resulted in the RH rising above 75% RH on the ground floor, 67% RH on the first floor and 65% RH on the second floor by 26 July.

On 27 July, as external nighttime temperatures had exceeded 15°C, the design engineer switched off the AHUs (Jankovic, 2013). From 27 July until 06 August, with a rise of internal temperature and no admittance of external air, the RH levels slowly dropped to a range around 58% RH in HMS 4 and 5 and 65% RH in HMS 6 (Figure 5.4). With the Hanwell telemetric system installed in the HMS on 23 July, the conservation team were finally able to closely monitor the internal conditions. The design engineer and contractors were warned that internal RH levels were still not acceptably low enough to allow deliveries of the ship models .

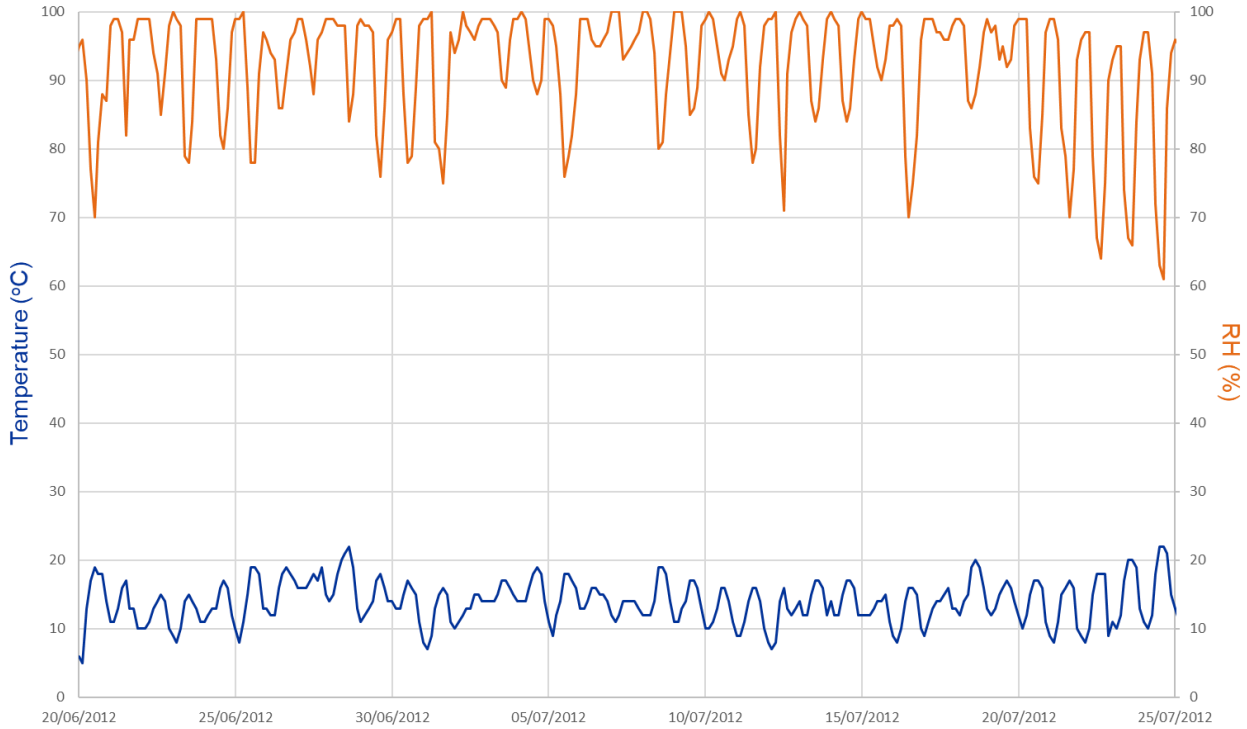

Figure 5.3 Swindon external RH & temperature ranges, June to July 2012
(Excel graph from CSV data www.worldweatheronline.com)

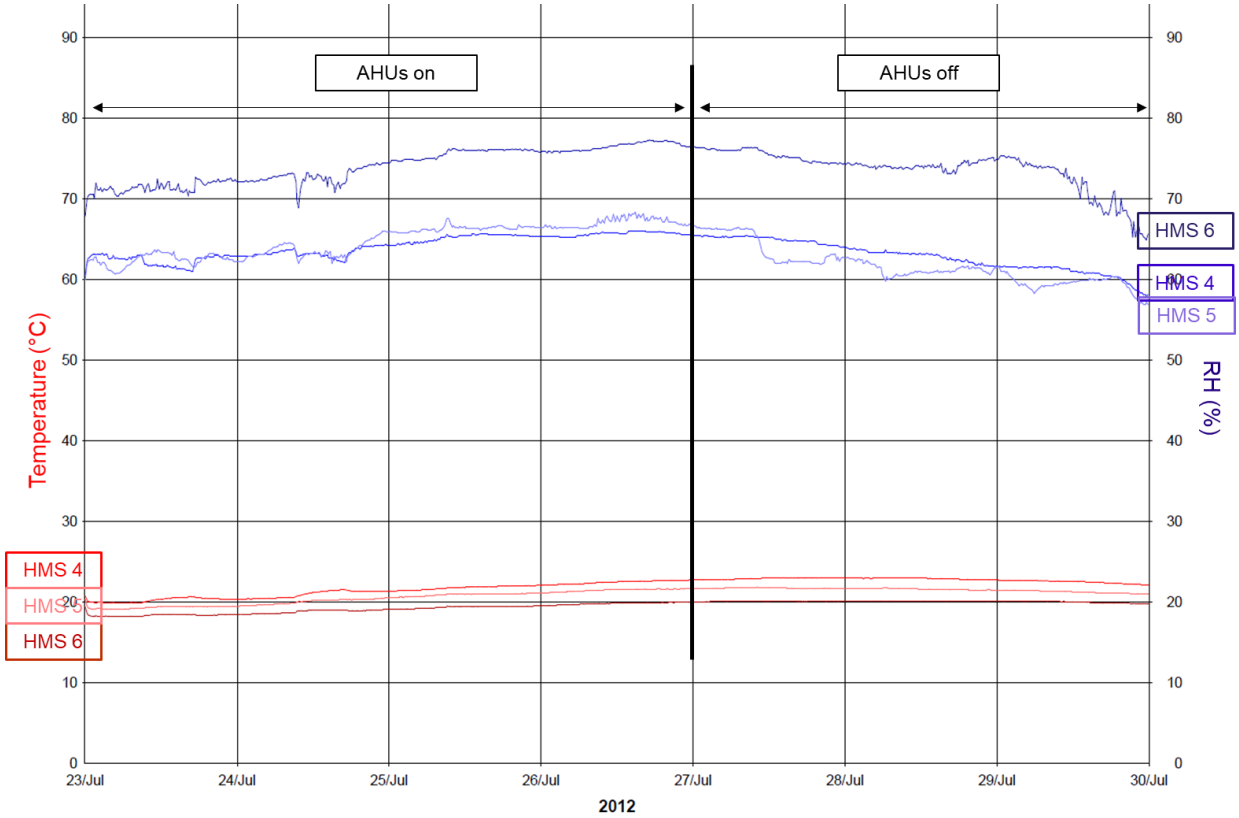

Figure 5.4 Effect of active vs passive control on RH & temperature in the HMS (Hanwell rl8)

On 06 August, as external nighttime temperatures had dropped below 14°C, the design engineer resumed internal cooling with nighttime operation of the AHUs.

Subsequently the RH rose by 22 August to a high of 78% RH in HMS 6, 68% RH in HMS 5 and 65% RH in HMS 4. The conservation team alerted the design engineer to the unwanted consequences of the free cooling and a series of attempts were made to rectify the problem. The internal temperature settings on the AHUs were reset. Control software for the AHUs was then updated and both units were set to work on the analogue signal from the BMS and according to the extract air temperature rather than the default supply air temperature. Filter pressure sensors were also manually adjusted to the maximum pressure setting of 300 Pa. Sporadic operation of the AHUs was traced to an issue with the HMS fire detection system which had been integrated with the existing hangar detection system. Random signals from the overhead detection beams shut off or turned on the AHUs until the fire alarm signal to shut down the AHUs was disengaged.

As it was now critical that the RH be reduced in the HMS, with the first deliveries of ship models scheduled for 24 August, the design engineer decided that external conditions were too mild to enable passive regulation. It was also acknowledged that there was more moisture in the building materials than anticipated (Jankovic, 2012). Two portable air conditioners (Daitsu APD12-AN, dry (dehumidifying) operation between 13°C to 35°C) and two dehumidifiers (EcorPro DH9500EW, typical extraction at 27°C/60% RH of 35 l/day) (Appendix C) were installed in HMS 6 on 22 August by the contractors to promote drying of that room. The AHUs were turned on to see if they would speed up cooling but their operation immediately resulted in an increase in the RH (Figure 5.5). They were turned off to allow dehumidification by the portable units. Additional dehumidifiers were installed in HMS 4 and 5 at the end of August and one of the two air conditioners moved to HMS 5 in September.

Although the portable units brought down both the temperature and the RH, the RH bounced upwards whenever the units filled up and stopped running (Jankovic, 2012). In order to continuously drain the dehumidifers and the air conditioners, the contractors connected hoses to the units and ran them out the personnel doors to the hangar’s internal drain. This left the doors slightly ajar, entailing a loss of security and airtightness.

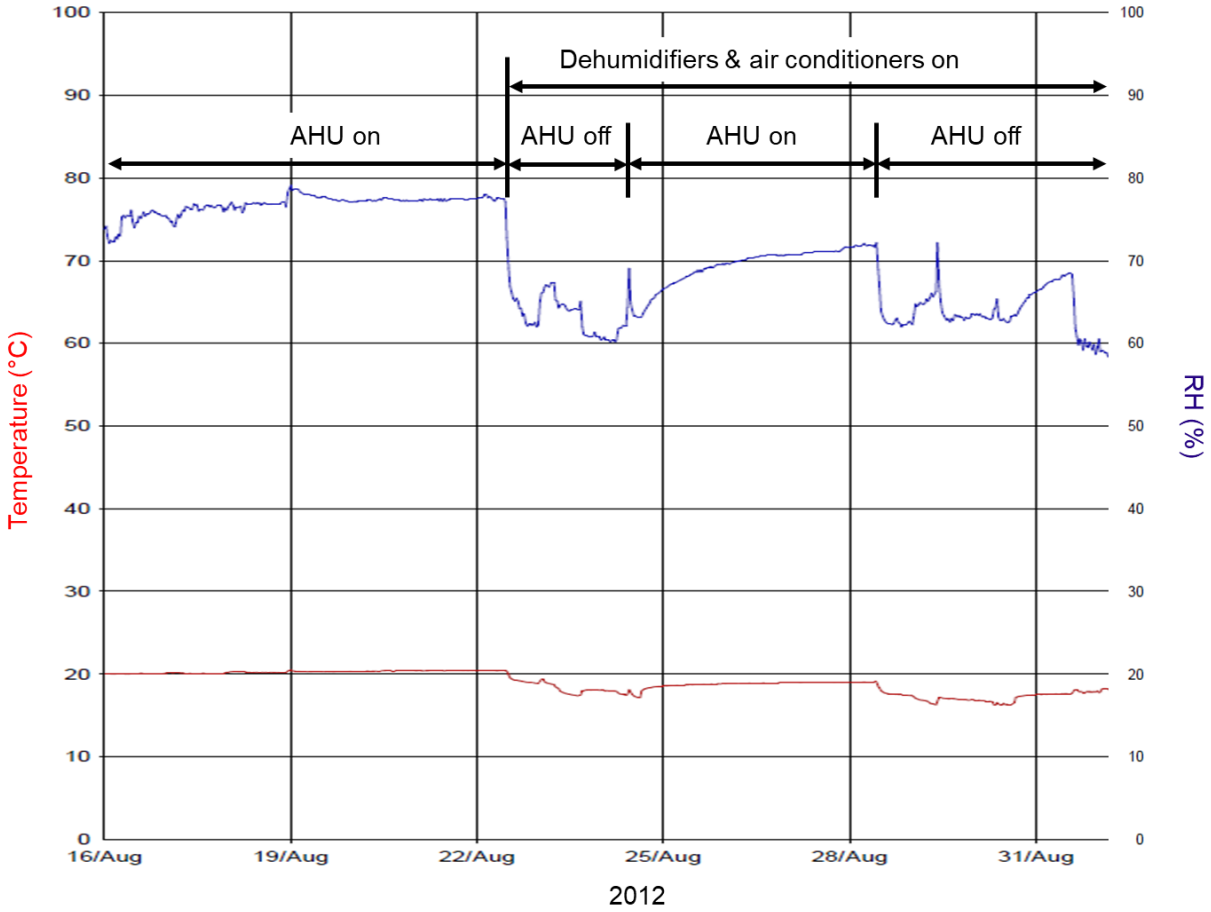

Figure 5.5 Effect of portable RH control units on RH & temperature, HMS 6 (Hanwell rl8)

By the time the deliveries of ship models started, on 24 August 2012, the RH levels in the building had dropped although conditions were still not as stable and levels as low as had been specified. Operation of dehumidifiers and air conditioners in the BOX storerooms continued while problems with the air handling system were investigated and rectified. From September through to November, the RH drifted between 40% RH to 65% RH in HMS 6 and between 40% RH to 60% RH on the other two floors. Daily fluctuations were minimal until the AHUs were put into heating mode in November at which point both the RH rose and fluctuations increased. Both heaters then required rewiring and the AHU software needed updating as neither unit responded to signals from the BMS. In HMS 4, the installation of art racking from 19 to 28 November caused rapid fluctuations in the RH during periods when room doors were open with a subsequent rise in the RH level.

In January 2013, the design engineer undertook trialing different modes of operation to find the most effective method of reducing the overall RH (Jankovic, 2013). Internal temperature variations in the BMS between 18°C ° to 19°C and in the AHUs between 15°C to 17°C allowed the AHU heaters to heat slightly above 15°C in order to bring down the RH and stopped the BMS putting the system into ventilation mode. Continuous heating was less effective as the BMS operated the AHUs with an excess of external air outside set temperature and humidity parameters. Various cycles of intermittent heating were trialled with a two hour on, four hour off cycle

seeming to retain internal temperature levels while increasing effective drying without going below 40% RH. A reduction in the RH levels was achieved using the different modes of the AHUs by the last week of January but this was significantly augmented by ventilating with low moisture content external air rather than low temperature external air. Monitoring external conditions for low RH periods was not written into the BMS software but was undertaken personally by the design engineer via the Carnego system and only during the transient period.

One dehumidifier in HMS 6 and the air conditioner in HMS 5 were left in operation at the start of the trials. Operation of the air conditioner, even though in dry mode, was found to have a noticeable effect on RH fluctuations due to the changing room temperature during intermittent heating trials (Figure 5.6). The level fluctuated between 30% RH and 40% RH and both the low level and the continuous ±10% RH fluctuations could have caused damage to the thin organic components of the ship models stored in the room. The fluctuations were noted by the conservation team when checking the Hanwell data and the air conditioner was turned off. Damage was averted as all models had remained in their packing crates, which were designed to mitigate RH fluctuations during transport. The air conditioner was removed and subsequently replaced with a dehumidifier. Monitoring data from HMS 6 during the same period showed very little fluctuation due to dehumidifier function during heating cycles (Figure 5.7).

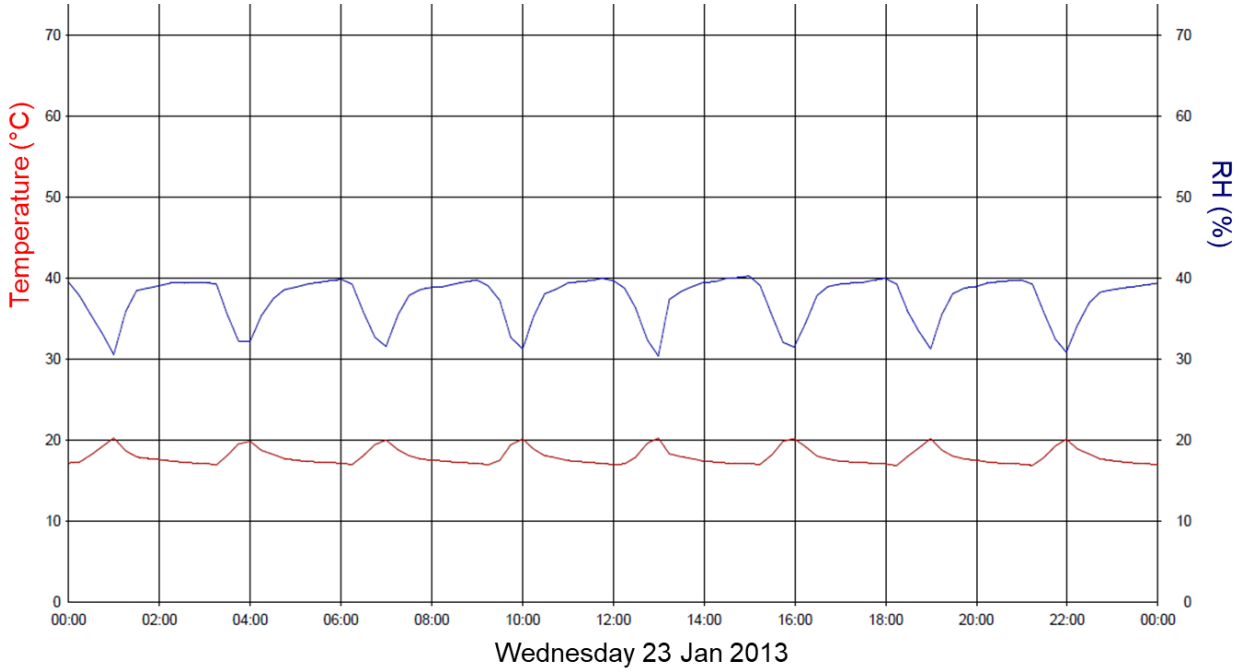

Figure 5.6 Effect of air conditioning with intermittent heating on RH & temperature, HMS 5 (Hanwell rl8)

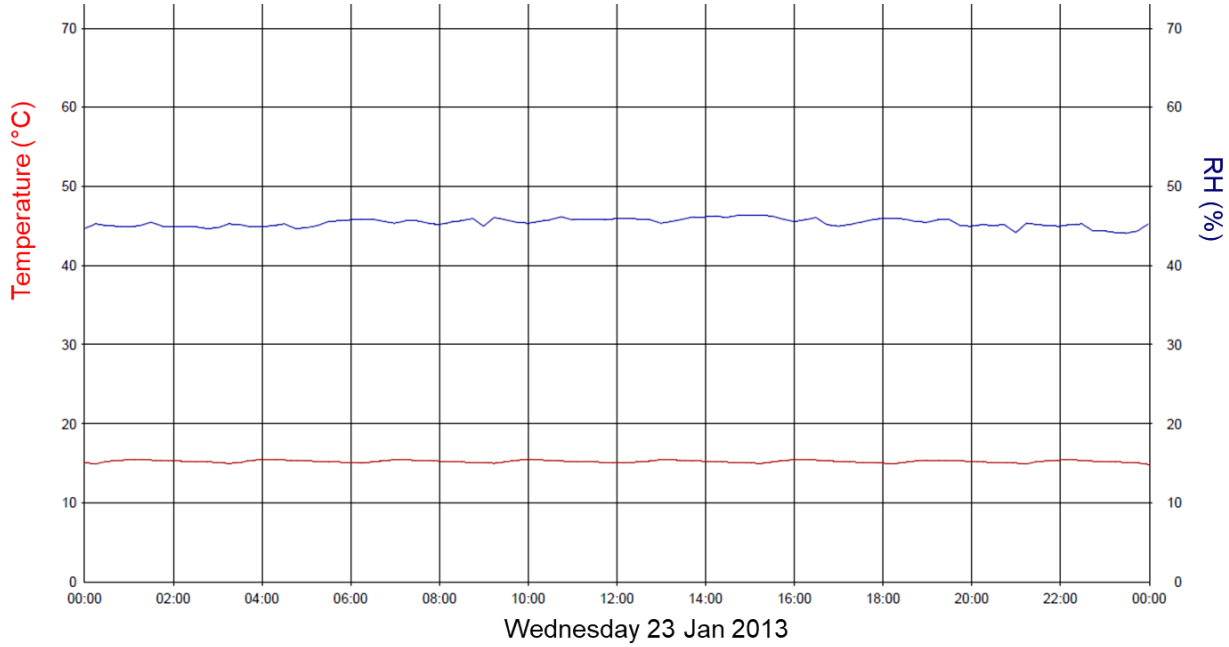

Figure 5.7 Effect of dehumidification with intermittent heating on RH & temperature, HMS 5 (Hanwell rl8)

With the RH being reduced to an acceptable level by the end of January, the BMS internal timer was set to automatically control the AHU operation. Underpressure due to faults with AHU2's supply fan and damper blades resulted in increased external air infiltration and a rise in the RH in HMS 6. The level was brought back down by lowering the RH setting on the dehumidifier. Ductwork rebalancing and replacement of all damper blades was undertaken between February and May 2013. All external air facing dampers had been found insufficiently airtight and the recirculation dampers faulty. The M&E system was finally re-commissioned as fully operational in May 2013 (Jankovic, 2013).

While RH levels were still at the higher end of the desired parameters, in the range of 55% RH in HMS 4 and 5 and 60% RH in HMS 6, the overall conditions in the building stabilised by mid-May with a total of only 6 hours of AHU operation from the beginning of the month. The design engineer concluded that there was less influence on internal conditions from moisture coming out of the new concrete slab although there was no practical test of moisture content (Jankovic, 2013). The museum requested the passive regulation period be initiated to see if the building would perform as anticipated. The regulation of RH was switched over from active to passive regulation mid-May, with the air handling system turned off (Figure 5.8). The dehumidifiers were also disconnected, allowing the personnel doors to be fully shut.

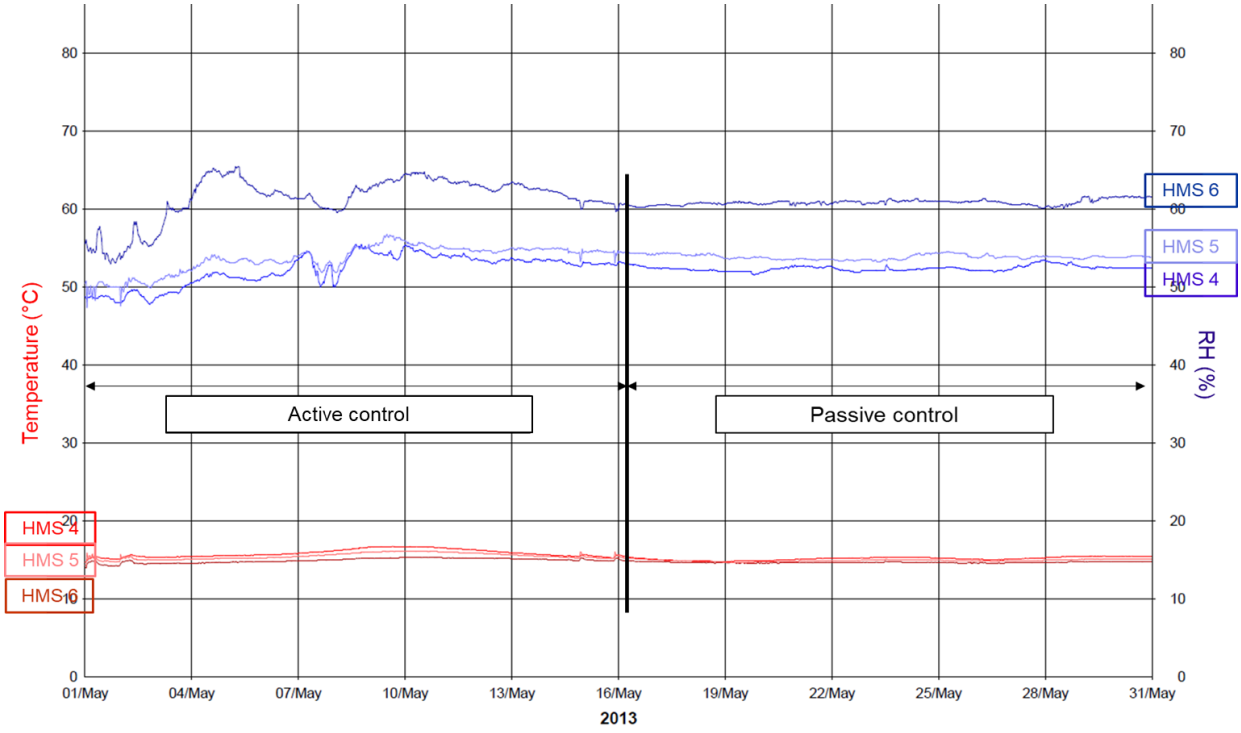

Figure 5.8 Effect of active vs passive control on RH in the HMS (Hanwell rl8)

A tabulated history of the mechanical and operational issues identified and rectified during the transient state and their effects on RH levels are to be found in Appendix E.

5.4 RH history during first steady state, June 2013 to May 2016

By the time control of the internal environment was switched to passive regulation, fifty large ship models had been moved into HMS 5 and three very large ship models into HMS 6. During the initial period of steady state operation, twenty horse-drawn carriages of various sizes were moved into HMS 6. Fifty-one framed art works had been installed on the art racking by the end of the transient period and a further three hundred and twenty-eight were moved from other SCM stores throughout June 2013 to May 2016. HMS 1, 2 and 3 remained empty. While the design engineer had recommended at the end of May that his services were retained to carry out an additional twelve months of monitoring and controlling the building in order to set the HMS onto "*a long term stable operation trajectory*" (Jankovic, 2013), operation of the M&E system was assigned to the site's Estates team and the contractor's monitoring programme ceased. There was no formal handover or training on the operation of the M&E system or on the seasonal schedule for active/passive regulation. As the Estates team did not have access to the conservation Hanwell monitoring system they used environmental information from the BMS sensors installed in the ducts, not in the storerooms. The conservation team were unaware the Estates team had not received training in operating the M&E programme and assumed that they would set the heating programme required for active regulation of RH during the winter period. The conservation team monitored the internal conditions of the HMS as part of the site's overall environmental monitoring system but only with monthly reviews of the

data. All the foregoing contributed to a time-lag in identifying and rectifying issues with regulating the RH levels during the first steady state.

The RH had remained stable on all three floors through May with limited heating but began drifting upward from June through July after the switch to passive regulation. A rise in temperature throughout the building occurred during a period of high external daytime temperatures. From mid-July into August, external daily temperatures were almost continuously higher than inside the HMS. While the internal temperatures rose in July, the internal RH levels also rose. Figure 5.9 shows the RH and temperature levels inside the HMS and externally from 10 July through August. Data from the site's external Tinytag data from 21 May to 10 July 2013 has been lost but, according to timeanddate.com, the cycle of external daily temperatures of more than 20°C began on 03 July.

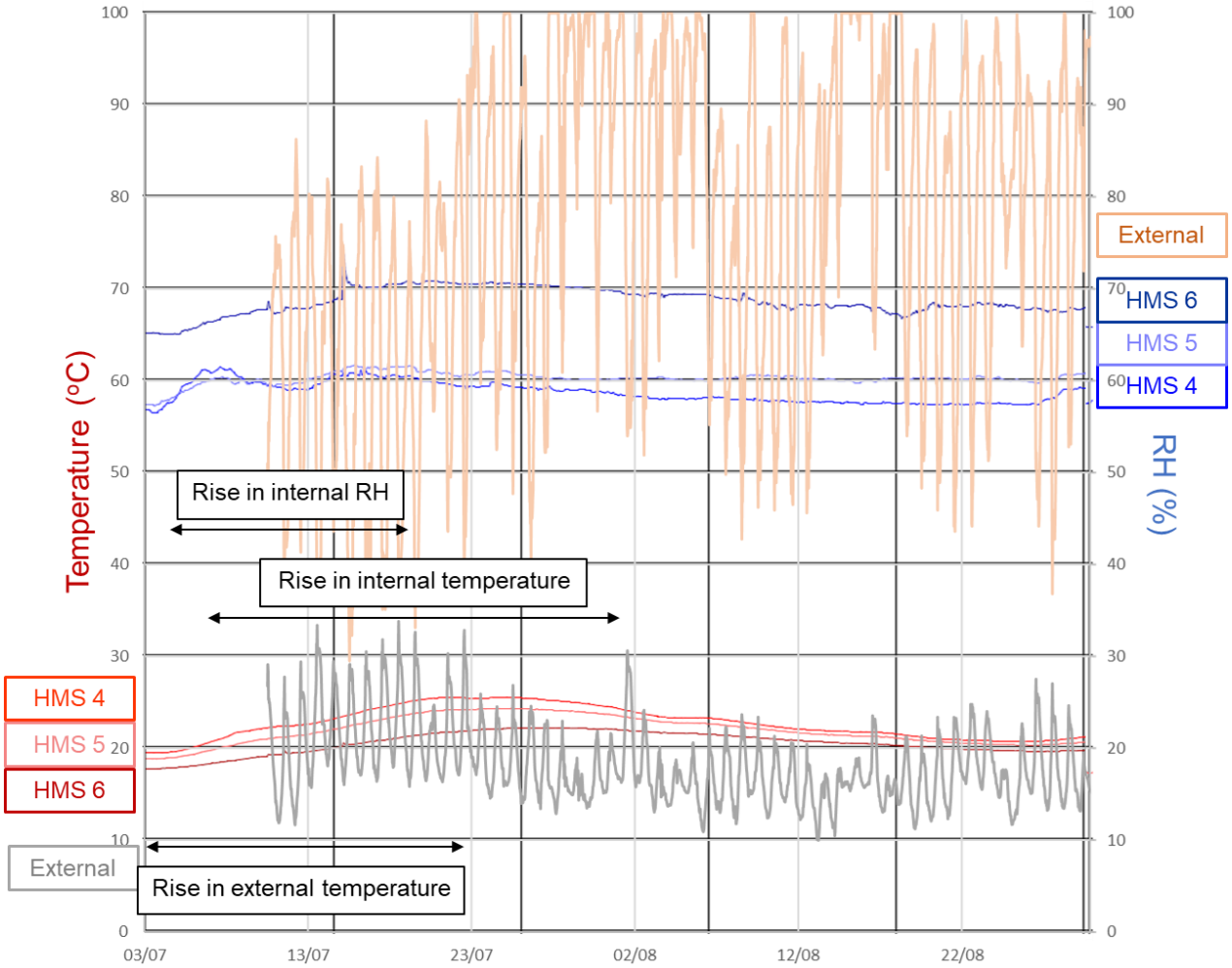

Figure 5.9 Internal & external RH & temperature ranges, July to August 2013 (Hanwell rl8; Tinytag)

The RH would have been expected to drop with the temperature increase as long as the humidity ratio had remained the same in the rooms. As there was no longer damp external air being drawn in by the air handling system and no damp hangar air infiltrating through ajar personnel doors, the increase in RH was caused from

moisture being drawn out of the porous building materials. This would have included construction moisture from the concrete slab, which would have accounted for the larger increase in the RH in HMS 6, as well as moisture desorbing from the HLC walls. The external temperature, being higher than the internal temperature, created an increasing temperature gradient across the HLC walls where moisture content was more or less in equilibrium due to passive operation. The moisture gradient, a difference in moisture content between a material's surface and inner matrix, and the temperature gradient, coupled heat and mass transport of the moisture to the wall/room interface as moisture was transported from the warmer to the colder side.

Mechanisms of moisture transport, which depend on the porous structure of the matrix as well as the environmental conditions, are the liquid phase, transported by capillarity, and the vapour phase, transported due to the gradients of parial pressure. According to Tran Le et al. (2010), the impact of the the mass transport coefficent associated with an increasing temperature gradient due to heating leads to an increase in the moisture flow through walls from the internal side to the external side during winter conditions. This results in a decreasing RH. During the period from July to August 2013, the increasing temperature gradient was external, causing an increase in the moisture flow towards the storerooms, leading to an increase in internal RH. The thermodiffusion phenomenon as observed in the HMS verified the observation of Padfield (1996) in the low energy storage building built at Ørholm, described in the literature review in Chapter 2.

The moisture was then transported out from the HLC walls and into the room through diffusion and evaporation, causing a rise in the RH level with the increase in absolute humidity. Using an online psychrometric calculator based on *ASHRAE Fundamentals*, *2001* (https://www.kwangu.com/work/psychrometric.htm) to calibrate the absolute humidity of HMS 6 from the dry bulb temperature and RH, it was found that the absolute humidity rose from 0.0065 kg/kg from 31 May (62% RH, 15°C) to 0.0116 kg/kg by 24 July (71% RH, 22°C) (Figure 5.10). The absolute humidity did not return to the May level until November 2013 when the external temperature finally dropped consistently below the temperature in HMS and the moisture content in the HLC walls reached a new equilibrium.

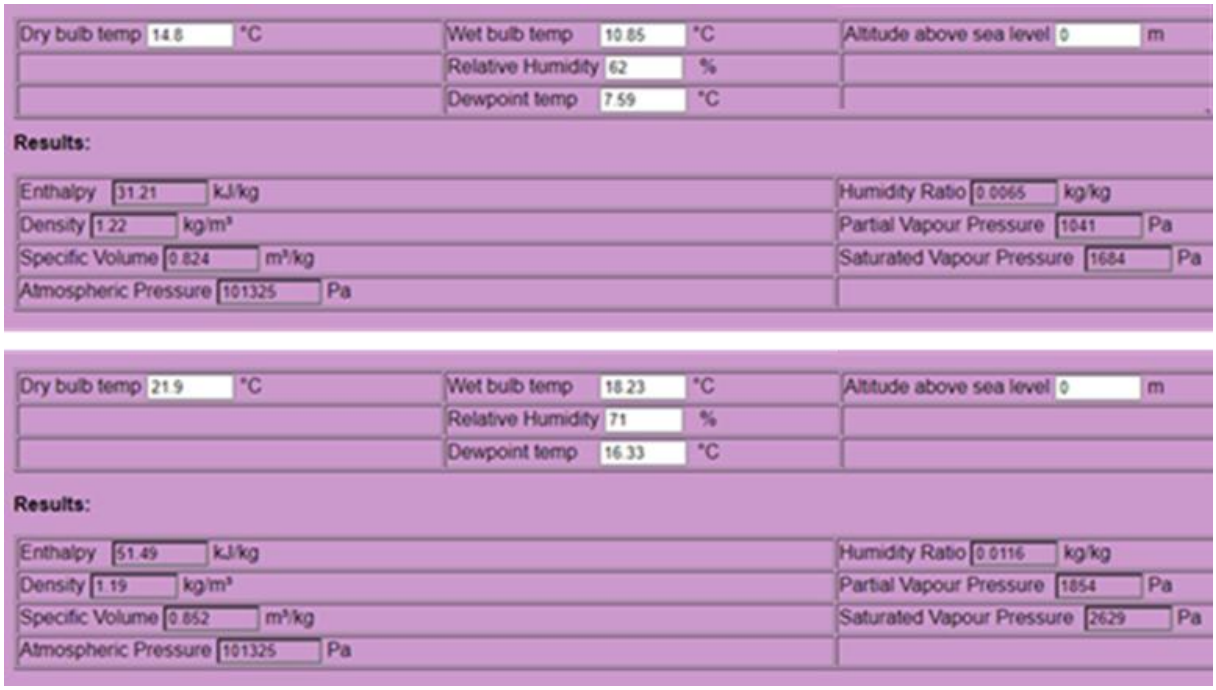

Figure 5.10 Example of absolute humidity values obtained using online psychrometric calculator

The mechanism of moisture storage buffered the fluctuations of RH during mechanical moisture regulation but contributed to the gradual rise in RH range during increasing temperature gradients due to external conditions. During the transient state, any enforced drying removed available liquid water by evaporation, in the first stage of drying. The drying rate fell when there was no longer sufficient liquid to sustain a continous capillary action as the speed of evaporation exceeded the speed at which the water diffused through the HLC pores. This point seemingly occurred in May 2013 as the rate of drying slowed down and the RH level became constant. Then the second stage of drying began after the switch to passive RH regulation was implemented in the first steady state. Water vapour diffused to the surface very slowly but as there was no mechanism to remove the moisture vapour out of the rooms, the ambient RH gradually rose. As the rate of the temperature gradient increased across the HLC walls, the RH rose at a faster rate until equilibrium was reached again within the walls, with the RH in HMS 4 and 5 levelling out at the higher end of the desired parameters, around 58% RH and 60% RH respectively and, in HMS 6, around 65% RH. Although the temperature continued to drop through December, the RH remained at the same level in HMS 6, indicating a very slight drying out. In HMS 4 and 5, as the temperature dropped, the RH rose, maintaining the humidity ratio.

The RH remained within 65% RH ±5% RH on the ground floor and 60% RH ±5% RH on the first and second floors until April 2014. Once-weekly operation of AHU2 from January 2014 resulted in abrupt RH fluctuations in HMS 5 and 6 but these had no effect on the overall RH level and did not last long enough to adversely affect objects stored in the rooms. From April to mid-June 2014, the external temperature rose almost daily above the temperatures in the HMS, promoting an increase in internal RH with levels eventually reaching up to 70% RH in HMS 4 and 5 and 75% RH in HMS 6. As sustaining this level of RH would have put the objects in the storerooms

at risk, the heaters in both AHUs were turned on for a short period of time. This rapidly dropped the RH by 10% in all three rooms but the Estates team was hesitant to operate the heating system as external temperature were above 22°C. Portable dehumidifiers were placed in HMS 5 and 6 and the heating system turned off. The dehumidifiers gradually brought the levels down to just below 60% RH in HMS 6 and 50% in HMS 5. No dehumidifier was placed into HMS 4 and the RH drifted between 60% RH and 65% RH.

In December 2014, the design engineer returned to site to assist the Estates team in reinstating the programme of heating and ventilation. Another drying period with intermittent heating and ventilation with external air was carried out to lower the internal RH. However, as there was no software programme in the BMS to use external humidity data for timing the operation of the AHUs, once the Estates team took over full operation in February 2015, the AHU heaters were set automatically to run from 00:00 – 06:00. AHU2's heater was set to run at 2°C higher than ambient in order to keep the RH in HMS 6 between 50% RH and 60% RH. In HMS 4, with the RH being reduced to 50% by the drying period, the RH was stabilised around that level with only a 1°C temperature increase from ambient during the daily 6 hour operation of AHU1. The Estates team felt confident that the 6 hour on, 18 hour off heating cycle would ensure that the RH parameters would be met without causing significant fluctuations and once again the portable dehumidifiers were removed. The cyclical operation of AHU2 caused daily RH fluctuations around ±5% in HMS 5 and 6 but AHU1 caused virtually no fluctuations in HMS 4 and the RH remained around 50% (Figure 5.11). The RH was still consistently higher in HMS 6 than the other two rooms but in an accepted range of 60% RH ±5% RH.

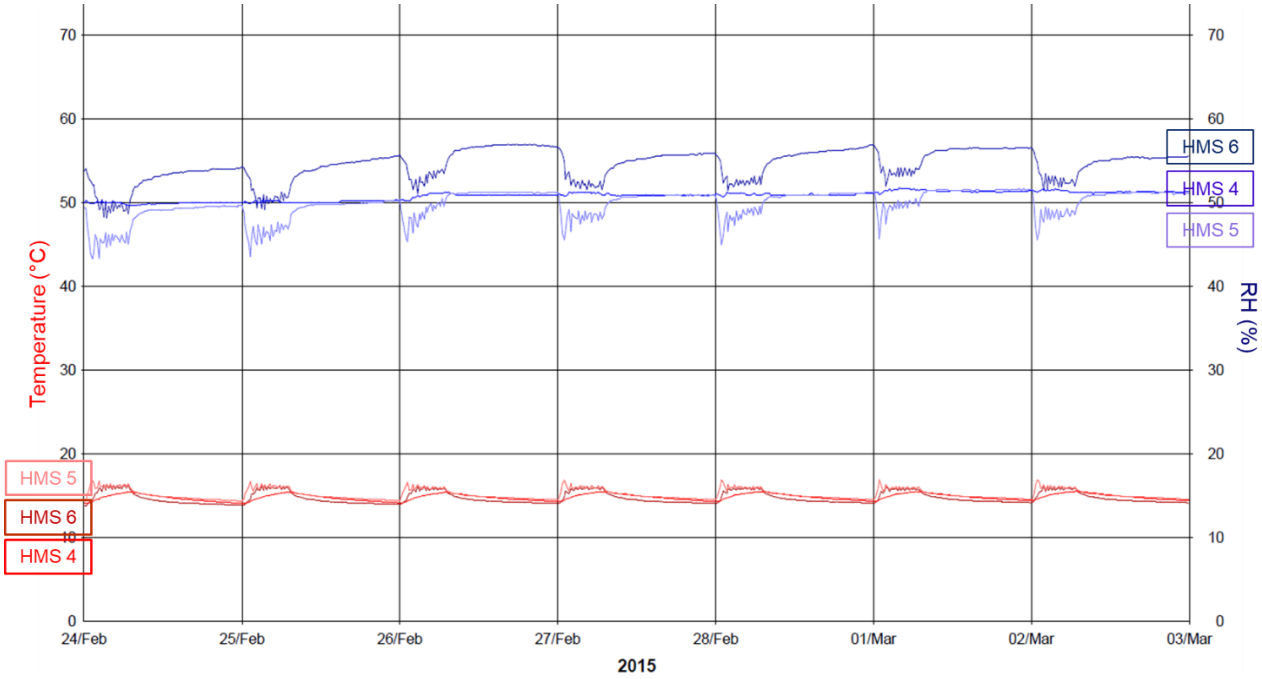

Figure 5.11 Effect of heating & ventilation programme on RH in the HMS (Hanwell rl8)

In June 2015 the original plan, to allow passive RH control during more temperate seasons, was reinstated and the heating system turned off. As in the previous

attempt to regulate the RH passively, the RH fluctuations virtually ceased but the RH level began to drift upwards once again. By mid-July 2015, the RH reached 68% in HMS 6, 8% higher than in HMS 4 or 5. As it was a very wet summer, the external air was continuously too damp to offer any possibility of passive drying through ventilation. A portable dehumidifier unit was returned to HMS 6 and the RH was brought down to 55%. Another attempt at total passive regulation in September resulted in the RH drifting back up to 62% and so operation of the dehumidifier became routine.

From January to mid-May 2016, AHU2 was operated for two hours, from 10:00 to 12:00, once a week, with the same operational cycle for AHU1 introduced from April to mid-May. The short periods of heating helped maintain an RH around 60% in HMS 5. The RH level in HMS 4 had been around 3% higher than in HMS 5, both with and without heating. When the heating was turned off in mid-May, as the external temperature rose to over 20°C, the RH in both rooms began an upward drift, with the RH in HMS 4 reaching 67%. In HMS 6, the RH remained within the range 55% RH ±5% RH to the end of May 2016, except when sporadic heating bursts occurred causing downward spikes in the RH. Whenever the dehumidifier stopped working in HMS 6, as seen in Figure 5.12, the RH began to drift upwards as long as the room temperature remained consistent.

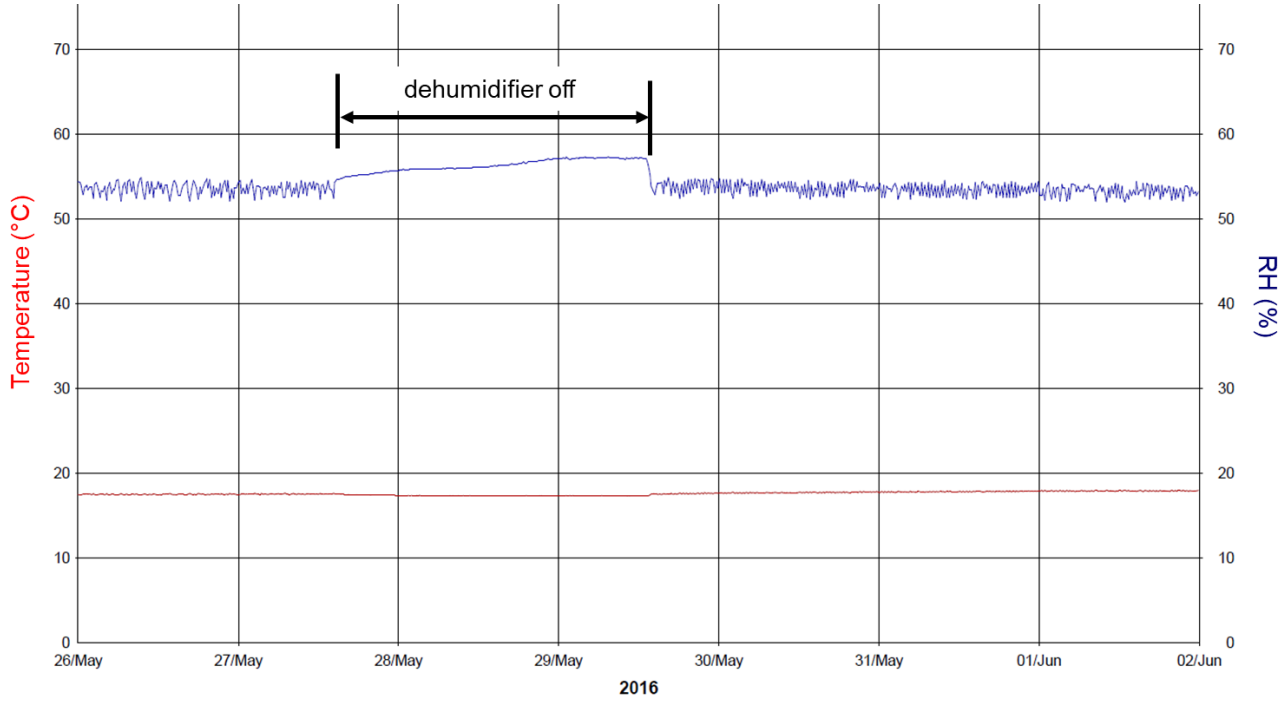

Figure 5.12 Effect of dehumidifier failure on RH, HMS 6 (Hanwell rl8)

5.5 Assessment of the RH moderation to June 2016

The building had required a year to obtain stable RH conditions, far more than the original estimate of one month. While the RH was kept overall within a range throughout the steady state to June 2016, so that stored museum collections were not at risk from deterioration by either too high or too low RH levels or by excessive and sustained RH fluctuations, the regulation in HMS 6 required the use of a

portable dehumidifier whether or not the air handling system was operated. Based on the monitoring data, which showed that there was a gradual upward drift of RH on all floors whenever passive operation was implemented, either intentionally or through mechanical failure, the HMS appeared to be still in the second phase of drying out throughout the first steady state period of operation. Since no active humidity regulation module was installed in the air handling system, the ancillary solution of a portable dehumidifier in the ground floor storeroom to control the higher level of RH had to be implemented. More effective secondary drying would have resulted if the dehumidification module had been retained as part of the total M&E system.

Moisture content in the ground floor storerooms might have been less of a problem if the construction programme had allowed for a longer drying-out period for the concrete pad before enclosing it within an airtight hygroscopic building envelope. The porosity of the construction materials, specifically the HLC walls, affected both the primary and secondary drying operations throughout the building as moisture diffusion and evaporation rates were accelerated whenever there was a rise in the temperature gradient through the walls. This caused a rise in the internal RH whenever the external temperature was higher than the internal temperature. Moisture was readsorbed by the hygroscopic materials once the phenomenon of the temperature gradient ceased. As Padfield pointed out (Padfield, 1996), RH control by heating would only have been achieved in the HMS if the temperature had been consistently held about 5°C above the expected external temperature in the hangar. This could have been achieved by consistently heating with very slow temperature changes but not by the intermittent heating cycles which became established for the air handling system.

5.5.1 Buffering effects of HLC

The environmental conditions inside the HMS were more stable than those inside the hangar during the intial steady state, with RH fluctuations being significantly buffered. Data was obtained using Tinytag data loggers which could then be compared to Hanwell data by converting the CSV data files from both systems to Excel spreadsheets. In Figure 5.13, comparative data from HMS 4 and hangar D2 during minimal (one-weekly) operation of AHU1 through February to April 2014 showed that the temperature range inside the HMS was similar to that in the hangar but more stable. The internal RH was significantly lower and more stable compared to the hangar RH. Similar buffering of the RH conditions occurred in HMS 5 during operation of AHU2. In HMS 6, it was more difficult to assess buffering performance of the HLC due to the operation of the portable dehumidifier. In the period from February through May 2014, when no dehumidification occurred, the monitoring data from HMS 6 showed very similar RH fluctuation moderation to that occurring in HMS 5 (Figure 5.14), with an exceptional spike in RH in HMS 6 on 02 May due to the overhead sectional door being opened when the external RH was above 90%. However, the RH level in HMS 6 was 5% higher than in HMS 5 without dehumidification.

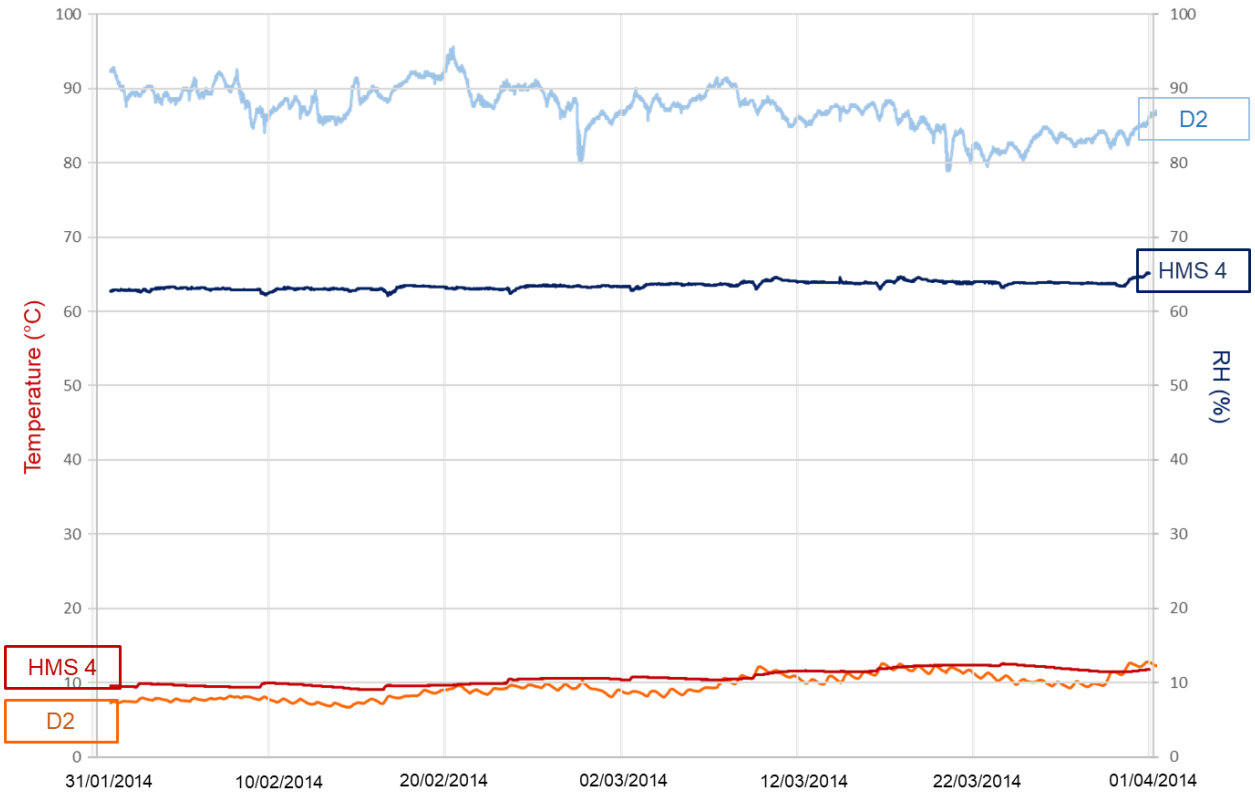

Figure 5.13 Stability of RH in HMS 4 compared to hangar D2, February to April 2014 (Hanwell rl8; Tinytag)

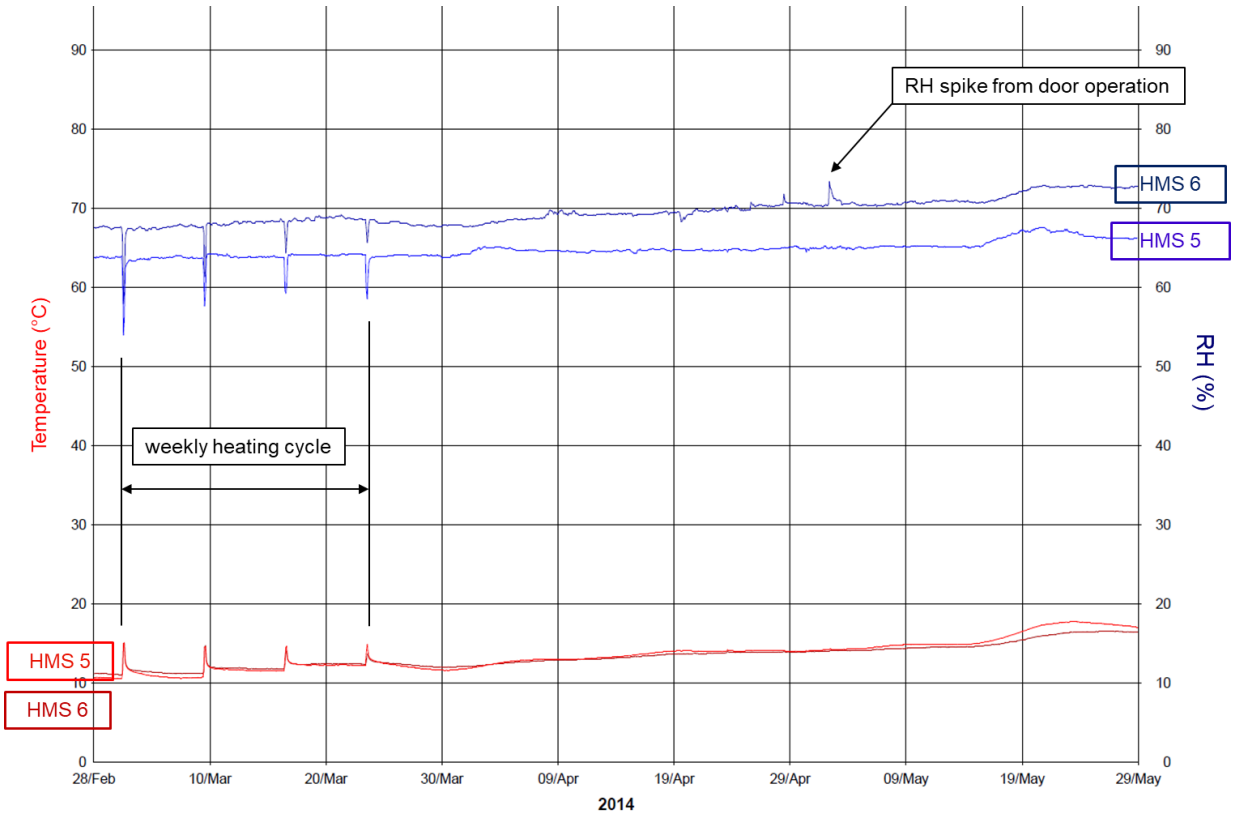

Figure 5.14 Comparison of RH levels & fluctuations in HMS 5 & 6 without dehumidification (Hanwell rl8)

Both heating and ventilation cycles and dehumidifier operation during the initial stable state caused RH fluctuations. Fluctuations caused by heating and ventilation were in the ratio of 1°C increase or decrease to a 3% decrease or increase in the RH level, showing that the heating and ventilation programme was not having an effect on the absolute humidity in the rooms. Fluctuations produced from operation of the dehumidifier in HMS 6 were a consistent ±2% around the RH setpoint of the portable unit. Where heating and ventilation and dehumidification were used, as in HMS 6, both rates of RH fluctuation occurred although the lower rate caused by the dehumidifier was over-ridden by the larger rate during operation of the heating and ventilation programme.

Based on the monitoring data obtained during the initial steady state, RH in the HMS fluctuations were caused predominately by AHU operation, then dehumidifier function. It was concluded that the buffering capacity of the HLC wall panels reduced humidity changes caused by mechanical RH control as RH fluctuations were short-lived and RH levels were returned to previous levels at the cessation of each cycle. During passive control, while the monitoring data showed very little RH fluctuation, the very stable RH levels could also be attributed to the negligible air change rates. The RH levels and fluctuations throughout both phases of RH control were kept well within the acceptable parameters for museum storage.

Levels of RH continued to be at the high end of the specification parameters to the end of the first steady state. Localised dehumidification in HMS 6 had little effect on lowering the absolute humidity in that room and the heating and ventilation programme had no drying effect. The thermodiffusion caused by the moisture gradient created whenever the external hangar temperature was higher than the internal storeroom temperature resulted in an increase in internal absolute humidity and a rise in internal RH. Moisture that had been stored in the porous structure of the HCL as a result of damp external air brought through the air handling system was transported into the rooms by the positive Soret coefficient. Moisture content in the HLC walls appeared to remain constant as RH levels did not decrease over time. During the initial steady state of operation, different solutions were tried to reduce the moisture gain from the transient state operation and to enhance control of RH levels.

The M&E malfunctions which were responsible for the introduction of moist external air during the transient period were identified and rectified throughout a year-long *“soft landing approach”* by the engineering design consultant and engineering contractors (Jankovic, 2013) although an fault in the BMS setting allowed random heating cycles to continue into the initial steady state of operation. Focus on achieving temperature parameters was redirected to attaining stable RH by using the results of the research literature review on RH recommendations to clarify the specifications required for the HMS. It was decided that internal temperature levels could be slightly higher than originally specified without having any significant deleterious effects on the cultural heritage collections stored in the HMS. Sustained levels of RH above 65% would, on the other hand, have damaging effects as both mould growth and corrosion could occur in relatively short periods of time. Wider fluctuation bands (±10% RH/24 hrs within the RH parameters) were allowed under revised SMG guidance, also based on the results of the literature review. These changes resulted in a programme of minimal cyclical heating to be used to reduce and maintain RH levels. Although raising the temperature to a continuous 25°C to

control the RH level was suggested (Jankovic, 2012), this was contrary to the intent of the project, which was to deliver low energy environmental control. Supplementing the heating and ventilation programe with dehumidification units connected to hangar drainage was a more energy-efficient solution. As there was no programme in the BMS to identify when external RH was lower than internal RH, attempts to lower internal RH through ventilation were abandoned. As external RH was lower when the external temperature wwas high enough to cause a thermal gradient across the HLC walls, increased ventilation during that time might have reduced the internal RH gain. However, increased ventilation would have led to increased fluctuations in RH.

The higher level of RH on the ground floor was identified through analysis of the RH monitoring data from the three rooms. The difference did not seem to be due solely to temperature thermodynamics or to RH stratification throughout the building, as the RH could be higher on the second floor than on the first. While the ratio of RH to temperature on the first and second floors remained about 3% RH to a change of 1°C, on the ground floor the ratio of change was 7% RH to 1°C during the transient period, as in August 2012 when the temperature on the second floor was 22°C and 65% RH, on the first floor 21°C and 68% RH but on the ground floor was 19°C and 78% RH. The RH in HMS 6 would have been expected to be 73% RH if there was no additional moisture to increase the absolute humidity. The regain of RH to the higher level when the dehumidifier stopped working also indicated continuing moisture influence. While no moisture content testing of the concrete floor slab was undertaken, by the end of the first year of steady state operation it was concluded by the design consultant that the *“initial high moisture content in the building concrete slab”* (Jankovic, 2013) had contributed to the *“teething”* problems of the HMS. Higher RH levels in HMS 6 continued through the first steady state and into the second.

Retrofit and overhaul of the M&E system, refocus on RH control rather than on temperature control and continued active removal of moisture, as illustrated by the flowchart in Figure 5.15, resulted in the RH within HMS 5 and 6 stabilising just within the SMG recommended range for hygroscopically sensitive materials but just above the recommended range in HMS 4, by the end of the fourth heating year. Daily fluctuations of RH were minimal but continued to be caused by intermittent heating and dehumidifier operation. (Figure 5.16).

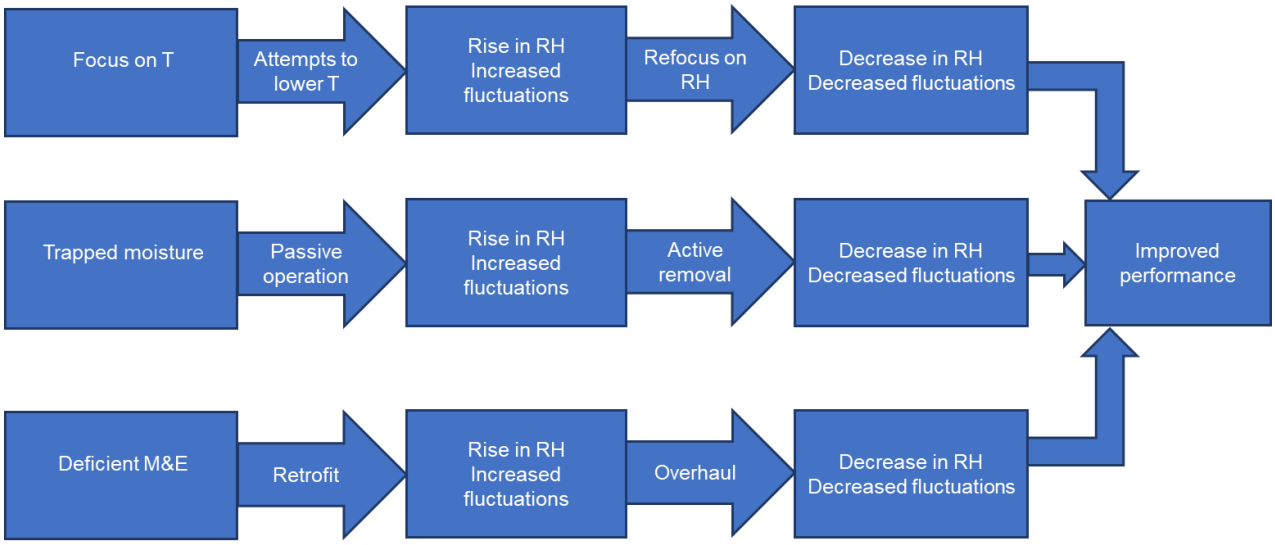

Figure 5.15 Flowchart of issues to solutions for improved RH control

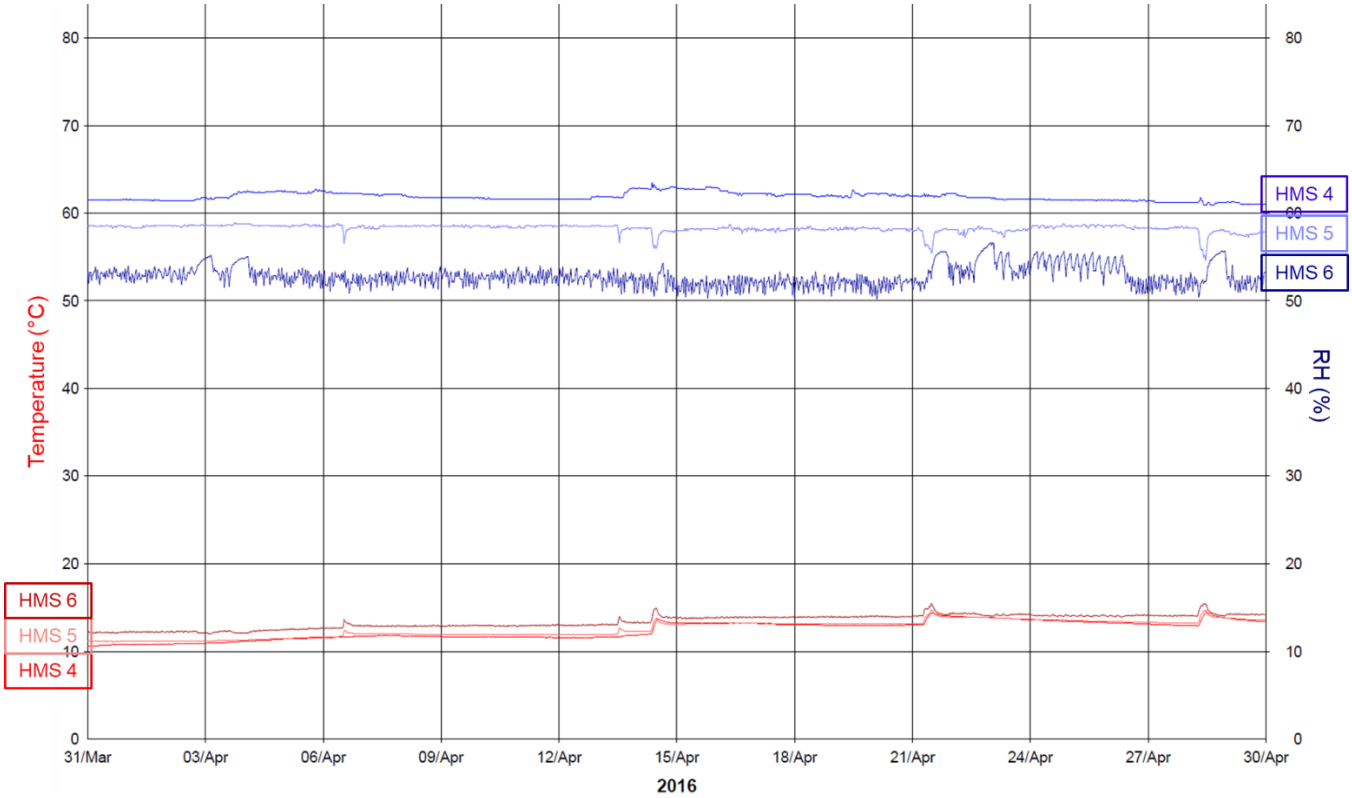

Figure 5.16 RH regulation in the HMS at end of 1st steady state (Hanwell rl8)

5.5.2 Energy expenditure in the transient & 1st steady state periods

The operation of the M&E system during the transient period to April 2013 was reported to have an electrical consumption of of 23.5 kWh/m^2/yr or 23,030 kWh/yr (Moore, 2013) against a predicted annual consumption of 24.8 kWh/m^2/yr or 24,320 kWh based on the seasonal operation of the reduced M&E system. This equated to 10.57 kWh/m^3/yr for the useable storage volume of 2,179 m^3. It was hoped that the

electrical consumption would decrease as the building further stabilised (Moore, 2013).

By the end of the initial steady state period, the annual electrical consumption had risen to 26,139 kWh (Hopkins (pers. comm.), 02.03.2017) as a result of running the AHU programme throughout the year in order to prevent the RH increases which ocurred whenever the building was put into passive mode. This equated to an electrical consumption of 12 kWh/m^3/yr or 30.4 kWh/m^2/yr for the usable storage space, predominately for maintaining the RH around the acceptable upper limit under SMG guidelines. Lighting needs were insignificant due to only occasional access and activity. According to Hopkins (2017), NCC site electricity costs in 2015 were 9.54p per kWh, costs which were in line with published electricity prices for very large non-domestic consumers (BEIS, 2013, updated annually). Electricity costs for maintaining the HMS in 2015 were £2,078.77.

Moore (2013) graded electrical running consumption for conventional museum storage, where mechanical means were relied on to control environment within 40% to 50% RH, with an excellent consumption averaging 44 kWh/m^2/yr, a mid-grade consumption averaging 70 kWh/m^2/yr and a poor consumption averaging 120 kWh/m^2/yr. He graded the HMS energy consumption of 28 kWh/m^2/yr as better than excellent. Moore's grades were similar to the UK museum energy benchmarks of 57 kWh/m2/yr (good) and 70 kWh/m2/yr (typical) (CIBSE, 2004; 2008). It should be noted that these energy usage benchmarks also included lighting usage and that the benchmarks were for exhibition rather than for storage climate control. Benchmarks were based on information from the Museums and Galleries Association and the Department for Culture, Media and Sport. According to a 2015 report on energy usage in SMG buildings, the annual energy expenditure for the museum's A Store averaged 380,000 kWh/yr for the 3,150 m^2 building footprint, equating to 120 kWh/m^2/yr, which placed it into Moore's poor grade, and for the L&A store, 1968 m^2, averaged 209,271 kWh/yr, equating to 106 kWh/m^2/yr which placed it in Moore's mid-grade.

However, more useful energy consumption data is obtained using storage volume which allows the comparison of energy use versus RH moderation in the usable storage space. Comparisons have been made with data obtained during more in-depth storage research projects in Denmark. Padfield (2010) developed an on-line calculator to simulate energy consumption for constant exhibition climate control (50% RH, no fluctuations), variable (seasonal drift) exhibition climate control (40% RH to 60% RH), "leaky" (3 air changes/hr) storage and airtight (0.5 air changes/hr) storage (both 50% RH to 60% RH), using data from museums and storage buildings in Denmark. His calculator assumed 30 kWh/m^3/yr for light energy for exhibition spaces but no light energy consumption for storage. Energy requirements for heating and cooling the airtight store was shown to be one-fifth of that needed by the controlled climate exhibition space, at 21 kWh/m^3/yr as opposed to 108 kWh/m^3/yr. Heating and cooling energy requirements for the variable climate control was 72 kWh/m^3/yr with the "leaky" store consuming 71 kWh/m^3/yr. He noted that consumption levels of less than 3 kWh/m^3/yr should be possible by including the use of abundant humidity buffering materials in the construction of the airtight store.

The energy consumption of the HMS, constructed of abundant humidity buffering material and airtight, was lower than Padfield's airtight model but not as low as results obtained during a 4-year study undertaken by the Department of Conservation at the National Museum (Ryhl-Svendsen et al., 2012) on energy usage of purpose-built low energy museum storage buildings in Denmark, at Vejle, Ribe, Randers and Ørholm (Chapter 2, section 2.4.3) with data collected from 2006 to 2010. The storerooms at Ribe and Randers had dehumidification but no direct heating. The shared facility at Vejle had both basic unheated but dehumidified storerooms as well as one storeroom with a drier environment provided by direct heating as well as dehumidification. Ørholm Hall P was provided with heating and ventilation and eventually dehumidification. Table 5.4 show the typical main trends for environment and energy use (Padfield, 2010; Ryhl-Svendsen et al., 2012):

Table 5.4 Typical environmental & energy performance levels for comparative low energy museum storage buildings

Building	RH (%)	Temperature (°C)	Energy use (kWh/m³/yr)
Ribe (basic storage	47-69	8-17	1.5
Vejle (basic storage)	45-63	7-17	1.5
Vejle (dry storage)	35-53	10-18	4
Randers (basic storage)	40-63	7-19	3
Randers (dry storage)	25-40	7-21	9
Ørholm Hall P	44-65	8-24	10 (est.)
HMS (all storerooms)	48-64	8-23	12
Padfield (airtight storage)	50-60	10-17	21

Energy consumption was higher in the HMS for average environmental performance trends comparable to three of the four Danish museum stores by the end of the initial steady state period (Figure 5.17) but was similar to that of Ørholm Hall P. The HMS differed from Ørholm Hall P in that it had an insulated floor slab and mechanical intake of external air. Both buildings initially relied on mechanical heating and ventilation to control RH levels with both having dehumidification provision added at a later date.

By comparing the energy consumption with the RH levels attained at the end of the first steady state period, it can be seen that RH moderation was tighter in the HMS than in the basic Danish museum stores but it still did not succeed in completely meeting the museum's specification of 40% RH to 60% RH despite the higher energy expenditure. While it would seem that allowing a wider range of RH levels would have reduced the energy consumption in the HMS, the tendency for the RH to drift to the upper range was continually an issue. Reducing the amount of heating and, in the case of HMS 6, dehumidification resulted in the inevitable rise in the RH level to over the acceptable limit of 65% RH.

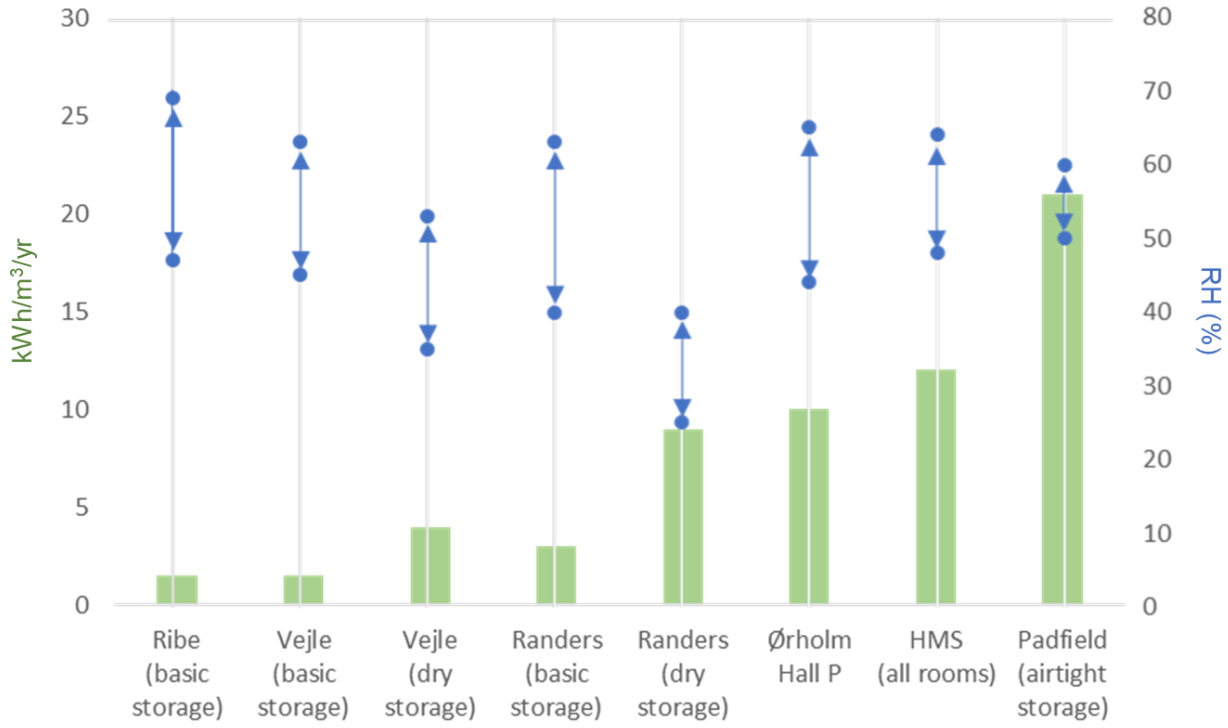

Figure 5.17 RH moderation vs energy usage for the HMS & comparative low energy museum stores

In the original plans for the HMS, a renewable energy system had been intended to reduce both energy costs and carbon emissions. The preferred option had been to install a solar photovoltaic array to produce 24.7 MWh/yr, or enough energy to off-set the entire annual consumption required to maintain environmental conditions. The outlay costs of the array were assumed to be fully paid for by the ninth heating year and then to subsequently yield a profit with a pay-back of £96,710 in 25 years (Jankovic, 2012e). While the installation never happened, the annual operation of the building without the array still came in under the original annual running cost estimate of £3,392.31 which had been predicted on an energy price of 13.7p per kWh. If, as indicated by the research results from Denmark, a more effective low energy system using dehumidification rather than heating had been installed, energy costs might have been closer to those found for the four Danish stores and mitigation of costs anticipated by the never-installed solar array not missed.

For the usable storage volume in the two other NCC purpose-built stores, the A Store required an average of 18 kWh/m^3/yr and the L&A store an average of 28 kWh/m^3/yr to moderate the environment. Neither building met the museum's specifications consistently either in terms of RH levels or RH fluctuations (Table 5.5).

Table 5.5 Average annual environment & energy performance in NCC low energy storage buildings

Building	RH (%)	Temperature (°C)	Energy use (kWh/m^3/yr)
HMS (all storerooms)	48-64	8-23	12
A Store	32-73	10-22	18
L&A store	55-80	10-21	28

Figure 5.18 shows the comparison between the control of RH and the energy consumption in the three low energy stores on the NCC site. All three stores regulated RH levels using mechanical heating and ventilating systems but only HMS had RH levels regularly within the museum's specifications. A Store performed better than the L&A store in that the RH levels were not excessively high but the range of RH throughout the year was much greater despite maintaining similar storeroom temperatures. The RH levels in the L&A store were consistently too high, leading to the issues of mould growth previously mentioned. RH data for both stores are presented and discussed in Chapter 6, Section 6.3.2.

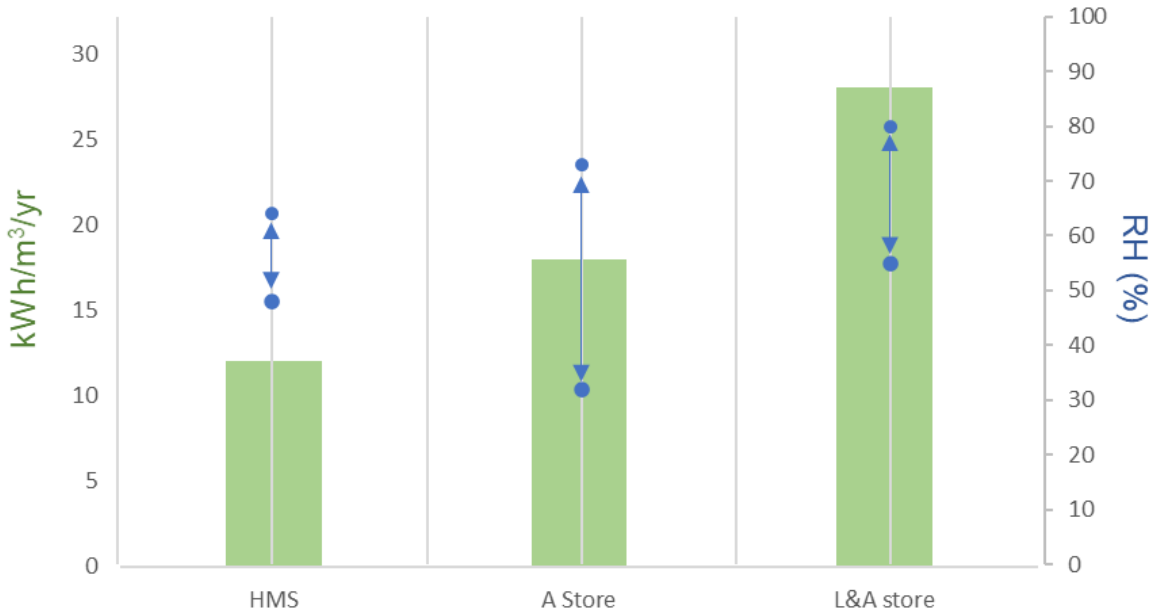

Figure 5.18 RH moderation vs energy use for NCC low energy museum stores

By the end of the first phase of steady state operation, the museum considered that the energy expenditure of 26,139 kWh/yr required to maintain the environment in the HMS fulfilled the institutional mandate for low energy environmentally-controlled storage. While energy use was higher than originally estimated, overall expenditure throughout the first steady state was lower as average energy costs for the NCC site was between 7.94p in 2012 to 9.54p per kWh in 2015. While the RH still tended to drift to the upper end of the range, the environment was much more stable than in either of the museum's other two purpose-built stores. Table 5.6 shows the annual energy costs from 2012 through 2015 required to regulate the RH in each of the three low energy stores. For the HMS and the A Store, costs are based on BEIS annual statistics on combined energy costs per pence per kWh for very large sites.

Costs for the L&A store are combined annual electricity costs and the biomass fuel costs, which were £7,000/yr (Hopkins (pers. comm.), 02.03.2017).

Table 5.6 Annual energy costs for NCC low energy stores, 2012-2015

Year	£ per kWh/yr	Annual energy cost		
		HMS	A Store	L&A store
2012	0.0794	£2,075.44	£30,172.00	£10,289.78
2013	0.0893	£2,334.21	£33,934.00	£10,699.97
2014	0.0929	£2,428.31	£35,302.00	£10,849.13
2015	0.0954	£2,493.66	£36,252.00	£10,952.71

While overall volume of the A Store was 32,000 m^3, the usable storage space was 22,000 m^3, making the percentage difference for energy costs per storage volume an annual 44% increase of the energy costs for the HMS. The usable storage volume in the L&A store, from floor to the top of shelving at 3.75 m, was 7,380 m^3. Annual energy consumption for electricity was 41,433 kWh and for biomass fuel was 177,838 kWh/yr. Overall, while costs per usable storage space in the L&A store were higher than in the HMS, the percentage difference dropped from an annual 46% increase to an annual 30% increase of the HMS energy costs as the price for wood pellets remained static. Table 5.7 shows the costs per usable storage volume for the three stores from 2012 to 2015.

Table 5.7 Annual energy costs per m^3 usable storage space, 2012-2015

Storage building	Energy costs per volume of usable storage space £/m^3			
	2012	2013	2014	2015
HMS	0.95	1.07	1.11	1.14
A Store	1.37	1.54	1.60	1.65
L&A store	1.39	1.44	1.47	1.48

In terms of low energy expenditure, all three stores met the museum's requirements based on kWh/m^3 usage but the HMS consistently provided the most stable environment for collections care with the lowest energy costs.

Further investigation into the hygroscopic performance of the HLC was carried out in the second steady state period, from 2016 to 2020, in order to clarify and validate findings from the first phase of research. Data were acquired on the effects of moisture content, secondary drying, ventilation velocity, duration of activity and AHU operation on the regulation of internal RH. This data is presented and discussed in Chapter 6.

5.6 Chapter summary

In Chapter 5, objectives were to describe the monitoring strategy for the case study and to assess RH data acquired during the transient and first steady state.

The use of HLC in the construction of the HMS was intended to reduce the need to rely on RH control by means of a full HVAC system. A full HVAC system was proposed based on simulation modelling using very tight specifications of RH and temperature but this led away from the museum's call for a low energy repository. A smaller and less energy-intensive air handling system, using heating and ventilation for mechanical RH control and the hygroscopic capacity of HLC for passive regulation for RH fluctuations, was modelled and installed.

During the transient state, mechanical and operational issues with the M&E system along with moisture content in the HLC and concrete, resulted in RH levels above an upper parameter of 60% RH. During pre-conditioning, the focus on temperature rather than RH and the M&E issues pushed the RH level to 80%. Enforced drying using the heating and ventilation system was insufficient to bring RH levels down to acceptable levels and portable dehumidifiers and air conditioners were required. Environmental monitoring data revealed the extent to which the mechanical issues impacted on RH control. Throughout the first steady state, the air handling operation was modified in efforts to resolve the tendency for the internal RH on all floors to rise to the upper limit of the specified range. Monitoring data from the first steady state showed that the operational modifications contributed to achieving an overall stability of the RH, meeting the SMG parameters for RH levels and fluctuations during dynamic operation.

Assessment of RH data from the HMS through the first steady state demonstrated that buffering from the HLC reduced the RH fluctuations caused by the mechanical system. The rise in internal RH occurring during periods of high external temperature was identified as the thermodiffusion phenomenon, resulting from a positive moisture gradient through the porous HLC matrix caused by a thermal gradient from warmer outside to colder inside temperatures. Thermodynamic reactions from increasing the internal temperatures were seen to reduce RH gains but only when internal temperatures exceeded external temperatures. Heating proved to be necessary in summer months, contrary to results from the M&E simulation which had informed a mechanical RH control programme using heating only during winter months.

Comparison with low energy stores in Denmark showed the HMS to be on the high end of low energy use but with better RH control. Comparison with RH data from two other low energy stores on site indicated that augmentation of RH regulation by HLC enabled RH control by mechanical means to be reduced, thereby reducing energy use and costs. Overall RH control was improved, with more stable diurnal and seasonal RH in the HMS than the other stores. Findings of the first phase of research were that the costs of controlling RH control to museum specifications could be reduced by utilising the buffering capability of HLC but that cost reduction was compromised by choice of the mechanical control system.

Chapter 6 Case study - the HMS: 2nd period of steady state performance, June 2016 to January 2020

6.1 Introduction

This chapter analyses the monitoring data obtained through the 5th to 8th heating seasons of the case study, from June 2016 until January 2020, and the second phase of the PhD research. The monitoring strategy was further developed and extended by this researcher to assess moisture content, ventilation and duration of activity effects on RH control. During this period, additional monitoring equipment was acquired through the museum and installed in the HMS and other areas within hangar D2 as described in Chapter 4. The data was assessed and used to clarify and verify conclusions based on RH and temperature monitoring during the first steady state period, that there was validity in assuming a techno-economic viability of HLC construction to provide low energy moisture control in museum storage.

Within the HMS, the Hanwell environmental monitoring system was extended to monitor MC (%) within the HLC walls and air flow from the ventilation system. RH was monitored at different levels within HMS 6 to confirm and assess effects of RH stratification. Access into the storerooms in use was recorded to see if there was any impact from duration of activity on buffering performance.

Data provided on the condition of collections objects prior to installation in the HMS was reviewed during the second steady state to assess for physical, chemical and/or biological deterioration. No visible damage from RH levels or fluctuations could be identified during the assessment period and it was determined that RH levels were regulated sufficiently to prevent deterioration of all objects stored in the building.

6.2 RH history during second steady state, June 2016 to January 2020

RH/T monitoring graphs comparing the external and internal environments through pre-conditioning through transient state and into first steady state (Figure 6.1; Figure 6.2) showed that the fluctuations in RH in the HMS were caused predominately by issues with the M&E system but that changes in RH levels could be caused by external temperatures. Graphical views using CSV data from the external Tinytag data logger and the Hanwell ML4106 unit in HMS 6 showed the deviation between internal and external RH. Figure 6.2 shows that there was significant buffering of RH fluctuations in HMS 6 during the start of passive operation with the RH level dropping down to the upper parameter. Overlay of external with internal data shows that this coincided with a period of lower external temperature. However, data acquisition for comparable purposes was limited during the first steady state due to the unreliability of the Tinytag data collection and the extent of the effect of external conditions on internal RH was not clearly identified.

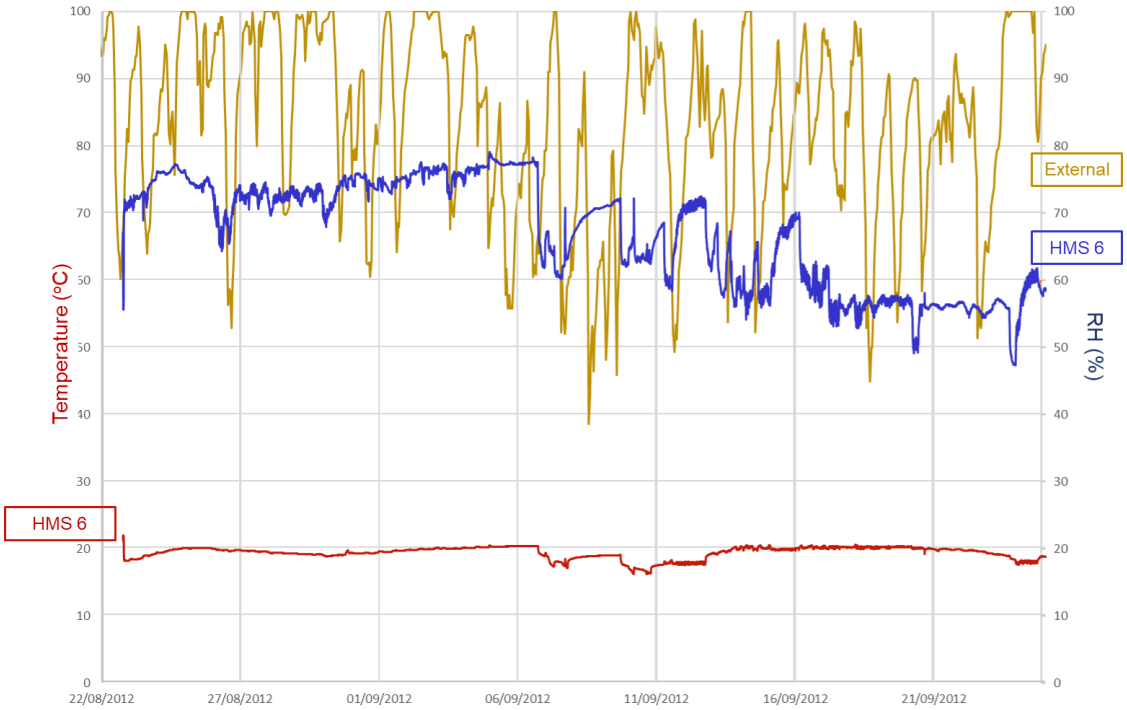

Figure 6.1 Deviation between internal & external RH, no external temperature data, beginning of transient state (Tinytag)

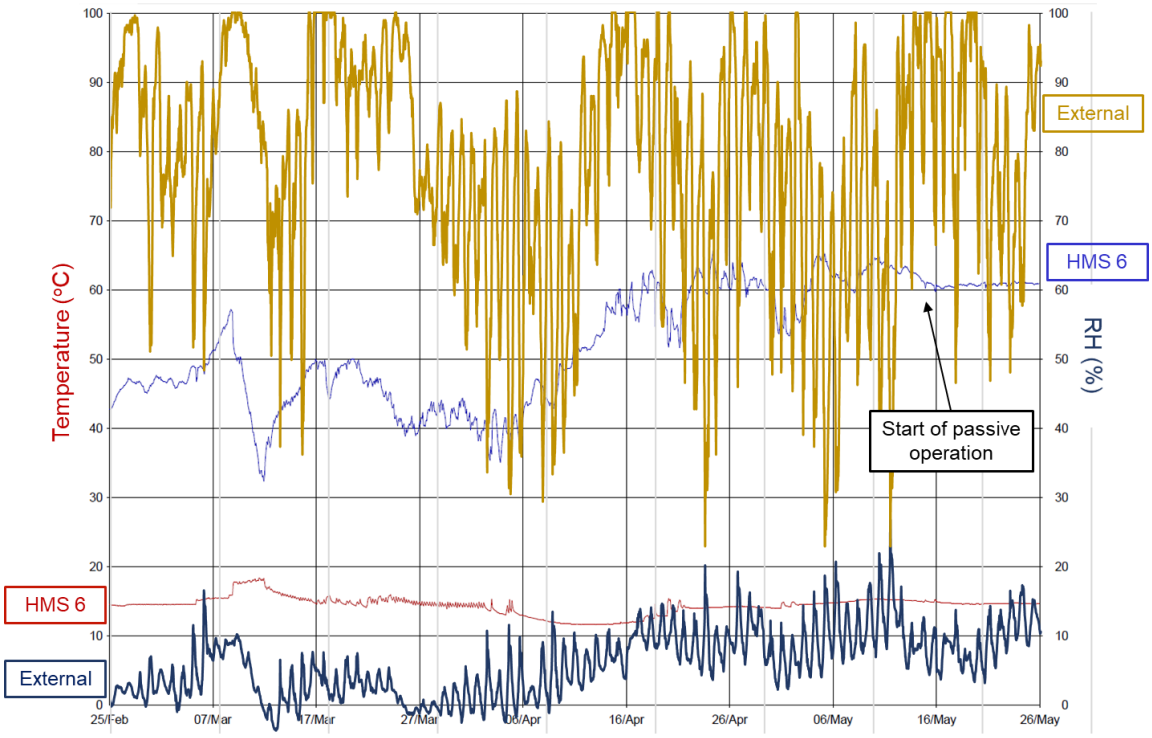

Figure 6.2 Deviation between internal & external RH, external temperature data, end of transient state (Tinytag)

6.2.1 RH history of the HMS

By the end of the first steady state period RH regulation in HMS 6 was within the range 55% RH ±5% RH, with continuous operation of one portable dehumidifier. RH levels had stabilised in HMS 5 and 4 in the ranges 60% RH ±3% RH and 65% RH ±3% RH respectively. Sporadic operation of the AHUs was halted at the end of May 2016, allowing for passive control of RH in HMS 5 and 4. Deviation between external and internal RH in all three large storerooms was more easily identified using the Hanwell ML4109 external unit as the availability of multiple layer graphical views made it easier to identify the effect that higher external temperatures had on internal RH in the HMS.

From June 2016 to May 2017, the RH was regulated through the passive performance of the hygroscopic building materials with the addition of portable control units rather than the air handling system. The dehumidifier was moved from HMS 6 to HMS 4 on 26 July to 5 August 2016 to bring down the RH which had risen through thermodiffusion phenomenon to almost 70%. The initial setting of the dehumidifier dropped the RH too rapidly so the unit was reset to a higher level on the same day, then lowered again 2 days later. Removing the dehumidifier from HMS 6 resulted in the RH in that room rising to almost 65% so a portable air conditioner in dry mode was installed. The dehumidifier was returned to the ground floor on 5 August as the air conditioner had no effect in regulating the RH level in HMS 6. The air conditioner in dry mode was then installed in HMS 4. The RH, which had dropped to around 55% by the operation of the dehumidifier, initially dropped but then rose, stabilising at just over 60%. The unit was switched off on 12 August to see if the RH could be passively regulated but operation was reinstated on 26 August as the RH started to rise in response to higher external temperatures. Regulation of RH using the air conditioner was ineffective and the unit switched off at the beginning of September. The RH rose to 68%, then drifted back down to 60% once the external temperature dropped below the internal temperature. Figure 6.3 is a timeline showing how the portable units affected RH levels and fluctuations in HMS 4.

Figure 6.4 is an overlay graph of external conditions on RH and temperature in HMS 4 in the same time period. It can be seen that thermodiffusion phenomenon affected RH levels despite the regulation attempts using mechanical controls. During passive operation, the RH reached a new equilibrium around 60% once the dynamic change in external temperature ceased. The RH remained around 60% until March 2017. The internal temperature had gradually dropped from 20°C to 8°C from September 2016 through to January 2017 which did not affect the RH level but a rise in external temperature starting in March resulted in an internal rise to 66% RH by mid-April.

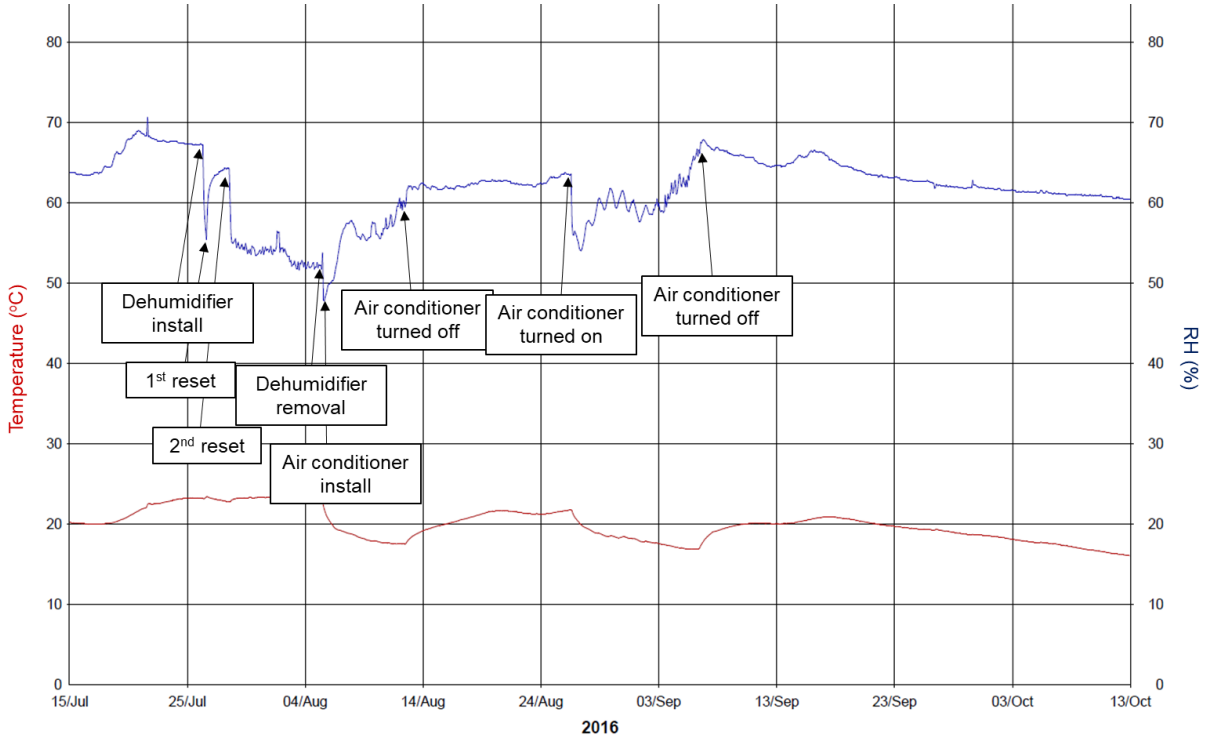

Figure 6.3 Timeline for portable unit operation, HMS 4 (Hanwell rl8)

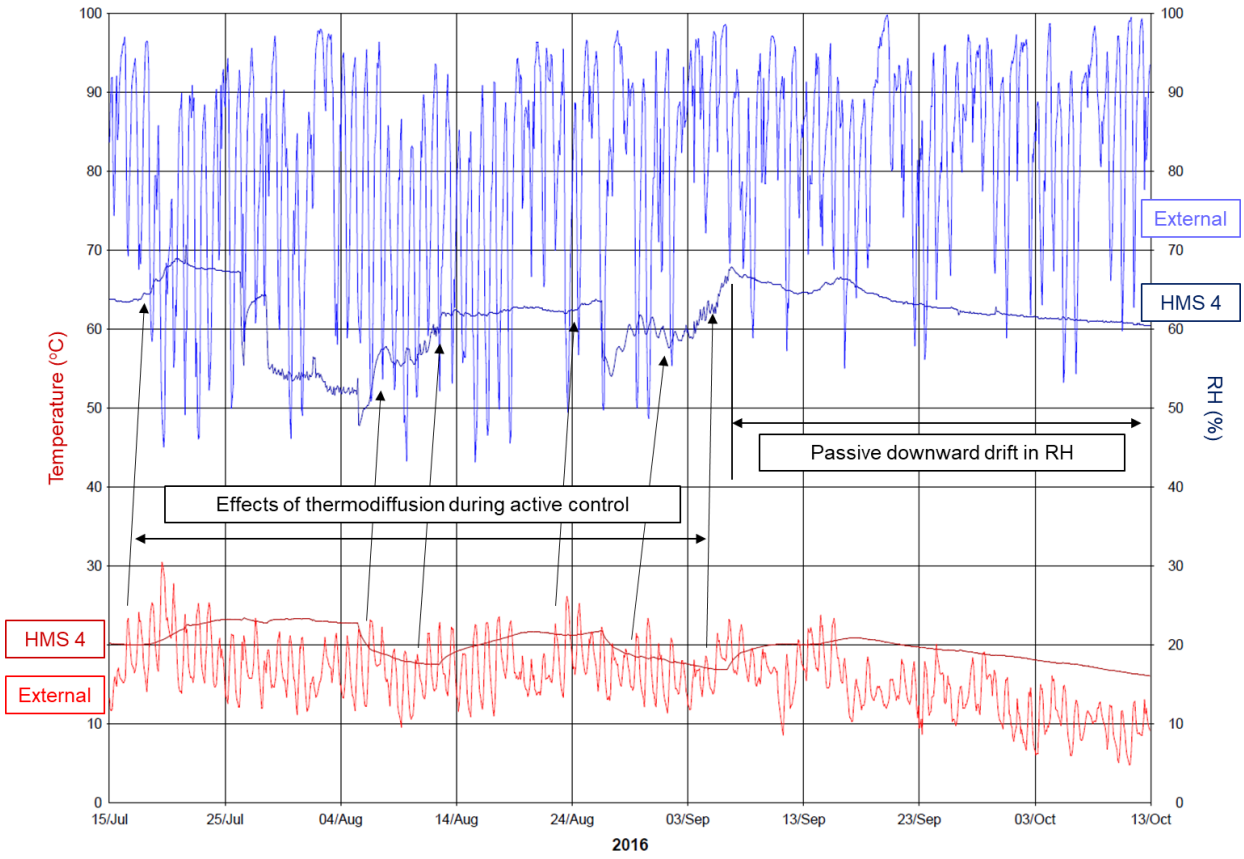

Figure 6.4 Effect of thermodiffusion on RH, HMS 4 (Hanwell rl8)

The external temperature rise in March caused the RH to rise in all three rooms. The dehumidifier in HMS 6 malfunctioned in March and the RH gradually rose to and

stabilised around 64% (Figure 6.5). With the dehumidifier function restored, the RH stayed in the range of 55% even during the period of high external temperature in April. The portable dehumidifier was more successful in mechanically moderating RH levels than the air conditioner in dry mode.

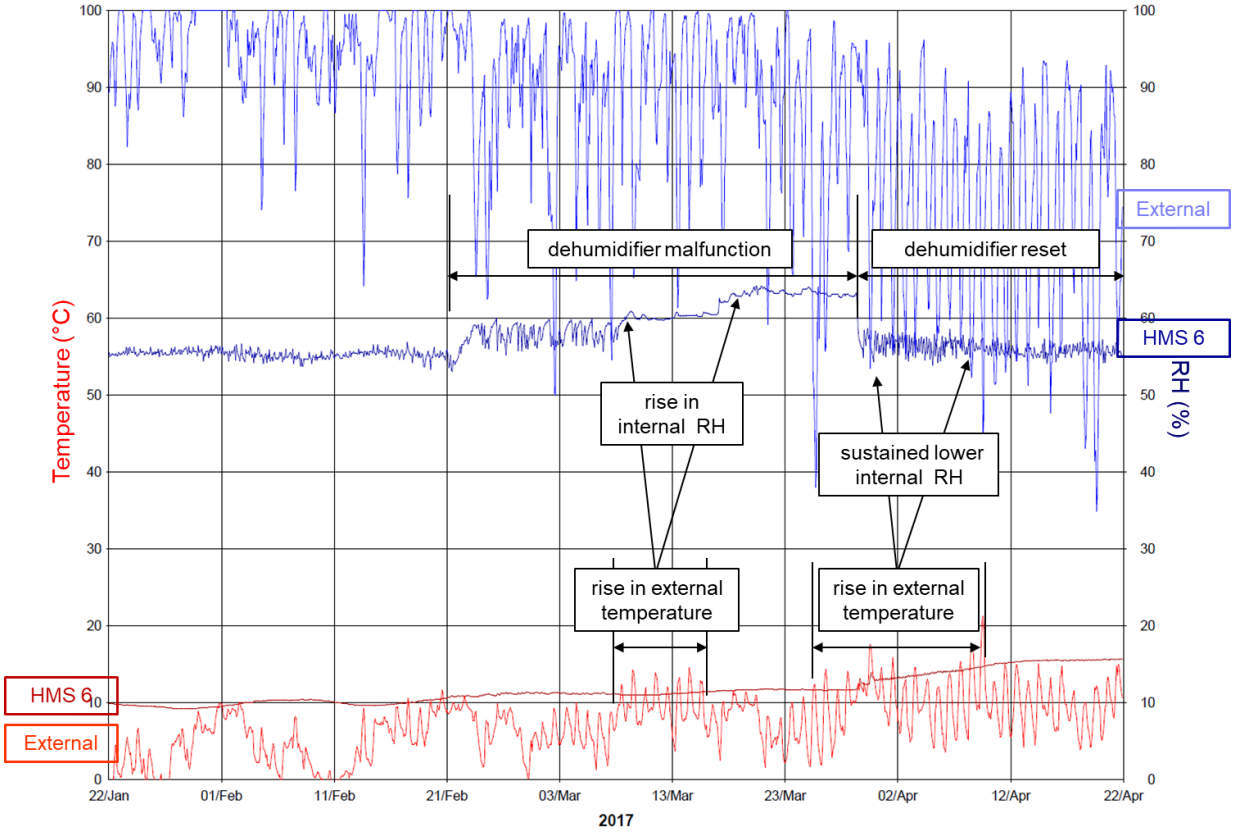

Figure 6.5 Effect of dehumidifier operation on RH during high external temperatures, HMS 6 (Hanwell rl8)

At the end of May, the heating cycles were reinstated to bring down the RH levels. The heat setpoint was raised by two degrees to 17°C with the aim of bringing the RH under 60%, although monitoring data showed room temperatures exceeding 20°C until mid- September. Both AHUs were set to run for two cycles of three hours each, from 21:30 to 00:30 and 03:30 to 06:30. The dampers were left open "*so there will be some fresh air exchange*", (Hopkins, (*pers. comm*.) 24.05.2017). This mode of operation caused minimal diurnal RH fluctuations with the RH levels in both HMS 4 and 5 drifting within the RH band of 40% RH to 60% RH, depending on influence of external temperatures, until August 2018.

Data from the ML41104 units showed the extent of RH stratification in HMS 6, with the RH level at ceiling height 5% to 10% lower than just above the floor (Figure 6.6). The RH at ceiling height was much more affected by the daily operation of the AHU than the other levels in the room, fluctuating by more than 5% during ventilation cycles. The RH at the median level showed minor fluctations of 2% RH to 3% RH over the entire AHU cycle. The RH at floor level was even less affected by the AHU operation but did rise slightly at the end of each heating cycle in response to the reduction in temperature as the unit turned off.

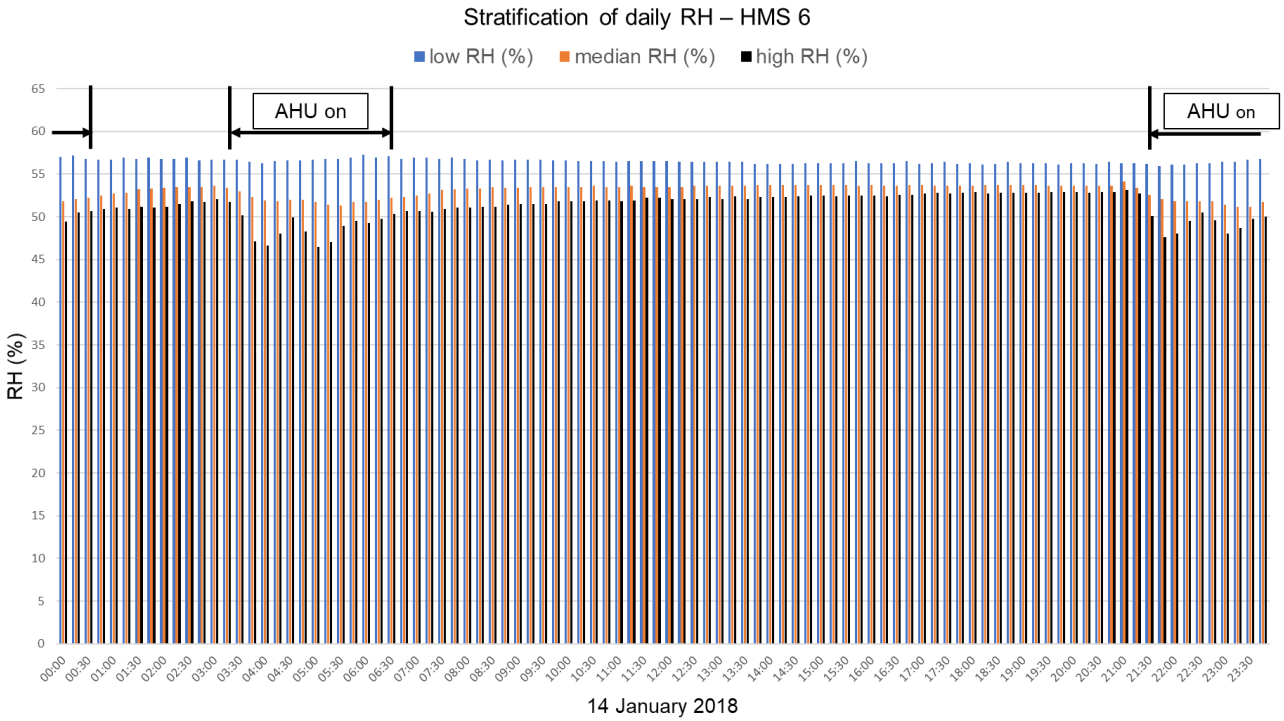

Figure 6.6 Effect of daily AHU operation on RH levels throughout HMS 6 (Hanwell rl8)

There was a drop in internal RH levels through February and March 2018, with a significant drop of 17% RH occurring between 28 February and 03 March (the period known as *the Beast from the East*), when external temperatures on site dropped to -7°C. This caused a negative thermal gradient across the HLC walls. A second less severe drop of 8% RH occurred a few days later, from 19 to 22 March, when the external temperature again dropped below 0°C. Figure 6.7 shows the effects caused by the very low external temperatures on the median RH in HMS 6. Moisture transfer in the HLC walls moved away from the warmer interior towards the colder exterior, resulting in a negative Soret coefficient and a drop in internal RH. The RH reached equilibrium around 50% RH once the external temperature had stabilised but then was affected by a sudden rise in external temperature in mid-April. The RH rose by more than 10% and stayed in that range until July 2018. Monitoring data showed that the internal RH responded more to less extreme external temperature rises than less extreme external temperature decreases, corresponding to the typical hysteresis loop in a porous material moisture isotherm.

RH/T monitoring data showed that internal temperatures also rose along with higher external temperatures as there was no cooling mechanism in the HMS. Higher internal temperatures eventually resulted in thermodynamically reducing internal RH once they reached the same degree range as externally.

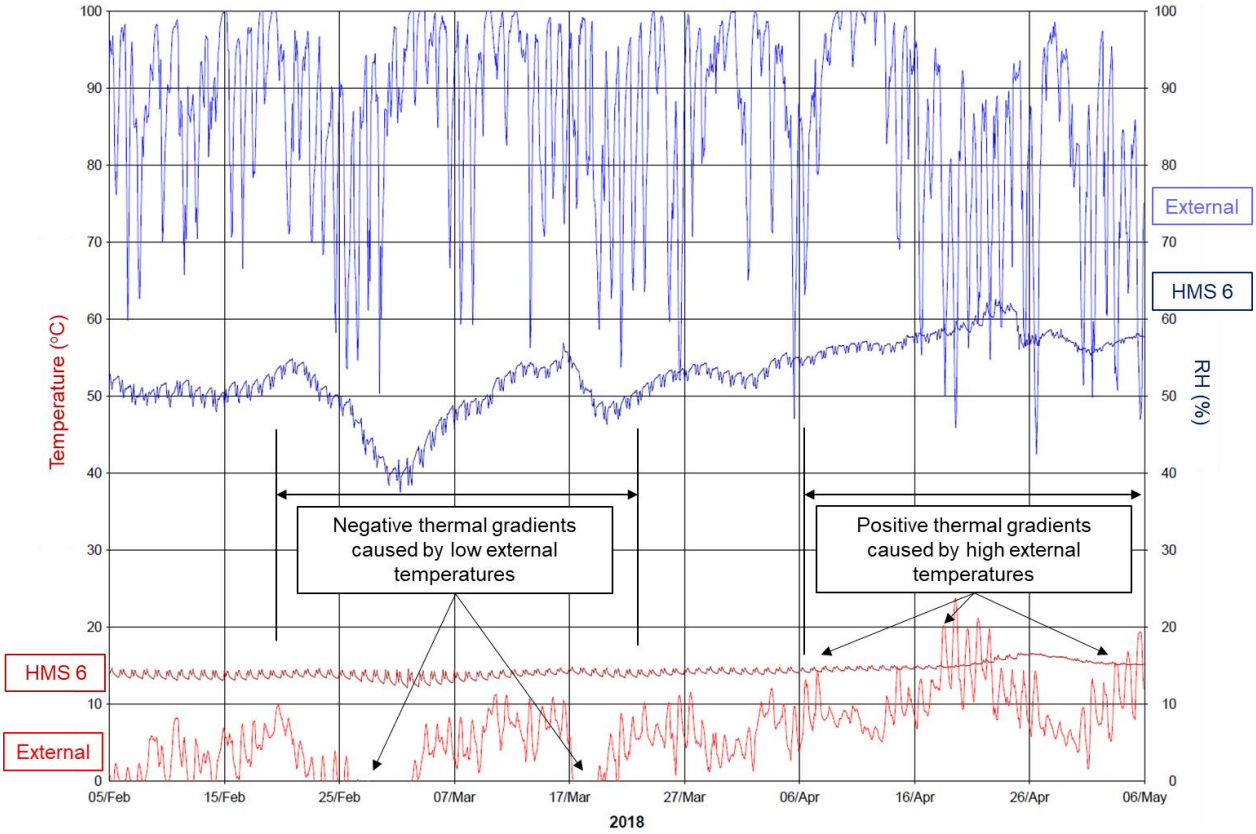

Figure 6.7 Effect of thermal gradients on RH, HMS 6 (Hanwell rl8)

On 21 July both AHUs stopped responding to the preset cycle from the BMS signal. Both AHUs started to run heating and ventilation cycles from 22:00 to 07:00, which introduced significantly more external air into the storerooms. The alteration to the AHU operation went unnoticed for several months as it unfortunately coincided with the changeover in software from rl8 to EMS. Dynamic access to the monitoring data by this researcher was lost from 18 August 2018 to 17 January 2019, with the alteration to AHU operation only being discovered once Hanwell and the SMG ICT department had resolved all the access issues to the new software. Review of the system by the Estates team via the BMS did not reveal operational issues.

While the RH generally remained within the band of 40% to 60% in HMS 5 and 6, the gradual seasonal drift was lost and RH fluctuations were more rapid, with changes up to 10% over twenty-four hours. In HMS 6, the median RH occasionally rose as high as 69% but also dropped as low as 39%. The overall level in HMS 5 was generally lower than in the ground floor room but still rose as high as 67% and dropped as low as 40%. In HMS 4, the RH range was lower, with levels within a band of 35% to 50%. The internal RH appeared to be affected by two factors. The first was continued response to thermal gradients. The RH would rise slightly when external temperatures were greater than internal temperatures. The second was increased ventilation. The RH would drop whenever cold external air was introduced as the cold air admitted into the rooms lowered the RH as it lost moisture content through heating, reducing the overall RH.

Based on psychrometric charts (Figure 6.8), with the external air at a temperature of 6.5°C and RH at 90.6% on 13 September, the median RH in HMS 6 would have been expected to be just under 35% when heating raised the temperature to 22°C.

Monitoring data showed it to be 35.5%, a 2% difference which was within the stated sensor accuracy of ±3% RH. RH stratification within HMS 6 was shown to be significant as the floor level RH was 10% higher than at ceiling height. Predicted RH was expected to be just under 40% at floor level but was in fact almost 49% RH (Figure 6.9), a difference of 25% which was not attributable to sensor inaccuracy. While the heating cycle raised the temperature at median level by 2°C and at ceiling level by 1.5°C it had no effect on the floor level which remained steady at 20°C. There was more effective buffering of the RH at the floor level. This might have been due to moisture leaching from the concrete slab but was more likely due to the desorption of moisture from the HLC walls as there was no thermodynamic response to increasing temperature and therefore more humidifying at floor level.

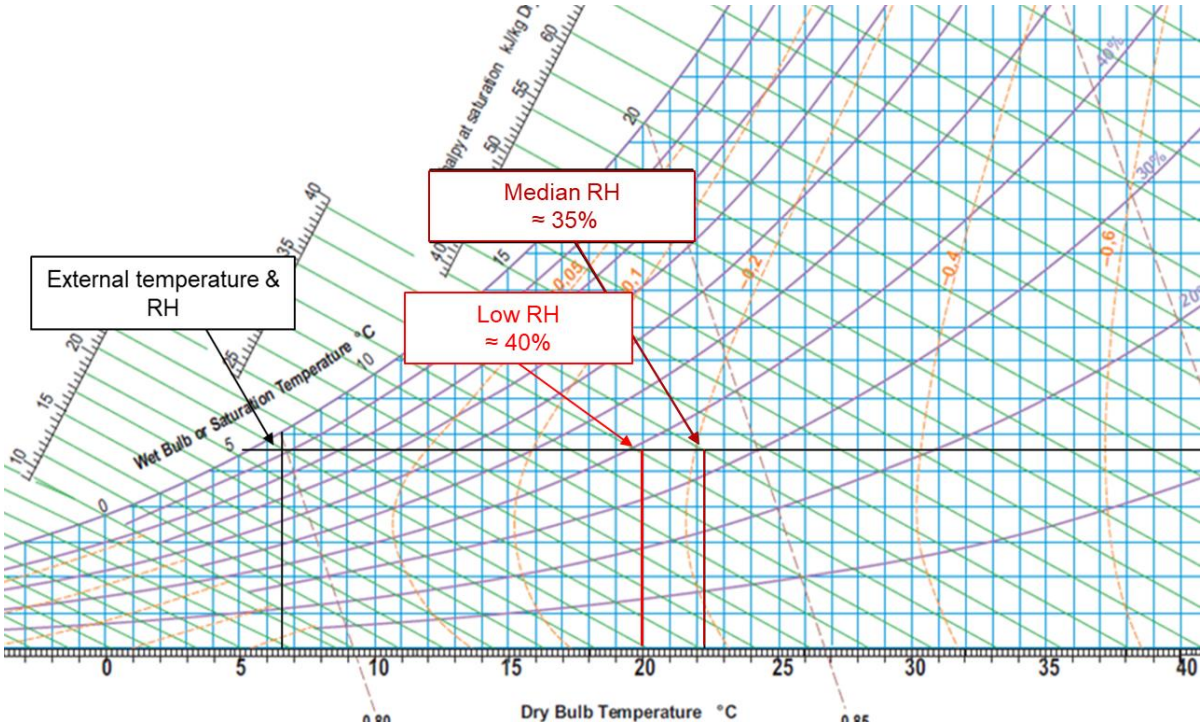

Figure 6.8 Predicted RH, HMS 6, 13 September 2018

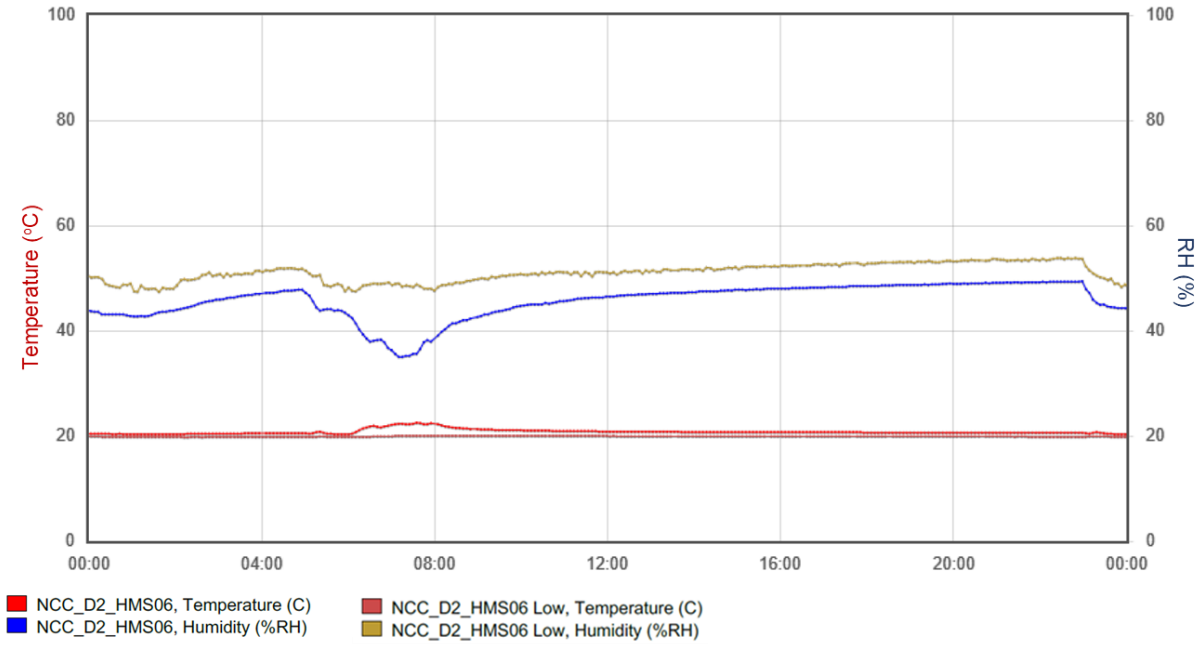

Figure 6.9 Measured RH, HMS 6, 13 September 2018 (Hanwell EMS)

In HMS 5, when room temperature was 22°C, the RH was 35.7%. In HMS 4, when room temperature was 21°C, the RH was 40.7%. The difference between measured and predicted RH for RH in HMS 5 was 2.3%, again within the ±3% sensor accuracy but in HMS 4, the difference between predicted and measured RH was 7% (Figure 6.10). As the temperature in HMS 4 rose by less than 1°C, the moisture desorbed from the HLC walls buffered any drop in RH caused by the introduction of cold external air with the result that the RH level was more stable.

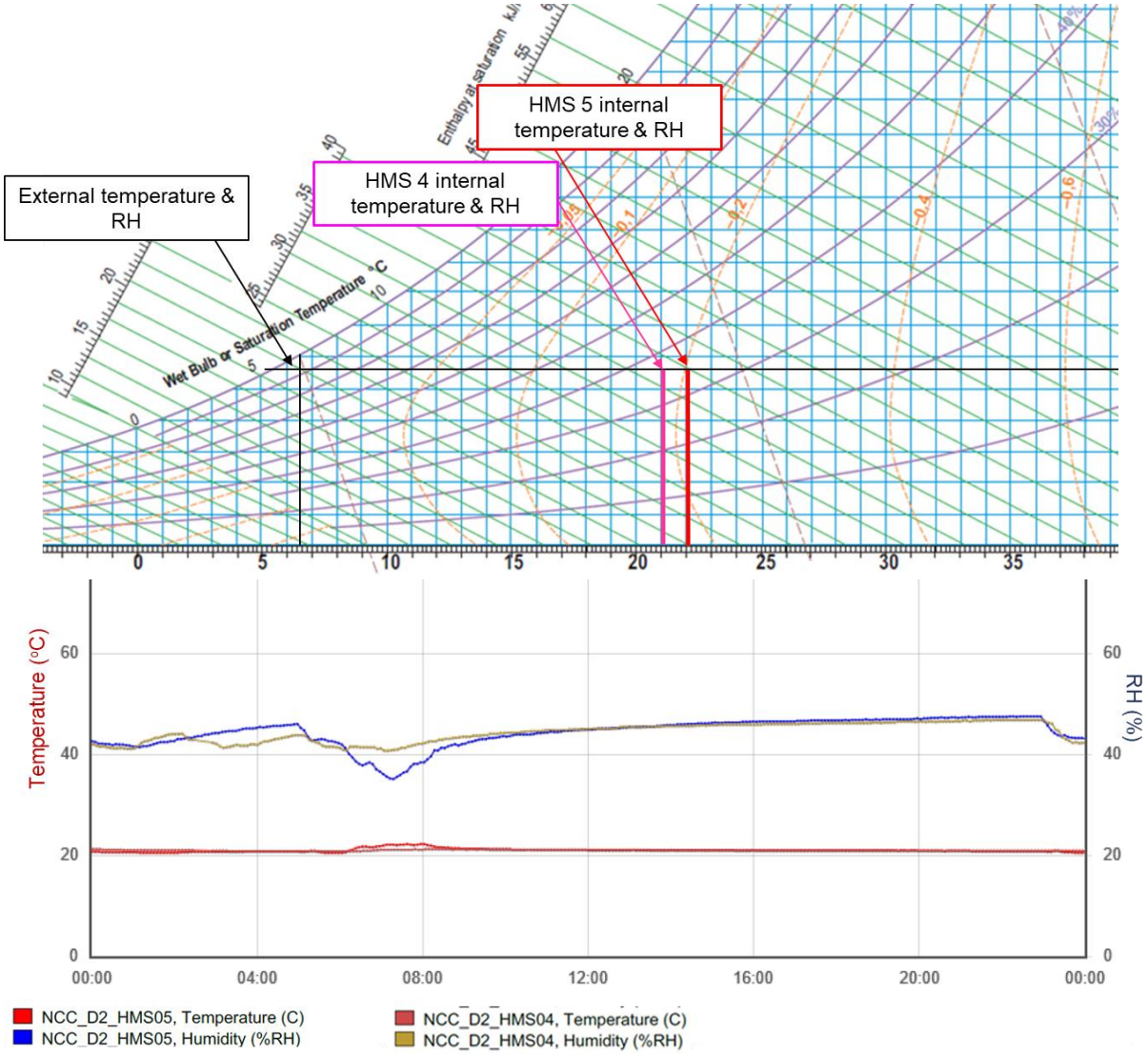

Figure 6.10 Predicted & measured RH, HMS 4 & 5, 13 September 2018

Fluctuations caused by both factors continued until 05 February 2019 when the AHUs were turned off with the external dampers fully closed. The environmental control in the HMS returned to a passive state with the exception of the one dehumidifier in HMS 6. The RH settled within hours to 53% on the ground floor, 51% on the first floor, and 42% on the second floor (Figure 6.11), and the levels stabilised until the end of February. A period of higher external temperature resulted in a rise of RH 2% to 3% in HMS 5 and 6 and 7% in HMS 4. Other periods of higher external temperature in April and May resulted in the RH reaching just over 60% at floor and median levels in HMS 6 and in June it was decided to reinstate operation of the AHUs (Figure 6.12). The BMS was set to run both AHUs on a cycle of two hours on and two hours off, between 21:00 and 07:00, at a temperature of 15°C and with 10% fresh air intake (Hopkins, (*pers.comm*.), 04.06.2019). The cyclic operation continued for the remainder of this research period, to January 2020, and resulted in the RH remaining in the range of 50% to 60% but with seasonal fluctuations consistent with external conditions, as shown in Figure 6.13. Although the BMS was set to operate the AHUs at a temperature of 15°C, this was not achieved until November 2019. The

RH rose initally in the HMS due to the temperature decrease but then stabilised within the range of 50% to 56% on all floors.

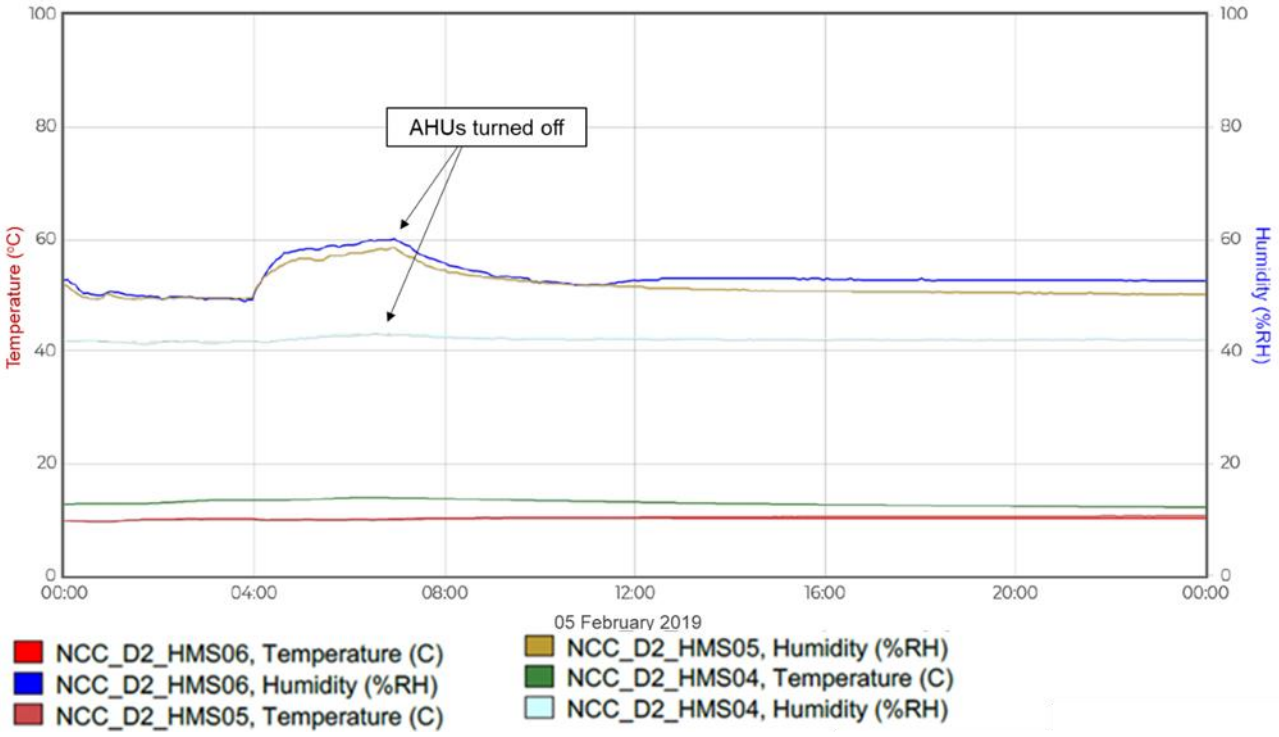

Figure 6.11 Effect of passive operation on RH, February 2019 (Hanwell EMS)

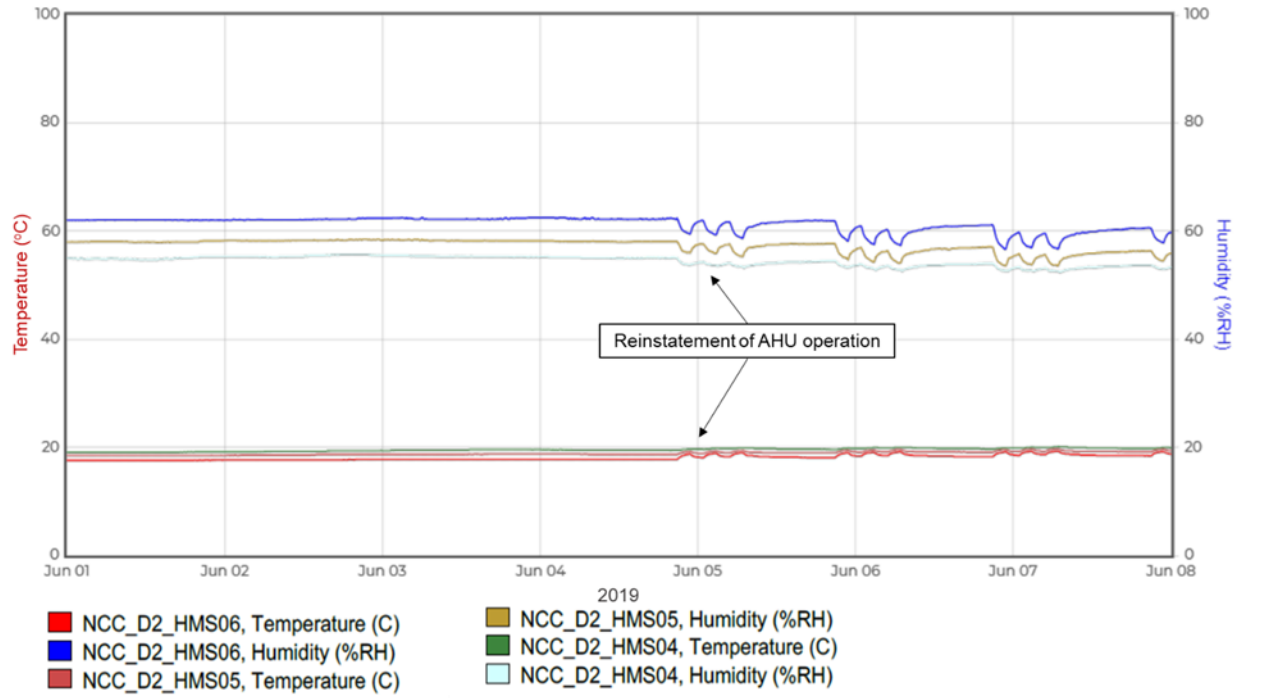

Figure 6.12 Effect of cyclical AHU operation, June 2019 (Hanwell EMS)

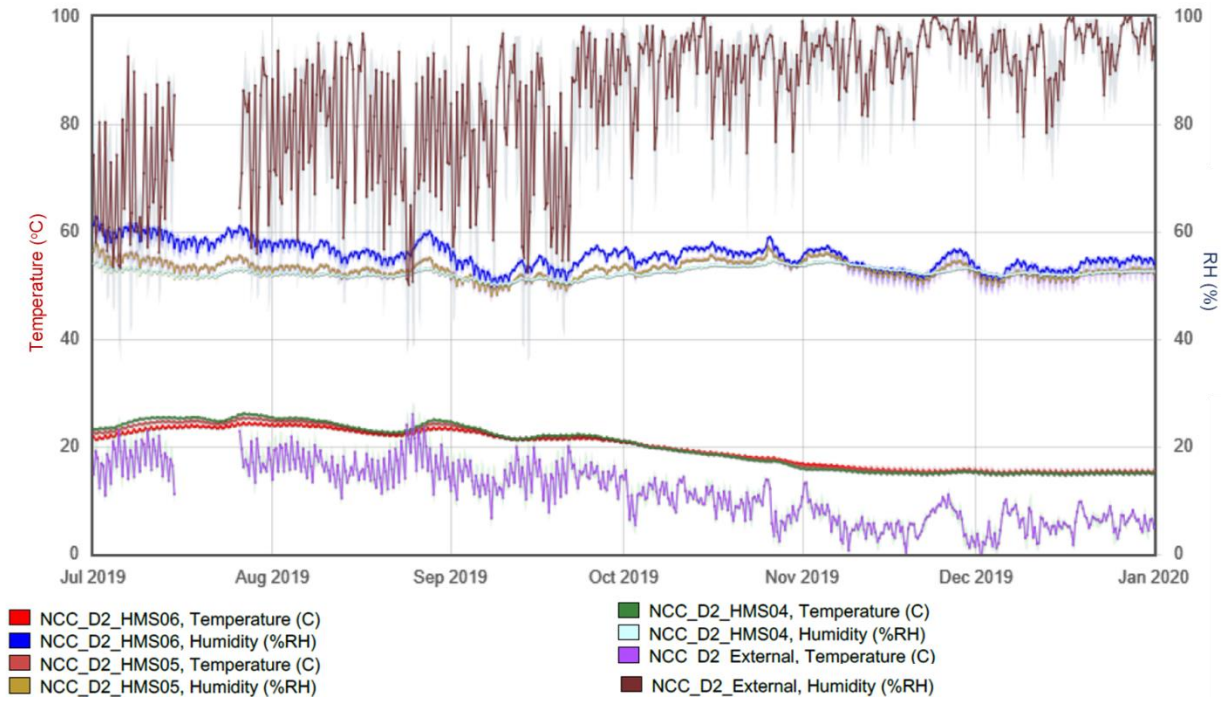

Figure 6.13 RH ranges in the HMS to end of research period (Hanwell EMS)

Data from the ML4106 unit (labelled Test_01) on the east (exterior) wall of HMS 6, sealed under polythene, showed less RH response to AHU operation. Although located at the same height as the median sensor, the polythene-covered sensor showed RH levels between 3% to 8% higher than in the room at median and ceiling levels, in a range between 56% RH and 62% RH (Figure 6.14). RH in the room at floor level was lower than at the sealed wall when the room temperature was above 20°C but higher once the room temperature stabilised at the BMS setpoint of 15°C. Data showed that the RH level was more stable with diurnal RH fluctuations buffered under the sealed polythene layer (Figure 6.15). Limited seasonal fluctuation in RH level occurred during the test period as there were few dynamic changes in external temperatures other than one period of higher temperature at the end of August 2019. The response under the polythene was much less than the response in the room. Using the RH and temperature data from the covered sensor enabled determination of moisture content at the room face of the east wall. Moisture content was at 0.011 kg/kg at the end of August 2019, following a period of higher external temperatures, but averaged between 0.055 kg/kg and 0.062 kg/kg during the prolonged cold period from mid-November through to the end of the research period (Figure 6.16). Data showed that in the section of wall covered by polythene sheeting the RH returned to equilibrium between 56% to 58% under stable temperatures. The RH in the room as a whole was stratified between 53% to 61%, with the highest RH at floor level.

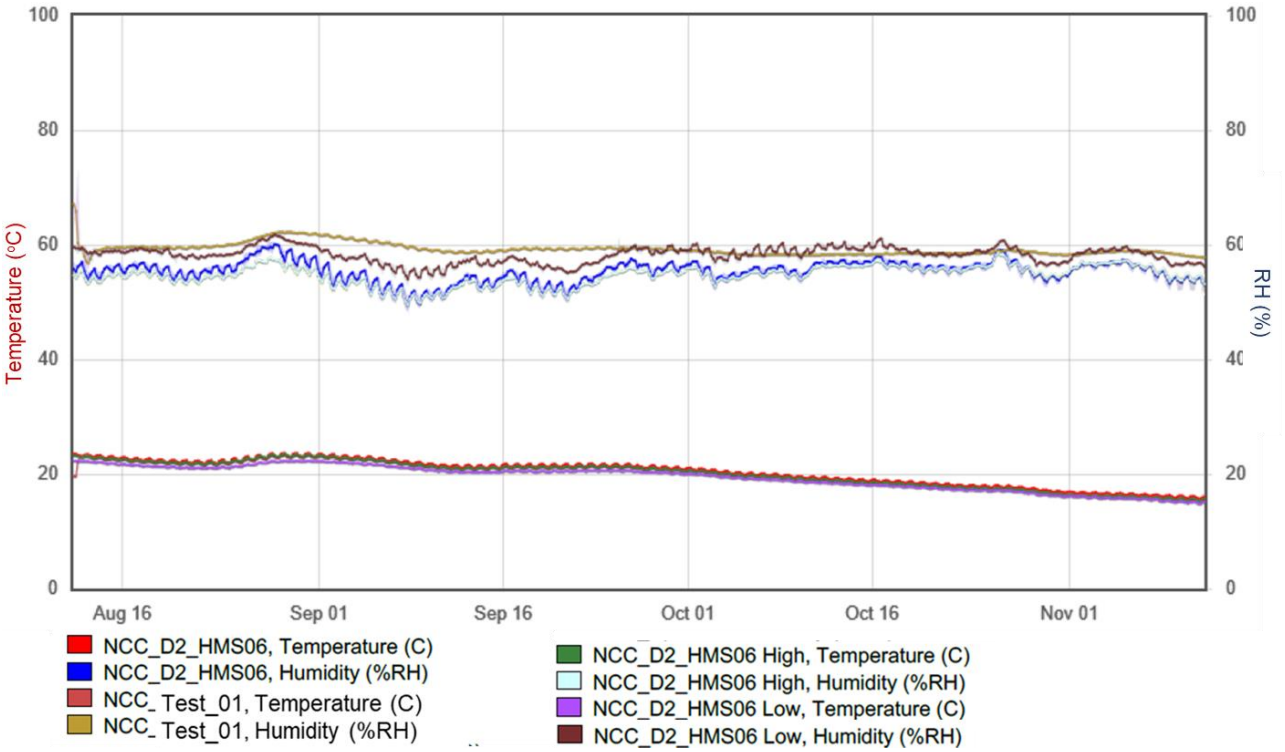

Figure 6.14 RH levels & fluctuations throughout HMS 6 (Hanwell EMS)

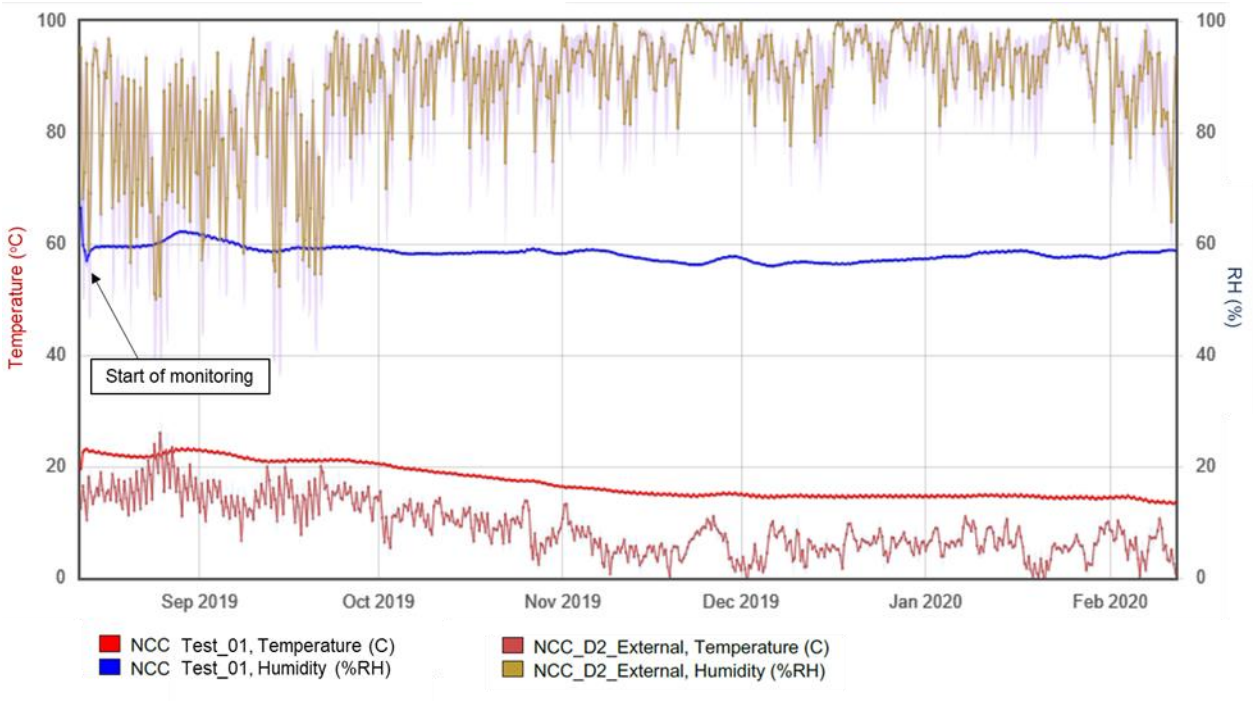

Figure 6.15 RH range under polythene sheeting (Hanwell EMS)

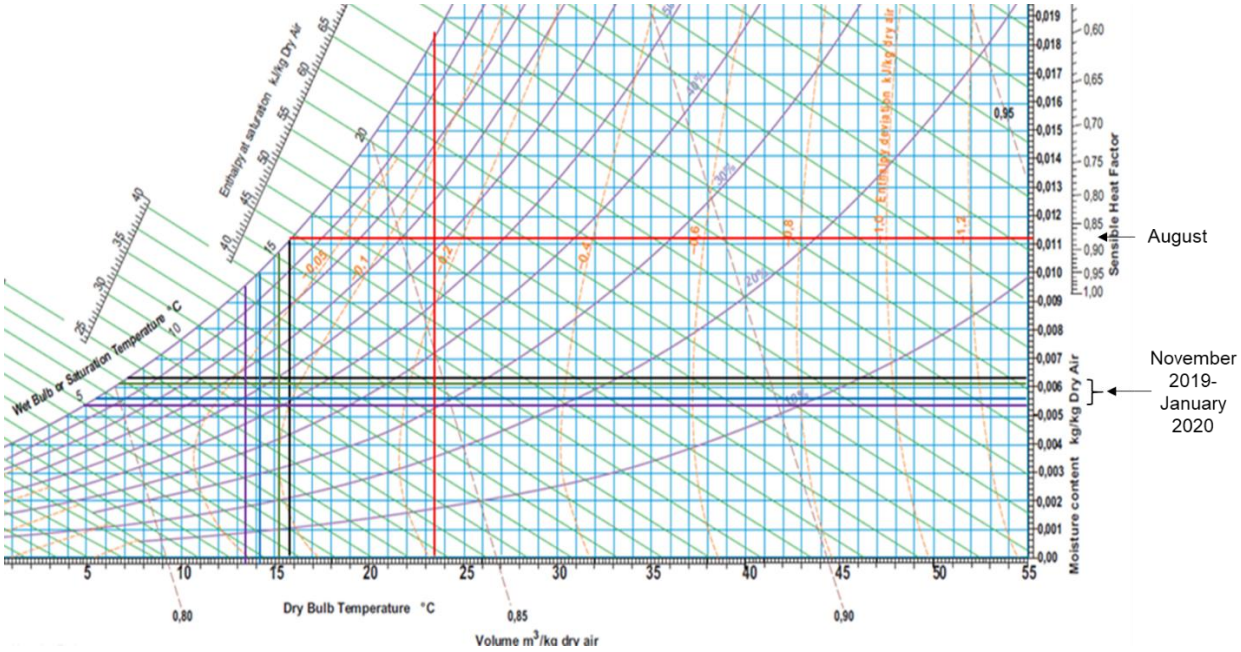

Figure 6.16 Predicted moisture content under polythene sheeting

6.2.2 RH history of other museum stores on NCC site

During the research period from June 2016 to February 2020 RH monitoring data was assessed from the L&A reserve store, the other storage facility in hangar D2. Details of the construction and M&E system of this repository have been given in Chapter 4, Section 4.4.2.2. The RH levels in the store were controlled by an HVAC system but without systematic dehumidification. Ventilation was set at 5% to 10% fresh air intake, a minimum rate of 5 air changes per hour and an air infiltration rate of 4 air changes per day (Hopkins, (*pers.comm*.), 13.02.2018).

Data from the two RH/T transmitters in the L&A store showed that the RH range did not meet published recommended guidelines for the storage of library and archival materials, either those from the period of construction (2006), which were "*a fixed point between "45% - 60% ±5%"* (BSI, 2000), or later revisions, which were "*no more than 60% and no less than 35%"* (BSI, 2017a). The specifications had called for the construction of a well-insulated and airtight facility with an energy expenditure of no more than 80 kWh/m^2 which would assist in maintaining a stable storage environment for books and paper (Leitch, 2006). Although recommendations were given at the time by the SMG Sustainability Development team for passive or low energy humidity regulation using hygroscopic building materials such as rammed earth or straw bales and natural ventilation (Zammit, 2006), mechanical plant was installed for environmental control. The system chosen was unable to maintain a suitable RH level at temperatures below 20°C and so, as temperature control between 16°C and 19°C took precedence, the RH was frequently too high (>60%). At no point was modelling or testing carried out to assess the passive contribution of the building to assist in maintaining stable storage conditions without mechanical control.

The RH range fluctuated mostly within the range of 60% RH to 70% RH at the south end of the store. At the north end, the range was frequently higher, between 65% RH

to 75% RH, with dissimilar fluctuation patterns at times despite internal temperatures being kept consistent, as can be seen in Figure 6.17 which shows monitoring data from June through August 2016.

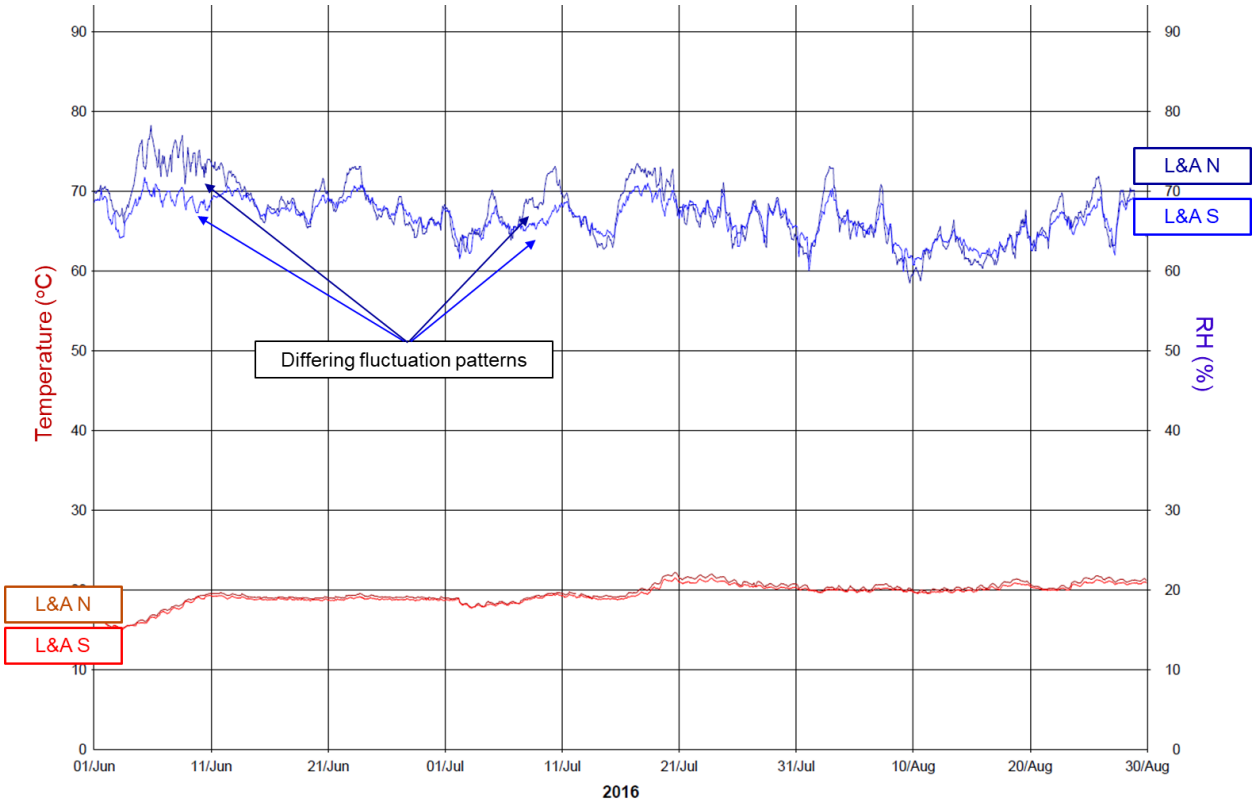

Figure 6.17 RH levels & fluctuations in the L&A store (Hanwell rl8)

The stability of the RH range in the L&A store was affected by external conditions. The northern, eastern and western sides of the store were separated from the hangar walls only by the narrow perimeter fire corridor which offered little buffering from high external temperatures. At the south end of the store, the open air volume of the hangar, approximately 20,500 m^3, helped to buffer external conditions, resulting in a variation in RH fluctuations from one end of the store to the other (Figure 6.18).

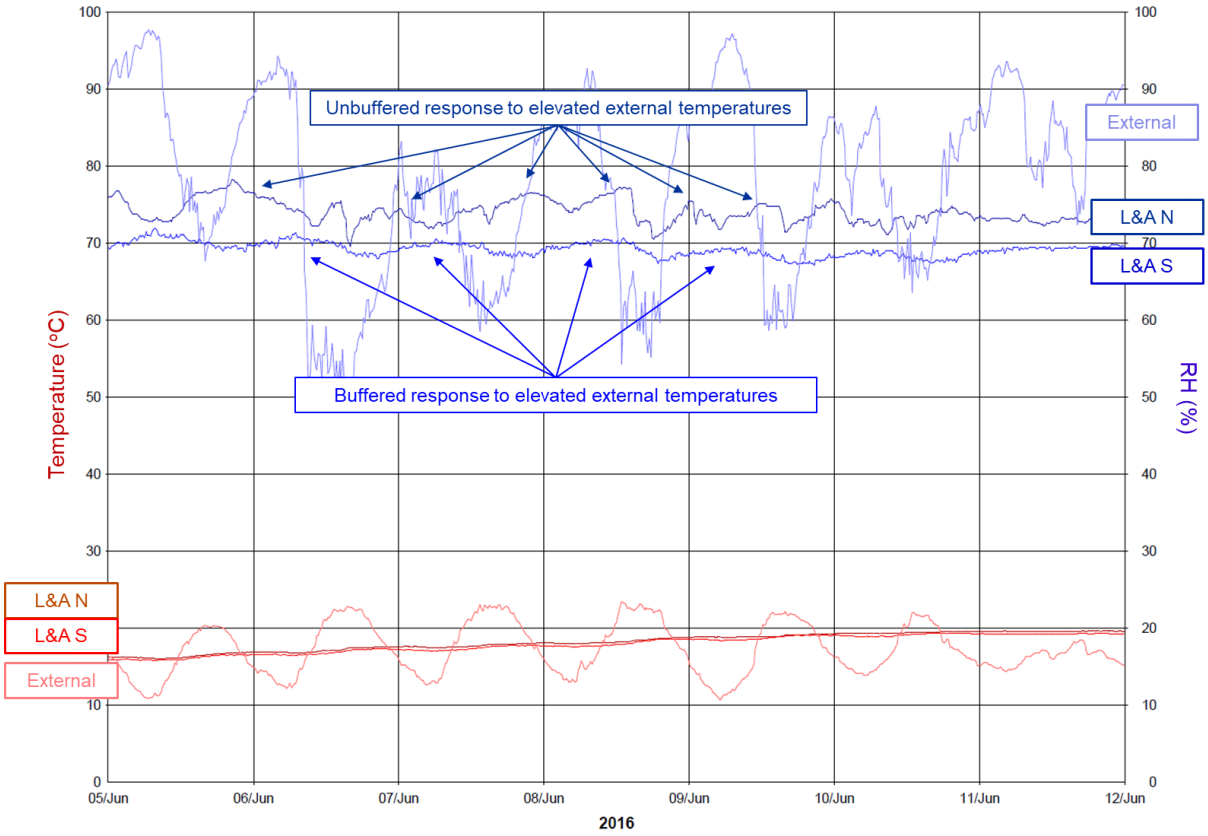

Figure 6.18 Effect of location on RH, L&A store (Hanwell rl8)

Ventilation contributed to the RH fluctuations and also brought in damp external air so that the overall RH remained high despite continuous heating. In October 2017, an outbreak of mould on book bindings was observed. Two industrial dehumidifiers were leased and installed mid- point along the west wall. At the same time, the HVAC system was switched off in response to a potential health issue from the wood pellets. This resulted in the RH levels gradually decreasing, although the range was still 3% to 5% higher at the north end of the building. Fluctuations also decreased in the period from October 2017 to January 2018 as no external air was admitted and as external temperatures were consistently low.

The dehumidifier units extracted 82 litres of water per day from air volumes up to 300 m^3. As the total L&A store volume was 8,856 m^3, the two units made slow progress in lowering the RH level. When the HVAC system was reinstated in January 2018, the RH levels dropped to between 40% and 60% but fluctuations increased due to ventilation admitting external air and to periods of high external temperatures. At the end of May 2018, due to the admittance of very damp air, the RH rose to 70% at the north end of the store and 65% at the south end. The levels were brought down to the 55% to 60% range by raising the temperature from 18°C to 22°C.

Mould outbreaks continued into 2020, but occurances were reduced. The percentage moisture content of books in the store had been measured in 2018, using a Stihl moisture gauge, and found to be between 11% to 16% RH at 22°C, against a typical percentage moisture content for dry paper of 4% to 6%. A programme to reduce the RH included purchasing dehumidifier units and locating them in the centre aisle to improve air circulation. The room temperature setpoint

was altered to between 18° to 22°C. These measures resulted in bringing the RH to 40% ±5% RH by January 2019. The RH rose throughout the building from June to October 2019 during an extended period of warm weather (Figure 6.19). When the external temperature finally remained steadily below the internal temperature, the thermodynamic pattern of RH and temperature inside the store resumed. The RH dropped back down to 40% at the south end of the room and 45% at the north end with room temperature lower at the north end than the south end and remained as such to the end of the research period. Moisture content percentages in the books were then measured between 9% to 11% so some drying out had been achieved. The thermodiffusion reaction could be attributed, as predicted by Padfield (2013), more to the movement of the moisture content of the 17,063 linear metres or approximately 1,400 m^3 of hygroscopic paper items within the building, rather than to any moisture content of the building materials.

Monitoring data revealed that RH levels and fluctuations were influenced by the operation of the HVAC system admitting external air and by external temperatures even with revised internal temperature settings and dehumidifier operation. Data showed the north end of the store was more affected when external temperatures exceeded hangar temperatures. The RH level throughout the store did remain within the band of 40% to 60% as long as both the HVAC system and the dehumidifiers were run continuously.

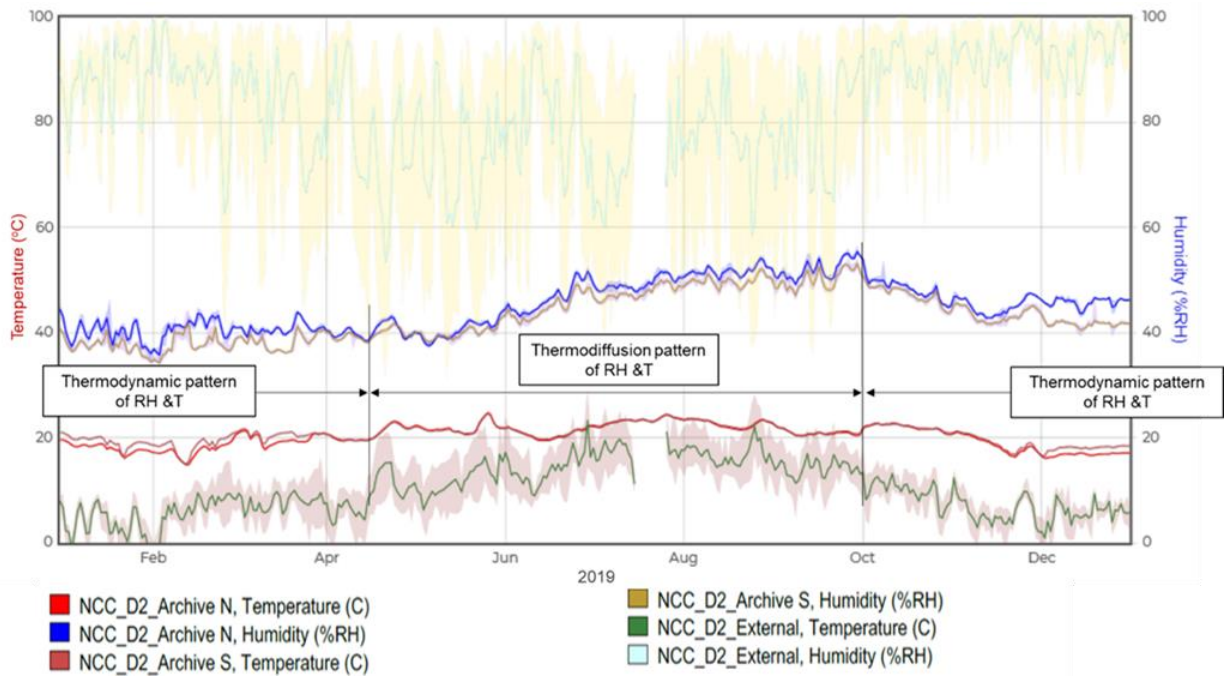

Figure 6.19 Effect of external conditions on RH, L&A store (Hanwell EMS)

The RH levels in the A Store were regulated only by a continuous low level heating system since the dehumidification plant had become inoperable within the first two years of building operation. Fresh air ventilation rates were set at 12 l/s per person to provide an air change rate of 1.35 per hour per person and a minimum air infiltration rate of 0.15 per hour in the ground floor storage rooms and 1.0 per hour in the mezzanine rooms (Read, 2011). The Hanwell monitoring data showed that RH levels were different in the three storage areas. In A1, the RH was consistently higher than

in A2 with the temperature 2°C to 3°C lower, although never as low as the original specification of 14°C ±2°C. In A3, the RH was less stable despite being on the same heating pattern as A1 and A2 (Figure 6.20). The room had not originally been intended for the storage of museum collections and had large glass doors leading onto the balcony running across the south face of the building, making the internal conditions more susceptible to changes in the external environment.

Data from Tinytag data loggers in A1 demonstrated that the eight metre tall high density mobile racking, with only one aisle, reduced air flow from the forced air supply at ceiling height so, while mid and low levels were more stable, the temperature was lower and the RH higher (Figure 6.21). The RH in the two main stores was kept within a seasonal drift band of 30% to 70% by continuous low level heating. Conditions in the two loading bays were less stable on a day to day basis but the overall RH range followed the same pattern as in the two main stores. RH in the mezzanine storeroom had a similar daily fluctuation pattern as in the loading bays with a RH range slightly higher than in the bays but lower than in the main stores. Monitoring data from 2016 on revealed that internal RH in the two main stores would change from a thermodynamic pattern to a thermodiffusion pattern during periods when the external temperature exceeded room temperature, which was unexpected as the construction materials of the building were not hygroscopic. Seemingly this was a result of moisture content in materials in the stores, particularly that from the large quantity of wooden pallets (566 m^3 in A1 and 332 m^3 in A2) used to store collections in the racking as well as from organic materials in the museum objects. Figure 6.22 shows the RH response in A1 and A2 during the same period as shown in Figure 6.20. RH levels rose higher than the recommended 60% in A1 despite a room temperature of 20°C from July to September. A return to thermodynamic patterns of RH and temperature occurred in both stores once the external temperature stabilised below the internal building temperatures.

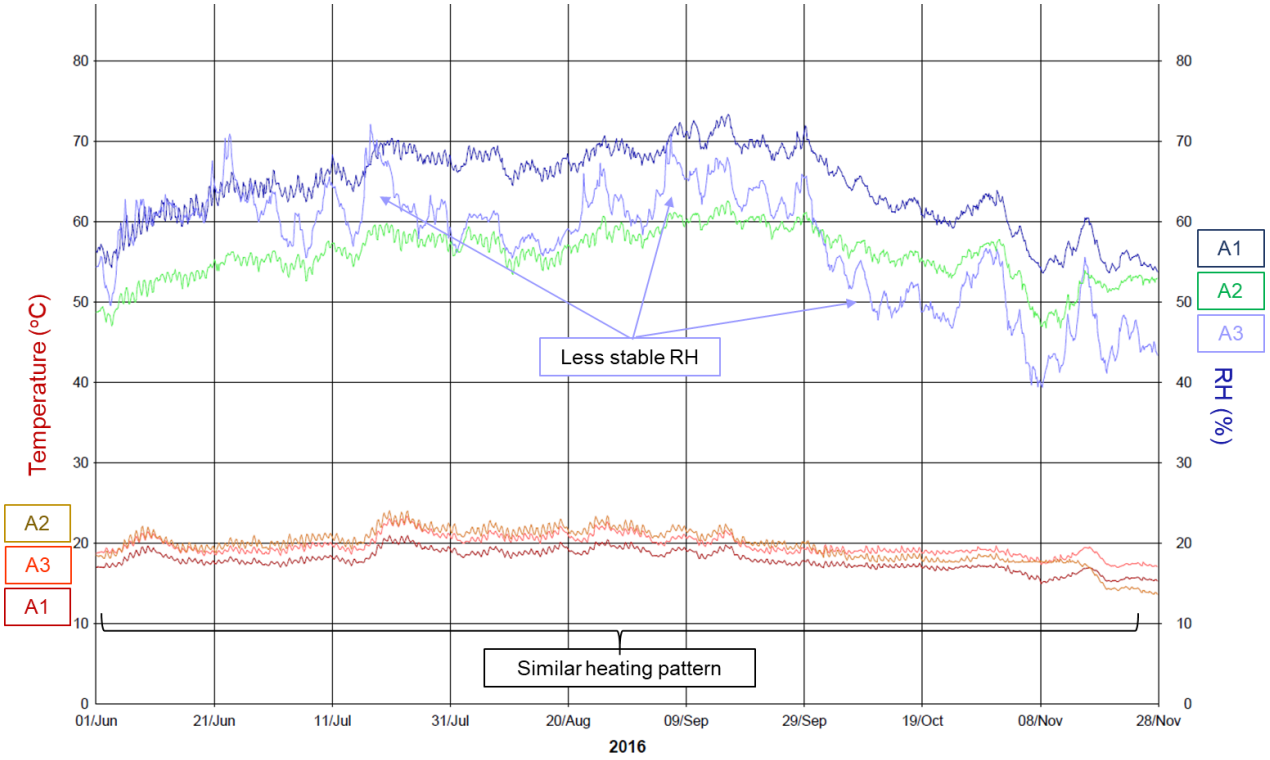

Figure 6.20 Effect of location on RH, the A Store (Hanwell EMS)

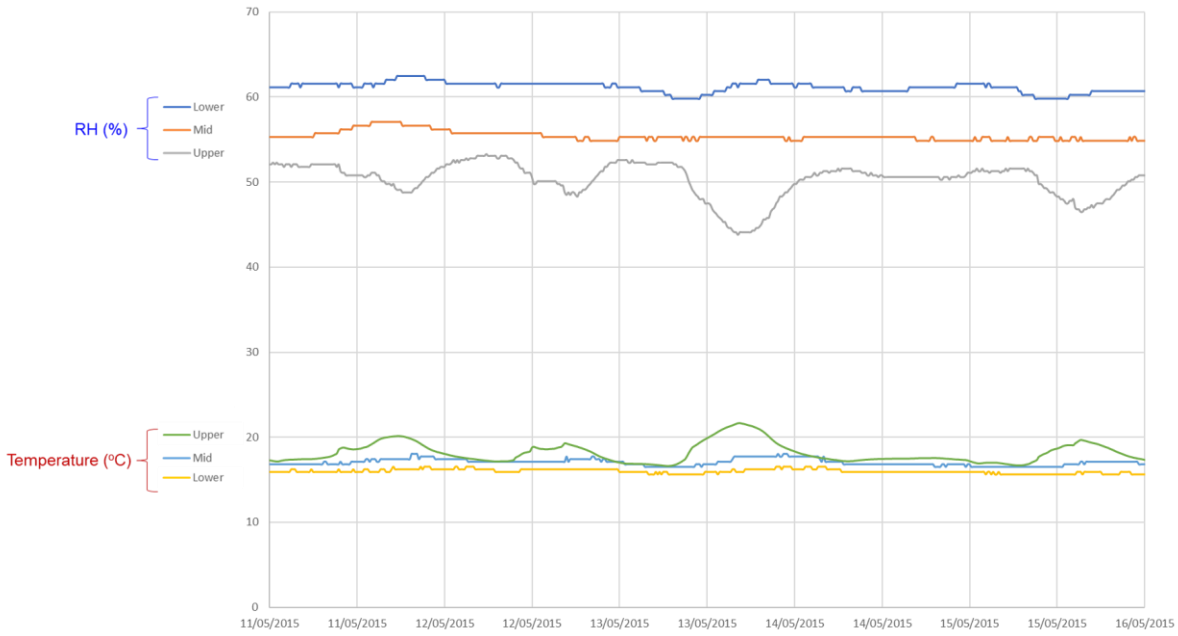

Figure 6.21 Stratification of RH & temperature in A1 (Tinytag)

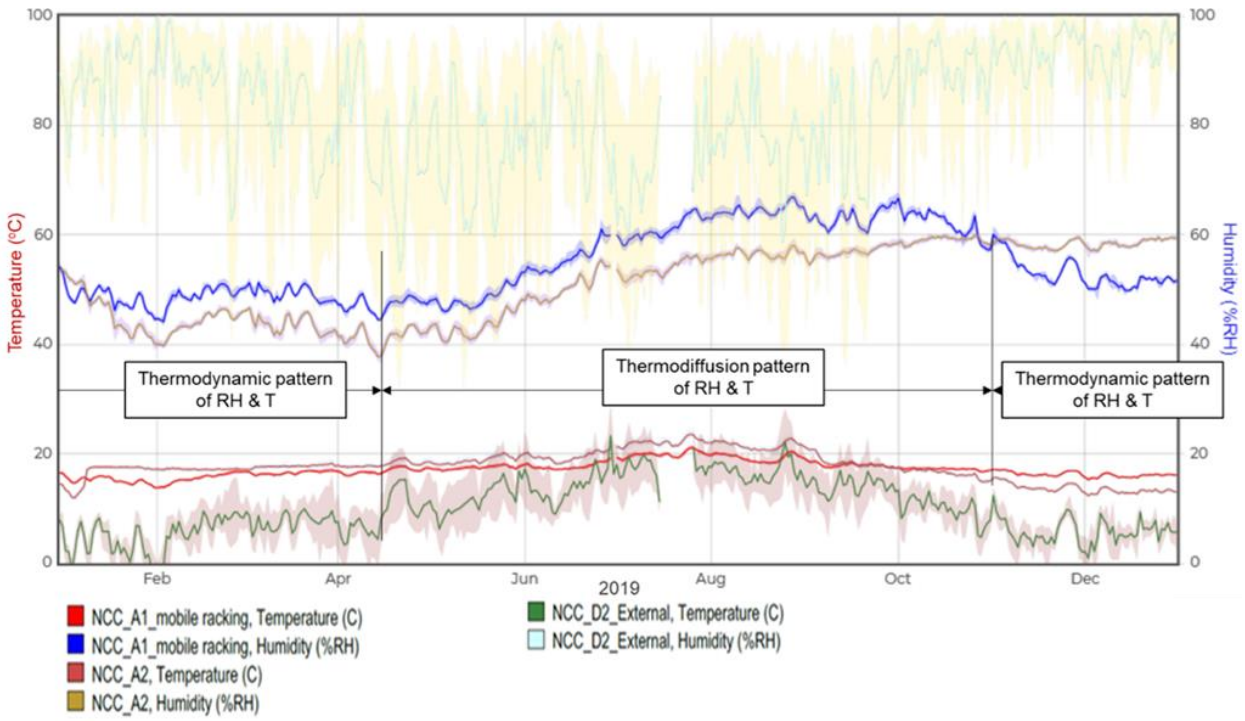

Figure 6.22 Effect of external conditions on RH, the A Store (Hanwell EMS)

While all three purpose-built SMG stores were intended to provide low energy environmental control, different levels of active control of the RH were needed in each building. All three storage buildings had been built to be as airtight as possible. At end of construction, air filtration in the HMS had measured at <1.0 $m^3/(h \cdot m^2)$ @ 50 Pa and at 0.84 $m^3/(h \cdot m^2)$ @ 50 Pa in the L&A store. The air leakage rate of the A Store was considered to be excellent, meeting the then-current BSRIA standard (Laurin & Scott, 1994) which was 2.0 $m^3/(h \cdot m^2)$ @ 50 Pa (BSRIA, 1998). Air change rates were set at four per hour in A1 and A2 storage areas (one per hour per person with a minimum of four people); eight per hour in the L&A store and five per hour (HMS 6) or seven per hour (HMS 4 and 5). Airflow was set at 1.08 m^3/s for the HMS AHUs with a supply fan pressure of 180 Pa and 3.3 m^3/s for the L&A AHU with a supply fan pressure of 250 Pa.

By comparing the RH monitoring data from the L&A store (Figure 6.19) and A Store (Figure 6.22) to data from the HMS during the period from February 2019 to January 2020 (Figure 6.23), the effectiveness of each environmental control system in regulating the response of RH levels and fluctuations to external conditions could be demonstrated. The monitoring data showed that there was a thermodiffusion reaction in each store during the period when the external temperature exceeded the internal temperature but it was more effectively buffered in the HMS.

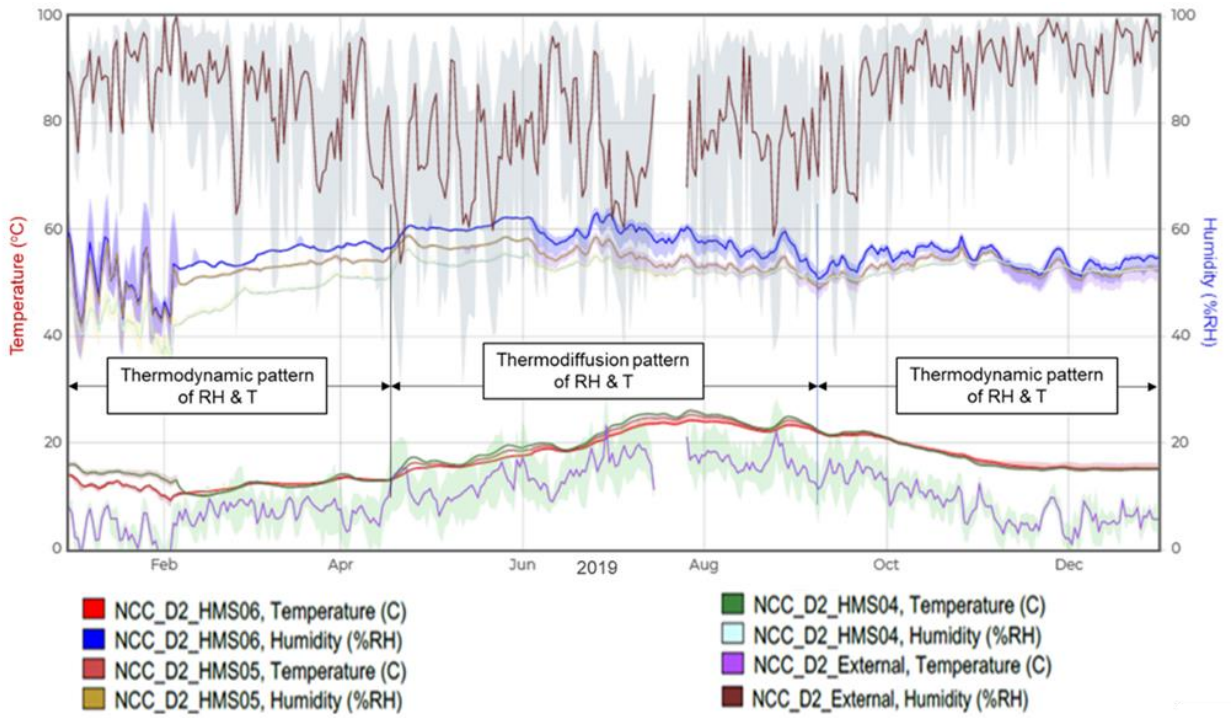

Figure 6.23 Effect of external conditions on RH, the HMS (Hanwell EMS)

Overlaying graphs, one each from HMS 6 (median), L&A N and A1 (Figure 6.24), shows that the overall RH range in HMS 6 was buffered more successfully than in the other two areas, as it stayed in the range of 50% RH ±5% RH except during the period prior to February 2019 when the ventilation system was drawing in too much external air. During February to June 2019, the RH in HMS 6 was regulated by one portable dehumidifier which did not prevent an upward response of 3% caused by a short period of elevated external temperature at the end of April. The RH in L&A N and A1 had a negligible response to the short duration rise of external temperature but both were significantly affected by the longer period of warm weather, with a rise from 38% to 54% in L&A N and from 46% to 66% in A1. The RH in HMS 6 stayed within 58% to 62% until September then dropped as the external temperature dropped, stabilising in the range of 50% to 55% through to February 2020. RH levels dropped by almost 10% to 45% in L&A N and by 16% in A1 by November 2019. Monitoring data showed that the RH in HMS 6 fluctuated as much as in the other stores once the AHU cycle was reinstated. Buffering of the RH level was more effective than buffering of RH fluctuations.

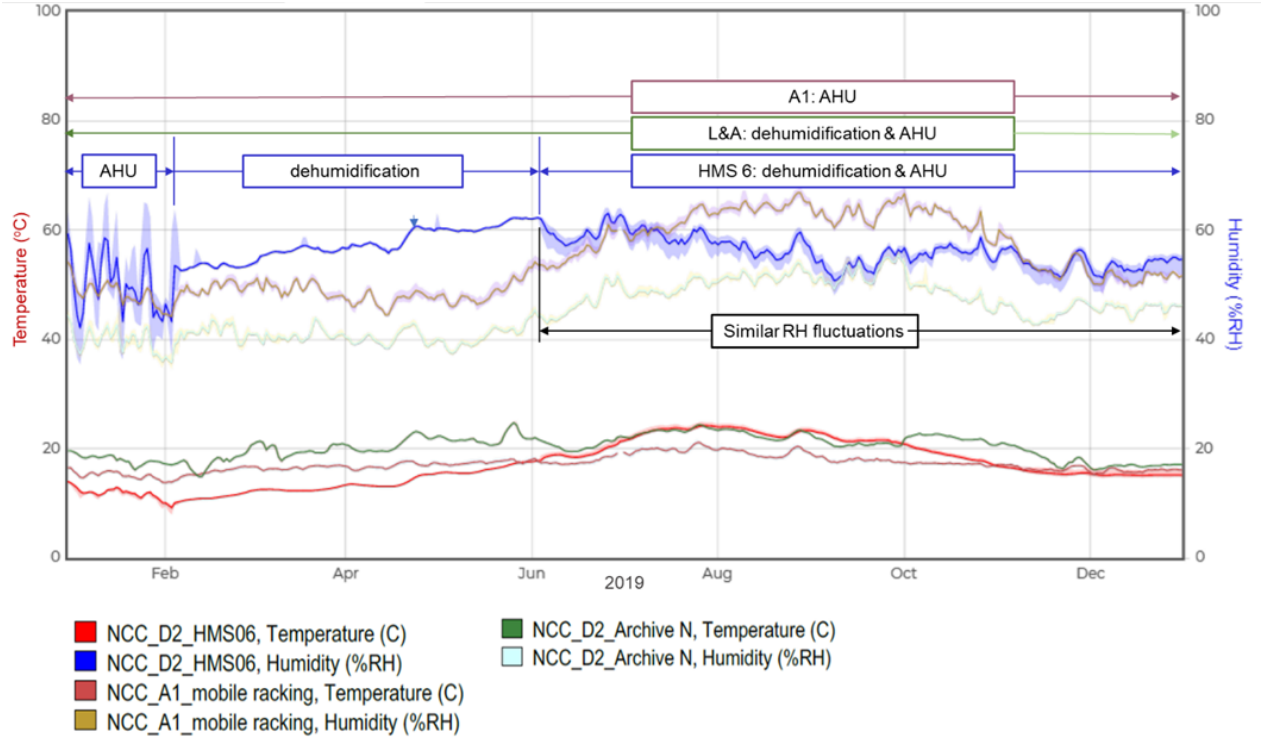

Figure 6.24 Comparison of RH, HMS 6, A1, L&A N (Hanwell EMS)

The RH was more stable in L&A S and A2 throughout the same period although it rose in L&A S from 39% to 52% and in A2 from 38% to 60% during the warm weather from June to October. The RH level remained around 60% in A2 through to the end of the research period. In L&A S, it dropped to around 40% by November. Comparing data from A2 and L&A S with data from HMS 4 showed that HMS 4 had the most stable RH in all three stores after April 2019 (Figure 6.25) and the most stable environment in the HMS, despite identical AHU operational cycles and heating levels (Figure 6.26). RH fluctuations in HMS 5 duplicated those in HMS 6 although RH levels were 1% to 3% lower. After a 6% rise in April 2019, due to external temperatures reaching 20°C, the RH in HMS 4 stabilised between 51% and 54% until the end of the research period, with negligible daily fluctuations. Both RH levels and fluctuations were buffered effectively.

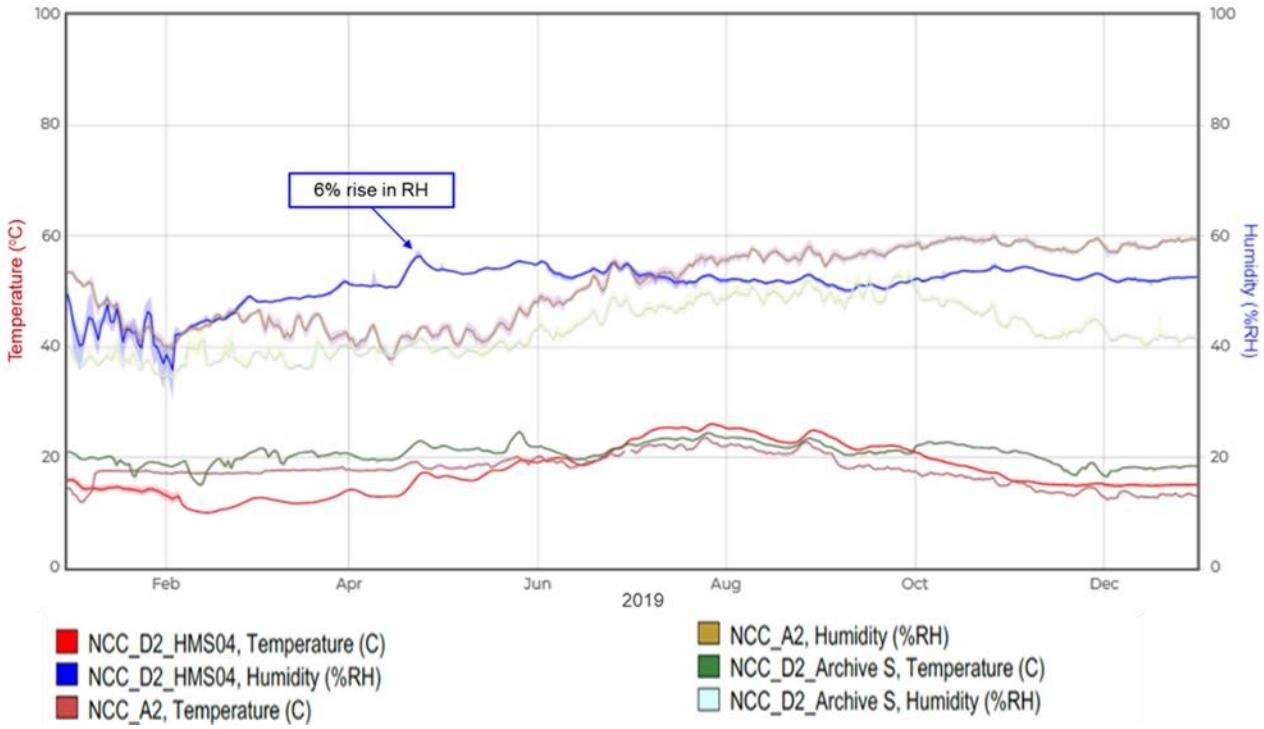

Figure 6.25 Comparison of RH, HMS 4, A2, L&A S (Hanwell EMS)

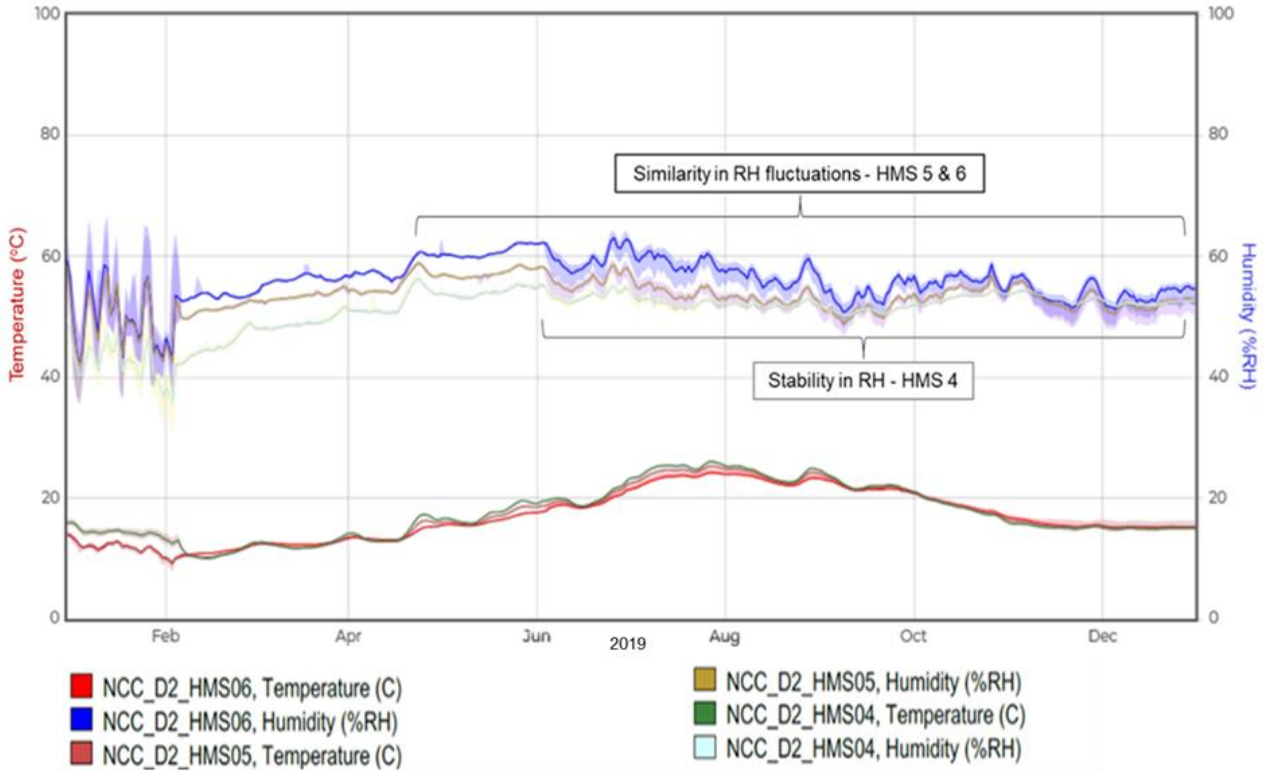

Figure 6.26 Comparison of RH, HMS 4, 5, 6 (Hanwell EMS)

Monitoring data from the hangar D2 ML4106 unit, positioned between the back of the HMS and the east wall of the hangar, showed that internally the thermodynamic response to external conditions affected the overall internal RH and temperature

(Figure 6.27) rather than a response to the thermodiffusion phenomenon. RH levels followed external patterns although they were generally 20% lower, ranging from a low of 55% RH to a high of 85% RH, depending on the time of year, and with more moderate fluctuations.

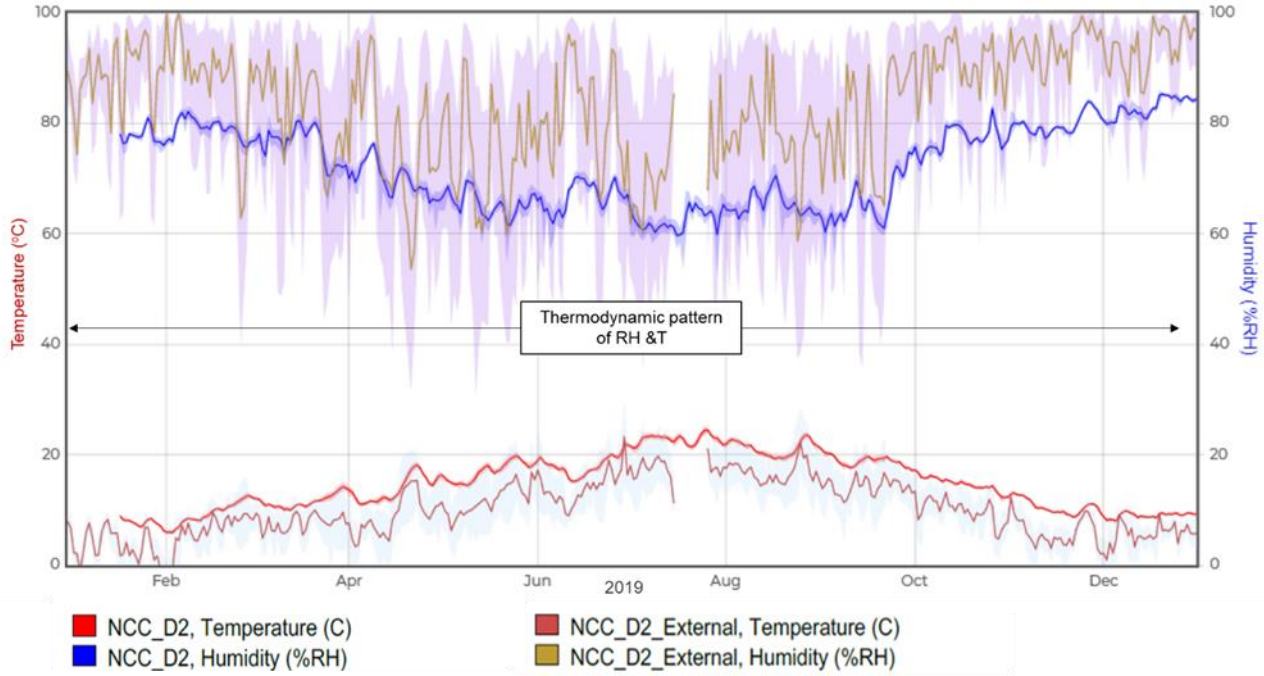

Figure 6.27 Effect of external conditions on RH, hangar D2 (Hanwell EMS)

RH monitoring data from the storage shelter next to the south-west corner of the L&A store from March 2017 to April 2018 showed moderately different RH levels but similar RH fluctuations to those recorded by the hangar sensor. Temperatures were moderated by one or two degrees so that RH levels were slightly more consistent within the tent. During the period from April 2018 to January 2019, the unit was accidentally left out on a stack of pallets in the open area of the hangar between the north-west corner of the HMS and the central fire door of the L&A store. Data from this period demonstrated that the RH level in the centre of the hangar varied from the RH between the HMS and exterior hangar wall by 2% to 6%. Temperatures also varied with more moderate temperatures in the centre of the hangar. As RH data showed no change when the ML4106 unit was replaced in the shelter, it was determined that it was location within the store and not the construction and airtightness of the shelter that provided any RH mitigation. Overall conclusions were that RH mitigation in the hangar was provided to a limited extent by the thermal mass of the hangar's concrete construction, as described in Chapter 4, Section 4.4.2.1, but there was also heat seeping from the AHU ductwork along the perimeter corridor of the L&A store which had a direct effect on the RH in the centre of the hangar.

6.3 Moisture content data assessment

The data gathered from the monitoring of moisture content in the east (exterior) and north (interior) walls of HMS 6 and 5 were assessed to see if a relationship between internal RH and moisture content within the HLC walls could be established. Data from the Hanwell Dampwatch unit was acquired from HMS 6 from August to December 2017 and from HMS 5 from January 2018 to February 2020. Data was acquired from the north and east walls of both rooms, with sensors placed at equal intervals to allow assessment of the percentage of MC from just above floor level to just below ceiling level.

In HMS 6, the pairs of sensors were spaced 410 mm apart with the bottom sensor 160 mm from the floor and the top sensor at 280 mm from the ceiling (Figure 6.28).

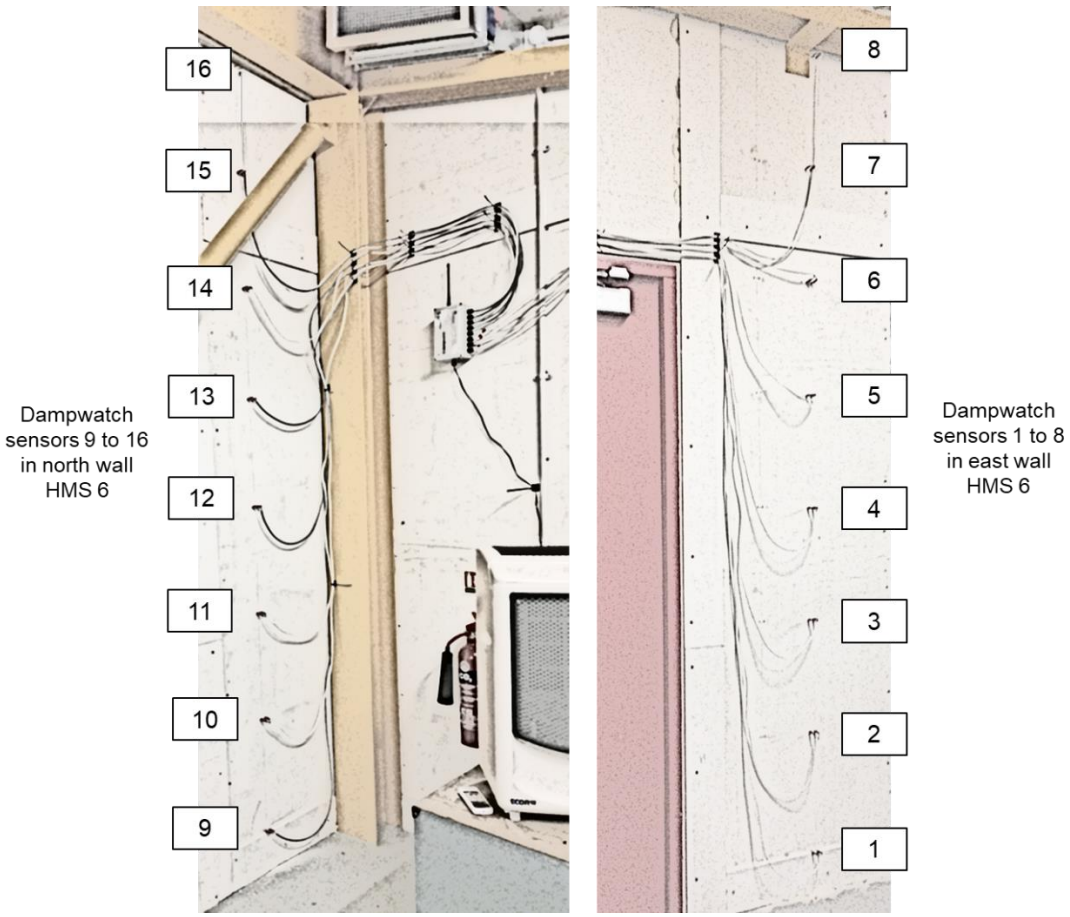

Figure 6.28 Dampwatch sensor locations, HMS 6

In HMS 5, due to the lower ceiling height, sensors were spaced at 300 mm intervals, with the bottom sensor at 140 mm from the floor and top sensor at 270 mm from the ceiling (Figure 6.29). Sensors were inserted to a depth of 50 mm in the HLC matrix.

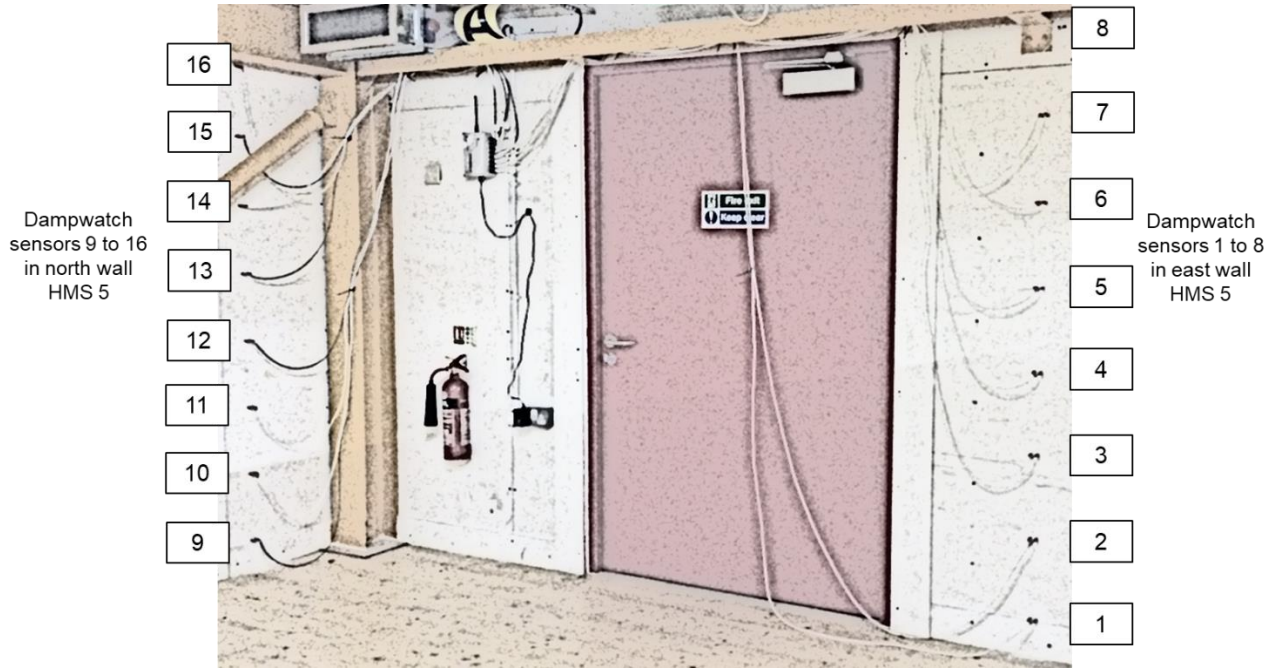

Figure 6.29 Dampwatch sensor locations, HMS 5

In HMS 6, there was a marked similarity to the pattern of MC (%) values obtained from each location in both walls throughout the monitoring period, as can be seen in Figure 6.30, which compares the MC (%) pattern obtained for 22 August and 29 December. The highest MC (%) value always came from Channel 7, located close to the ceiling in the east wall The MC (%) values revealed the specific capacity for moisture storage at each location throughout the walls, highlighting the heterogeneous porosity of the HLC matrix.

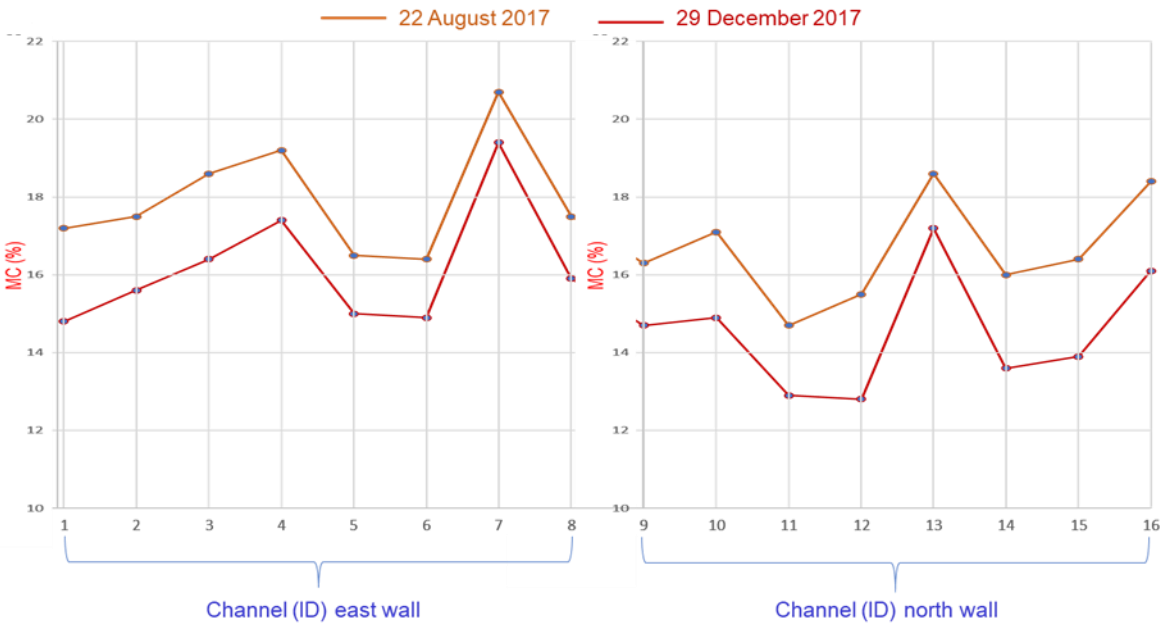

Figure 6.30 Range of MC (%), E & N walls, August & December 2017

Overall MC (%) from both walls was 17.29% on 22 August and 16.44% on 29 December. The daily HMS 6 median RH percentages were an average of 58.7% on 22 August and 53.4% on 29 December (Figure 6.31). As the internal temperature in HMS 6 was lower in December by almost 7°C it would have been anticipated that the RH would have been higher than in August. However, by plotting the RH and temperature for both days on a psychrometric chart , it can be shown that the absolute humidity could be estimated at 0.009 kg/kg on 22 August and at 0.0055 on 29 December (Figure 6.32). Monitoring data from the Dampwatch sensors demonstrated that there was a correlation between the overall MC (%) in the walls within 50 mm of the interface with the room and the RH (%) in HMS 6. RH and temperature data from the external and hangar units in August showed that there had been a preceeding period of high external temperatures which created a rise in HMS RH levels, allowing the moisture in the wall to move towards the wall/room interface and to desorb into the room, with a resultant higher absolute humidity. During the period from 27 to 29 December, external temperatures dropped below 0°C and moisture moved away from the wall/room interface, initiating absorption and reducing the absolute humidity.

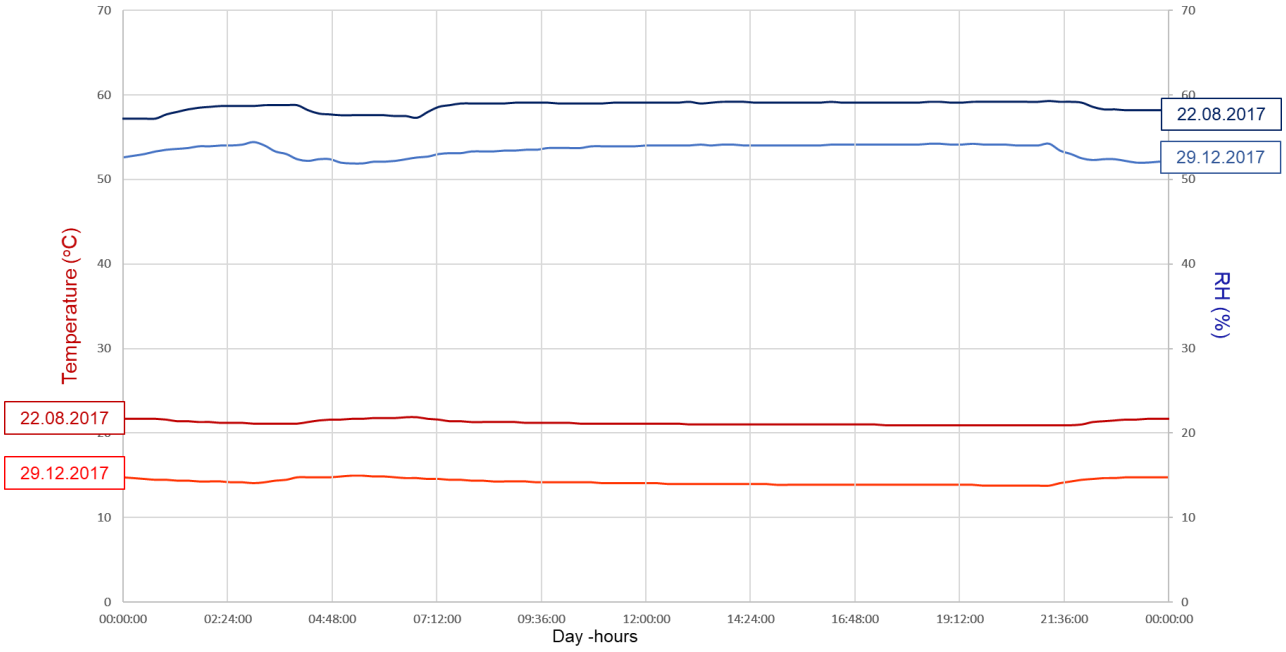

Figure 6.31 Comparison of daily RH & temperature, HMS 6, August & December 2017 (Hanwell rl8)

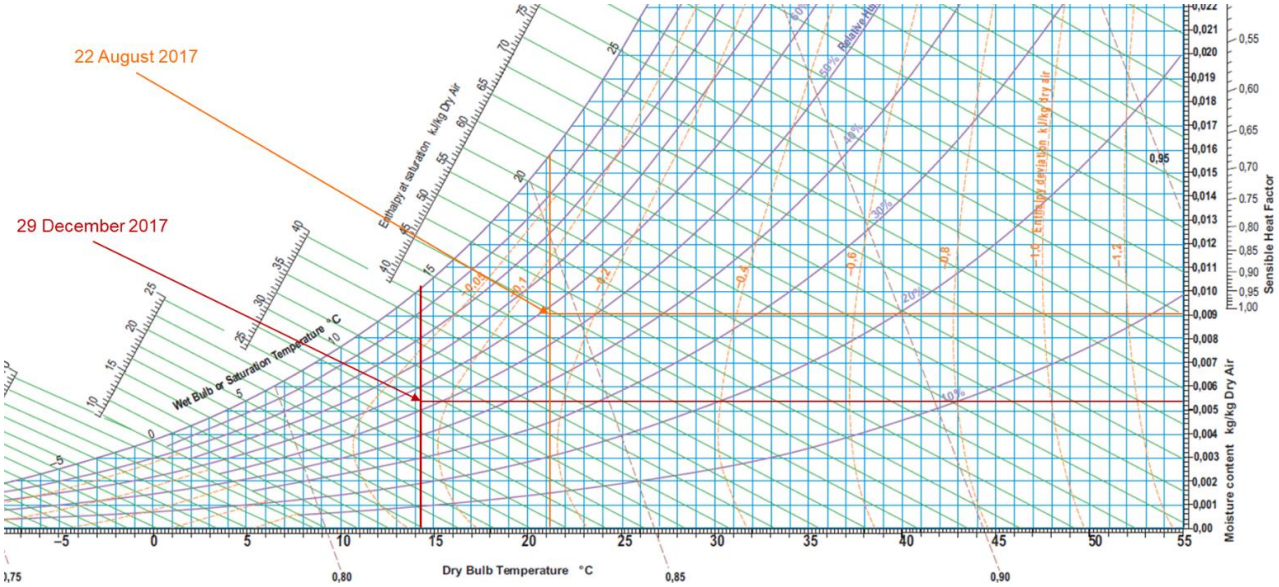

Figure 6.32 Calculation of absolute humidity, HMS 6, August & December 2017

Averaged overall wall MC (%) was always higher in the east wall. On 22 August, there was a percentage difference of 7.69% between the averaged readings from the east (17.95%) and north (16.62%) walls and on 29 December, a percentage difference of 14.09% between the east (16.71%) and north walls (14.51%) (Figure 6.33). There was a percentage difference of 7.16% within the east wall from the August reading compared to the December reading but a percentage difference of 13.56% within the north wall between the two dates (Figure 6.34). While overall moisture content had dropped in both walls as a result of the continuous operation of the dehumidifier and cyclical operation of the AHU, moisture content in the exterior wall was likely affected by the higher RH in the hangar. In the period around 22 August, the average RH level in hangar D2 was just above 70%; in December, the average RH was 85%. Moisture would have been transferred through the building envelope with the moisture penetration depth being sufficient to account for the increase in MC (%) in the east wall to within 50 mm of the wall/room interface.

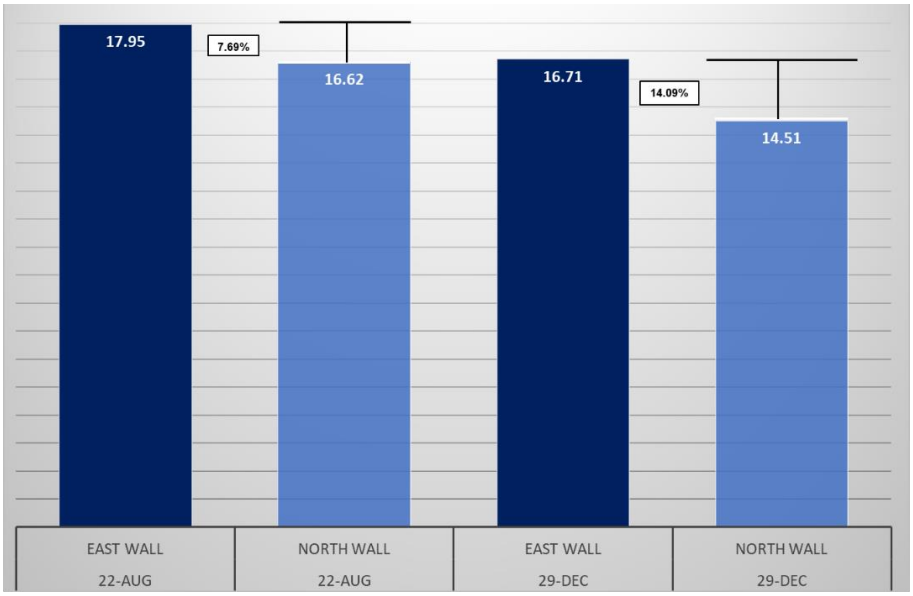

Figure 6.33 MC (%) difference between walls, HMS 6, August & December 2017

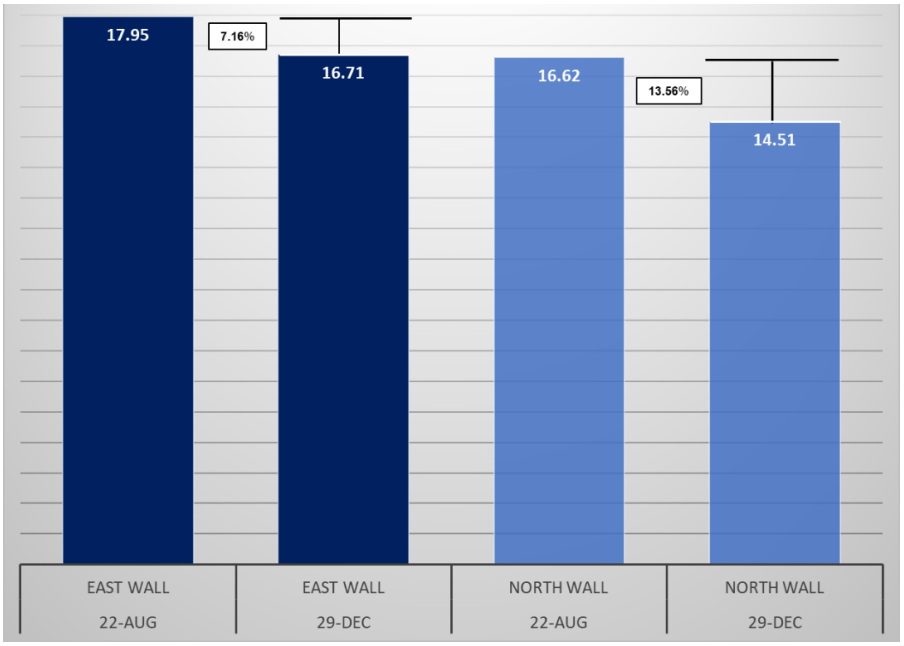

Figure 6.34 MC (%) difference within walls, HMS 6, August & December 2017

As the dehumidifier was closer to the sensors in the north wall than in the east wall, dehumidification could have accounted for the difference in wall moisture content. The dehumidifier was connected to hangar drainage so it could not be moved and there was limited access to other wall areas. It was decided to relocate the Dampwatch to HMS 5 to see if the MC (%) difference between the walls was consistent with the data obtained from HMS 6 as well as to determine if the difference in RH levels between the two storerooms had an effect on overall moisture content.

MC (%) values obtained on 07 January 2018 from HMS 5 were compared to those obtained from HMS 6 on 29 December 2017 as both external and internal conditions were similar. Data showed that the average values of MC (%) in the north and east walls in HMS 5 were closer to each other than the values had been in HMS 6 but again MC (%) was higher in the east wall. Average overall MC (%) in the east wall was 17.66% and 16.425% in the north wall, a percentage difference of 7.25% (Figure 6.35). MC (%) was higher in both the east and north walls of HMS 5 than in HMS 6, with a percentage difference of 5.52% between the two east walls and of 12.38% between the two north walls (Figure 6.36). It was determined that dehumidification affected the MC (%) in the areas monitored in both walls in HMS 6 but more so in the north wall.

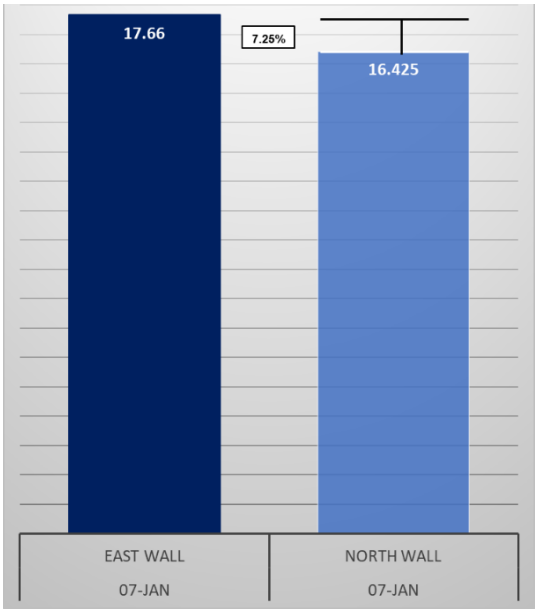

Figure 6.35 MC (%) between walls, HMS 5, January 2018

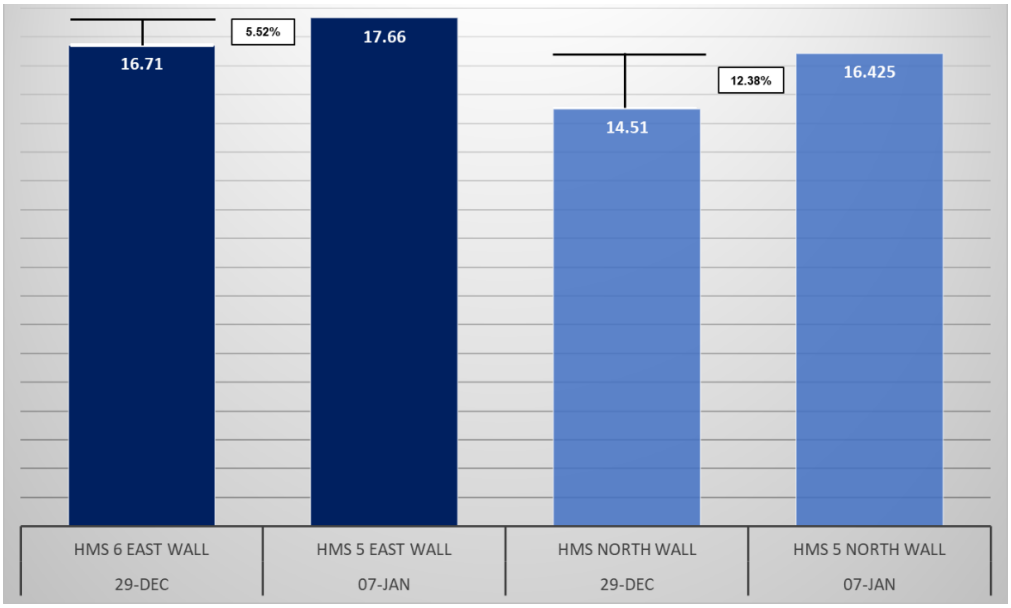

Figure 6.36 Comparative MC (%) at 53% RH, HMS 5 & 6

Excel graphs using the CSV data show the patterns of moisture storage in the walls. From 07 January to 07 March 2018, the air handling system ran reliably with daily RH fluctuations of ±2%. The MC (%) pattern remained consistent, with the highest reading coming from Channel 1 and 3, sensors in the east wall, but overall MC (%) decreased. By 07 May, the RH was stable at 57% as the AHU drew in almost no external air after the March cold snap. There was a shift in the MC (%) pattern in the interior wall but the pattern in the exterior wall was virtually the same as in January and MC (%) values in both walls regained the January level (Figure 6.37). As the external temperature exceeded the store temperature in the beginning of May 2018, the internal RH began to drift upwards. The AHU was reset at a higher temperature to offset the RH gain, resulting in RH fluctuations twice a day of ±3% but an overall reduction in internal RH by 5%. MC (%) levels increased in July but then dropped through August with the MC (%) pattern shifting more in the interior wall (Figure 6.38). Higher MC (%) values now came from Channel 7 rather than Channels 1 and 3.

As discussed in Section 6.3.1, the air handling system failed to respond to the BMS signal from July and both AHUs operated erratically until January 2019. Dampwatch data showed that, despite the erratic operation of the AHU, the MC (%) in HMS 5 settled into a more consistent pattern in the interior wall. With the re-establishment of the normal AHU operation and an internal RH stabilised between 52% to 60%, with daily fluctuations of no more than ±2%, the pattern of MC (%) also became more consistent in the east wall from January 2019 (Figure 6.39). Similar high MC (%) values came from Channels 7 and 8 after July 2019 (Figure 6.40).The changing patterns of moisture storage showed that moisture could move vertically as well as laterally but vertical movement was more likely under fluctuating internal conditions. Overall MC (%) values revealed the interconnected porosity of the HLC matrix as the moisture moved back and forth within the walls depending on external and internal pressures. Patterns persisted despite the overall MC (%) rising and falling, revealing the capacity for moisture storage and thus pore size in the HLC matrix, with the lowest MC (%) indicating smaller pores with less moisture storage capacity.

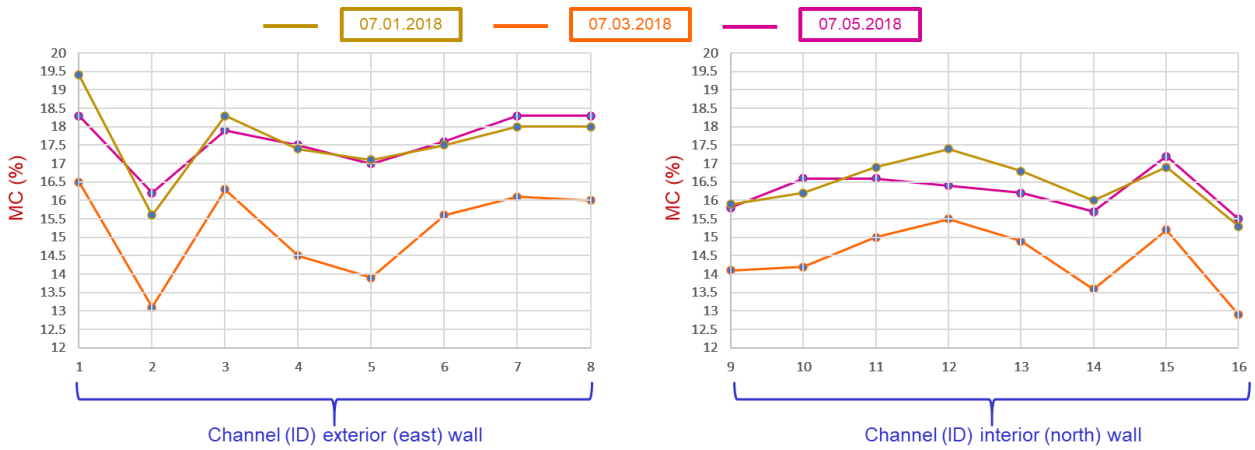

Figure 6.37 MC (%) patterns from January to May 2018

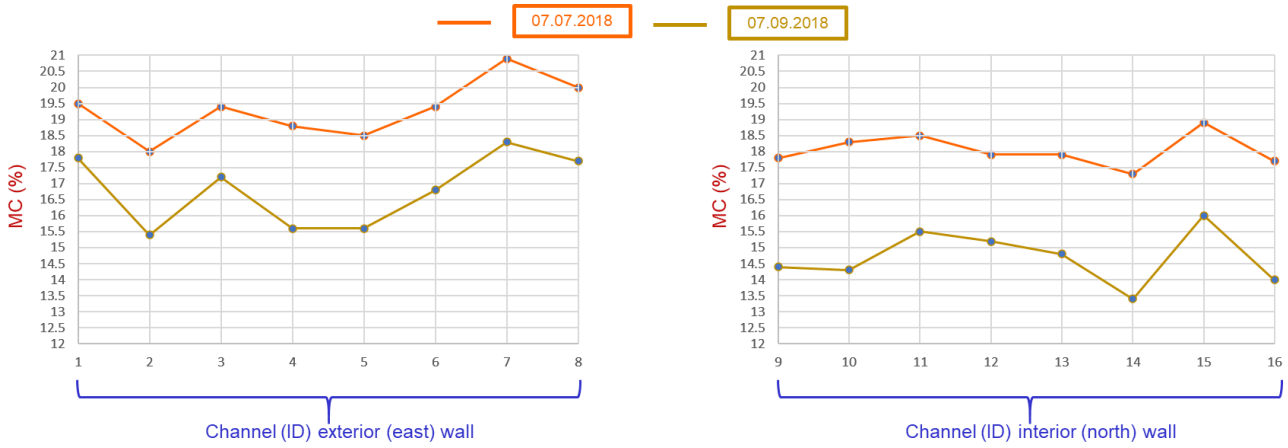

Figure 6.38 Shifting MC (%) patterns during loss of AHU stability

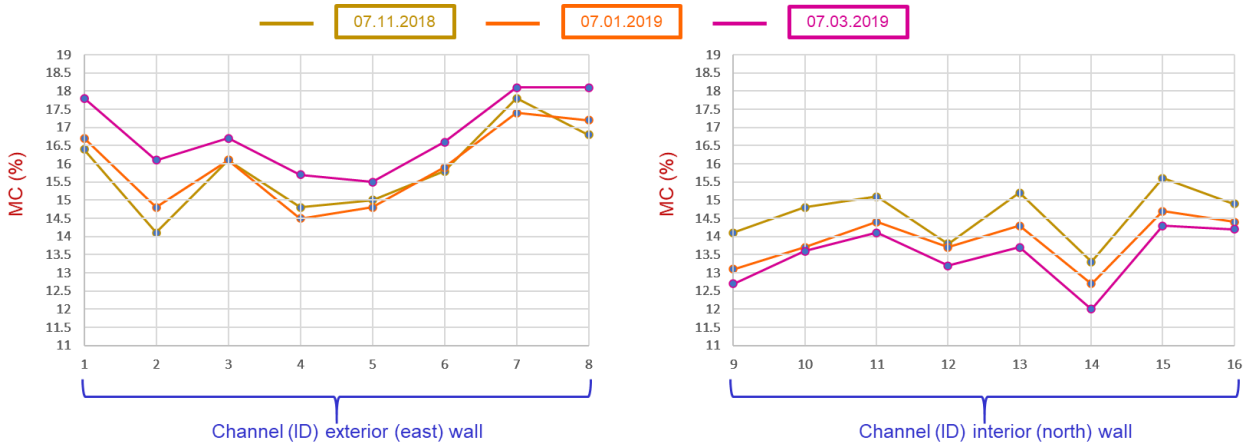

Figure 6.39 MC (%) under fluctuating internal conditions

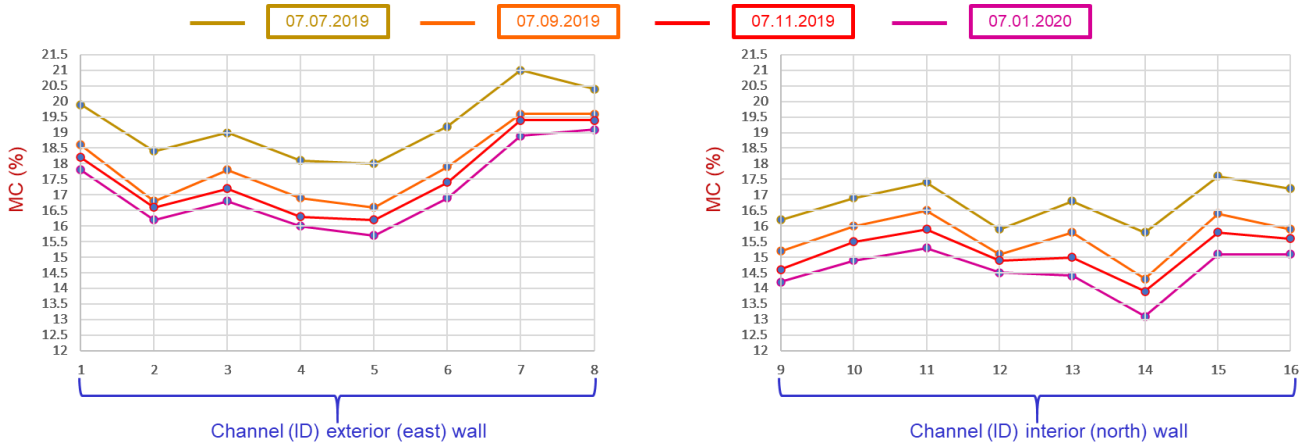

Figure 6.40 MC (%) under stable internal conditions

According to the sorption curve of HLC, MC (%) increases with RH (%). Thus an increase in the RH (%) in HMS 5 should have corresponded to an increase in MC (%) in the walls. The MC (%) of HLC, based on typical moisture sorption isotherms, should be about 5% when at equilibrium with 50% RH at 20°C (Fabbri et al., 2015)

(Figure 6.41). According to Evrard (Evrard, 2006), the MC (%) of HLC at 50% RH would be 22.31 kg/m^3 or 4.65%. As the %WME used by the Dampwatch system is a theoretical measurement, not a definitive one, the higher MC (%) values obtained by the Dampwatch did not represent the true moisture content within the HLC walls but established the moisture content capacity within the interconnected porous matrix. The MC (%) values obtained also demonstrated that MC (%) of the interior wall decreased at a faster rate than that of the external wall, which was to be expected with drying processes occurring on both sides of the wall.

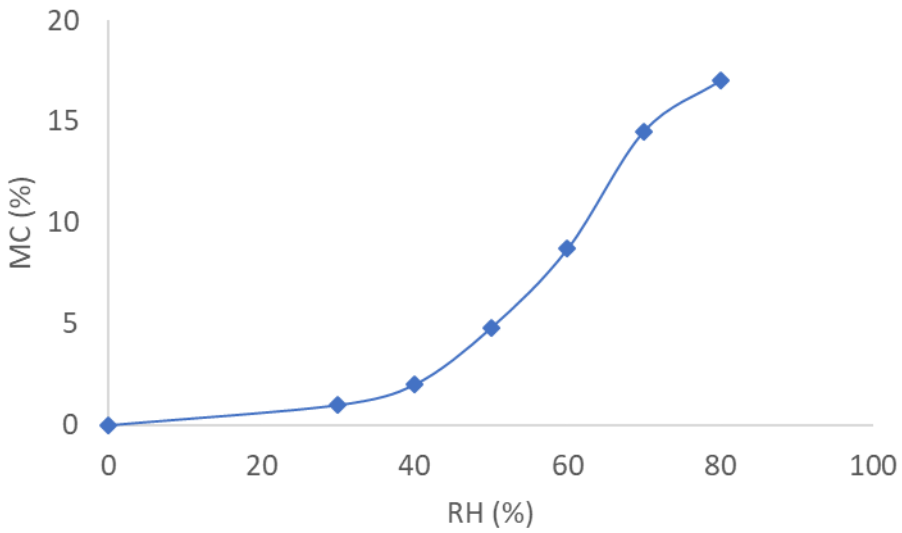

Figure 6.41 Typical HLC moisture sorption isotherm at 20°C, after Fabbri et al., 2015

A comparison of the graphical data from the ML 4106 and the Dampwatch sensors showed that, as RH rose or fell within HMS 5, the MC (%) of the walls appeared to have a correlated rise and fall. In order to explain the relationship between MC (%) at each location in either wall and room RH (%), regression analysis using a simple linear regression model was undertaken. Simultaneous RH (%) and MC (%) data was used from different operational modes during the monitoring period from August 2018 to February 2020. Correlation coefficients were used to measure the strengths of the relationship between each set of variables at each location in the interior (north) and exterior (east) wall of HMS 5. A correlation coefficient can be any value between -1 and 1, with the larger its value indicating a stronger relationship. A correlation coefficient greater than zero would indicate a positive relationship, showing that both variables moved in the same direction and supporting the theory that MC (%) in the HLC walls increased with increasing RH (%) in the room.

The correlation coefficients were calculated using the Excel Data Analysis ToolPak. The results provided the correlation coefficient as well as the R-squared (R^2) value, the p-value and the Standard Error. R^2 value, the coefficient of determination, is a statistical measure of the percentage of the variance of the dependent (response) variable that is predicable from the independent (predictor) variable. R^2 is always between 0% and 100% and generally it is considered that the higher the R^2 value, the better the fit of the model to the data. However, a low R^2 value can still allow

conclusions to be drawn about how changes in the independent variable are associated with changes in the dependent variable. The significant coefficients still show the standard change in the response for one unit of change in the independent variable. The p-value measures the probability that the observed difference has occurred randomly, with the lower the p-value (< 0.05), the greater the statistical significance of the observed difference. Standard Error is another way to measure goodness of fit, showing the average distance that the data points fall from the regression line.

The period from 16 August to 08 September 2018 included intervals of RH instability when the internal RH fluctuated rapidly below a norm of 50% to 53% due to the AHU drawing in significant quantities of cold external air (Figure 6.42) Calculated linear regression values, rounded to two places, for each location are given in Table 6.1. Correlation coefficients ranged between 0.73 for Channel 2 to 0.92 for Channel 13, indicating that there was a strong relationship between MC (%) and RH (%) at all locations. The lowest R^2 value was found for Channel 6, with 53% of the values fitting the regression analysis model, followed by Channels 2 and 12 at 54%. The highest R^2 value was found for Channel 13, with 84% of the values fitting the model, followed by Channel 10 at 83%. As the goal of the regression model was to determine how changes in the independent variable related to changes in the dependent variables, the R^2 value was not considered to be greatly significant other than indicating that the data was fitting the regression model. P-values indicated that all predictor variables were significant. The residual plot for each location was checked to ensure that patterns were random, helping ensure that the regression model was valid.

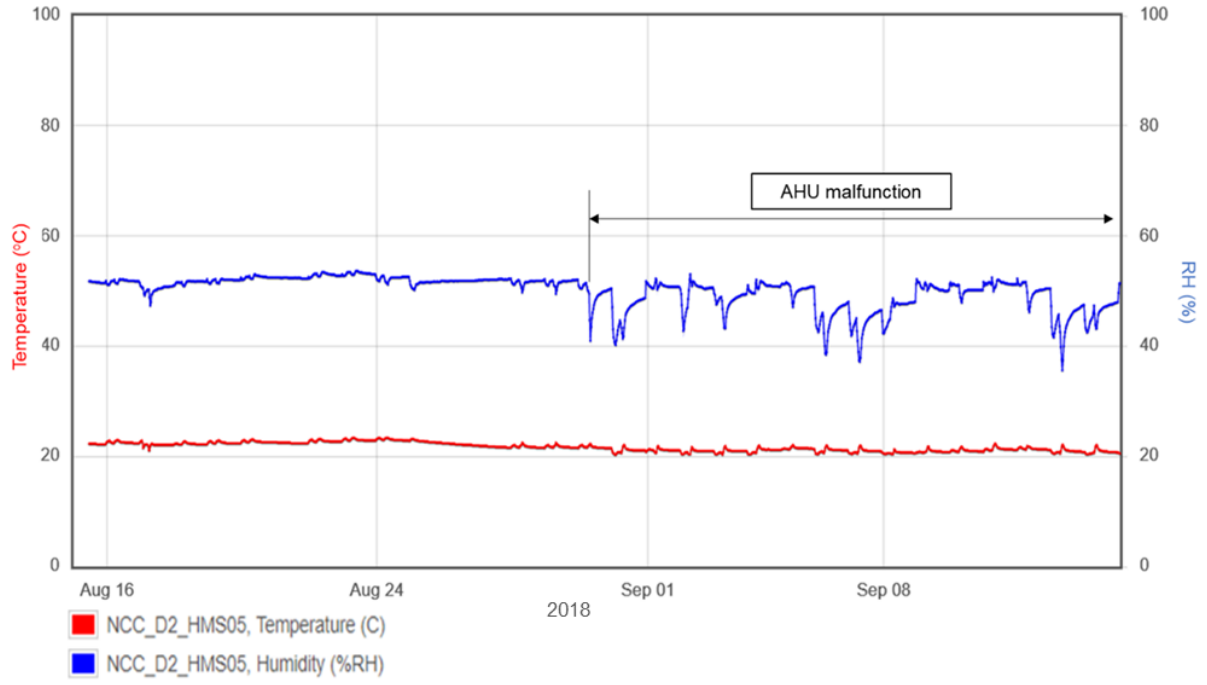

Figure 6.42 RH pattern, HMS 5, August to September 2018 (Hanwell EMS)

Table 6.1 Calculated linear regression values, 16 August to 08 September, 2018

Channel	Correlation coefficient	R^2 value	P-value	Standard error
1	0.85	0.72	4.83E-10	0.14
2	0.73	0.54	1.34E-06	0.19
3	0.84	0.70	1.22E-09	0.18
4	0.87	0.76	3.92E-11	0.22
5	0.82	0.67	5.44E-09	0.24
6	0.73	0.53	1.43E-06	0.23
7	0.85	0.72	4.3E-10	0.22
8	0.75	0.57	4.06E-07	0.19
9	0.85	0.73	2.53E-10	0.23
10	0.91	0.83	2.77E-13	0.30
11	0.82	0.68	4.04E-09	0.26
12	0.74	0.54	1.2E-06	0.17
13	0.92	0.84	6.45E-14	0.23
14	0.89	0.80	1.73E-12	0.27
15	0.87	0.75	6.72E-11	0.22
16	0.85	0.72	5.48E-10	0.29

Scatter plots using data from each location were created to see if there was a linear relationship between the dependent variable, MC (%), on the X-axis and the independent variable, RH (%), on the Y-axis. All data showed a linear relationship with residuals showing a constant variance around the true line. Data from locations in the interior wall were generally a better fit to the model than data from locations in the exterior wall in this period. Figure 6.43 shows the linear regression graphs for Channels 6 and 13. Data fit the model better when the RH was between 50% to 55% than when the RH fluctuated rapidly downward but the outliers indicated that MC (%) responded to rapid downward RH fluctuations as well as gradual changes in RH (%).

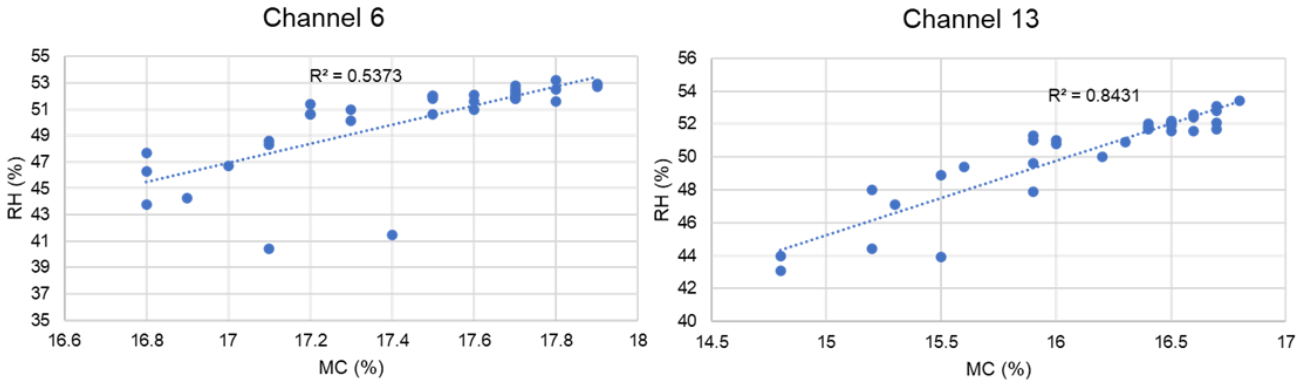

Figure 6.43 Linear regression graphs, Channels 6 & 13, August to September 2018

During the period from 03 to 28 November 2018, excessive daily fluctuations in the internal RH increased with levels rising above 70% as well as falling below 40%. This resulted in the overall RH range no longer remaining between 50% RH to 53%

RH but fluctuating from 40% RH to 60% RH. Linear regression modelling showed lower correlation coefficients and R^2 values but p-values were still statistically significant and residual plots showed random patterns. Data from the interior wall fit the regression model better than data from the exterior wall. Channel 2 had the lowest R^2 value, with only 20% of the data fitting the model, with Channel 8 next lowest at 23%. The R^2 values for the other exterior wall channels fell between 31% and 55%. In the interior wall, R^2 values ranged between 49% for Channel 11 to 70% for Channel 13. Figure 6.44 compares the linear regression graphs for Channels 2 and 13. The poorer fit of data from the exterior locations to the regression model indicated increased outward moisture movement in the exterior wall. Monitoring data from the external ML4109 unit showed that the period of lower internal RH corresponded to a period of very low (to 0°C) external temperatures so that the MC (%) in the exterior wall was not only affected by the internal RH response to the influx of colder temperatures via the AHU but also by a negative thermal gradient across the wall (Figure 6.45). There was an increased inward movement of MC (%) in all locations in both walls during the periods of high RH, with the cause being the action of the AHU operation drawing in external air with an RH between 90% to 100%.

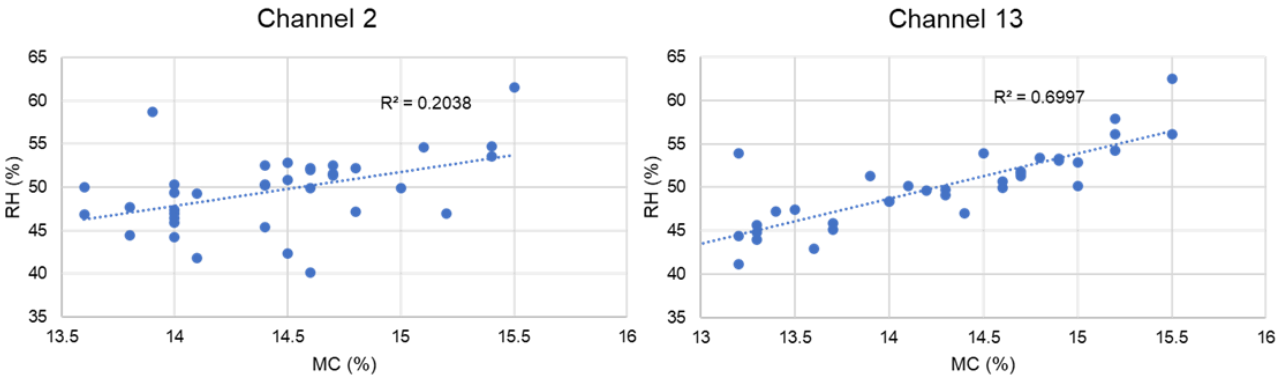

Figure 6.44 Linear regression graphs, Channels 2 & 13, November 2018

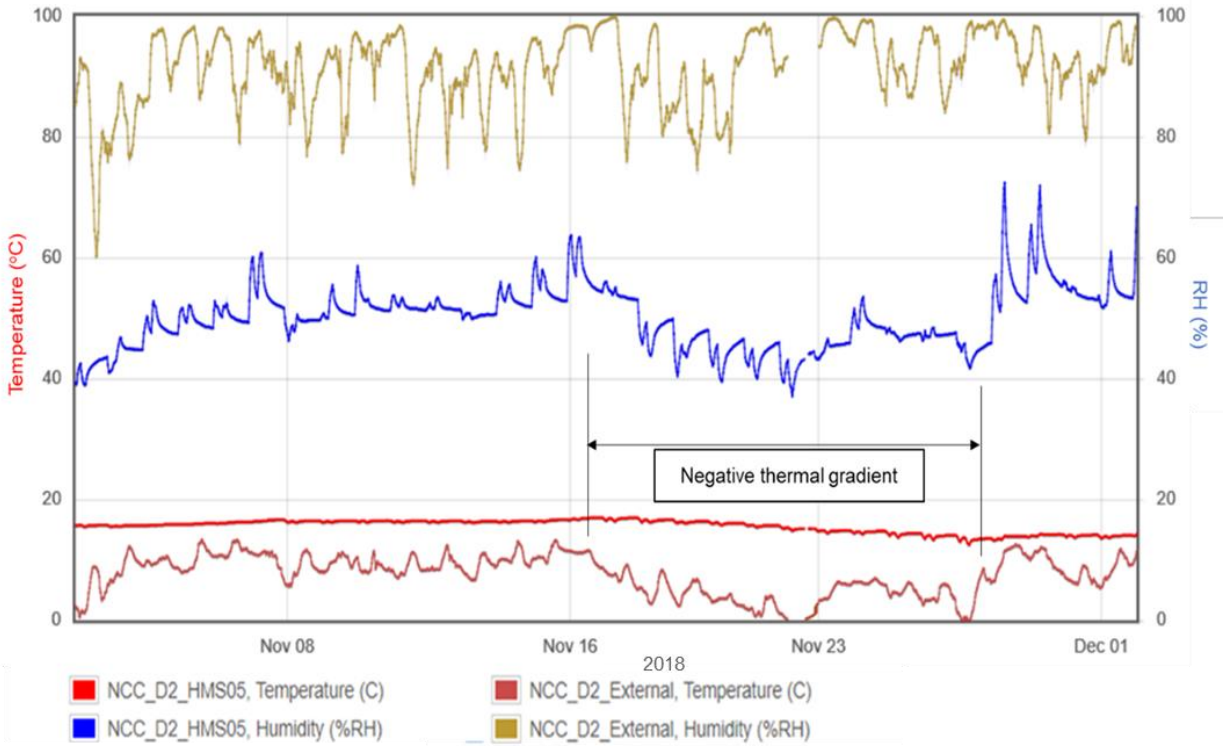

Figure 6.45 Effect of external conditions on RH, HMS 5, November 2018

From February until June 2019, the HMS was operated passively. The RH level was without daily fluctuations although the level rose gradually under the thermal gradient caused by higher external temperatures (Figure 6.46). From 13 to 24 April, the RH rose 5%, with external temperatures exceeding internal temperatures, and then dropped as external temperatures dropped. MC (%) for each channel plotted against the RH measured for each channel reading showed a slight rise along with the RH rise, as seen from the values obtained for each channel from 13 April to 01 May shown in Figure 6.47. Data from all locations in both walls showed a good to very good fit with the linear regression model, with the lowest R^2 value coming from Channel 16 at 69% and the highest from Channel 12 at 91% (Figure 6.48). All linear regression graphs showed MC (%) did not increase until there was a continuous daily increase in RH (%). At the end of the cycle, MC (%) then remained constant while the RH drifted back down by 2% over a period of days.

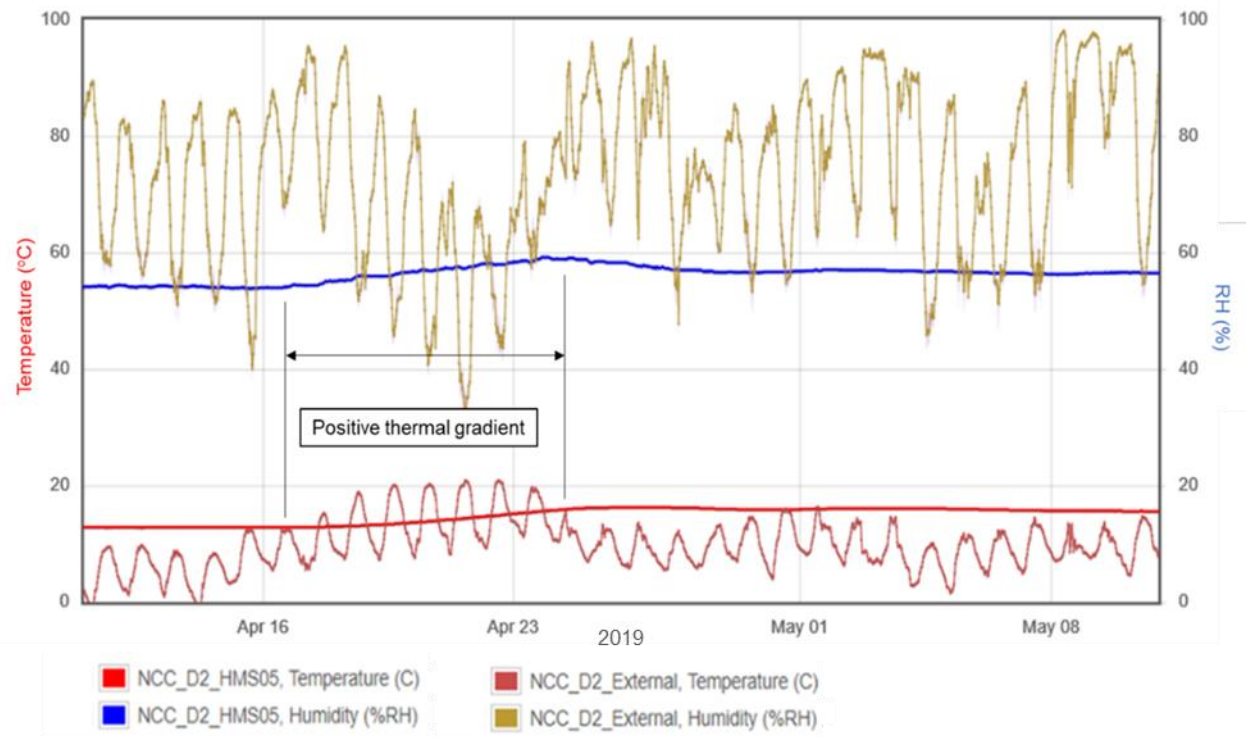

Figure 6.46 Effect of external conditions on RH, HMS 5, April 2019 (Hanwell EMS)

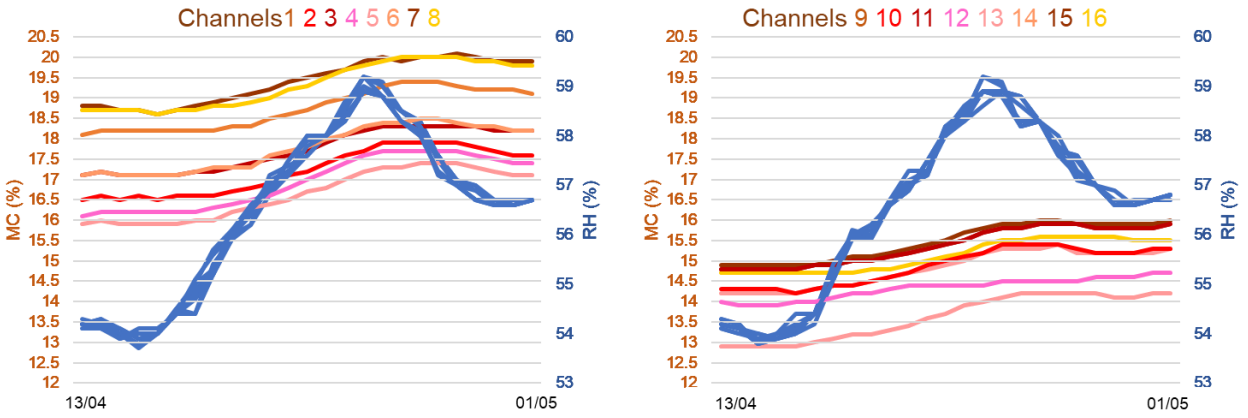

Figure 6.47 MC (%) values obtained for each channel compared with RH, HMS 5, April 2019

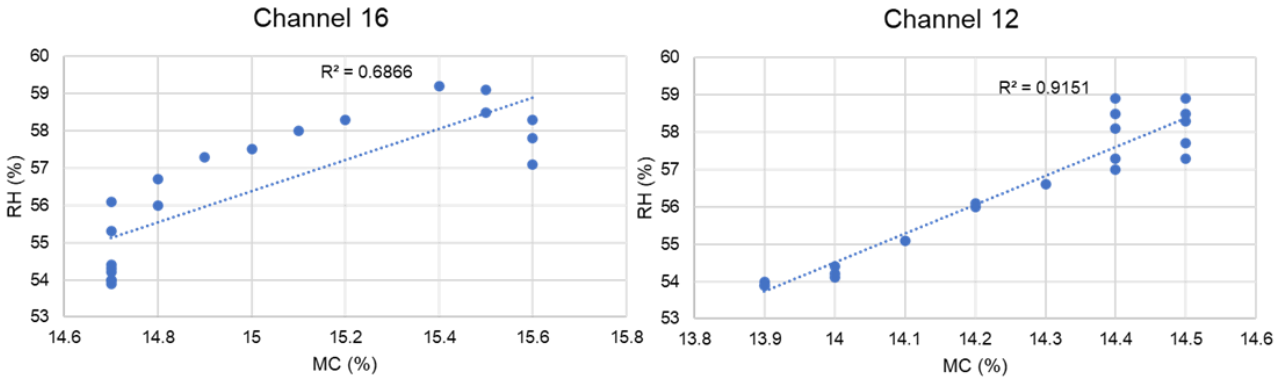

Figure 6.48 Linear regression graphs, Channels 16 & 12, April 2019

With the reinstatement of the consistent heating cycles from June 2019, data from all locations no longer fit the linear regression model. Graphs from all locations in the interior wall showed MC (%) reaching equilibrium despite slight RH fluctuations occurring during AHU operation. Diurnal fluctuations of ± 2% RH had a limited effect on the levels of moisture storage, as shown in the graph from Channel 11 where MC (%) fluctuated between 16.3% to 16.6% as the RH fluctuated around 55% but where it also remained constant at different RH (%) (Figure 6.49). Data from the interior wall supported the conclusion that the MC (%) of the HLC had reached an equilibrium MC (%) with the room RH (%) with the drying mechanism virtually ceasing, as described in Chapter 3, Section 3.2.1.

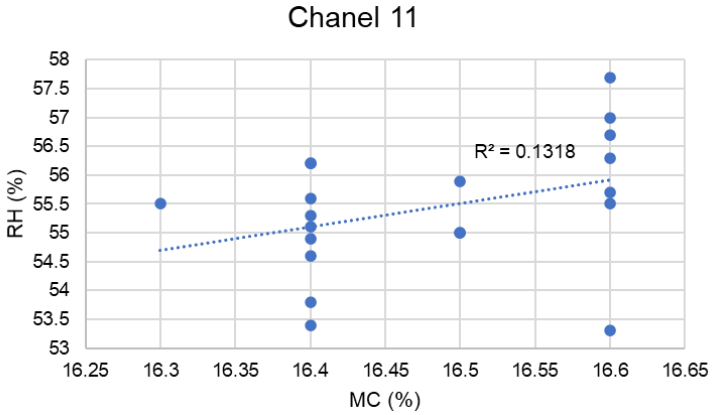

Figure 6.49 Linear regression graph showing end of drying phase in Channel 11, June 2019

Data from the channels in the exterior wall showed less stability in MC (%) with MC (%) more responsive to changes in internal RH and taking longer to reach equilibrium, shown in the linear regression graph for Channel 4 in Figure 6.50. The overall MC (%) remained at a higher level than the interior wall.

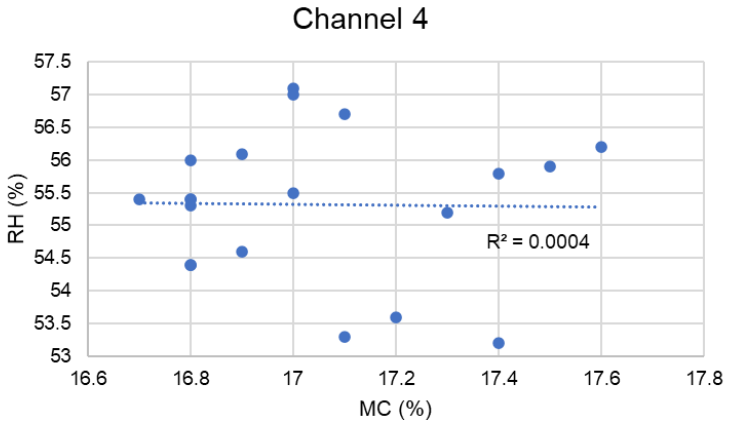

Figure 6.50 Linear regression graph showing mobile MC (%) in exterior wall

At the beginning of the monitoring period in HMS 5, average MC (%) values in the interior and exterior walls were close, being 16.4% and 17.7% respectively. At the end of the two year monitoring period, the average MC (%) value from the exterior wall was virtually the same as at the beginning, being 17.2%. Average MC (%) from the interior wall had dropped by almost 2%, from 16.4% to 14.6%, confirming that the drying processes had been more effective in that wall.

6.4 Air flow data assessment

The air flow sensor was suspended from the ceiling on the north side of HMS 6, mid-way between the east and west corners, 8700 mm from the closest supply grille and directly above the median ML4106 unit. There were no velocity measurements from February until mid-March 2018 as the BMS did not operate in ventilation mode during cold periods. From mid-March until May, data from the air flow sensor showed that velocity rates were very low, with readings of 0.1 m/s to 0.4 m/s being obtained from AHU operation. In May, the AHU settings were altered and velocity measurements were obtained between 0.4 m/s to 1.2 m/s. When the system started malfunctioning in August 2018, with AHU cycles running outside time settings, the lower velocity rate increased to 0.7 m/s. In late October, low external temperatures again stopped the ventilation mode. When ventilation mode was resumed, the air velocity dropped to 0.1 m/s to 0.2 m/s, then gradually rose to 0.4 m/s to 1.0 m/s by December. There were no velocity rates recorded from February until June 2019 as the AHUs had been shut off. With the air handling system reset in June 2019, the velocity rate only reached a maximum of 0.9 m/s per cycle and remained within this range until the end of the research period.

A correlation between velocity rate and daily fluctuations in RH could be made by overlaying data from the ML4106 median unit and the ML4810 unit. Fluctuations in the median RH (%) range began when velocity was measured at 0.4 m/s (Figure 6.51). Increased velocity had no effect on the extent of the fluctuations, with the RH (%) beginning to recover part-way through the ventilation cycle. Data from the high and low ML4106 units also showed initiation of RH fluctuation around a velocity of 0.4 m/s with a much greater degree of RH fluctuation being measured by the sensor at ceiling level. Correlation of the effect of air velocity on RH fluctuations was

obtained from data obtained during the period from February to June 2019, when the air handling system was shut down (Figure 6.52).

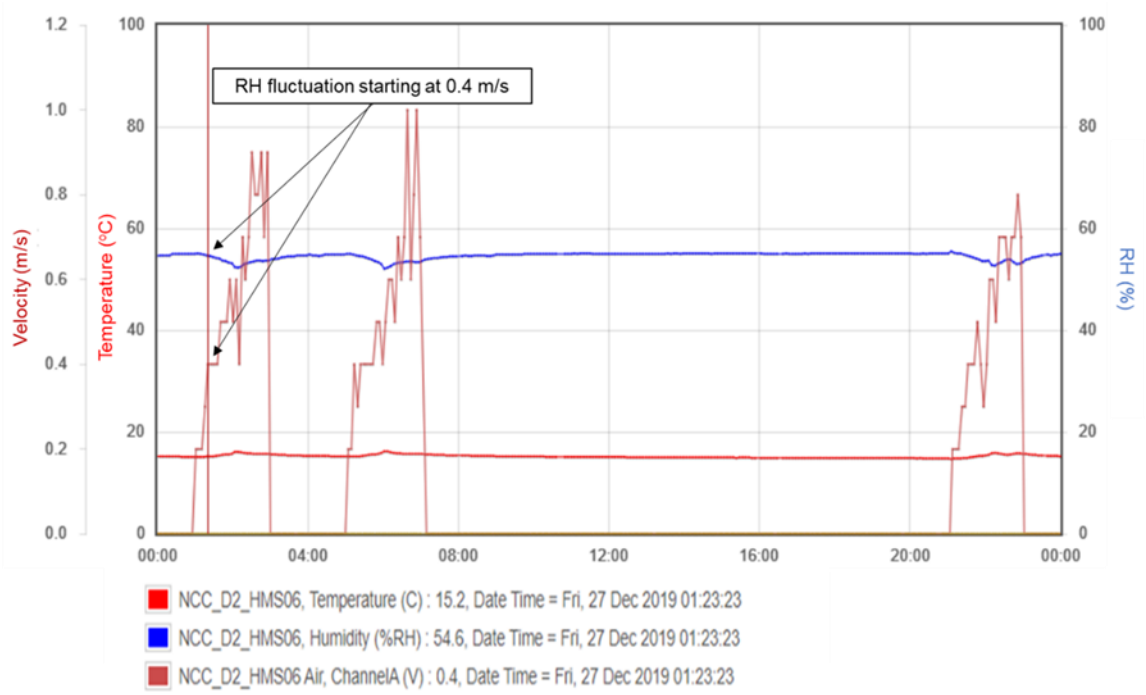

Figure 6.51 Relationship between air velocity & median RH, HMS 6 (Hanwell EMS)

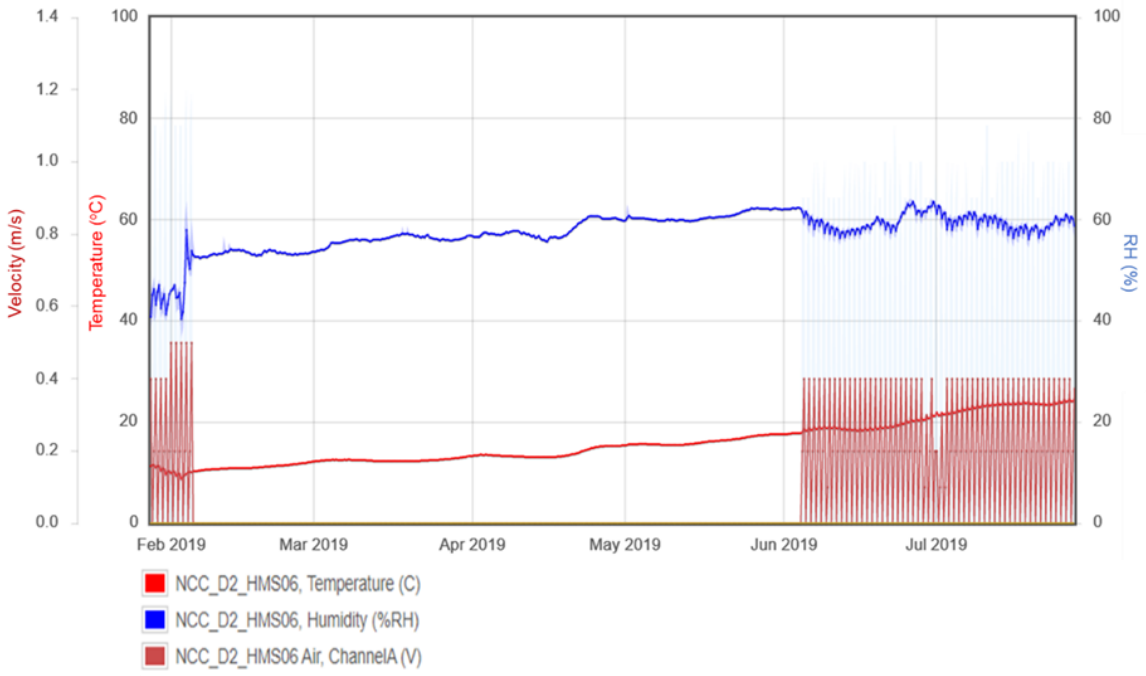

Figure 6.52 Correlation of air velocity to RH fluctuations (Hanwell EMS)

6.5 Access and duration of activity

The period of greatest activity in the HMS was in the first steady state. During the Shipping Gallery decant from October to December 2012, ship models were delivered into HMS 5 and 6 through the sectional overhead doors. Monitoring data showed that storeroom temperature and RH levels reacted almost immediately to the colder temperature and higher RH levels of the hangar but regained previous levels shortly after the door was closed, although duration of activity with the overhead door open affected the length of time for the internal RH to return to the level before activity (Figure 6.53).

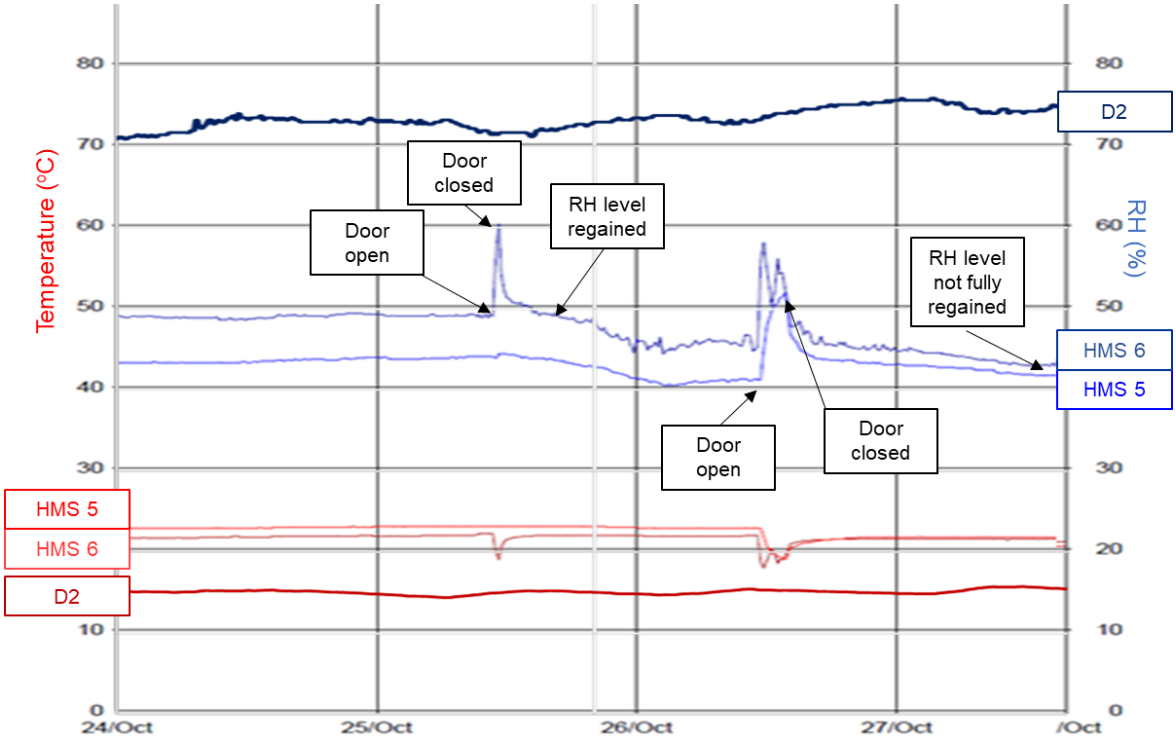

Figure 6.53 Effect of activity on RH, HMS 5 & 6, 2012 (Hanwell rl8)

Art racking installation took place in HMS 4 during November 2012 when RH in the hangar ranged between 85% and 93% but the temperature was only 2°C lower than in the HMS. The sectional overhead door was frequently opened and closed to load in the racking units. The periods when the door was open could be detected from the RH monitoring data, establishing the installation working periods (Figure 6.54). There was a 1°C drop in internal temperature when the overhead door was opened but the RH rose between 5% to 12%, depending on the length of time the overhead door was left open. The RH in HMS 4 did not recover to the level before the installation began throughout the work period but did drop every time the door was closed. At the end of the working week, the RH dropped back to the earlier range in 24 hours but then drifted back up due to an influx of damp air resulting from the second wettest week in the UK in 50 years (www.metoffice,gov,uk).

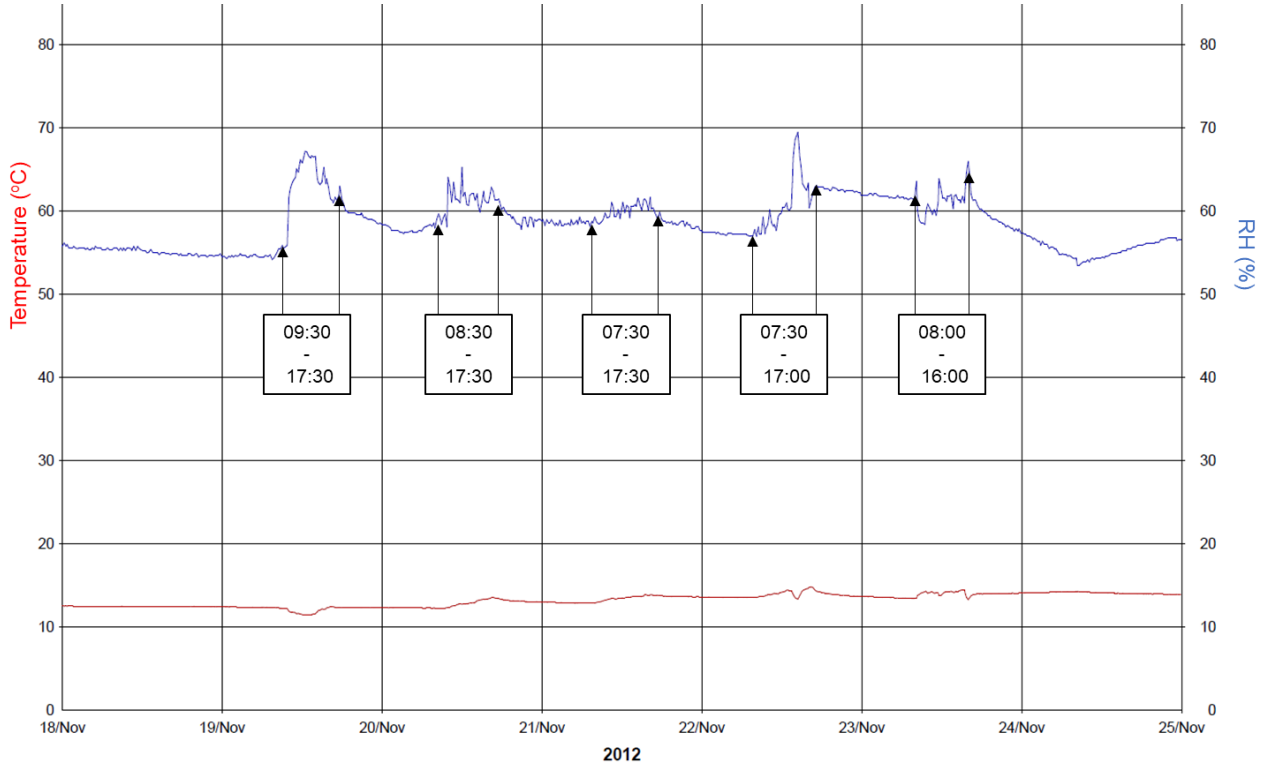

Figure 6.54 Art rack installation working hours revealed by RH fluctuations (Hanwell rl8)

During the passive operation period of HMS in 2013, periods of activity when overhead doors were opened were clearly identified through the RH monitoring as these caused the only RH fluctuations. RH levels recovered within seven to 12 hours depending on the duration of the activity. While the move of the framed art collection from the SCM, during January to March 2015, occurred during operation of the heating system, it was possible to determine from the monitoring data how quickly the RH of the room recovered after access into HMS 4. The RH level would rise less than 3% within 15 minutes of the door being opened, then return to the previous level within seven to eight hours of the door being closed.

Access and duration of activity could also result in the RH in the HMS dropping. On 21 June 2018, a carriage was removed from HMS 6 between 11:05 and 12:00. This required opening the hangar sectional overhead door at the same time as the storeroom overhead door. The external RH, introduced through the open hangar door, was between 40% to 43%, 20% lower than the RH within the HMS. The RH in HMS 6 dropped from 60% to 49% during the hour the doors were open. It took two hours to rise back up by 5% RH but more than 48 hours to reach the previous level of 60% RH.

Sign-in sheets were intended to facilitate the correlation between access and the RH levels and fluctuations. However, it was discovered by the current author that the facilities maintenance contractors did not understand that they too were expected to sign in and out every time they accessed one of the rooms in the HMS. This meant that correlating data with all known periods of access with the RH data was not possible as had been planned.

6.6 Assessment of buffering performance during second steady state, 2016 to 2020

The moisture buffering performance of an ideal construction material for museum storage purposes should fall in the Good-Excellent MBV range. A critical buffering property is the rate of adjustment to changes in RH over time in order to reach equilibrium, with an ideal material adsorbing and desorbing quickly to moderate abrupt peaks and drops of internal ambient RH. The moisture storage capacity is also key to the buffering performance, so that an ideal material is able to store a significant volume of water vapour at very high RH without becoming saturated. Vapour permeability being a function of porosity, a very porous material will have a high vapour permeability, providing a better buffer performance. A material with a significant interconnected porous structure will have a more effective penetration depth, allowing for the long-term buffering required to maintain stable storage conditions.

Analysis of the HMS monitoring data from June 2016 to January 2020 was used to determine whether the buffering performance of HLC was effective under various operational modes in the storage building. RH and temperature data showed the daily and seasonal variations in RH within the building during all operational modes. Data provided from the ML4106 units installed at different heights in HMS 6 identified the range of RH stratification and the various RH fluctuation patterns. The external RH data identified the thermodiffusion phenomenon and the extent of the effect caused by positive and negative thermal gradients across the HLC walls. MC (%) values from interior and exterior walls confirmed that MC (%) did increase with increasing RH (%) but also confirmed that there was significant moisture storage capacity in the HLC matrix. MC (%) values also demonstrated the interconnected porous structure of the HLC matrix. The effective penetration depth was shown to be at least 50 mm, the depth to which the Dampwatch sensors had been inserted into the HLC matrix, as moisture transfer was detected at each sensor location. Indications were that the penetration depth was greater than 50 mm with moisture transfer occurring from the hangar into the exterior HLC walls as far as the Dampwatch sensors, as monitoring data showed the MC (%) to be higher in the exterior walls of both HMS 5 and 6. Linear regression modelling of MC (%) and RH (%) data demonstrated the rate of adjustment to changes in RH and the buffering capability from the absorption and desorption rates.

Air flow and access activity monitoring provided limited data for assessing the buffering performance of the HLC construction but did give some indication of time-related response to changes in RH. Comparison with RH/T monitoring data from other storage structures on the site showed that the RH was buffered more effectively within the HMS in all regulation modes. Due to the difficulties encountered with obtaining data from the environmental monitoring system during the latter part of the research study, there was an opportunity to observe buffering capability under abnormal M&E operation as well as during regular AHU cycles, dehumidification and passive drift.

6.6.1 Evaluation of HLC buffering capability

Passive control of the RH in HMS 4 and 5 eliminated fluctuations caused by heating, ventilation and dehumidification but was unable to prevent the gradual upward drift of RH from May 2016 until May 2017. The dehumidification provided by one unit was sufficient to keep the RH level at 55% ±2% in HMS 6 but any cessation of dehumidification resulted in a 5% rise over 5 to 10 days, depending on the relationship of room temperature with external temperature. High external temperatures, starting in early May 2016 and lasting through to mid-September, had an impact on the internal RH on all floors but the buffering capacity of the HLC resulted in a delayed upward response as moisture desorbed slowly into the rooms. Moisture was reabsorbed as external temperatures dropped to or below room temperatures and RH levels brought back down to previous levels. Periods of low (< 0°C) external temperatures through November 2016 to January 2017 were too short to have an effect on moisture movement and the RH in HMS 4 and 5, although above the recommended upper limit of 60%, remained stable, buffered by the consistent MC (%) in the HLC matrix. The RH in HMS 6 was regulated by the dehumidifier and remained at 55% ±2% unless its operation ceased, at which point the room RH rose to the same level as in the other rooms.

From June 2017, active reduction of the RH gain was required to reduce the upward drfit of RH caused by consistently higher external temperatures. Because dehumidification was not designed into the M&E system, active control had to be achieved using cycles of heating and ventilation. Daily RH fluctuations caused by the heating cycles were buffered to less than ±3% RH in all rooms, keeping them below the museum's specification for fluctuations not exceeding ±10%/24hrs. In HMS 6, the dehumidifier function was triggered when the floor level RH reached 60%. When RH regulation by room temperature proved to be ineffective at reducing rises in RH level caused by thermodiffusion, the dehumidifier setting was lowered. Fluctuations caused by the dehumidifier were minimal, being less than ±2%. By November 2017, daily RH fluctuations in each room were buffered to ±2% RH and the RH levels drifted between 50% to 60% until the cold snap in March 2018. RH levels were restabilised from April 2018 although at a higher level than previously, again due to higher external temperatures.

By July 2018, the malfunction of both AHUs interrupted the stability of the RH level and fluctuations that had been achieved through the regular cycles of heating and ventilation. Initially all floors were equally affected by the faulty operation. The fault appeared to sporadically introduce external air, which caused fluctuations in RH of ±8% to ±20% over two hours. The RH levels in the HMS would recover once ventilation ceased. Overall the RH range remained between 40% to 60% with some exceptional fluctuation spikes, with the buffering capability of the HLC mitigating the fluctuations. By November, the RH fluctuations in HMS 4 differed from the pattern in the other two storerooms as the two AHUs operated in completely different cycles. Despite the abnormal cycles of both AHUs, the RH levels continued to be buffered sufficiently to recover previous levels whenever the influx of external air ceased. When the airhandling system was shut down in February 2019, the RH in the HMS 6 rose fractionally and then stabilised. The internal temperature remained stable at 11°C. RH fluctuations were negligible in all three rooms due to elimination of ventilation with external air. From March to June , there was a gradual upward drift in

the RH level in all rooms whenever the external temperature rose above the storeroom temperatures. While RH levels did not exceed the upper RH recommendation of 60% in HMS 4 and 5, the AHU operation was resinstated in order to reduce the RH in HMS 6, which still remained 5% to 7% higher than in the other storerooms. Continuous regular operation of the AHUs, with two hour on-cycles starting at 01:00, 05:00 and 21:00, kept the RH levels within a range of 50% to 60%, even during periods of thermodiffusion, to the end of the research study. Daily RH fluctuations were less than ±2%. By January 2020, the RH level in HMS 6 was in the same range as in HMS 5 with the level slightly lower in HMS 4 (Figure 6.55).

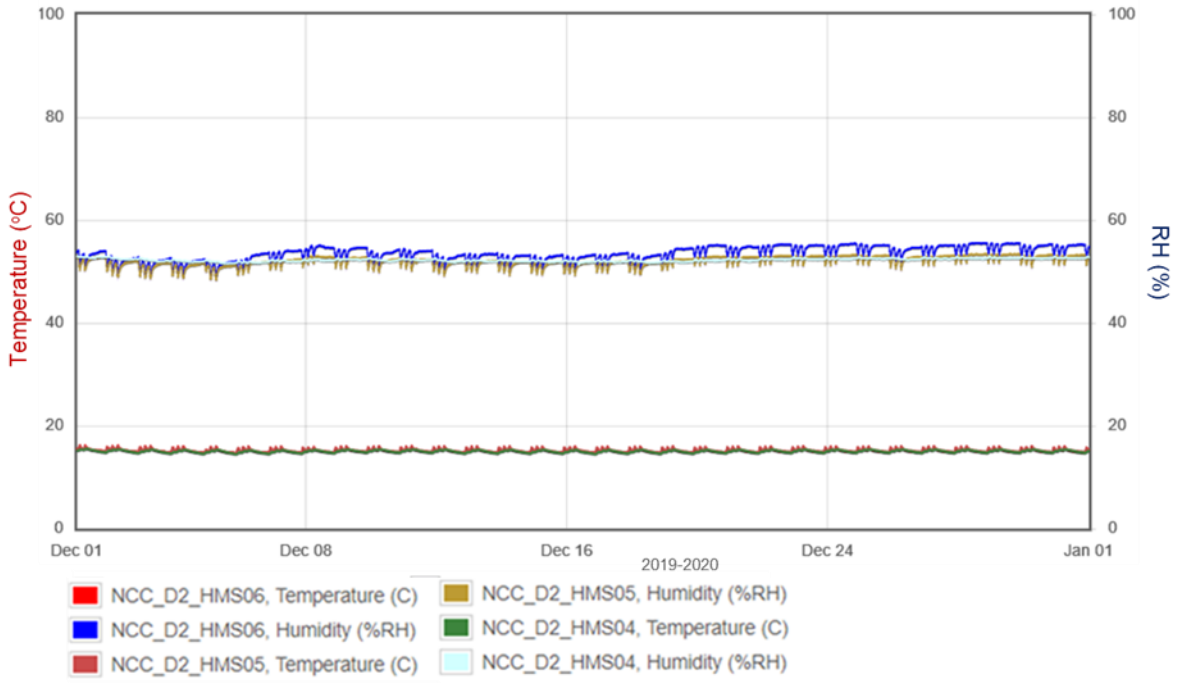

Figure 6.55 Stabilisation of RH in the HMS by end of research period (Hanwell EMS)

The malfunctioning of the air handling system highlighted operational issues that could have had serious consequences for the collections stored in the HMS if the buffering capacity of the HLC had not been effective. The loss of access to the environmental monitoring system meant faults in the system went unnoticed for a considerable period of time. Once system breakdown was noted, the system had to be turned off until a review could be carried out and issues rectified. While AHU operation was reinstated by the site's facilities team, the dampers continued to draw in 10% fresh air as no-one knew how to alter the damper drives. Despite the operational issues, the RH range in the HMS was kept within the museum's specifications for more than 95% of the time, with recovery from daily fluctuations occurring as soon as active control cycles ceased and with no fluctuations during passive control.

The buffering capability of the HLC mitigated effects from activity when hangar air was introduced into the HMS through an open sectional overhead door. The monitoring data showed that RH fluctuations could be correlated to activity but that

recovery of RH levels occurred shortly after storeroom overhead doors were closed as long as the hangar door was not open. With the storeroom overhead doors opening directly into the hangar, if the external hangar door was open at the same time, more than 24 hours would be required for the RH levels to fully recover. Buffering capability of the HLC allowed a recovery of 3% RH to 5% RH to previous levels within two hours.

The monitoring data from periods of extreme external conditions, periods of high or very low external temperatures, showed that the HLC buffered but did not prevent internal environmental response to external conditions as both positive and negative thermal gradients across the HLC walls caused thermodiffusion of the moisture content. Any corresponding internal rise or fall of RH within the HMS was delayed by the buffering performance.

The pattern of MC values obtained from all walls showed that MC (%) was affected more by thermodiffusion through thermal gradients than by RH fluctuations caused by AHU operation. Linear regression modelling showed that MC (%) did follow changes in RH (%) levels. MC (%) patterns obtained by the sensors at each location in both the interior (north) and exterior (east) wall in HMS 5 remained similar despite overall increases or decreases in MC (%) values. The MC (%) patterns revealed the heterogeneous porous structure of the HLC matrix as well as demonstrating how moisture moved through the walls. Moisture movement tended to be lateral although vertical movement was also noted.

The MC (%) in the exterior walls of both HMS 5 and 6 was higher than in the interior walls. In HMS 6, the difference was attributed to the location of the dehumidifier. Initial overall MC (%) values obtained for the interior and exterior walls in HMS 5 showed an average difference of 1.3% but by the end of the research period, overall values for MC (%) were 2.6% higher in the exterior wall. The drying process was demonstrated through linear regression modelling which showed when MC (%) reached equilibrium with room RH (%). Although the difference in drying extent was likely due to the interior wall being between two heated rooms, there may also have been moisture penetration from the hangar through the exterior wall through the sorption mechanisms, interconnected porosity and high water vapour permeability of the HLC. Average MC (%) in the interior wall remained around 14.5% and average MC (%) in the exterior wall around 17.5%, enabling the long-term buffering required to maintain an internal RH between 55% to 60%.

6.6.2 Comparison of low energy storage building performances

The buffering performance of the HMS was compared to the L&A reserve collections store built within the same hangar. While the construction specifications for the L&A store were similar to those of the HMS in that they called for a well-insulated and airtight structure, there were no other low energy control initiatives incorporated in the final design. M&E systems were installed in both buildings but neither system utilised dehumidification to reduce the external RH of external air used for ventilation or to regulate the internal RH. The HVAC system in the L&A store supplied both heating and cooling as well as ventilation. The RH range rise and fall patterns in the L&A store followed external and hangar D2 RH patterns despite the HVAC system. The RH levels were more unstable than in hangar D2 with continuous but

inconsistent fluctuations caused by both heating and ventilation, different at either end of the store. The HVAC system ultimately proved incapable of maintaining the level of RH required to prevent mould growth and it had to be augmented with the purchase and full-time operation of industrial dehumidification units. RH fluctuations were slowly reduced once the dehumidifiers were installed. There was no indication from the monitoring data that any buffering was contributed by design or materials of construction. The monitoring data during periods of extreme external conditions showed that RH levels in the L&A store responded almost immediately to extreme external RH and temperature conditions, with fluctuations between ±10% RH to 15% RH, depending on location within the building.

The buffering performance was also compared to the A Store, a purpose-built storage building on the NCC site. Built in the 1990s, it was intended to be a low energy storage facility and was considered at the time of construction to be well-insulated and airtight. Failure over time of the desiccation dehumidification system as well as other parts of the environmental control system meant that the RH in all three storage areas was regulated only by heating and seasonal drift. Daily RH fluctuations in both A1 and A2 stores remained within acceptable limits at ground and median levels but the RH was less stable at the upper level of the eight meter high racking, closer to the jet nozzle diffusers. The RH range was between 30% RH to 70% RH despite internal temperatures remaining steady, with the range lower in A2 than A1. The RH in the A3 storeroom fluctuated more as the room was less insulated due to presence of large windows. When compared to data from the ML4109 external sensor, it was shown that the RH within the building responded to highs and lows of external temperature almost immediately, rather than being buffered as in the HMS, so that the pattern of internal RH appeared to mirror the pattern of external temperature. Floor sweating was also an issue in both A1 and A2, and was thought to be result of condensation on cold concrete floors due to the design of the ventilation system, with insufficient velocity from the supply jet nozzles. As there was no humidification from the HVAC system, no natural ventilation and air locks provided for all overhead doors into the storerooms, moisture was brought in through the ventilation system. Moisture also would have been present in the large quantities of wooden pallets used in the racking as well as in the cultural heritage collections themselves.

In the HMS, the M&E system provided heating and ventilation, but not cooling. A cyclical operation of the AHU units was used to reduce gradual upward drifts of RH. Fluctuations were generated only during the AHU cycles with stability of level being regained during passive periods. Successful regulation of RH levels in the HMS was achieved by the cyclical programme until faults developed with the AHU units. Portable dehumidification units supplied by the contractor were required in the HMS in the second steady state as in the first steady state. One was used, along with a portable air conditioner, for a short period in 2016 in HMS 4 to reduce an exceptional rise in RH as buffering by the HLC along with seasonal drift was insufficient to reduce levels adequately. Another unit was retained throughout the second steady state and used in the ground floor storeroom to reduce the persistent higher RH level. Its function was triggered when the floor level RH reached 60%. A second and extensive period of AHU malfunction resulted in wider and more frequent RH fluctations and a wider range of RH levels. The immediate resolution to the AHU malfunction was to turn off the system. This resulted in minimal RH fluctuations but

the RH level rose as a result of thermodiffusion and AHU operation was reinstated. Final cyclical operation of the system was to run it for two hours at three intervals over 24 hours which resulted in a reduced RH range and minimal RH fluctuations.

Figure 6.56 shows a comparison of annual RH regulation in the NCC stores from 2016 to 2020. Graphical data from 2018 to 2019 displays the effect that the extensive malfunction of the AHU units in the HMS had on overall RH control in that period. Once the system had been reset, RH fluctuations were reduced and RH levels returned to the 2017 to 2018 range. There was an annual seasonal fluctuation in the RH range in A1 and A2 of ±20% RH to ±30% RH, with overall RH lower in A2 than in A1. In the L&A store, graphical data shows the effect of the industrial dehumidifiers, with the RH levels reduced gradually over three years from more than 70% RH to a band low enough to prevent further mould outbreaks.

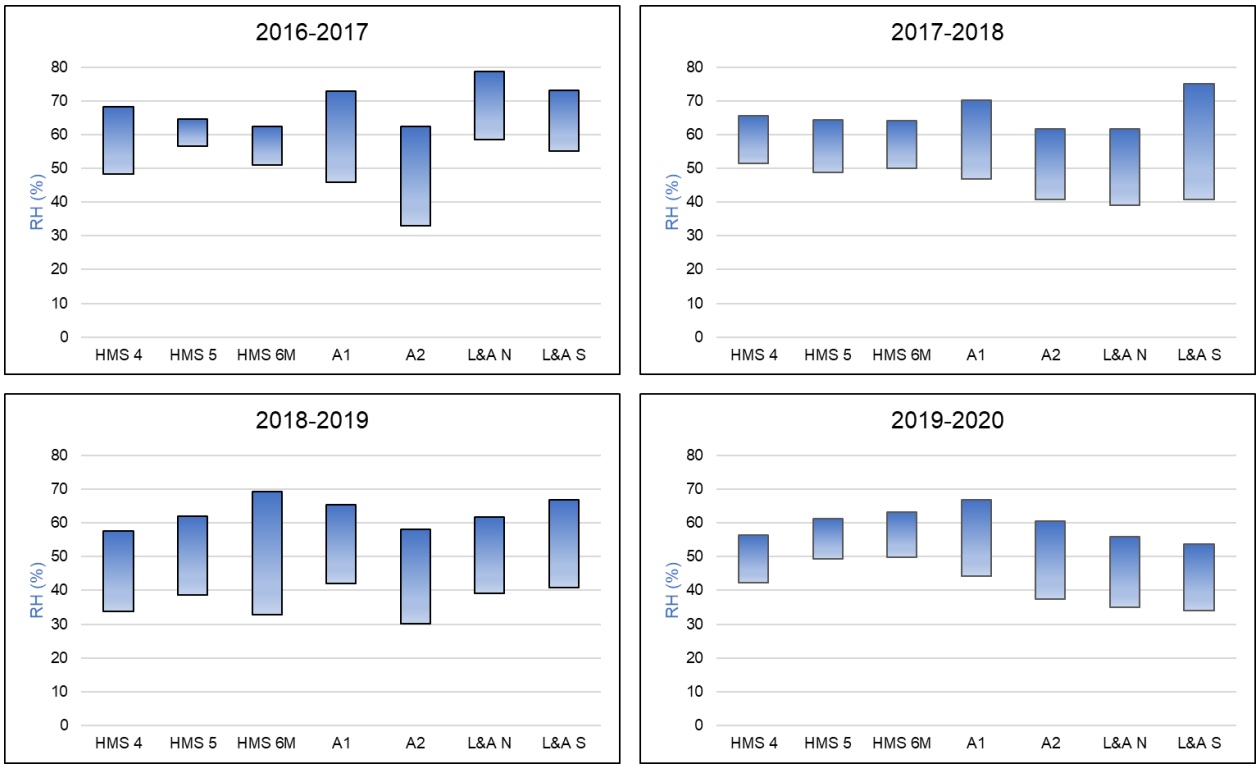

Figure 6.56 Comparison of RH regulation in three low energy stores by year, 2016 to 2020

During the second steady state, the RH in the L&A store was regulated by continuous operation of the biomass boiler and the HVAC unit, augmented by two industrial dehumidifiers. Annual wood pellet costs for the boiler rose around 19% from 2016 to 2020, from £185/tonne to £220/tonne. Total energy consumption remained around 209,270 kWh/yr. Dehumidifier equipment costs were £2400/yr for two years, from 2017 to 2019, with leased units being replaced with purchased units in the second year. In the A Store, regulation of RH was by continuous operation of the oil-fueled boilers and the AHUs with annual energy consumption remaining around 380,000 kWh/yr. A cyclical operation of the two AHUs along with one dehumidifier was used to maintain the RH level in the HMS. Electricity usage in the second steady state was 26,139 kWh/yr. This was still slightly higher than the

predicted annual electrical consumption of 24,320 kWh, which had been estimated on a seasonal operation of the M&E system, with heating and ventilation only during winter months. The seasonal mode was never established and the daily cycle of AHU operation continued through to the end of the research period. Total annual energy costs for each store from 2016 up to 2020 are presented in Table 6.2. Annual energy costs for the HMS and the A Store are similar to BEIS statistical data for electricity, gas and oil but are lower for the L&A store due to the lower costs for biomass fuel.

Table 6.2 Annual energy costs for NCC low energy stores, 2016-2020

Year	£ per kWh/yr	Total annual energy cost		
		HMS	A Store	L&A store
2016	0.0966	£2,525.03	£36,708.00	£11,002.43
2017	0.1024	£2,676.63	£38,912.00	£13,896.74
2018	0.1037	£2,710.61	£39,406.00	£14,186.60
2019	0.1134	£2,964.16	£43,092.00	£12,783.50

Based on energy costs per volume, the total annual energy costs for RH regulation in the usable storage space in the A Store had an increase of 45% over the energy costs for the HMS. In the L&A store, annual costs had an increase over the HMS costs from 29% in 2016 to 54% in 2017 and 57% in 2018 due to the dehumidifier equipment costs. After dehumidifier cost payback, the percentage increase dropped to 27% by January 2020 as non-domestic costs of energy dropped in the UK. Table 6.3 shows the annual energy costs for regulating RH per volume of usable storage space in the three low energy storage buildings on the NCC site.

Table 6.3 Annual energy costs per m^3 usable storage space, 2016-2020

Storage building	Energy costs per volume of usable storage space £/m^3			
	2016	2017	2018	2019
HMS	1.15	1.22	1.24	1.36
A Store	1.67	1.77	1.79	1.96
L&A store	1.49	1.88	1.92	1.73

The buffering capacity of the HLC ensured a more effective RH regulation in the HMS when compared to the two other low energy stores on the NCC site, as determined through analysis of the environmental monitoring data. There was a cost benefit to the use of HLC in regulating RH in the storage environment when compared to the operation of the A Store and the L&A store. Despite continuing to operate the AHU units in the HMS throughout the year, rather than utilising seasonal drift as part of a low energy RH regulation programme as originally intended, energy consumption per volume of usable storage space fell within design projections.

6.7 Assessment of the environmental monitoring system

The environmental monitoring system used for this research programme was the one already in use by SMG for monitoring RH and temperature in gallery and storage spaces. The research programme offered an opportunity to extend the

system with additional monitors for moisture content and air flow. The research programme also offered an opportunity to evaluate the Hanwell hardware and software for accuracy, flexibility and user-friendliness.

The Hanwell environmental monitoring system could be used with both telemetric units and data loggers. The system was capable of data analysis and reporting and could be used to map environmental parameters of RH, temperature, air flow and MC (%). Installation into the HMS extended a monitoring system already in use in both the SCM galleries and cultural heritage collections store in Kensington Olympia. The Hanwell ML4106 and ML4114 had LCD data displays for immediate reference. On-site calibration of the Hanwell units was carried out by conservation staff, using calibration salts, eliminating the costs of calibration services and allowing calibration to be carried out annually or as required. Data sheets for Hanwell monitoring equipment are found in Appendix E.

During the transient and first steady state of the HMS, telemetric data could only be accessed through the museum server. The RadioLog8 software displayed data in three formats: Tabular, Graphical and Plan. Tabular view provided the list of sensors with alarm traffic light status. Graphical view provided line or bar graphs with multiple sensor overlay options. Drag and view was available to obtain sensor reading dates and times but only data from the first sensor could be obtained on overlays. Data for other sensors could be viewed at the same time by exporting CSV data and converting to graphs using Excel spreadsheets. Views could be daily, weekly, monthly, three-monthly, six- monthly or yearly. Graphical views could be printed to PDF format but chart keys were difficult to see.

EMS provided all the same features as RadioLog8 but was a more robust and flexible platform, as it was not restricted to either cloud or server-based configuration. In addition to the original views, an Overview provided overall system status as well as the potential to customise the dashboard. It was easier to interrogate sensor data in Graphical view as a mouse pointer replaced drag and view. Viewing periods were the same as in RadioLog8. Sensor data was accurate to the second and to 0.1°C and 0.1% RH. All sensor data could be overlaid in Graphical view, enabling comparative analysis. Chart keys had a wider range of colours. Historic data from .rl8 software was not uploaded to EMS due to on-going issues with the archival link until late into the second phase of data assessment. Archived data was still available as .rl8 files. This resulted in different Graphical views being used when documenting the monitoring history.

6.8 Summary of the second steady state of the case study, 2016 -2020

During the second steady state of operation, from 2016 to 2020, an expanded monitoring strategy assessed the buffering capability of the case study. In the transient and first steady states, consistent RH monitoring data was acquired from only three ML4106 units, one placed in each of the BOX storerooms. Comparative RH/T data obtained from other storage facilities on site or externally was not assessed at length.

Objectives for Chapter 6 were to present the findings from the expanded monitoring strategy, supplying a more rigorous dataset for longer-term analysis. Comparative RH data from the other low energy storage buildings on the site were used to determine the effectiveness of HLC's buffering performance during dynamic operation. Long-term data on the effects of moisture content, air velocity and duration of activity on buffering capability were also obtained. External monitoring data revealed the extent to which internal environment in the HMS responded to positive and negative thermal gradients across the HLC walls, resulting in thermodiffusion as opposed to thermodynamic reactions of internal RH. RH and temperature data needed to be analysed in conjunction with external data in order to fully understand the implications of thermodiffusion on internal conditions. MC (%) sampling of the tested walls demonstrated moisture storage capacity and moisture movement under changes of internal RH (%). Linear regression modelling confirmed the relationship between MC (%) and RH (%). The heterogeneous porosity of the HLC matrix was revealed by the percentage of moisture storage at each sensor location.

The monitoring strategy and data acquisition were evaluated throughout operational variations and assessed for reliability and veracity. Additionally, the functional performance of the monitoring system was evaluated in order to confirm its selection as appropriate environmental monitoring hardware and software.

Assessment of the wider dataset showed that the buffering performance of the HLC contributed to a more stable and sustainable storage environment when compared with the two other low energy buildings on the NCC site. Both effectiveness of RH regulation and energy costs were compared through the second steady state. There was improved regulation of both RH range and daily fluctuations with a lower energy consumption in the HMS despite full-time cyclic operation of the AHU units.

Chapter 7 Discussion of research results

7.1 Introduction

The research hypothesis for this study was based on key performance criteria required to maintain suitable control of RH levels and fluctuations in museum storage buildings while reducing the operational energy costs of storage building operation. The research hypothesis that was formulated and tested was:

> *Does hemp lime concrete have the hygroscopic performance potential to augment the regulation of relative humidity within museum storage buildings in temperate climates?*

The qualitative approach to research analysed environmental monitoring data obtained during dynamic operation of SMG museum storage facilities on the NCC site, using the museum's environmental monitoring system. Longitudinal and in-depth studies on the effectiveness of the regulation of RH levels and fluctuations were carried out on the case study, the HMS, through transient, first and second steady states of operation. Analysis of comparative RH data from the two other low energy stores during the second steady state period supported the hypothesis that the hygroscopic performance of the HLC augmented the regulation of relative humidity within the HMS. Available numerical data on energy usage for the three low energy storage facilities were cross tabulated for costs against effectiveness of RH regulation. Data on moisture storage in the HLC walls, air velocity and duration of access to the storerooms of the case study were recorded and assessed for correlations to the RH data. Quantitative analysis on numerical data acquired on moisture content was carried out using linear regression modelling to correlate the MC (%) relationship to RH (%).

7.2 Statistical significance of data

Statistical significance is the likelihood that a relationship between two or more variables is caused by something other than chance. It is used to accept or reject a null hypothesis which postulates that there is no relationship between variables. A data set is statistically significant when it accurately represents the phenomenon being tested.

7.2.1 Results of monitoring data sets

In the first phase of data assessment, during the transient and first steady state period from 2012 to 2016, three Hanwell ML4106 transmitters units were used to obtain RH and temperature monitoring data from each BOX storeroom in the HMS, in order to test the research hypothesis. RH and temperature data obtained from Hanwell and Tinytag data loggers placed in both the BOX and RINA storerooms, in hangar D2 and externally as part of the SMG conservation environmental monitoring programme were compared to the data obtained from the HMS. CSV data from sensors were converted to Excel files in order to obtain comparative graphical views.

External data obtained from weather stations in the area were also assessed in order to augment the limited data set from the external Tinytag data logger.

In order to determine whether the data sets obtained during the transient, first and second steady state periods were statistically significant in the testing of the research hypothesis, the null hypothesis was formulated:

> *Hemp lime concrete construction does not augment the regulation of RH in museum storage buildings in temperate climates.*

Analysis of the data set concluded that the null hypothesis was unlikely, given the relationship observed between the RH and operational histories during the transient and first steady state. Monitoring data demonstrated that there were buffering effects on the RH fluctuations caused by variations in active operation of the air handling system, dehumidifiers and air conditioners when compared with periods of passive operation.

Monitoring data from the transient and first steady state demonstrated that measured RH varied from floor to floor in the HMS. Although the same AHU served both HMS 5 and 6, monitoring data showed that the RH was persistently higher in HMS 6 despite similar room temperatures. On the second floor, in HMS 4, the RH rose throughout the first steady state, from less than 60% RH in June 2013 to almost 70% RH by June 2016, a level higher than in either HMS 5 or 6. It seemed possible that, as measured RH variables had been limited to room median RH, levels of RH might also vary within a single room rather than being consistent throughout.

In the second steady state of building operation, the Hanwell telemetric monitoring system was extended. The RH data set was expanded to examine the extent of RH regulation at different levels within one room. Two Hanwell ML 4114 units were installed at floor and ceiling levels in HMS 6. The data revealed the degree of RH stratification within the three metre floor to ceiling range and the extent to which buffering of fluctuations induced by ventilation and heating was achieved in each stratum. Data from ML4016 units installed in the two other low energy storage building were compared with data from the HMS to test the extent of augmentation of RH regulation and reduction of energy consumption. Analysis of the data year on year confirmed the extent to which constructing a storage building with HLC rather than with conventional building materials augmented effectiveness and offset failures of regulation by mechanical plant while reducing the energy load in a temperate climate.

External RH data obtained using an ML4109 unit revealed the effect that thermal gradients had on the RH within the HMS. Both positive and negative thermal gradients caused by external temperatures either higher than internal temperatures or much lower than internal temperatures caused moisture gradients across the porous HLC, driving moisture content either towards or away from the wall/room interface. This resulted in the phenomenon known as thermodiffusion, with internal RH levels increasing with rising external temperature or decreasing with falling external temperature, instead of the thermodynamic reaction of RH rising with falling temperature or falling with rising temperature. Internal temperatures were shown to be less affected by thermal gradients than internal RH.

MC (%) monitoring data was obtained using the Hanwell Dampwatch unit in order to see if a dynamic relationship between MC (%) and RH (%) could be verified. Values obtained showed that porosity of the HLC wall matrix had more influence on moisture storage capacity at each location than RH stratification within the room as values were not consistent from floor to ceiling but varied from location to location in each wall. MC (%) values demonstrated the extent and effect of moisture transfer, confirming the thermodiffusion phenomenon caused by moisture gradients and the thermodynamic reactions caused by RH regulation by mechanical means. Both the RH and MC (%) analysis verified the observations of Padfield and Jensen (1990), Padfield (1996; 2008) and Tran Le et al. (2010) on thermodiffusion phenomenon effects on porous media during dynamic operations. Analysis of the data obtained under dynamic conditions confirmed the theoretical relationship of MC (%) with RH (%), that as RH (%) rises, MC (%) rises. Data also demonstrated the drying processes in internal and external walls and the complex porosity of the HLC matrix.

Air flow monitoring in HMS 6 verified the ventilation schedule of the air handling system and the effect of air velocity from the supply grilles on RH fluctuations at three levels.

Analysis of the expanded data sets in the second steady state confirmed that there were a sufficient number and range of sensors per test building to measure key variables in order to reject the null hypothesis. The data sets were deemed statistically significant.

7.2.2 Results from observation of cultural heritage collections

Observation of the cultural heritage collections stored in the HMS was used to determine if variables in operation had any deleterious effects. Periodic visual assessment of the stored objects revealed no changes to condition throughout either the first or second steady state of operation, with no occurrence or recurrence of visible physical, chemical or biological damage. Prior to storage in the HMS, deterioration of the carriage collection had occurred while in storage in unheated hangars, with RH levels that drifted seasonally from a low of 45% RH to a high of 100% RH but generally between 80% RH to 100% RH. There had been biological deterioration caused by mould growth on textiles, leather and wood and chemical deterioration through corrosion of iron and brass components. Surface varnishes and waxes had turned cloudy under exposure to prolonged periods of high RH. The carriages had undergone conservation treatments to remove dust, dirt, discoloured waxes, mould, moth infestation and corrosion products. Comparison of condition assessments made after conservation treatment and at the end of the research project found no changes in condition. There was no recurrence of metal corrosion, mould or moth infestation and no indication of further physical deterioration. There was minimal dust even on the uncovered carriages..

The large ship models, which had acclimatised to a stable low RH over decades, were at risk of physical deterioration by material response to fluctuating RH, with thin organic materials held under tension lifting, warping or splitting. Inspection found no changes in condition in those that were removed from shipping crates over the period of research. Fluctuations caused by excessive ventilation from August 2018 to January 2019 were insufficient to cause material damage as they were buffered

quickly enough to prevent material response. Conditions were significantly more stable in HMS 4 than in the areas previously used for the storage of framed art works and half-block ship models. Even during the period of excessive ventilation, daily fluctuation rates were buffered within ±10% RH. Upon examination, none of the framed art works or the half-block ship models showed any changes in condition from delivery into HMS 4 to the end of the research project.

Results of observation concluded that the provision of stable RH reduced the potential for deterioration through physical, chemical or biological degredation caused by too low or high RH levels. The buffering capability of HLC reduced the potential effect of RH fluctuations by limiting material response times.

7.3 Implications of the case study

Research implications infer the potential for impact that the findings of a study might have on future theory, policy and practice in the relevant field of interest. The rationale for this study was based on directives to provide long-term sustainable storage for cultural heritage collections, reducing energy use while still ensuring continuous stability of the preservation environment. The main aim of the research was to assess the potential of a selected hygroscopic building material to augment the regulation of RH. This was achieved through monitoring and observing a case study, the HMS, constructed by the SMG. As the HMS was intended to be a prototype for sustainable museum storage for the SMG, implications from the study have bearings on practical applications for future development of museum storage for the group.

The anticipated outcomes of the research were:

- To define the potential of the hygroscopic ability of HLC to moderate the RH fluctuations caused by mechanical environmental control of RH levels.

- To identify the extent to which HLC can control levels of RH within optimal museum storage ranges.

- To confirm that the hygroscopic performance of HLC can augment control of RH in order to support the design of low energy museum storage facilities.

- To quantify the dynamic relationship between RH (%) in the storage environment and MC (%) of the HLC matrix

The research found that the RH fluctuations caused by the air handling system were moderated by the hygroscopic ability of HLC. Fluctuations were generally kept below SMG guidelines of ±10%/24 hrs for sensitive and hygroscopic materials. Average fluctuations rarely exceeded ±3% except when the air handling system malfunctioned but fluctuations were still buffered within the allowable ±10% parameters. Issues arising from the choice of mechanical RH control system installed in the HMS clearly illustrated that heating and ventilation were the predominant source of RH fluctuations as activity was limited once collections had been stored.

The external influence of high or low temperatures on moisture movement did affect the range of RH in all stages of operation although effects were more significant during passive operation. In the first attempt at passive operation, RH levels throughout the building eventually rose over the top of the SMG guideline range. However, daily fluctuations were negligible under passive operation. In order to reduce RH gain, mechanical means were required as the original intent to use drier external air to lower the internal RH was never implemented. Low-level operation of a dehumidifier was continued on the ground floor as the overall RH remained slightly higher than on the other two floors. However, the hygroscopic performance of the HLC augmented control of RH to the extent that operation of the air handing system was required only part-time to maintain the RH within the optimal museum storage range. Comparison with the conditions achieved in the two other low energy stores on the NCC site showed that on an annual basis the regulation of RH was more effective in the HMS in meeting the specifications of the museum.

Based on the energy costs per volume of usable storage space in the SMG low energy storage buildings, the annual cost of RH regulation in the HMS were calculated to be 45% less than the annual cost for the A Store. Cost differences varied for the L&A store due to the leasing and purchasing of industrial dehumidifiers and the costs for biomass fuel. Energy costs for the HMS compared to the L&A store were calculated to be 30% lower in 2016, 50% lower in 2017 and 2018 and 22% lower in 2019 and 2020. Energy usage in the HMS was not as low as in some low energy stores identified through the literature review but overall performance in regulating RH within the current specifications of 40% RH to 60% RH was equal to or better than all other stores cited.

Lower energy costs could have resulted if the mechanical RH control system had utilised dehumidification instead of heating and ventilation to reduce RH gain. The thermodiffusion phenomenon, identified through the comparative analysis of external and internal RH and temperature data, caused seasonal RH gain in the HMS. In order to reduce RH during summer months, it was necessary to heat the storerooms to a temperature above the external temperature. This resulted in energy expenditure in a period when it would normally not be required. As there was no programme to use natural ventilation to remove desorbed moisture whenever the external RH was lower than internal RH, moisture was absorbed back into the HLC walls once internal temperatures were higher than external temperatures. Only in HMS 6 was there some gradual moisture removal through the continuous use of one portable dehumidifier. The modelling undertaken during the design of the mechanical system had resulted in the programme of heating and ventilation during winter months without taking into account the thermodiffusion phenomenon, despite research as identified in the literature reviews to suggest that there would be increases in internal RH in an airtight storage building with positive thermal gradients causing moisture movement from warmer to colder sides of porous hygroscopic walls. Monitoring data from the passive period of operation from February to June 2019 also showed that it was unnecessary to heat in the winter months as the temperature in the HMS remained around 10°C with the RH stabilising between 50% (HMS 4) and 58% (HMS 6). The RH only rose once the external temperatures rose in April to 20°C. Assessment of the monitoring data supplemented the conclusions made by Ryhl-Svendsen et al. (2010) that dehumidification in hygrothermally buffered airtight stores could maintain a stable RH at temperatures between 10°C to

15°C. Assessment also verfied the conclusions of Ryhl-Svendsen et al. (2010) and Barclay et al. (2014) that a material's moisture buffering ability to mitigate peaks of high RH, allowing more stable internal conditions and reducing risk of mould, decreases the need for humidification or dehumidification with consequent improved energy performance.

The theoretical relationship between RH (%) and MC (%) was quantified through analysis of the data acquired under dynamic conditions, correlating the increase in MC (%) with the increase with RH (%) and demonstrating when MC (%) of the HLC had reached equilibrium with room RH due to drying mechanisms. The patterns of moisture storage capacity and moisture movement confirmed the heterogeneous nature and interconnected porosity of the HLC matrix. Moisture movement patterns also confirmed the effects of thermodiffusion and thermodynamic reactions when correlated with external RH data and air handling operational history.

Results of the research study show that, by using HLC in the construction of the HMS, the SMG specifications for a sustainable, low energy storage building with a stable environment suitable for the storage of moisture-sensitive materials was met. Implications from the study suggest that control of RH to museum guidelines cannot be achieved using hygroscopic construction materials alone when building in a temperate climate but that construction materials with an Excellent MBV, such as HLC, will significantly augment the regulation of RH to provide a sustainable low energy control programme, as suggested by Padfield (2008). Extremely good airtightness, a benefit of HLC's homogeneous monolithic construction method, and reduction in ventilation with external air also contribute to the regulation of RH. The buffering capability of HLC can be compromised by the failure of any mechanical plant installed as part of a total environmental control system. However, the research study shows that the buffering capability of HLC ensures that, during periods of mechanical plant malfunction or failure, environmental conditions can be held within the museum's specifications of 40% RH to 60% RH for at least the minimum of 48 hours as stipulated in *BS EN 16893:2018 – Conservation of cultural heritage – specifications for location, construction and modification of buildings or rooms intended for the storage or use of heritage collections.* Identification of the influence of thermodifussion phenomenon verifies the assumption that dehumidification is a more effective mechanical control mechanism than heating and ventilation for an airtight storage building with porous hygroscopic walls.

7.4 Practical considerations

The data from this study reveal practical considerations which must be examined in respect of the storage requirements of the SMG.

While building a storage facility within an existing building such as a hangar seems to be a sensible approach, as it reduces the costs and time of construction by utilising the structure as an external envelope, it limits the size of the facility. Compromises have to be made on orientation, height of building and internal spaces, and access routes. The external building must be in good condition or it will decrease the estimated life span of the storage building. This restricts the choice of existing building as necessary repairs and renovations can increase costs beyond

those incurred by new builds. Unheated buildings in temperate climates will have cold and damp environments similar to external conditions during winter months. Building within a building does offer the opportunity to upgrade storage conditions for smaller distinct cultural heritage collections which might otherwise deteriorate under uncontrolled RH levels and fluctuations. The use of HLC for the construction of storage units within existing unheated buildings could improve conditions for other distinct collections which presently are stored under unsuitable ranges and fluctuations of RH and are at risk of deterioration. Prefabricated HLC panels installed on a steel or timber framework could be used to build units that would provide stable RH. A single dehumidifier would provide sufficient control of RH for at least 200 m^2 of storage to museum RH guidelines, as demonstrated by monitoring data from HMS 6.

The 195 mm thickness of the HLC in the wall panels used for the HMS may have been equal to the true moisture penetration depth of the material. Values for moisture penetration depth have ranged from 58 mm to 120 mm (Collet & Pretot, 2012; Latif et al., 2015), obtained from testing samples under laboratory conditions. Data from the MC (%) monitoring showed that the moisture penetration depth was up to 50 mm as moisture movement to and from the wall/room interface was observed using sensors inserted to a depth of 50 mm. The MC (%) of the tested exterior walls in HMS 5 and HMS 6 was always higher than in the interior walls with percentage values remaining static through the testing period. This was thought to be due to an increased rate of drying in the interior wall than in the exterior wall. However, moisture from the usually higher RH in hangar D2 may have penetrated through the 80 mm outer layer of wood fibre insulation board and into the HLC matrix. The moisture penetration depth of wood fibre board insulation has been calculated by Kaczorek (2019) to be 109.4 mm so moisture could have moved through the wood fibre board into the HLC walls. Moisture could penetrate through the HLC matrix from the warmer to the colder side when moisture transfer through the interconnected porosity was prompted by the thermodiffusion phenomenon caused by a moisture gradient during a positive thermal gradient across the HLC walls.

A high MC (%) would contribute to thermal stability within an HLC unit, with the phase change between the liquid and vapour storing or releasing energy (Bevan & Woolley, 2008), slowing down the flow of heat from warmer interior to colder exterior environments. While MC (%) values obtained during the research study were Wood Moisture Equivalent measurements and not exact measurements of the moisture content in the HLC walls, they were at the higher end of what is considered the wood air-dry (safe) condition. Assessment of the thermal performance of the store under dynamic conditions showed that internal RH was affected by positive thermal gradients across the walls even during heating operation. This resulted in the thermodiffusion phenomenon of rising internal RH with rising internal temperature with the expected thermodynamic reaction being superseded. Negative thermal gradients had less effect on internal temperatures during heating operation even during the very cold period in March 2018 as internal temperatures in the storerooms remained steady. During passive operation, internal temperatures followed seasonal drift without responding to sudden changes in external temperatures. During the longest period of passive operation, from May 2016 to May 2017, internal temperatures stabilised between 10°C to 12°C on all three floors through the winter months despite external temperatures dropping as low as -4°C. The MC (%) in the

HLC matrix slowed the flow of heat from the warmer interior to the colder exterior environment as predicted by Bevan and Woolley. As long as dehumidification was provided to counteract the rise in RH caused by thermal gradients, heating would be unnecessary in HLC storage units.

As the MBV of HLC can be affected by surface linings or coatings (Latif et al., 2015), it might be beneficial to reconsider the need for and type of internal linings and coatings. Internally, the HLC walls in the HMS were faced with a medium density magnesium silicate board (Multi-Pro) with a stated μ-value of 8.4 (Resistant Building Products, 2017), similar to that of gypsum. From the literature review, HLC has a tested μ-value ranging from 1.8 to 8.98. The vapour permeability of both materials might have been similar enough that there was no effect on the capability of the HLC to buffer internal RH but it is possible that the Multi-Pro board reduced the MBV to some extent. Testing to determine whether the facing boards affected the potential capability was not possible as the boards were part of the panel construction and could not be removed. The facing boards were considered essential to eliminate potential dusting from the HLC matrix. The assumption that there would be dust from the HLC walls was based on the behaviour of conventional construction materials such as concrete and gypsum board, rather than on research into the characteristics of HLC. It would be valuable to determine whether on-going dusting from HLC is an issue, since the carbonation process should encapsulate and mineralize the hemp shiv. The airtight monolithic walls should actually exclude dust and pollutants. Practically, a surface lining or coating is desirable as exposed HLC walls are neither puncture-resistant nor smooth, due to the porous structure. Using a biobased coating such as a clay-based paint, which has a very similar MBV, would minimise any reduction in the HLC MBV and also contribute to the sustainability of construction while providing a level of protection. Wall protection within museum storage facilities need only be minimal compared to that in commercial storage units since movement of cultural heritage collections is infrequent and carried out with care at all times.

HLC storage units could potentially act as passive regulators of the RH in unheated hangars. However, cladding the external walls with wood fibre insulation board as in the HMS might reduce the extent of buffering. Roels & Janssen (2006), Latif et al. (2015) and Kaczorek (2019) have demonstrated that using a material less thick than its penetration depth in a wall assembly can compromise the overall MBV. By making the HLC walls thicker, closer to 300 mm to 500 mm as recommended by the industry for free-standing buildings (www.ukhempcrete,com; hemptechglobal.com; www.stastier.co.uk) rather than the 195 mm as used in the prefabricated HLC panels of the HMS, a degree of RH regulation in the hangar environment could be provided in addition to the buffering of the internal environment. As wall protection needs only to be minimal in museum storage, with logistical procedures different from commercial storage activities, possibly only the areas at greater risk of damage, such as corners and door openings, would need cladding. Although Bevan and Woolley (Bevan & Woolley, 2008) have stated that HLC is inedible and not attractive to rats, rat-proof mesh was installed over the exterior of the HMS. As the mesh in no way compromised the buffering capacity of the HLC, this could serve as wall protection as well.

The design of the HMS eliminated internal loading bays with air locks in order to achieve more storage space within the available footprint. Monitoring data compared

with access activity showed that access into a storeroom through the personnel door had limited effect on the RH levels and fluctuations. Opening a storeroom's overhead door did result in changes to RH levels. The resultant rise or drop in RH was buffered with previous ranges recovered without the need for mechanical intervention. However, if the overhead door of hangar D2 was opened at the same time, buffering of the HMS RH took up to three times longer. Optimally, the standard procedure for accessing an HLC unit of similar design should require the external hangar door to be closed before opening any large access door into the unit. Ideally, this operating procedure would be observed by all SMG staff and contractors by co-ordinating activities in order to reduce RH recovery periods.

The potential failure of mechanical control systems that are relied upon to regulate storage environment is a concern to museum professionals (BSI, 2018b) and has led to the recommendation that the building envelope should be capable of maintaining specified conditions for a minimum of 48 hours in the event of equipment failure. The research case study has show that the building envelope, incorporating the insulative and hygroscopic properties of HLC, augmented the regulation of RH when the mechanical control system was turned off. RH fluctuations were reduced to a minimum, less than ±1% RH over 24 hours, and RH ranges followed seasonal drift as driven by thermal gradients across the porous HLC walls. However, the malfunction of a heating and ventilation system can have effects on internal RH levels and fluctuations that HLC buffering capability cannot fully mitigate. Damper issues and periodic loss of AHU control by the BMS resulted in daily fluctuations between ±5% RH and ±10% RH depending on the amount of external air introduced through the air handling system. Recovery of RH levels occurred when ventilation ceased. While the extent of RH fluctuations during the period from August 2018 to January 2019 pushed the RH level outside the specified range of 40% RH to 60% RH, the buffering capacity of the HLC enabled the RH range to recover as soon as the mechanical system was turned off.

Because of the phenomenon of thermodiffusion, which has an evident effect on the RH range within a building constructed of very porous hygroscopic material, some form of mechanical climate control is indicated. A practical modification of the mechanical system used in the HMS would be to replace heating with dehumidification. While the original plan for a passive approach, using drier external air to lower internal RH, was commendable, in practice it was never achieved as the BMS lacked a programme to identify acceptable external conditions. In addition, a temperate climate such as Wiltshire has an average annual RH of 82% (weather-and-climate.com). It would be more reliable to install a dehumidification system with humidistat. As the need for ventilation is diminished in storage areas, a low air filtration rate such as the recommended rate of 0.5 m^3/(h.m2) @ 50 Pa (BSI, 2019b) rather than the 1.0 m^3/(h.m2) @ 50 Pa achieved for the HMS would reduce both RH fluctuations and the energy use. Requirement for fresh air intake is minimum as activity within storage areas is limited but circulation of filtered recycled air is necessary to reduce potential for condensation or the build-up of pollutants emanating from the stored collections.

Prior to the construction of the HMS in hangar D2, the SMG had used the building within a building approach to provide low energy environmentally-controlled storage for the reserve library and archive collections. The research study showed that the

HLC construction of HMS augmented regulation of RH better than the conventional construction materials used in the L&A. Buffering of both hangar and external conditions was more effective with less reliance on mechanical means of RH control. As the current storage plan includes retaining hangar D2 for the L&A reserve collections, consideration could be made to add modules to the HMS, moving the L&A collections into the more sustainable and stable conditions, or to replace the current L&A store with a two or three storey HLC repository.

7.4.1 Cost considerations

If the SMG were to consider constructing more HLC storage units within the hangars on the NCC site as a practical solution for current collections storage needs, cost implications for repairs to the hangars would have to be taken into account. As all hangars are considered to be at end of life, having been built for short-term use in the 1940s and having had little maintenance since the 1990s, significant refurbishment is required to extend their use. Cost estimates received in 2017 for hangar upgrades, including recovering roofs and gullies, replacing hangar doors and insulation, repairing spalling concrete and upgrading water and drainage systems, were between £1m to £2m per hangar, depending on type of construction and condition (Pegasus Group, 2017). Other costs might include the replacement of the concrete slab since structural load testing has found, as in the case of the HMS, that the load bearing of original concrete floors is inadequate for full-height structures or for warehouse racking of archival materials. Based on the UK National Statistics Building Cost Index (BCI) increases in construction costs year on year (Office for National Statistics, 2020), current (2020) costs for the HMS groundwork, foundations and slab would cost in the region of £230/m^2. Building services upgrades to hangar D2 were required for the HMS in 2012 in addition to those undertaken for the construction of the L&A store in 2006 in order to install the M&E plant. These included electrical infrastructure, fire and security alarms and ICT cabling and switching. Costs in 2006 were £88,593 (2020 = £108,083) with additional costs of £25,000 in 2012 (2020 = £28,875) for a total cost of £30/m^2 (2020 = £36/m^2). Estimated 2020 upgrade costs for hangar D4, considered to be the hangar in best condition on site, would be in the region of £1.92m (Table 7.1) based on previous costs for enabling works for the HMS and current costs for hangar repair.

Table 7.1 Estimated 2020 upgrade costs for hangar D4

Nature of works		**Cost £**
Hangar refurbishment	roof & drainage	1,158,300
	hangar doors	326,430
	concrete	231,660
Groundworks- 307m^2 footprint		70,610
Services upgrade		136,958
Total		1,923,958

Total construction costs of the HMS including enabling groundwork and services costs, professional fees and contingencies were £1,153/m^2 in 2012. Breakdown of the costs has been detailed in Chapter 4. Using the BCI of a 15.5% increase in construction costs to 2020, updated costs to replicate the construction of the HMS

would be between in the region of £1,332/m^2 or £1.3m. Adding the major hangar refurbishment costs to the enabling costs would revise the total cost to £3.14m or £3,200/m^2. As can be seen in Figure 7.1, the projected enabling costs required to construct another HLC unit within one of the hangars on the SMG site could require more than 60% of total project costs.

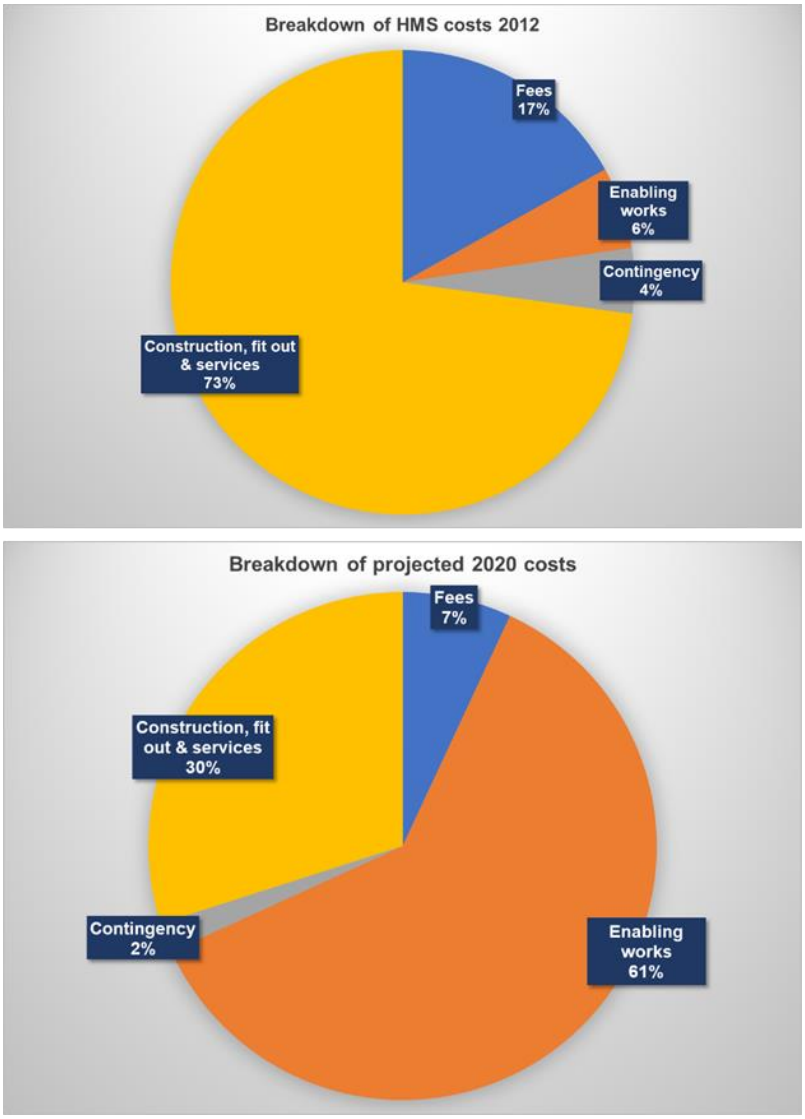

Figure 7.1 Breakdown of costs to construct HLC unit within hangar, 2012 project & 2020 projection

Benchmark construction costs typically add 10% to 20% of the building costs for a free-standing building for external works such as site preparation, external drainage and external services, 5% to 15% for professional fees and 10% to 15% for contingencies in order to establish a total project budget (https://costmodelling.com/building-costs). A free-standing building would require weather protection, unlike the HMS which was protected from the elements by the hangar building envelope. While the Hembuild panels used for the construction of the HMS could be supplied as a whole envelope solution including external render, the production company is dissolved. Current suppliers recommend outer finishes such as plaster, brick facing or cladding. Rainscreen cladding, a two layer system

with a durable outer layer such as steel and a ventilated cavity that allows vapour movement, commonly adds 40% to 45% to the construction costs for materials, delivery and assembly (https://www.approvedindex.co.uk/steel-buildings/steel-building-prices). In the 2012 project, professional fees were 17%, contingencies were 4% and enabling works 6% of the construction costs. A revised cost modelling for a free-standing HLC building, adding 40% to 45% for cladding and using benchmarks of 15% professional fees, 10% contingency and 20% enabling works (Figure 7.2) would result in a cost of £1,948/m^2 to £2,018/m^2, for an overall cost of £1.9m to £1.97m for a 980 m^2 building. Projected construction costs for building a free-standing building instead of constructing a unit inside a refurbished and retrofitted hangar would be 36% to 40% less expensive. Not factored in is a redesign of the building which could not be replicated as a free-standing storage building without putting the collections at risk whenever a door was opened.

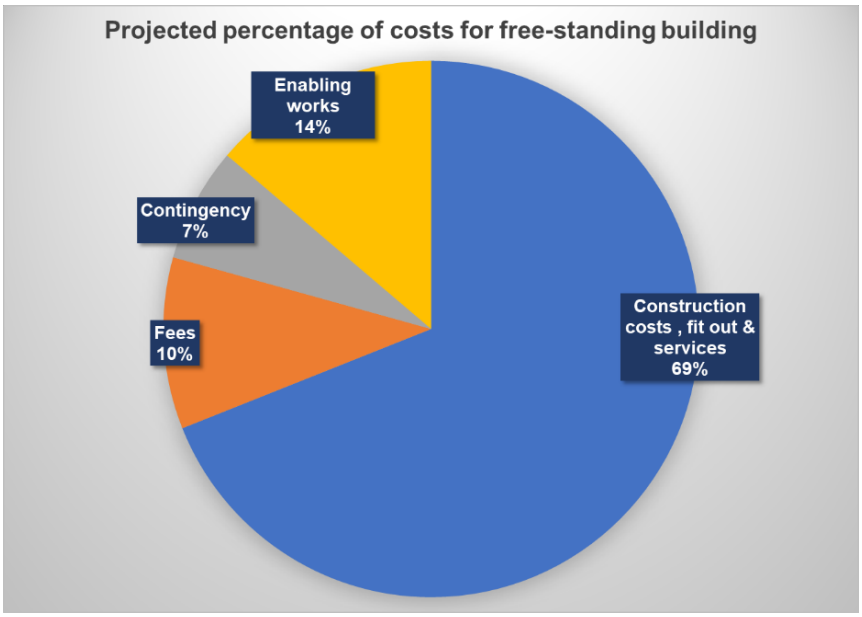

Figure 7.2 Breakdown of costs for projected free-standing storage building

Overall projected construction costs are similar to benchmarks for the construction of light industrial/office building (Turner & Townsend, 2019): shell and core with heating and ventilation (£1,986/m^2 to 2,218/m^2) and less than for light industrial/office: shell, core, heating, ventilation and air conditioning (£2934/m^2 to £3,436/m^2) but would deliver a building on the NCC site suitable for the storage of cultural heritage collections due to the augmented RH regulation by the hygroscopic performance of HLC.

The issues with the design and operation of the mechanical plant installed in the HMS revealed by this research study would need to be addressed. The research case study has demonstrated that some form of mechanical RH regulation is required in order to counteract the effects of thermodiffusion from positive moisture gradients across the HLC walls caused by thermal gradients between external and internal temperatures. The plant as finally installed in the HMS relied on heating and ventilation to reduce RH gain rather than on dehumidification. While heating cycles reduced RH levels that resulted from positive thermal gradients, internal temperatures would have to be continuously higher than external temperatures.

During periods in summer months, this meant that the heating system had to be operated at temperatures above 24°C. Under SMG environmental guidelines this temperature is acceptable for 5% of the year but in 2019 this temperature was exceeded for almost 10%, for five weeks through July to September. Increased temperatures due to global warming will mean that periods of higher external temperature are likely to be longer. While raising internal temperatures above external temperatures allows the thermodynamic relationship between RH and temperature to be re-established, heating during summer months is not a sustainable solution.

Fluctuations in RH caused during the operational cycles of the air handling system were attributable to both thermodynamic reactions and velocity of air flow. Design of the system allowed for five to seven air changes per hour, instead of the currently recommended upper limit of 0.5 air changes per hour (BSI, 2018b) so fan operation during operational cycles caused fluctuating air movement. While fluctuating air movement can contribute to cooling, the short cycles of the air handling system had no effect on internal temperatures but did affect internal RH. Reducing the fan speed to decrease the air changes per hour to 0.5 would reduce the extent of RH fluctuations. Lowering the fan speed would also lower energy consumption.

While operational costs and energy expenditure of an HCL storage building could be reduced by replacing electricity with a renewable fuel source for a heating and ventilation system, data from the research case study has corroborated findings from the literature review that dehumidification is more effective than heating and ventilation for regulating RH in museum storage. Dehumidification could be carried out using an MVHR system with partial recirculation with heating and two-stage heat recovery and dehumidification provided by outside air and heat pump cross-flow heat exchanger. Costs obtained from supplier websites indicate in the region of £8,000 to £12,000 for smaller commercial buildings. If the new HLC building replicated the HMS volume of storage space, a maximum ventilation rate of 1186 m^3/hr would be required to obtain with a maximum air volume of 3500 m^3/hr would be sufficient as the unit should run at less than 70% of total output for maximum efficiency. Maximum total power consumption is in the region of 4.6 kWh/hr (https://www.danthermgroup.co.uk/product/dantherm-danx-1-2-3-xd) which would bring annual operational costs to £1,066 if the system was run with the same frequency as the system in the HMS. However, operational costs could be further reduced by installing a humidistat so that the system would run only when required, as in periods when the phenomenon of thermodiffusion causes internal rise in RH levels.For the remainder of the time, the RH would be regulated by the buffering capability of the HLC.

Storage requirements of the SMG are under review in order to determine how much environmentally-conditioned space is required to ensure all cultural heritage collections are cared for and preserved as set out in the National Heritage Act, 1983 (UK Public Generals Acts: Science Museum). Building individual HLC units such as the HMS within end-of-life structures would likely not provide sufficient space for all current and/or future needs but would provide stable RH regulation for the storage of distinct at-risk collections at a cost similar to heated and ventilated light industrial structures. Refurbishing and retrofitting hangars to enable construction of HLC units would give the buildings a new lease of life, contributing to the sustainable directives

of the SMG, but would come at a cost. It would be more cost-effective to build a larger free-standing storage building. As the SMG owns the 545 acre NCC site, there are no land purchase costs and there are many potential building locations with road and services access.

7.4.2 Replication of HLC manufacture

The company that produced the prefabricated HLC panels to SMG requirements is no longer in business in the UK. There is off-site production of panels for the housing markets (Greencore Construction Group) but there is very limited availability of prefabricated panels for large-scale commercial building application. One panel currently being developed through the Biond project (previously the HEMPSEC Project), is aimed at developing a prefabricated closed panel system in order to expand the market for a pre-fabricated, pre-dried, panelised system of HLC construction, again for housing. The project has developed, tested and produced an accredited panel system for franchisement within the UK and the EU (Biond, 2019). The product was tested at the University of Bath's Building Research Park, based on the NCC site, during a 24-month testing phase (Latif et al., 2018). Because the panels are manufactured in a factory under franchise, it might not be possible to alter the specifications to replicate the HMS model. However, the company literature claims a flexible approach to design and construction to allow a bespoke custom build.

The Biond (originally Hempcell) panel is a timber-framed composite panel with an HLC and wood fibre core that attempts to use the excellent hygric mass of HLC and good hygric mass of wood fibre to improve the hygrothermal performance of the building envelope. The Biond panel (Figure 7.3) differs from the Lime Technology Hembuild® HLC panels used in the construction of the HMS in that it is a complete system and does not require an external facing board.

The Biond panel has a rainscreen and open cavity on its outer face which would not be required if HLC units were constructed inside hangars on the NCC site. The plasterboard inner lining might hamper buffering capability of the HLC/ wood fibre core. Latif et al. acknowledged that, while the Biond panel demonstrated the least degree of RH fluctuation within the panel when compared to Mineral Wool and Wood Fibre panels, the role of plasterboard in controlling moisture flow might affect the operational hygrothermal performance. The Biond panel as supplied, which presently seems to be the only prefabricated HLC available in the UK, might not replicate the manufacture of the HMS within existing buildings. However, there are characteristics that complement conclusions drawn from this research study, including essential wall thickness (Biond 300 mm, HMS 285 mm), the advantages of wood fibre, and the exclusion of vapour barriers. These suggest that, if the linings, particularly the plasterboard, could be removed or altered, the panels could be used to construct an HLC unit capable of similar regulation of RH.

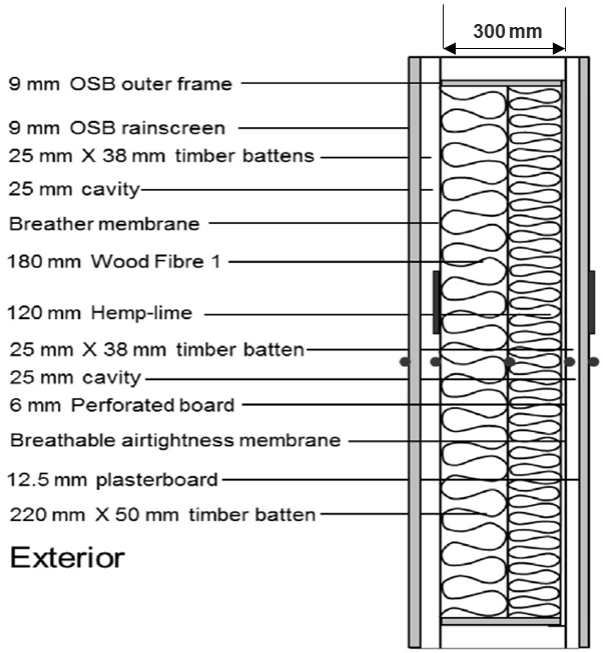

Figure 7.3 Schematic of Biond panel (Latif et al., 2018)

In the UK and the EU, there are a number of companies which supply hemp and lime components for on-site manufacture or who produce HLC blocks. It would be possible to replicate the HLC panels on site, either through spraying or casting into shutters, although the overall construction period would be longer than that required for the erection of the HMS. Drying time would likely be more than 28 days as conditions on the NCC site are generally between 80% RH to 90% RH, even in summer months. Replication of the HMS model within a hangar would entail installing the panels on a steel framework, applying a breathable airtight membrane and wood fibre board on the exterior and a hygroscopic lining or coating on the interior. A free-standing building would require external cladding to prevent damage from driving wind and rain.

Pre-dried modular HLC blocks could be used. A five-storey, 10,000 m^2 free-standing warehouse using interlocking modular HLC blocks was constructed in Kelowna, British Columbia in 2019 (Radford, (pers. comm.), 18.04.2019). The design used Super Structural R-Value (SSR) “Just Biofiber” HLC construction blocks (JustBioFiber, 2019) with an internal structural frame. The blocks are 542 mm long x 272mm wide by 203 mm high so would create a wall depth similar to that of the HMS without the addition of external cladding. There are several other HLC block systems available but all require a supporting structure. All HLC blocks are stated to deliver similar hygrothermal performance to the panels used in the construction of the HMS. External cladding and internal finishes can be applied after construction of the blockwork.

Current prices (2019) for HLC pre-dried block, 500 mm by 200 mm by 300 mm thick, density of 330 kg/m^3, is £99/m^2 and for 400 mm thick is £132/m^2 (ukhempcrete.com amongst other suppliers). In the 2012 project, 742 m^2 of HCL was used for the pre-cast panels, at a cost of £159/m^2, accounting for 11.5% of the budget. Panels included timber framing, magnesium silicate board interior facing and vapour

permeable airtightness membrane. At current prices, 742 m^2 pre-dried HLC blocks would cost would be between £73,457 and £97,944, or between 4% to 5% of the total projected construction cost for a free-standing building. HLC block requires external and internal finishes which would increase the cost per m^2 depending on choice.

7.5 Environmental impact

Through the SMG Sustainable Development policy, the Science Museum has been committed to reducing energy consumption. An integral part of the success of the policy is sustainability of the built environment. The HMS was designed in response to a mandate from the SMG to find a sustainable solution for the storage of hygroscopically-sensitive cultural heritage collections, both archival and three-dimensional. It was intended to be a blueprint for future storage structures by championing the use of biobased hygroscopic building materials in order to augment the regulation of RH through the buffering of humidity changes, reducing the need for mechanical plant. The choice of HLC as the infill material for the building envelope resulted in a reduction of the operational environmental impact of the building by removing the need for energy intensive air conditioning for humidity control. Further decreases in energy consumption could be achieved by following the original intent of operation by running the air handling system only during periods when seasonal changes affected internal conditions. The decrease in air change rates and fan operation would also contribute to the overall stability of the storage environment.

Environmental impact was also reduced during the construction of the HMS as the choice of HLC contributed to lowering overall energy cost and carbon footprint. Buildings and construction together account for more than 35% of global energy use and almost 40% of global energy-related CO_2 emissions (UN Environment & International Energy Agency, 2017). While progress has been made implementing energy-efficiency, the increasing global growth of the construction sector has resulted in rising energy demands and a year on year growth of CO_2 emissions. In 2018, global energy demand rose by 2.3%, the fastest pace in a decade. Despite major growth in renewable energy sources, CO_2 emissions were up 1.7% (IEA, 2019). In order to reduce global energy consumption, government policy change and legislation has focused on the use of energy in the construction industry. Building energy codes and standards for minimum requirements for operational energy sufficiency and renewable energy sources are now mandatory or voluntary in over 60 countries. In order to reduce energy intensity, the measure of the energy inefficiency of an economy, focus needs to be not only on reducing operational energy use but also on reducing the embodied energy of construction materials.

Embodied energy (EE) is the total energy consumed either directly or indirectly with all the processes associated to produce any goods or service. The embodied impact of a building takes into consideration all the energy use during its life-cycle excluding the operational energy requirements. It can be defined by the cradle-to-grave approach (McAlinden, 2015), which includes a number of stages:

- Initial EE- the energy used for abstraction, processing and manufacture of materials, transport and assembly on site.

- Recurring EE- the energy used for refurbishment and maintenance over lifetime

- Demolition EE- the energy used for demolishment and disposal of all building components

Commonly recommended steps to reduce EE include specification of alternative low energy biobased materials in place of conventional materials, reduction and optimisation of materials and minimisation of waste. Design should take into account minimal material quantities, deconstruction and reuse, future use, adaptability and flexibility to increase material and building life spans.

Industrial hemp is a renewable material as its rate of consumption is lower than its renewal rate due to a growing season of only four months. Drying and chopping the stalk into shiv for use as aggregate in agro-concrete makes the amounts of water and fertiliser required for fibre and seed production more defensible as the entire plant is used. Hemp absorbs atmospheric CO_2 during photosynthesis in the growing phase and sequesters it for the material's lfetime. The cultivation EE of hemp is low, estimated at 0.0014 MJ/kg (Pervais & Sain, 2003).

The production of lime binder has a higher environmental impact as it is a mined finite resource, a heavy material and is processed away from mining operations using fossil fuels. While the production of lime cause CO_2 emissions through the calcination of the mineral, it requires less energy to produce than cement as the raw material is burned at a lower temperature. The CO_2 created through calcination is reabsorbed by the lime as it hardens through recarbonation but not the CO_2 from the burning of fuel. The EE of lime is estimated in the range of 4.0 MJ/kg to 9.0 MJ/kg (Rhydwen, 2006).The use of 20% to 30% pozzolans, low energy recycled materials such as fly ash and granulated blast furnace slag, in the binder in order to improve hydration can decrease production EE by 6% to 12% (Kupwade-Patil et al., 2018).

Overall, the manufacture of HLC has a significantly lower initial EE to mineral-based construction materials due to reduced energy requirements during its production. Busbridge and Rhydwen (2010) reported an EE value of 3.5 MJ/kg for a density of 330 kg/m^3. A value of 5.3 MJ/kg for lime was given by Hammond and Jones in *ICE V3.0* (2019), and quoted as the value for HLC by Florentin et al. (2017) and will be used in this study, as a 3.5 MJ/kg value would be under the lowest estimated EE for lime production. Walker and Pavia (2014b) noted production of 1 m^2 by 260 mm thick HLC with a density of 380 kg/m^3 required 370 MJ to 394 MJ of energy compared to 560 MJ for an equivalent cellular concrete wall. Based on the foregoing, each one metre by one metre by 195 mm panel of HLC produced for the HMS would have required between 169 MJ to 295.5 MJ of energy, a reduction in EE between 251 MJ and 124.5 MJ compared to an equivalent cellular concrete wall. The density of the HLC used in the HMS construction was estimated at 330 kg/m^3 by the supplier and thus close to the density used by Walker and Pavia.

Steel, concrete, timber, inorganic minerals and fibreglass were also used in the construction of the building envelope of the HMS. Concrete has a low EE but is generally used in large quantities. Steel is considered to have a high EE as it is highly processed. The use of concrete and steel was minimised in the design of the

HMS. Concrete was only required to replace the floor slab and for foundations. Cross-laminated timber could have been used for the structural framework as CLT beams are comparable to steel in strength and have excellent dimensional stability, which would have reduced the EE of the framework. However, the steel beams allowed greater span lengths with fewer uprights, giving more useable storage space within the storerooms. CLT was used for the internal floors. Wood fibre insulation board used as cladding has an EE close to that of steel despite being made from mostly waste material as the production process has a high energy use (Bianco et al., 2016). The initial EE of the Mulit-Pro XS board is quoted by the supplier to be low as the boards are cured using a cold process but the embedded glass fibre mesh has an embodied energy of 13 MJ/kg to 32 MJ/kg (Composites UK, 2019). Table 7.2 lists the initial EE for the materials used to construct the building envelope of the HMS. Figure 7.4 is a comparative graph of initial EE, showing that, after concrete, HLC has the next lowest initial EE, due mostly to the EE of lime production.

Table 7.2 Initial EE values for HMS construction materials (from Busbridge & Rhydwen, 2010; Hammond & Jones, 2011)

Material	MJ/kg
HLC	5.3
CLT	12
Concrete (GEN 3)	0.81
Steel (general)	20.1
Magnesium silicate board	30
Wood fibre board	16

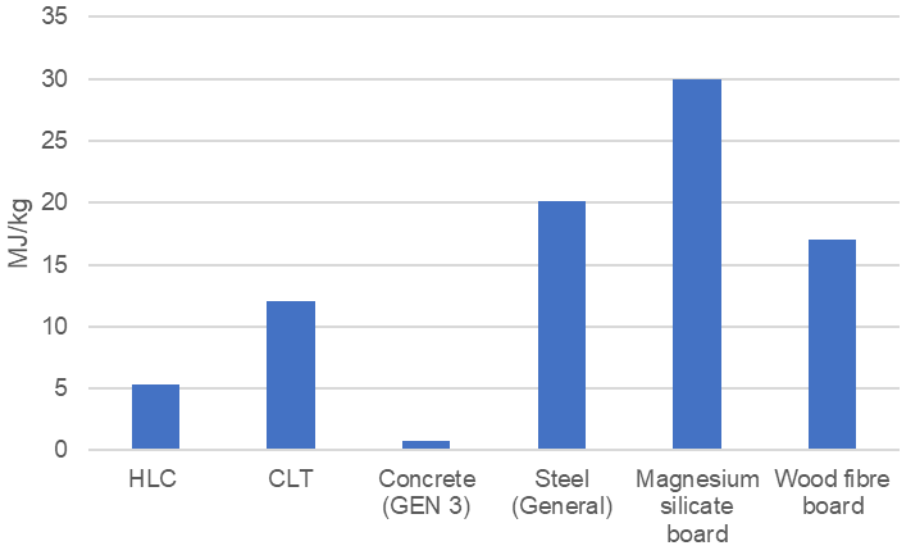

Figure 7.4 Comparison of initial EE values for HMS building envelope materials

Energy use directly causes emissions of greenhouse gases (GHGs). As CO_2 is not always the only GHG, emissions are measured in CO_2e or carbon dioxide equivalents when other gases are given off. Calculation of CO_2e depends on the timescale which is generally calculated as 100 years. Reducing the carbon output of

construction is considered one of the principal outputs of using sustainable resources.

The main source of CO_2 emissions from HLC production is the processing of the lime mortar. According to Shea et al. (2012), hemp shiv sequesters 2.1 $kgCO_2e$ whereas lime is estimated to produce 0.78 $kgCO_2e$ (Hammond & Jones, 2019). Carbonation of the lime binder during mixing and 240 days of curing along with the CO_2 absorbed by the hemp plant results in a negative value. Arrigoni et al. (2017) calculated that a 1 m^2 by 330 mm HLC block would absorb 12.09 $kgCO_2e$ and after full carbonation would be equal to -26.01 $kgCO_2e/m^2$. Lawrence (2013) cited a carbon footprint of -35.5 $kgCO_2e$ for a 1 m^2 by 260 mm sprayed timber-framed and rendered HLC wall with a density of 380 kg/m^3, compared to the 110 $kgCO_2e$ footprint from a similar-sized traditional cavity wall brick and block construction. Walker and Pavia (2014b) reported that 1 m^2 of 260 mm thick HLC sequestered 14 kg to 35 kg of CO_2 over a 100-year lifespan, making it a carbon-negative material. Using the last figures, as the HMS panels are 1 m^2 by 195 mm thick, they should sequester 10.5 kg to 26.25 kg of CO_2, for a total between 7,791 $kgCO_2$ and 19,425 $kgCO_2$ for 742 m^2 with a lifespan of 100 years. With the HMS expected to have a 40 year lifespan (to 2050), this would reduce the initial EE between 3,116.4 $kgCO_2$ to 7,770 $kgCO_2$.

Table 7.3 CO_2 emission from HMS construction materials (from Lawrence, 2013; Hammond & Jones, 2019)

Materials	**$kgCO_2e$**	**$kgCO_2$**
HLC		-35.5
CLT (sustainably sourced)	-1.2	
Concrete (GEN 3)	0.113	
Steel (structural)	1.55	
Magnesium silicate board		1.35
Wood fibre board		0.98

There has been minimal recurring EE of the structure due to repair, refurbishment or maintenance to the end of this research period. Small areas of concrete have spalled off the floor in HMS 6 close to the overhead sectional door and patches of floor paint have lifted off from the movement of the heavier carriages but there have been no repairs carried out to date for either issue. No damage has occurred to either CLT floor or to the varnish layer. There are no paint coatings to renew as both the interior panel facings of white Multi-Pro board and the external wood fibre insulation boards were left uncoated. The steel frame and doors were powder-coated then sprayed with intumescent paint and the steel decking was galvanised. Condensation dripping from the open edges of the Multi-Pro XS board used as door trim has discoloured the wooden boards overlying the decking and caused some minor corrosion of the protective metal door plates but this is cosmetic rather than structural damage and has not been repaired. Restricted access and careful movement of cultural heritage collections has prevented damage to walls, doors and door frames during use. There has been no rodent damage. There is no regular room cleaning programme as none is required due to the limited activity that takes place in the storeroom. Being a

building inside a building has protected the HMS from the usual deterioration caused by wind, sun and rain.

The projected lifespan of the HMS was 40 years at project initiation due to the expected useful lifespan of hangar D2. However, until major repairs are done to the hangar roof, the lifespan of the HMS may be compromised if it is exposed to external weather conditions for which it was not designed. Refurbishment and repairs to the hangar would therefore add to the recurring EE of the HMS. At end of life, the building could be disassembled thanks to its modular design. Materials such as the steel framework, doors, balconies and staircases could be reused as well as being recycled. The HLC panels could be broken down and recycled, with the HLC being used as mulch on the fields of the NCC site.

7.6 Cost effectiveness of the case study

The capital expenditure invested by the SMG in 2012 to build a low energy storage building was £1,129,700. The museum budgeted 14% over the costs of a conventional museum storage building in order to achieve the long-term low operational costs expected as a result of the augmentation of RH regulation by the buffering capacity of HLC. Final capital expenditure was 1% higher than budget, at £1,152.75/m^2.

Costs of the HLC panels have been calculated as 24% of the material costs or 11.5% of the total project costs. Comparison of indicative costs for conventional infill materials for a structural steel frame building, such as brick and block or concrete block with insulation and internal facing of plasterboard, based on 2020 benchmarks (Doherty, 2020) to costs for HLC panels upifted to 2020 demonstrates that the HLC panels as used in the HMS were significantly more expensive, with a percentage difference between 33.4% and 58.6%. Lifetime operational expenditure savings between £51,950 and £81,340 would be required to offset the capital expenditure of the HLC panels. Comparison can be made with the L&A store. Built within hangar D2 to a low energy specification, the infill walls on the steel framework were constructed of two layers of wallboard, a cavity filled with insulation, another layer of wallboard and a layer of plasterboard. The percentage difference for the capital expenditure for the L&A walls was 83.7% to the HMS. Lifetime operational savings would need to be £105,840.

For accurate comparison of capital expenditure against operational expenditure to obtain effective RH regulation, costs would need to obtained from low energy museum storage buildings built with conventional infill walls to the same environmental specifications as the HMS. Projected costs per m^2, total costs and percentage difference for some conventional infill materials based on 2020 benchmarks are given in Table 7.4 along with updated costs for the HMS and L&A store infill materials.

Table 7.4 Costs per m², total costs & % difference for infill materials

Infill layers	Indicative 2020 prices £/m²	£ 980 m²	% difference
HLC panels, wood fibre board skin, magnesium silicate facing	183	179,340	
Brick & block cavity wall, mineral wool insulation, plasterboard	105-130	102,900-127,400	54 - 33.8
Rendered concrete block cavity wall, insulation, plasterboard	100-103	98,000-100,940	58.6 - 56
Rendered externally insulated block, plasterboard	100	98,000	58.6
L&A store- 3 layers wallboard, 1 layer plasterboard, insulation	75	73,500	83.7

Using the total annual energy costs for the HMS and the L&A store, the annual operational expenditure can be calculated for 980 m^2 from 2012 up to January 2020 (Table 7.5). After eight years, operational expenditure for 980 m^2 of the HMS has been £20,205 compared to £47,137 for 980 m^2 of the L&A store, an average annual savings of £3,366. Payback for the additional capital expenditure required for the HLC panels will be reached by the 31st year of use. As has been demonstrated by the case study, the hygroscopic capacity of HCL augments RH regulation to meet the requirements of the museum, requirements which are not achieved in the L&A store despite the continual use of mechanical plant at more than double the cost on an annual basis.

Table 7.5 Comparison of annual OPEX for HMS & L&A store

Year	HMS £	L&A £
2012	2,075	5,124
2013	2,334	5.328
2014	2,428	5,402
2015	2,493	5,454
2016	2,525	5,479
2017	2,676	6,920
2018	2,710	7,064
2019	2,964	6,366

The annual energy expenditure for the HMS has remained in the region of 26,139 kWh/yr from 2012 through to 2020 since the programme of continuous cyclical operation of the air handing system has persisted. Total annual costs have been computed from site consumption information received from the SMG Estates department, using the statistical data complied by the BEIS on non-domestic consumers in the UK (Table 7.4). Costs per m^3 have been calculated on usable storage storage space in order to compare the three environmentally-controlled storage spaces on the NCC site. Both the L&A store and the A Store were designed

as low energy storage buildings. The case study compared the annual energy consumption and costs of both buildings to the HMS.

Between the HMS and the A store there was a 37% difference in the annual costs per volume of usable storage space and between the HMS and L&A store there was an annual 30% to 42.5% difference, depending on outlays for biofuel and necessary additional mechanical control. Annual energy consumption of the HMS was not as low as originally projected as the intended seasonal RH regulation programme was not followed during the period of the research study. However, based on the monitoring data from 2012 to 2020, heating during the winter months is not required. Operation of the heating system is required during periods when the external temperature exceeds the internal temperature. Operational expenditure could be reduced if heating is only used in those periods but the extent of expenditure reduction will depend on climate change and future seasonal temperatures. Table 7.6 shows the annual energy consumption costs and costs per volume of usable storage space for the HMS through the transient, first and second steady states of operation up to January 2020.

Table 7.6 HMS annual energy consumption costs, 2012-2019

Year	Annual average energy consumption 26,139 kWh/yr	
	annual energy cost	£/m^3
2012	£2,075.44	0.95
2013	£2,334.21	1.07
2014	£2,428.31	1.11
2015	£2,493.66	1.14
2016	£2,525.03	1.15
2017	£2,676.63	1.22
2018	£2,710.61	1.24
2019	£2,964.16	1.36

CO_2 emissions from electricity, the operational energy source for the HMS, has dropped by 56% from 2012, when it was quoted as 0.59 kgCO_2e/kWh (Carbon Trust, 2012), due to the downward trend in emissions caused by power stations moving away from coal and towards renewable sources.The UK 2019 government report on carbon emissions (BEIS, 2019, updated 2020) quotes 0.256 kg of CO_2e per kWh of electricity. Annual operational emissions for the HMS have dropped from 15,422 kgCO_2e/kWh in 2012 to 6,691.6 kgCO_2e/kWh in 2019.

Contractor-based annual operational costs, for maintenance, servicing and inspection of the M&E system, cannot be teased out as they are included in the site-wide contractor contracts. There have been minimal upgrade costs when replacing security door locks, changing passive infrared sensors (PIR) to light switches in HMS 4 and adding external PIRs to improve lighting on the staircases and decks. Regular servicing and frequent repairs have been required for the external lift which has proved inadequate for purpose, with a typical annual cost of £1,500 to repair same.

7.7 Benefits to the Science Museum Group

According to *PAS 198*, the expected cultural heritage collections lifetime is the length of time over which the usable life of collection items can be prolonged by means of preservation measures (BSI, 2012a). An organisational collections management strategy must take into account the significance, planned use and expected rate of deterioration of collections in order to determine the resources required for preservation purposes. Institutional environmental guidance is used to estimate the impact of RH, along with temperature, light and pollutants, on component materials or complex structures of collection items. At the same time, resources are limited so museums must find ways to reduce energy use while providing the required environmental conditions. The expected lifespan of collections in museum storage can be increased to centuries if it is possible to sustain a low energy moisture control system.

The HMS was built in response to specific collections storage needs, both for collections objects and for archives. The original intent of the HMS project was to construct an archive store, specifically for the storage of the RINA archives. These were intended to become part of the collection of the NRM but the archive store in York was at capacity. As there was also insufficient space in the Science Museum's archival store, built within hangar D2 in 2006, it was proposed to build another store beside the existing store. Specifications for the L&A store had been for a low energy facility but conventional building materials with limited buffering capability had been used for construction and the regulation of the environment was achieved only with continuous operation of an HVAC system. Any dehumidification provided by the air conditioning system was ineffective and the RH range frequently was 10% to 20% above the recommended upper parameter of 60% RH. This resulted in mould growth on some of the collections particularly at the north end of the room, as the store had varying environmental conditions from one end to the other.

The HMS project was revised through storage needs for three object collections. Prior to the construction of the HMS, environmentally-controlled cultural heritage collections storage was limited to one building on the NCC site. All other object storage buildings on the site were unheated WWII-era aircraft maintenance hangars. There was insufficient space in the A Store for the object collections with both the carriages and very large ship models needing floor-standing space and the framed art works requiring vertical art racking. Some of the fixed racking could have been removed but the racking was at capacity and alternative storage space would have had to be provided for those objects. Even if sufficient space could have been made available, the environmental conditions did not fully meet the RH regulation of 40% RH to 60% RH ±5% RH stipulated by the museum. The building, constructed between 1992 to 1993, had been intended to be a low energy facility with airtight construction and a dehumidification system. RH regulation originally was provided by a desiccant system which ceased to be operational by 1995. RH regulation after that was provided by the heating and ventilation system. Environmental conditions within the two large storerooms seasonally drifted below and above RH parameters. A feasibility study for the heating and ventilation system was undertaken in 2011 with the boilers and AHUs both considered to be nearing end of life. Quotes were £270,000 for a like-for-like replacement of the two oil-fuelled boilers, £583,500 for a ground source heat pump, £506,50 for an air source heat pump and £452,000 for a

biomass boiler system (Read, 2011). Higher costs for the three alternative systems were due to insufficient space within the existing plant room, entailing additional construction costs. Annual operational costs were calculated with running costs of the three alternative systems approximately half of those for a like-for-like system. All installations included replacement of the AHUs with DX condensers. Replacement of the dehumidification system was not included in the survey. As it was not possible to provide enough space in the A Store for the three specific collections requiring environmentally-controlled storage, capital funds for replacing the heating and ventilating system were allocated to the HMS project.

The issues arising from the design and operation of the L&A store and A Store were taken into consideration during the planning and design of the HMS. Focus was on providing low energy storage through enhanced hygroscopic and thermal capabilities of biobased construction materials in order to augment the regulation of the internal environment. This was intended to reduce operational loads for heating, ventilation and air conditioning. Stable conditions within the parameters of 40% RH to 60% RH would ensure that the preservation needs of the three object collections and the archive would be met and deterioration rates decreased.

While the RINA Archive as yet to arrive, to date there have been 401 framed art works, 30 carriages and 238 rigged and half-block ship models moved into the HMS. The carriage collection had originally been stored in one of the unheated hangars where they were subjected to high levels and extreme fluctuations of humidity, mould growth and pest activity. All had sustained some level of physical, chemical and biological damage to their component materials and complex structures from the storage conditions. Retaining the collection in uncontrolled storage would have negated all conservation treatment and resulted in further and possibly irreversible damage. The ship models had been on display in the Shipping Gallery in the SCM for more than forty years, in low but stable RH. While crated before removal to reduce the impact of changes in RH, the crates were intended only to buffer short-lived RH fluctuations and would not prevent eventual rise in internal RH levels. The rigged ship models were at great risk of physical deterioration from RH fluctuations due to the sensitivity of the organic component materials and the complex structures and uncontrolled storage would result in deterioration leading to loss of components and, potentially, entire objects. Storage of framed art works had been in locations where the RH ranged between 35% RH to 60% RH with daily fluctuations between 3% RH and 10% RH. Only one store had vertical art racking and there was no additional capacity. Storage on art racking was recommended to allow viewing without handling which would reduce the risk of physical damage. Uncontrolled storage would have resulted in damage to paint and support layers. Provision of storage with stable RH would enhance the preservation of all three collection types.

Condition assessments of the objects were carried out as objects were put into storage, and entered into the SMG object database. To date, no visible deterioration of any object has been noted. Individual objects from each of the three object collections have been assessed for use in exhibitions and for loans. The requirement for further conservation treatment has been minor for all objects, being limited to light cleaning. There has been no corrosion, no mould growth and no physical deterioration caused by incorrect levels or excessive fluctuations of RH. Under such regulated RH conditions, the longevity of even the most sensitive materials will be

extended as deterioration, although inevitable, has been significantly slowed down. The anticipated lifespan of the SMG collections, 95% of which are in storage, is in the hundreds of years when under a programme of collections care which provides controlled and buffered environmental conditions.

While the majority of the stored collections of the SMG are not in the HMS, the results of the HMS project has enabled the development of the collections management strategy for the group, which is now storing all its reserve collections at the NCC. The project has demonstrated how external conditions on the NCC site can affect internal conditions not just through thermodynamic reaction of RH to changes in temperature but also through thermodiffusion phenomenon of moisture movement caused by temperature gradients. This knowledge can be used to inform the design and operation of future mechanical control systems in order to reduce energy use and operational expenditure. The use of a very hygroscopic building material does augment the regulation of RH and consideration should be made in future to find ways to incorporate construction materials such as HLC despite initial increased capital expenditure. The buffering capacity of HLC reduces the risk of deterioration to and loss of collections through the failure of any mechanical system by maintaining the specified RH levels for at least the minimum of 48 hours as recommended in *BS EN 16893:2018* (BSI, 2018). RH fluctuations induced by ventilation and air changes are also reduced through the capacity of the material to absorb and desorb moisture.

As a result of the case study undertaken in this research project, SMG RH guidance has been revised to better reflect the preservation needs of collection materials and structures. This in turn has been used to inform the performance specification for the M&E of a new storage facility, Building ONE (B1) which utilises dehumidification and reduced ventilation in the regulation of RH. Construction with wall infill using HLC proved to be impossible due to contractor reluctance and lack of panel production in the UK. Wool insulation was used in the hope that some buffering capacity might be provided by its hygroscopic properties.

7.8 Limitations of the research study

The research study is subject to several limitations, potential issues caused by the research study's methodology, instruments and techniques used to collect data.

The case study was limited to one museum storage building using HLC in pre-cast panel form as a very hygroscopic construction material. While there have been warehouses built in the UK using HLC pre-cast panels, any available environmental monitoring data was limited to temperature as the focus of those projects was on thermal insulation to maintain internal temperatures for the storage of food and beverages. The research project required RH data in order to determine whether the use of HLC augmented the regulation of RH in order to achieve the specified parameters of the museum storage environment.

The case study was built within another building, hangar D2, so it was not possible to determine the direct effects of weather on the building envelope or on the internal environment. While external data was collected and assessed for impact, there was

likely to have been mitigation of the effects of external conditions by the hangar structure. Future research on free-standing museum storage buildings built using HLC walls would determine the extent that direct thermal gradients driven by solar or wind have on the thermodiffusion phenomenon or moisture transfer through the very porous matrix.

Environmental monitoring data was collected and assessed from two other low energy museum storage buildings constructed from conventional materials on the NCC site in order to obtain comparative information on the effectiveness of RH regulation processes. Monitoring in the two other buildings was limited to obtaining RH and temperature data. Comparable costs for operational expenditure were limited to energy usage and operational costs had to be calculated against the annual site energy costs per kWh. Information on energy use and costs was limited to personal communication and there was no access to bills for the site. Energy usage data from other low energy stores in the EU was limited to the literature review.

The number of telemetric sensors available to obtain RH and temperature data from the HMS was a factor as was the timeframe for obtaining them. They were purchased through the museum's conservation budget as and when funds were available. This affected data collection for the empty storerooms as telemetric sensors were not available during the research period. Data was therefore only obtained and evaluated ftom the three rooms storing object collections and stratified RH data obtained and evaluated from one storeroom. RH and temperature data was obtained and evaluated from two sensors in the L&A store, from six sensors in the A Store and from two sensors in hangar D2. There was only one Hanwell external RH and temperature sensor. Data collection from Tinytag data loggers was sporadic and data was not robust.

Time constraints as a result of this researcher in full-time employment limited data comparison analysis to the NCC site. Time constraints as a result of equipment acquisition meant MC (%) values were only obtained for four sections of HLC wall, two from the ground floor and two from the first floor. MC (%) monitoring was only carried out on the HLC matrix and not on the concrete floor slab where data might have confirmed that the concrete moisture content was responsible for the higher level of RH on the gound floor.

Increasing the number of sensors in future long-term monitoring of the RH and MC (%) in the HMS could reveal if the HLC has continued to dry out over time as a result of the intermittent heating programme and whether there is any effect on the regulation of RH levels. Analysis of the effect of thermodiffusion phenomenon could be further studied by longer periods of passive operation during winter months in order to assess full effects of negative thermal gradients on internal RH. Without heating, the lower temperatures in the HMS would potentially provide data on interstitial mould growth and the risk of condensation while the recommended RH band of 40% RH to 60% RH was maintained. Future research could expand the MC (%) data obtained to all walls throughout the building in order to verify the findings from the limited research sample size. Parallel studies could be carried out with additional low energy museum storage buildings in order to obtain side by side

comparisons of capital expenditure, operational expenditure and effectiveness of RH regulation.

7.9 Summary of the discussion of results

In order to test the research hypothesis of this study, key performance criteria for maintaining suitable and sustainable control of RH levels and fluctuations within museum storage in temperate climates were assessed through environmental monitoring of the case reference study, the HMS. The data acquired from 2012 to 2020 demonstrated that the hygroscopic performance of the HLC construction supported the design for low energy storage.

The statistical significance of the datasets from the research study was assessed after formulating a null hypothesis. The monitoring results were found to be statistically significant with the data demonstrating the positive relationship between the regulation of RH in the HMS and the buffering performance of HLC. Observation of objects' condition were found to support the conclusion that the buffering performance of HLC had augmented the regulation of RH to ensure that no deterioration had occurred during storage in the HMS.

Implications were that the anticipated outcomes of the research were met, showing that the hygroscopic ability of HCL could moderate RH fluctuations caused by mechanical environmental controls and identifying the extent to which HCL could contribute to the control of RH levels. The hygroscopic performance of HCL was shown to augment RH control in a low energy museum storage facility. The dynamic relationship between RH and MC (%) of HLC was clearly demonstrated. Identification of the influence of thermodifussion phenomenon verified the assumption that dehumidification would be a more effective mechanical control mechanism than heating and ventilation for an airtight storage building with porous hygroscopic walls.

Practical and cost considerations, including capital and operational expenditures, for future practical applications of the research were identified specifically for the SMG from the implications of the case study. Options for replication of the HMS both within another building and as a free-standing building were explored.

Detailing the environmental impact, both embodied energy and carbon emissions from processing and manufacture of HLC and other building materials used for the structure of the HMS, showed that construction with HLC contributes to reducing the overall impact of construction as HLC can be considered to be carbon-negative. Consideration of the potential for HLC to support effective low energy RH control to museum specifications outweighed the increased cost of construction compared to conventional materials.

Benefits to the SMG collections stored within the HMS and to the SMG stored collections as a whole came from outcomes of the research study which demonstrated that using a hygroscopic building material such as HLC would ensure that obligations for long-term sustainable preservation would be met.

Impact from the limitations of the research project were described and suggested improvements to future studies proposed.

Chapter 8 Conclusions and recommendations for future research

8.1 Conclusions

One of the current recommendations to enable sustainability in the preservation of cutural heritage collections in storage has been to reassess how RH control has been achieved. While the control of both RH levels and fluctuations is considered necessary for long-term preservation, museum and collecting institutions have been encouraged to reduce carbon footprint and environmental impact by reducing energy use by finding alternative ways to maintain RH than reying on mechanical methods of air conditioning. One proposal has been to employ the hygrothermal capacity of the building, through the use of hygroscopic building materials, to augment RH control through passive means of moisture transfer and moisture buffering. While more conventional materials such as concrete block or unfired brick have been suggested as potential buffering materials, the production of biobased materials has less impact on the environment, with lower imitial embodied energy. Biobased materials can have significant transient hygrothermal behaviour which would enhance buffering capacity. However, the key knowledge gap is the lack of assessment to identify the extent to which such hygrothermal behaviour can moderate RH levels and fluctuations to museum specifications under dynamic museum storage conditions.

This thesis has contributed to filling the gap in knowledge on the hygrothermal performance of hemp lime concrete (HLC) in augmenting the regulation of RH within a museum storage building in a temperate climate. The key objectives of the investigation were to assess the moisture management capacities of HLC through a literature review of relevant studies and *in situ* monitoring of a museum store utilising HLC as part of a low energy RH control system and to put the findings of the assessment into the context of conventional museum RH control practices by comparing performance and operational costs with other low energy museum stores. The assessments were carried out using a case study, the HMS.

The moisture content of the HLC was found to support the RH levels in the stores so that they were maintained within the required band of 40% RH to 60% RH throughout normal steady states of operation. Dynamic equilibrium through absorption and desorption of water vapour caused by temperature and pressure changes across the porous HLC matrix buffered the effects on room RH so that the extent of diurnal RH fluctuations was minimised. The duration of extreme RH fluctuations caused when the AHUs drew in too much external air was limited to the period of ventilation with the interaction of the buffering capability of the HLC enabling almost immediate recovery of RH to the required range. Most importantly, this research has verified the thermodiffusion phenomenon effect across the porous HLC walls. Both positive and negative Soret coefficients were shown to influence RH levels in the storerooms as long as the the dynamic change in external temperature outlasted the dynamic change in moisture concentration. The effect of the temperature gradient became more significant as the temperature gradient increased and the thermodynamic relationship between temperature and RH altered. In the HMS, while there was a seasonal drift in internal temperature, the moisture storage capacity of the HLC eliminated the need for winter heating or humidification in order

to maintain required RH levels. But heating was required during summer months to reduce the RH gain that resulted from desorbed moisture from the HLC walls. It is concluded that where there is a predominance of hygroscopic material, whether construction materials or cultural heritage collections themselves, the design of any low energy mechanical RH control system needs to take thermodiffusion into consideration in an airtight storage building with limited air change rates. It is also important to note that, in any analysis of RH regulation in museum storage, the influence of external conditions on the building envelope must be taken into account.

The operational expenditure required to regulate the RH to museum specifications was reduced by at least a third when compared to other low energy storage buildings on the same site although OPEX was comparatively high in contrast to low energy stores in Denmark. Energy usage was reduced by the cyclical operation of the AHUs but could have been decreased further by only running the system when required. More efficient and cost-effective RH control would have been provided by a dehumidification system with humidistat rather than a heating and ventilation system.

Capital expenditure for construction using HLC wall panels was higher than using conventional infill materials with a 30-year payback period for a building with a minimal expectation of a 40-year lifespan. Conventional infill materials, as used in the construction of the other low energy storage buildings, were shown to have comparatively poor buffering capacity under dynamic operation with a continuous need for active RH control and no passive buffering of RH fluctuations.

8.2 Recommendations for future work

Long-term monitoring of the RH in the HMS would reveal the extent to which HLC might mitigate RH levels in addition to buffering RH fluctuations. Assessing RH from the smaller storerooms would determine if RH buffering was more effective in smaller spaces with more internal HLC wall surface per volume. Data from HMS 1, on the ground floor, would help verify the effect of the concrete floor slab on room RH as well as confirm the effect of continuous dehumidification over several years on the RH in HMS 6.

It was demonstrated that the initial MC (%) of the building materials resulted in significant moisture storage within the HLC matrix resulting in elevated RH levels. Over time, the RH levels on all floors have dropped slightly and the MC (%) in the interior wall in HMS 5 has lessened, although the MC (%) in the external wall has remained at the same level from the beginning of monitoring to the end of the research period. Longer monitoring of MC (%) would clarify whether the linear regression modelling truly identified the end of the drying process. MC (%) monitoring of all rooms would further define the relationship between RH and MC (%) as the RH level in each storeroom was slightly different. MC (%) monitoring of the outer walls could also potentially determine the moisture penetration depth of HLC.

As lower temperatures (below 10°C) have been shown to contribute to the preservation of cultural heritage collections, long-term monitoring would provide data for studies on potential interstitial mould growth and the risk of condensation while

maintaining the recommended band of 40% RH to 60% RH. Monitoring data has shown that humidification is not required through the duration of temperatures around 10°C but investigation into potential mould growth was not undertaken. Eliminating heating during the winter would provide data on energy consumption and operational expenditure.

Side by side studies could be undertaken to define the thermal stability of the HMS which would verify the thermal properties of HLC, as found through numerical, simulation and experimental studies, under dynamic museum storage operation.

Research areas which fell outside the remit of this research study were:

- The quantification of potential off-gassing of volatile compounds from HLC.
- The alkalinity, particle size and particle shape of dust and debris from the HLC and any potential effects on cultural heritage collections.
- An assessment of the effects of the coatings and linings on the hygroscopic capability of HLC.
- An assessment of the effect on RH from hygroscopic cultural heritage collections.
- The potential effectiveness of natural versus forced ventilation in moderating RH levels affected by the thermodiffusion phenomenon.

References

Abbott, T., 2014. *Hempcrete factsheet- essential hempcrete info* [Online]. Available from: http://limecrete.co.uk/hempcrete-factsheet/ [Accessed 23.08.2017]

Aidan, A., Shareefdeen, Z., Bogdanov, B., Markovska, I., Rusev, D., Hristov, Y. & Georgiev, D., 2009. Preparation and properties of porous aerated concrete. *Scientific Work of the Russian University*, 48 (9), pp.24-28.

Ait Oumeziane, Y., Bart, M., Moissette, S., Lanos, C., Pretot, S. & Collet, F., 2011. Hygrothermal behaviour of a hemp concrete wall: influence of sorption modelling. *9th Nordic Symposium on Building Physics- NSB 2011*. Tempere, Finland.

Ait Oumeziane, Y., Bart, M., Moissette, S. & Lanos, C., 2014. Hysteretic behaviour and moisture buffering of hemp concrete. *Transport in Porous Media*, 103(3), pp.515-533.

Ait Oumeziane, Y., Moissette, S., Bart, M. & Lanos, C., 2016. Influence of temperature on sorption process in hemp concrete. *Construction and Building Materials*, 106, pp.600-607.

American Limetechnology, 2012. *What is hempcrete?* [Online]. Available from: http://www.americanlimetechnology.com/what-is-hempcrete/ [Accessed 14.10.2019].

Amziane, S., Collet, F., Lawrence, M., Magniont, C., Picandet, V. & Sonebi, M., 2017. Recommendation of the RILEM TC 236-BBM: characterisation testing of hemp shiv to determine the initial water content, water absorption, dry density, particle size distribution and thermal conductivity. *Materials and Structures*, 50:167, pp.1-11.

Andrew, R., 2018. Global CO_2 emissions from cement production. *Earth System Science Data*, 10, pp.195-217.

Appel, K., 2010. *The plain truth about relative humidity sensors*. [Online]. Available from: www.qualitydigest.com/inside/twitter-ed/plain-truth-about-relative-humidity-sensors. [Accessed 24.01.2017].

Arizzi, A., Cultrone, G., Brummer, M. & Viles, H., 2015. A chemical, morphological and mineralogical study on the interaction between hemp hurds and aerial and natural hydraulic lime particles: implications for mortar manufacturing. *Construction and Building Materials*, 75, pp.375-384.

Armstrong, T., ed., 2018. A review of global cement industry trends. *International Cement Review.*

Arnaud, L. & Cerezo, V., 2001. *Qualification physique des materiaux de construction a base de chanvre*. Departement Genie Civil et Batiment. Vaulx-en-Velin: Ecole Nationale des Travauz Publics de l'Etat.

Arnaud, L. & Gourlay, E., 2012. Experimental study of parameters influencing mechanical properties of hemp concretes. *Construction and Building Materials*, 28, pp.50-56.

Arrigoni, A., Pelosato, R., Melia, P., Ruggieri, G., Sabbadini, S. & Dotelli, G., 2017. Life cycle assessment of natural building materials: the role of carbonation, mixture components and transport in the environmental impacts of hempcrete blocks. *Journal of Cleaner Production*, 149, pp.1051-1061.

Ashley-Smith, J., Umney, N. & Ford, D., 1994. Let's be honest- realistic environmental parameters for loaned objects. *Preventive conservation practice, theory and research*. Ottawa: International Institute for Conservation of Historic and Artistic Works, pp.28-31.

ASHRAE, 1964. *ASHRAE guide and data book: 1964 applications*. New York: American Society of Heating, Refrigerating and Air Conditioning Engineers.

ASHRAE, 2011. Chapter 23: museums, galleries, archives, and libraries. *2011 ASHRAE handbook: HVAC applications*. American Society of Heating, Refrigerating and Air Conditioning Engineers, Inc., 23, pp.23.1-23.11.

Ashraf, W., 2016. Carbonation of cement-based materials: challenges and opportunities. *Construction and Building Materials*, 120, pp.558-570.

Athen Sustainable Materials Institute, 2019. *Appendix D:NRMCA member national and regional LCA benchmark (industry average(report.* V 3.0. NRMCA.

ATTMA, 2010. *Measuring air permeability of building envelopes (non-dwellings)*. Technical standard L2, October 2010 issue. Northamption: The Air Tightness Testing & Measurement Association.

Ayres, J. M., Haiad, J. C. & Lau, H., 1988. *Energy conservation and climate control in museums*. Los Angeles: The Getty Conservation Institute.

Ayres, J. C., Druzik, J., Haiad, J. C., Lau, H. & Weintraub, S., 1989. Energy conservation and climate control in museums: a cost simulation under various outdoor climates. *The International Journal of Museum Management and Curatorship*, 8, pp.299-312.

Balabanov, P.V. & Mishchenko, S.V., 2016. Methods and means of determining the thermal properties of heterogeneous materials. *Measurement Techniques*, 59 (6), pp.649-655.

Balogh, A., 2018. *What makes concrete a sustainable building material?* [Online]. Available from: https://www.concretenetwork.com/concrete/greenbuildinginformation/what_makes.html [Accessed 14.10.2019].

Banks, P. N., 1999. What makes records deteriorate? *ASHRAE Journal*, 41 (4), pp.64-68.

Barclay, M., Holcroft, N. & Shea, A., 2014. Methods to determine whole building hygrothermal performance of hemp lime buildings. *Building and Environment*, 80, pp.204-212,

BBC, 2016. *Hottest day of 2016 recorded at Gravesend in Kent* [Online]. Available from: https://www.bbc.co.uk/news/uk-37178746

BCMAF, 1999. *Industrial hemp (cannabis sativa L.)*. Specialty Crops Factsheet, Kamloops, B.C.: Government of British Columbia, Ministry of Food & Agriculture.

BEIS, 2013. *Tables of gas and electricity prices in the non-domestic sector: prices of fuels purchased by non-domestic consumers in the United Kigdom excluding/including CCL* [Online]. Available from: https://www.gov.uk/government/statistical-data-sets/gas-and-electricity-prices-in-the-non-domestic-sector

Benfratello, S., Capitano, C., Peri, G., Rizzo, G., Scaccianoce, G. & Sorrentino, G., 2013. Thermal and structural properties of a hemp-lime biocomposite. *Construction and Building Materials*, 48, pp.745-754.

Berardi, U., 2017. A cross-country comparison of the building energy consumptions and their trends. *Resources, Conservation and Recycling*, 123, pp.230-241.

Betts, B., 2010. Beer comes clean. *Engineering & Technology*, July 10, 2010.

Bevan, R. & Woolley, T., 2008. *Hemp lime construction: a guide to building with hemp lime composites*. IHS BRE Press.

Bianco, L., Pollo, R. & Serra, V., 2016. Wood fiber vs synthetic thermal insulation for roofs energy retrofit: a case study in Turin, Italy. *8th International Conference on Sustainability in Energy & Buildings*, SEB-16, 11-12 September 2016, Turin, Italy,

Bickersteth, J., 2014. Environmental conditions for safeguarding collections: what should our set points be? *Studies in Conservation* 59 (4). London: International Institute for Conservation of Historic and Artistic Works (IIC), pp.218-224.

Biond, 2019. *The Biond construction system: a layman's guide* [Online]. Available from: https://www.biond.co.uk/wp-content/uploads/biond_laymans-guide.pdf [Accessed 25.03.2019].

Bizot Group, 2009. *Revised loan guidelines: executive summary*. International Exhibition Organizers (IEO). Budapest, pp.1-9.

Blengini, G. & Di Carlo, T., 2010. The changing role of life cycle phases, subsytems and materials in the LCA of low energy buildings. *Energy & Buildings*, pp.869-880.

Bomberg, M., Kisilewicz, T. & Nowak, K., 2016. Is there an optimum range of airtightness for a building? *Journal of Building Physics*, 39 (5), pp.395-421.

Bordass, B., 1996. *Museum collections in industrial buildings*: a *selection and adaptation guide*. M. Cassar, ed. Museums & Galleries Commission: The Conservation Unit.

Bradley, S., 1989. Environmental monitoring and control in the galleries of the British Museum. *Preprints: Environmental Monitoring and Control*. Dundee: Scottish Society for Conservation & The Museums Association, pp.68-77.

Bradley, S. M., 1991. The implementation of environmental standards. In M. Norma & V. Todd, eds. *Storage Preprints for UKIC conference, Restoration '91*. London: United Kingdom Institute for Conservation of Historic and Artistic Works of Art, pp.22-26.

Bratasz, Ł., Camuffo, D. & Kozłowski, R., 2007. Target microclimate for preservation derived from past indoor conditions. In T. Padfield & K. Borchersen, eds. *Museum Microclimates,* National Museum of Denmark, pp.129-134.

Bratasz, Ł., 2013. Allowable microclimatic variations for painted wood, *Studies in Conservation*, 58:2, pp.65-7.

Bratasz, Ł., Łukomski, M., Klisińska-Kopacz, A., Zawadzki, W., Dzierżęga, K., Bartosik, M., Sobczyk, J., Lennard, F.J. & Kozłowski, R., 2015. Risk of climate-induced damage in historic textiles. *Strain*, 51(1), pp.78-88.

BRE, 2011. *Hemp lime: an introduction to low-impact building materials*. Information Paper IP 14/11, IHS BRE Press.

BRE, 2012. *SAP 2012: the government's standard assessment procedure for energy rating of dwellings.* BRE Press.

Brick Industry Association, 2006. Manufacturing of brick. *Technical notes on brick construction*, 9. Reston, Virginia: The Brick Industry Association.

Brophy, S. S. & Wylie, E., 2008. *The green museum*. Altamira Press.

Brown, J. P., 1994. Hygrometric measurement in museums: calibration, accuracy, and the specification of relative humidity. *Studies in Conservation*, 39 (Supp 2), pp.39-43.

Brown, J. P. & Rose, W. B., 1996. Humidity and moisture in historic buildings: the origins of building and object conservation. *APT Bulletin*, 27(3), pp.12-23.

Brown, J. P. & Rose, W. B., 1997. *Development of humidity recommendations in museums and moisture control in buildings* [Online]. Available from: http://cool.conservation-us.org/byauth/brownjp/humidity1997.html [Accessed 04.01.2014].

BSI, 1989. *BS 5454:1989: Recommendations for storage and exhibition of archival documents.* London: BSI.

BSI, 2000. *BS 5454:2000: Recommendations for the storage and exhibition of archival documents.* London: BSI.

BSI, 2010. *BS EN 15757:2010- Conservation of cultural property: specifications for temperature and relative humidity to limit climate-induced mechanical damage in organic hygroscopic materials*. London: BSI.

BSI, 2012a. *PAS 198:2012: Specification for managing environmental conditions for cultural collections*. London: BSI.

BSI, 2012b. *PD 5454:2012: Published document: guide for the storage and exhibition of archival materials*. London: BSI.

BSI, 2013. *BS EN ISO 1257:2013: Hygrothermal performance of building materials- determination of hygroscopic sorption properties*. London: BSI.

BSI, 2014. *BS EN ISO 11274:2014: Soil quality- determination of the water retention characteristic; laboratory methods*. London: BSI.

BSI, 2015. *BS ISO 11799:2015: Information and documentation: document storage requirements for archive and library materials.* London: BSI.

BSI, 2016. *BS EN ISO 12572:2016: Hygrothermal performance of building materials and products- determination of water vapour transmission properties: cup method*. London:

BSI, 2017a. *BS 4971:2017: Conservation and care of archive and library collections.* London: BSI.

BSI, 2017b. *BS EN ISO 13786:2017 Thermal performance of building components- Dynamic thermal characteristics- Calculation methods*. London: BSI.

BSI, 2018a. *BS EN 15759-2:2018: Conservation of cultural heritage: indoor climate. Part 2: ventilation management for the protection of cultural buildings and collections*. London: BSI.

BSI, 2018b. *BS EN 16893:2018: Conservation of Cultural Heritage: specifications for location, construction and modification of buildings or rooms intended for the storage or use of heritage collections*. London: BSI.

BSRIA, 1998. *Air tightness specifications*. Specification 10/98. Bracknell: BSRIA.

BSRIA, 2018. *The BSRIA blue book*. Bracknell: BSRIA.

Buck, R. D.,1964. Part I: a specification for museum airconditioning. *Museum News* , 43(4, December), pp.53-56.

Building, 2018. *Costing steelwork: cost models update*. [Online]. Available from: www.building.co.uk/focus/costing-steelwork-cost-models-update/5094738.article [Accessed 20.07.2018]

Burmester, A. & Eibl, M., 2014. *Stable is safe: the Munich position on climate and cultural heritage*. Munich: Doerner Institute, pp.1-9.

Burrell, E., 2015. *What is airtight construction?* [Online]. Available from: https://elrondburrell.com/blog/passivhaus-airtight-construction/ [Accessed 26.08.2019].

Burridge, J. & Clear, C., 2014. Specifying sustainable concrete. *Concrete Quarterly*, 248, pp.16-18.

Busbridge, R. & Rhydwen, R., 2010. An investigation of the thermal properties of hemp and clay monolithic walls. *Proceedings of Advances in Computing and Technology*, *(AC&T) The School of Computing and Technology Annual Conference*. University of East London, pp.163-170.

Cameron, D., 1968. Environmental control: a theoretical solution. *Museum News*, 46(8), pp.17-22.

Cammalleri, V. & Lyon, E., 2003. Condensation in the building envelope: expectations and realities. *SSPC 2003: The Industrial Protective Coatings Conference and Exhibit*, New Orleans, pp.210-219.

Canadian Conservation Institute, 1993. *Environmental and display guidelines for paintings*. Ottawa: Communications Canada.

Canadian Council of Archives, 2003. Chapter 3 – Environment. In *Basic Conservation of Archival Materials* (revised edition), pp.11-25.

Carbon Trust, 2012. *Carbon neutral calculator* [Online]. Available from: www.carbonneutralcalculator.com/carbon%20offset%factors.pdf

Carmeliet, J., De Wit, M. & Janssen, H., 2005. Hysteresis and moisture buffering of wood. *Symposium of Building Physics in the Nordic Countries*, pp.55-62.

Carrier Corporation, 2005. *Psychrometrics*. Technical Development Program. Syracuse, NY: Carrier Corporation.

Cassar, M., 2009. Sustainable heritage: challenges and strategies for the twenty-first century. *APT Bulletin: Journal of Preservation Technology*, 40(1), pp.3-11.

Cassar, M. & Hutchings, J., 2000. *Relative humidity and temperature pattern book*. London: Museum & Galleries Commission.

Cérézo, V., 2005. *Propriétés mécaniques, thermiques et acoustiques d'un matériau à base de particules végétales: approche expérimentale et modélisation théorique*. Thesis (PhD), Institut National des Sciences Appliquées, Lyon.

Cerolini, S., D'Orazio, M., Di Perna, C. & Stazi, A., 2009. Moisture buffering capacity of highly absorbing materials. *Energy and Buildings*, pp.164-168.

CFA, 2005. *Concrete cracking* [Online]. Available from: http://www.cfawalls.org/foundations/cracking.htm [Accessed 27.02.2018].

Chambers, S., 2012. *Highlight report 10- RINA project highlight report*. Science Museum. Unpublished.

Chen, C. & Wangaard, F. F., 1968. Wettability and the hysteresis effect in the sorption of water vapor by wood. *Wood Science and Technology*, 2, pp.177-187.

Chen, T.Y., Burnett, J. & Chau, C.K. (2001). Analysis of embodied energy use in the residential building of Hong Kong. *Energy,* 26, pp.323-340.

Child, R. E., 2007. Insect damage as a function of climate. In T. Padfield & K. Borchersen, eds. *Museum Microclimates*, National Museum of Denmark, pp.57-60.

Christensen, J. E. & Janssen, H., 2011. Passive hygrothermal control of a museum storage building. *Proceedings of Building Simulation 2011:12th Conference of International Building Performance Simulation Association*, Sydney, pp.1848-1854.

Christensen, J. E. & Kollias, C., 2015. Hygrothermal evaluation of a museum storage building based on actual measurements and simulations. *Energy Procedia*, 78, pp.651-656.

Christensen, J. E., Knudsen, L. R. & Kollias, C. G., 2016. New concept for museum storage buildings: evaluation of building performance model for simuation of storage. *4th Annual International Conference on Architecture and Civil Engineering*, Singapore, Singapore.

Christoffersen, L. D., 1993. Resource-saving storage of historical material*. 10th Triennial Meeting of the Committee for Conservation of the International Council of Museums*: *Preprints* 2, 22-27 August 1993, Washington, DC, USA. Allen Press, James and James Science Publishers Ltd, London, pp.601-604.

Christoffersen, L. D., 1995. *Zephyr: Passive climate controlled respositories; storage facilities for museum, archive and library purposes.* Thesis (Licentiate). University of Lund, Sweden, Department of Building Physics.

Church, A. H., 1872. Chemistry of the fine arts- VI: preservation and restoration of paintings in oil: oil paintings - painting with wax and paraffin. In: *The technical educator*. London: Cassell, Petter & Galpin, pp.246-248.

CIBSE, 2006. *CIBSE Guide A: Environmental design*. 7th ed., issue 2. London: CIBSE.

Cigasova, J., Stevulova, N., Schwarzova, I. & Junak, J., 2014. Innovative use of biomass based on technical hemp in building industry. *Chemical Engineering Transactions*, 37, pp.685-690.

Clarke, K. M., 1943. News and views: science in the service of art. *Nature* 3822, pp.133-133.

CMA, 2013. *A study of the economics of museum collections*. Ottawa: Canadian Museums Association.

Cohan, L. H., 1938. Sorption hysteresis and the vapor pressure of concave surfaces. *Journal American Chemical Society*, 60(2), pp.433-435.

Colinart, T., Glouannec, P. & Chauvelon, P., 2012. Influence of the setting process and the formulation on the drying of hemp concrete. *Construction and Building Materials*, 30, pp.372-380.

Colinart, T., Glouannec, P., Pierre, T. & Chauvelon, P., 2013. Hygrothermal behaviour of a hemp concrete wall: comparison between experimental and numerical results. *Proceedings of BS2013: 13th Conference of International Building Performance Simulation Association*, Chambery, France, pp.2852-2859.

Colinart, T. & Glouannec, P., 2014. Setting and drying of biobased building materials. In: *Drying and wetting of building materials and components*, 4. Springer International Publishing, pp.91-112.

Colinart, T. & Glouannec, P., 2016. Accounting for the temperature dependence in the sorption isotherms in the prediction of hygrothermal behaviour of hemp concrete. *Proceedings of Central European Symposium on Building Physics*. Dresden (Germany).

Colinart, T. & Glouannec, P., 2017. Temperature dependence of sorption isotherm of hygroscopic building materials. Part 1: experimental evidence and modeling. *Energy and Buildings*, 139, pp.360-370.

Colinart, T., Lelievre, D. & Glouannec, P., 2016. Experimental and numerical analysis of the transient hygrothermal behaviour of multilayered hemp concrete wall. *Energy and Buildings*, 112, pp.1-11.

Collet, F., Bart, M., Serres, L. & Miriel, J., 2008. Porous structure and water vapour sorption of hemp-based materials. *Construction and Building Materials*, 22, pp.1271-1280.

Collet, F. & Pretot, S., 2012. Experimental investigation of moisture buffering capacity of sprayed hemp concrete. *Construction and Building Materials*, 36, pp.58-65.

Collet, F., Chamoin, J., Pretot, S. & Lanos, C., 2013. Comparison of the hygric behaviour of three hemp concretes. *Energy and Buildings*, 62, pp.294-303.

Collet, F. & Pretot, S., 2014. Thermal conductivity of hemp concretes: variation with formulation, density and water content. *Construction and Building Materials*, 65, pp. 612-619.

Collins, J., 2012. *Science Museum Archive, RAF Wroughton, Swindon.* Structural Design Intent Document. Sylva Group Ltd. Unpublished.

Colville, J., Kilpatrick, W. & Mecklenburg, M.M., 1982. A finite analysis of multi-layered orthotropic membranes with application to oil paintings on fabric. *Studies in Conservation*, 27 (sup1), pp.146-150.

Composites UK., 2019. *Composites/FAQS/embodied energy* [Online]. Available from: https://compositesuk.co.uk/composite-materials/faqs/embodied-energy [Accessed 14.10.201].

Conrad, E. A., 2007. Climate control systems design and climate change. *Contributions to the experts' roundtable on sustainable climate management strategies*. Tenerife, Spain. The Getty Conservation Institute, p.6.

Crawford, R. H., Bartak, E., Stephan, A. & Jensen, C., 2016. Evaluating the life cycle energy benefits of energy efficiency regulations for buildings. *Renewable and Sustainable Energy Reviews*, 63, pp.435-451.

Daly, P. R. & Woolley, T., 2009. *Hemp lime composite as a building material in Irish construction*. Wexford: Environmental Protection Agency.

Dartois, S., Mom, S., Dumontet, H. & Hamida, A., 2017. An iterative micromechanical modeling to estimate the thermal and mechanical properties of polydisperse composites with platy particles: application to anisotropic hemp and lime concretes. *Construction and Building*, 152, pp.661-671.

de Bruijn, P., Jeppsson, K.-H., Sandin, K., & Nilsson, C., 2009. Mechanical properties of lime-hemp concrete containing shives and fibres. *Biosystems Engineering*, pp.474-479.

de Bruijn, P. & Johansson, P., 2013. Moisture fixation and thermal properties of lime–hemp concrete. *Construction and Building Materials*, 47, pp.1235-1242.

Dedesko, S. & Siegel, J. A., 2015. Moisture parameters and fungal communities associated with gypsum drywall in buildings. *Microbiome,* 3:71, pp.1-15.

Delgado, J., Barreira, E., Ramos, N. & de Freitas, V., 2013. Inputs for hygrothermal simulation tools. In *Hygrothermal numerical simulation tools applied to building physics*. Berlin, Heidelberg: Springer, pp.7-19.

Desco, 2017. *Report on the resilience of the engineering plant- Building ONE Wroughton*. Desco (Design & Consultancy) Ltd. Unpublished.

de Selincourt, K., 2013. The cost of building passive. *Passive house Plus* 3, pp.70-73.

Doherty, T., 2020. *Cost Guide: Walls and Insulation* [Online] Available from: https://www.self-build.co.uk/cost-guide-walls-and-insulation. [Accessed 20.01.2021].

Donahue, M.D. & Aranovich, G.L., 1998. Classification of Gibbs adsorption isotherms. *Advances in Colloid and Interface Science*, 76-77, pp.137-152.

Dubois, S., Evrard, A. & Lebeau, F., 2012. Hygrothermal modelling of lime-hemp concrete used as building material and indoor climate buffering characterization. *Structures and Environmental Technologies: International Conference of Agricultural Engineering- CIGR-AbEng 2012*. Valencia.

Dubois, S. & Lebeau, F., 2013. Hygrothermal behavior modeling of different lime-hemp concrete mixes. *ICCS13 Conference Proceedings.*

Dubois, S., Evrard, A. & Lebeau, F., 2014. Modeling the hygrothermal behavior of biobased construction materials. *Journal of Building Physics*, 38(3), pp.191-213.

Ducman, V. & Mirtič, B., 2014. Water vapour permeability of lightweight concrete prepared with different types of lightweight aggregate. *Construction and Building Materials*, 68, pp.314-319.

Duffy, E., Lawrence, M. & Walker, P., 2013. Hemp lime: highlighting room for improvement. *Civil and Environmental Research: Special Issue for International Congress on Materials & Structural Stability*, 4, Rabat, pp.16-21.

E + E Elektronik, 2018. *EE07-02 low power humidity/ temperature probe with digital output: data sheet*. [Online] Available from: https://www.epluse.com/en/sevice-support/download-centre/?filterDownload=EE07%2Datasheet [Accessed 30.08.2018].

Eberlin, M. & Carter, P. A., 2011. *Science Museum Archive: initial proposal*. Unpublished.

Eibl, M. & Burmester, A., 2013. Learning from history: historic indoor climate conditions and climate control strategies. In J. Ashley-Smith, A, Burmester & M. Eibl, eds. *Climate for Collections: Standards and Uncertainties. Postprints of the Munich Climate Conference*, 7 to 9 November 2012. Doerner Institut, pp.217-232.

Emission Zero, 2012. *Proposed new archive storage facility: option 1*. Unpublished.

Enercorp, 2008. *Which sensor? Thermistor, RTD or thermocouple*. [Online] Available from: http://www.enercorp.com/temp/Thermistors_comparison.html [Accessed 21.05.2018].

Erhardt, D. & Mecklenburg, M., 1994. Relative humidity re-examined. *Studies in Conservation,* 39 (sup2): Preventive Conservation Practice, Theory and Research. Ottawa: International Institute for Conservation of Historic and Artistic Works, pp.32-38.

Erhardt, D., Mecklenburg, M. F., Tumosa, C. S. & McCormick-Goodhart, M., 1995. Determination of allowable RH fluctuations. *Western Association for Art Conservation Newsletter*, pp.19-23.

Erhardt, D., Tumosa, C. S. & Mecklenburg, M. F., 2007. Applying science to the question of museum climate. In T. Padfield & K. Borchersen, eds. *Museum Microclimates,* National Museum of Denmark, pp.11-18.

Eshøj, B. & Padfield, T., 1993. The use of porous building materials to provide a stable relative humidity. *10th Triennial Meeting of the Committee for Conservation of the International Council of Museums: Preprints*, 2, 22-27 August 1993, Washington, DC, USA. Allen Press, James and James Science Publishers Ltd, London, pp.605-609.

European Commission, 2017. *Development and demonstration of highly insulating, construction materials from bio-derived aggregates* [Online]. European Commission. Available from: https://cordis.europa.eu/project/rcn/193427/factsheet/en [Accessed 28.03.2019].

Evrard, A., 2003. *Betons de chanvre- synthese des proprieties physique*. Saint Valerian: Association Construire en Chanvre.

Evrard, A. & De Herde, A., 2005. Bioclimatic envelopes made of lime and hemp concrete. *CISBAT 2005*, 28 to 29/9/2005. Lausanne (Switzerland).

Evrard, A., 2006. Sorption behaviour of lime-hemp concrete and its relation to indoor comfort and energy demand. *PLEA2006 - The 23rd Conference on Passive and Low Energy Architecture*, 6-8 September 2006, Geneva, Switzerland.

Evrard, A., 2008. *Transient hygrothermal behaviour of lime-hemp materials*. Thesis (PhD). Ecole Polytechnique de Louvain, Unité d'Architecture, Universite Catholique de Louvain.

Evrard, A., & De Herde, A., 2010. Hygrothermal performance of lime-hemp wall assemblies. *Journal of Building Physics*, 34(5), pp.5-25.

Fabbri, A., Chabriac, P-A., Ngo, D.C., Sallet, F., Gourdon, E., Wong, H. & Morel, J., 2015. Hygrothermal behaviour of hemp concrete: experimental evidences and modelling. In Schreler, B, Onate, E. Papadrakakis, eds. *Coupled Problems: VI International Conference on Computational Methods for Coupled Problems in Science and Engineering*, pp.1-12.

Fang, L., Clausen, G. & Fanger, P., 1998. Impact of temperature and humidity on the perception of indoor air quality. *Indoor Air* (8), pp.80-90.

Faure, P., Peter, U., Lesueur, D. & Coussot, P., 2012. Water transfers within hemp lime concrete followed by NMR. *Cement and Concrete Research*, 42(11), pp.1468-1474.

Ferdyn-Grygierek, J., 2014. Indoor environment quality in the museum building and its effect on heating and cooling demand. *Energy and Buildings*, 85, pp.32-44.

Ferdyn-Grygierek, J., 2016. Monitoring of indoor air parameters in large museum exhibition halls with and without air-conditioning systems. *Building and Environment*, 107, pp.113-126.

Florentin, Y., Pearlmutter, D., Givoni, B. & Gal, E., 2017. A life-cycle energy and carbon analysis of hemp-lime-bio-composite building materials. *Energy and Buildings* 156, pp.293-305

Florian, M.-L. E., 2000. Aseptic technique: a goal to strive for in collection recovery of moldy archival materials and artifacts. *Journal of the American Institute for Conservation,* 39 (1): Disaster preparedness, response and recovery, pp.105-115.

Flower, D. R., 2018. *Initial assessment of microbiological contamination within library archive buildings of the Science Museum Library*. IOM Consulting. Unpublished.

Fraser, M., 2009. Increasing thermal mass in lightweight dwellings using phase change materials – a literature review. *Built Environment Research Papers*, 2 (2), pp.69-83.

Freyburg, S. & Schwarz, A., 2007. Influence of the clay type on the pore structure of structural ceramics. *Journal of the European Ceramic Society*, 27, pp.1727-1733.

Frueh, A., 2017. *A cheap soil moisture sensor* [Online] Available from: http://gardenbot.org/howTo/soilMoisture/ [Accessed 03.03.2017].

Gemini Data Loggers, 2014. *Data sheet:TGU-4500(10)* [Online]. Available from: https://www.geminidataloggers.com/ [Accessed 23.04.2019].

Getty Conservation Institute, 2007. *Edited transcript: experts' roundtable on sustainable climate management strategies*. Tenerife, Spain. GCI.

Ghosal, P.S. & Gupta, A.K., 2017. Development of a generalized adsorption isotherm model at solid-liquid interface: a novel approach. *Journal of Molecular Liquids*, 240, pp.21-24

Grattan, D. & Michalski, S., 2014. *Environmental guidelines for museums* [Online]. Canadian Conservation Institute. Available from: http://www.cci-icc.gc.ca/resources-ressources/carepreventivecons-soinsconspreventive/controls-niveaux-eng.aspx [Accessed 05.02.2015].

Greenspec, 2019a. *Insulation materials and their thermal properties* [Online]. Available from: www.greenspec.co.uk/building-design/insulation-materials-thermal-properties/ [Accessed 25.08.2019].

Greenspec, 2019b. *Hemcrete @M&S Cheshire Oaks: Marks & Spencer: Cheshire Oaks retail store* [Online]. Available from: http://www.greenspec.co.uk/building-design/hemcrete-at-ms-cheshire-oaks/ [Accessed 14.10.2019].

Groom, P. & Panisset, T., 1933. Studies on penicillium chrysogenum thom, in relation to temperature and relative humidity of the air. *Annals of Applied Biology*, 20, pp.633-660.

Groskopf, C., 2016. Museums are keeping a ton of the world's most famous art locked away in storage. *Quartz* [Online]. Available from: http://qz.com/583354 [Accessed 20.06.2016].

Gualtieri, M., Gualtieri, A., Gagliardi, S., Ruffini, P., Ferrari, R. & Hanuskova, M., 2010. Thermal conductivity of fired clays: effects of mineralogical and physical properties of the raw materials. *Applied Clay Science*, 49(3), pp.269-275.

Gypsum Association, 2014. EPA concludes FGD gypsum in gypsum board contributes significant environmental and economic benefits; affirms environmental, health and safety studies. *Gypsumation* [Online]. Available from: https://www.gypsum.org/press-roomfgd-gypsum-board/ [Accessed 17.04.2018].

Hagentoft, C., Kalagasidis, A., Adl-Zarrabi, B., Roels, S., Carmeliet, J., Hens, H., Grunewald, J., Funk, M., Becker, R., Shamir, D. & Adan, O., 2004. Assessment method of numerical prediction models for combined heat, air and moisture transfer in building components: benchmarks for one-dimensional cases. *Journal of Thermal Envelope and Building Science*, 27(4), pp.327-352.

Hammond, G. & Jones, C., 2011. *Inventory of carbon & energy (ICE)*. Version 1.6a, University of Bath.

Hammond, G. & Jone, C., 2019. *Inventory of carbon and energy (ICE).* Version 3.0, Circular Ecology & University of Bath.

Hansen, E. F., Lee, S. N. & Sobel, H., 1991. The effects of relative humidity on some physical properties of modern vellum: implications for the optimum relative humidity for the display and storage of parchment. *The Book and Paper Group Annual*, Volume 10, American Institute for Conservation, pp. 1-19.

Hanwell, 2018. *Hanwell EMS comprehensive software platform* [Online]. Available from: http://hanwell.com [Accessed 28.02.2019].

Hanwell, 2018. *IM5666 - 16 channel WME sensor unit (Dampwatch) user guide*. [Online]. Available from: www.hanwell.com [Accessed 10.03.2019].

Hanwell, 2018. *Technical data sheet- SR2 base station* [Online]. Available from: http://hanwell.com [Accessed 16.10.2018].

Hassanpour, M., Shafigh, P. & Mahmud, H., 2012. Lightweight aggregate concrete fiber reinforcement: a review. *Construction and Building Materials*, 37, pp.452-461.

Hawkins, G., 2011. *BG 9/2011 Rules of thumb: guidelines for building services*. 5th Edition. Bracknell: BSRIA.

He, Y., Zhang, X., Zhang, Y. & Zhou, Y., 2014. Effects of particle characteristics of lightweight aggregate on mechanical properties of lightweight aggregate concrete. *Construction and Building Materials*, 72, pp.270-282.

Heissler, G., 1998. Engineering an interior environment for the National Archives. *Canadian Consulting Engineer*, October/November 1998, pp.34-40.

Hill, C., Norton, A. & Newman, G., 2009. The water vapor sorption behavior of natural fibers. *Journal of Applied Polymer Science* 112, pp.1524-1537.

Hirst, E.A.J., Walker, P., Paine, K.A. & Yates, T., 2010. Characterisation of low density hemp lime composite building materials under compression loading. *The 2nd international conference on sustainable construction materials and technologies,* Ancona, Italy.

Hirst, E.A.J, Walker, P., Paine, K.A. & Yates, T., 2012. Characteristics of low-density hemp lime building materials. *Proceedings of the Institution of Civil Engineers-Construction Materials*, 165(1), pp.15-23.

Hoadley, R. B., 1978. The dimensional response of wood to variation in relative humidity. *Conservation of wood in painting and the decorative arts: preprints of the contributions to the Oxford congress*, Oxford: IIC, pp.1-6.

Holcroft, N. & Shea, A., 2013. Moisture buffering and latent heat effects in natural fibre insulation materials. *Portugal SB13-Contribution of Sustainable Building to meet the EU 20-20-20 Targets*, pp.221-228.

Holcroft, N. & Shea, A., 2014. Heat of sorption and moisture buffering properties of building insulation materials. In: R. Hassan et al., eds. *CIEC 2013,* Singapore. Springer, pp. 649-661.

Holcroft, N. & Shea, A., 2015. Effect of compaction on moisture buffering of hemp-lime insulation. *First International Conference on Biobased Building Materials*, June 22-24, Clermont-Ferrand, France.

Holliday, A., 2007. *Doing and writing qualitative research*. London: SAGE Publications Ltd., pp. 42-59.

Hong, S.H., Strlič, M., Ridley, I., Ntanos, K., Bell, N. & Cassar, M., 2012. Climate change mitigation strategies for mechanically controlled repositories: the case of the National Archives, Kew. *Atmospheric environment*, 49, pp.163-170.

Hong, T., Sun, K. & Langevin, J., 2018. Building simulation: ten challenges. *Building Simulation.* Tsinghua University Press and Springer-Verlag GnbH Germany.

House of Commons, 2018. *Environmental Audit Committee: UK progress on reducing F-gas emissions.* HC 469, Fifth report of session 2017-19.

Hussain, A., Calabria-Holley, J., Jiang, Y. & Lawrence, M., 2018. Modification of hemp shiv properties using water-repellant sol-gel coatings. *Journal of Sol-Gel Science and Technology*, 86:187-197.

ICCROM-UNESCO, 2011. *International storage survey: summary* [Online]. Available from: http://www.unesco.org/new/en/culture/themes/dynamic-content-single-

view/news/stored_but_not_safe_museum_collections_are_at_risk_worldwide/#.V2j7YbiU3nE [Accessed 09.01.2014].

International Council of Museums, 2007. *Statutes* [Online]. Vienna: ICOM. Available from: http://archives.icom.museum/statutes.html [Accessed 23.04.2014].

International Energy Agency, 2019. *Global Energy & CO_2 Status Report: the latest trends in energy & emissions in 2018* [Online]. IEA. Available from: https://www.iea.org/geco [Accessed 25.03.2019].

International Institute for Conservation of Historic and Artistic Works, 2010. *Dialogues for the New Century: the plus/ minus dilemma: a way forward in environmental guidelines*. 13 May 2010, Milwaukee, Wisconsin, USA. IIC.

International Institute for Conservation of Historic and Artistic Works & International Council of Museums, 2014. *Environmental guidelines – IIC and ICOM-CC declaration*. London: IIC.

IMC Group Ltd., 2007. *Radiolog data sheet* [Online]. Available from: www.the-imcgroup.com [Accessed 29.03,2018].

IPI, 2014. *The who, why, when and how of moisture equilibration* [Online]. IPI: Rochester Institute of Technology. Available from: https://www.imagepermanenceinstitute.org/resources/newsletter-archive/v4/moisture-equilibration [Accessed 04.02.2015].

IPI, 2016. Summary of the museum preservation environment summit. *Environmental management: climate notes newsletter* [Online]. Available from: https://www.imagepermanenceinstitute.org/resources/newsletter-archive/v19/preservation-environment-summit [Accessed10.06.2016].

ISO, 2003. *ISO 11799: 2003(E): Information and documentation: document storage requirements for archive and library materials*. Geneva: ISO.

ISO, 2018. *PD ISO/TR 19815 Information and documentation: management of the environmental conditions for archive and library collections*. Geneva: ISO.

Issaadi, N., Nouviaire, A., Belarbi, R. & Ait-Mokhtar, A., 2015. Moisture characterization of cementitious material properties: assessment of water vapor sorption isotherm and permeability variation with ages. *Construction and Building Materials,* 83, pp.237-247.

Jakieła, S., Bratasz, L. & Kozłowski, R., 2008. Numerical modelling of moisture movement and related stress field in lime wood subjected to changing climate conditions. *Wood Science and Technology*, 42(1), pp.21-37.

Jami, T. & Kumar, S., 2017. *Assessment of Carbon Sequestration of Hemp Concrete*. Thesis (MA). IR&D, Gujarat Forensic Sciences University.

Jankovic, L., 2012a. *M&E design intent document: Science Museum archive*. (1st issue revised). Birmingham: Emission Zero LLP. Unpublished. Jan.

Jankovic, L., 2012b. *M&E detailed design document: Science Museum archive*. Birmingham: Emission Zero LLP. Unpublished.

Jankovic, L., 2012c. *Science Museum archive M&E redesign design document*. Birmingham: Emission Zero LLP. Unpublished.

Jankovic, L., 2012d. *Operation analysis of hemcrete museum store at Wroughton*. Emission Zero R&D Ltd. Unpublished.

Jankovic, L., 2012e. *Renewable Energy Analysis, Science Museum Archive, NMSI Wroughton, Swindon*. Emission Zero LLP. Unpublished.

Jankovic, L., 2013. *Hemcrete Museum Store at Wroughton: first year of operation*. Zero Emission R&D Ltd. Unpublished.

Jankovic, L., 2014. A method for eliminating simulation performance gap in buildings built from natural fibrous materials. In L. Malki-Epsthein et al., eds. *Proceedings of the 2013 Building Simulation and Optimization Conference*, 23-24 June, London. London: UCL.

Jankovic, L., 2016. Reducing simulation performance gap in hemp-lime buildings using Fourier filtering. *Sustainability*, 8 (9): 864, pp.1-16.

Janssen, H. & Roels, S., 2009. Qualitative and quantitative assessment of interior moisture buffering by enclosures. *Energy and Buildings*, 41, pp.382-394.

Janssen, H. & Christensen, J. E., 2013. Hygrothermal optimisation of museum storage spaces. *Energy and Buildings*, 56, pp.169-178.

Janz, M., 2001. Technique for measuring moisture storage capacity at high moisture levels. *Journal of Materials in Civil Engineering*, pp.364-370.

Janz, M. & Johannesson, B. F., 2001. Measurement of the moisture storage capacity using sorption balance and pressure extractors. *Journal of Thermal Environment and Building Science,* 24, pp.316-334.

Jiang, Y., Lawrence, M., Ansell, M. & Hussain, A., 2018. Cell wall microstructure, pore size distribution and absolute density of hemp shiv. *Royal Society Open Science*, 5:171945.

Johansson, P., Ekstrand-Tobin, A., Svensson, T. & Bok, G., 2012. Laboratory study to determine the critical moisture level for mould growth on building materials. *International Biodeterioration & Biodegradation*, 73, pp.23-32.

Johnson, E. V. & Horgan, J. C., 1979. *Museum collections storage*. Paris: Unesco.

JustBioFiber, 2019. *EcoLock* [Online]. Available from: justbiofiber.ca/ecolock/ [Accessed 23.04.2019].

Kaczorek, D., 2019. Moisture buffering of multilayer internal wall assemblies at the micro scale: experimental study and numerical modelling. *Applied Sciences*, 9, 3436, pp.1-15.

Karus, M. & Vogt, D., 2004. European hemp industry: cultivation, processing and product lines. *Euphytica*, 140, pp.7-12.

Keeley, T. & Rawlins, F.I.G., 1951. Air conditioning at the National Gallery, London: its influence upon the preservation and presentation of pictures. *Museum International*, 4(3), pp.194-197.

Kennett, S., 2006. *Innovative Adnams distribution centre minimses environmental impact* [Online]. Available from: https://www.building.co.uk/innovative-adnams-distribution-centre-minimises-environmental-impact/3072978.article [Accessed 28.10.2019].

Kerschner, R. L., 1991. A practical approach to environmental requirments for collections in historic buildings. *Journal of the American Institute for Conservation*, 31(1), pp.65-76.

Kerschner, R. L., 2013. AIC working group informs IIC and ICOM-CC work on museum environmental guidelines. *AIC News,* 38 (5), p.8.

Kim, Y.-Y., Lee, K.-M., Bang, J.-W. & Kwon, S.-J., 2014. Effect of w/c ratio on durability and porosity in cement mortar with constant cement amount. *Advances in Materials Science and Engineering*, pp.1-11.

Korecký, T., Keppert, M., Maděra, J. & Černý, R., 2015. Water transport parameters of autoclaved aerated concrete: experimental assessment of different modelling approaches. *Journal of Building Physics, 39*(2), pp.170-188.

Korolija, I., 2011. *Heating, ventilating and air-conditioning system energy demand coupling with building loads for office buildings*. Thesis (PhD). Institute of Energy and Sustainable Development, De Montfort University, Leicester.

Koronthalyova, O., Matiasovsky, P., Szabo, D. & Puskar, A., 2008. Simulation of dynamic moisture response of autoclaved aerated concrete. *Proceedings of the 8th Symposium on Building Physics in the Nordic Countries.*

Kozłowski, R., 2007. Climate-induced damage of wood: numerical modeling and direct tracing. *Contributions to the experts' roundtable on sustainable climate management strategies*. Tenerife, Spain. The Getty Conservation Institute, pp.1-12.

Kraus, M. & Kubečková, D., 2014. *Airtightness of energy efficient buildings*. VSB-Technical University of Ostrava, Faculty of Civil Engineering.

Kurpinska, M. & Ferenc, T., 2017. Effect of porosity on physical properties of lightweight cement composite with foamed glass aggregate. *ITM Web of Conferences, CMES'17*, 15, article no. 0600515, pp. 1-5.

Kumaran, M. K., 2006. A thermal and moisture property database for common building and insulating materials. *ASHRAE Transactions*, 112(Part 2), pp.485- 497.

Kumaran, M.K., Lackey, J.C., Normandin, N., Tariku, F. & Van Reenen, D., 2003. *Variations in the hygrothermal properties of several wood-based building products.* NRCC-46090. Ottawa: National Research Council of Canada.

Kupwade-Patil, K., De Wolf, C., Chin, S., Ochsendorf, J., Hajiah, A.E., Al-Mumin, A. & Büyükőztürk, O., 2018. Impact of embodied energy on materials/buildings with partial replacement of ordinary Portland Cement (OPC) by natural pozzolanic volcanic ash. *Journal of Cleaner Production* 177, pp.547-554.

Kwiatkowski, J., Woloszyn, M. & Roux, J.-J., 2009. Modelling of hysteresis influence on mass transfer in building materials. *Building and Environment*, 44, pp.633-642.

Lafontaine, R., 1979. *Environmental norms for Canadian museums, art galleries and archives*. Ottawa: Canadian Conservation Institute.

Lafontaine, R. H. & Wood, P. A., 1982. The stabilization of ivory against relative humidity fluctuations. *Studies in Conservation*, 27(3), pp.109-117.

Larsen, P. K., 2004. Moisture measurement in Tirsted Church. *Journal of Architectural Conservation*, 1(1), pp.22-35.

Larsen, P. K., Ryhl-Svendsen, M., Jensen, L. A., Bøhm, B. & Padfield, T., 2014. *Ten years experience of energy efficient climate control in archives and museum stores*. [Online]. Available from: http://www.conservationphysics.org/musdes/tenyearexp.php [Accessed 17.10.2014].

Larsson, B., Sandberg, P.I., Bankvall, C., Sikander, E. & Wahlgren, P., 2007. The effects and cost impact of poor airtightness: information for developers and clients. *The 10th international conference on Thermal Performance of the Exterior Envelopes of Whole Buildings,* 2-7 December 2007, Clearwater Beach, Florida.

Latif, E., Lawrence, M., Shea, A. & Walker, P., 2015. Moisture buffer potential of experimental wall assemblies incorporating formulated hemp lime. *Building & Environment*, 93, pp.199-209.

Latif, E., Lawrence, M., Shea, A. & Walker, P., 2018. An experimental investigation into the comparative hygrothermal performance of wall panels incorporating wood fibre, mineral wool and hemp lime. *Energy & Buildings*, 165, pp.76-91.

Laurin, G. & Scott, P., 1994. New storage facility for the National Museum of Science and Industry. *Preventive Conservation Practice, Theory and Research: Preprints of the contributions to the Ottawa Congress,* 12-16 September, 1994. IIC, pp.154-158.

Lawrence, M., Fodde, E., Paine, K. & Walker, P., 2012. Hygrothermal performance of an experimental hemp lime building. *Key Engineering Materials*, 517, pp.413-421.

Lawrence, M., 2013. The use of biobased materials to reduce the environmental impact of construction. *Civil and Environmental Research Special Issue for International Congress on Materials and Structural Stability*, 5, Rabat, pp.136-141.

Lawrence, M., Shea, A., Walker, P. & De Wilde, P., 2013. Hygrothermal performance of biobased insulation materials. *Proceedings of the Institution of Civil Engineers: Construction Materials*, 166(4), pp.257-263.

Lawrence, M., 2014. Growing our way out of climate change by building with hemp and wood fibre [Online]. *Guardian Sustainable Business, The Guardian*, 25 Sept 2014. Available from: https://www.theguardian.com/sustainable-business/2014/sep/25/hemp-wood-fibre-construction-climate-change [Accessed 02.04.2020].

Lawrence, M. G., 2005. The relationship between relative humidity and the dew point temperature in moist air: a simple conversion and applications. *Bulletin of the American Meteorological Society*, 86(2), pp.225-234.

Learmonth, G. S., 1968. *Air-conditioning and the museum environment*. University of London, Institute of Archaeology, London. Unpublished.

Leene, J., ed., 1972. *Textile conservation*. International Institute for Conservation of Historic and Artistic Works. Butterworths and Smithsonian Institution.

Legnér, M. & Luciani, A., 2013. The historical indoor climate: a long-term approach to conservation environments within heritage buildings. *Built Heritage 2013: Monitoring Conservation Management*, 18-20 November 2013, Politecnico di Milano; Italy, pp.1321-1328.

Leitch, A., 2006. *Specification for tender: temporary deep storage structure*. NMSI, Planning & Development Unit. Unpublished.

Lelievre, D., Colinart, T. & Glouannec, P., 2015. Modeling the moisture buffering behaviour of a coated biobased building material by including hysteresis. *Energy Procedia*. 78, pp. 255-260.

Leskard, M., 2015. A sustainable storage solution for the Science Museum Group. *Science Museum Group Journal* [Online], Autumn(04). Available from: http://journal.sciencemuseum.ac.uk/browse/issue-04/sustainable-storage/

Linden, J., 2014, Research on mechanical system shutdowns in collection storage areas. *AIC 42nd Annual Meeting: Collections Care + HVAC Session* [Online]. San Francisco. Available from: https://aic42ndannualmeeting2014.sched.com/event/18tkAQS/collection-care-hvac-session [Accessed 03.02.2017].

Lo, T. & Cui, H. Z., 2004. Effect of porous lightweight aggregate on strength of concrete. *Materials Letters*, 58, pp.916-919.

Lo, T., Tang, W. & Nadeem, A., 2008. Comparison of carbonation of lightweight concrete with normal weight concrete at similar strength levels. *Construction and Building Materials*, 22, pp.1648-1655.

Löwgren, B.H., Bergmann, J. & Alves-Filho, O., 2020. A numerical implementation of the Soret Effect in drying processes. *ChemEngineering* 4, 13, 14pp.

Łukomski, M., 2012. Painted wood: what makes the paint crack? *Journal of Cultural Heritage*, 13S, pp.S90-S93.

Lull, W. P., 1994. Further comments on climate control guidelines. *The Abbey Newsletter* [Online], 18(7). Available from: http://cool.conservation-us.org/byorg/abbey/an/an18/an18-7/an18-707.html [Accessed 25.08.2014].

Maalouf, C., Lachi, M., Mai, T. H. & Wurtz, E., 2013. Numerical and experimental study of the hygric inertia of a hemp lime concrete. *International Journal of Mathematical Models and Methods in Applied Sciences*, 7(2), pp.149-156.

Maalouf, C., Tran Le, A.D., Umurigirwa, S.B., Lachi, M. & Douzane, O., 2014. Study of hygrothermal behaviour of a hemp concrete building envelope under summer conditions in France. *Energy and Buildings*, 77, pp.48-57.

MacIntyre, J. A., & Buckley, H., 1930. The fading of water-colour pictures. *The Burlington Magazine for Connoisseurs*, 57(328), pp.31-34.

MacIntyre, J. A., 1934a. Some problems connected with atmospheric humidity. *Atmospheric humidity in relation to works of art*. London: Courtauld Institute, pp.7-16.

MacIntyre, J., 1934b. Air conditioning for Mantegna's cartoons at Hampton Court Palace. *Technical Studies in the Field of Fine Arts*, 2(4), pp.171-177.

Macleod, K., 1975. *Relative humidity: its importance, measurement and control in museums*. Ottawa: National Museums of Canada, pp.1-15.

Matsushita, F., Aono, Y. & Shibata, S., 2004. Calcium silicate structure and carbonation shrinkage of a tobermorite-based material. *Cement and Concrete Research*, 34, pp.1251-1257.

May, N., 2005. *Breathability: The key to building performance.* Oxford.

McAlinden, B., 2015. *Embodied energy and carbon* [Online]. ICE. Available from: https://www.ice.org.uk/knowledge-and-resources/briefing-sheet/embodied-energy-and-carbon [Accessed 26.03.2019].

McCabe, J. F., 1917. Report of James T. McCabe superintendent of buildings and grounds submitted at the anniversary meeting: new building. *The Bulletin of the Cleveland Museum of Art*, pp. 131-133.

McCabe, J. W., 1931. Humidification and ventilation in art museums. *Museum News*, September, pp. 7-8.

McCrady, E., 1994. Temperature & RH guidelines challenged by Smithsonian. *Abbey Newsletter*, 18(4-5, Aug-Sept) [Online]. Available from: http://cool.conservation-us.org/byorg/abbey/an/an18/an18-4/an18-404.html [Accessed 17.08.2014].

McCrady, E., 1995. Indoor environment standards: a report on the NYU Symposium. *Abbey Newsletter*, 19(6-7) [Online]. Available from: http://cool.conservation-us.org/byorg/abbey/an/an19/an19-6/an19-602.html [Accessed 25.08.2014].

McGregor, F., Heath, A., Shea, A., & Lawrence, M., 2014. The moisture buffering capacity of unfired clay masonry. *Building and Environment*, 82, pp.599-607.

McLaren, D. (2109). The problem with net-zero emissions targets. *Carbon Brief* [Online]. Available from: https://www.carbonbrief.org/guest-post-the-problem-with-net-zero-emissions-targets [Accessed 30.09.2019].

McManus, N. C., 2003. *ASHRAE Guidelines* [Online] Available from: http://cool.conservation-us.org/byform/mailing-lists/cdl/2003/0997.html [Accessed 30.09.2019].

Mecklenburg, Marion F. 1991. Applied mechanics of materials in conservation research. In P.B. Vandiver, J.R. Druzik & G.S. Wheeler, G. S., eds. *Materials Issues in Art and Archaeology II*. Pittsburgh, Pennsylvania: Materials Research Society, pp.105-122.

Mecklenburg, M. F., McCormick-Goodhart, M. & Tumosa, C. S., 1994. Investigation into the deterioration of paintings and photographs using computerized modeling of stress development. *Journal of the American Institute for Conservation, 33 (2): papers from the conservation research and technical studies update session and the general session on collections in historic buildings of the 21st annual meeting of the AIC*. Denver, Colorado, May 31- June 6, 1993, pp.153-170.

Mecklenburg, M. F. & Tumosa, C., 1999. Temperature and relative humidity effects on the mechanical and chemical stability of collections. *ASHRAE Journal* 41, pp.69-74.

Mecklenburg, M. F., 2007. *Determining the acceptable ranges of relative humidity and temperature in museums and galleries: part 1, structural response to relative humidity.* Smithsonian Museum Conservation Institute.

Melia, P., Ruggieri, G., Sabbadini, S. & Dotelli, G., 2014. Environmental impacts of natural and conventional materials: a case study on earth plasters. *Journal of Cleaner Production*, 80, pp.179-186.

Merriman, N., 2008. Museum collections and sustainability. *Cultural Trends,* 17(1), pp.3-21.

Met Office, 2018. *Past weather events:snow and low temperatures February to March 2018* [Online]. Available from: https://www.metoffice.gov.uk/weather/learn-about/past-uk-weather-events [Accessed 18.03.2019].

Meyer, C., 2001. A case in case study methodology. *Field Methods*, 13(4), pp.329-352.

Michael, C., 2013. *Using a dehumidifier in a museum (or archive, or gallery)* [Online]. Available from: https://www.meaco.com/blog/using-a-dehumidifier-in-a-museum-or-archive-or-art-gallery/ [Accessed 08.09.2019].

Michalski, S., 1990. An overall framework for preventive conservation and remedial conservation. *9th Triennial Meeting of the Committee for Conservation of the International Council of Museums: Preprints,* 2, 26-31 August 1990, Dresden, German Democratic Republic. Los Angeles: ICOM Committee for Conservation, pp, pp.589-591.

Michalski, S., 1993. Relative humidity: a discussion of correct/incorrect values.*10th Triennial Meeting of the Committee for Conservation of the International Council of Museums: Preprints*, 2, 22-27 August 1993, Washington, DC, USA. Allen Press, James and James Science Publishers Ltd, London, pp.624-628.

Michaski, S., 2000. *Technical Bulletin No. 23: guidelines for humidity and temperature in Canadian archives*. Ottawa: Canadian Conservation Institute.

Michalski, S., 2007. The ideal climate, risk management, the ASHRAE chapter, proofed fluctuations, and toward a full risk analysis model. *Contributions to the experts' roundtable on sustainable climate management strategies.* Tenerife, Spain. The Getty Conservation Institute, pp.1-19.

Michalski, S., 2011. Museum climate & global change: doing the right thing for both. *Reflections on Conservation*. Ottawa: Canadian Conservation Institute, pp. 9-11.

Mitchell, S., 2019. Outside the comfort zone: energy consumption and museums. *The Australian Museum Blog* [Online]. Available from: https://australianmuseum.net.au/blog-archive/at-the-museum/outside-the-comfort-zone-energy-consumption-and-museums/ [Accessed 02.08.2019].

Moore, M., 2010. *NMSI sustainable development policy*. NMSI. Unpublished.

Moore, M., 2013. *Science Museum, Hemcrete Museum Store: entry for museums and heritage awards*. Unpublished.

Morse, A., 2014. Crizzling. *AIC wiki: a collaborative knowledge resource* [Online]. Available from:https://www.conservation-wiki.com/wiki/crizzling [Accessed 05.102019].

Mukhopadhyaya, P., Kumaran, K., Normandin, N. & Goudreau, P., 2002. Effect of surface temperature on water absorption coefficient of building materials. *Journal of Thermal Envelope and Building Science,* pp.179-195.

Murphy, F., Pavia, S. & Walker, R., 2010. An assessment of the physical properties of lime-hemp concrete. *Proceedings of the bridge and concrete research in Ireland, Cork.* Cork.

Museums + Heritage, 2014. *Sustainability in the museum sector*. Available from: https://advisor.museumsandheritage.com [Accessed 23 May 2014].

Myrefelt, S., 2004. Reliability and functional availability of HVAC systems. *Proceedings of the 4th International Conference for enhanced building operations (ICEBO 2004).* October 18-19, Paris, France, pp.2-18.

Nallaperumal, K. & Krishnan, A. 2013. *Engineering research methodology: a computer science and engineering and information and communication technologies perspective* [Online]. Available from: https://www.researchgat.net/publication/259183120 [Accessed 26.04.2018].

National Gallery of Art, 2016. *NGA then and now: air conditioning* [Online]. Available from: https://www.nga.gov/feature/thenandnow/air.shtm [Accessed 21.11.2016].

NatSCA & ICON, 2013. *Care and conservation of geological specimens* [Online]. Available from: https://icon.org.uk [Accessed 27.08.2015].

Neuhaus, E. & Schellen, H.L., 2007. Conservation heating for a museum environment in a monumental building. *Thermal Performance of the Exterior Envelopes of Whole Buildings X, Proceedings*. Atlanta, GA, USA: American Society of Heating, Refrigerating and Air-Conditioning Engineers, pp.02-07.

Neuhaus, E., 2012. A criticial look at HVAC-systems in the museum environment. In J. Ashley-Smith, A, Burmester & M. Eibl, eds. *Climate for Collections: Standards and Uncertainties. Postprints of the Munich Climate Conference*, 7 to 9 November 2012. Doerner Institut, pp.117-126.

Ngala, V. & Page, C., 1997. Effects of carbonation on pore structure and diffusional properties of hydrated cement pastes. *Cement and Concrete Research*, 27(7), pp.995-1007.

NCS Suffolk, 2017. Conservation plan for the archive collections of the Suffolk record office. *The Hold: A Suffolk Archives Service for the 21st Century* (HG-014-08167 The Hold 14.Conservation Plan). National Conservation Service.

NMDC, 2003. *Too much stuff? Disposal from museums*. National Museum Directors' Conference.

NMDC, 2008. *NMDC guiding principles for reducing museums' carbon footprint*. National Museums Directors' Conference.

Noblecourt, A., 1958. *Protection of cultural property in the event of armed conflict*. Paris: Unesco .

Ntanos, K. & Van Snick, S., 2010. Environmental assessment without limits. *The National Archives: choices in conservation: practise versus research.* ICOM-CC Graphic Documents Working Group Interim Meeting, Copenhagen.

Ntanos, K., 2014. The road to sustainable environmental management of storage conditions at the National Archives. *AIC 42nd Annual Meeting: Conscientious Conservation: sustainable choices in collection care: abstract book.* Collections Care + HVAC Session, San Francisco, p.38.

Odbcontracts, 2006. *Building manual (Part 1) at deep store library facility at Wroughton Wiltshire.* Unpublished.

Oddy, A., 2011. Harold Plenderleith and the conservation of antiquities and works of art. *Intervention*, International Journal of Conservation, Restoration and Museology, pp.56-62.

Office for National Statistics, 2020. *Construction Output Price Indices*. Brewster, I. (ed). [Online]. Available from: https://www.ons.gov.uk/businessindustryandtrade/constructionindustry/datasets/interimconstructionoutputpriceindices [Accessed 13.01.2021].

Office International des Musees, 1938. La conservation des peintures. *Mouseion*, 41-42, pp.1-11.

Office of Public Affairs, 1994. *Work of Smithsonian scientists revises guidelines for climate control in museums and archives*. Washington, DC: Smithsonian Institution.

Omega Engineering, 2018. *pt1000 temperature sensor* [Online]. Available from: https://www.omega.co.uk/prodinfo/rtd.html [Accessed 25.05.2018].

Omega Engineering, 2018. *Thermistor* [Online]. Available from: https://www.omega.co.uk/prodinfo/thermistor.html [Accessed 25.05.2018].

Omega Engineering, 2018. *What temperature probe is better for you?* [Online]. Available from: https://www.omega.co,uk/temperature/z/thermocouple-RTD.html [Accessed 25.05.2018].

Osanyintola, O., Talukdar, P. & Simonson, C., 2006. Effect of initial conditions, boundary conditions and thicknesses on the moisture buffering capacity of spruce plywood. *Energy and Buildings*, 38, pp.1283-1292.

Osanyitola, O. F. & Simonson, C. J., 2006. Moisture buffering capacity of hygroscopic building materials: experimental facilities and energy impact. *Energy and Buildings*, pp.1270-1282.

Pacheco-Torgal, F., Jalali, S. & Fucic, A., eds, 2012. *Toxicity of building materials*. Woodhead Publishing.

Padfield, T. & Landi, S., 1966. The light-fastness of the natural dyes. *Studies in Conservation*, 11(4), pp.181-196.

Padfield, T.& Jensen, P., 1990. Low energy climate control in museum stores. *9th Triennial Meeting of the Committee for Conservation of the International Council of Museums: Preprints,* 2, 26-31 August 1990, Dresden, German Democratic Republic. Los Angeles: ICOM Committee for Conservation, pp.596-601.

Padfield, T., Bøllingtoft, P., Eshøj, B. & Christensen, M.C., 1994. The wall paintings of Gundsømagle church, Denmark. *Studies in Conservation*, 39(sup2), pp.94-98.

Padfield, T., 1996. Low energy climate control in museum stores- a postscript. *11th Triennial Meeting of the Committee for Conservation of the International Council of Museums: Preprints,* 1, 1-6 September 1996, Edinburgh, Scotland. London: James and James Science Publishers, pp.68-71.

Padfield, T., 1998. *The role of absorbent building materials in moderating changes of relative humidity*. Thesis (PhD), The Technical University of Denmark, Department of Structural Engineering and Materials, Lyngby.

Padfield, T., 1999a. Humidity buffering of interior spaces by porous absorbent insulation. *Report: hygrothermal properties of alternative insulation materials*. (series R, No.61). Department of Structural Engineering and Materials, Technical University of Denmark, Lyngby, Denmark.

Padfield, T., 1999b. On the usefulness of water absorbent materials in museum walls.*12th Triennial Meeting of the Committee for Conservation of the International Council of Museums: Preprints,* 29 August - 3 September, 1999, Lyon, France. James and James Science Publishers Ltd, London, pp. 83-87.

Padfield, T., 2007. Exploring the limits for passive indoor climate control. *Contributions to the experts' roundtable on sustainable climate management strategies.* Tenerife, Spain. The Getty Conservation Institute, pp.1-12.

Padfield, T., Larsen, P. K., Jensen, L. A. & Ryhl-Svendsen, M., 2007. The potential and limits for passive air conditioning of museums, stores and archives. In T. Padfield & K. Borchersen, eds. *Museum Microclimates*, National Museum of Denmark, pp.191-198.

Padfield, T., 2008. Simple climate control in archives. *Nordic Symposium on Building Physics*, June 2008.

Padfield, T. & Jensen, L. A., 2009. *Humidity buffer capacity of some building materials* [Online]. Available from: www.conservationphysics.org [Accessed 20.10.2014].

Padfield, T., 2010. *The psychrometric chart explained* [Online]. Available from: www.conservationphysics.org/mollier/moll1.htm [Accessed 02.07.2020].

Padfield, T. & Jensen, L. A., 2010. *Humidity buffering by absorbent materials* [Online]. Available from: www.conservationphysics.org [Accessed 07.102.104].

Padfield, T. & Jensen, L., 2011. Humidity buffering of building interiors by absorbent materials. *9th Nordic Symposium on Building Physics - NSB 2011*, pp. 475-482.

Padfield, T., 2013. *Conservation physics*. An online textbook in serial form.

Padfield, T., Larsen, P.K., Ryhl-Svendsen, M. & Jensen, L.A., 2013. Low energy museum storage. *Papers delivered at the Paris Conference of the Centre de Recherche sur la Conservation des Collections* [Online]. Available from: www. conservationphysics. org/storage/low energy-museum-storage. php. [Accessed 05.09.2014].

Pallot, A. C., 1946. Améneagement de refuges destines a recevoir les oeures d'art et objects de musee en temps de guerre. *Mouseion*, 55-56 (I-II), pp.17-33.

Payraudeau- Le Roux, N., Meille, S., Chevalier, E. & Adrien, J., 2016. In situ observation of plaster microstructure evolution during thermal loading. *Fire and Materials*, 40, pp.973-984.

Pegasus Group, 2017. *Building One pre-application planning statement- the Science Museum Group at Wroughton*. Unpublished.

Pel, L., Kopinga, K., Bertram, G. & Lang, G., 1995. Water absorption in a fired-clay brick observed by NMR scanning. *Journal of Physics D: Applied Physics*, 28, pp.675-680.

Pervais, M. & Sain, M., 2003. Carbon storage potential in natural fiber composites. *Resources Conservation & Recycling*, 39, pp.325-340.

Plenderleith, H. J., 1943. Preservation of museum objects in war-time. *Nature*, 152 (3847), pp.94-97.

Plenderleith, H. J., 1956. *The conservation of antiquities and works of art: treatment, repair and restoration*. Oxford University Press.

Plenderleith, H. J. & Philippot, P., 1960. Climatology and conservation in museums. *Museum*, (4), pp.243-289.

Plenderleith, H. & Werner, A., 1971. *The conservation of antiquities and works of art* (2nd ed.). Oxford University Press.

Plenderleith, H. J., 1998. A history of conservation. *Studies in Conservation* 43 (3), pp.129-143.

Poelmans, N., 2016. *Hempcrete as a sustainable material for heritage storage: applicability and transition*. Thesis (MSc). Engineering Sciences, University of Leuven.

Portland Cement Association, 2017. *How cement is made* [Online]. Available from: http://www.cement.org/cement-concrete-applications/how-cement-is-made [Accessed 27.02.2018].

Preusser, F. D., 1997. Meeting on collections environments, Washington, D.C., Sept. 3-5, 1997. *Abbey Newsletter* [Online].. Available from: LISTSERV 16.0 - MUSEUM-L Archives [Accessed 26.01.2017].

Prislan, Š. J., Cerar, E. & Živković, V., 2014. Who cares? We do: a nationwide survey of museum storage in Slovenia. *17th Triennial Meeting of the Committee for Conservation of the International Council of Museums: Preprints,* 15-19 September 2014*,* Melbourne, Australia. Paris: ICOM Committee for Conservation.

Pritchett, I., 2012. *Contractor's proposals prelims document for NMSI project*. Hemcrete Projects Ltd. Unpublished.

Proctor, K., 2016. *Energy efficient membranes: minimising condensation within buildings*. A. Proctor Group Ltd.

Pullen, T., 2016. *Which wall material has the best U Value?* [Online]. Available from: https://www.homebuilding.co.uk/which-wall-material-has-the-best-u-value/ [Accessed 27.01.2020].

Qu, X. & Zhao, X., 2017. Previous and present investigations on the components, microstructure and main properties of autoclaved aerated concrete: a review. *Construction and Building Materials*, 135, pp.505-516.

Quay, J., 2019. *Building ONE, Wroughton low and zero carbon technology report*. London: Desco Ltd. Unpublished.

Rahim, M., Douzane, O., Tran Le, A., Promis, G., Laidoudi, B., Crigny, A., Dupre, B. & Langlet, T., 2015. Characterization of flax lime and hemp lime concretes: hygric properties and moisture buffer capacity. *Energy and Buildings*, 88, pp.91-99.

Rajasekar, S., Philominathan, P. & Chinnathambi, V., 2006. *Research methodology* [Online]. arXiv:physics/0601009 [physics.gen-ph]. Cornell University. Available from: arxiv.org [Accessed 22.05.2018].

Rawlins, F. I. G., 1942. Care of works of art in war-time. *Nature*, 150, pp.112-114.

Rawlins, F. I. G., 1943. The National Gallery in war-time. *Nature*, 151, pp.123-128.

Rawlins, F. I. G., 1947. Natural science and the fine arts. *Nature*, 159, pp.628-630.

Read, J., 2011. *Feasibility study for boiler replacement of A Store*, Bexley: C.J. Design Partnership Ltd. Unpublished.

Real, W. A., 1994. Some thoughts on the recent CAL press release on climate control for cultural collections. *Abbey Newsletter*, 18(7) [Online]. Available from: http://cool.conservation-us.org/byorg/abbey/an/an18/an18-7/an18-706.html [Accessed 25.08.2014].

Resistant Building Products, 2015. *Multi-Pro XS*.Technical Data Sheet RESXSTD0310/001.

Resistant Building Products, 2017. *Multi-Pro XS*. Technical Data Sheet RESMPTD1113/001.

Rhydwen, R., 2006. *Building with hemp and lime*. Center for Alternative Technology, Graduate School of the Environment.

Rode, C., Holm, A. & Padfield, T., 2004. A review of humidity buffering in the interior spaces. *Journal of Thermal Envelope and Building Science*, 27, pp.221-226.

Rode, C., ed, 2005. *Moisture buffering of building materials*. Department of Civil Engineering, Technical University of Denmark.

Rode, C., Peuhkuri, R., Time, B., Svennberg, K. & Ojanen, T., 2006. Moisture buffer value of building materials. *Symposium on Heat-Air-Moisture Transport: Measurements on Building Materials*, Toronto, Ont., pp.1-15.

Rode, C., Peuhkuri, R., Time, B., Svennberg, K. & Ojanen, T., 2007. Moisture buffer value of building materials. *Journal of ASTM International*, 4(5), pp.1-12.

Roels, S. & Janssen, H., 2005. Is the moisture buffer value a reliable material property to characterise the hygric buffering capacities of building materials? *Conference paper, Laboratory of Building Physics,* KU Leuven, Belgium.

Roels, S. & Janssen, H., 2006. A comparison of the Nordtest and Japanese test methods for the moisture buffering performance of building materials. *Journal of Building Physics*, 30, pp.137-161.

Roels, S., Janssen, H., Carmeliet, J., Diepens, J. & de Wit, M., 2006. Hygric buffering capacities of uncoated and coated gypsum board. In G. R. Fazio, ed. *3rd International Building Physics Conference: research in Building Physics and Building Engineering*, pp.27-32.

Roveti, D. K., 2001. *Choosing a humidity sensor: a review of three technologies* [Online]. Available from: https://www.sensorsmag.com/components/choosing-a-humidity-sensor-a-review-three-technologies [Accessed 21.05.2018].

Rubene, S., Vilnītis, M. & Noviks, J., 2014. Monitoring of the aerated concrete construction drying process by electrical impedance spectrometry. *Proceedings of 4th International Conference "Advanced Construction 2014",* Lithuania, Kaunas, 9-10 October 2014. Kaunas: Kaunas University of Technology, pp.216-220.

Ryhl-Svendsen, 2007. The role of air exchange rate and surface reaction rates on the air quality in museum storage buildings. In T. Padfield & K. Borchersen, eds. *Museum Microclimates*, National Museum of Denmark, pp.221-226.

Ryhl-Svendsen, M. & Clausen, G., 2009. The effect of ventilation, filtration and passive sorption on indoor air quality in museum storage rooms. *Studies in Conservation* 54 (1), pp.35-48.

Ryhl-Svendsen, M., Jensen, L.A., Larsen, P.K. & Padfield, T., 2010. Does a standard temperature need to be constant? *Meddelelser om konservering*, *1*, pp.13-20.

Ryhl-Svendsen, M., Jensen, L. A., Larsen, P. K., Bøhm, B. & Padfield, T., 2011. Ultra low energy museum store. *16th Triennial Meeting of the Committee for Conservation of the International Council of Museums,* 19-23 September 2011, Lisbon, Portugal. Paris: ICOM Committee for Conservation, pp.19-23.

Ryhl-Svendsen, M., Jensen, L.A., Bøhm, B. & Larsen, P.K., 2012. Low energy museum storage buildings: climate, energy consumption and air quality. *UMTS Research Project 2007-2011: Final Data Report: Project no. 10821521*. Conservation: Research, Analysis & Consulting, National Museum of Denmark.

Sachs, R., 2015. *Pt100, Pt1000 or NTC- which is the right sensor?* [Online]. Available from: https://blog.wik.com/knowhow/pt100-pt1000-or-ntc-which-is-the-right-measuring-element/# [Accessed 21.05.2018].

Saeidpour, M. & Wadso, L., 2016. Moisture diffusion coefficients of mortars in absorption and desorption. *Cement and Concrete Research*, 83, pp.179-187.

Samri, D., 2008. *Analyse physique et caractérisation hygrothermique des matériaux de construction: approche expérimentale et modélisation numérique.* Thesis (PhD). L'Institut National des Sciences Appliquees de Lyon.

Schober, G., 2011. Porosity in autoclaved aerated concrete (AAC): a review on pore structure, types of porosity, measurement methods and effects of porosity on properties. *5th International Conference on Autoclaved Aerated Concrete*, pp.351-359.

Schoch, T. & Kreft, O., 2011. The influence of moisture on the thermal conductivity of AAC. In *5th International conference on Autoclaved Aerated Concrete: securing a sustainable future,* Bydgoszcz, Poland, pp. 361-370.

Scribner, B. W., 1934. The preservation of records in libraries. *The Library Quarterly*, 4(3), pp.371-383.

Shea, A., Lawrence, M. & Walker, P., 2012. Hygrothermal performance of an experimental hemp lime building. *Construction and Building Materials*, 36, pp.270-275.

Simonson, C., Salaonvaara, M. & Ojanen, T., 2004. Heat and mass transfer between indoor air and a permeable and hygroscopic building envelope: part II- verification and numerical studies. *Journal of Thermal Enviroment and Building Science*, 28(2), pp.161-185.

Simpson, W., 1993. Determination and use of moisture diffusion coefficient to characterize drying of northern red oak (Quercus rubra). *Wood Science and Technology*, 27, pp.409-420.

Sinka, M., Sahmenko, G., Korjakins, A., Radina, L. & Bajare, D., 2015. Hemp thermal insulation concrete with alternative binders, analysis of their thermal and mechanical properties. In *IOP Conference Series: Materials Science and Engineering* 96. 2nd International Conference on Innovative Materials, Structures and Technologies
30 September to 2 October 2015, Riga, Latvia**.** IOP Publishing Ltd.

SMG, 2017. *One collection facility: design team and project team brief*. Unpublished.

SMG Conservation & Collections Care, 2018. *SMG collections environment guidance*, Conservation & Collections Care, Science Museum Group. Unpublished.

Smith, R., 2018. End grain, edge grain, face grain. *Woodworker's Journal* [Online]. Available from: https://www.wagnermeters.com/end-edge-and-face-grain/ [Accessed 23.05.2018].

Staniforth, S., 2008. Conservation heating to slow conservation: a tale of the appropriate rather than the ideal. In *Contributions to the experts' roundtable on sustainable climate management strategies.* Tenerife, Spain. The Getty Conservation Institute, pp.1-19.

Staniforth, S. & Hayes, B., 1987. Temperature and relative humidity measurement and control in National Trust houses. *8th Triennial Meeting of the Committee for Conservation of the International Council of Museums: Preprints,* 6-11 September 1987, Sydney, Australia. Los Angeles: Getty Conservation Institute, pp.915-926.

Staniforth, S., Hayes, B. & Bullock, L., 1994. Appropriate technologies for relative humidity control for museum collections housed in historic buildings. *Studies in Conservation*, 39(Supplement 2), pp.123-128.

Stauderman, S. & Tompkins, W.G., eds, 2016. Summit on the museum preservation environment. *Proceedings of the Smithsonian Institution on the Museum Preservation Environment*. Washington, D.C.: Smithsonian Institution Scholarly Press

Sterflinger, K., 2010. Fungi: their role in deterioration of cultural heritage. *Fungal Biology Reviews*, 24 (1-2), pp.47-55.

Stillwell, S. & Knight, R., 1931. *An investigation into the effect of humidity variations on old panel paintings on wood*. Forest Products Research Laboratory, Department of Scientific and Industrial Research. Controller of His Majesty's Stationery Office.

Strandberg-de Bruijn, P. & Johansson, P., 2014. Moisture transport properties of lime-hemp concrete determined over the complete moisture range. *Biosystems Engineering*, pp.31-41.

Straube, J., 2006. Moisture and materials. *Building Science Digest*(138), pp.137-139.

Sun, G., Sun, W., Zhang, Y. & Liu, Z., 2011. Relationship between chloride diffusivity and pore structure of hardened cement paste. *Journal of Zhejiang University-Science A (Applied Physics & Engineering)*, 5, pp.360-367.

Sutton, A., Black, D. & Walker, P., 2011. *IP 14/11: Hemp lime: an introduction to low-impact building materials*, BRE. ISBN 978-1-84806-225-2

Sylva Group, 2011, November. *D2 storage facility foundation plan*. Unpublished.

Terzic, E., Terzic, J., Nagarajah, R. & Alamgir, M., 2012. Capacitive sensing technology. In *A Neural Network Approach to Fluid Quantity Measurement in Dynamic Environments*, Springer-Verlag, pp.11-37.

The National Gallery, 2016. *Improving our environment_research_paintings* [Online]. Available from:https://www.national gallery.org.uk/paintings/research/improving-our-environment?viewPage=4 [Accessed 21.11. 2016].

Royal Ontario Museum, 1978. *In search of the black box: a report on the proceedings of a workshop on micro-climates held at the Royal Ontario Museum*. Toronto: ROM.

Thickett, D., Csefalayova, L. & Strlič, M., 2011. Smart conservation: targeting controlled environments to improve sustainability. *16th Triennial Meeting of the Committee for Conservation of the International Council of Museums* 19-23 September 2011, Lisbon, Portugal. Paris: ICOM Committee for Conservation, pp.19-23.

Thomson, G., 1978. *The museum environment*. London: Butterworth & Co.Ltd.

Thomson, G., 1986. *The museum environment*. 2nd ed. London: Butterworth & Co. Ltd.

Time, B., 1998. *Hygroscopic moisture transport in wood.* Thesis (PhD). Trondheim: Norwegian University of Science and Technology.

Tradical, 2014. *Building lime innovation; hemp lime technology* [Online]. Available from: www.tradicalcom/pdf/Tradical_Information_Pack_small.pd [Accessed 23.07.2014].

Tran Le, A., Maalouf, C., Mai, T., Wurtz, E. & Collet, F., 2010. Transient hygrothermal behaviour of a hemp building envelope. *Energy and Buildings*, pp.1797-1806.

Turner & Townsend, 2018. *International construction market survey*. [Online]. Available from: https://www.turnerandtownsend.com. [Accessed 05.02.2019].

UK Hempcrete, 2019. *Better than zero carbon buildings* [Online].Available from: https://www.ukhempcrete.com/services/better-than-zero-carbon-buildings/ [Accessed 11.08.2019].

UN Environment & IEA, 2017. *Towards a zero-emission, efficient, and resilient buildings and construction sector.* International Energy Agency; Global Alliance for Buildings and Construction (Global Status Report 2017). United Nations Environmental Programme.

UNESCO, 1968. The conservation of cultural property- with special reference to tropical conditions. *Museums and Monuments XI*. Switzerland: UNESCO.

University of Bath, 2010. *Low carbon hemp house put to the test* [Online] Available from https://www.bath.ac.uk/announcements/low-carbon-hemp-house-put-to-the-test/ [Accessed 02.01.2019].

V&A, 2015. *Sustainability at the V&A- Victoria & Albert Museum* [Online]. Available from: http://www.vam.ac.uk/content/articles/s/v-and-a-sustainability/ [Accessed 14.10.2014].

Vici, P.D., Mazzanti, P. & Uzielli, L., 2006. Mechanical response of wooden boards subjected to humidity step variations: climatic chamber measurements and fitted mathematical models. *Journal of Cultural Heritage*, 7(1), pp.37-48.

Vereecken, E., Saelens, D. & Roels, S., 2011. A comparison of different mould prediction models. *Proceedings of Building Simulation 2011: 12th Conference of International Building Performance Simulation Association*, Sydney, pp.1934-1941.

Vereecken, E. & Roels, S., 2012. Review of mould prediction models and their influence on mould risk evaluation. *Building and Environment*, 51, pp.296-310.

Vici, P. D., Mazzanti, P. & Uzielli, L., 2006. Mechanical response of wooden boards subjected to humidity step variations: climatic chamber measurements and fitted mathematical models. *Journal of Cultural Heritage*, 7(1), pp.37-48.

Walker, R, & Pavia, S., 2014a. Influence of the type of binder on the properties of lime-hemp concrete. In C. Llinares-Millán et al., eds. *Construction and Building Research*. Switzerland: Springer International Publishing, pp. 505-514.

Walker, R. & Pavia, S., 2014b. Moisture transfer and thermal properties of hemp lime concrete. *Construction and Building Materials*, 64, pp.270-276.

Walker, R., Pavia, S. & Mitchell, R., 2014. Mechanical properties and durability of hemp lime concretes. *Construction and Building Materials*, 61, pp.340-348.

Waller, R., 1985. Pyrite disease: cause and treatment. In *Abstracts from the AIC Preprints, 13th annual meeting.* Washington, D.C., p.1.

Waller, R. & Shelton, S., 1989. Risk management strategies applied to the development of pragmatic solutions to collections storage problems. *Society for the Preservation of Natural History Collections 4th Annual Meeting Programme and Abstracts*. Calgary: SPNHC, p.32.

Waller, R., 1994. Conservation risk assessment: a strategy for managing resources for preventive conservation. *Studies in Conservation*, 39(2), pp.12-16.

Waller, R., 1995. Risk management applied to preventive conservation. In C. L. Rose, C. A. Hawks, H. H. Genoways, eds. *Storage of natural history collections: a preventive conservation approach.* Pittsburgh, Pa: Society for the Preservation of Natural History Collections, pp. 21-27.

Waller, R., 2002. A risk model for collection preservation. *13th Triennial Meeting of the Committee for Conservation of the International Council of Museums*, 22-27 September 2002, Rio de Janeiro. London: James and James Science Publishers Ltd., pp.22-27.

Waller, R. & Michalski, S., 2004. Effective preservation: from reaction to prevention. *Conservation Perspectives*, The Getty Conservation Institute Newsletter,19.1 Spring 2004 [Online]. Available from: http://www.getty.edu/conservation/publications_resources/newsletters/19_1/feature.html [Accessed 27.08.2014]

Wan, H., Xu, Xinhua, Goa, J.J. & Li, A., 2017. A moisture penetration depth model of building hygroscopic material. *Procedia Engineering,* 205, pp.3235-3242.

Wang.Y. & Xi, Y., 2017. The effect of temperature on moisture transport in concrete. *Materials*, 10, 926.

Waterhouse, E. K., Collins Baker, C. H. & MacIntyre, J., 1934. Mantegna's cartoons at Hampton Court. *The Burlington Magazine for Connoisseurs*, 64(372), pp.102-115.

Weaver, J., Stout, G. & Coremans, P., 1950. The Weaver report on the cleaning of pictures in the National Gallery. *Museum*, 3(8), pp.113-135.

Weintraub, S., 2006. The museum environment: transforming the solution into a problem. *Collections: A journal for museum and archives professionals*, 2(3), pp.195-218.

Wendler, E. & Charola, A., 2008. Water and its interaction with porous inorganic building materials. *Hydrophobe V: 5th International Conference on Water Repellant Treatment of Building Materials,* Aedificatio Publishers, pp.57-74.

Willmott Dixon, 2010. *The impacts of construction and the built environment*. Briefing Note 33, Willmott Dixon, pp.1-6.

Wilson, W. K., 1995. *Environmental guidelines for the storage of paper-based records in libraries and archives*. (Technical Report NISO TR01-1995), Bethesda, Maryland: National Information Standards Organisation.

Woloszyn, M., Kalamees, T., Abadie, M., Steeman, M. & Kalagasidis, A., 2009. The effect of combining a relative-humidity-sensitive ventilation system with the moisture-buffering capacity of materials on indoor climate and energy efficiency of buildings. *Building and Environment*, 44, pp.515-524.

World Nuclear Association, 2011. *Comparison of lifecycle greenhouse gas emissions of various electricity generation sources*. (WNA report). London: WNA.

WorldWeatherOnline, 2018. *Historical weather data* [Online] Available from: https://www.worldweatheronline.com/' title='Historical average weather'>Data provided by WorldWeatherOnline.com [Accessed 15.01.2018].

Wu, T., Wei, X. & Xing, G., 2016. Factors influencing the mechanical properties of lightweight aggregate concrete. *Indian Journal of Engineering & Materials Sciences*, 23, pp.301-311.

Younes, C., Abi Shdid, C. & Bitsuamlak, G., 2011. Air infiltration through building envelopes: a review. *Journal of Building Physics*, 35 (3), pp.267-302.

Yu, Q. & Brouwers, H., 2012. Thermal properties and microstructure of gypsum board and its dehydration products: a theoretical and experimental investigation. *Fire and Materials,* 36, pp.575-589.

Zammit, D., 2006. *Wish list from Sustainability Development*. SCM Library contractors brief. Unpublished.

Zhang, M., Qin, M. & Chen, Z., 2017. Moisture buffer effect and its impact on indoor environment. *Procedia Engineering: 10th International Symposium on Heating, Ventilation and Air Conditioning.* ISHVAC 2017, 19-22 October 2017, Jinan, China, pp. 1123-1129.

Appendix A Tables of thermal and hygroscopic values for HLC and conventional building materials

Table of thermal values as found in the literature for HLC and for conventional materials used in museum storage building applications

Material group	Density ρ Kg/m^3	Thermal conductivity λ W/(m·K)	Specific heat capacity c K/kg·K	Thermal diffusivity α m^2/s	Thermal effusivity ξ J/s$^{1/2}$·m^2·K
HLC[1,4,5,6,8]	220-600	0.06-0.13	1000-1560	1.4E-07	320
Concrete[2,3,7]	1700-2400	1.04-2.06	1000	3.0E-07 - 7.61E-07	1700-2006
AAC[3,7]	400-1300	0.15-0.70	840-1000	3.33E-07	330-346
Brick[3,7]	1200-2000	0.36-0.77	850-1000	4.4E-07	1161-1230
Gypsum board[2,3]	700-800	0.16-0.25	840-1000	3.4E-06	383
Wood[2,3]	480-720	0.072-0.14	1680	1.5E-07	
Plywood[2,3,9]	300-700	0.050-0.73	1210-1800		
Fibre board[2,3]	200-800	0.052-0.18	1700		

References:

[1] Arnaud & Gourlay, 2012
[2] BS EN ISO 10456:2007
[3] CIBSE, 2006
[4] Collet & Pretot, 2014
[5] Evrard & De Herde, 2005
[6] Evrard, 2008
[7] Evrard & De Herde, 2009
[8] Lawrence et al., 2012
[9] Osanyintola et al., 2006

Table of hygroscopic values as found in the literature for HLC and for conventional hygroscopic building materials used in museum storage building applications

Material group	**Total porosity %vol**	**Moisture penetration depth mm**	**Water vapour diffusion resistance factor μ**	**Water vapour permeability value δp kg/(m·s·Pa)**	**Moisture absorption coefficient kg/m^2/h$^{1/2}$**	**Moisture diffusivity m^2/s**
HLC[2,3,4,5,7,8,9]	0.711-0.85	70-120	4.84-8.98	2.23E-11-1.0E-08	4.44-4.5	1.4E-07
Cement[6,8,9,15]	0.18	6	180	0.005E-09	0.018-1.5	5.5E-11 - 6.0E-07
AAC[8,9,15]	0.73-0.82	52	8	6.21E-11 - 2.76E-11	3.96	4.6E-10 - 3.3E-05
Brick[6,8,9,15]	0.23-0.31	104	15	0.03E-09	0.00083-21.6	1.8E-08
Gypsum board[6,12,14,15]	0.52	33	7.3-13.5	0.025E-09	960	1.9E-09
Wood[9,15]	0.73	16	130-200	0.015E-09	0.24	1.35E-07
Plywood[9,10,11,13,14,15]	0.70	12.5-16	130-142	0.015E-09 - 1.6E-07	0.70-0.23	4.3E-10 - 4.10E-07
Fibre board[6,10,11,14]	0.98	6.87	4.6-6.1	1.7E-05 - 3.1E-05	0.083-0.312	1.48E-10 - 2.54E-09

References:

[1] CIBSE, 2006
[2] Cerezo, 2005
[3] Collet et al., 2008
[4] Collet et al., 2013
[5] Collet & Pretot, 2014
[6] Delgado et al., 2013
[7] Evrard & De Herde, 2005
[8] Evrard, 2008
[9] Evrard & De Herde, 2009
[10] Kumaran et al., 2003
[11] Kumaran, 2006
[12] Latif et al., 2015
[13] Osanyintola et al., 2006
[14] Roels & Janssen, 2000
[15] Rode et al., 2005

Appendix B Library & Archives Store: Building & Plant Designs

Stack and ducting design

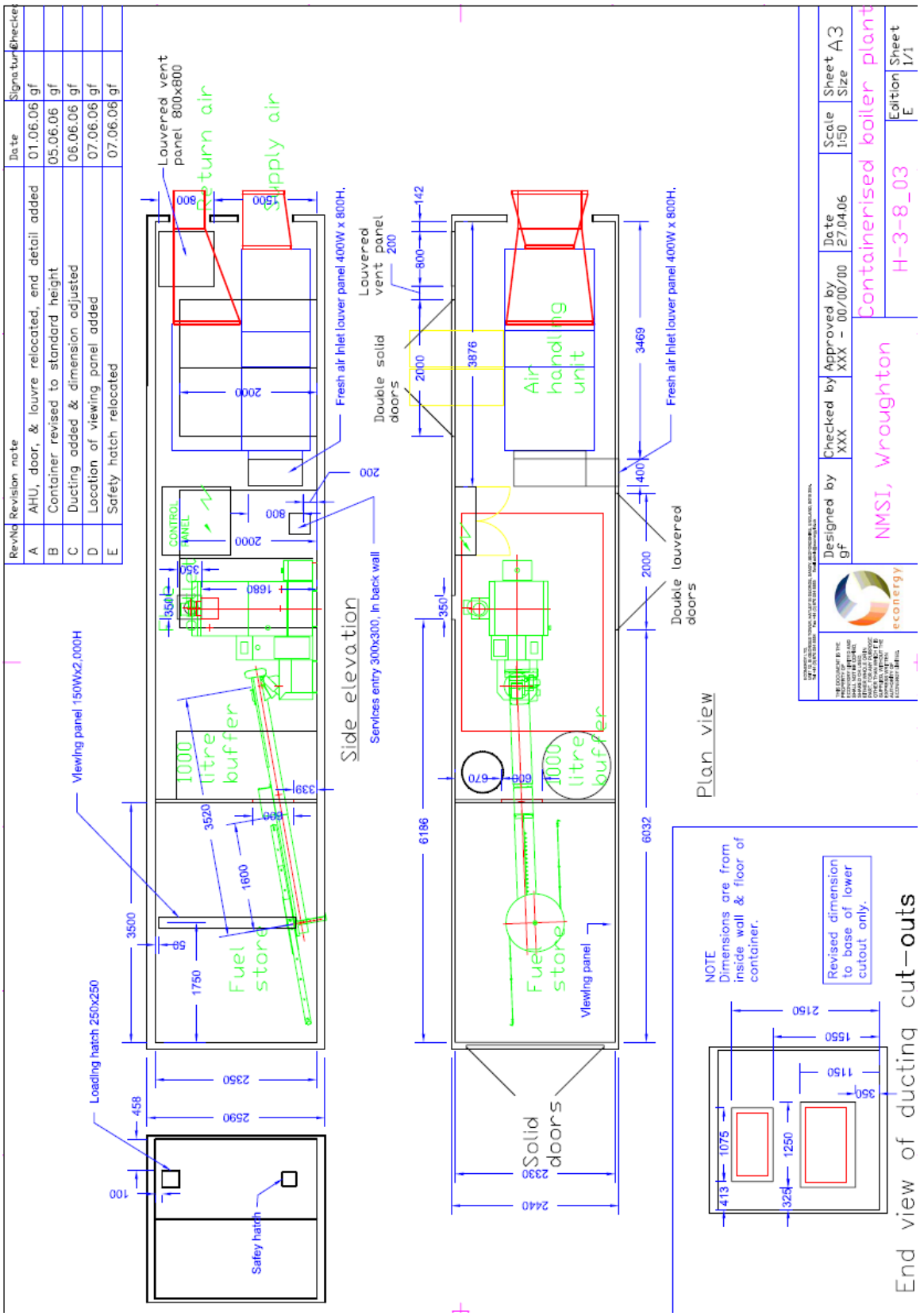

Container, boiler side and front plan views

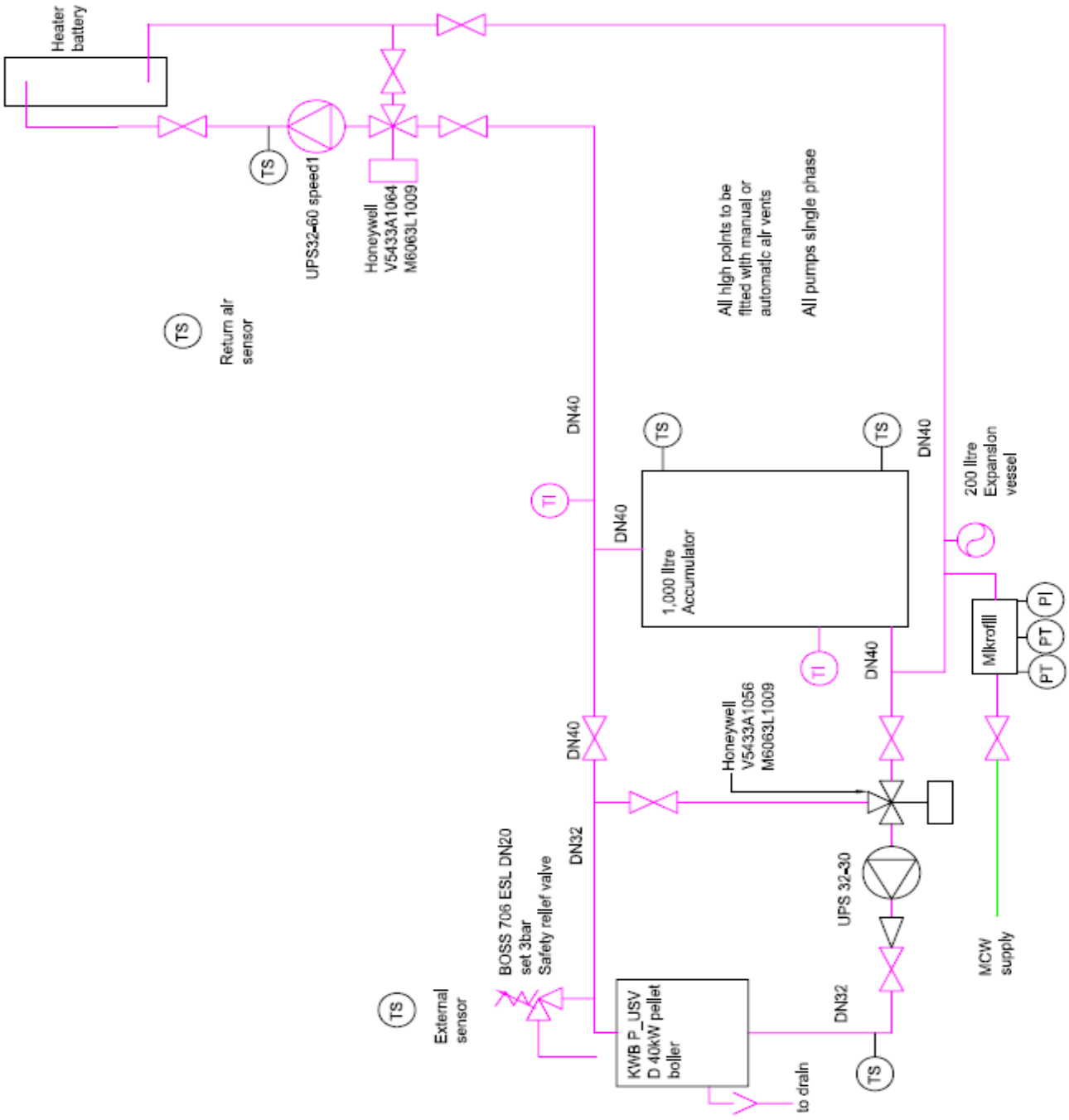

M&E schematic

Appendix C Data sheets: Construction materials & HVAC equipment

Hembuild® Pre-cast Wall Systems

Hembuild® Systems

Hembuild®, the factory produced, off-site system incorporating the structural frame into the timber cassette, creating a building envelope solution for 1 – 3 storey buildings.

Lime Technology can supply and install factory made (pre-dried) Hembuild® panels to site to offer the following options:-

- Panel supply and erection together with the upper floors and roof.
- Whole envelope solution that includes the render, doors and windows to leave a fully tested airtight shell, ready for services and second fix.

By using Hembuild® customers get a quick build and a predictable programme at all times of the year giving the thermal advantages of solid wall construction in a programme time of lightweight timber frame.

Like Hemclad®, Hembuild® can be supplied in a range of U-values from 0.10 to 0.22 W/m²K to provide a thermally efficient building envelope. Its unique combination of thermal inertia and insulation buffers changes in temperature to create a stable environment and greatly reduce energy usage.

The system can be used to meet high levels of the code for sustainable homes and for BREEAM excellent buildings such as schools and commercial buildings.

Hembuild® is a registered Trademark of Lime Technology and has patents pending on the system.

Hemp Lime Technology

Tradical® Hemcrete® Information Downloads

Introduction to Tradical® Hemcrete®

1. Introduction

Tradical® construction materials are developed products of the Lhoist Group based on high purity manufactured lime materials. The Lhoist Group is an international business focussed on the supply of high purity lime products to many industries including the construction industry.

Tradical® Hemcrete® is a unique, highly sustainable construction product for the creation of insulating walls as well as insulation layers for floors and roofs. Hemcrete® is a blend of specially prepared hemp shiv (Tradical® HF) and a special lime based binder (Tradical® HB). Together these products form a bio-composite building material that can be used both for the creation of buildings that have excellent thermal and acoustic properties as well as creating a healthy living and working environment.

Additionally Tradical® Hemcrete® has the ability to make an impact on the future of sustainable building. Helping to reverse the damaging effects of greenhouse gases, Tradical® Hemcrete® locks up approximately 110kg of CO_2 per m^3 of wall and provides one of the best value materials for low impact, sustainable and commercially viable construction.

Produced mainly from renewable sources, Tradical® Hemcrete® is mixed on site for fast track construction and delivers high levels of insulation, air-tightness and vapour permeability.

Properties:

- Low density
- High thermal insulation
- High sound insulation
- High thermal inertia
- Good vapour permeability
- Good flexibility
- Fire and pest resistant
- Can significantly reduce CO_2 emissions
- Inherently airtight structures
- Low waste

Hemcrete® Products' Components

Tradical® HF
Tradical® HF is a hemp aggregate made from the stem of the hemp plant. It is chopped, graded and de-dusted to give a natural, sound and breathable product. Cultivated in the UK without agrochemicals, it is harvested annually. A renewable primary material, the industrial processing is mechanical and requires little energy and zero toxic products.

Tradical® HB
Tradical® HB is a special binder based on the purest hydrated air lime blended manufactured to BS EN 459 part 1 with selected cementitious, hydraulic and inorganic materials. This ensures the perfect particle size distribution and setting characteristics to create the correct binder for use with Tradical® HF hemp shiv.

Hemcrete® is available thanks to the collaboration of Lhoist UK Ltd., Lime Technology Ltd and Hemcore Ltd. Lhoist bring their expertise as the largest manufacturers of lime in the world and also the benefit of many years' research and development of binders for hemp in France. Lime Technology specialise in the development of lime based construction materials for environmental building uses. Hemcore are the pioneers of growing and processing industrial hemp in the UK.

Hemp Lime Technology

Tradical® Hemcrete® Information Downloads

3. Materials

Tradical® Hemcrete® is a bio-composite building material made by mixing specially prepared hemp shiv (Tradical® HF) with a lime based binder (Tradical® HB).

a) Lime

Lime is produced by heating calcium carbonate (limestone, chalk, shells, coral etc.) in a kiln to a temperature of approx. 900°C. At this temperature the calcium carbonate is chemically changed, or calcined, to form calcium oxide (known as quick lime or lump lime).

Air Limes and Hydraulic Limes

The raw material - calcium carbonate, will vary according to its point of origin. Calcium Carbonate sources that are pure are used to produce high purity limes and these are known as air limes. These high purity limes are used in applications that require the characteristics of consistently manufactured chemical products. Calcium Carbonate sources that are contain impurities are inevitably the more common in geology. Some of these impurities provide the characteristic of hydraulicity in limes. Hydraulicity is a term that relates to the nature of the setting mechanism of lime in a mortar form.

Setting of Lime Mortars

The setting mechanism for mortars with hydraulic limes is a combination of the principal setting where water is required for the formation of cementitious compounds incorporating the impurities; and air where carbon dioxide is absorbed in the recarbonation of the lime to calcium carbonate.

Water and quicklime are combined in a process known as hydration to produce hydrated lime. If only an exact amount of water is added, the end product is a dry powder and is generally known as hydrated lime or lime hydrate. If an excess of water is used (always putting the quick lime into the water) the process is normally referred to as slaking or slacking and the end product is a colloidal gel, often sold in plastic tubs and known as lime putty.

The setting mechanism for high purity air limes is where only the carbon dioxide absorption provides the setting process.

Tradical® air lime is one of the purest air limes produced anywhere in the world.

b) Tradical® HB – Hemp binder

Tradical® HB is a pre-formulated binder based on a high purity air lime manufactured in accordance with the requirements of BS EN 459. It is a blend of UK produced Tradical® lime, Cement and other pozzolanic and mineral additions. It has been carefully formulated and tested over many years to ensure consistent, quality results when used with hemp.

Other Binders

Please note that cementitious or hydraulic binders that have not been designed to be used with hemp may produce unacceptable results. The failure is often related to there being a competition for water between the binder and the hemp. If the binder has insufficient moisture for the hyrdraulic components to set, then the result can be a mixture of damp hemp and/or dry powder.

RESISTANT Building Products

multi-pro XS

RESXSTD0310/001

Technical Data Sheet

Multi-Pro XS is a Medium Density Magnesium Silicate panel which has been developed to provide the System Build and Off-Site Construction Markets with a new fire rated external wall panel system. Multi-Pro XS is tested to BS EN 594 (Racking), is Non-Combustible, has a low environmental impact and provides a stable substrate to bond various finishes.

Externally, Multi-Pro XS can be faced with Plastisol Steel, acrylic based render systems, or brick slips, providing your design team with unlimited options. Internally, Fire rated laminated plasterboard using Cova PVC coverings can be used to provide the internal finish of your choice.

60 minute Fire Wall
for modular construction

Key:

1 12mm Fireline plasterboard with COVA PVC finish
2 9mm **MultiPro XS**
3 Plasticol coated 0.5mm steel
4 Timber Floor
5 RWA 45 Insulation
6 Window Opening
7 Timber Floor
8 Timber Frame

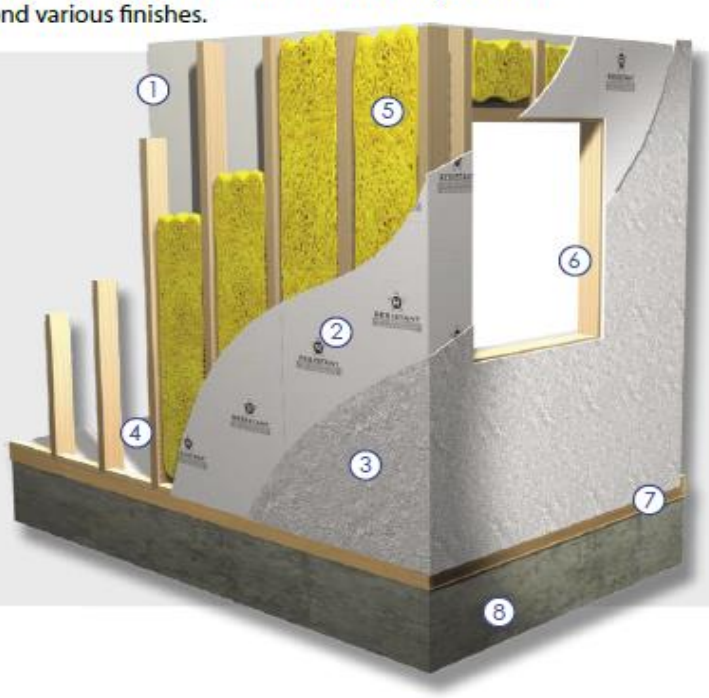

MANUFACTURE

RESISTANT Multi-pro XS is manufactured using inorganic substances, Si02, CaCO3,Mgo, MgCl2, and alkaline resistant fibreglass mesh.

The product is naturally cured using no energy through cold fusion unlike similar competitive products on the market which use autoclaving technology. This ensures that RESISTANT Multi-Pro XS has a relatively low impact on the environment. Multi-Pro XS achieves its superior strength and flexibility by the introduction of four layers of alkaline resistant glass fibre mesh. Consistent high quality of the product is maintained and monitored through a sophisticated digitally controlled process to ensure a superior finished board always reaches our commitment to quality assurance.

TYPICAL USES

It is ideal for applications requiring a combination of these properties, for example:

- Closed Cell Timber Frame
- Fire Rated Modular Construction
- Prisons
- Park Homes
- Anti-Vandal Units
- False Chimney Breasts

RESISTANT

multi-pro

RESMPTD1113/002

Technical Data Sheet

Technical SPECIFICATION

Test Subject	Test	Result
Density Dry (ex works)		1050 kg/m ^{3} (+/- 10%)
Modulus of Rupture	BSEN 310	20 Nmm ^{2}
Modulus of Elasticity	BSEN 310	4540 Nmm ^{2}
Impact Strength (Brinell)		34 Nmm ^{2}
Vapour Resistance	BSEN 12086:1997	2.0 MNs/g
Durability	BSEN 12467 : 2012	Category B - PASSED
Thermal Conductivity at 50°	BSEN 594	0.307 w/m/°k
Fire Test	A1 Euroclass	Class Non-Combustible
Change in thickness (After immersion in water)	BSEN 317	0 - 0.1% Nmm ^{2}
Tensile Strength (Perpendicular to plane)	BSEN 319	2.11 Nmm ^{2}
Screw Withdrawal Strength	BSEN 320	81.1N/mm
Pull through Resistance of Fixings	BSEN 1383:199	1.267 KN
Average Thickness Swelling	BSEN 321	0
Average Tensile Strength	BSEN 321	2.04 Nmm ^{2}
Moisture Content	BSEN 322	3.6%
Fire Resistance Steel	BSEN 1364 - 1	60 minutes

DIMENSIONS

Resistant Multi-pro is supplied as a rectangular board with square edges and white in colour.

Thickness: 3, 6, 9 & 12 mm

Sizes: 1200 x 2400 mm, 600 x 2400 x 3mm

Special size requirements and thicknesses are available upon request depending on quantity.

TOLERANCES

Length and Width:	+ / - 2mm
Thickness:	+ / - 0.2mm
Edge Straightness:	1mm / metre
Squareness of edge:	< 3mm

PAVATHERM

Universal Wood Fibre Insulation for Internal Use on Walls, Roofs, Floors and Ceilings

pavatex

Construct. Insulate. Relax.

Pavatherm Characteristics

Produced According to EN 13171

Pavatherm wood fibre thermal insulation rigid panels have a variety of interior uses, for example they can be used flush against rafters, walls and floors, as well as insulating the cavity between the rafters, studs and floor joists. Thanks to their high density they also improve the acoustic insulation of walls, floors, ceilings and roofs. When the Pavatherm insulation panels are fixed flush to studs or rafters they will significantly reduce thermal bridging through the timber elements and so will save on energy costs.

Pavatherm boards are natural, breathable rigid insulation boards with a high thermal mass and a long thermal lag time. This means they keep buildings warmer in winter and cooler in summer in all climates. Pavatherm has a specific heat capacity of 2100 J/kgK which is very favourable compared to mineral wool (800 J/kgK approx) or expanded polystyrene insulation (1400 J/kgK approx). It is very important to take summer heat protection into account particularly if the attic space of a house is to be used as a living or working space or if the property has a lot of south facing glazing which often contributes to excess solar gain during the warm weather. The building will remain at a more ambient, comfortable temperature all year round, because the excess heat will be stored in the wood fibre, and released slowly as the temperature drops.

Pavatherm insulation boards, with a vapour diffusion factor of $\mu = 3$, are open to diffusion and ensure effective water vapour transmission through the structure, to provide a comfortable, healthy living space. The condensation will not get trapped in the middle of the structure which could cause mould growth, wet rot or dry rot.

The CE marked Pavatex wood fibre insulation panels are made from new timber off-cuts sourced from local sawmills. In turn this timber is sourced from sustainable FSC and PEFC certified forests and the wood fibre boards are made almost entirely from natural raw materials and so will not emit any toxic chemicals into the interior environment as denoted by their Natureplus certification. The wood fibre boards are carbon neutral, which means that during their lifetime, they will not release any extra carbon dioxide into the atmosphere than the trees absorbed during their growing period.

Pavatherm

Thickness (mm)	Weight (kg / m²)	Board Size (cm)	No. Boards Per Pallet	M² per Pallet	KG per Pallet	Edge Profile
40	4.6	102 x 60	112	68.54	333	Square Edge
60	6.9	102 x 60	72	44.06	322	Square Edge
80	9.2	102 x 60	48	29.38	288	Square Edge
100	11.5	102 x 60	40	24.48	300	Square Edge
120	13.8	102 x 60	32	19.58	288	Square Edge
140	16.1	102 x 60	32	19.58	333	Shiplap
160	18.4	102 x 60	28	17.14	333	Shipap

Technical Details	Pavatherm
Density (kg / m³)	110
Declared Thermal Conductivity λ D (W/mK)	0.038
Vapour Diffusion Factor μ	3
Specific Heat Capacity - C (J/kgK)	2100
Tensile Strength Perpendicular to Plane of Board (kPa)	2.5
Compression Strength at 10% (kPa)	50
Fire Behaviour (EN 13501-1)	Class E
Building Material Class (DIN 4102-1)	B2
Waste Code According to European Waste Catalogue	030105 - 170604
Identification Code	WF-EN13171-T4-CS(10/Y)50-TR2.5-WS2,0-MU5-AF100

Application

Insulating Roofs

Pavatherm can be installed below the roof rafters in renovation projects to very effectively reduce the risk of thermal bridging. It can also be placed in between the rafters if cut carefully to ensure a tight fit. If insulating above the rafters with Isolair or Pavatherm-Plus sarking boards, Pavatherm can be placed on top of the rafters first and then the water resistant Isolair or Pavatherm-Plus boards can overlay the Pavatherm, to provide rain protection during construction. This will give greater thermal efficiency if required. The underside of the rafters should be sealed with an airtight membrane. Pavatherm wood fibre will protect the property from overheating during summer-time which is particularly critical in buildings where the attic space is used for living accommodation and in dormer bungalows, as well as in buildings with lots of south facing windows.

Insulating Walls

Pavatherm is suitable for interior timber stud or cavity masonry wall insulation and can be even used externally behind a ventilated façade so long as it is protected by the more water resistant Isolair or Pavatherm-Plus products. However it is not suitable for direct plastering so must be finished with plasterboard or other similar wall board. The wood fibre boards can also be inserted in between the stud cavity, but it is much easier to use the flexible wood fibre batts, Pavaflex, to ensure a tight fit. A cavity should not be left between the wall and the Pavatherm insulation because this will cause interstitial condensation. Masonry walls must be dry and flat before insulating so if the wall is uneven it must be re-plastered first with a breathable plaster. If insulating solid walls, we recommend using Pavadentro or Pavadry which are specifically made for this purpose as they control the passage of water through the structure, due to their integral mineral layer.

Breathable insulation is particularly important when insulating solid walls (SWI) on historic or heritage properties because these walls were built to be vapour-open structures. Covering these walls with a waterproof material will affect the building physics of the wall structure and may cause untold damage to the wall. The optimum solution for solid wall insulation is to use Diffutherm externally or Pavadentro or Pavadry internally along with lime plaster or render, as this is very vapour open, and mould does not grow on it due to it being alkaline. Pavatherm wood fibre boards have a high vapour permeability which means that they absorb and desorb moisture efficiently, as relative humidity changes. This avoids interstitial condensation, mould growth, dust mite populations and humidity in buildings, so a pleasant living environment will be created. As well as significantly improving the thermal efficiency and mass, it will also enhance the sound insulation.

Insulating Floors

Pavatherm can be used to insulate both solid and timber joist floors and it will also reduce both impact and airborne noise transmission through floors. Because of its reasonable compression strength (50 kPa), Pavatherm is recommended as a thermal insulator as well as an impact sound insulator under screed floors, so long as there will be no excessive loading on the floor. Pavaboard offers greater compression strength if there will be heavy loading on the floor. Pavatherm can also be inserted in between the timber floor joists if cut carefully to avoid air gaps. A very effective thermal and acoustic insulation result will be achieved if the Pavatherm panels are laid floating on top of a timber sub-deck which can then be covered with timber flooring.

Cutting and Storing the Wood Fibre Softboards

The panels can be cut with normal timber cutting tools e.g. a jigsaw with Pavatex blades, a circular saw or reciprocating saw. It is recommended to use suction equipment to minimize dust. If a hole or gap occurs in the wood fibre due to a construction error, ensure that it is filled in with wood fibre pieces. Keep the boards dry when in storage and protect from damage. Do not stack any more than 4 pallets on top of each other.

Acara Concepts Ltd
Killossery
Kilsallaghan
Swords
Co. Dublin, Ireland
Tel UK: 020 7998 1690
Tel IRL: +353 (0)1 8409 286
info@acaraconcepts.com

www.acaraconcepts.com

ENVIROGRAF® PRODUCT 92

FIRE RETARDANT COATING FOR TIMBER

DESCRIPTION

A water-based clear or white coating for internal/external application by brush, roller or spray. Achieved Class 0/Class 1 protection with two applications at 12-15m² per litre. Coverage on the first coat may vary according to the density and type of timber. UV protection is available.

USE

Can be used on bamboo, chipboard, decorative laminates, furniture, plywood, MDF, melamine, timber, etc. ES/VFR can be applied first and then be coated over with a range of coatings. If using QVFR externally, a top coat is required to seal the flame retardant layer. See separate coatings booklet for more details and colour charts.

PERFORMANCE

VFR coatings have had numerous tests on many surfaces and over coated surfaces to meet BS476 Part 6 (1989) Spread of Flame and BS476 Part 7 (1989) Spread of Flame, and **this coating system now complies with Classification B/S1/d0 of European Standard EN13501 Parts EN13823 (2002) single burn test (SBI) and EN11925-2 (2002) ignitability.**

ORDERING REFERENCES:

Reference	Coating	Based on	Int/Ext	Finishes
QVFR/C	Clear protection	Water	Both	M
QVFR/W	White protection	Water	Both	M
ES/VFR/C	Clear protection	Water	Both	M
ES/VFR/W	White protection	Water	Both	M
ES/VFR/P	Primer	Water	Both	–
AEC	White acrylic top coat	Water	Internal	SG

A range of top coats is available. Please see new data sheet for full details.
Finishes: M=matt, SG=semi-gloss, G=gloss)

KS1000 RW Trapezoidal

Product Data Sheet

Kingspan Insulated Panels

Applications

The KS1000 RW is a metre wide through-fix trapezoidal profiled insulated wall panel which is ideal for both horizontal and vertical applications.

Available Lengths

Standard Lengths	1.8m - 12m
Longer Lengths (non-standard)	12m – 29.3m
Shorter Lengths (non-standard)	Below 1.8m

Notes:
Additional costs and transport restrictions may apply for non-standard lengths. All lengths may change for export (outside of the UK).

Dimensions, Weight & Thermal Performance

Core Thickness (mm)	40	50	60	70	80	100	115	120	137	150
Overall Thickness (mm)	71	81	91	101	111	131	146	151	168	181
U-value (W/m²K)	0.46	0.38	0.35	0.30	0.25	0.20	0.18	0.16	0.15	0.14
Weight kg/m² 0.5/0.4 Steel	9.9	10.3	10.7	11.0	11.5	12.3	12.8	13.1	13.7	14.2
Weight kg/m² 0.7/0.5 Alum	5.5	5.9	6.3	6.7	7.1	7.9	8.5	8.7	9.4	9.9

Notes:
The U-values have been calculated using the method required by the Building Regulations Part L2 (England & Wales) and Building Standards Section 6 (Scotland).

KS1000 RW Trapezoidal

Product Data Sheet

Insulation Core
KS1000 RW insulated wall panels are manufactured with an ECO*safe* and FIRE*safe* polyisocyanurate (PIR) core.

Fire
The external and internal faces of the panel to be Class 0 in accordance with the Building Regulations when tested to BS 476: Part 6: 2009 and Part 7: 1997.

This FIRE*safe* system has passed all the requirements of LPS 1181: 2005: Part 1: Issue 1.1, ceiling lining tests by the Loss Prevention Certification Board (LPCB) certified to LPS 1181 Grade EXT – B and achieves periods of fire resistance (EXT-A), for further information please contact Kingspan Technical Services. This system is also FM approved to FMRC 4880 & 4881 Class 1 fire classification, unlimited height, for wall applications.

Environmental
This ECO*safe* system achieves a Green Guide A+ rating as per the BRE Global "The Green Guide to Specification", Green Guide 2008 ratings. Green Guide element no. 806600001.

Air Leakage
An air leakage rate of $3m^3/hr/m^2$ at 50Pa or less can be achieved when using Kingspan insulated roof and wall panels.

Acoustic
Sound Reduction Index (SRI)

Hz*	63	125	250	500	1K	2K	4K	8K
SRI (dB)	20	18	20	24	20	29	39	47

* Frequency

The KS1000 RW insulated wall panel has a single figure weighted sound reduction Rw = 25dB.

Biological
Kingspan panels are normally immune to attack from mould, fungi, mildew and vermin. No urea formaldehyde is used in the construction, and the panels are not considered deleterious.

Materials
Substrate
- Kingspan XL Forté, Kingspan Spectrum, Kingspan AQUA*safe* and Kingspan CLEAN*safe*: S220GD+ZA hot-dip zinc / aluminium Galfan coated steel to BS EN 10346: 2009. Standard external sheet thickness 0.5mm, standard internal sheet thickness 0.4mm.
- Bright White Polyester: Hot dip zinc coated to BS EN 10346: 2009, Standard internal steel thickness 0.4mm.
- Stainless Steel: Austenitic Grade 304 stainless steel to BS EN 10088: Part 2: 2005, thickness 0.4mm.
- Aluminium: Please contact Kingspan Technical Services.

Coatings - External Weather Sheet
- Kingspan XL Forté: Consists of a multi-layer organic coating, embossed with a traditional leather-grain finish.
- Kingspan Spectrum: Consists of a coated semi-gloss finish with slight granular effect.

Coatings - Internal Liner Sheet
- Bright White Polyester: The coating has been developed for use as the internal lining of insulated panels. Standard colour is "bright white" with an easily cleaned surface.
- Kingspan AQUAsafe: The coating has been developed for use as the internal lining of insulated panels to suit high humidity internal environments (class 5 as defined by the Building Regulations).
- Kingspan CLEANsafe: The coating has been developed for use as the internal lining of insulated panels where a high level of cleanliness and hygiene is required, and the panels are to be cleaned down on a regular basis.
- Stainless Steel: The stainless steel liner has been developed for use as the internal lining of insulated panels in buildings with a very aggressive/corrosive internal environment.

Gyproc FireLine

Product Data Sheet

Introduction

Used in British Gypsum partition, wall lining and ceiling systems to give increased fire protection. Also used for protection to structural steel.

Product description

Gypsum plasterboard with glass fibre and other additives in the core. Gyproc FireLine consists of an aerated gypsum core with glass fibre and other additives encased in, and firmly bonded to, strong paper liners. Gyproc FireLine is a plasterboard that is suitable for drylining internal surfaces.

This plasterboard is one of the products within our plasterboard range that is certified to BES 6001 achieving a rating of 'Very Good'.

BES 6001 Responsible Sourcing www.greenbooklive.com

Board performance

Fire protection

Plasterboard linings provide good fire protection owing to the unique behaviour of the non-combustible gypsum core when subjected to high temperatures. The inclusion of glass fibre and other additives in the core of Gyproc FireLine improves its fire protective properties when compared with standard plasterboard. For the purposes of the national Building Regulations, plasterboard is designated a 'material of limited combustibility' (Approved Document B). The surfaces of Gyproc FireLine are designated Class 0 (for the purposes of national Building Regulations). Please refer to the table below.

Fire resistance / sound insulation

Please refer to the appropriate **White Book** product or systems section for information on the fire resistance and sound insulation of building elements lined with Gyproc FireLine, available to download at www.british-gypsum.com.

Reaction to fire test performance

Standard	Performance
BS 476: Part 6: 1989 Method of test for fire propagation for products.	*Index of performance (I) not exceeding 12 and a sub-index (i1) not exceeding 6.*
BS 476: Part 7: 1997 Surface spread of flame tests for materials.	*Class 1 (both sides).*
EN 520: 2004 + A1: 2009	*Classified without further testing as A2-s1, d0.*

Thermal conductivity

λ Gyproc FireLine - 0.24W/mK

Effect of temperature

Gyproc FireLine is unsuitable for use in areas subject to continuously damp or humid conditions, i.e. above 70% RH unless intermittent and must not be used to isolate dampness. Plasterboards are not suitable for use in temperatures above 49°C but can be subjected to freezing conditions without risk of damage.

Effect of condensation

The thermal insulation and ventilation requirements of national Building Regulations aim to reduce the risk of condensation and mould growth in new buildings. However, designers should take care to eliminate all possibility of problems caused by condensation, particularly in refurbishment projects.

Board colour

☐ Pink face paper
☐ Brown reverse side paper

Board printing

Face - screw centre markings 'x'.
Edge - product code, EAN number, board thickness x width x length, edge type.
Reverse - standard and certification

Board range

Width mm	**Length** mm	**Edge type**
12.5mm Board		Kg/m² = 9.8 R (m²K/W) = 0.05
900	1800	T/E S/E
1200	2400	T/E S/E
	2700	T/E
	3000	T/E
15mm Board		Kg/m² = 11.7 R (m²K/W) = 0.06
900	1800	T/E
1200	2400	T/E S/E
	2700	T/E
	3000	T/E

T/E – Tapered Edge S/E – Straight Edge

Board types

T/E - with Gyproc jointing materials for taped and filled joints or application of Thistle Board Finish or Thistle Multi-Finish plaster.

S/E - for plaster application, artex texture finish or undecorated applications

Application and installation

General

It is important to observe appropriate health and safety legislation when working on site i.e. personal protective clothing and equipment, etc. The following notes are intended as general guidance only. In practice, consideration must be given to design criteria requiring specific project solutions.

Handling

Manual off-loading of this product should be carried out with care to avoid unnecessary strain. For further information please refer to the Manual Handling section of the Site Book or Manual Handling Guide, available to download from www.british-gypsum.com.

Gyproc WallBoard DUPLEX

Product Data Sheet

Introduction

Used for wall and ceiling linings where vapour control and plasterboard lining are required in one fixing operation.

Product description

Gyproc WallBoard backed with a vapour control membrane. Gyproc WallBoard DUPLEX consists of an aerated gypsum core encased in, and firmly bonded to, strong paper liners and backed with an additional metalised polyester film. Gyproc WallBoard DUPLEX is a plasterboard that is suitable for drylining internal surfaces.

This plasterboard is one of the products within our plasterboard range that is certified to *BES 6001* achieving a rating of 'Excellent'.

BES 6001 Responsible Sourcing www.greenbooklive.com

Board performance

Fire protection

Plasterboard linings provide good fire protection owing to the unique behaviour of the non-combustible gypsum core when subjected to high temperatures. For the purposes of the national Building Regulations, plasterboard is designated a 'material of limited combustibility' (Approved Document B). The surfaces of Gyproc WallBoard DUPLEX are designated Class 0 (for the purposes of national Building Regulations). Please refer to the table below.

Fire resistance

Please refer to the appropriate **White Book** product or systems section for information on the fire resistance of building elements lined with Gyproc WallBoard.
The substitution of Gyproc WallBoard with the same thickness of Gyproc WallBoard DUPLEX will not change the fire performance.

Reaction to fire test performance

Standard	Performance
BS 476: Part 6: 1989 Method of test for fire propagation for products.	*Index of performance (I) not exceeding 12 and a sub-index (i1) not exceeding 6.*
BS 476: Part 7: 1997 Surface spread of flame tests for materials.	*Class 1 (both sides).*
EN 13501-1: 2007 + A1: 2009.	*Classified without further testing as B-s1, d0.*

Thermal conductivity

? Gyproc WallBoard DUPLEX - 0.19W/mK

Effect of temperature

Gyproc WallBoard DUPLEX is unsuitable for use in areas subject to continuously damp or humid conditions and must not be used to isolate dampness. Plasterboards are not suitable for use in temperatures above 49°C, but can be subjected to freezing conditions without risk of damage.

Effect of condensation

The thermal insulation and ventilation requirements of national Building Regulations aim to reduce the risk of condensation and mould growth in new buildings. However, designers should take care to eliminate all possibility of problems caused by condensation, particularly in refurbishment projects.

Board colour

☐ Ivory face paper
☐ Metalised polyester film reverse

Board printing

Face - screw centre markings 'x'.
Edge - product code, EAN number, board thickness x width x length, edge type.

Board range

Width mm	Length mm	Edge type
12.5mm Board		Kg/m² = 8.0 R (m²K/W) = 0.41
900	1800	S/E
1200	2400	T/E S/E
	2700, 3000	T/E
15mm Board		Kg/m² = 9.8 R (m²K/W) = 0.42
1200	2400	T/E

[1] Including 25mm minimum air space.
T/E – Tapered Edge S/E – Square Edge

Board types

T/E - with Gyproc jointing materials for taped and filled joints or application of Thistle BoardFinish or Thistle MultiFinish plaster.
S/E - for plaster application, Artex Texture Finish or undecorated applications.

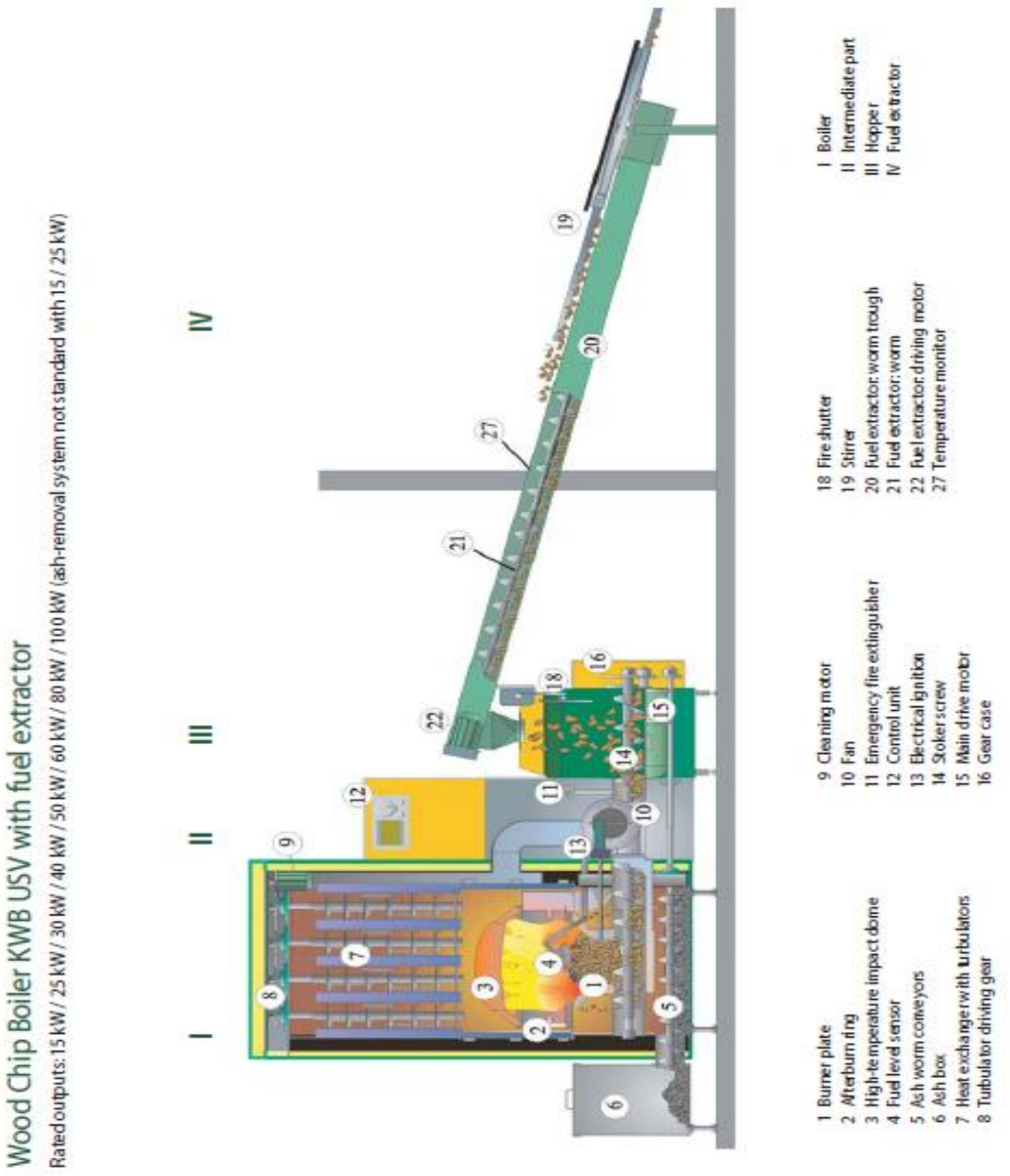

Figure 2: Sectional drawing with fuel extraction system

Wood Chip Boiler KWB USV with storage container

Rated outputs: 15 kW / 25 kW / 30 kW / 40 kW (ash-removal system not standard with 15 / 25 kW)

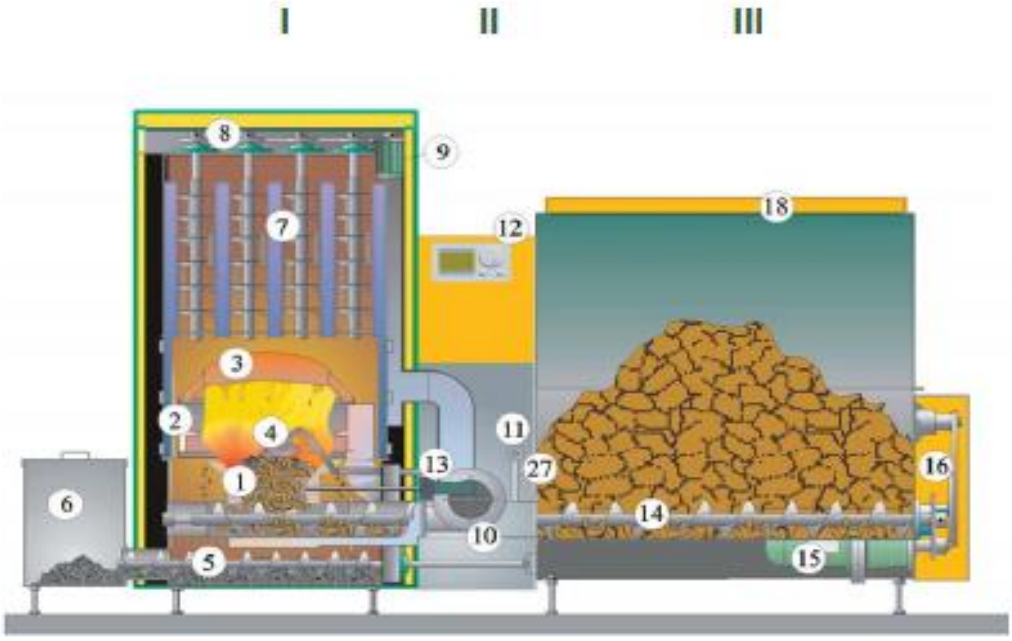

1 Burner plate
2 Afterburn ring
3 Afterburn dome
4 Fuel level sensor
5 Ash worm conveyors
6 Ash box
7 Heat exchanger with turbulators
8 Turbulator driving gear
9 Cleaning motor
10 Fan
11 Emergency fire extinguisher
12 Control unit
13 Electrical ignition
14 Stoker screw
15 Main drive motor
16 Gear case
18 Container cover
27 Temperature monitor

I Boiler
II Hopper
III Storage container

Figure 3: Sectional drawing with storage container

Call 01757 289067
Email info@shelterit.co.uk

SHELTER IT
PORTABLE INDUSTRIAL CANOPY SHELTERS

26H Series - 7.9m Width

£4,995
Excluding VAT & Delivery

Select the Length NEED A DIFFERENT LENGTH?

Select

ADD TO CART

Delivery

Our delivery costs vary dependant on location. Contact us to receive a bespoke quotation for the shelter, delivery and any further requirements.

Installation

An install manual will be provided with each shelter. This provides instruction on building the steel frame and securing the canopy; along with dimensions and an inventory that will aid you if the building was de/reconstructed.

Shelter dimensions Width 7.9m Height 6.2m
Door dimensions Width 3.8m Height 4.7m

- Hot Galvanised Steel Frame Structure
- Heavy duty Quality 610g/m2 PVC Cover
- Front and Back end panels Included
- Winch-up door System on end panels
- Colour options - White, Grey and Green

Call or E-mail Us for a tailored quotation
Although we hold many of our products in stock **certain shelters listed require a manufacturing period.** This time can vary so please **contact us** for a tailored quote and we will advise dependant on your needs.

Data Sheet

IQ3
Web Enabled Controller

IQ3 Web Enabled Controller

BACnet™ is a trademark of ASHRAE.

Description

The IQ3 controllers are Building Management System controllers that use Ethernet and TCP/IP networking technologies; they are optionally able to use BACnet protocol over IP. Each controller incorporates a web server which can deliver user-specific web pages to a PC or mobile device running internet browser software. Using Wide Area Networking technologies, such as the Internet, with the appropriate levels of device and network security in place, a user could monitor or adjust the controller from anywhere in the world. Please refer to the security section of the IQ3 Configuration manual for advice on security best practice. It is also compatible with the traditional IQ system protocol. The IQ3 range consists of DIN rail mounting controllers with from zero to 16 input/output points (expandable up to 128 points by adding DIN rail mounting I/O modules). This flexibility makes them suitable for a broad range of applications. A local PC or display (SDU-xcite) can be connected to the RS232 port.

Features

- Ethernet 10 Mbps main network with TCP/IP protocol
- Embedded web server with security protected monitor/control
- Embedded XML Web Services option
- BACnet over IP option (BTL Listed)
- Compatible with existing IQ system protocol
- IQ3xact with 12 I/O points and IQ3xcite with 0 or 16 I/O points
- IQ3xcite with 80 or 112 additional points by DIN rail I/O modules
- I/O bus allows separate placement of I/O modules
- Flexible number of software strategy modules
- RS232 local supervisor port
- 100 to 240 Vac, or 24 Vac and 24 to 60 Vdc input power supply versions
- Small footprint with DIN rail mounting
- Battery backup, current loop Lan, or serial auxiliary board options
- DHCP enabled.

Physical

Diagram shows IQ3XCITE/96 or /128 (other versions may have less I/O connectors)

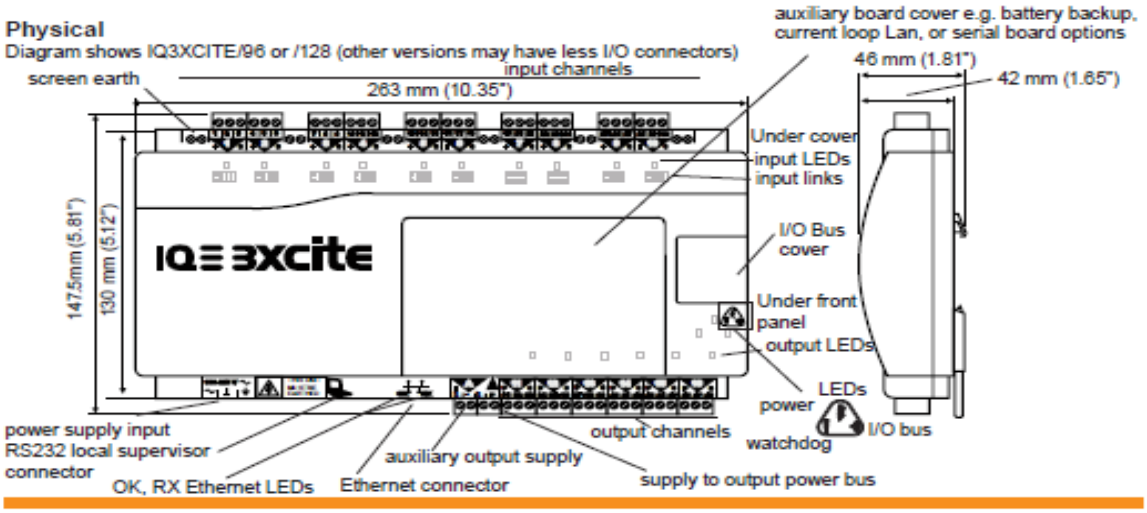

Physical (continued)

I/O Module (e.g. 8 universal input)

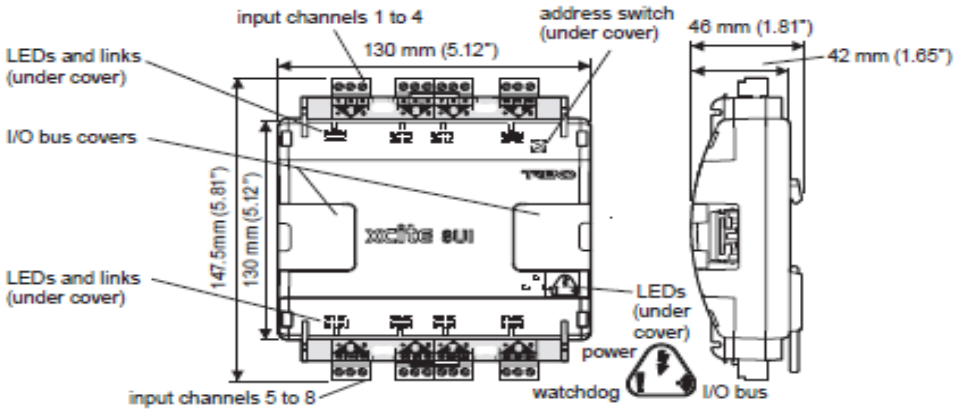

FUNCTIONALITY

This data sheet gives a general description of IQ3, it does not provide information on the /BINC or /XNC options. For details of the /BINC option see the IQ3../MSTP/BINC/.. Data Sheet (TA201095). For details of the /XNC option see the IQ3.../.../XNC/... Controller/Interface Data Sheet (TA200912). Detailed information is given in the following manuals:

- IQ3/4 Configuration Reference Manual (TE20076) covers IQ3's communications, hardware, configuration and modules.
- SET Manual (TE200147) covers IQ3's configuration using SET
- IQ System Ethernet Products Engineering Manual (TE200369) covers the use of Trend products with Ethernet
- IQ3 Web User Guide covers the use of IQ3 Web Pages
- IP Tool Manual (TE200638) describes the use of the IP Tool.
- IQ3 Graphical Display Page Editor Manual (TE200629).
- IQ3 Reset Applet Manual (TE200767)

The IQ3 functionality can be divided into four sections: system, hardware, firmware, and strategy.

SYSTEM

Standard Communications

The full standard IQ3 has Ethernet, I/O bus, and RS232 ports.

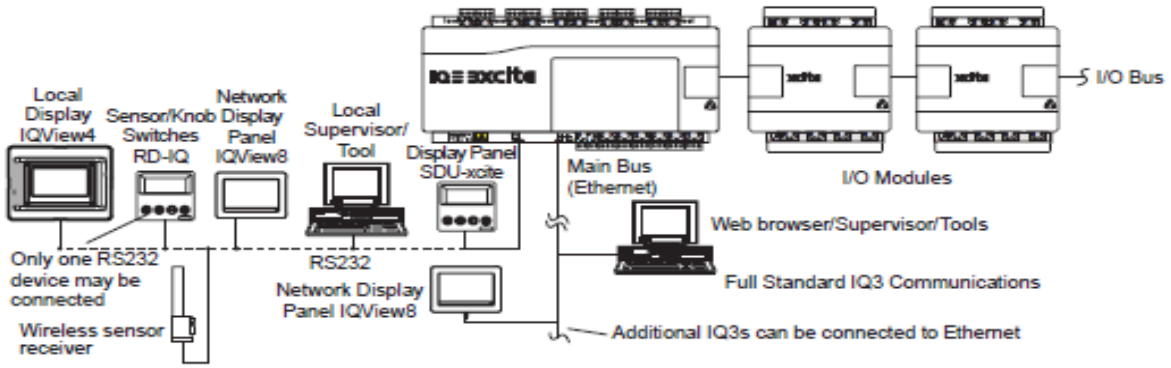

Ethernet: This is the main network for the IQ3 controller. It enables PCs to connect directly to Ethernet and communicate with the IQ3 using IP addressing. It also enables Inter-Controller Communications (IC Comms - peer to peer Ethernet communications) between controllers. Remote PCs can communicate through standard IT networks using IP, enabling communication from anywhere in the world.The IP connection will support a web browser (thin client) running in a PC, but communication with an IQ System supervisor or tool (thick client e.g. 963, IQView8) will require the use of the virtual CNC embedded in the IQ3 controller. The strategy and all other configuration files may be downloaded to the IQ3 from SET (System Engineering Tool) across Ethernet.

I/O bus: The controller has the option of a highly reliable I/O bus. This enables expansion I/O modules to be connected to add up to 112 additional I/O points (128 points in total with the 16 points in the IQ3). The bus can be up to 10 m (11 yds) or 30 m (33 yds) in length, and have a maximum of 15 I/O modules.

Standard Communications (continued)

RS232 port: A sensor/display (RD-IQ), 4 line display panel (SDU-xcite), network display (IQView8 or IQView4), a wireless sensor receiver (XW/R/IQ) or a local PC running a supervisor or a software tool may be connected to the RS232 port. Only one device may be connected.

This port can communicate directly with the IQ3 (address 0) or to the IQ system network using the local supervisor CNC (see below).

The RD-IQ or SDU-xcite communicates only with the local IQ3, so for the RS232 port to operate with RD-IQ or SDU-xcite, its address module local supervisor port address must be set to zero.

Stand Alone Mode: Stand alone mode can be enabled in the Ethernet IP network module. Enabling stand alone mode will stop the IQ3 from attempting to build networks with other IQ3s or EINCs, but it will still communicate as a single IQ3 (with supervisor, web browser, and local supervisor). A controller is set to stand alone mode to reduce Ethernet network traffic (i.e. to disable polling messages trying to find other Trend devices).

An IQ3 prior to firmware version 1.2 could be set to 'Stand Alone' by the IP Tool. If a controller's firmware prior to v1.2 is upgraded it will be taken out of stand alone mode. It is recommended that no IQ3 controller prior to version 2.2 should be operated in stand alone mode.

Networks: The IQ3 will create its own internal Lan which includes a node for its own controller, a CNC for its local supervisor port (sCNC - if supervisor port address is set non-zero), a virtual CNC (vCNC), and a virtual INC (vINC - address 126).

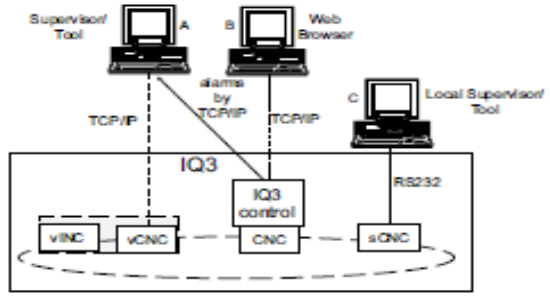

internal Lan

If multiple IQ3s with the same Lan number are connected to Ethernet, then an Ethernet Lan will form to include these IQ3s and their internal nodes. They must be on the same Ethernet segment, in the same subnet, and use same UDP port.

The IQ3 with the lowest IP address on the Lan also assumes the INC functionality (the other vINCs disappear) and is responsible for maintaining the Lan across the IQ3s.

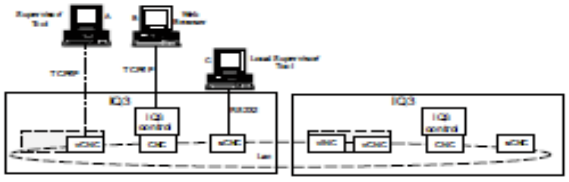

shared Lan

If multiple IQ3s with different Lan numbers are connected to Ethernet then their INCs will form an internetwork (along with any EINCs/3xtends on the network).

Note that Trend Ethernet devices (e.g. IQ3, EINC, 3xtend/ EINC L) on the same Ethernet segment must all be on the same subnet.

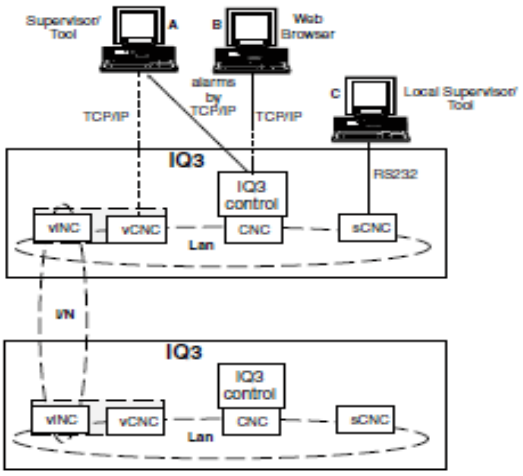

multiple Lans

IC Comms: The IQ3s may communicate with each other IQ4, IQeco and earlier IQ (and IQL) controllers using Inter Controller Communications (peer to peer communications). This will use IQ System Lan/node addressing (not direct IP addressing).

Alarm Delivery: Alarms can be delivered to the local supervisor port or to a supervisor making a permanent connection to the virtual CNC by normal IQ system comms. Alarms can be delivered to supervisors making temporary connections to the virtual CNC using TCP/IP by setting the supervisor's IP address and port number in the alarm destination module (i.e. IP alarms). Alarms may also be sent by email.

Note that network alarms are sent to any connected port (e.g. supervisor connected to local supervisor port, or supervisor connected to virtual CNC).

Optional Communications

IQ System Current Loop Lan Auxiliary Board
The optional IQ system current loop Lan auxiliary board enables the IQ3 to become a device on an IQ system current loop Lan. It can no longer be part of an Ethernet Lan (or internetwork). However, it will still support access using a web browser or a supervisor or tool by way of a virtual CNC, and it can still send IP or email alarms across Ethernet. The current loop Lan auxiliary board is fitted in IQ3../.../LAN versions of IQ3 (henceforth referred to as IQ3/LAN).

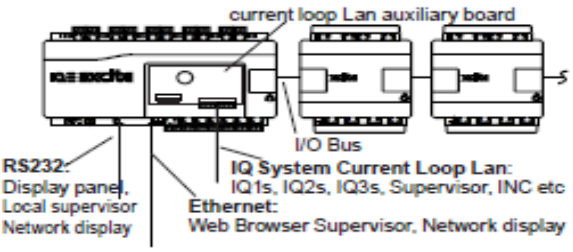

Optional Communications (continued)

Once another IQ (IQ1, IQ2, IQ3, or IQ4) is connected to the current loop, the two IQs form a Lan. This can then be extended onto an internetwork in the normal way using an INC type node (e.g. INC2, LINC, 3xtend/EINC L).

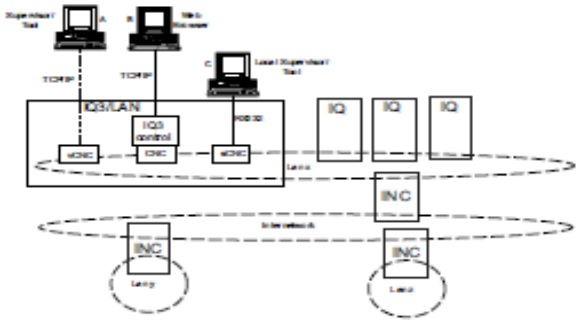

If a 3xtend/EINC L is used instead of an INC, then the internetwork (or a segment of it) can exist on Ethernet. This would enable Ethernet Lans of IQ3s to be part of the same system network as an IQ3/LAN.

Serial Auxiliary Board
The serial auxiliary board provides an additional RS232 or RS485/422 serial port for communicating with other devices. This board is used in some versions of the IQ3.../.../XNC/.. (referred to as IQ3/XNC/SER, see IQ3../../XNC/... Data Sheet for more details).

BACnet Protocol Option
IQ3/BAC versions of IQ3 support BACnet protocol; BACnet is an open protocol that enables the products of a number of different manufacturers of building automation and control equipment to communicate with each other.

Each BACnet device has a number of objects (roughly corresponding to Trend modules) and each module has a number of properties (roughly corresponding to Trend module parameters). The mapping of the BACnet properties to the Trend parameters is covered in the IQ3/4 Configuration Reference Manual (TE20076).

BACnet communications can only occur if the BACnet Network module (Network module 3, type 5) is enabled and set up as this defines the controller's communication parameters on the BACnet network.

The network module's default settings normally allow BACnet communications to operate correctly, but under certain circumstances they may need to be changed - see IQ3/4 Configuration Reference Manual (TE20076).

SET is able to browse the BACnet system, and this can be used to confirm that the IQ3's BACnet communications are operating.

A specification of the objects, properties, and BIBBS (BACnet Interoperability Building Blocks) supported by the IQ3 are given in the IQ3 Product Implementation Conformance Statement (TP201002). This describes the IQ3 functionality which is submitted to the BACnet Testing Laboratory for conformance testing.

The IQ3 controller is BTL listed as a BACnet Application Specific Controller (B-ASC) because it complies with all the BIBBS required, but it supports more than this, and on a practical system can be treated as a BACnet Advanced Application Controller (B-AAC).

BACnet Alarms: IQ3/BAC is able to send alarms using BACnet protocol by way of the BACnet Device type of Alarm Destination Module. This will only accept Sensor, Digital Input, Driver (digital readback), and Plot (buffer ready) alarms (other alarms will be ignored).

BACnet IC Comms: IQ3/BAC controllers support BACnet IC comms. This enables it to send IC Comms to a BACnet device using BACnet protocol.

The Protocol parameter in the IC Comms module can be set to either Trend, or BACnet.

BACnet IC Comms supports Data From, Data To, and Global To Direction Classes, but not Minimum, Maximum, Sum, or Average.

The Data From, Data To, and Global To BACnet IC Comms supports Analogue and Digital Bit Variable Types, but not Digital Byte.

In order to send a BACnet IC Comms a Non-Trend Device module (NTD) must be set up for the BACnet device being communicated with.

The NTD module is allocated a Lan number (for the Lan of BACnet NTDs), a node address on that Lan, and address attributes so that the controller selection process operates similarly for both Trend and BACnet protocol IC Comms. BACnet IC Comms Global To IC Comms are restricted to a specific Lan, so the Remote Lan cannot be set to 128 (signifying a global message to every Lan, i.e. a global global).

BACnet item selection is similar to that for the Trend protocol, except that BACnet variables must be specified absolutely (i.e. item selection by item label matching may not be used).

BACnet with Automatic IP Addressing: Certain issues exist when using automatic IP addressing and BACnet protocol. These are described in the IQ3/4 Configuration Reference Manual (TE20076).

System Configurations

Routers: IQ3s are able to construct an internetwork (but NOT a Lan) across a router. However, it is possible for PCs to connect to IQ3s across routers, and to treat IQ3s separated by routers as separate sites.

Using a Supervisor with Multiple Sites: In the diagram below there are two IQ3s either side of a router.

If the IQ3s are not configured to cross the router as described below, they will construct two separate networks, one each side of the router.

Only one internetwork is allowed on a site, but the Supervisor can treat the networks as separate sites and so each site may have an internetwork. The supervisor will change the IP address of the IQ3 virtual CNC it is using as it switches sites. *Note that there cannot be any IC comms between the sites.*

Alarms can be sent to the supervisor directly using TCP/IP.

System Configurations (continued)

Configuring IQ3s to Cross Routers: This is done by setting up the IQ3's network module with the 'Router 1' (default router) IP address (for a router on its own subnet) and with a Remote Device's IP address, and subnet mask (for an IQ3 on the other side of the router).

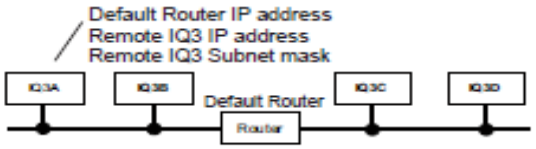

If several IQ3s are connected one side of a router, the unit with the lowest IP address (cross-router master) will attempt to construct the network across the router. In the above diagram, IQ3A is the cross-router master and is configured with the default router IP address and a remote IQ3's (e.g. IQ3C's) IP address and subnet mask. It will now send a message to IQ3C's subnet through the default router. IQ3C will then reply and the IQ3A will construct the internetwork between the two IQ3s.

Because IP addresses may not be fixed (see Automatic IP Addressing Mode - below) it may not be possible to specify which controllers have the lowest IP addresses, so the details should be set up in every device on the subnet, so that any device may be able to become the cross-router master. If Automatic IP Addressing mode is being used, the remote devices will be identified by host names rather than IP addresses.

It is recommended that the details of two devices (either IQView8s, 3xtend/EINC Ls, or IQ3s) in the network from each subnet the other side of a router should be set up in every device in the network (either IQView8s, 3xtend/ EINC Ls or IQ3s) on the local subnet. For increased reliability, details of additional devices should also be set up. *Note that up to 20 device's details may be entered in the network module.*

Internet Access: Because the Internet uses TCP/IP addressing, the 963/IQ3 communication can operate over the Internet. Company Internet access is normally protected by a firewall which is usually the responsibility of the company's IT department. The firewall will need to be set up to allow messages through the port addresses being used for sending and receiving IQ System messages. Additionally the firewall may be set up either to pass messages through or to redirect them. If redirection is being used, then the messages are sent to the firewall IP address and the firewall must be set up with the relevant IQ System IP address (e.g. IQ3 vCNC, 3xtend/EINC L vCNC, or IQ3's own IP address for web pages) so it can pass them on. If using an impermanent ISP connection (e.g. using a dial up modem) at either 963 or IQ3 end, the ISP (Internet Service Provider) must support reverse dial up.

Note that IQ3 to IQ3 networking communications will not operate across a firewall (i.e. virtual networks cannot be built across firewalls).

IQ3 with 3xtend/EINC L: The diagram below shows the addition of an 3xtend/EINC L to Ethernet. The 3xtend/EINC L supports an IQ System current loop Lan which may contain IQ1 IQ2 or IQ4 series controllers.

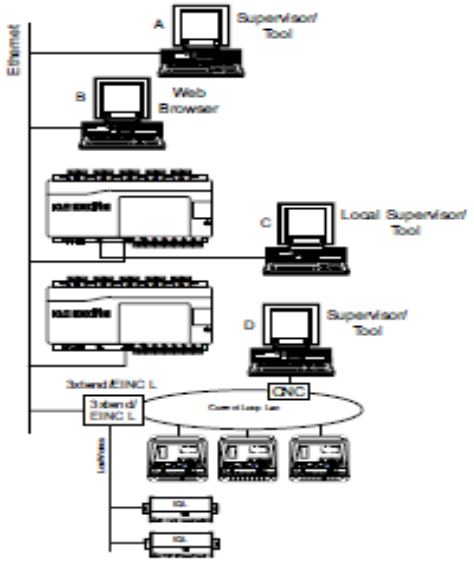

The 3xtend/EINC L differs from the EINC in that it can operate in an automatic IP addressing environment (e.g. with DHCP) and has a LonWorks® bus connection enabling the extension of the internetwork over the LonWorks network, and communication with IQLs.

Note that the LonWorks network is not to be used where a high level of network traffic is expected e.g joining internetworks or where there are many IQ system devices on many IQ system Lans being accessed across an internetwork routed through the LonWorks network. An alternative topology should be used such as an Ethernet network.

Note that the IQ3 and the 3xtend/EINC L cannot have the same Lan number since the EINC's Lan number (set up on its address switches) is reserved for its current loop Lan.

IQ3 and TMN: The IQ3 can use a TMN connected to an 3xtend/EINC L's current loop network. The 3xtend/EINC L should operate in internetwork extension mode (i.e. device address =>100) which provides a current loop internetwork with an extension on Ethernet. However, this will only give normal IQ System Communications (i.e. text communications), it cannot provide web pages.

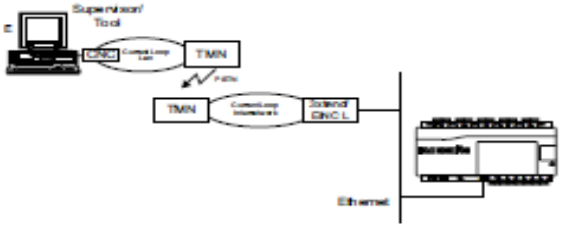

System Configurations (continued)

Automatic IP Addressing Mode: The IQ3 is able to operate in a system where the IP addresses are automatically allocated by a DHCP (Dynamic Host Configuration Protocol) server (i.e. the IP addresses are not fixed).

The IP Addressing Mode parameter (in network module) is set to 'Enter Manually' for traditional manual entry with a fixed IP address, and is set to 'Obtain Automatically' (default setting) for the IP address to be set automatically by the DHCP server.

DHCP Operation: If set to 'Obtain Automatically', when the controller powers up it will inform the DHCP server which can then provide it with:

IP Address
Subnet Mask
Router 1 (default router)
WINS Servers (1 to 5)
DNS Servers (1 to 5)

(These parameters cannot now be changed by SET unless IP Addressing mode parameter is set to 'Enter Manually'.)

Link/Local Operation: If the controller is in automatic IP addressing mode and the DHCP server fails to respond, the IQ3 will enter link/local mode where it will negotiate its IP address with the other devices on its Ethernet segment.

A PC (running supervisor or tool software) should be set up for auto-addressing. On DHCP failure it may take a very long time to enter link/local and be able to communicate with the IQ3s. This can be avoided by power cycling the PC which will cause it to enter link/local on power up. To communicate with an IQ3 it must be on the same segment.

IP Addressing Mode	IP addressing set up by	
Obtain Automatically	DHCP	IP address may vary
	Link/local	
Enter Manually	Manual	IP address fixed

Summary of IP Addressing Modes

Note that it is recommended that link/local only be used as the default method of operation on a single segment system, (not across a router).

Host name: Because the IP address is no longer fixed in automatic IP addressing mode, the IQ3 uses a Host name, which is fixed. When the IQ3 powers up it sends its host name to a WINS (Windows Internet Naming Service) server. If a device wishes to communicate with the IQ3 it will send the IQ3's host name to the WINS server which will return the associated IP address.

If a WINS server does not exist, the host name can be used over the local segment only (i.e. not across routers).

The host name can also be used to communicate with the IQ3 if the IP Addressing Mode parameter (in network module) is set to '**Enter Manually**'. This provides a user-friendly way of identifying the controller rather than remembering its IP address.

Default Host Name: If the host name has not been set up, the IQ3 will power up with a default host name which is a function of its MAC address ('Trend' plus the last six digits of the MAC address e.g. TREND_00_14_D0). The default host name will always be operational (as well as its Host name if it has been set up), unless the Default Host name parameter in the network module has been set to 'Disabled'.

Communication across the Internet: If a device (e.g. supervisor) wishes to communicate across the Internet with an IQ3 on a system with automatic IP addressing, then the firewall server either has to be able to use the host name, or the IQ3's IP address must be fixed.

Fixing the Controller's Address on a DHCP controlled System: It is possible for the IQ3 to operate in a DHCP regime with a fixed IP address by setting up the DHCP server so that it always gives that particular IQ3 the same IP address. An alternative is to set the IQ3 IP Addressing Mode parameter to 'Enter Manually', and set its IP address outside the range of the DHCP server.

Email Server Address: Because the Email Server Address is no longer fixed on a DHCP system, it must be set up (in the network module) to a host name or an Internet domain name. Thus when an email alarm is to be sent the Email Server IP Address is resolved by either a WINS server or a DNS (Domain Name System) server.

Crossing Routers if DHCP is operating: In the DHCP regime, if the internetwork is to cross a router(s), the Remote Devices (1 to 20) IP addresses should be set up as host names. This will enable the IP addresses to be obtained from the WINS servers.

Note that if any communication using a host name crosses a router(s), then a WINS server address must be set up.

Servers: If the IQ3's IP address settings are to be supplied by a DHCP server, the server must be installed on the same segment as the IQ3. On a multi-segment system a single DHCP server may be use providing it has a connection to each segment, i.e. multiple connections.

The server must be capable of downloading either or both (as appropriate, see below) the WINS server address, and the DNS server address.

If host names are being used for IP addressing across a router, then a WINS server must be installed somewhere on the system.

If email alarms are being sent, and the email server address is identified by Internet domain name, then a DNS server must be installed somewhere on the system.

HARDWARE

IQ3

Box: The controller box is DIN rail mounting and must be fitted inside a cabinet. The input channel links are accessible by means of a clear polycarbonate cover which can be unclipped using a screwdriver. The I/O bus connector has a hinged plastic cover. The auxiliary board cover can be levered off by inserting a screwdriver between the back of the cover and the main unit. It has a rear DIN rail clip.

The digital input LEDs, the output LEDs, and the three controller status LEDs can be viewed through the clear polycarbonate.

I/O Bus: This feature is only available on the expandable IQ3s (IQ3XCITE/96, /128). The IQ3xcite is connected to an adjacent I/O module by a rigid connector. It can be connected to a remote I/O module by a flexible cable. The connection is made by opening the flap, plugging in the connector, and then closing the flap over the cable. The last module on the I/O bus must be correctly terminated (see I/O Modules section). The IQ3xcite is provided with a terminator, and each I/O module is provided with a rigid interconnector.

IQ3 (continued)

Connectors: Other than the screen terminals, which are single part, two part connectors are used throughout to facilitate installation. The screw terminals are of a rising cage clamp type to facilitate good connections. Each input channel has a terminal for cable screen connection. The internal cable screen earthing (grounding) terminal bus is connected to the controller earth (ground) by a soldered link on the board. If required to segregate the screen earth (ground) from the controller input power supply earth (ground), it may be connected to a separate external earth (ground) by lifting the cover and cutting the screen earth (ground) track and making a connection between the internal screen bus terminal and an external earth (ground).

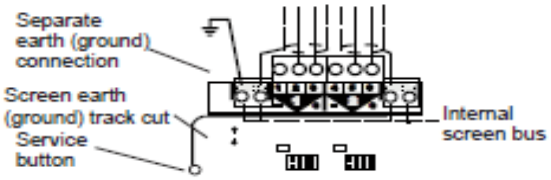

Service Button: The IQ3 can be restored to defaults by holding down the service button for greater than 2 s (but less than 15 s) as the IQ3 is powered up. For earlier hardware versions without the service button it can be restored to defaults by using the Reset Applet (part of SET). *Note that this will clear the strategy; the data cleared down is defined in the Firmware/Strategy section below.*

Power Supply: The IQ3 can be supplied in two input power supply versions.

/100-240 :100 to 240 Vac at 50 or 60 Hz. Power requirement is 56 VA maximum.

The 230V supply must include a dedicated 5A fuse complying with BS1362 and a suitably rated switch in close proximity and be clearly marked as the disconnecting device for the unit. A 5A circuit breaker with high breaking capacity may be used as an alternative.

/24 :24 Vac at 50 or 60 Hz, 24 to 60 Vdc (36 Vdc maximum for /UL versions). Power requirement is 40 VA maximum.

The 24V supply must include a suitably rated switch in close proximity and be clearly marked as the disconnecting device for the unit.

A summary of the minimum and maximum power requirements is given below:

	Supply					
	240 Vac (nominal)		24 Vac		24 Vdc (nominal)	
	min	max	min	max	min	max
IQ3xcite/000	6 VA	15 VA	5 VA	11 VA	4 VA	8 VA
IQ3xact/012	6 VA	28 VA	5 VA	25 VA	4 VA	16 VA
IQ3xcite/016	6 VA	39 VA	5 VA	28 VA	4 VA	18 VA
IQ3xcite/096, /128	6 VA	56 VA	5 VA	40 VA	4 VA	27 VA

The minimum power is for the core electronics without any I/O auxiliary power or additional I/O modules. The maximum power for the IQ3xcite/000 includes core electronics and maximum auxiliary supply consumption, for the IQ3xact/012 and IQ3xcite/016 it also includes maximum I/O consumption; the maximum for the IQ3xcite/96 and /128 includes core electronics, maximum I/O consumption, and maximum auxiliary supply of 700 mA (which includes power to the I/O bus).

Fusing: The 24 Vdc combined supply to the IQ3's own I/O channels, the I/O bus, the RS232 connector (e.g. to power SDU-xcite), and the auxiliary supply output is protected by a self-resetting electronic circuit breaker. The part of the 24 Vdc combined supply which supplies the RS232, and the 24 V auxiliary supply output is limited to 150 mA. The 0V return of this supply (in A terminals set) of this supply is limited at 500 mA by a self resetting fuse, so that if this 0V terminal is mistakenly used for high currents, the fuse will blow and protect the 0V line; when the fault is removed the IQ3 will return to normal operation.

The analogue output P bus is protected by a 1.6 A self resetting multifuse.

The power supply is protected against catastrophic failure by a non-replaceable fuse. The analogue output circuitry is protected against the wrong connection of a non-isolated external supply by a non-replaceable fuse. If either non-replaceable fuse blows, the controller should be sent back for repair.

The I/O modules have protection as described in the I/O module section.

Battery Backup: The strategy configuration and data (logs, alarms) are stored in the unit in nonvolatile memory (Flash). A 'supercap' is used to maintain the real time clock (time and date). In the event of power failure this will support the clock for 6 days (typically). *Note that the supercap needs about 2 minutes to reach full charge after power is applied.*

Optionally a battery board (XCITE/BBC) can be fitted into the unit; this will support the clock for several years in the event of power failure (e.g. for Timemaster, see Firmware/Timemaster).

If the battery hasn't been discharged, it should be replaced routinely every 5 years. The battery (type CR2032) can be replaced after turning the power off and removing the auxiliary board cover (while the battery is not in circuit the supercap will maintain the real time clock).

IQ system Current Loop Lan Optional Auxiliary Board: The IQ3/LAN (IQ3.../.../LAN) is supplied complete with a Lan auxiliary board fitted in the auxiliary board slot, and with a special auxiliary board cover which enables access to the auxiliary board switches and connectors.

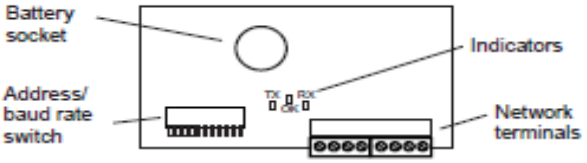

The auxiliary board also contains the circuit for a backup battery so it can also fulfil the function of XCITE/BBC as described above. However, the CR2032 battery is not supplied so must be purchased separately if a battery backup option is required.

The board contains the normal hardware for an IQ system current loop Lan node:

Address/Baud rate switch: The address on the Lan is set by poles 1 to 7 in range 1, 4 to 9, 11 to 119 and must be unique on the Lan. The strategy address module Local Address parameter monitors the address switch settings and is read only for IQ3/LAN. The baud rate is set by poles 8 to 10 in the range 9k6, 19k2 and must match the other nodes on the Lan (it can also be read in Network Module 2).

Note that zero address reset is not implemented on IQ3.

Network terminals: The network terminals facilitate connection of 4 wire cables (enabling a 'weaving' connection method).

IQ3 (continued)

Indicators: The standard LEDs are fitted (TX, RX, and network OK).

Bypass relays: The board contains 2 changeover relays which bypass the receive and transmit circuitry and maintain network integrity during power fail.

Serial Auxiliary Board: This board is fitted to IQ3/XNC/SER (IQ3../.../XNC/SER) versions of IQ3, see IQ3../.../XNC/... Data Sheet for details. This board also supports the battery backup facility in the same way as the IQ system current loop Lan auxiliary board (see previously).

Indicators:
I/O Channels

Input LEDs: (yellow) Each input channel has an LED to monitor the input state when the input channel is set to a digital input. The LED will illuminate when the associated input contact is closed.
Output LEDs: (yellow) Each output channel has an LED whose light intensity increases with output voltage.

Core function

Watchdog (): (red) On if controller has a software fault (i.e. strategy or firmware).
I/O bus error (): (red, not fitted on IQ3xact) On if there is an I/O bus fault, (e.g. check for short circuit between Data Hi or Data Lo and either of the power lines).
Power (): (green) On when input power supply is connected. Flashes briefly at 1 second intervals if input power supply fault; return unit to supplier.

Ethernet

OK: (green) Normally called LINK on Ethernet systems. ON indicates a good Ethernet connection. If OFF indicates faulty Ethernet connection.
RX: (yellow) Flashes when packet of data is being received across the Ethernet.

24 Vdc Combined Supply: The 24 Vdc combined supply supplies the IQ3's own input/output channels, the I/O bus, the RS232 connector (e.g. to power SDU-xcite), and the 24 Vdc auxiliary output supply terminals. The total available current is 700 mA (reducing to 550 mA for /100-240 version if the 230 Vac input power supply is less than 200 Vac). The PSU has thermal overload protection and the combined supply is protected by a self resetting electronic circuit breaker.

The input and output channels are current limited at 22 mA each. The part of the combined supply used by the RS232 connector and the auxiliary output supply is current limited to 150 mA (typical). The auxiliary output supply can be linked into the P connector to supply auxiliary power for use by output devices.

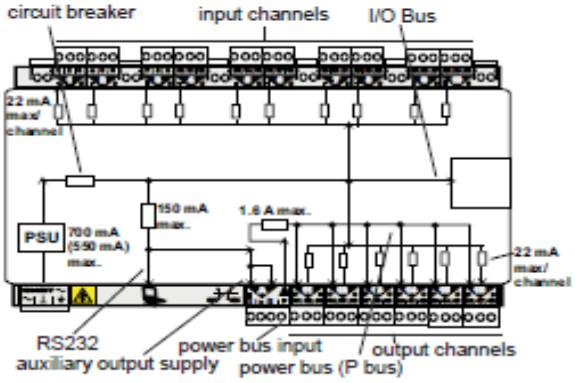

The P output terminals are used to supply the power to output devices. The internal power bus (P bus) is protected by a 1.6 A self-resetting multifuse. The power bus input terminal is normally supplied from the IQ3 24 Vdc auxiliary output supply by using an external link but it can be supplied from an external, dedicated, isolated, 24 Vac/Vdc power supply. The controller is protected against the wrong connection of a non-isolated external supply by a non-replaceable fuse.

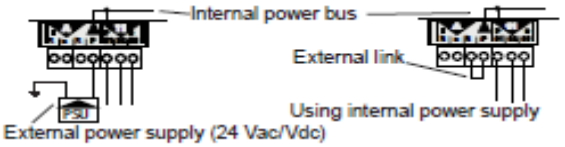

Note that if an external 24 Vac/dc power supply is used, it must be dedicated to I/O channel use, and it must comply with the relevant EMC and safety standards.

The external supply can be either 24 Vac or 24 Vdc, but if the output devices require a mix of 24 Vac and 24 Vdc a decision will have to be made over which supply to connect to the P bus; the other supply will need to be provided by external wiring.

Note that the installer should note whether the P bus is 24 Vac, or 24 Vdc and only connect the appropriate loads.

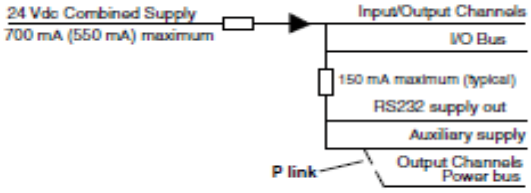

The following checks should be made:

- The maximum current 700 mA (550 mA) available from 24 Vdc combined supply is not exceeded.
- The 150 mA supply to the RS232 and Auxiliary output supply is not exceeded.

The calculation to perform these checks is described in the IQ3/4 Configuration Reference Manual (TE20076).

I/O Channels: The various models of IQ3 have differing numbers of I/O channels as shown below:

IQ3XCITE/00	Zero input/output channels
IQ3XACT/12	6 universal inputs and 6 analogue outputs
IQ3XCITE/16	10 universal inputs, and 6 analogue outputs
IQ3XCITE/96 IQ3XCITE/128	10 universal inputs, and 6 analogue outputs plus additional I/O channels can be provided by connecting I/O modules to the I/O bus to provide up to a maximum of 96 or 128 channels.

Universal Inputs: (Channels 1 to 10)
Linkable for digital (D), current (I), thermistor (T), or voltage (V) inputs.

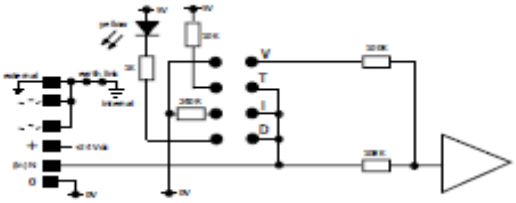

For D, Ix, V, and T connect between (in)N and 0 V. For IL, connect between 24 Vdc and (in)N.

Duplexvent FLEXI DV3600

Flexi Line Side Entry -
Up to 5620 m³/hr air volume

KEY FEATURES

- Air volume up to 5340 m³/hr @ 200 Pa
- Excellent heat recovery efficiency, up to 93%
- Versatile unit positioning with floor and ceiling suspended mounting options
- Low SFP with energy saving EC fans
- Low noise, refer to NR35 and BB93 standards
- 100% adjustable digital controller with internet and BMS connection
- BREEAM, Passive House and ErP 2016 / 2018 compliant
- 2 year warranty +

PERFORMANCE

Sound Power Level Lw (dB)	dB (A)	63	125	250	500	1 k	2 k	4 k	8 k
Outdoor air e1	50	67	65	45	36	35	28	<25	<25
Supply air e2	70	71	83	72	62	61	54	48	53
Extract air i1	50	66	65	45	38	34	28	<25	<25
Exhaust air i2	69	69	82	71	61	59	53	47	52
Breakout noise	54	56	67	56	49	44	35	<25	<25
Sound Pressure Level Ld	**dB (A)**	**63**	**125**	**250**	**500**	**1 k**	**2 k**	**4 k**	**8 k**
To the surrounding	33	36	46	36	28	<25	<25	<25	<25

Sound pressure level is measured at 3m distance

Ventilation		Supply Air	Extract Air
Maximum air volume @ 200 Pa	m³/hr / l/sec	5340 / 1483	5400 / 1500
Air volume @ 250 Pa*	m³/hr / l/sec	2000 / 556	2000 / 556
Nominal voltage	V	400	400
Voltage (at operation point)*	V	400	400
Nominal Power (at operation point)*	W	446	397
Max connection power	W	1480	1480
Max current	A	2.4	2.4
Filters		F7	M5
Fan type		EC	EC

* Note: ● The figures above have been measured at 2000 m³/hr and 250 Pa. Please use the Duplexvent Selection Software to calculate measurements at other performance levels.

Heat Recovery		Supply Air	Extract Air
Maximum air volume @ 200 Pa	m³/hr / l/sec	5340 / 1483	5400 / 1500
Air volume @ 250 Pa*	m³/hr / l/sec	2000 / 556	2000 / 556
Temperature at inlet*	°C	-10	22
Temperature at outlet*	°C	18	1
Humidity at inlet*	%rh	90	40
Humidity at outlet*	%rh	11	100
Thermal efficiency in winter / summer	%	88 / 84	
Performance in winter / summer	kW	19.4 / -2.3	
Condensation	l/h	6.5	
Type of heat exchanger		Counter Flow, Plastic	
Part No.		80000070	

* Note: ● The figures above have been measured at 2000 m³/hr and 250 Pa. Please use the Duplexvent Selection Software to calculate measurements at other performance levels.

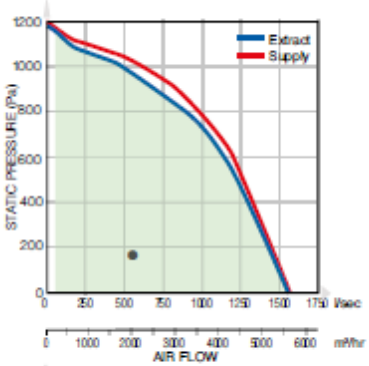

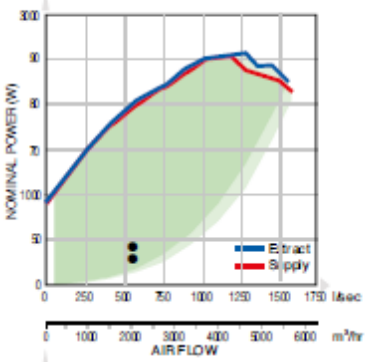

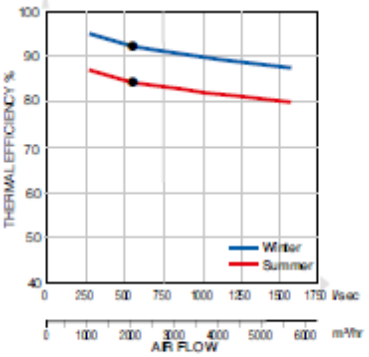

+ excludes motors. Motor warranty one year from date of purchase.

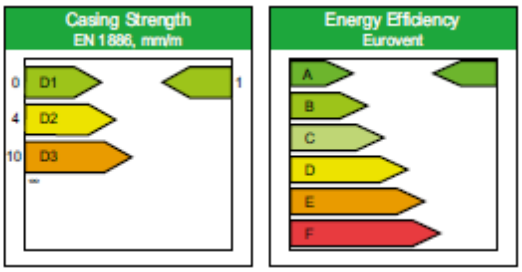

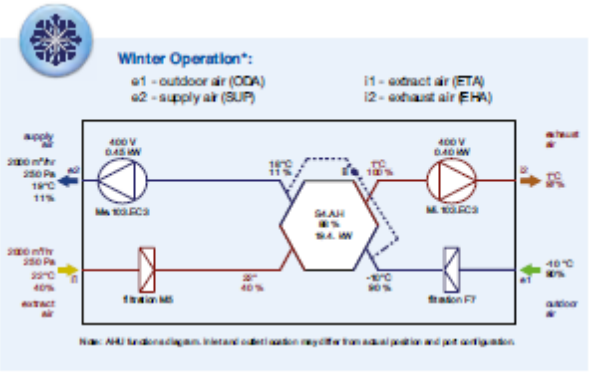

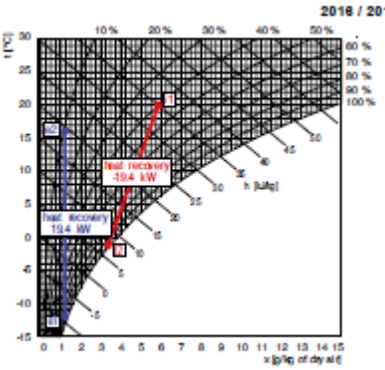

Supply

	Description	t [°C]	rh [%]
e1	Outdoor Air	-10.0	90
e2	Supply Air	18.0	11

Exhaust

	Description	t [°C]	rh [%]
i1	Extract Air	22.0	40
i2	Exhaust Air	1.0	100

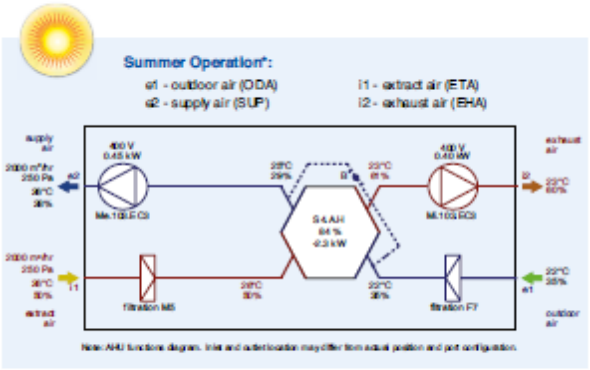

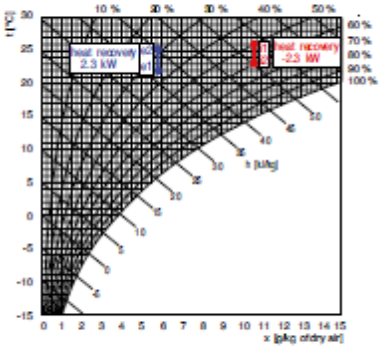

Supply

	Description	t [°C]	rh [%]
e1	Outdoor Air	22.0	35
e2	Supply Air	25.0	29

Exhaust

	Description	t [°C]	rh [%]
i1	Extract Air	26.0	50
i2	Exhaust Air	23.0	61

DIMENSIONS

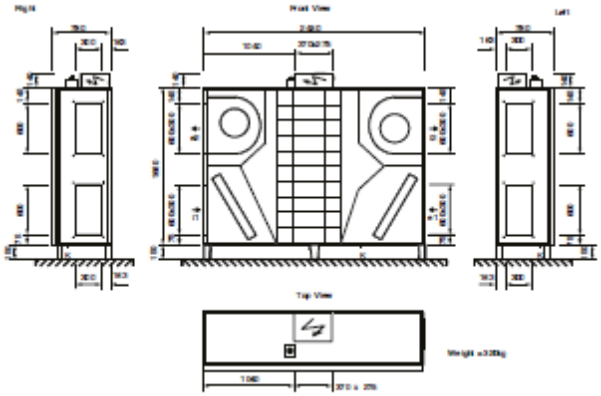

Connections	Type	Diameter	Accessories
e1	Outdoor Air	600 x 300 mm	Shut-off Damper, Flexible Connector
e2	Supply Air	600 x 300 mm	Flexible Connector
i1	Extract Air	600 x 300 mm	Flexible Connector
i2	Exhaust Air	600 x 300 mm	Flexible Connector
K	Condensate Outlet	Ø 21 mm	Condensate Trap

ACCESSORIES

See Duplexvent accessories pages for more details.

* The above figures are example performance measurements. Please use the Duplexvent Selection Software to calculate measurements at other performance levels.

Call: 01494 560800 **Visit: airflow.com**

80000673 Issue 1 06/17

AIRFLOW

Airflow Developments Limited
Aidelle House, Lancaster Road,
Cressex Business Park,
High Wycombe, Buckinghamshire,
United Kingdom, HP12 3QP

E-mail: info@airflow.com
Telephone: +44 (0) 1494 525252

airflow.com

GB

TECHNICAL DATA

Specifications	DH8500EW	DH9500EW
Typical Extraction @ 30°C 85%rh	47 l /day	57 l /day
Typical Extraction @ 30°C 80%rh	43 l /day	55 l /day
Typical Extraction @ 27°C 60%rh	24 l /day	35 l /day
Air Flow (High Speed)	430 m^3/hr	430 m^3/hr
Voltage	230 V	230 V
Current @ 27°C/60%rh	3.5 A	4.1 A
Frequency	50 Hz	50 Hz
Power @ 27°C/60%rh	0.78kW	0.91kW
Phase	1ph	1ph
Dimensions (mm)	500 x 306 x 680	500 x 306 x 680
Weight (NET)	25kg	26.5kg
Weight (GROSS)	26.5kg	28kg
Operating Temperature	7°C / 35°C	7°C / 35°C
Condensate pump head (Option)	1.8m	1.8m
Refrigerant R410A Hermetically sealed		

* (EC) No 842/2006: R410A is a preparation of fluorinated greenhouse gases covered by the Kyoto Protocol. Its global warming potential (GWP) is 1725.

Disposal

This marking indicates that this product should not be disposed with other household wastes throughout the EU.To prevent possible harm to the environment or human health from uncontrolled waste disposal, recycle it responsibly to promote the sustainable reuse of material resources. To return your used device, please use the return and collection systems or contact the retailer where the product was purchased. They can take this product for environmental safe recycling.

Appendix D Data sheets: Research environmental monitoring equipment

Technical Data sheet

Hanwell

SR2 Base Station

Pro Network Receiver

Base Unit

The SR2 is the Hanwell Pro network enabled smart receiver, designed for collecting environmental monitoring data from multiple points within a site, or across multiple sites. The unit can receive data from up to 253 Hanwell Pro transmitters.

Features

- ✓ British made high performance technology
- ✓ Incorporates standard TCP/IP comms protocols for rapid data handling
- ✓ Each SR2 can obtain data from up to 253 sensors
- ✓ Unlimited number of SR2's can be used on a single system
- ✓ Data is automatically sorted and filed
- ✓ Long-distance radio transmission when accompanied with receiver

Always ask for a long-range signal strength test.

We can prove ours to be unrivalled.

Product code: SR2-E-P4/5/7 (P4 = UK, P5 = EU and P7 = Aus power supply)

Instrumentation specification	
Dimension (Excl. ancillaries)	300 x 200 x 85mm
Weight	1.2 kg
Power supply	110V AC or 240V AC. On-board 12V battery backup supplying 2.3A/hr
Case material	Powder coated mild steel
Memory capacity	512kb
Clock accuracy (logging)	40ppm @ 25°C
Operating temperature range	5°C to +40°C
Operating humidity range	0-100% RH non-condensing
Storage temperature	-40°C to +60°C
IP Rating	IP54

Accessories	
RX-xx	Remote receiver - please specify the frequency required
SR2-E-7.0-UPS	7.0Ah external wall mounted UPS
SR2-E-15-UPS	15Ah external wall mounted UPS

Outputs	
Alarm outputs	1 x nominal 12V, 2 x changeover relays (energised when no alarms exist)
MS1000 cards	4 core signal cable

Technical Data sheet

Hanwell

How it works

The Hanwell Pro SR2 logs all received data in its on-board 512kb memory. The Hanwell EMS software continually interrogates the SR2 for the most recent data, and downloads the data according to user-defined logging periods to the server or operating PC. Software users can view live and historic data, produce out of spec and summary reports and set alarms on both the data levels and the rate of change.

The SR2 is designed to be in constant communication with the software but has user-configurable fallback behaviour in the event of network or power failure. An on-board battery provides a UPS with 2.3A/hour life to carry it through up to 12 hours' power disruption (larger external UPSs are available as an optional extra).

Alarm relays are included: these can indicate that the readings are out of specification, and can be optionally set to indicate a network failure. MS1000 cards can be used to to drive beacons, sounders and control systems on sensor alarm events.

Schematic - SR2

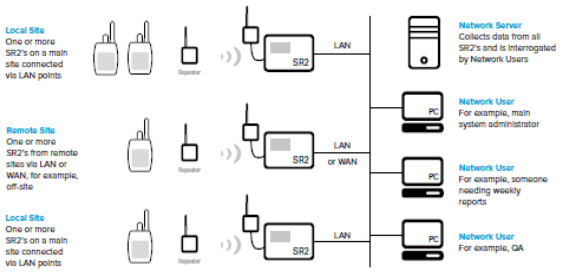

One system can comprise an unlimited number of sites.

Hanwell

ML4106 transmitter

Pro ML4000RH/T Series

Temperature

Humidity

Radio transmitter

Part of the **Hanwell Pro** ML4000RHT Series, the ML4106 combines temperature and humidity measurement using onboard sensors. The instrument includes LCD display and 434.075MHz frequency as standard.

Features

- ✓ Combined temperature & humidity measurement
- ✓ LCD display with 50,000 data readings per channel & up to 2 years battery life
- ✓ Superior performance hardware & high accuracy sensors
- ✓ Easily accessible battery & USB socket
- ✓ Low power radio for long distance transmission (3km over open ground)
- ✓ Complies with RoHS, EU & WEEE directives
- ✓ Carries CE Marking

Typical Applications

- Showcases
- Ambient room conditions
- Stored collections

Always ask for a long-range signal strength test.

We can prove ours to be unrivalled.

Product code: ML4106-434.075

Instrumentation specification	
Dimension (Excl. ancillaries)	110 x 80 x 35mm
Weight	200 grams
Power supply	1 x 3.6V AA Lithium battery
Case material	ABS & PC
Memory capacity	50,000 readings per channel (unit will wrap when full)
Clock accuracy (logging)	20 ppm at 25°C
IP Rating	IP30
Instrument operating range	-20°C to +65°C in a non-condensing RH environment
Storage temperature	-40°C to +60°C
Resolution	0.1°C (temp), 0.1%RH (humidity)

Radio transmitter functions	
Frequency options	A range of frequencies are available between 433-458MHz. Country specific regulations apply.
Radio power	10mW
Radio range	3km over open ground
Battery life	Up to 2 years (dependent on conditions of use and instrument settings)
Software required	W900 – Standard EMS Software Package *See EMS datasheet for further options
Hardware required	CR2 / CR3 – Controller SR2 – Smart Receiver REP – Repeater

Accessories	
Y119	Wall mounting bracket
88706	AA Lithium battery

Sensor options (supplied with unit)

Internal temperature sensor	Precision Thermistor
Operating range	-20°C to +60°C (restricted by instrument operating range)
Accuracy	+/- 0.3°C
Long term drift	< 0.1°C per year

Fixed humidity sensor	Capacitive Polymer
Operating range	10-90% RH non condensing
Accuracy	+/- 3% RH
Temperature dependence	<(0.025+0.0003xRH)[%RH/°C]

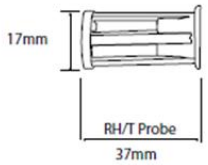

Technical Data sheet

RL4109 transmitter

Pro RL4000RH/T Series

Part of the **Hanwell Pro** RL4000RHT Series, the RL4109 outdoor transmitter combines temperature and humidity measurements and is configured to 434.075MHz frequency as standard.

Temperature

Humidity

Radio transmitter

Features

- ✓ Combined temperature & humidity measurement for outdoor use
- ✓ LCD display with 50,000 data readings per channel & up to 2 years battery life
- ✓ Superior performance hardware & high accuracy sensors
- ✓ Easily accessible battery & USB socket
- ✓ Low power radio for long distance transmission (3km over open ground)
- ✓ Complies with RoHS, EU & WEEE directives
- ✓ Carries CE Marking
- ✓ Supplied with wall bracket

Typical Applications

- Outdoor comparative data

Always ask for a long-range signal strength test.

We can prove ours to be unrivalled.

Product code: RL4109-OD-434.075

Instrumentation specification	
Dimension (Excl. ancillaries)	150 x 88 x 50mm
Weight	485 grams
Power supply	1 x 3.6V AA Lithium battery
Case material	ABS & PC
Memory capacity	50,000 readings per channel (unit will wrap when full)
Clock accuracy (logging)	20 ppm at 25°C
IP Rating	IP30
Instrument operating range	-20°C to +65°C in a non-condensing RH environment
Storage temperature	-40°C to +60°C
Resolution	0.1°C (temp), 0.1%RH (humidity)

Radio transmitter functions	
Frequency options	A range of frequencies are available between 433-458MHz. Country specific regulations apply.
Radio power	10mW
Radio range	3km over open ground
Battery life	Up to 2 years (dependent on conditions of use and instrument settings)
Software required	W900 – Standard EMS Software Package W906 – Validated EMS Software Package *See EMS datasheet for further options
Hardware required	CR2 / CR3 – Controller SR2 – Smart Receiver REP – Repeater

Accessories	
Y119	Wall mounting bracket
88706	AA Lithium battery

Technical Data sheet

Sensor options (supplied with unit)

J140 EE07-02 RH/T probe	
Temperature Probe	PT1000 (Tolerance class A)
Temperature operating range	-40°C to +80°C (restricted by instrument operating range)
Cable operating range	-40°C to +80°C
Temperature accuracy	+/- 0.1°C at 20°C (see temp accuracy chart)
Long term drift	+/- 0.05°C per year
Humidity Probe	Capacitive Polymer
Recommended range	0-100% RH non condensing
Accuracy	+/- 2% (0-90%) +/- 3% (90-100%)
Temperature dependance	<(0.025+0.0003xRH[%RH*C]

Temperature accuracy chart for EE07 probe

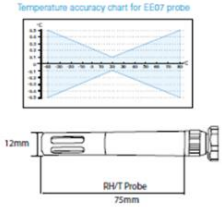

Solar and rain shield

T351-G18	
Operating environment	
Operating/Storage temperature	-40°C to +80°C
Maximum wind speed	75 m/s (168mph)
Shielding performance	
Shielding efficiency *(temperature rise/error due to incident solar radiation)*	2.3°C/KW/m² at 1m/s typical
Mechanics	
Diameter	76mm
Shield materials	Nylon/polyamide, polycarbonate, ABS, aluminium, stainless-steel
Overall height	118mm
Typical weight	110g

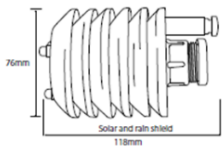

Technical Data sheet

ML4114 Radio Transmitter

Pro ML4000RH/T Series

Temperature

Radio transmitter

Humidity

Part of the **Hanwell Pro** ML4000RHT Series, the ML4114 combines high accuracy temperature and humidity measurement using an EE07 probe. The instrument includes LCD display and 434.075MHz frequency as standard.

Product code: ML4114-434.075

Features

- ✓ Combined temperature & humidity measurement
- ✓ LCD display with 50,000 data readings per channel & up to 2 years battery life
- ✓ Superior performance hardware & high accuracy sensors
- ✓ Easily accessible battery & USB socket
- ✓ Low power radio for long distance transmission (3km over open ground)
- ✓ Complies with RoHS, EU & WEEE directives
- ✓ Carries CE Marking

Typical Applications

- Dry storage
- Ambient room conditions

Always ask for a long-range signal strength test.

We can prove ours to be unrivalled.

Instrumentation specification	
Dimension (Excl. ancillaries)	110 x 80 x 35mm
Weight	200 grams
Power supply	1 x 3.6V AA Lithium battery
Case material	ABS & PC
Memory capacity	50,000 readings per channel (unit will wrap when full)
Clock accuracy (logging)	20 ppm at 25°C
IP Rating	IP30
Instrument operating range	-20°C to +65°C in a non-condensing RH environment
Storage temperature	-40°C to +60°C
Resolution	0.1°C (temp), 0.1%RH (humidity)

Radio transmitter functions	
Frequency options	A range of frequencies are available between 433-458MHz. Country specific regulations apply.
Radio power	10mW
Radio range	3km over open ground
Battery life	Up to 2 years (dependent on conditions of use and instrument settings)
Software required	W900 – Standard EMS Software Package *See EMS datasheet for further options
Hardware required	CR2 / CR3 – Controller SR2 – Smart Receiver REP – Repeater

Accessories	
Y119	Wall mounting bracket
88706	AA Lithium battery
Y421-3	EE Probe extension lead 3 meters
Y421-5	EE Probe extension lead 5 meters

Technical Data sheet

Sensor options (supplied separately)

J40 EE07-02 RH/T probe	
Temperature Probe	PT1000 (Tolerance class A)
Temperature operating range	-40°C to +80°C (restricted by instrument operating range)
Cable operating range	-40°C to +80°C
Temperature accuracy	+/- 0.1°C at 20°C (see temp accuracy chart)
Long term drift	+/- 0.05°C per year
Humidity Probe	Capacitive Polymer
Recommended range	0-100% RH non condensing
Accuracy	+/- 2% (0-90%) +/- 3% (90-100%)
Temperature dependance	<(0.025+0.0002xRH)[%RH/°C]

Temperature accuracy chart for EE07 probe

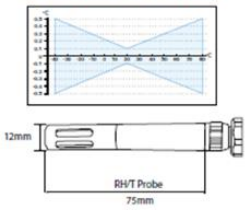

EE07-02

Low Power Humidity / Temperature Probe with Digital Output

EE07-02 is a version of the well-proven EE07 humidity (RH) and temperature (T) probe, optimized for very low power consumption and ideal for battery powered measurement devices. It is available in polycarbonate or metal enclosure and features the well-proven E+E HC105 humidity sensor.

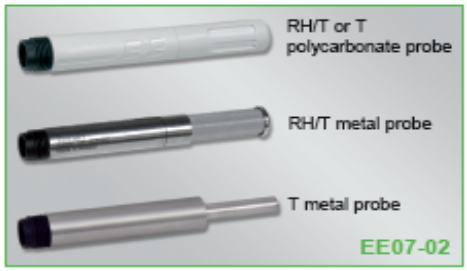

The wide T working range, the T compensation and the choice of filter caps make EE07-02 appropriate for both indoor and outdoor use. The E+E proprietary coating protects the humidity sensor against corrosion and dirt, which leads to best long term stability even in harsh environment.

The measured values are available on the serial E2 interface. The M12 connector allows for probe replacement within seconds. The user can perform the RH and T adjustment of the probe with the optional configuration kit.

Typical Applications

- Battery powered measurement devices
- Data loggers
- Hand held meters

Features

- Very low power consumption
- Outstanding RH and T Accuracy
- Excellent long term stability
- Pluggable and interchangeable

Technical Data

Measured values

Relative Humidity		
Sensor element	E+E HC105	
Digital output (2 wire E2 interface)[1]	output value: 0.00...100.00 % RH	
Working range	0...100 % RH	
Accuracy incl. hysteresis and nonlinearity	±2 % RH (0...90 % RH)	±3 % RH (90...100 % RH)
	Traceable to intern. standards, administrated by NIST, PTB, BEV...	
Supply voltage dependency at UB < 3.3 V DC	typ. -0.0026 % RH/mV	
Temperature dependence	< (0.025 + 0.0003 x RH) [$\frac{\%RH}{°C}$]	

Temperature	
Sensor element	Pt1000 (tolerance class A, DIN EN 60751)
Digital output (2 wire E2 interface)[1]	output value: -40.00...+80.00 °C (-40...176 °F)

Accuracy
(at 20 °C (68 °F): ±0.1 °C (±0.18 °F))

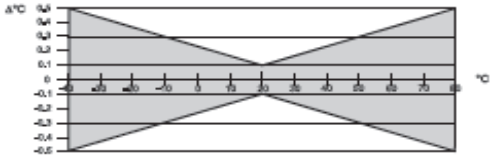

General

Supply voltage (Class III)	2.7 V DC - 5.5 V DC	
Voltage level digital interface	≤ Supply voltage, but max 3.5 V	
Current consumption	< 6 µA, in sleep mode 1.5 - 2.5 mA during measurement (150 ms)	
Average current consumption	< 200 µA at sampling rate 1 s	
Housing	polycarbonate or stainless steel / IP65	
Electromagnetic compatibility[2]	EN 61326-1 EN 61326-2-3	CE
Temperature range	working temperature:	-40...80 °C (-40...176 °F)
	storage temperature:	-40...60 °C (-40...140 °F)
Max. cable length[3]	30 m (98.4 ft)	

1) See details at support literature at www.epluse.com/EE07
2) No protection against surge
3) Depends on the bus frequency

Dimensions (mm/inch)

EE07-02-P

EE07-02-MFTx

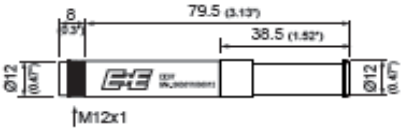

EE07-02-MT

Connection Diagram

EE07-02:

1...GND
2...+UB
3...DATA
4...CLOCK

M12x1 flange coupling with 50 mm (2") flying leads (HA010705):

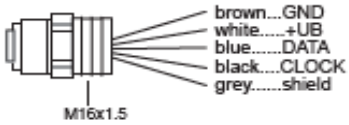

E+E Sensor Coating

The E+E proprietary sensor coating is a protective layer applied to the sensing elements. The coating extends substantially the lifetime and the measurement performance of EE07-02 in **corrosive environment**. Additionally, it improves relevantly the long term stability in **dusty, dirty or oily applications** by preventing stray impedances caused by deposits on the active sensor surface.

Ordering Guide

HOUSING		MODEL		FILTER		COATING[1]	
metal[2]	(M)	humidity and temperature	(FT)	membrane	(1)	without	(no code)
polycarbonate	(P)	temperature	(T)	metal grid	(6)	with	(HC01)
				stainless steel grid[2]	(9)		
EE07-02-							

1) Only available for model humidity & temperature (FT).
2) The metal housing (M) is only available with stainless steel grid filter (9). The stainless steel grid filter (9) is only available with metal housing (M).

Order Example

EE07-02-PFT6

Housing:	Polycarbonate
Model:	Humidity and temperature
Filter:	Metal grid
Coating:	without

EE07-02-MT

Housing:	Metal
Model:	Temperature

Scope of Supply

- EE07-02 probe according to ordering guide
- Inspection certificate according to DIN EN10204 - 3.1

Accessories (See data sheet "Accessories")

- M12x1 flange coupling with 50 mm (2") flying leads	HA010705
- Connecting cable M12x1 - flying leads (1.5 m (59.1") / 5 m (196.9") / 10 m (393.7"))	HA010819/20/21
- Filter caps	HA0101xx
- Radiation shield with cable gland (M20x1.5)	HA010502
- Configuration adapter	see data sheet EE-PCA

DampWatch

Moisture and rising damp detection

HANWELL

Long-term moisture penetration of structural timbers, porous brickwork and masonry walls can be the cause of major deterioration in a buildings structure.

Often damp can go unnoticed until it becomes clearly visible through 'tide marks' on walls, jeopardising internal contents thereafter.

Detecting moisture before visible damage occurs is crucial to early identification of leaks, issues with draining systems and so on -ultimately preventing expensive and time-consuming building repairs.

The Hanwell DampWatch unit can be used to detect this moisture well before long-term damage can set in.

With up to 16 dampness sensors per unit, DampWatch uses Wood Moisture Equivalent (WME) measurements to detect moisture in multiple areas.

Product Features

- Uses industry recognised WME measurements.
- Device accepts up to 16 dampness sensors per unit.
- Uses unrivalled radio technology.
- Superior performance hardware with high accuracy dampness sensors.
- Complies with RoHS, EU and WEEE directives.
- Carries CE Marking

Benefits

- Provides users with critical moisture data.
- Prevents expensive and time-consuming building repairs caused by moisture.
- Assist with mould growth reduction.
- Assists with reducing health hazards caused by mould and air moisture

Always ask for a long-range signal strength test.

We can prove ours to be unrivalled.

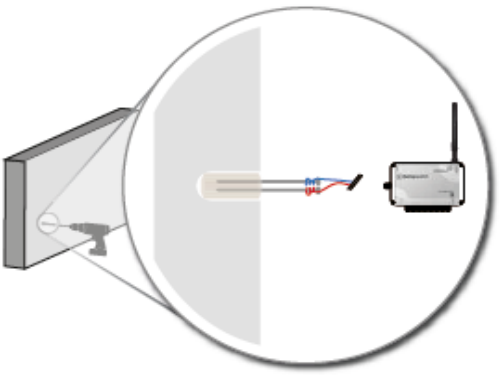

The dampness sensors can be inserted into timber, brickwork or masonry walls. Data is transmitted using radio to Synergy software.

CE RoHS

imc

BRITISH MADE for Quality

Another solution from **The IMC Group Ltd.**
Pendle House, Jubilee Road, Letchworth, Hertfordshire SG6 1SP
Tel: +44 (0)1462 686070 | Email: sales@the-imcgroup.com | Visit: www.the-imcgroup.com

Graphical Data

The below graph shows successive channel readings (channel no. is shown in blue) returning to zero after every loop round as a marker.

The red trace shows the WME of each channel, all showing 15% in this example. Alarms can be generated from this data in all the normal ways.

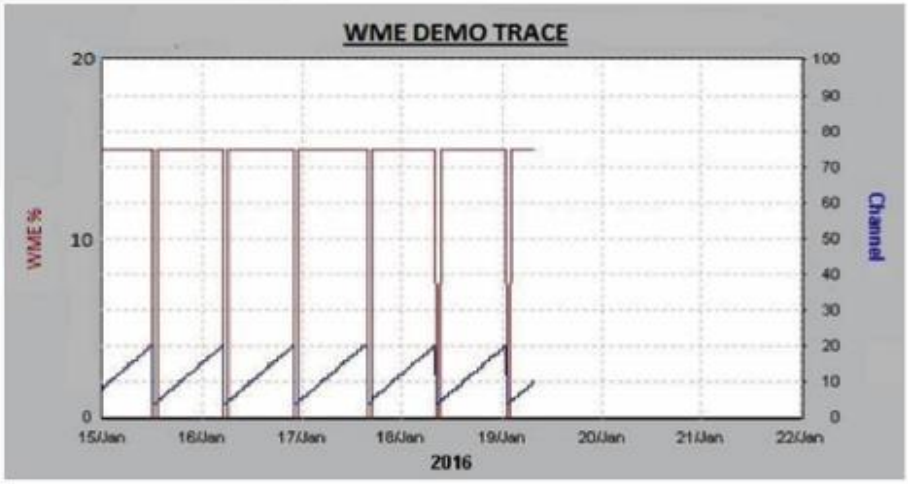

SPECIFICATIONS

Part number:	16-MSM-434.075
Frequency options:	A range of frequencies are available between 426 - 458MHz. Country specific regulations apply.
Radio power:	10mW
Radio range:	3km over open ground
Software required:	W700 – Standard Synergy Software Package W706 – Validated Synergy Software Package
Hardware required:	CR2 – Controller or SR2 – Smart Receiver REP – Repeater (not always needed) Ask for a signal strength test
Environmental:	Instrument operating range -20°C to +65°C in a non-condensing RH environment
Dimensions:	200 x 120 x 80mm
Power supply:	12V DC Power Supply
Case material:	ABS
Sensor specification:	Resistive, range equivalent of 7%WME to 35%WME (6340M ...37.6k)

imc
BRITISH MADE for Quality
Another solution from **The IMC Group Ltd.**
Pendle House, Jubilee Road, Letchworth, Hertfordshire SG6 1SP
Tel: +44 (0)1462 686070 | Email: sales@the-imcgroup.com | Visit: www.the-imcgroup.com

AIR FLOW METER

Air flow monitoring

HANWELL

The Hanwell 4000 series of radio transmitter units are well established as being the most flexible on the market today. The RL4810 air flow unit is a reliable 4000 wireless transmitter with air flow sensor that provides users with the tools for preventative maintenance within refrigeration units, filtration systems and air handling systems etc.

The Hanwell RL4810 wirelessly transmits directly to a local SR2/CR2 and PC or Network for immediate alarm notification and long-term analysis. This wireless device also includes a logging function that guarantees against gaps in data during the unlikely event of radio communication loss.

Product Features

- Detects early signs of failure within refrigeration plants
- Identifies reduced air flow through blocked filters
- Low power radio for long distance transmission (over 3km over open ground)
- Identifies problems in air handling systems
- Supports (optional) hidden wall brackets
- Complies with RoHS, EU directives and WEEE
- Carries CE Marking

Benefits

- Cuts maintenance costs and enables users to introduce optimised maintenance plans
- Reduces downtime and associated costs
- Reduces errors and hassle associated with manual checks
- Eliminates the risk of damage to stock and prevents process failures

Radio System (requires radio receiver)

Always ask for a long-range signal strength test.

We can prove ours to be unrivalled.

CE RoHS

imc

BRITISH MADE for Quality

Another solution from **The IMC Group Ltd.**
Pendle House, Jubilee Road, Letchworth, Hertfordshire SG6 1SP
Tel: +44 (0)1462 686070 | Email: sales@the-imcgroup.com | Visit: www.the-imcgroup.com

Air Flow Meter
DATASHEET

HANWELL

4810

Radio transmitter code: RL4810-434.075 *(other frequencies are available)*

SPECIFICATIONS

Instrumentation Specification:

Dimensions:	110 x 80 x 35mm
Weight:	200 grams
Power supply:	External 12V DC
Case material:	ABS & PC
Memory capacity:	100,000 readings
IP Rating:	IP50

Radio Transmitter Functions:

Frequency options:	A range of frequencies are available between 433-458MHz. Country specific regulations apply.
Radio power:	10mW
Radio range:	3km over open ground
Software required:	W700 – Standard Synergy Software Package W706 – Validated Synergy Software Package *See Synergy datasheet for further options
Hardware required:	CR2 – Controller SR2 – Smart Receiver REP – Repeater
Accessories:	Y119 – Wall mount bracket

This product can be calibrated to your specifications, contact us for further details. N.B Instrument operating range-20°C to +65°C in a non-condensing RH environment (operating range dependant on sensor).

4810 – Radio transmitter & data logger

Airflow transmitter with 1 x 0-5v input

Probe Options Available

Option 1: J202-07
Air flow sensor: 0-5m/s (0... 1000ft/min)
Working range temperature: 0°C to +60°C
Storage Temperature: -30°C to +60°C
Working range: 0-5m/s (0... 1000ft/min)
Accuracy: ±(0.2m/s / 40ft/ min +3% of measuring value)

Option 2: J189-07
Air flow sensor: 0-10m/s (0...2000ft/min)
Working range temperature: 0°C to +60°C
Storage Temperature: -30°C to +60°C
Working range: 0-10m/s (0...2000ft/min)
Accuracy: ±(0.3m/s / 60ft/ min +4% of measuring value)

Option 3: J211-07
Air flow sensor: 0-20m/s (0...4000ft/min)
Working range temperature: 0°C to +60°C
Storage Temperature: -30°C to +60°C
Working range: 0-20m/s (0...4000ft/min)
Accuracy: ±(0.4m/s / 80ft/min +6% of measuring value)

imc

BRITISH MADE for Quality

Another solution from **The IMC Group Ltd.**
Pendle House, Jubilee Road, Letchworth, Hertfordshire SG6 1SP
Tel: +44 (0)1462 686070 | Email: sales@the-imcgroup.com | Visit: www.the-imcgroup.com

RADIOLOG SOFTWARE

RadioLog8 is the software platform that supports all Hanwell hardware.

All Hanwell transmitters are configured through RadioLog8 which enables users to set thresholds and alarms before transmitters are positioned throughout a site. Data is captured within RadioLog and stored on a user server for historical analysis and audit trails (where required).

The software is a forms application which ensures fast and comprehensive access to stored data and a rapid response to user requests. RadioLog provides the functionality to view data using graphs, tables and plan view layouts as well as set user notifications and report on alarms generated. A typical system will use distributed clients to view data held on a central server but stand alone operation is also possible.

Software Features

- Runs on a variety of Microsoft based platforms including: Windows 98, 2000, 2003, 2008, XP and 7
- Can accommodate multiple users with permission functionality
- Devices can be added at will with no interruption to logging
- Users can be added as required
- Supports multiple geographical locations in a single organisation, seamlessly
- Access to historical data
- Extensive reporting tools available
- User access control
- Supports GPRS transmitters
- Variety of alarm features available including email and SMS notifications
- Full history of recorded data available for analysis by users at all times
- Export data files to CSV format

Benefits

- Ensures alarms conditions are notified to the relevant responsible personnel
- Assists with national regulatory compliance such as HACCP, MRHA and 21 CFR Part 11
- Free up staff time by removing manual checking processes
- Eliminate errors associated with manual checks
- Improve speed of preventative action with immediate email and SMS alarms
- Generate a complete environmental monitoring solution for multiple parameters in multiple locations using RadioLog8
- Easily expand or change the system as and when required
- No cost obligation following purchase of the system and software
- Post purchase support available

Data Accessibility

PC	✓
Web	✗

PC Prerequisites

Standalone PC

- Processor Intel® Pentium® or equivalent
- Memory 1GB minimum 2GB recommended
- Hard drive 80GB +
- USB ports minimum 2 spare
- Ethernet network port
- Windows® XP Pro (32 or 64bit)
- Vista not recommended

Server

- Processor Intel® Pentium® or equivalent
- Memory 2GB minimum 4GB recommended
- Hard drive 130GB +
- USB ports minimum 2 spare
- Ethernet network port
- Windows® Server 2000 or later (32 or 64bit)

Compatible Hardware:
The RadioLog8 software is compatible with all Hanwell Radio and GPRS hardware*.
*W600 also required for GPRS devices

Data Viewing Options
Tabular
Graphical
Plan View

Regulatory Assistance
HACCP
FDA 21 CFR Part 11
And other national regulatory bodies

Tabular View

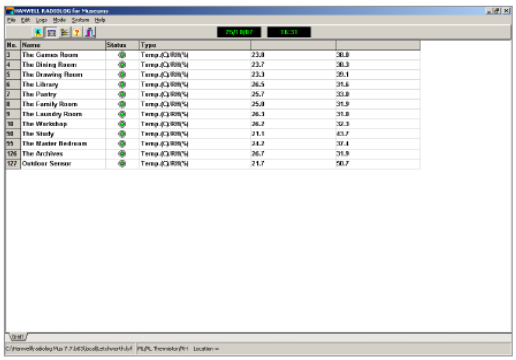

Graphical View

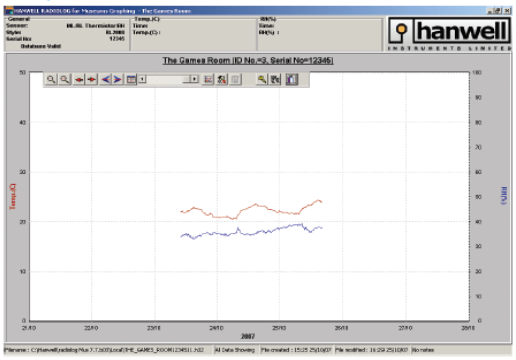

Plan View

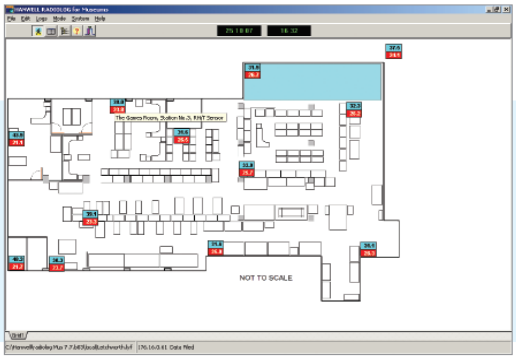

Tabular View
View list of sensors with traffic light status:
Red – Alarmed sensor
Orange – Acknowledged alarm
Green – No alarm

Graphical View
Line or bar graph with multiple sensor data overlay options for environmental comparison.

View sensor intervals and drag and view sensor reading date and times.

Plan View
Upload building floorplans and view sensor alarms and values in situ.

Flexible drag and drop sensors to new locations when they are required to be moved.

Sales sheet

Hanwell EMS

Comprehensive Software Platform

EMS is a leading edge software platform that combines and supersedes Synergy and Notion Pro onto a single integrated software solution.

EMS is a scalable and offers a contemporary browser-based user interface. This enables the data from both Hanwell Pro and Hanwell IceSpy hardware to be seamlessly fed into one system, providing an industry leading software and hardware combination.

Multisite/Group | Audit trails | Historical data | Email/SMS alerts | Report Scheduling | RAG Alarms

Developed to give maximum flexibility and control of data and events, EMS has made significant advances in how, where and when data can be viewed and managed across the widest spectrum of customers from the single site/single user through to multiple site/multiple user situations. EMS also has both standard and bespoke reporting options to meet the simplest and most complex customer requirements.

Software Features & Benefits

- Browser based technology with SQL database
- Top level pictorial overview of site activity and alarms on start up
- Devices can be added at will with no interruption to logging
- User access management and control via simple permissions process
- Seamlessly supports multiple geographical locations
- Easy navigation to alarms, reporting tools and administration areas
- Easy access to historical data
- Supports all Hanwell Pro & Hanwell IceSpy current and future hardware
- Option to design additional bespoke reports
- Various software installation configurations available
- Allows flexible grouping of sensors to customise views even across multiple sites
- Variety of alarm features available including email and SMS notifications, including mobile app
- Full history of recorded data available for analysis by users at all times
- Export data files to CSV formats
- Automated reporting directly to PDF format at user defined timescales
- Interactive graphical and tabular data
- Gives the user maximum control of how, when and where the data is managed and presented
- Simple to use and manage providing instant alarm notification to relevant personnel
- Assists with national regulatory compliance such as MRHA and 21 CFR Part 11
- Frees up staff time and eliminates errors by removing manual checking processes
- Improves speed of preventative action with immediate email and SMS alarms
- Generates a complete environmental monitoring solution for multiple parameters in multiple locations
- Easily expandable/changeable system as and when required with minimal disruption
- Post purchase support available
- Integration of data from handheld and data logging devices, creating centralised and paperless monitoring.

Sales sheet

Hanwell

OVERVIEW

Overview provides users with an overview of overall system status, while the dashboard can be customised per user.

TABULAR VIEW

Tabular View provides list of sensors with clear indication of alarm, battery status and live data

GRAPHICAL VIEW

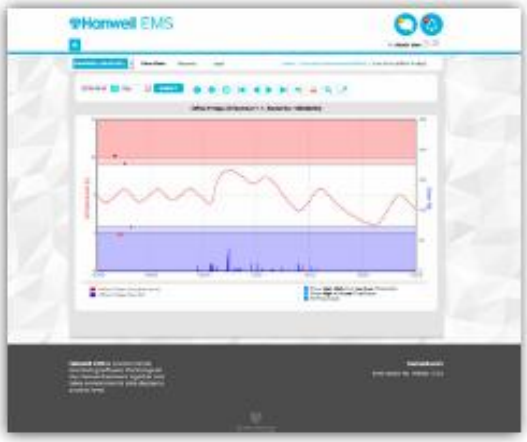

Graphical View provides line graphs with optional door position indicator, alarm level indication. Data overlays, zoom plus many more features.

PLAN VIEW

Plan View provides visual indication of sensor location within a facility. Sensor icons show real-time data and alarms and interaction by double clicking icon.

Sales sheet

Hanwell

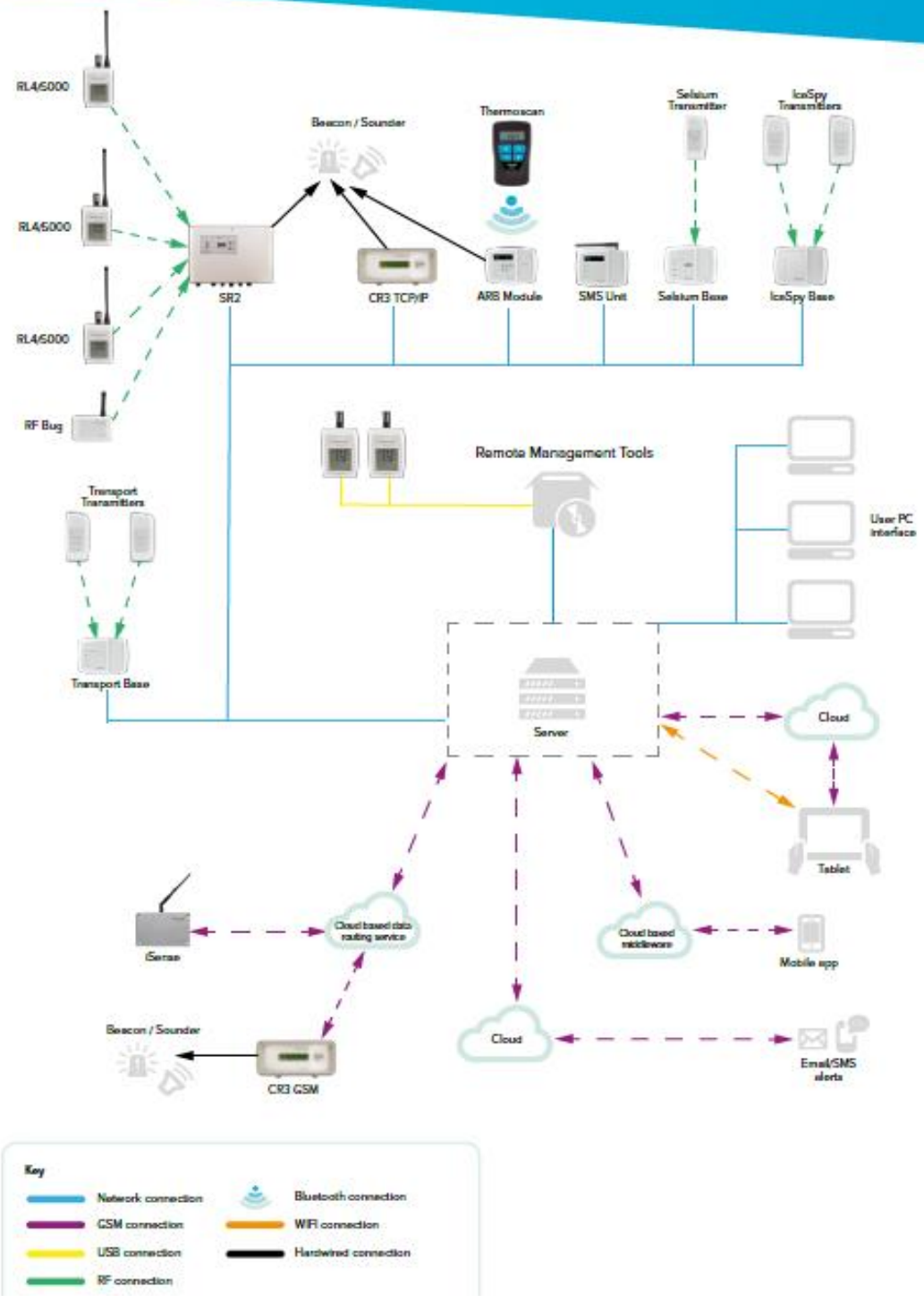

Table of specifications for monitoring equipment used during research project

Monitor	Sensor Type	Range of measurement	Required accuracy	Optimum sample rate	Record rate	Supplier	Unit Specification	System Hardware	System Software	Number of Units	Location(s)
Air flow	Thermoelectric Anemometer (J189-07)	0 - 10 m/s	±(0.3m/s +4% of measuring value)	5 - 10 sec	every 15 mins	Hanwell	RL4810	Smart Receiver SR-2	RadioLog8 (replaced by EMS Aug 2018)	1	HMS 6
Temperature	Pt1000 tolerance class A (EE07-02)	-40 to +80°C	±0.1°C at 20°C	10 - 30 sec	every 15 mins		ML4109			1	D2 external
	Precision Thermistor	-20 to +60°C	±0.3°C	10 - 30 sec	every 15 mins		ML4106			7	D2; HMS,4,5,6; L&A; D2 tent
	Pt1000 tolerance class A (EE07-02)	-40 to +80°C	±0.1°C at 20°C	10 - 30 sec	every 15 mins		ML4114			2	HMS 6
Relative Humidity	Capacitive polymer	0% to 100%	±2% (0-90%)	10-30 sec	every 15 mins		ML4109			1	D2 external
	Capacitive polymer	10% to 90%	±3%	10-30 sec	every 15 mins		ML4106			7	D2; HMS 4,5,6; L&A; D2 tent
	Capacitive polymer	0% to 100%	±2% (0-90%)	10-30 sec	every 15 mins		ML4114			2	HMS 6
Moisture Content	Electrical resistance	7%WME to 35%WME	±2.5%	10-30 sec	every 60 mins		Dampwatch			1	HMS 4,5,6

Sensor specifications for Hanwell RH/T transmitters

Model	**ML4106**	**ML4109**	**ML4114**
Portable or fixed	Portable or wall mount bracket	Portable or wall mount bracket	Portable or wall mount bracket
Internal/ external	internal	external	internal
Display	Yes - LCD	no	Yes - LCD
Dimensions	110 x 80 x 35mm	150 x 88 x 50mm	110 x 80 x 35mm
Power supply	3.6 V Lithium battery	3.6 V Lithium battery	3.6 V Lithium battery
Resolution	0.1% RH	0.1°C, 0.1% RH	0.1% RH
Calibration	In-house or on-site Supplier or user	In-house or on-site Supplier or user	In house or on-site Supplier or user
Frequency	433-458MHz	433-458MHz	433-458MHz
Radio range	3km/ open ground	3km/ open ground	3km/ open ground
Probe- T	NTC Thermistor	RTD-Pt1000	RTD-Pt1000
Probe – RH	Capacitive polymer	Capacitive polymer	Capacitive polymer
Sensor- CO_2	N/A	N/A	N/A
Range – T	-20°C - +60°C	-40°C - +60°C	-40°C - +60°C
Range – RH	10%-90%	0%-100%	0%-100
Accuracy -T	±0.3°C	±0.1ºC at 20 ˚C	±0.1ºC at 20 ˚C
Long term drift	<0.1°C/yr	±0.05°C/yr	±0.05°C/yr
Accuracy – RH	±3% RH	±2% (0 -90%); ±3% (90-100%)	±2% (0 -90%); ±3% (90-100%)
T dependence	<(0.025 + 0.0003 x RH) [$[(\%RH)/°C$]	<(0.025 + 0.0003 x RH) [$[(\%RH)/°C$]	<(0.025 + 0.0003 x RH) [$[(\%RH)/°C$]
Operating T	-20°C - +65°C	-20°C - +65°C	-20°C - +65°C
Wind speed	N/A	75m/s (168mph)	N/A
Data transmission	User defined;10 s - 24hrs	User defined;10 s - 24hrs	User defined;10 s - 24hrs
Memory capacity	50,000	50,000	50,000

Gemini DATA LOGGERS

Tinytag

DATA SHEET

Tinytag Ultra 2 Temperature/Relative Humidity Logger (-25 to +85°C/0 to 95% RH)

TGU-4500

Issue 10
17th October 2014
E&OE

Tinytag Ultra 2 data loggers are ideally suited to monitor interior applications where there is little or no moisture.

Tinytag Ultra 2 data loggers have a high reading accuracy and resolution, large memories, a fast offload speed and a low battery monitor.

The TGU-4500 is a self contained temperature and humidity recorder.

Popular Applications

- Office and housing monitoring
- Pharmaceutical manufacture
- Dry food storage
- Museum display and repository
- Incubators

Features

- Temperature and relative humidity recorder
- 32,000 reading capacity
- High accuracy
- High reading resolution
- Fast data offload
- Splash-proof case
- Low battery monitor
- User-replaceable battery

Appendix E Figures reproduced from Jankovic (various)

Design year simulated weather data (Jankovic, 2012b):

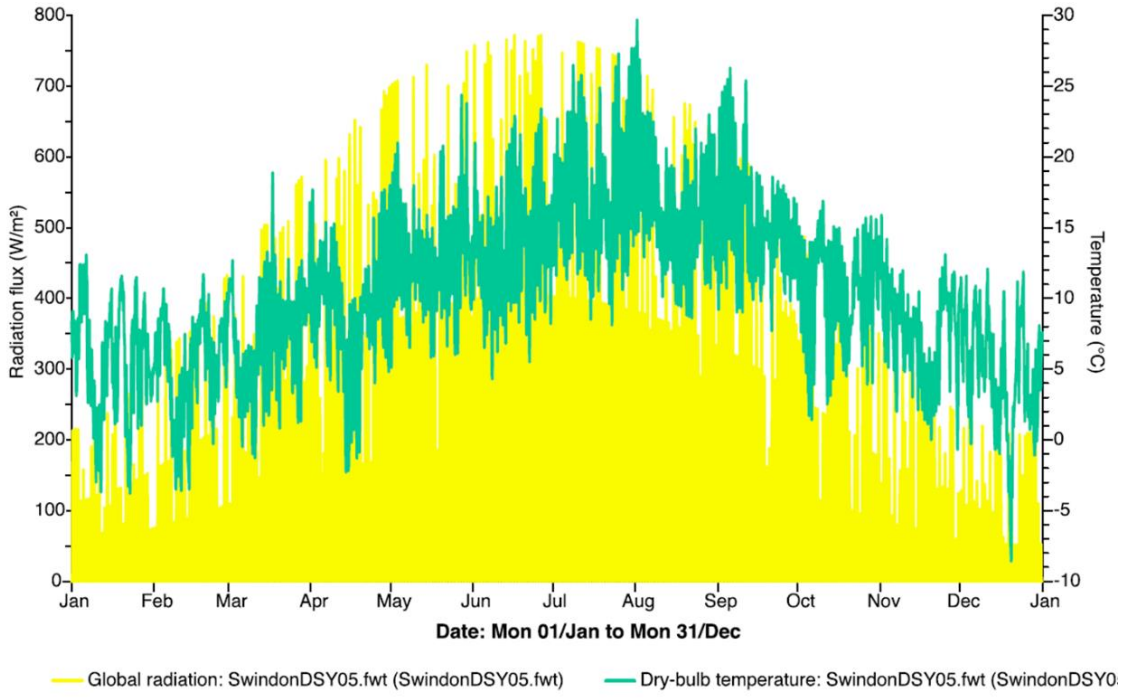

a) 2005

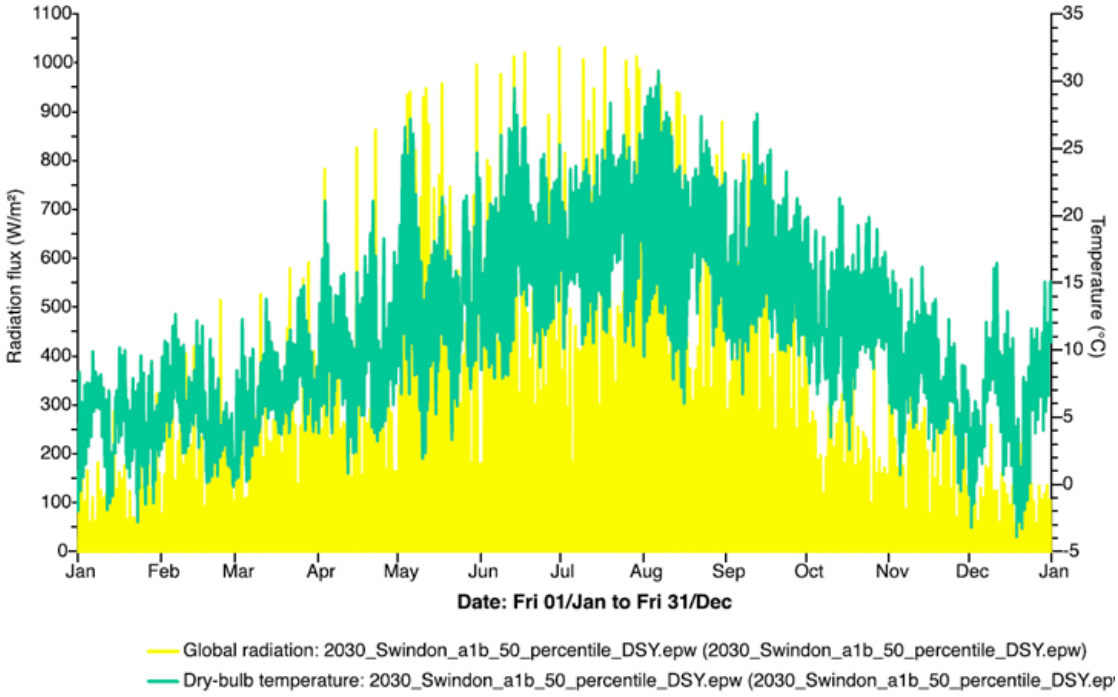

b) 2030

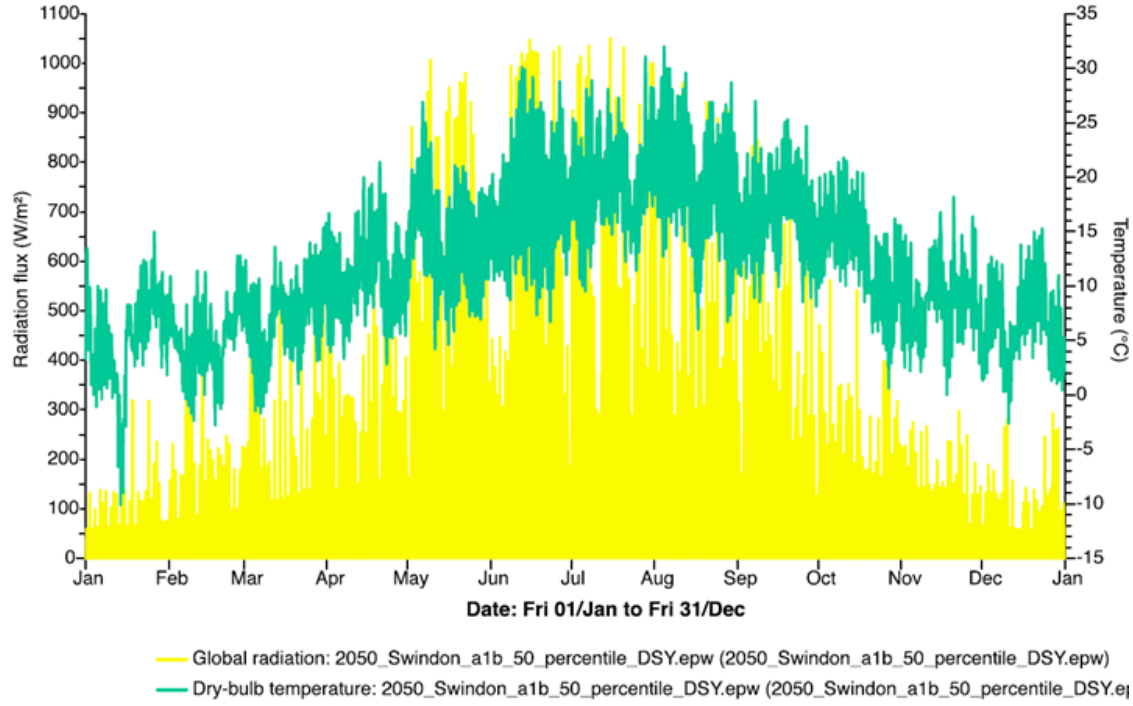
Radiation flux (W/m²)
Temperature (°C)
Jan
Feb
Mar
Apr
May
Jun
Jul
Aug
Sep
Oct
Nov
Dec
Jan
Date: Fri 01/Jan to Fri 31/Dec
Global radiation: 2050_Swindon_a1b_50_percentile_DSY.epw (2050_Swindon_a1b_50_percentile_DSY.epw)
Dry-bulb temperature: 2050_Swindon_a1b_50_percentile_DSY.epw (2050_Swindon_a1b_50_percentile_DSY.ep

c) 2050

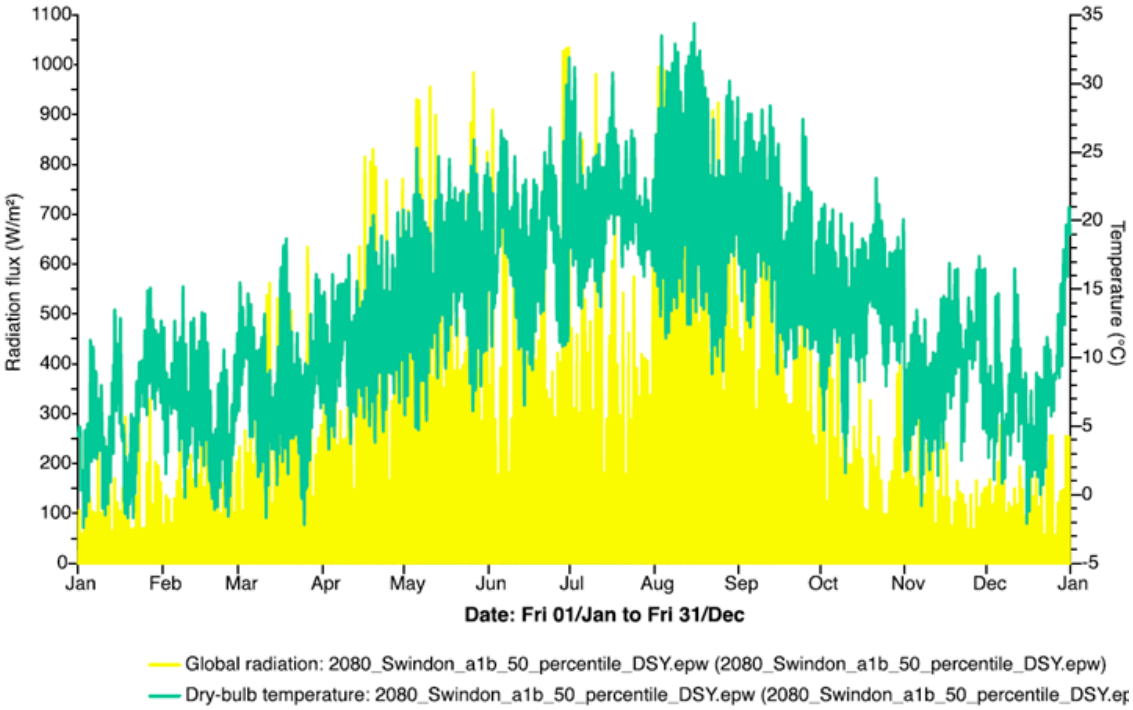
Radiation flux (W/m²)
Temperature (°C)
Jan
Feb
Mar
Apr
May
Jun
Jul
Aug
Sep
Oct
Nov
Dec
Jan
Date: Fri 01/Jan to Fri 31/Dec
Global radiation: 2080_Swindon_a1b_50_percentile_DSY.epw (2080_Swindon_a1b_50_percentile_DSY.epw)
Dry-bulb temperature: 2080_Swindon_a1b_50_percentile_DSY.epw (2080_Swindon_a1b_50_percentile_DSY.ep

b) 2080

Simulation model geometry showing the HMS within hangar D2 (Jankovic, 2012a):

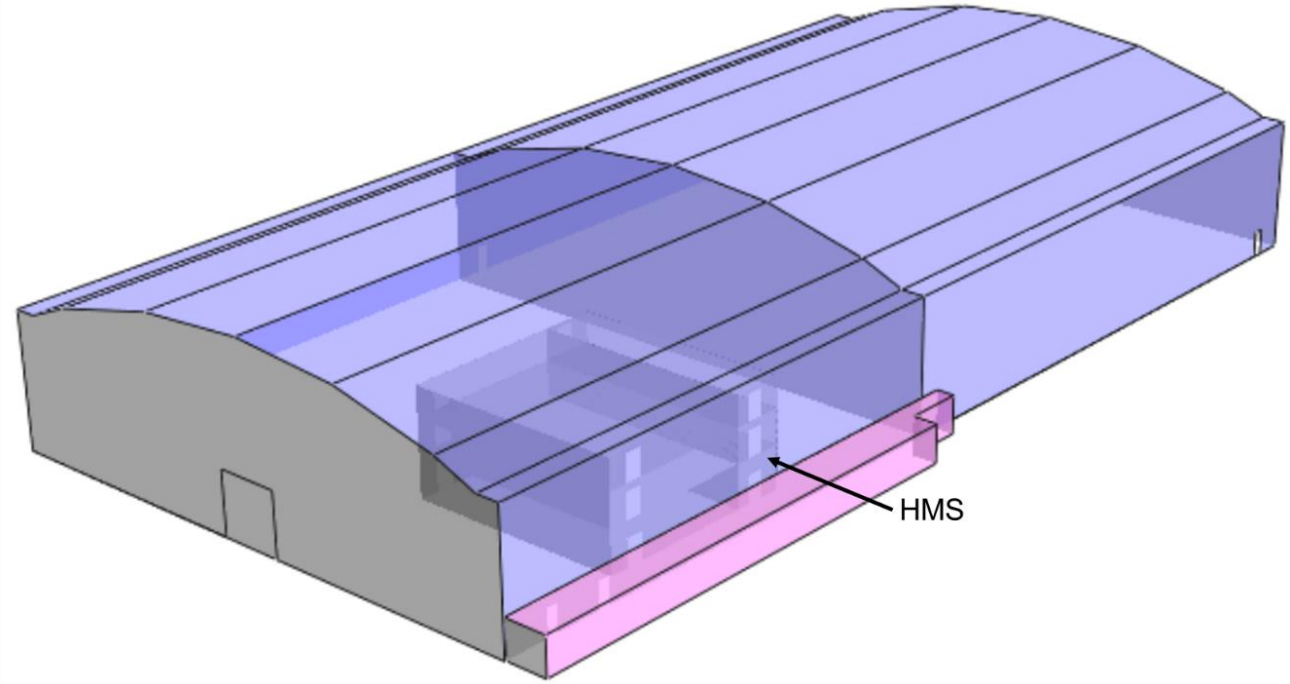

Tables of data used in simulations (Jankovic, 2012b):

Summary of changes in solar radiation and external air temperature

Year	Radiation flux (W/m^2)			Temperature (°C)		
	Min.Val.	Max. Val.	Mean	Min.Val.	Max. Val.	Mean
2005	0.0	772.0	113.8	-8.6	29.7	10.4
2030	0.0	1031.8	121.5	-3.9	30.8	11.6
2050	0.0	1050.7	125.6	-10.1	32.0	12.2
2080	0.0	1034.9	120.2	-2.4	34.4	13.3

Density of material in the RINA

Floor	Length (m)	Height (m)	Depth (m)	Number of sides	Number of shelves at 0.5 m height	Number of rows per shelf 0.25 m row depth	Utilisation factor	Volume of paper (m^3) = 0.5 m x 0.25 m x (1) x (4) x (5) x (6) x (7)
	(1)	(2)	(3)	(4)	(5)	(6)	(7)	(8)
Ground	17.45	3.35	1.5	2	5	6	0.95	124.33
First	17.45	2.67	1.5	2	4	6	0.95	99.47
Second	17.45	2.40	1.5	2	3	6	0.95	74.70
							Total	298.40

Density of material in the BOX

Floor	Length (m)	Height (m)	Depth (m)	Volume (m^3)	Volume Utilisation factor	Display unit utilisation factor	Volume of stored material (m^3) = (4) x (5) x (6)
	(1)	(2)	(3)	(4)	(5)	(6)	(7)
Ground	17.45	3.35	12.58	735.39535	0.6	0.3	132.37
First	17.45	2.67	12.58	586.12107	0.6	0.3	105.50
Second	17.45	2.40	12.58	526.8504	0.6	0.3	94.83
						Total	332.71

Thermal properties of storage contents, from CIBSE Guide A

Material	Thermal conductivity (W/m·K)	Density (kg/m^3)	Specific heat (J/kg·K)
Paper	0.07	480	1380
Softwood/ Pine	0.12	510	1380

Material thickness used in simulation

Material	Layer thickness in the party wall representing the full room loading (m)
Paper	1.92
Softwood/Pine	2.15

General lighting gains from ambient lighting

RINA	Floor	Lighting energy use (W/m^2)	Lighting energy use (W/m^2/100 lux)
	ground	7.63	3.22
	1^{st}	5.47	2.39
	2^{nd}	5.47	2.39
BOX	ground	5.32	2.21
	1^{st}	5.32	2.02
	2^{nd}	5.32	2.02

Equipment rating based on cooling and heating loads

		Base case – 98%
		kW
RINA	Heating	2.2
	Cooling	23.0
BOX	Heating	2.2
	Cooling	6.0

AHU sizing from flow rate and fan pressure

	Volume flow rate (m^3/s)	Fan total pressure Supply/Extract (Pa)	Max. power per fan (kW)
RINA	0.516	137/121	2.2
BOX	1.512	209/161	5.5

Plan showing initial layout of M&E plant on roof (Jankovic, 2012a):

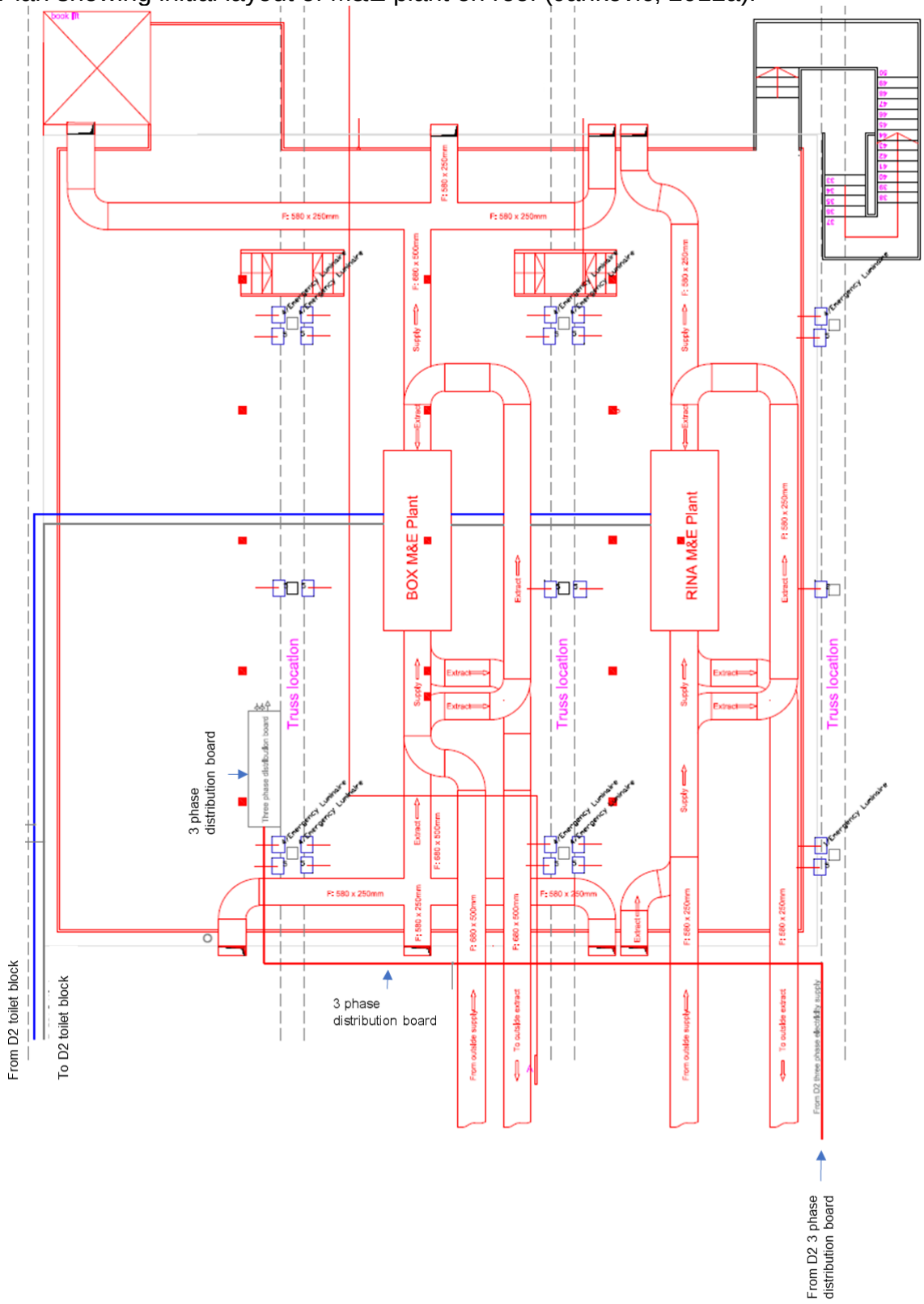

Plan showing initial layout of ducting and luminaires (Jankovic, 2012a)

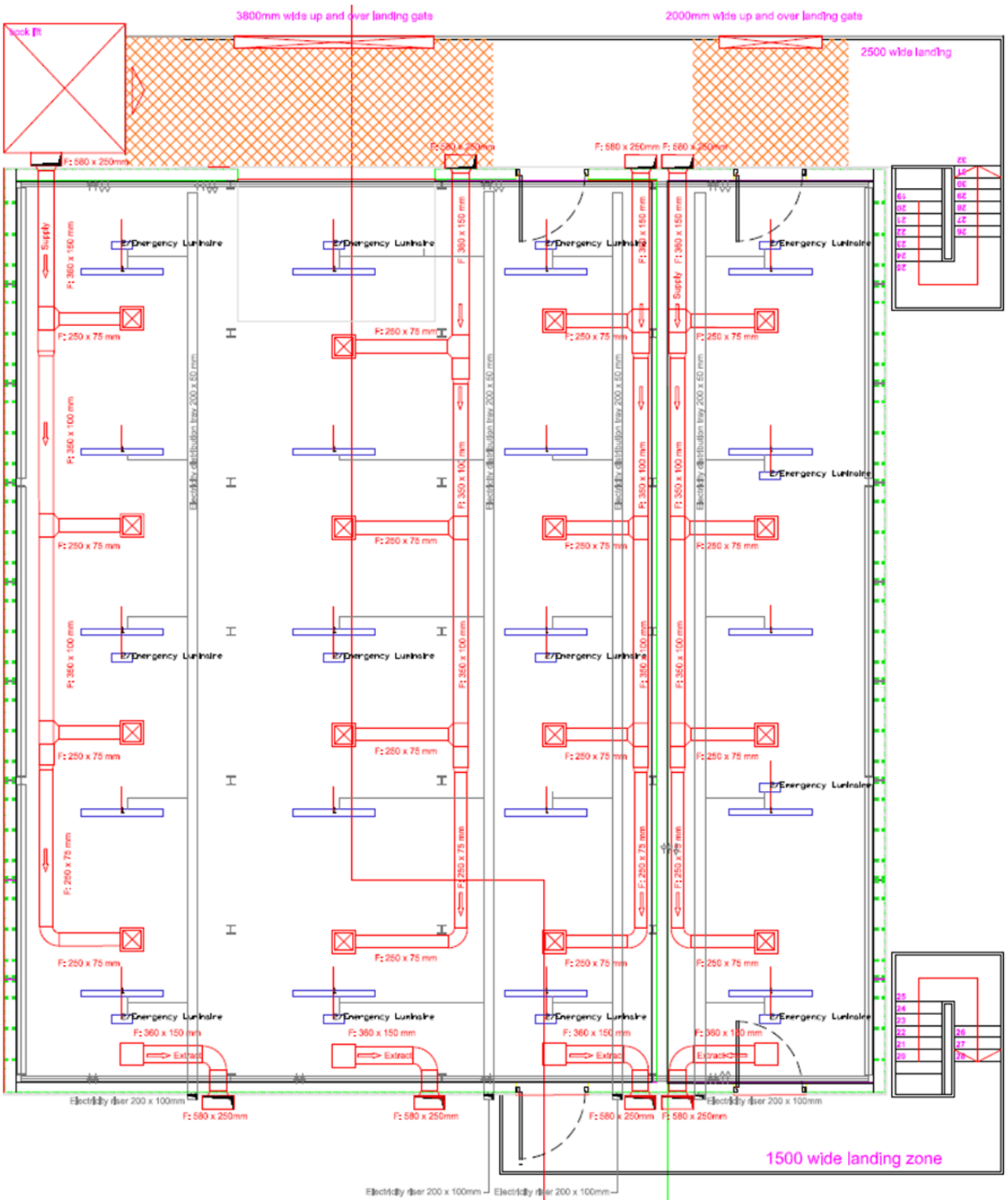

Measured and simulated internal conditions, HemPod, University of Bath (Jankovic, 2014):

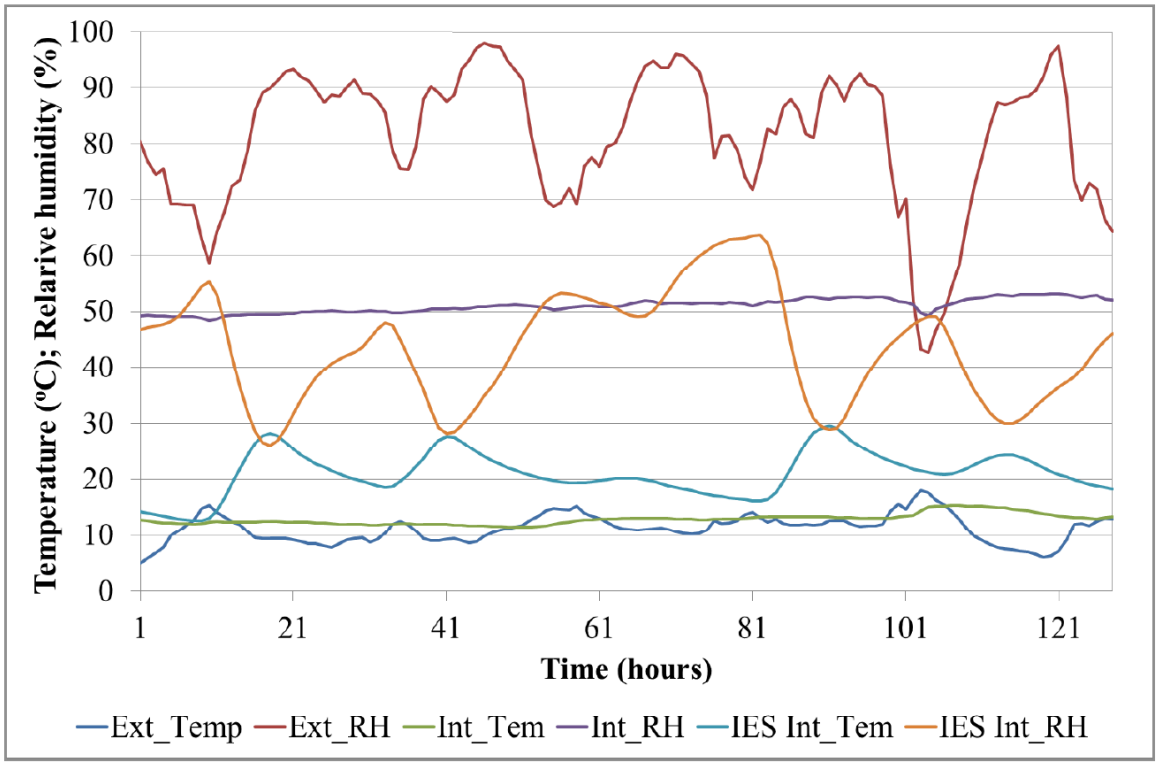

Results of Fourier filter on IES simulated temperature in the RINA (Jankovic, 2012c):

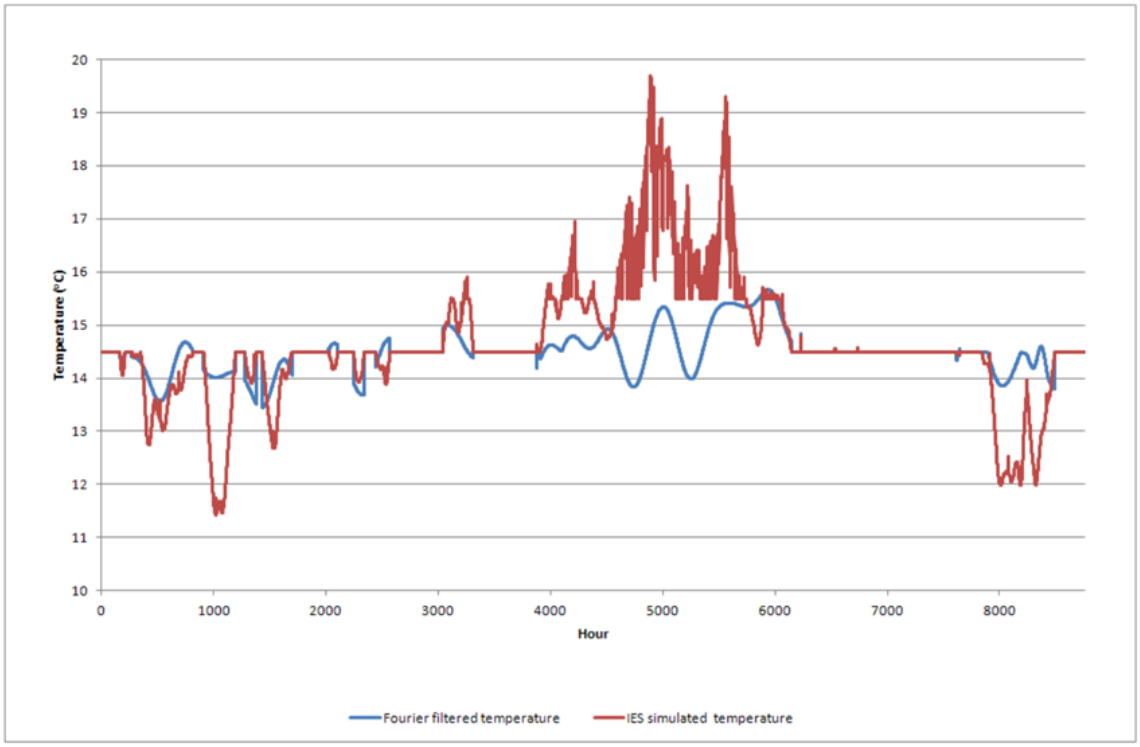

Results of Fourier filter on IES simulated RH in the RINA (Jankovic, 2012c):

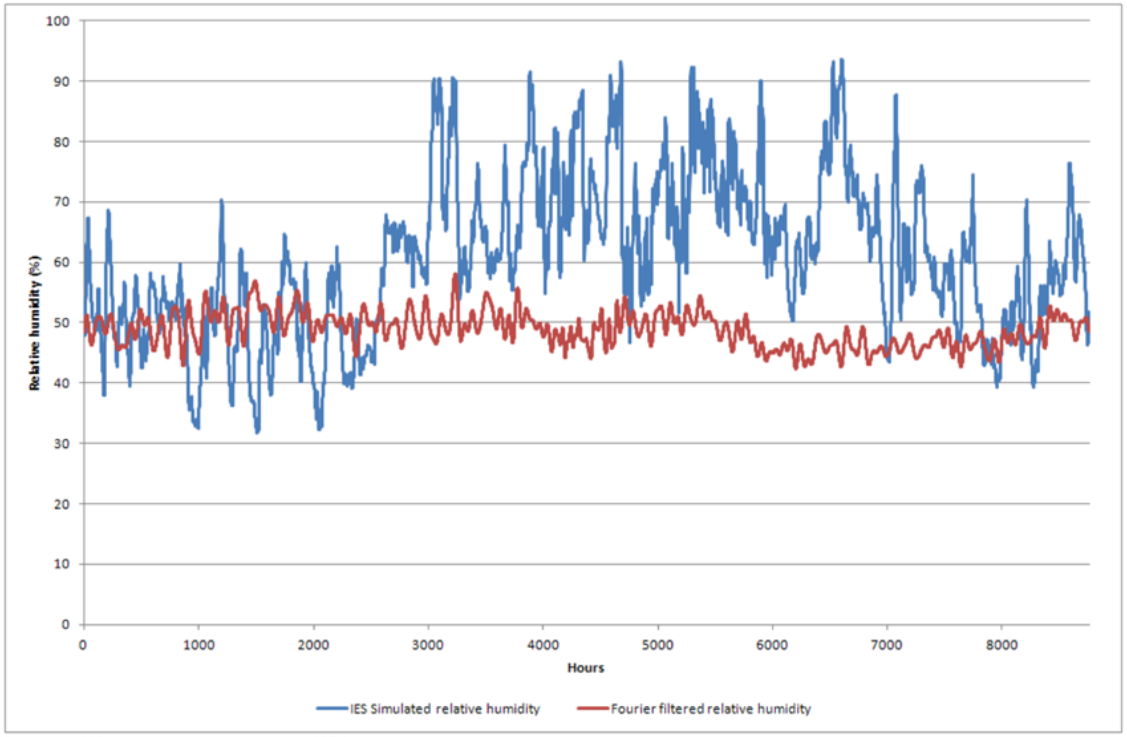

Tabulated transient state M&E & RH history (from Jankovic, 2013)

Date	Issue	Consequence	Solution	Date	Result	RH ground floor
05/12	M&E install delayed	Pre-conditioning delayed	Delivery schedule revised		Allowance for 2-month pre-conditioning period	No RH data
05/12	Carnego monitoring system accessible only by project consultant	No consistent monitoring history available for first three months No monitoring by museum	SMG Hanwell system extended to monitor three BOX stores	07/12	SMG RH monitoring from 23/07 Monitoring history started	
05/12	Technical problem with one of printed circuit boards (PCB)	Delay in full AHU operation	Replace PCB	05/12	Technical issue resolved	
05/12	Missing duct sensors in AHUs	AHU operational parameters not met	Install missing sensors	05/12	Improved monitoring of external air supply	
05/12	No internet connection to BMS	No remote commissioning or communication by subcontractor	SMG ICT supply VPN access to subcontractor	07/12	BMS operational and fault diagnosis started	RH at 80% ±5%
05/12	No internet connection to Airflow AHUs	No remote commissioning	Engineers carry out 1st commissioning on-site Internet connection	06/12 07/12	AHUs operated Fault diagnosis started	RH drops to 65% ±5%
05/12	No internet connection to AHUs	No remote communication by system designer	SMG ICT supply VPN access to system designer	06/12	AHUs set to operate from 22:00-04:00 to lower temperature	RH starts to rise to 70% ±5%
06/12	BMS external RH/T sensor readings incorrect: T at 35°C instead of <20°C	No heating to reduce RH from intake air	Sensors replaced & connected to BMS	06/12	Air intake RH reduced by heating	RH drops to 70% ±5%
06/12	Air flow rates exceeded	RH rises as moisture is drawn in from outside	Units set into manual override	06/12	RH rises	RH rises to 75% ±10%
06/12	Carnego system not monitored regularly	RH readings rising unnoticed to 75% by contractors & consultant	Hanwell system installed	07/12	Rise in RH noted by SMG staff monitoring Hanwell	RH rises to 80% ±10%
06/12	Unpredictable behaviour of AHUs even in manual override	Flow rate unpredictable RH/T fluctuations	Zero speed signal set on BMS	07/12	RH fluctuates 20%	RH fluctuates between 55% -75%

07/12	AHUs operate at 30% fan speed 04:00-22:00 despite zero speed signal from BMS	Night time drying benefits reversed; RH levels continually rise during day to reach 77% by 27/07	Hanwell system functional with SMG staff weekly surveillance Night-time operations of AHUs ceased on 26/07 as T>15°C AHUs turned on 06/08 as night-time T's <14°C	07/12 08/12	Consultant alerted to high RH by SMG site staff	RH drifts from 71% ±3% to 75% ±3% RH rises to 78%
07/12	Fan speed operates at 30% at all times, despite zero signal	Moist air continues to be drawn into system	Unit settings changed by contractor	08/12	Increased RH fluctuations but RH level drops	RH 70% ±5%
08/12	AHU1 shuts down as inhibited by fire alarm signal	RH remains around 75%	Control software updated in both AHUs Units set to work on analogue signal from BMS Units set to work on extract air T rather than default supply air Filter pressure sensors manually adjusted to max pressure 300Pa from default setting of 200Pa	08/12	RH fluctuations reduced but level remains high	RH 75 ±2%
08/12	AHUs random operation tracked to STOP contact receiving ON/OFF signals from fire alarm system	RH levels rise when moist air is drawn in	As above	08/12	As above	
08/12	No RH regulation from AHUs Passive control system inadequate to rectify high RH levels	RH levels in excess of 70% and continuing to drift upwards	Portable air conditioners and dehumidifiers installed	08/12	RH drops 10% in 1 hour, then another 10%/ 1 hr drop 3 days later	RH drops from high of 77% ±3% to low of 58% ±2%
08/12	Sporadic emptying of portable dehumidifiers	RH drops while units are functional but bounces back when units are full & cease operating	AHUs turned on at night AHUs turned off	08/12 09/12	RH level & fluctuations increase RH levels decrease; fluctuations decrease	RH fluctuates between 58% ±2% - 70% ±2% RH drops from 65% ±5% to 45%±5%

			Hoses connect dehumidifiers to internal hangar drain			
End of pre-conditioning phase						
10/12	Drop in external temperatures	RH fluctuates rapidly due to sudden temperature changes	BMS runs heaters		Temperature increases but does not return to earlier levels;	RH rises to 48% ±2%
11/12	No connection to Hanwell	No independent RH/T data from 07 - 14/11/12	SMG ICT & Hanwell notified	11/12	Connection re-established	RH rises to 60% ±5%
11/12	AHUs set into heating mode Dampers set into recirculation mode	RH rises from 50% to over 60% then drops to 55%±5%	AHUs continue to operate	11/12	RH levels start to drop	RH drops to 55% ±5%
12/12	AHU1 showing overheated status & not working AHU2 running at 67% max speed but supply heater failed	RH rises to 65%±3%	Software updated Heaters rewired	12/12	System operational;	RH drops to 60% ±5%
12/12	Continuous ventilation & heating modes reduce effectiveness of RH control	RH fluctuations over 20% depending on mode	Various modes of operation trialled including limited use of drier external air & intermittent heating	01/13	RH levels continue to drop but fluctuations range between 10 -20%	RH drops to 45% ±5%
12/12	Zone conditions unbalanced	No documentation for control algorithm	Software control algorithm reverse-engineered & functionality checked remotely	01/13	Control specialist required to attend site for further investigation to rectify controller issues	
02/13	Zone conditions unbalanced	RH was compared to T and not to RH so setpoints imprecise	Plotting channels engineered for all T sensors & controller reconfigured	02/13	Controller with precise setpoints for T	
02/13	Ductwork unbalanced AHU2 supply fan providing only 50% of flow compared to extract fan	Considerable under pressure with corresponding heat loss	Ductwork unable to be rebalanced due to faulty dampers	02/12	RH fluctuations are erratic	RH 50% ±2% – 15%

02/13	Faulty bypass damper with non-working blade	Unbalanced air flow	As above	02/13	RH levels fluctuate	RH fluctuates between 40% ±10% to 50% ±10%
04/13	Online access to BMS controller suddenly read-only	No external control of building conditions by system designer	Password access enabled	04/13	System designer able to externally control conditions	
04/13	BMS controller no longer responds to internal timer signals	Requires manual override to run AHU1	AHU1 ENABLE signal switch identified & turned from OFF to ON	05/13	Fan signal responding to timer	
04/13	All outside air facing dampers substandard with non-working blades or poor airtightness	RH rises from 40% ±5% to 60% ±5% due to external air leakage even in full recirculation mode	Outside air facing dampers (4) replaced with ones with higher airtightness Bypass dampers (4) replaced reusing replaced outside dampers	05/13	Dampers commissioned as fully operational RH stabilises at higher range	RH 60% ±5%
04/13	AHU2 exhaust working out of sync with supply and recirculation damper Both exhaust dampers with non-working blades	RH gain due to reverse operation on OPEN and CLOSE signals	Exhaust dampers(2) replaced Ductwork rebalanced	05/13	System commissioned as fully operational M&E system turned off to allow passive regulation RH stabilises until mid-06/13	RH 60 ±2%